

Sheffield Hallam University

The role of citrullination of central nervous system proteins in multiple sclerosis.

BRADFORD, Claire Margaret.

Available from the Sheffield Hallam University Research Archive (SHURA) at:

<http://shura.shu.ac.uk/19387/>

A Sheffield Hallam University thesis

This thesis is protected by copyright which belongs to the author.

The content must not be changed in any way or sold commercially in any format or medium without the formal permission of the author.

When referring to this work, full bibliographic details including the author, title, awarding institution and date of the thesis must be given.

Please visit <http://shura.shu.ac.uk/19387/> and <http://shura.shu.ac.uk/information.html> for further details about copyright and re-use permissions.

ProQuest Number: 10694268

All rights reserved

INFORMATION TO ALL USERS

The quality of this reproduction is dependent upon the quality of the copy submitted.

In the unlikely event that the author did not send a complete manuscript and there are missing pages, these will be noted. Also, if material had to be removed, a note will indicate the deletion.



ProQuest 10694268

Published by ProQuest LLC (2017). Copyright of the Dissertation is held by the Author.

All rights reserved.

This work is protected against unauthorized copying under Title 17, United States Code
Microform Edition © ProQuest LLC.

ProQuest LLC.
789 East Eisenhower Parkway
P.O. Box 1346
Ann Arbor, MI 48106 – 1346

Learning and Information Services
Adsetts Centre, City Campus
Sheffield S1 1WD

102 040 847 2



Sheffield Hallam University
Learning and Information Services
Adsetts Centre, City Campus
Sheffield S1 1WD

REFERENCE

**The role of citrullination of central nervous
system proteins in multiple sclerosis**

Claire Margaret Bradford

A thesis submitted in partial fulfilment of the requirements of Sheffield Hallam
University for the degree of Doctor of Philosophy

October 2012

For mum

Multiple sclerosis (MS) is a chronic inflammatory neurodegenerative disease of the central nervous system (CNS) characterised by focal lesions of inflammation and demyelination, with subsequent axonal damage. Although the cause is not yet known, it is thought to be autoimmune in origin. Antibodies are implicated in the disease process, as these are detectable in the cerebrospinal fluid (CSF) seen as oligoclonal bands (OCBs) following isoelectric focussing. However, the target antigen of these antibodies has not yet been fully characterised. Post-translational modification of myelin basic protein (MBP) and other CNS-specific proteins, including citrullination of arginine residues, results in conformational changes in the protein. This leads to increased degradation by proteases and exposure of new epitopes, which may then cause the production of autoantibodies targeting the myelin sheath. The process of citrullination is carried out by a family of enzymes known as peptidylarginine deiminases (PADs) with PAD2 and PAD4 expressed in the brain. Excess citrullination occurs in MS, with MBP isolated from MS white matter being more highly citrullinated than in healthy control white matter. This thesis aimed to investigate the *in vitro* expression of PAD2 and PAD4 by cells of the CNS to gain a better understanding of how these enzymes might be regulated and their possible role in the pathogenesis of MS. Cells were treated with pro-inflammatory cytokines *in vitro*, to mimic *in vivo* inflammatory conditions, and following this, PAD2 and PAD4 mRNA expression was determined using real-time PCR. PAD2 mRNA was significantly decreased in the presence of pro-inflammatory cytokines IL-1 β , TNF- α and IFN- γ in three preparations of primary human astrocytes, a human foetal microglial cell line (CHME3) and a brain endothelial cell line (hCMEC/D3). Furthermore, treatment of CHME3 cells with anti-inflammatory cytokines IL-4, IL-10 and TGF- β also resulted in the down-regulation of PAD2 mRNA. PAD4 was undetectable. Thus pro- and anti-inflammatory cytokines down-regulate expression of PAD2 mRNA *in vitro*, which indicates that increased citrullination of CNS proteins in MS is not due to the inflammatory milieu in the CNS, suggesting additional mechanisms must be involved in the up-regulation of PAD2 and PAD4 enzymes reported in MS tissue.

Subsequently, *in vivo* studies were carried out investigating the distribution and expression of PAD2 and PAD4 enzymes, and citrullinated proteins, in post-mortem control, MS normal appearing white matter (NAWM) and MS lesional brain tissue by immunohistochemistry. Higher levels of citrullinated proteins were observed in MS lesions compared to control and NAWM brain tissue, and were associated with areas of myelin thinning with on-going demyelination, and was co-localised to GFAP-positive astrocytes. PAD2 expression was difficult to detect. Western blotting of proteins extracted from these MS brains showed citrullination of multiple proteins, two of which were identified as glial fibrillary acidic protein (GFAP) and MBP, the latter also confirmed by mass spectrometry. This agrees with previous studies implicating citrullination in the pathogenesis of MS. Lastly, an enzyme-linked immunosorbant assay (ELISA) method was developed to detect anti-citrullinated protein antibodies (ACPAs) against citrullinated MBP peptides in the CSF and serum of patients newly diagnosed with MS, other neurological diseases (ONDs) and controls, to determine whether higher levels of antibodies were observed in individuals with MS. No significant increases in the levels of ACPAs were found in the CSF and serum of individuals with MS compared to ONDs and controls. Although not significant, increased reactivity of MS patient CSF immunoglobulins towards citrullinated MBP peptides was observed. Furthermore, an association was found between reactivity towards citrullinated MBP peptides and patients testing positive for OCBs. Evidence presented in this thesis demonstrates an important role of citrullination in the pathogenesis of MS. The results of this thesis indicate that further investigations into the role of citrullination in MS, particularly with regards to assessment of further citrullinated peptides as antigenic targets in ELISA assays, are warranted.

Contents

Dedication.....	ii
Abstract	iii
Contents	iv
List of Figures	xi
List of Tables	xv
Abbreviations.....	xvii
Published Abstracts	xxii
Published Papers.....	xxiii
Acknowledgements.....	xxiv
Chapter 1 General Introduction	1
1.1 Innate and adaptive immunity.....	2
1.1.1 Innate immunity	2
1.1.2 Adaptive immunity	5
1.1.2.1 Major histocompatibility complex class I and II	6
1.1.2.2 T cell receptor.....	8
1.1.2.3 T cell activation.....	9
1.1.2.4 B cell development	10
1.1.2.5 B cell isotype switching.....	11
1.1.3 Immunological tolerance	11
1.1.3.1 Central tolerance	12
1.1.3.2 Peripheral tolerance	13
1.1.3.3 Dendritic cells and tolerance.....	14
1.2 Autoimmunity	14
1.2.1 Breakdown of tolerance in autoimmunity.....	14
1.2.2 Autoimmunity	14
1.2.3 Multifactorial nature of autoimmunity.....	15
1.2.3.1 Genetics	15
1.2.3.2 Environment	17
1.2.3.3 Epigenetics.....	18

1.2.3.4 Gender	20
1.2.3.5 Geoepidemiology	21
1.3 Multiple sclerosis	21
1.3.1 Clinical presentation and disease course of MS	22
1.3.2 Diagnosis	22
1.3.3 Genetics and MS	23
1.3.4 Epidemiology	25
1.3.5 Pathology of multiple sclerosis	26
1.3.5.1 White matter pathology	26
1.3.5.2 Grey matter pathology	28
1.4 Immune responses within the central nervous system	29
1.4.1 T cells	29
1.4.2 B cells	30
1.4.3 Glial cells	30
1.4.3.1 Microglia	30
1.4.3.2 Astrocytes	33
1.4.3.3 Oligodendrocytes (OLGs)	35
1.4.4 Endothelial cells (ECs)	36
1.4.5 The blood brain barrier (BBB)	37
1.4.5.1 BBB disruption and multiple sclerosis	39
1.5 Autoimmune mechanisms in MS	40
1.5.1 T cells in MS	40
1.5.2 B cells in MS	41
1.5.3 Peptidylarginine deiminases (PADs) and citrullination	42
1.5.3.1 PADs and citrullination in MS	43
1.5.3.2 Citrullination and experimental autoimmune encephalomyelitis (EAE) ..	46
1.5.3.3 Proteolytic enzyme action on citrullinated MBP	47
1.5.3.4 Regulation of PAD and citrullination	49
1.5.3.5 Citrullination in rheumatoid arthritis (RA)	50
1.5.3.6 Citrullination in other neurological diseases (ONDs)	51

1.5.4 Hypothesis	53
1.5.5 Aim of the thesis	53
1.5.6 Objectives of the thesis	53
Chapter 2 <i>In vitro</i> investigation of the effects of pro-inflammatory cytokines on the expression of PAD2 and PAD4	54
2.1 Introduction	55
2.1.4 Aim of the study	57
2.1.5 Objectives of the study	57
2.2 Materials and methods	58
2.2.1 Suppliers used in this chapter	58
2.2.2 Cell culture	58
2.2.2.1 Collagen coating	59
2.2.2.2 Recovery of cryofrozen cells	59
2.2.2.3 Cell harvesting and serial passage of cells	59
2.2.2.4 Cell counting	60
2.2.2.5 Reconstitution of cytokines	60
2.2.2.6 Cytokine treatment of cells	63
2.2.2.7 Cell viability and proliferation assay	63
2.2.3 The principles of standard polymerase chain reaction (PCR) and quantitative real-time PCR (qPCR)	64
2.2.3.1 Total RNA extraction	68
2.2.3.2 Agarose gel electrophoresis of total RNA	69
2.2.3.3 cDNA synthesis	69
2.2.3.4 qPCR	71
2.2.3.5 Relative quantification using comparative CT method	71
2.2.3.6 Determination of primer efficiencies	73
2.2.3.8 Selection of housekeeping genes	74
2.2.4 Traditional PCR	75
2.4.4.1 Optimisation of traditional PCR for PAD4	75
2.4.4.2 Agarose gel of PCR products	75
2.2.5 Immunocytochemistry	77

2.2.5.1 Indirect immunofluorescence	78
2.2.6 Statistical analysis	79
2.3 Results	82
2.3.1 Effect of pro-inflammatory cytokines on the viability of CNS cells.....	82
2.3.1.1 U373-MG astrocytoma cell line.....	82
2.3.1.2 EP14 primary human astrocyte cells	82
2.3.1.3 EP15 primary human astrocyte cells	82
2.3.1.4 MS16 primary human astrocytes	86
2.3.1.5 CHME3 human foetal microglial cell line.....	86
2.3.1.6 hCMEC/D3 human brain endothelial cell line.....	86
2.3.2 RNA integrity.....	90
2.3.3 Selection of housekeeping genes	90
2.3.4 Primer efficiencies	90
2.3.5 Modulation of gene expression by pro-inflammatory cytokines	96
2.3.5.1 Basal expression of PAD2 and PAD4 in cells of the CNS.....	96
2.3.5.2 U373-MG astrocytoma cell line.....	99
2.3.5.3 Primary astrocytes derived from normal white matter (EP14 and EP15)	101
2.3.5.4 Primary astrocytes derived from white matter from a case of MS (MS16)	101
2.3.5.5 CHME3 human foetal microglial cell line.....	104
2.3.5.6 hCMEC/D3 brain endothelial cell line	106
2.3.6 Standard PCR of PAD4	106
2.3.7 Immunocytochemical detection of PAD2 and PAD4.....	109
2.4 Discussion.....	114
2.4.1 IL-1 β , TNF- α , IL-6 and IFN- γ differentially affect cellular proliferation in an astrocytoma cell line, primary human astrocytes, microglial cell line and brain endothelial cell line	114
2.4.2 IL-1 β , TNF- α and IFN- γ differentially modulate the gene expression of PAD2 and PAD4 in an astrocytoma cell line, primary human astrocytes, microglial cell line and brain endothelial cell line	115

2.4.3 Conclusion	122
Chapter 3 <i>In vivo</i> investigation of citrullinated proteins and PAD expression in post-mortem brain tissue	125
3.1 Introduction	126
3.1.1. Aim of the study	127
3.1.2 Objectives of the study	127
3.2 Materials and methods	128
3.2.1 Suppliers used in this chapter	128
3.2.2 Source of MS and control tissue and ethical approval	128
3.2.3 Characterisation of tissue blocks	132
3.2.3.1 Haemotoxylin and eosin (H&E)	132
3.2.3.2 Oil Red O (ORO)	134
3.2.3.3 Sudan black B staining	135
3.2.4 Tissue grading	135
3.2.4.1 H&E and ORO stains	135
3.2.4.2 HLA-DR expression	138
3.2.4.3 MOG expression	138
3.2.4.4 Classification of lesion type	138
3.2.5 Immunohistochemistry	140
3.2.5.1 Single label immunofluorescence	140
3.2.5.2 Dual labeling immunofluorescence	141
3.2.5.3 Semi-quantification of citrullination immunoreactivity	145
3.2.6.1 Image analysis and capture	145
3.2.6.2 Light and fluorescence microscopy	148
3.2.6.3 Confocal scanning laser microscopy	148
3.2.3 qPCR using Taqman® probes	148
3.2.3.1 Statistical analysis for qPCR data	148
3.2.4 Western blotting	148
3.2.4.1 Protein extraction	151
3.2.4.2 Bicinchoninic Acid (BCA) assay for measurement of protein concentration	153

3.2.4.3 Optimisation of western blotting.....	153
3.2.4.4 Sodium Dodecyl Sulphate Polyacrylamide Gel Electrophoresis (SDS-PAGE).....	155
3.2.4.5 Protein electroblotting.....	155
3.2.4.6 Immunoprobng	155
3.2.4.7 Statistical analysis of western blot data	156
3.3 Results	158
3.3.1 Tissue classification.....	158
3.3.2 Isotype and negative controls	158
3.3.3 Expression of citrullinated proteins in MS, NAWM and control tissue.....	164
3.3.4 Expression of PAD2 in MS, NAWM and control tissue.....	164
3.3.5 qPCR analysis of mRNA expression of PAD2 and PAD4 in MS, NAWM and control tissue	165
3.3.6 Western blot analysis of expression of citrullinated proteins in MS, NAWM and control tissue	165
3.4 Discussion.....	179
3.4.1 The expression of citrullinated proteins is increased in MS	179
3.4.2 PAD2 protein expression is associated with microglia and the lumen of blood vessels	182
3.4.3 Conclusion.....	183
Chapter 4 Investigation of the presence of anti-citrullinated protein antibodies in MS and other neurological conditions	184
4.1 Introduction	185
4.1.1 Aim of the study.....	188
4.1.2 Objectives of the study.....	188
4.2 Materials and methods	189
4.2.1 Suppliers used in this chapter.....	189
4.2.2 Reconstitution of human MBP.....	189
4.2.3 Sodium Dodecyl Sulphate Polyacrylamide Gel Electrophoresis (SDS-PAGE)	189
4.2.4 In-gel digest and extraction of peptides.....	189

4.2.5 Mass spectrometry	190
4.2.5.1 Principles of MALDI mass spectrometry	191
4.2.5.2 Matrix requirements for MALDI mass spectrometry	196
4.2.5.3 Use of Zip Tips® in sample preparation for analysis by mass spectrometry	196
4.2.2.4 MALDI-MS/MS of peptides	198
4.2.6 Enzyme-linked immunosorbant assay (ELISA)	198
4.2.6.1 CSF and serum samples and ethical approval.....	199
4.2.6.2 Preparation and storage of CSF and serum samples	199
4.2.6.3 Detection of ACPAs using a commercial ACPA ELISA used for detection of these antibodies in RA	202
4.2.6.4 Antigens	202
4.2.6.5 Optimisation of ELISA	202
4.2.6.6 ELISA.....	202
4.2.6.7 Statistical analysis	203
4.3 Results	205
4.3.1 Identification of citrullinated peptides	205
4.3.2 Detection of RA-specific ACPAs	218
4.3.3 Optimisation of MBP ELISA	218
4.3.4 Detection of MS-specific ACPAs.....	223
4.4 Discussion.....	237
4.4.1 Citrullinated peptide detection by mass spectrometry	237
4.4.2 ACPAs were not significantly different in MS	240
4.4.3 Conclusion.....	242
Chapter 5 General Discussion	243
5.1 General Discussion	244
5.1.1 Future work.....	249
5.1.2 Conclusions	250
Chapter 6 References	254

Chapter 1

Figure 1.1: The three levels of the human immune system.	4
Figure 1.2: Clinical disease course in multiple sclerosis.....	24
Figure 1.3: Schematic diagram of the blood-brain barrier (BBB).	38

Chapter 2

Figure 2.1: Chemical structures showing the conversion of MTS tetrazolium salt to formazan product.	65
Figure 2.2: qPCR amplification plot.....	66
Figure 2.3: A schematic diagram showing the principles of qPCR using Taqman® probes.	70
Figure 2.4: Direct and indirect immunofluorescence staining of a membrane antigen (Ag).....	80
Figure 2.5: Effect of cytokine treatment on viability of an astrocytoma cell line (U373-MG)..	83
Figure 2.6: Effect of cytokines on the viability of primary adult human astrocytes (EP14)..	84
Figure 2.7: Effect of cytokines on the viability of primary adult human astrocytes (EP15)..	85
Figure 2.8: Effect of cytokines on the viability of primary adult human astrocytes (MS16).....	87
Figure 2.9: Effect of cytokines on the viability of CHME3..	88
Figure 2.10: Effect of cytokines on the viability of hCMEC/D3 cells.....	89
Figure 2.11: RNA extractions of CNS cells following treatment with varying concentrations (0, 1, 10 and 100 ng/mL) of single cytokines; IL-1 β , TNF- α , IL-6 and IFN- γ	91
Figure 2.12: RNA extractions of CNS cells following treatment with varying concentrations (0, 1, 10 and 100 ng/mL) of dual cytokines; IL-1 β + TNF- α , IL-1 β + IFN, and TNF- α + IFN- γ	92
Figure 2.13: Standard curves showing the primer efficiencies following qPCR of serially diluted cDNA from CHME3..	95
Figure 2.14: Amplification curves generated following qPCR of target and housekeeping genes.	97

Figure 2.15: Basal expression of PAD2 mRNA in different preparations of primary human astrocytes, a human foetal microglial cell line (CHME3) and a human brain endothelial cell line (hCMEC/D3).	98
Figure 2. 16: Relative fold change in mRNA levels of PAD2 and PAD4 in U373-MG astrocytoma cells following cytokine treatment.	100
Figure 2.17: Relative fold change in mRNA levels of PAD2 in primary astrocytes from two control cases (EP14 and EP15) following cytokine treatment.. . . .	102
Figure 2.18: Relative fold change in mRNA levels of PAD2 in primary astrocytes from an MS case (MS16) following cytokine treatment.....	103
Figure 2.19: Relative fold change in mRNA levels of PAD2 in CHME3 following cytokine treatment.	105
Figure 2.20: Relative fold change in mRNA levels of PAD2 in hCMEC/D3 endothelial cells following cytokine treatment.....	107
Figure 2.21: Agarose gel electrophoresis of standard PCR products.	108
Figure 2.22: Single label immunofluorescence for GFAP and S-100 β in EP14 primary human astrocytes.. . . .	110
Figure 2.23: Single label immunofluorescence for PAD2 in different preparations of primary human astrocytes and an astrocytoma cell line.	111
Figure 2.24: Single label immunofluorescence for PAD4 in different preparations of primary human astrocytes and an astrocytoma cell line.. . . .	112
Figure 2.25: Single label immunofluorescence for PAD4 using a different primary antibody from Sigma, UK in EP14 primary human astrocytes.. . . .	113

Chapter 3

Figure 3.1: Schematic diagram illustrating the coronal slicing of brains and preparation of tissue blocks by the UK MS Society Tissue Bank.. . . .	133
Figure 3.2: Haematoxylin and eosin (H&E) staining showing the different grades of inflammation observed in CNS white matter.. . . .	136
Figure 3.3: Haematoxylin and eosin (H&E) staining showing the hypercellular border surrounding a lesion and the hypocellular centre of the same lesion (MS058 P1C3).. . . .	137
Figure 3.4: Oil red O (ORO) showing the different grades of lipid-laden macrophages in the white matter tissue.....	139
Figure 3.5: Levels of citrullinated protein (pep cit) in control, NAWM and multiple sclerosis lesions by single staining immunofluorescence and confocal microscopy..	146
Figure 3.6: Schematic diagram showing the optical pathway and principal components in a laser scanning confocal microscope.....	147

Figure 3.7: Schematic representation of western blotting and detection procedure...	149
Figure 3.8: Schematic diagram showing the principle components of the Odyssey Infrared Imaging System.	152
Figure 3.9: An example of a standard curve used in the determination of the protein concentration of unknown samples using BSA as a standard..	154
Figure 3.10: The levels of non-specific staining using isotype controls.....	163
Figure 3.11: Level of citrullinated proteins scored from each block of control white matter, NAWM and lesions from MS cases.....	166
Figure 3.12: Citrullinated protein expression in an active MS lesion.....	167
Figure 3.13: Differential citrullinated protein expression in an active MS lesion.....	168
Figure 3.14: Citrullinated protein expression in areas of demyelination in an active MS lesion..	169
Figure 3.15: Citrullinated protein expression in a chronic active MS lesion..	170
Figure 3.16: Citrullinated protein expression in MS NAWM.	171
Figure 3.17: Citrullinated protein expression in control white matter.	172
Figure 3.18: Localisation of peptidylarginine deiminase 2 (PAD2) in MS lesions, visualised using double staining immunohistochemistry and confocal microscopy.	173
Figure 3.19: Expression of PAD2 and PAD4 in NAWM MS103 P1D3..	174
Figure 3.20: qPCR analyses showing PAD2 and PAD4 mRNA expression in control, NAWM and lesion brain tissue (Log scale).....	175
Figure 3.21: Coomassie blue stain of SDS-PAGE and subsequent western blotting of proteins extracted from control white matter, MS NAWM and MS lesional brain tissue..	176
Figure 3.22: Western blotting of proteins extracted from control white matter, MS NAWM and MS lesional brain tissue.	177
Figure 3.23: Levels of citrullinated GFAP and MBP in control white matter, MS NAWM and MS lesional brain tissue..	178

Chapter 4

Figure 4.1: Schematic diagram demonstrating MALDI-TOF mass spectrometer and a TOF mass spectrometer.	193
Figure 4.2: Nomenclature for the product ions generated in the fragmentation of peptide molecules.....	197
Figure 4.3: Indirect ELISA.	200
Figure 4.4: MALDI mass spectrum obtained following in-gel digestion of recombinant human MBP.....	206

Figure 4.5: Western blotting of MS brain tissue showing citrullinated proteins identified with F95 mAb and corresponding Instant Blue® SDS-PAGE gel.	207
Figure 4.6: MALDI mass spectrum obtained following in-gel digest of MS brain tissue.. ..	208
Figure 4.7: MALDI MS spectrum produced when using different buffers during in-gel digestion and subsequent peptide extraction.	210
Figure 4.8: Comparison between MS spectra produced with and without sample clean-up using Zip Tips®.....	212
Figure 4.9: An example of peptide identification of GFAP.. ..	214
Figure 4.10: An example of peptide identification of MBP.. ..	216
Figure 4.11: Analysis of immune response to RA-specific citrullinated peptides in patients with MS, other neurological disorders and controls.....	219
Figure 4.12: Optimisation of citrullinated MBP peptide 1 ELISA.....	221
Figure 4.13: Optimisation of citrullinated MBP peptide 2 ELISA.	222
Figure 4.14: Analysis of immune response to different citrullinated MBP peptides in the sera of patients with multiple sclerosis (MS), other neurological disorders and controls.	225
Figure 4.15: Analysis of immune response to different citrullinated MBP peptides in the CSF of patients with MS, other neurological disorders and controls.....	227
Figure 4.16: Correlation between patient sera antibodies against different cit-MBP peptides.....	229
Figure 4.17: Correlation between patient CSF antibodies against different cit-MBP peptides.....	230
Figure 4.18: CSF Absorbance values from patients with and without oligoclonal bands.	231
Figure 4.19: Correlation between patient albumin/IgG ratio and patient serum antibodies to cit-MBP peptides.....	233
Figure 4.20: Correlation between patient albumin/IgG ratio and patient CSF antibodies to cit-MBP peptides.....	233
Figure 4.21: Correlation between patient serum IgG concentration and patient serum antibodies to cit-MBP peptides.....	235
Figure 4.22: Correlation between patient CSF IgG concentration and patient CSF antibodies to cit-MBP peptides.....	236

List of Tables

Chapter 1

Table 1.1: Overview of the innate and adaptive immune system. 3

Chapter 2

Table 2.1: Human primary and secondary cell lines used in this study and their culture medium composition..... 61

Table 2.2: qPCR housekeeping and target gene information 72

Table 2.3: Details of PAD4 primers tested in standard PCR, including details of the primer sequences for the forward and reverse primers used..... 76

Table 2.4: Details of primary and secondary antibodies used for immunocytochemical detection of GFAP, PAD2 and PAD4. 81

Table 2.5: Validation of reference genes using the GeNorm analysis programme. 93

Table 2.6: Summary of the primer efficiencies of all housekeeping and target genes used in qPCR. 94

Table 2.7: Summary of significant effects of cytokines, single and co treatment on proliferation of CNS cells. 123

Table 2.8: A summary of the significant data obtained by qPCR for PAD2 and PAD4 mRNA expression following cytokine treatment, single and dual treatment, on CNS cells used in this study. PAD4 expression was only assessed in U373-MG cell line. 124

Chapter 3

Table 3.1: Clinical data of patients with multiple sclerosis included in this study. 129

Table 3.2: Clinical data of control cases included in this study..... 131

Table 3.3: Details of the primary and secondary antibodies used in immunohistochemistry. 142

Table 3.4: Details of the primary and secondary antibodies used in western blotting for analysis of protein expression in MS and control tissue. 157

Table 3.5: Tissue classification of MS and control blocks based upon H&E, ORO, HLA-DR and MOG staining. 159

Chapter 4

Table 4.1: Summary of clinical details of patients participating in this study. 201

Table 4.2: Citrullinated MBP peptides used as the antigenic substrate in ELISA assays. 204

Table 4.3: List of peptides identified using MALDI-IMS-MS/MS and Mascot. 217

Abbreviations

Ab	Antibody
ACN	Acetonitrile
ACPA	Anti-citrullinated protein antibody
AD	Alzheimer's disease
ADEM	Acute disseminated encephalomyelitis
AJ	Adherens junction
Ag	Antigen
AICD	Activation-induced cell death
AIRE	Autoimmune regulator
AITD	Autoimmune thyroid disease
ALP	Alkaline phosphatase
AMP	Anti-microbial peptide
APC	Antigen presenting cell
AQP-4	Aquaporin-4
ATP	Adenosine triphosphate
BAEE	Benzoyl-L-arginine ethyl ester
BCA	Bichinchoninic Acid
BCSFB	Blood-CSF barrier
BM	Basement membrane
BSA	Bovine serum albumin
CARM1	Coactivator-associated arginine methyltransferase 1
cDNA	Complementary deoxyribonucleic acid
CD	Cluster of differentiation
CHCA	Cyano-4-hydroxycinnamic acid
CID	Collision-induced dissociation
CIS	Clinically isolated syndrome
Cit	Citrulline
CCP	Cyclic citrullinated peptide
CLSM	Confocal laser scanning microscopy
CNS	Central Nervous System
CRP	C-reactive protein
CSF	Cerebrospinal fluid
CT	Cycle Threshold
CTL	Cytotoxic T lymphocyte
Da	Dalton

DAMPs	Damage-associated molecular patterns
DAPI	4',6-diamidino-2-phenylindole
DC	Dendritic cell
2-DE	Two-dimensional gel electrophoresis
DEPC	Diethylpyrocarbonate
DNA	Deoxyribonucleic acid
dNTP	Deoxyribonucleotide triphosphate
DP	Double positive
DPBS	Dulbecco's phosphate buffered saline
DR-3	Death receptor-3
DTT	Dithiothreitol
EAE	Experimental autoimmune encephalomyelitis
EBV	Epstein-Barr virus
EC	Endothelial cell
ECM	Extracellular matrix
EDTA	Ethylenediaminetetraacetic acid
EGF	Endothelial growth factor
EGM	Endothelial growth media
ELISA	Enzyme-linked immunosorbent assay
ETD	Electron-transfer dissociation
FCS	Foetal calf serum
FGF	Fibroblast growth factor
FRET	Fluorescence resonance transfer
GAPDH	Glyceraldehyde 3-phosphate dehydrogenase
GC	Germinal centre
GFAP	Glial fibrillary acidic protein
GLM	General Linear Model
GWAS	Genome-wide association studies
H&E	Haematoxylin and eosin
HAT	Histone acetyltransferase
HDAC	Histone deacetylase
HI	Heat inactivated
HK	House keeping
HLA	Human leukocyte antigen
HMGB1	High mobility group box 1 protein
HPLC	High-performance liquid chromatography
HPRT1	Hypoxanthine phosphoribosyltransferase 1
IC	Isotype control

ICC	Immunocytochemistry
IGF	Insulin-like growth factor
ID	Identification
IDO	2, 3-dioxygenase
IEF	Isoelectric focussing
IFN- γ	Interferon-gamma
Ig	Immunoglobulin
IHC	Immunohistochemistry
IIH	Idiopathic intracranial hypertension
IPEX	Immune dysregulation, polyendocrinopathy, enteropathy, X-linked syndrome
IL	Interleukin
IL-2R	Interleukin-2 receptor
IL7R	IL-7 receptor
IMS	Ion mobility separation
IRFS	Interferon regulatory factor S
JAMs	Junctional adhesion molecules
LBP	LPS binding protein
LC	Liquid chromatography
LFB	Luxol Fast Blue
LPS	Lipopolysaccharide
Lys C	Lysine C
M	Stability measure
mAb	Monoclonal antibody
MAG	Myelin associated glycoprotein
MALDI-MS	Matrix-assisted laser desorption/ionization-mass spectrometry
MBL	Mannose-binding lectin
MBP	Myelin basic protein
mC	Methyl cytidylic acid
MHC	Major histocompatibility complex
miRNA	Micro ribonucleic acid
MOG	Myelin oligodendrocyte glycoprotein
M_r	Relative molecular mass
MRI	Magnetic resonance imaging
mRNA	Messenger ribonucleic acid
MS	Multiple sclerosis
mTEC	Medullary thymic epithelial cells
MTS	(3-(4,5-dimethylthiazol-2-yl)-5-(3-carboxymethoxyphenyl)-2-(4-

	sulfophenyl)-2H-tetrazolium
MZ	Monozygotic
<i>m/z</i>	Mass-to-charge ratio
NAWM	Normal appearing white matter
NCM	Nitrocellulose membrane
NF-KB	Nuclear factor-kappa B
NHEK	Normal human keratinocytes
NI	Non-inflammatory
NK	Natural killer
NLR	NOD-like receptor
NLS	Nuclear localisation signal
NMO	Neuromyelitis optica
NOD	Nucleotide oligomerisation domain
OCB	Oligoclonal band
OD	Optical density
O/N	Overnight
OND	Other neurological disease
ORO	Oil Red O
PAD	Peptidylarginine deiminase
PAMP	Pathogen associated molecular pattern
PAS	Periodic acid-Schiff
PBC	Primary biliary cirrhosis
PBMC	Peripheral blood mononuclear cell
PBS	Phosphate buffered saline
PCR	Polymerase chain reaction
PD	Parkinson's Disease
PFA	Paraformaldehyde
PLP	Proteolipid protein
PMS	Phenazine methosulphate
pNPP	p-nitrophenyl phosphate
PPIA	Cyclophilin A
PPMS	Primary progressive multiple sclerosis
PR	Progressive relapsing
PRR	Pathogen recognition receptor
PtdSer	Phosphatidylserine
PTM	Post-translational modification
PTPN22	Protein tyrosine phosphatase non-receptor type 22
PVC	Perivascular cuff

Q	Quadrupole
qPCR	Quantitative real-time polymerase chain reaction
RA	Rheumatoid arthritis
RNA	Ribonucleic acid
RNS	Reactive nitrogen species
ROS	Reactive oxygen species
RP	Reverse phase
RRMS	Relapsing-remitting multiple sclerosis
RT	Room temperature
SBB	Sudan Black B
sCJD	Sporadic Creutzfeldt-Jakob disease
SDS-PAGE	Sodium dodecyl sulphate polyacrylamide gel electrophoresis
SFM	Serum free media
SLE	Systemic lupus erythematosus
SP	Single positive
SPMS	Secondary progressive multiple sclerosis
SS	Sjogren's syndrome
SST	Serum separator tube
TAE	Tris-acetate-EDTA
TBS	Tris-buffered saline
TBS-T	Tris-buffered saline-Tween
T1DM	Type 1 diabetes mellitus
T _{CM}	Central memory T cell
TCR	T cell receptor
T _{EM}	Effector memory T cell
TEP	Triethyl phosphate
TIR	Toll/IL-1 receptor-like domain
TFA	Trifluoroacetic acid
TGF- β	Transforming growth factor-beta
Th	T helper cell
TJ	Tight junction
TLR	Toll-like receptor
TNF- α	Tumour necrosis factor-alpha
TOF	Time-of-flight
Treg	Regulatory T cell
TREM2	Triggering receptor expressed on myeloid cells-2
UTP	Uridine triphosphate
UV	Ultraviolet

Published Abstracts

1. Bradford C, Ramos I, Cross AK, Haddock G, McQuaid S, Nicholas AP & Woodroofe MN (2012) The expression of citrullinated proteins in post-mortem tissue in multiple sclerosis *Neuropathology and Applied Neurobiology* **38**: 24-25. British Neuropathological Society Congress 2012, London, UK.
2. Bradford C, Cross, A, Haddock G & Woodroofe N (2010) The role of citrullination of central nervous system proteins in the pathogenesis of multiple sclerosis *Journal of Neuroimmunology* **228**: 113-114. International Society of Neuroimmunology Congress 2010, Sitges, Barcelona.
3. Bradford C, Cross A, Haddock G, Nicholas A. & Woodroofe N. (2010) The role of citrullination of central nervous system proteins in the pathogenesis of multiple sclerosis *Immunology* **131**: 160-161. British Society for Immunology Congress 2010, Liverpool, UK.

Published Papers

1. Frentzou, G.A., Bradford, C., Harkness, K.A., Haddock, G., Woodroffe, M.N., & Cross, A.K. (2012) IL-1 β down-regulates ADAMTS-13 mRNA expression in cells of the central nervous system. *Journal of Molecular Neuroscience* **46**(2): 343-351.
2. Bradford, C.M., Cross, A. K., Haddock, G., Woodroffe, N. & Sharrack, B. (2011) Citrullination of CNS proteins in the pathogenesis of multiple sclerosis. *Future Neurology* **6**(4): 521-530.
3. Bradford, C.M., Cross, A. K., Haddock, G. & Woodroffe, M.N. (2009) Citrullination in MS: Potential for a new diagnostic test *British Journal of Neuroscience Nursing* **5**(1): 13-15.

Acknowledgements

First and foremost I would like to thank Professor Nicola Woodroffe for giving me the opportunity to carry out this PhD in the first place, and providing me with guidance, support and encouragement throughout. Also, thank you to Dr. Alison Cross and Dr. Gail Haddock for their valuable advice and support. Thank you to the UK MS Society for funding this PhD.

Most importantly to all the donors at the UK MS Society Tissue Bank for choosing to donate your tissue to research, without you this thesis would not have been possible. Thank you also to all the patients at the Neurology Department at the Royal Hallamshire Hospital for kindly agreeing to donate their CSF and blood for this research. I will forever be grateful. Also, to the medical staff for collecting these samples and ensuring I reached my target of 200 patients, and adding to your already extensive work load. Thank you also to Dr. Basil Sharrack for his involvement in the patient study, and for funding the latter part of my PhD.

Special thank you to Dr. Stephen McQuaid at Queen's University, Belfast, for kindly giving up a day of your precious time to look at my histology slides and imparting your expert knowledge on MS pathology, I will forever be grateful for your time and kindness shown to me during my short stay in Belfast.

Thank you to all my friends and colleagues in the BMRC, especially my girls Helenne Nyamwaro, Laura Cole, Louise Vickers, Kate Phillips and Rachel Doherty for providing advice, friendship and most importantly a source of distraction. Thank you also to Rachel Waller, Inês Ramos and Mafalda Reiss for all your help during your placements in our laboratory. Thank you to Marguerite Lyons and Sarah Wright for all your help and support throughout the PhD. Thank you to Kevin Blake for all your IT support. Thank you to Dr. Karen Kilner for all your statistical help. Thank you to my life-long friends Dr. Harriet Nicholls and soon-to-be Dr. Nicholas Hooper for your friendship over the years, you have both helped me more than you will ever know.

Special thank you to my mum who has been my rock throughout this PhD, and given me the confidence to pursue my dreams, even at a time when it did not seem possible and most importantly for providing me with a constant supply of jelly babies whilst writing up. This PhD thesis is as much yours as it is mine. To my gran for supporting me, especially during these difficult last two months writing up, providing me with a place to stay and constant cups of tea. Last but not least, thank you to my 'little' brothers David and Carl and my sister Mandy, for always being there for me.

Chapter 1

General Introduction

1.1 Innate and adaptive immunity

The body is constantly exposed to pathogenic organisms and in order to combat this, the immune system has evolved to protect against infection of the host cells. The first line of defence against pathogens is the anatomical and physiological barriers, which include the skin, the cilia of the lungs and lysozyme in tears, and these prevent the entry of some pathogenic organisms into the body. However, many of these pathogens are able to evade these anatomical and physiological barriers, and this is where the adaptive immune system becomes paramount. The immune system is composed of two types: (1) innate immunity and (2) adaptive immunity (Table 1.1; Figure 1.1).

1.1.1 Innate immunity

Innate immunity was originally thought to offer non-specific immunity; however, recent advances in this field have led to considerable changes in this concept. The innate immune system relies on a limited number of receptors referred to as pathogen recognition receptors (PRRs) to detect invading pathogens but compensates for this limited number by targeting conserved microbial components that are shared by large numbers of pathogens (Turvey and Broide 2010). Speed is the most prominent characteristic of the innate immune system, as within minutes of pathogen exposure, the innate immune system starts generating a protective inflammatory response. The innate immune system also plays a vital part in activating the adaptive immune response.

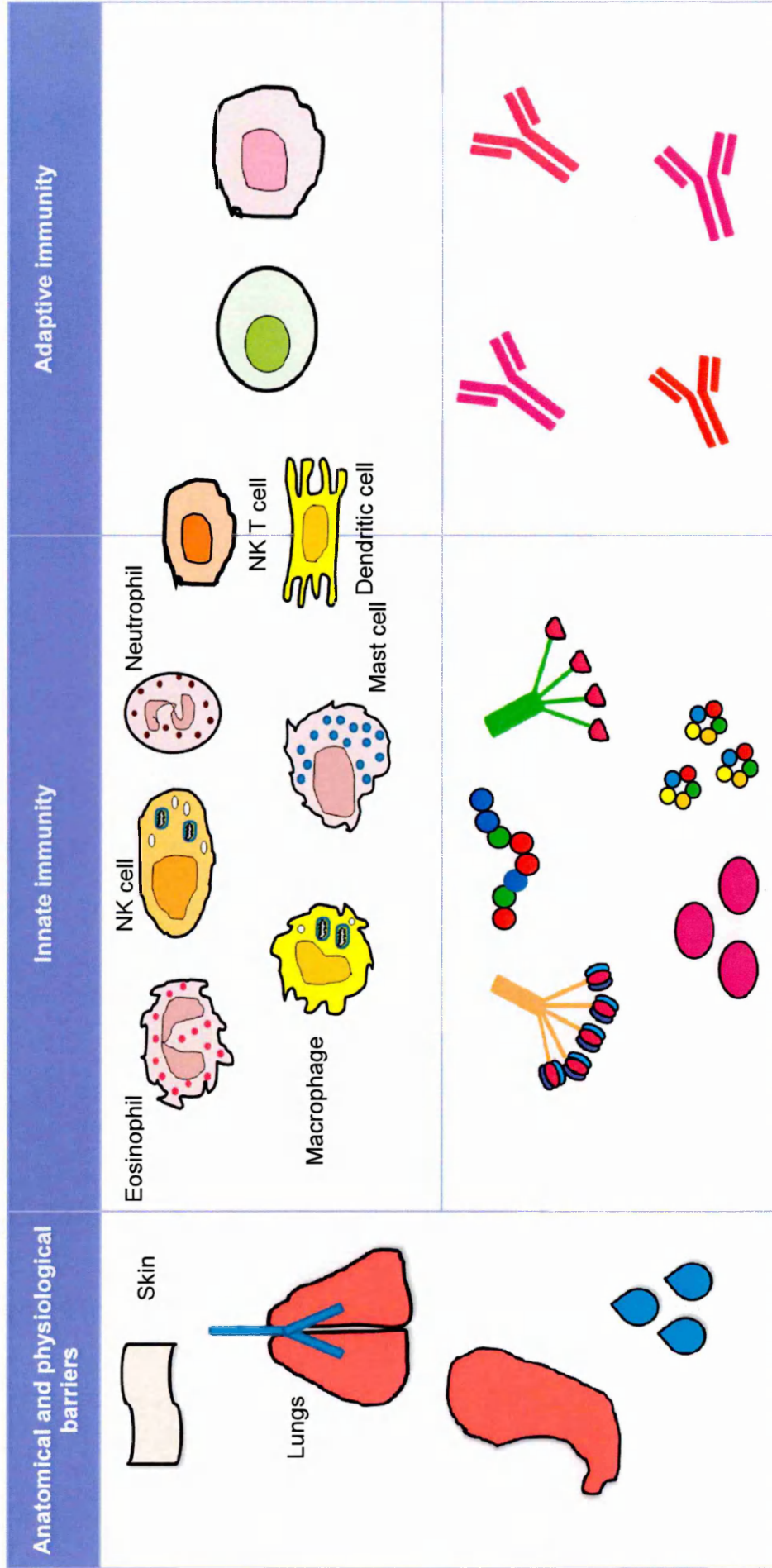
The innate immune system is composed of both cellular and humoral elements (Figure 1.2). A number of haematopoietic cells are involved, including macrophages, dendritic cells, mast cells, neutrophils, natural killer (NK) cell and NK T cells. In addition to haematopoietic cells, non-haematopoietic cells also play a role in innate immunity, including the skin and epithelial cells lining the respiratory, gastrointestinal, and genitourinary tracts. To enhance the effect of these cellular defences, innate immunity also has a humoral component that consists of well-characterised components, such as complement proteins, lipopolysaccharide (LPS) binding protein, C-reactive proteins and antimicrobial peptides (Turvey and Broide 2010).

Table 1.1: Overview of the innate and adaptive immune system. (adapted from Janeway and Medzhitov 2002).

	Innate immune system	Adaptive immune system
Cellular components	Haematopoietic cells: macrophages, dendritic cells, neutrophils, eosinophils, NK cells and NK T cells Non-haematopoietic cells: epithelial cells, such as those lining the skin, airways and gastrointestinal tract	Haematopoietic cells: T and B cells
Humoral components	Complement proteins, LBP, CRP, AMPs, and MBL	Immunoglobulins secreted by B cells
Receptors	Invariant and germline encoded Nonclonal	Generated by random somatic gene segment rearrangement Clonal
Types	TLR, NLR and complement	B and T cell receptors
Ligands recognised by receptors	Conserved microbial components	Specific details or epitopes of macromolecules, including proteins, peptides, and carbohydrates
Response time	Immediate	Hours to days
Immunological memory	None Response the same with each exposure	Yes Response enhanced by repeated exposure
Risk of autoreactivity	Low; self-tolerant receptors are selected during evolution	High; random gene rearrangement generates autoreactive receptors needing multitolerance mechanisms

Key: AMP; anti-microbial peptide, CRP; C-reactive protein, LBP; LPS binding protein, NK; natural killer, TLR; Toll-like receptor, MBL; mannose-binding lectin, NLR; NOD-like receptor.

Figure 1.1: The three levels of the human immune system. (Adapted from Turvey and Broide 2010).



Key: AMP; antimicrobial peptide, CRP; C-reactive protein, LPS; Lipopolysaccharide, MBL; Mannose binding lectin, NK; natural killer.

In addition to the detection of pathogens, the innate immune system is also able to detect immunologic danger through the detection of damage-associated molecular patterns (DAMPs), such as high mobility group box 1 protein (HMGB1) released from dying cells (Bianchi 2007). Finally, receptors of NK cells are also able to detect healthy cells expressing 'self' molecules and deliver an inhibitory signal to prevent activation of the immune response against host tissue (Joncker and Raulet 2008).

Neutrophils, macrophages, and monocytes are the major phagocytic cells of the innate immune system. Neutrophils engulf pathogens and localise them to intracellular vacuoles where they are exposed to toxic effector molecules, such as nitric oxide and degradative enzymes to destroy the pathogen, and play a major role in the clearance of microbial pathogens (Kennedy and DeLeo 2009). Macrophages and monocytes are also highly phagocytic for microbes and particles that have been marked for clearance either through opsonisation by antibodies and/or complement (Chaplin 2010). In addition to this important role in the innate immune response, monocytes and macrophages also play vital roles in the adaptive immune response by ingesting microbial antigens, processing them into peptide fragments, and presenting them to T cells (Chaplin 2010). The most potent antigen presenting cells (APCs) are the broad class of dendritic cells (DCs) that are present in most tissues of the body and concentrated in the secondary lymphoid organs (Lambrecht and Hammad 2009).

All APCs express both class I and II major histocompatibility complex (MHC) molecules that are required for recognition of processed antigen by the T cell receptor (TCR) on T cells; the key cellular components of the adaptive response (see section 1.2). All cells bearing MHC molecules have the ability to act as APCs if appropriately stimulated (Chaplin 2010).

DCs are important in initiating the adaptive immune response by migrating from the site of infection to regional lymph nodes where they present pathogen-derived antigen to naive CD4⁺ T cells. Activated DCs express co-stimulatory molecules essential to T cell activation and can instruct the differentiation of naive CD4⁺ T cells into T helper cells. In addition, this cross-talk between DCs and T cells can lead to clonal expansion and migration of T cells to B cell areas to assist with antibody production (Gallucci *et al.*, 1999).

1.1.2 Adaptive immunity

The adaptive immune system consists of T and B cells, and unlike the innate immune system, requires antigen exposure in order to mount an effective immune response hence 'adaptive' (Turvey and Broide 2010). In contrast to the limited number of PRRs

used by the innate immune system, the adaptive immune system has an extremely diverse, randomly generated repertoire of receptors that are encoded by gene elements that somatically rearrange to assemble antigen-binding molecules with great specificity for individual, unique foreign structures (Chaplin 2010). This great diversity in receptors enables these cells to recognise virtually any foreign antigen, however, due to this arm of the immune system requiring antigen exposure before mounting a response there is a delay of approximately 5 days, due to clonal expansion of antigen-specific T and B cells. In addition to the time delay of the adaptive immune response, there is also a risk of autoimmune disease, as receptors for self-proteins are created by means of the random process of gene rearrangement that generates receptors expressed by T and B cells (Turvey and Broide 2010). However, substantial tolerance mechanisms are in place to eliminate or regulate self-reactive cells (see section 1.1.3).

A key feature of the adaptive response is that it produces long-lived cells that persist as memory cells until a second exposure with their specific antigen, where they rapidly re-express effector functions (Chaplin 2010). The adaptive immune response therefore manifests immune memory, enabling it to contribute prominently to a more effective host response against specific pathogens following a second encounter.

The major role of the T-cell arm of the adaptive immune response is to identify and destroy infected cells and is responsible for cell-mediated immunity. T cells can also recognise peptide fragments of antigen that have been taken up by APCs through phagocytosis or pinocytosis. The immune system has evolved to enable T cells to recognise foreign antigens through recognising two molecules on the surface of these APCs: (1) a self-component i.e. MHC and (2) a foreign peptide. MHC molecules are cell surface glycoproteins that bind peptide fragments of proteins that have either been synthesised within the cell i.e. endogenous antigens (class I MHC molecule) or ingested by the cell and proteolytically processed i.e. exogenous antigens (class II MHC molecules) (Chaplin 2010).

1.1.2.1 Major histocompatibility complex class I and II

There are three HLA class I molecules; HLA-A, -B and -C. Class I MHC molecules are cell-surface heterodimers consisting of a polymorphic transmembrane α -chain and a nonpolymorphic β_2 -microglobulin protein, with the α chain determining whether the class I molecule is an HLA-A, B or C molecule (Bjorkman 1997). The genes for the α -chain and the β_2 -microglobulin protein are encoded on chromosome 6 and 15, respectively (Bjorkman 1997). The α_1 and α_2 domains of the α -chain forms a groove in which the antigenic peptides can bind producing a complex of both class I MHC molecule and antigenic peptide which is recognised by TCR present on the surface of

the T cell (Bjorkman 1997). This complex is vital for recognition by T cells, as the TCR shows no measurable affinity for the antigenic peptide alone and very low affinity for MHC molecules containing other peptides. This concept is now known as “MHC restriction” in which T cells can only recognise their specific antigen when it is presented by a specific self-MHC molecule (Zinkernagel and Doherty 1997). The α_3 domain of the MHC molecule interacts only with the CD8 molecule on cytotoxic T cells, which restricts the recognition of antigenic peptides that are presented in class I HLA molecules to CD8+ cytotoxic cells (Joshi and Kaech 2008).

So far, more than 650 alleles have been identified at the HLA-A locus, more than 1,000 alleles at the HLA-B locus and more than 350 alleles at the HLA-C locus (Immunogene). The highly polymorphic nature of the α -chain is predominantly in the amino acids in the peptide-binding groove, resulting in different peptide-binding specificities of different class I alleles. There are three distinct HLA class I genes, each is highly polymorphic, and heterozygous individuals have six distinct peptide-binding grooves. Each class I protein can bind many different peptides, having six peptide-binding molecules results in the ability to bind a very diverse collection of antigenic peptides (Chaplin 2010). Generally, the antigenic peptides that are found bound in the peptide-binding groove of the HLA class I molecules are derived from proteins synthesised within the cell bearing the class I molecules. MHC class I molecules are most effective in delivering viral peptides in a virus-infected cell to the cell surface for recognition and elimination by cytotoxic CD8+ T cells. Exogenous antigens can also be internalised by endocytosis and presented in class I molecules by APCs in a process called “cross-presentation” (Melief 2003). This is of great importance in the fight against virally infected cells in which the host is prevented from being able to present antigen (Sigal *et al.*, 1999).

There are three class II molecules: HLA-DR, -DQ and -DP (Bjorkman 1997). Similar to the class I molecules, class II HLA molecules also consist of an α and a β -chain (Bjorkman 1997). When the common α -chain is paired with the DRB1 chain it produces the HLA-DRB1 protein, so far more than 500 HLA-DRB1 alleles have been identified. This α -chain can also pair with DRB2-DRB9, where there are a total of 60 alleles. The HLA-DQ encodes one polymorphic α -chain which has 25 alleles and one polymorphic β -chain which has 72 alleles. Lastly, the HLA-DP encodes one polymorphic α -chain which has 16 alleles and one polymorphic β -chain which has 118 alleles (Chaplin 2010). An individual can express two different HLA-DQ and two different HLA-DP proteins, and HLA-DR α -chain can pair with both an HLA-DRB1 and an HLA-DRB3 chain, each person can express distinct HLA-DR proteins. Each of these HLA molecules can bind a large repertoire of antigenic peptides. The α_1 and β_1 domains

combine to form the peptide-binding groove and the β_2 domain interacts with the CD4 molecule present on the surface of the CD4⁺ T helper cell. The CD4 molecule enhances the interaction between the T cells and the class II expressing APCs (König *et al.*, 1996). Class II proteins are expressed on a number of immune cells, including B cells, DCs, monocytes and macrophages. Class II proteins are most effective in presenting antigenic proteins of extracellular pathogens, such as most bacteria, parasites, and virus particles that have been released from infected cells to CD4⁺ T helper cells.

Different HLA types have been associated with susceptibility to certain diseases. A recent epidemiological study has shown that more than 40 diseases are associated with certain HLA class I or HLA class II alleles, most of which are autoimmune in nature (see section 2.1) (Ghodke *et al.*, 2005). HLA presentation is limited to protein antigens, and in order to detect lipids a further molecule is used for presentation to T cells. CD1 molecules consist of α and β chains and are structurally similar to class I HLA molecules, but are important in the presentation of lipids to T cells (Balato *et al.*, 2009).

1.1.2.2 T cell receptor

The largest class of T cells express $\alpha\beta$ TCRs on their surface and recognise peptide antigens presented by either class I or II MHC proteins. These $\alpha\beta$ T cells differentiate into: (1) CD8⁺ T cells which act to kill cells infected with intracellular microbes or (2) CD4⁺ T cells which regulate both the cellular and humoral immune responses. A much smaller group of $\alpha\beta$ T cells express CD161 NK cell antigens rather than CD4 or CD8, and are called NK-T cells, and recognise glycolipid antigens presented by CD1 molecules rather than through HLA molecules. NK-T cells appear to play an immunoregulatory role and release numerous cytokines following activation, including interleukin-4 (IL-4) and interferon- γ (IFN- γ) (Godfrey *et al.*, 2004). These $\alpha\beta$ TCR T cells account for approximately 90-95% of T cells, with the remaining 5-10% expressing $\gamma\delta$ TCRs on their cell surface.

TCRs are somatically assembled from variable, diversity, and joining gene elements, with recombinase enzymes assembling these elements in a seemingly random process. This produces a wide range of receptor sequences, some of which are functional. In the thymus these T cells expressing functional TCR genes are selected (Miller 2002). The thymus consists of three compartments that are all important for the development of T cells: (1) subcapsular zone, (2) thymic cortex, and (3) thymic medulla. The subcapsular zone is where bone marrow-derived prothymocytes differentiate, proliferate and rearrange their TCR β -chains. Following this, the cells then move to the cortex where the α -chain gene segments rearrange to form functional,

mature $\alpha\beta$ receptors. Following positive selection these T cells become either CD4+ or CD8+ T cells.

CD4+ T cells are helper cells and are important in activating both the humoral and cellular responses; a proportion of these CD4+ T cells play an important role in down-regulating the immune response and are regulatory T (Treg) cells (LaRosa and Orange 2008). CD8+ T cells are important in directly killing cells infected with intracellular microbes and also contain a population of cells that suppress the immune response (Trapani *et al.*, 2000).

1.1.2.3 T cell activation

For T cell activation, in addition to the TCR, a cell surface molecule called CD3 is also required. The interaction of the CD3/TCR complex with MHC molecules presenting antigenic peptides only results in partial signal for cell activation. Full activation requires additional co-stimulatory molecules, including CD28 expression on the surface of T cells and the expression of CD80 or CD86 on the surface of the APC (Nurieva *et al.*, 2009).

Resting naive CD4+ T cells release very low levels of cytokines but following stimulation through the presentation of antigens by APCs, CD4+ T cells begin to produce IL-12 and are called Th0. Depending on cytokines present at the site of activation these T cells differentiate into Th1, Th2 or Th17 helper cells (Sallusto and Lanzavecchia 2009). Th1 cells support cell-mediated immune responses and Th2 cells support humoral and allergic responses. Th17 cells are induced early in the adaptive immune response to extracellular bacteria and help in the recruitment of neutrophils to eliminate these pathogens. Th17 cells are also involved in many autoimmune diseases.

The second branch of the adaptive immune response is the B-cell arm which is responsible for humoral immunity. B cells constitute approximately 15% of peripheral blood leukocytes and are defined by their capacity to produce immunoglobulins. Each B cell possesses specified immunoglobulin on its surface made up of two identical heavy (H) chains and two identical κ or λ light (L) chains. Each chain is encoded by variable (V), diversity (D), joining (J) and constant region genes. Each part of the VL and VH chains are made up of three hypervariable regions, and it is these regions which vary in sequence from one antibody molecule to another, and create the antigen-binding region of the molecule (Burnet 1976). The heavy chain constant regions of the antibody molecule pair to form the Fc domain which carries out the effector function, including binding to Fc receptors and activating the complement system (see section 1.3). The genes encoding the κ light chain, λ light chain and the heavy chain are

encoded on chromosomes 2, 22 and 14, respectively. The heavy chain gene contains exons which encode nine different constant regions that are used to produce the different classes and subclasses of immunoglobulins (Chaplin 2010).

1.1.2.4 B cell development

B cells differentiate from haematopoietic stem cells in the bone marrow and undergo antigen receptor assembly through somatic joining of genes (Nagasawa 2006). In the bone marrow CD19⁻ CD20⁻ stem cells go through many stages of maturation taking them from stem cells, pro-B-cells, then pre-B-cells and eventually naive CD20⁺ CD19⁺ IgD⁺ and IgM⁺ B (Nikbin *et al.*, 2007). Immunoglobulins are encoded by multiple genes, which rearrange during the pro-B-cell stage to create a unique cell surface receptor that defines its specificity for antigen. During this stage of B cell development, many B cells are generated with different specificities. This process of random somatic joining of genes occurs in the bone marrow in the absence of a pathogenic antigen. Whilst in the bone marrow these B cells are subjected to negative selection similar to T cell development in the thymus, where the majority die in the bone marrow by apoptosis during development due to their antigen receptors (antibodies, IgM) being assembled incorrectly or are directed against self-antigens.

Once these cells have survived negative selection in the bone marrow, these naive B cells expressing IgM and IgD on their cell surface, migrate via the bloodstream to the spleen and other lymphoid tissues, where they mature within the secondary lymphoid organs and germinal centres (GC). In an immune response to a pathogen, antigen-dependent development begins in the GC of secondary lymphoid organs under the influence of T cells (Liu *et al.*, 1992; MacLennan 1994; Schmidlin *et al.*, 2009). T cells provide “help” for B cells to mature, which includes both the induction of isotype switching by T cell cytokines and the activation of somatic mutation (Chaplin 2010). When naive B cells encounter their respective antigen they capture it through membrane bound IgM, internalise and process it intracellularly. These antigenic peptides are then presented on the B cell surface bound to the class II HLA molecule. Antigen uptake increases expression of MHC class II molecules and the expression of co-stimulatory molecules CD80 and CD86. CD4⁺ T cells then become activated through the binding of costimulators and peptide class II complex, which in turn then leads to the CD4⁺ T cell to signal to the B cell through the interaction of CD40 ligand on CD4⁺ T cells with CD40 on B cells. This signalling through CD40 is essential for the induction of isotype switching (Korthäuer *et al.*, 1993; Gray, Siepmann and Wohlleben 1994).

1.1.2.5 B cell isotype switching

T cells produce a number of cytokines which can influence isotype switching: (1) IL-10 results in switching to IgG₁ and IgG₃, (2) IL-4 and IL-13 results in switching to IgE, (3) transforming growth factor- β (TGF- β) results in switching to IgA, and (4) IFN- γ induces switching to IgG₂. During this period of isotype switching random somatic mutations in the antigen-binding portions of the heavy and light chains also occurs (MacLennan 1994; Klein and Dalla-Favera 2008). Inside the GC, these mature B cells undergo positive selection, whereby if these mutations result in a lowered affinity for the antigen then the cell undergoes apoptosis and if these mutations result in an increased affinity for the antigen, then this leads to extensive proliferation of this cell producing the antibody, also called clonal expansion.

Those B cells that survive the process of positive selection either become: (1) antibody-producing plasma cells or (2) memory B cells. The first subset undergoes clonal expansion, lose their surface immunoglobulin (Ig) molecules, and secrete antibodies of one class (Goldsby *et al.*, 2003; Avery *et al.*, 2005). The second subset do not release their surface antibodies and remain surface antibody-expressing cells; memory B cells. These memory B cells circulate in the peripheral blood and lymph nodes until subsequent encounter with the same antigen, when an extremely efficient secondary antibody response is mounted.

In addition to their ability to act as antigen presenting cells to T cells and their ability to produce antibodies, B cells are vital in driving the differentiation of T cells through producing an array of cytokines. Production of tumour necrosis factor- α (TNF- α) by B cells amplifies Th1 differentiation whereas IL-6 and TGF- β production promote Th17 production (Bettelli *et al.*, 2007; Menard *et al.*, 2007). Secretion of IL-4 and IL-10 by B cells results in the development of Th2 cells (Harris *et al.*, 2000).

The immune system has evolved to coordinate a variety of responses against numerous pathogens whilst remaining silent towards self-antigens and also those derived from commensal organisms that exist in the body (see section 1.1.3). However, if these processes are not strictly maintained, chronic inflammation and/or autoimmunity can develop (see section 1.2).

1.1.3 Immunological tolerance

In order to ensure that both the innate and adaptive immune system only responds to foreign pathogens and not self-proteins, a number of mechanisms are in place to ensure tolerance of self-proteins; these are divided into two types: (1) central tolerance

and (2) peripheral tolerance. Central tolerance is established in the thymus for T cells and in the bone marrow for B cells.

1.1.3.1 Central tolerance

Central tolerance is established within the thymus by purging self-reactive thymocytes, and thus reducing the propensity for autoreactivity among mature T cells in the periphery (Metzger and Anderson 2011). T cells are derived from hematopoietic stem cells but migrate to the thymus to undergo maturation. Upon entry into the thymus, the majority of T cell precursors commit to the $\alpha\beta$ T-cell lineage and at this stage are double negative i.e. do not express CD4 or CD8 coreceptors (Washburn *et al.*, 1997; Rothenberg and Dionne 2002; Wolfer *et al.*, 2002). However, once in the thymic cortex these thymocytes undergo TCR β chain rearrangement in a ligand-independent process, followed by rearrangement of the α chain, and upregulation of both CD4 and CD8 molecules; also called double-positive (DP) T cells (Fehling *et al.*, 1995; Irving *et al.*, 1998). These DP thymocytes are programmed to undergo apoptosis unless a 'rescue signal' is delivered via TCR and self-peptide-MHC ligation. DP thymocytes with a minimal threshold of reactivity to the particular self-MHC haplotypes survive, whereas those that fail to recognise self-MHC molecules undergo apoptosis. During this time prior to apoptosis there is a three day window in which rearrangement of the α -chain occurs, referred to as receptor editing, which aims to increase the likelihood of successful self-MHC restriction (Petrie *et al.*, 1993; McGargill *et al.*, 2000; Huang *et al.*, 2005). Around 95% of these DP thymocytes fail to demonstrate any specificity for an MHC ligand and undergo "death by neglect" or apoptosis (Egerton *et al.*, 1990; Surh and Sprent 1994). Those DP thymocytes that express TCR that are able to bind an MHC ligand with mild avidity are positively selected and mature into single-positive (SP) thymocytes expressing either CD4 or CD8 (Starr *et al.*, 2003). During this time chemokines are also produced which directs these T cells to undergo further maturation in the thymic medulla (Kwan and Killeen 2004; Misslitz *et al.*, 2004; Ueno *et al.*, 2004).

It is in the thymic cortex that positive selection occurs, whereby cells are tested to see if their receptors have sufficient affinity for self-MHC molecules, if not these cells undergo apoptosis and are cleared by macrophages. During this time cells express both CD4 and CD8, however, those that are selected based on their interaction with class I MHC become CD4⁻ CD8⁺ whereas those selected based on the interaction with class II MHC become CD4⁺ CD8⁻ (Boehmer *et al.*, 1989).

Once in the thymic medulla, these positively selected thymocytes must survive negative selection. During this process thymocytes are screened for any reactivity

against self, autoreactivity, by subjecting these cells to an array of tissue-specific proteins that are under the control of autoimmune regulator (AIRE) gene (Chaplin 2010). Medullary thymic epithelial cells express AIRE and it is these cells that are responsible for the negative selection of tissue-specific autoreactive T cells (Anderson *et al.*, 2002). Thymocytes that express high-avidity TCR for self-peptide-MHC complexes undergo apoptosis. This process of clonal deletion serves to reduce the frequency of strongly self-reactive T cells in the periphery. Less than 5% of these developing T cells survive both positive and negative selection, those that do are released into the circulation. In the blood and secondary lymphoid organs 60-70% of T cells are CD4⁺ CD8⁻ and the remaining are CD4⁻ CD8⁺. However, despite this mechanism of negative selection of thymocytes reacting to self proteins, this process is not complete and a number of autoreactive T cells have been shown to escape into the periphery (Walker and Abbas 2002).

1.1.3.2 Peripheral tolerance

The incompleteness of central tolerance in removing the mature T cells with self-antigen specificity necessitates additional mechanisms to maintain peripheral tolerance, where Tregs and tolerogenic DCs participate actively. These mechanisms include further clonal deletion of mature autoreactive T cells in the periphery, rendering these cells anergic, or actively suppressed (Arnold *et al.*, 1993; Parijs and Abbas 1998; Walker and Abbas 2002). Tregs are specialised for immune suppression and disruption in the development of Tregs is a primary cause of autoimmune and inflammatory diseases in humans (see section 2.2). In particular CD4⁺ CD25⁺ Tregs have emerged as important players in the maintenance of peripheral self-tolerance and down-regulation of various immune responses (Maloy and Powrie 2001; Sakaguchi 2004).

Although the exact nature of Treg-mediated immune suppression is unknown, a number of mechanisms have been proposed, which include release of immunosuppressive cytokines, IL-10 and TGF- β , cell-contact-dependent suppression and killing of APCs (Shevach, Thornton and Suri-Payer 1998; Takahashi *et al.*, 1998; Asseman *et al.*, 1999; Levings *et al.*, 2002; Sakaguchi *et al.*, 2008). Activated Tregs may also downregulate expression of CD80/86 on APCs or stimulate DCs to produce indoleamine 2, 3-dioxygenase (IDO), which is toxic to cells; both of which are dependent on CTLA-4 expressed on Foxp3⁺ CD25⁺ CD4⁺ Tregs (Cederbom *et al.*, 2000; Takahashi *et al.*, 2000; Mahnke *et al.*, 2007).

1.1.3.3 Dendritic cells and tolerance

In addition to Tregs, DCs, the professional APCs of the immune system (see section 1.1), also have the potential to induce immunity or tolerance, depending on the state of activation, activation signals, and cytokine milieu (Banchereau and Steinman 1998; Belz *et al.*, 2002). DCs exist in three functional stages: (1) immature, (2) semi-mature and (3) mature. Immature DCs scan self and foreign antigens but in the absence of inflammatory stimuli express low levels of MHC class II and costimulatory molecules, and are therefore unable to activate T cells (Mahnke *et al.*, 2002). Semi-mature DCs are loaded with antigen but in the absence of inflammatory stimuli are once again unable to stimulate T cells due to low expression of MHC class II and costimulatory molecules (Mahnke *et al.*, 2002). Therefore, self-antigen presented by either immature or semi-mature DCs are unable to activate T cells inducing a state of functional inactivation in naive T cells called anergy (Randolph *et al.*, 2008). In addition to this, when autoreactive T cells are repeatedly stimulated by immature DCs these cells may undergo apoptosis through activation-induced cell death (AICD) involving ligation of CD95 (Süss and Shortman 1996). Immature DCs may become activated in the presence of an antigen and inflammatory stimuli leading to maturation of DCs and activation of T cells (Gallucci *et al.*, 1999). As mentioned previously, DCs produce IDO which suppresses T-cell proliferation and promotes T-cell apoptosis, and therefore directly contributes to T-cell tolerance (Munn *et al.*, 2002; Terness *et al.*, 2002; Swanson *et al.*, 2004).

1.2 Autoimmunity

1.2.1 Breakdown of tolerance in autoimmunity

Breakdown of self tolerance leads to autoimmunity. Although the causes of autoimmunity remain to be elucidated, there are many studies documenting the link between breakdown of tolerance and development of autoimmune diseases.

1.2.2 Autoimmunity

The production and activation of autoreactive T and B cells leads to the development of autoimmunity. Autoimmune diseases are characterised by an inappropriate, excessive, inflammatory response against self, which results in destruction of tissue (Zenewicz *et al.*, 2010). Although there is usually one primary end-organ target in individuals afflicted by an autoimmune disease, such as destruction of the pancreatic islet cells in the autoimmune disease type I diabetes mellitus (T1DM), numerous other organs are often

also affected. Although the aetiology of autoimmune diseases remains to be elucidated, the causes are likely to be a combination of both genetic and environmental factors (Costenbader *et al.*, 2012).

1.2.3 Multifactorial nature of autoimmunity

1.2.3.1 Genetics

Within families, clustering of distinct autoimmune diseases has been reported, suggesting the presence of shared pathogenic factors across autoimmune conditions. Families with autoimmune diseases, rheumatoid arthritis (RA) or multiple sclerosis (MS) are more likely to also manifest other autoimmune diseases (Lin *et al.*, 1998; Broadley *et al.*, 2000). Families with multiple members with MS have a much higher frequency of other autoimmune diseases compared to families with only a single member affected by the disease (Broadley *et al.*, 2000). This suggests a cumulative enrichment of autoimmune susceptibility loci in these select cohorts.

Interestingly, monozygotic (MZ) twins show significantly higher concordance for autoimmunity than dizygotic twins, implicating genetics as an important factor in the development of autoimmune conditions. However, this concordance rate varies, with up to 70% in T1DM and only up to 30% concordance in MS (Ballestar 2010; Breton *et al.*, 2011), which demonstrates that there is a genetic predisposition to developing autoimmune diseases but also shows that environmental factors must also influence the precipitation of disease in these genetically predisposed individuals (Thorsby and Lie 2005). A number of genes have emerged as important in predisposing individuals to the development of autoimmune diseases, the most studied and greatest association has been found in genes within the MHC complex.

The MHC consists of 252 genes, many of which are highly polymorphic, in particular the human leukocyte antigens (HLA) class I and II genes encoding the peptide-presenting class I and II molecules (see section 1.1.2.1) (Thorsby and Lie 2005). A number of population studies have demonstrated strong associations between autoimmune diseases and HLA class I and II molecules. In some cases certain HLA molecules are associated with a specific autoimmune disease, such as HLA-DQ2 and coeliac disease, whereas some HLA molecules may be associated with a number of diseases, such as the HLA-DQ6 haplotype, which is associated with both MS and T1DM (Thorsby and Lie 2005). Although the reasons for this genetic predisposition to autoimmune disease in individuals expressing these particular HLA alleles is not yet fully elucidated, it is proposed that self-peptides are preferentially recognised and presented by these disease-predisposing HLA molecules.

The application of genome-wide association studies (GWAS) to the study of autoimmune diseases has identified an increasing number of disease-associated loci in addition to HLA genes. The association signals for many of these associated loci do not directly implicate a single protein-encoding gene, and the causative role for candidate genes can only be speculated. However, a large number of major loci have been observed to demonstrate genome-wide evidence for association in distinct autoimmune diseases (for review see Thorsby and Lie 2005; Zenewicz *et al.*, 2010). Associated loci include a broad array of immune-associated genes involved in lymphocyte activation, microbial recognition, and cytokine and cytokine receptors (Gregersen and Olsson 2009).

In individuals with an autoimmune disease, many tolerogenic mechanisms are altered by genetic loci implicated in autoimmunity. Some of these mechanisms are involved in central tolerance in the thymus and bone marrow that delete self-reactive B and T cells, whereas others involve peripheral mechanisms including Tregs (Wing and Sakaguchi 2009).

AIRE is essential in ensuring central tolerance (see section 1.1.3.1), mutations affecting *AIRE* lead to a relaxing of selection against self-reactive T cells in the thymus, resulting in a rare and aggressive autoimmune disease called autoimmune polyendocrine syndrome 1 (Shikama *et al.*, 2009). Tregs play a critical role in maintaining peripheral tolerance (see section 1.1.3.2) and mutations of the *FOXP3* gene, which is essential for the development and function of Tregs, causes the autoimmune disease immune dysregulation, polyendocrinopathy, enteropathy, X-linked syndrome (IPEX) which is fatal in the first two years of life (Bennett *et al.*, 2001; Torgerson and Ochs 2007).

Pre-B cells in the bone marrow are highly autoreactive but become less so on differentiation, which is activated by the gene encoding tyrosine phosphatase non-receptor type 22 expressed by lymphocytes (*PTPN22*) (Menard *et al.*, 2011). A substitution of the amino acid arginine by tryptophan within this *PTPN22* gene affects intracellular signalling inhibiting the activation of T and B cells, leading to failure to delete autoreactive T cells during thymic selection and impaired activation of Tregs (Vang *et al.*, 2005). This *PTPN22* tryptophan risk allele renders individuals more susceptible to developing a number of humoral autoimmune diseases, including T1DM, RA, and systemic lupus erythematosus (SLE) (Criswell *et al.*, 2005; Bottini, *et al.* 2006; Barrett *et al.*, 2009). In addition to *PTPN22*, there are a number of other associated loci containing candidate genes encoding molecules expressed by lymphocytes that modulate co-stimulatory functions, including *CTLA-4*, that contribute to genetic susceptibility to a number of common autoimmune diseases, including T1DM and RA

(Wellcome Trust Case Control Consortium, 2007). This highlights the central role of lymphocyte activation in humans in the adaptive immune response.

Cytokines and cytokine receptor genes have been associated with autoimmunity. IL-2 is a central mediator of T cell growth, and its signalling is regulated by its affinity to its receptors. Polymorphisms in the IL-2 receptor alpha (IL2RA or CD25) gene is associated with a number of autoimmune diseases, including T1DM, MS, RA and Crohn's disease (Hafler *et al.*, 2007; Lowe *et al.*, 2007; Franke *et al.*, 2010; Stahl *et al.*, 2010). This can affect the growth and survival of regulatory and pro-inflammatory T cells. MS has also been associated with IL-7 receptor alpha (IL7R) polymorphisms (Hafler *et al.*, 2007; Barrett *et al.*, 2009).

In addition to genetic variants altering lymphocyte activation and cytokine signalling, variants in genes related to innate immunity have also been identified with a number of autoimmune diseases. An example of this are variants of the *NOD2* gene and its association with Crohn's disease; explaining the heritability of this disease (Abraham and Cho 2009). *NOD2* is a pattern recognition receptor that is usually involved in the recognition of bacterial peptidoglycan and subsequently activation of NF- κ B. In addition to *NOD2*, variants in the autophagy gene *ATG16L1* have also been associated with Crohn's disease (Abraham and Cho 2009).

1.2.3.2 Environment

A number of environmental agents have been found to play a role in the pathogenesis of autoimmune diseases including infection, ultraviolet light, chemicals or other factors capable of modulating immune responses such as occupational/environmental pollutants or drugs, and behavioural factors, such as smoking and diet (Borchers *et al.*, 2010; Ranque and Mouthon 2010; Selmi *et al.*, 2010; Tobón *et al.*, 2010; Selmi *et al.*, 2011).

Infection has long been associated with the development of autoimmune diseases. During infection, DCs take up and process self-antigens as well as foreign antigens, and in genetically susceptible individuals this may lead to activation of low affinity autoreactive T cells. This is called the "adjuvant effect" of infection in the pathogenesis of autoimmunity (Israeli *et al.*, 2009). Another hypothesis involves molecular mimicry, whereby particular structures of certain pathogens imitate self-antigens resulting in the activation of autoreactive T cells, and attack of both foreign and self proteins (Blank *et al.*, 2007). A well-documented organism where molecular mimicry is known to take place is infection with *Streptococcus pyogenes* which leads to rheumatic fever and glomerulonephritis.

A number of occupational exposures have been linked to the development of a range of autoimmune diseases, in particular silica, solvents, and ionising radiation (Gourley and Miller 2007; Cooper *et al.*, 2010). A strong association has been found between silica exposure and risk of developing several rheumatic autoimmune diseases, including scleroderma, RA and SLE (Khuder *et al.*, 2002; Finckh *et al.*, 2006; Cooper *et al.*, 2010; McCormic *et al.*, 2010).

Various solvents have also been linked to an increased risk of developing autoimmune diseases, including RA and MS (for review see (Gourley and Miller 2007). Ionising radiation has been linked with an increased risk of developing autoimmune thyroid disease (AITD) (Völzke *et al.*, 2005). Ultraviolet radiation (UVR) resulting in more than one incidence of severe sunburn has been linked with an increased risk of developing lupus, whereas exposure to ultraviolet radiation has been found to significantly reduce the risk of developing MS (Freedman *et al.*, 2000; Bengtsson *et al.*, 2002).

In terms of behavioural factors, diet has also be linked to the development of autoimmune diseases, in particular gluten has been found to induce coeliac disease in genetically susceptible individuals and dietary meat and protein have been found to be associated with an increased risk of developing RA (Pattison *et al.*, 2004; Alaedini and Green 2005). Cigarette smoking has been shown to significantly increase the chances of developing RA, although the exact mechanisms for this are unclear. A number of epidemiological studies have shown strong gene-environment interactions between smoking and the presence of *HLA-DRB1* shared epitope (HLA SE) and *PTPN22*. Individuals who carry these susceptibility genes and smoke greatly increase their risk of developing RA (Costenbader *et al.*, 2010; Karlson *et al.*, 2010).

Environmental factors may also directly affect Tregs contributing to autoimmunity. Under normal physiological conditions Tregs display greater proliferation and higher metabolic activity than effector T cells and are therefore more sensitive to environmental agents such as ionising radiation, drugs and vitamins (Yamaguchi *et al.*, 2007; Costenbader *et al.*, 2010; Karlson *et al.*, 2010).

1.2.3.3 Epigenetics

Epigenetics is a new area of research in autoimmune diseases, and refers to changes in gene expression that do not involve changes in the actual DNA sequence (Lu *et al.*, 2010). These epigenetic mechanisms are sensitive to external stimuli and therefore environmental effects can be mediated by changes in epigenetic regulation. The major mechanisms of epigenetic gene regulation are through DNA methylation and histone modifications, which interact with one another in modulating chromatin architecture,

leading to either silencing or transcription of the gene. More recently micro RNAs (miRNA) have also been identified that are involved in epigenetics. miRNAs are non-coding RNA that can suppress translation by binding to complementary target mRNA species resulting in degradation of the target (Ruan *et al.*, 2009).

DNA methylation consists of the addition of a methyl group to the fifth carbon of cytosine residues, resulting in their conversion to 5-methylcytosines. DNA methylation occurs predominantly at CpG islands, which are regions in the genome exceeding 500 base pairs with a CG content higher than 55% (Gardiner-Garden and Frommer 1987; Illingworth and Bird 2009). These CpG islands have key regulatory functions, and are found at the promoter regions of approximately 50% of all genes (Bird 2002).

Histones are highly conserved proteins that reside within the nuclei of cells and provide DNA condensation and organisation in the nucleus, as well as modulating DNA accessibility to the transcription machinery. Modulation of transcription can be altered by chemical modifications of histones, including acetylation and methylation. In acetylation, histone acetyltransferase (HAT) promotes gene expression by transferring acetyl groups to lysine, whereas histone deacetylase (HDAC) remove acetyl groups resulting in gene repression (Gregory *et al.*, 2001; Roth *et al.*, 2001; Thiagalingam *et al.*, 2003). Histone methylation can result in both gene activation and repression depending on where in histones the methyl group is added to lysine residues (Bauer *et al.*, 2002; Schotta *et al.*, 2004).

The potential role of epigenetics in environmental/genetic interactions, where environmental changes produce modifications in gene expression has received much interest. Studies have shown an association between DNA methylation and exposure to prenatal tobacco smoke, alcohol consumption and environmental pollutants (Baccarelli *et al.*, 2009; Tarantini *et al.*, 2009; Breton *et al.*, 2011; Zhang *et al.*, 2011). Epigenetics may explain the discordance of autoimmune diseases in MZ twins, as differences in phenotype become greater as twins age, a termed referred to as 'epigenetic drift' (Fraga *et al.*, 2005; Ballestar 2010). This epigenetic drift occurs during life according with the different exposures to environmental stressors. Concordance rates among MZ twins vary widely depending on the autoimmune disease, but with the exception of primary biliary cirrhosis (PBC), T1DM and coeliac disease, are well below 50% indicating major environmental contributions (Meda *et al.*, 2011).

A number of autoimmune diseases have been shown to be associated with epigenetic changes, including SLE, RA, T1DM and MS (for review see (Meda *et al.*, 2011). An example of this is in RA, where it has been proposed that RA synovial fibroblasts have a major role in the initiation and perpetuation of the disease, either through decreased

global DNA methylation or hypomethylation of CpG islands (Neidhart *et al.*, 2000; Meinecke *et al.*, 2005; Karouzakis *et al.*, 2009). RA monocytes show increased resistance to apoptosis through changes in the methylation state of CpG islands within the promoter of death receptor 3 (Takami *et al.*, 2006), with unmethylated CpG islands within the IL-6 promoter gene in monocytes found to be associated with hyperactivation of the inflammatory response (Nile *et al.*, 2008).

1.2.3.4 Gender

Gender seems to play a crucial role in predisposition to developing an autoimmune disease, as more than 78% of individuals afflicted with an autoimmune disease are women (Fairweather *et al.*, 2008). Generally, women are almost three times more likely to acquire an autoimmune disease compared to men, with the ratio between women and men varying between different autoimmune diseases (Oliver and Silman 2009). In SLE, AITD and Sjogren's syndrome (SS) the ratio is 9:1, females to males, whereas in RA and MS this rate is lower at 2:1 (Whitacre 2001; Borchers *et al.*, 2010; Kivity and Ehrenfeld 2010; Sellner *et al.*, 2011). In addition to this, female gender is a risk factor for the development of multiple autoimmune diseases, also called polyautoimmunity (Rojas-Villarraga *et al.*, 2010). Although the exact reason for this gender association remains to be fully elucidated, there are a number of possible mechanisms that have been suggested.

The strongest evidence appears to be the influence of hormones and the association with autoimmune diseases. Women are known to elicit a stronger humoral and cellular response compared to men, with women displaying a higher CD4:CD8 ratio, and increased number of both circulating CD4+ T cells and antibodies (Amadori *et al.*, 1995). A number of different hormones have been investigated for their association with the development of autoimmunity in women. Oestrogens have been shown to direct the immune system to a Th2 response rather than a Th1 response, resulting in increased B cell activation and the production of autoantibodies whereas prolactin stimulates both cell and humoral based immunity (McCarthy 2000; McMurray 2001). A number of autoimmune diseases have been shown to be negatively affected by the hormones oestrogen and progesterone, including SLE, RA and MS (for review see (Quintero *et al.*, 2011)). An example of this is in RA, where synovial fluid levels of oestrogens are significantly elevated in both male and female patients with RA resulting in the activation of macrophages and the proliferation of fibroblasts (Castagnetta *et al.*, 2003; Cutolo *et al.*, 2004).

Pregnancy and hormones are another important association with gender. The signs and symptoms of MS and RA are reduced during pregnancy but are exacerbated

following delivery of the baby, with this improvement during pregnancy thought to be linked to a shift from a Th1 to a Th2 response and worsening on return to this Th1 response (Wegmann *et al.*, 1993; Marzi *et al.*, 1996). Other hormonal influences have also been studied including menses, menopause and hormonal contraceptives, in addition to possible genetic factors, such as X-chromosome inactivation and X chromosome monosomy (for review see (Quintero *et al.*, 2011)).

1.2.3.5 Geoepidemiology

There is an overall North-South gradient for immune disorders in North America, Europe and also in China (Yang *et al.*, 1998; Bach 2002; Wallin *et al.*, 2003). In Europe there is also a West-East gradient; an example of this is T1DM which has a lower incidence in Bulgaria and Romania compared to Western Europe, however incidence in these countries is increasing (Green and Patterson 2001). This gradient cannot be explained by genetic differences; an example of this is the incidence of T1DM is six-fold higher in Finland compared to Russia, even though the genetic background of the population is the same (Kondrashova *et al.*, 2005). Migration studies have shown that offspring of immigrants coming from a country with a low incidence acquire the same incidence as the host country for both T1DM and MS (Leibowitz *et al.*, 1973; Bodansky *et al.*, 1992; Hammond *et al.*, 2000). This is well demonstrated in the case of T1DM where there is increasing frequency of T1DM in immigrants from Pakistan to the United Kingdom and also in the case of MS where there is increasing frequency of this disease in immigrants from Asia to the United States (Detels *et al.*, 1972; Staines *et al.*, 1997). In addition to these examples, the prevalence of SLE is much higher in African Americans compared to West Africans (Symmons 1995).

1.3 Multiple sclerosis

MS is a chronic inflammatory neurodegenerative disease, which predominantly affects the white matter of the central nervous system (CNS) and is the most common neurological disease in young adults, with a mean age of onset of 30 years (Trapp *et al.*, 1998). The disease is characterised by destruction of the myelin sheath, which insulates the axons of nerves, resulting in lesions of demyelinated axon fibres (Lassmann 2004). Within these lesions there is infiltration of macrophages, activated astrocytes and microglia, in addition to T and B lymphocytes (Musse and Harauz 2007). It is this demyelination and subsequent axonal damage that leads to irreversible disability in people with MS (Musse and Harauz 2007). Symptoms of the disease vary depending on the area in the CNS where these lesions are formed, but include loss of sensation and motor control in addition to visual, speech, swallowing and sphincter

disturbances, cognitive impairment, pain and fatigue. Despite considerable research, the cause of MS is still not known, although genetic and environmental factors influence disease incidence and it is thought to be autoimmune in origin (Musse and Harauz 2007).

1.3.1 Clinical presentation and disease course of MS

There are four different clinical subtypes of MS, which are divided based on the clinical course of the disease (Figure 1.2) (Lublin and Reingold 1996). Relapsing-remitting MS (RRMS) is the most common form of the disease, accounting for approximately 90% of cases initially (Schwarz *et al.*, 2006; Zuvich, *et al.* 2009). RRMS is characterised by acute attacks where there are periods of a worsening in neurological function (relapses) followed by either a partial or full recovery (remission), with recurrent attacks over a period of time (Podojil and Miller 2006; Zuvich, *et al.* 2009). However, approximately 60% of these patients find that as the disease progresses complete recovery from these attacks does not occur, leading to secondary progressive MS (SPMS). SPMS is similar to RRMS as there are periods of acute attacks where there is an increase in disability, however, during remission of this attack there is only partial recovery of symptoms leading to progressive disability over time (Lublin and Reingold 1996). This progression from RRMS and SPMS takes an average of 19 years from the initial onset of the disease (Rovaris *et al.*, 2006). Primary progressive MS (PPMS) is much less common, accounting for approximately 10% of cases, and is characterised by progressive disability from onset of disease, with no significant periods of relapse and/or remission (Podojil and Miller 2006; Miller and Leary 2007). Lastly, progressive relapsing MS (PRMS) is the least common subtype, occurring in less than 5% of cases, and is similar to PPMS as it is characterised by progressive onset of disability from disease onset, however, with clear periods of relapses without remission (Lublin and Reingold 1996; Podojil and Miller 2006).

1.3.2 Diagnosis

A diagnosis of MS is based on showing lesion dissemination in space and time, i.e. that clinical episodes affecting separate sites within the CNS have occurred at least 30 days apart, and involves excluding other neurological disorders that can clinically and radiologically mimic MS (Charil *et al.*, 2006). The principle of diagnosis is to establish from clinical evidence, supplemented by laboratory investigations, that disease activity, which is consistent with focal demyelination, has affected more than one part of the CNS on more than one occasion (McDonald *et al.*, 2001; Polman *et al.*, 2005; Compston and Coles 2008). Diagnosis can be made based on clinical assessment

only, but usually involves the use of magnetic resonance imaging (MRI) to visualise enhancing and non-enhancing lesions in the brain and/or spinal cord and the presence of oligoclonal bands (OCBs) on isoelectric focusing (IEF) of cerebrospinal fluid (CSF) (McDonald *et al.*, 2001). MRI shows white matter lesions in more than 95% of MS patients. However, their presence alone cannot be used in the diagnosis of MS, as characteristic radiological lesions can appear in people with other neurological conditions, such as acute disseminated encephalomyelitis (ADEM), and older individuals have non-specific white matter cerebral lesions (Compston and Coles 2008). The finding of OCBs in CSF remains the most reliable immunological test used to support the clinical and radiological features in establishing the diagnosis of MS (Weber and Hemmer 2010). However, OCBs are not disease specific and therefore can only be used in conjunction with other neurological tests. Variants of MS include neuromyelitis optica (NMO), Balo's concentric sclerosis and acute MS (Marburg type) can also overlap substantially with MS by clinical, laboratory and imaging measures. Based on this important exclusion of other disorders is carried out by combining the clinical history, physical examination, MRI and presence of OCBs to establish a firm and clear diagnosis of MS (Polman *et al.*, 2005).

1.3.3 Genetics and MS

There have been many studies carried out to investigate the genetics of MS within affected families. It is known that individuals belonging to a family with an affected individual carry an increased risk of developing the disease, with a familial recurrence rate of approximately 20% (Ebers *et al.*, 1995; Sadovnick *et al.*, 1996). Siblings, parents, and children carry an increased risk of developing MS if a family member is affected, of 3, 2 and 2%, respectively (Sadovnick *et al.*, 1996). The age-adjusted risk of developing MS as a white northern European is 0.3% (Robertson *et al.*, 1996). Studies in twins have also proven invaluable, with MZ twins showing a recurrence rate of 25-34% compared to 2-5% in dizygotic (DZ) twins, indicating a high heritability (Sadovnick *et al.*, 1993; Willer *et al.*, 2003). Half-siblings have a lower age-adjusted risk of developing MS than full siblings, and this risk factor does not change whether they are reared together or apart from one another (Sadovnick *et al.*, 1996). In children where both parents are affected by MS the recurrence risk is higher than in children who only have one affected parent (Robertson *et al.*, 1997; Ebers *et al.*, 2000).

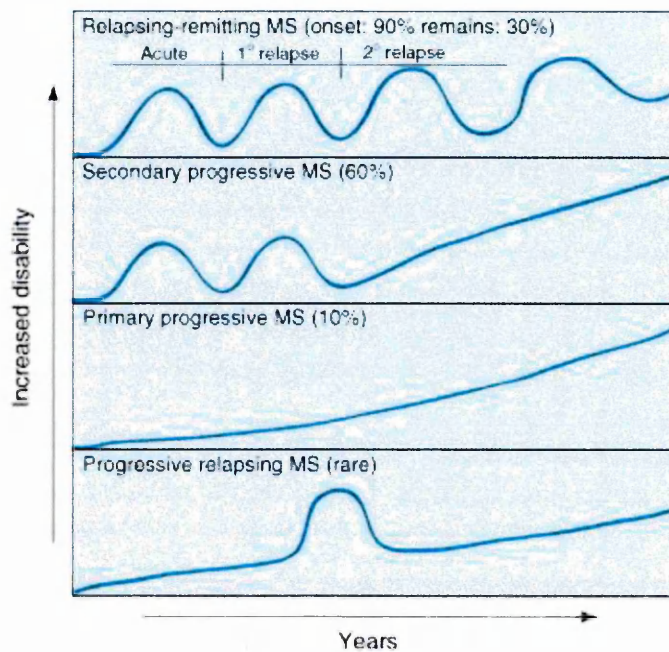


Figure 1.2: Clinical disease course in multiple sclerosis. There are four disease courses of MS. The most common disease course is relapsing remitting MS (RRMS) which is characterised by an acute attack followed by a full recovery and then subsequent attacks over time. The majority of patients with RRMS progress to secondary progressive MS (SPMS) which is characterised by fewer attacks and incomplete recovery as the disease becomes more progressive. Primary progressive MS (PPMS) is characterised by an increase in disability over time in the absence of any well-defined relapses and remissions. Progressive relapsing MS (PRMS) is the most rare disease course and is characterised by progressive disability from disease onset with clear relapses, in the absence and presence of a full recovery (Podojil and Miller 2006).

There have been many genetic studies carried out to identify particular genes that may be associated with a risk of developing MS. The greatest achievement in genetics was the identification of variants in the HLA genes and associated risk of developing MS, in particular inheritance of the *HLA-DRB*1501*, *DRB5*0101*, *DQB1*0602*, and *DQA1*0102* haplotypes (Bertrams *et al.*, 1972; Naito *et al.*, 1972; Fogdell *et al.*, 1995; Oksenberg and Barcellos 2005)

In a recent large-scale genetic study, *DRB1*15/08* genotypes were identified as high-risk for MS whereas *DRB1*15/14* genotypes were identified as protective for MS (Barcellos *et al.*, 2006). In addition, protective effects have been reported to be conferred by both HLA-5 and HLA-DRB1*11 (Ramagopalan *et al.*, 2007; Yeo *et al.*, 2007; Dean *et al.*, 2008). Additional genes have also recently been identified as having MS susceptibility loci associated with single nucleotide polymorphisms, including interleukin-7 receptor, interleukin-2 receptor, ecotropic viral integration site 5 and kinesin family member 1 β (Hafler *et al.*, 2007; Lundmark *et al.*, 2007; Aulchenko *et al.*, 2008; Hoppenbrouwers *et al.*, 2008).

1.3.4 Epidemiology

MS affects approximately 2.5 million people globally. It affects 1:1000 in the UK, costing £1.2 billion per year in the UK alone (Holmes *et al.*, 1995; Compston and Confavreux 1998). Onset of disease is most common between the ages of 20 and 40 years, reaching highest incidence at around 24 years of age, with females twice as likely to develop the disease than males (Noseworthy *et al.*, 2000). In some countries this 2:1 ratio has increased, as demonstrated in Canada where a recent study showed that 3.2 women were affected for every man (Orton *et al.*, 2006). Childhood MS is rare with disease onset occurring before the age of 18 in only 3-10% of cases (Banwell *et al.*, 2007). Both the incidence and prevalence of MS appears to increase with increasing distance from the equator, with the most northern and southern countries identified as most high risk (Goldacre *et al.*, 2004; Alonso and Hernan 2008). Clear increases in both the incidence and prevalence have been found in America (Noonan *et al.*, 2002), Australia (Barnett *et al.*, 2003), Canada (Orton *et al.*, 2006), and the UK (Alonso and Hernan 2008) supporting the theory that there is an increase in countries furthest from the equator. This gradient of increasing MS risk with increasing latitude has been strongly linked with lack of UVR and vitamin D deficiency. It has been suggested that UVR exposure, which is the primary source of vitamin D, may offer protection against the development of MS, therefore accounting for this latitudinal effect of MS prevalence (Acheson *et al.*, 1960; Kurtzke *et al.*, 1979). In support of this a

recent study found that individuals with MS have a much lower risk of developing skin cancer than individuals without MS (Goldacre *et al.*, 2004).

1.3.5 Pathology of multiple sclerosis

1.3.5.1 White matter pathology

In 1868, Charcot first described the pathological hallmarks of MS, including focal demyelination, inflammation, formation of a scar, and varying degrees of axonal damage. There are two major types of plaques in MS: the active lesion and the chronic inactive lesion. The active lesion consists of active inflammatory demyelination, which is typically restricted to white matter and characterised by the accumulation of both lipid-laden macrophages and large reactive astrocytes, accompanied by varying degrees of perivascular inflammation. Luxol fast blue staining reveals loss of myelin with the preservation of axons in most cases, although where there is extensive damage, axons may become lost or fragmented (Lucchinetti *et al.*, 2005). Typically macrophages become engorged with phagocytosed myelin remnants and debris, resulting in the appearance of classic Gitter cells. These cells are characterised by spherical round nuclei, vacuolated cytoplasm, and discrete cell bodies. Reactive astrocytes are also prominent, displaying polymorphic nuclei and an eosinophilic cytoplasm, and are distributed evenly throughout the active lesion (Lucchinetti *et al.*, 2005). By investigating the structural profile and degradation products within macrophages, demyelinating activity within a plaque can be determined: minor myelin proteins, including myelin oligodendrocyte (MOG) and myelin-associated glycoprotein (MAG), are rapidly degraded within 1 to 2 days following phagocytosis; whereas, major myelin proteins, including myelin basic protein (MBP) and PLP, can persist in macrophages for up to 10 days in biopsies; and in the later stages, macrophages contain sudanophilic and periodic acid-Schiff (PAS)-positive granular lipids that can persist in the lesion for several months (Brück *et al.*, 1995).

The chronic lesion involves predominantly the white matter and consists of demyelinating foci or plaques, which are found throughout the CNS, but most commonly develop in the periventricular white matter, varying in both size and number between individuals. These lesions also have a predilection for the optic nerves, brainstem, cerebellum and spinal cord. The chronic inactive plaque is sharply defined and hypocellular with no evidence of active demyelination or axonal loss (Lucchinetti *et al.*, 2005). There is prominent fibrillary gliosis, along with a substantial reduction or complete loss of mature oligodendrocytes, with varying degrees of inflammation sometimes still present, particularly in the perivascular region (Prineas 1985). There

can be obvious areas of remyelination but this is often incomplete and restricted to the plaque edge. However, more extensive remyelination throughout a chronic MS plaque may also be observed; referred to as shadow plaques (Lucchinetti *et al.*, 2005). These remyelinated lesions can then become targets for further demyelination (Prineas *et al.*, 1993). Oligodendrocyte progenitor cells have been identified in completely demyelinated plaques devoid of mature oligodendrocytes (Wolswijk 1998), suggesting that remyelination may not be limited by an absence of oligodendrocyte progenitors but that damaged neurons may not be receptive to remyelination signals (Chang *et al.*, 2002).

At present MS lesions are classified based on either stage (for review see (Van der Valk and De Groot 2000) or underlying pathology (Lucchinetti *et al.*, 2000). To date, four staging systems for MS lesions have been defined (for review see (Van der Valk and De Groot 2000)(Berger and Reindl 2007). The Bö/Trapp staging system encompasses the cellularity to determine the type of lesion, which is split into the following three categories: (1) active demyelinating lesions, defined as hypercellular; (2) chronic active lesions have a hypocellular centre with a hypercellular rim; and (3) chronic inactive lesions are hypocellular (Bö *et al.*, 1994; Trapp *et al.*, 1998). This system works best when applied to frozen sections and paraffin embedded tissue from post-mortem acquired lesions, but does not recognise early changes that occur in lesions. A modification of the Bö/Trapp staging system is the De Groot-van der Valk system which includes the following additional categories: (1) 'pre-active' lesions defined by clusters of microglial cells with little inflammation and no demyelination; (2) active demyelinating; (3) active but not demyelinating; (4) chronic active (as with the Bö/Trapp system); and (5) chronic inactive (as with the Bö/Trapp system). This system has been shown to work best on MRI-sampled material (Van Waesberghe *et al.*, 1999). The Lassman/Brück staging system used a high number of biopsy samples and therefore has been deemed most useful for classifying early lesions, and consists of five categories: (1) early active; (2) late active; (3) inactive; (4) early remyelinating; (5) late remyelinating (Brück *et al.*, 1994; Brück *et al.*, 1995). The Vienna consensus was brought about at a conference in Vienna when a group of MS pathology experts convened to discuss staging of MS, led by Professor Hans Lassman (Ferguson *et al.*, 1997). The Vienna consensus incorporated both the Bö/Trapp and Lassman/Brück staging system and identified six lesion types, as follows: (1) inflammatory and demyelinating; (2) inflammatory but not demyelinating; (3) hypocellular centre with inflammatory rim and demyelinating; (4) hypocellular centre with inflammatory rim, but not demyelinating; (5) no inflammation, but demyelinating; and (6) no inflammation and not demyelinating. The Vienna consensus is a more descriptive way to describe MS lesions rather than a staging system.

1.3.5.2 Grey matter pathology

MS is traditionally thought of as a disease of the white matter, however, there is increasing interest in grey matter pathology, as demyelinating lesions have been found in both the cerebral cortex and the cerebellum of post-mortem tissue taken from the brains of patients with MS (Kutzelnigg *et al.*, 2005; Kutzelnigg *et al.*, 2007). The reason for this traditional view of MS as a disease of the white matter appears to be due to the fact that grey matter lesions are much more difficult to detect than those that occur in the white matter using traditional T2-weighted MRI scanning, for a number of reasons including location of lesion, size of lesion and the intrinsic properties of the grey matter, and therefore are often missed (Schmierer *et al.*, 2010). A recent study also found that MRI for the detection of cortical lesions has a sensitivity of only 3-5% (Geurts *et al.*, 2005). In addition, although there is axonal injury, the global tissue texture is preserved better in grey matter lesions compared to white matter lesions, which can make it more difficult to determine cortical demyelination on visual inspection of the post-mortem brain or with MRI (Kidd *et al.*, 1999).

In a study carried out by Lumsden and colleagues examining 60 MS post-mortem brain tissue cases, 93% of cases showed involvement of the cortex to a varying degree, with some showing involvement of only a few cortical lesions whilst in one case there were 465 lesions (Lumsden 1970). Using post-mortem tissue from 52 patients with MS and 30 control brains with immunohistochemistry, Kutzelnigg *et al.* (2005) identified cortical demyelination as a characteristic feature of progressive MS. Demyelination in the cerebral cortex was mainly observed in tissue taken from patients with SPMS and PPMS, and was rare in patients with acute or relapsing disease course (Kutzelnigg *et al.*, 2005). This has confirmed previous studies which also showed the presence of cortical demyelination in SPMS and PPMS patients (Brownell and Hughes 1962; Peterson *et al.*, 2001).

Furthermore, in a more recent study, Gilmore and colleagues used 14 MS post-mortem MS cases and 3 control brain cases to quantify grey and white matter demyelination through staining for proteolipid protein (PLP) (Gilmore 2008). Overall, 28.8 % of the grey matter was demyelinated compared with only 15.6 % of the white matter, which was most extensive in the spinal cord and cerebellum. Consistent with the study by Kutzelnigg *et al.* (2005) this demonstrated that the cerebellar cortex is a predilection site for demyelination (Gilmore 2008). Grey matter lesions differ significantly from white matter lesions, as they are less inflammatory, with less infiltration by both macrophages and lymphocytes (Bö *et al.*, 2006).

1.4 Immune responses within the central nervous system

1.4.1 T cells

T cells arise from haematopoietic stem cells in the bone marrow and mature in the thymus, and play an important part in cell mediated immunity. Unlike B cells, T cells are only able to recognise peptide antigens that are displayed on MHC molecules expressed on other cells. All nucleated cells express MHC class I proteins, which are able to bind specifically to TCRs on T cells expressing the CD8 co-receptor (Friese and Fugger 2009). T cells expressing the CD4 co-receptor on their surface are restricted to interaction with MHC class II proteins, which are mainly expressed on specialised APCs (LaRosa and Orange 2008).

T cells can be divided into two main populations; effector and memory. Effector T cells encompass CD8⁺ T cells; CD4⁺ T helper (Th) 1, Th2, Th17, regulatory T cells (Tregs), whereas memory T cells consist of central memory (T_{CM}) and effector memory (T_{EM}) populations. CD4⁺ T helper cells produce the largest numbers of cytokines with Th1-type cytokines including IL-1 β , TNF- α and IFN- γ producing pro-inflammatory responses specific for killing intracellular parasites and for exacerbating autoimmune responses, and Th2-type cytokines IL-4, IL-5 and IL-13, facilitating B-cell antibody responses, with IL-4 driving B-cell proliferation against extracellular pathogens and IL-4/IL-5 enabling production of IgE and eosinophilic inflammation, which is important for the clearance of helminth infections and atopy (Berger 2000; LaRosa and Orange 2008). CD4⁺ T cells differentiate into the different subsets upon priming and are distinguished by the cytokines they produce and their effector functions. Although not yet completely understood, it is thought that the cytokine milieu is the major factor that determines the differentiation of these subsets (LaRosa and Orange 2008).

T cells are able to enter the CNS in order to carry out immune surveillance, but are found in relatively low numbers in the CNS of healthy individuals (Hickey 1999), with higher efficiency in the spinal cord compared to the brain (Phillips and Lampson 1999; Yeager *et al.*, 2000). The amount of immune surveillance in the CNS is much less than that occurring in other tissues.

Cytotoxic lymphocytes (CTLs) are found in low numbers in the CNS of healthy individuals, but are recruited during inflammation. CD8⁺ T cells are implicated in the direct killing of resident cells in host tissues through the release of perforin and granzymes which are toxic to the cells, resulting in specific killing of target cells (Shresta *et al.*, 1998; Trapani *et al.*, 2000; LaRosa and Orange 2008).

1.4.2 B cells

B cells comprise the humoral part of the adaptive immune response, originating from haematopoietic stem cells in the bone marrow, and are imperative in controlling microbial infections (Cepok *et al.*, 2006). B cells respond to protein targets in the GC of the lymph node, with the support of antigen-specific T cells. Upon contact with a specific protein presented on DCs B cells undergo affinity maturation during which high affinity receptors directed towards the target antigen are generated and eventually Ig class-switch is induced (see section 1.1.2.4). These high-affinity B cells can either mature into memory B cells or become antibody-secreting plasma cells, secreting antibodies of IgA, IgD, IgE, IgG or IgM class (Rajewsky 1996). These antibodies can bind specifically to antigens where they undergo phagocytosis by macrophages and can also activate the complement system (Dunkelberger and Song 2009). B cells can also act as APCs (Batista and Harwood 2009).

In non-inflammatory conditions, B cells are largely absent from the CNS and CSF, however, in acute and chronic inflammatory disease B cells can constitute up to 30% of cells of the CSF (Cepok *et al.*, 2003; Cepok *et al.*, 2005). These accumulated B cells in the CSF are predominantly IgM-IgD-CD27+ class switched memory B cells rather than short-lived immature plasma blasts (Cepok *et al.*, 2006).

1.4.3 Glial cells

Virchow in 1846 was the first to coin the term neuroglia when he described cells other than neurons in the brain. This term has been used since the 1850s as a generic name for these cells, or in its shortened form 'glia'. These major glial cell types were further characterised as the result of microscopic studies whereby Cajal first identified astrocytes, which was followed by Hortega identifying oligodendrocytes and microglia (Kettenmann and Verkhratsky 2008).

1.4.3.1 Microglia

Microglia are derived from myeloid cells in the periphery and are the resident long-lived macrophages of the CNS, accounting for approximately 12% of cells in the brain and 10-20% of glial cells (Lawson *et al.*, 1990; Gandhi *et al.*, 2010; Zhang *et al.*, 2010). There is significantly higher microglial density in white matter versus grey matter, with as little as 0.5% microglia in the grey matter compared to 16.6% in the white matter of the non-diseased human brain (Mittelbronn *et al.*, 2001).

Microglia are responsible for the first line of defence against bacterial, viral, parasitic and fungal infections in the CNS (Napoli and Neumann 2009). In order to carry out this

task microglia have a large number of processes which cover the entire CNS parenchyma (Napoli and Neumann 2009). Traditionally microglia were thought to be in a “resting” state under normal physiological conditions, however, *in vivo* live imaging of fluorescently-tagged microglia in the rodent brain showed that microglia processes are very motile and are constantly surveying their environment through projection and retraction of their processes (Davalos *et al.*, 2005; Nimmerjahn *et al.*, 2005). This high motility enables microglial processes to immediately perceive their microenvironment and carry out important homeostatic activity in the normal CNS, including the constant phagocytosis of cellular debris and apoptotic cells (Napoli and Neumann 2009; Neumann *et al.*, 2009). In this state, microglia are characterised by a ramified morphology and the expression of certain cell surface antigens, such as MHC molecules (Mittelbronn *et al.*, 2001; Rock *et al.*, 2004). Based on the above findings microglia are now thought of more as “surveillance” cells when not yet activated. Microglia are quickly activated following injury or infection and migrate towards the site of damage or infection within hours (Davalos *et al.*, 2005; Haynes *et al.*, 2006). In this state, microglia are characterised by an amoeboid morphology, along with up-regulated expression of cell surface markers, such as MHC molecules and chemokine receptors, and also the expression of CD14 which is not found on ramified microglia (Rock *et al.*, 2004).

Microglia express distinct types of receptors, which have a role in phagocytosis of pathogenic organisms through the expression of their Toll-like receptors (TLRs) or scavenger receptors which recognise phosphatidylserine (PtdSer) on the surface of apoptotic cells (Napoli and Neumann 2009).

The first line of defence in the elimination of microbes in the CNS is mediated by the recognition of pathogen associated molecular patterns (PAMPs) by TLRs expressed by microglia, which are widely expressed on many cells of the immune system and exist on both the surface and on internal membranes. TLRs respond rapidly to microbial pathogens through binding to these PAMPs (Napoli and Neumann 2009). TLRs are a type I transmembrane pattern recognition receptors (PRRs) that act as endogenous sensors for PAMPs produced by bacteria, viruses, parasites and fungi (Glezer *et al.*, 2007). Microglial cells express TLRs 1-9 and expression of these receptors is pivotal for generation of neuroimmune responses (Aravalli *et al.*, 2007; Jack *et al.*, 2007). Upon a PAMP binding to a specific TLR a downstream signalling pathway is initiated whereby adapter proteins are recruited leading to the activation of protein kinases and activation of transcription factors resulting in the secretion of pro-inflammatory cytokines (such as IL-1 β and IL-6) and chemokines (such as CCL2 and CCL5) and production of reactive oxygen and reactive nitrogen species (ROS and RNS) (Takeda

and Akira 2005; O'Neill 2008; O'Neill *et al.*, 2009; Huang and Pope 2010). This results in both phagocytosis of infected cells and inflammation limited to the area of infection. TLR signalling plays a significant role not only in the innate immune response to CNS infections but also in inflammatory and demyelinating disorders including MS, ischaemic injury, and neurodegeneration (Aravalli *et al.*, 2007; Lehnardt 2010). An example of this is injury to tissue within the CNS results in the release of DAMPs which are also recognised by TLRs and activate the same downstream signalling pathway as PAMPs.

In addition to TLRs, microglia express receptors able to detect pathogens, including nuclear oligomerisation domain-like receptors (NLRs) (Shaw *et al.*, 2010; Bielig *et al.*, 2011; Kepp *et al.*, 2011; Lamkanfi 2011). NLRs are located within the cytoplasm and recognise cytosolic viruses and bacterial products, which like TLRs bind many different ligands leading to gene transcription and production of pro-inflammatory cytokines, chemokines and proteases. However, NLRs also recruit cytoplasmic proteins to form an inflammasome capable of activating caspase-1, leading to the conversion of cellular proteins such as those transcribed by TLR activation (e.g. IL-1 β and IL-18) to their active forms that upon secretion contribute to the inflammatory cascade. These pathways involving TLRs and NLRs are important for helper T cell type I responses in killing of intracellular pathogens (Ross 2010). TLRs and NLRs both activate signalling pathways, however microglia also express PRRs which have immediate effects resulting in binding and subsequent internalisation of either pathogens or apoptotic cells without subsequent activation of signalling pathways (Ross 2010).

Dying cells in the CNS recruit phagocytes from both close proximity and greater distances, through the release of DAMPs. These signals facilitate the recruitment of microglia, include the release of nucleotides adenosine triphosphate (ATP) and uridine triphosphate (UTP) from damaged neurons, which have been shown to be key mediators in the recruitment of microglia through activation of purinoreceptors following injury, leading to the removal of dying cells or their debris (Davalos *et al.*, 2005; Haynes *et al.*, 2006).

Within days following injury, microglia undergo a process called reactive microgliosis whereby microglia proliferate extensively and upregulate the expression of the stem cell-associated surface molecule CD34 (Ladeby *et al.*, 2005). In comparison, cells undergoing apoptosis i.e. programmed cell death express signals which act as markers for microglia leading to ingestion and subsequent elimination of these cells. The most studied of these signals is PtdSer, which is redistributed to the outer leaflet of the plasma membrane to enable recognition by phagocytes followed by subsequent internalisation (Ravichandran 2003; Ravichandran and Lorenz 2007; Napoli and

Neumann 2009). Apoptotic neurons have also recently been shown to upregulate their expression of TREM2 ligand (triggering receptor expressed on myeloid cells-2) resulting in efficient clearance of these damaged neurons by microglia expressing TREM2, without inducing gene transcription of pro-inflammatory mediators or up-regulating the expression of receptors involved in antigen presentation (Takahashi *et al.*, 2005; Piccio *et al.*, 2007).

Microglia are also important antigen presenting cells in the CNS and are able to interact with B and T cells through the expression of MHC class II and co-stimulatory molecules CD83 and CD40 (Benveniste 1997; Raivich and Banati 2004; Aravalli *et al.*, 2007).

Besides their role in both innate and adaptive immunity, microglia are also important in embryogenesis whereby cells of the immune system undergo developmental apoptosis, in particular twice as many neurons are produced then are retained in the mature individual. Microglia are thought to play a role in both promoting cell death and the phagocytosis of developing neurons (Marín-Teva *et al.*, 2004; Bessis *et al.*, 2006; Ransohoff and Perry 2009). In addition to this, microglia are also important as promoters of neurogenesis in adults through secretion of neurotrophic factors such as brain-derived neurotrophic factor, insulin-like growth factor (IGF-1) and neurotrophin 3 (Napoli and Neumann 2009; Napoli and Neumann 2010). Microglia are also thought to carrying out synaptic stripping in pathological processes (Bessis *et al.*, 2006; Trapp *et al.*, 2006). Therefore, microglia can be both neuro-protective and neuro-destructive (Aravalli *et al.*, 2007).

1.4.3.2 Astrocytes

Astrocytes are the most abundant glial cells in the CNS and are defined by their characteristic star-shaped morphology and the expression of the intermediate filament GFAP within their cytoplasm (Eng 1985). Two types of astrocytes exist within the brain: (1) stellar fibrillary astroglia and (2) protoplasmic astroglia. The former have elongated cell processes and are predominantly found in the white matter of the brain (Bignami *et al.*, 1972), whereas the latter have short and ramified cell processes and are usually found in the grey matter (Didier *et al.*, 1986; Cammer and Tansey 1988). Until recently, these cells were thought to merely play a role as supportive cells within the brain and in forming a structural part of the blood-brain barrier (BBB). However, this view has now changed with recent publications showing that astrocytes play a number of important complex roles within the brain, including monitoring and modulating the neuronal microenvironment and information processing and signalling in the brain (for review see Penkowa *et al.*, 2008).

Astrocytes have a number of housekeeping duties within the CNS, including the formation and maintenance of the BBB as part of the glia limitans, which prevents the entry of potentially harmful molecules into the brain and facilitates the entry of essential nutrients into the CNS, in addition to the formation of tight junctions (TJs) between the endothelial cells (ECs) of the BBB (Aschner 2000). Astrocytes are able to preserve the stability of the extracellular environment by regulating extracellular pH and removing neurotransmitters, excess ions, ammonia, free radicals and water from the brain microenvironment (Tsacopoulos and Magistretti 1996; Benveniste 1997; Aschner *et al.*, 1999). Under normal conditions, astrocytes maintain homeostasis in the CNS to support survival and information processing functions of neurons through providing neurotrophic and protective factors (Ridet *et al.*, 1997; Raivich *et al.*, 1999).

Due to their large numbers within the brain and their extended processes, astrocytes are also important surveillance cells within the CNS and react to brain damage or disease by increasing in both their number and size in a process called reactive astrogliosis (Penkowa *et al.*, 2008). Cell hypertrophy of these reactive astrocytes is a consequence of an increase in intracellular filaments and cytoskeleton proteins (Ridet *et al.*, 1997) in order to stabilise the brain tissue surrounding the site of injury. In particular, there is an upregulation of the intermediate filament protein GFAP within the cytoplasm of the astrocytes, which is a hallmark of reactive astrogliosis and GFAP immunostaining is the most commonly used marker for reactive astrogliosis, and is a sensitive and early biomarker of astrogliosis following injury (O'Callaghan and Sriram 2005).

Trauma, ischaemia, infections and neurological diseases are all known to have the capacity to induce astrogliosis i.e. conversion of astrocytes into their "reactive" form (Malhotra *et al.*, 1997; Okamoto *et al.*, 2005; Sofroniew 2009; Wakasa *et al.*, 2009). Reactive astrocytes initiate and regulate CNS inflammatory and immune response through the expression and secretion of a number of important neuroimmunological factors, including adhesion molecules, MHC class I and II, cytokines, neurotrophic factors, growth factors and signalling molecules (Penkowa *et al.*, 2008). Reactive astrocytes modulate the CNS microenvironment by producing and secreting molecules of the extracellular matrix (ECM) (Eddleston and Mucke 1993; Aschner *et al.*, 1999). In addition to the above roles, reactive astrocytes are also pivotal in the maintenance and repair of the BBB following CNS injury (Zhang *et al.*, 2010).

Reactive astrocytes provide support for axonal growth and help improve the recovery of axons following injury (Privat 2003). Initially astrocytes encase themselves around damaged neurons with thin sheet-like lamellar cell processes (Graeber and Kreutzberg 1988) resulting in the loss of synapses, but then retract from the neurons prior to

neuroregeneration, with neuronal surface membranes eventually re-establishing synapses (Raivich *et al.*, 1999). However, following a particularly traumatic injury to the CNS, hypertrophic astrocytic processes encase the lesion site and deposit an inhibitory ECM, which results in the formation of a dense structure that prevents neuroregeneration and is referred to as a glial scar (Cafferty *et al.*, 2007). CNS neurons are unable to neuroregenerate due to both an inhibitory physical and chemical barrier, as it is thought that astrocytes may also produce growth-inhibitory factors (Stichel and Müller 1998; Rolls *et al.*, 2009).

Reactive astrocytes are also a major source of both pro- and anti-inflammatory cytokines, and are therefore able to activate other immune-responsive cells, such as monocytes/macrophages/microglia and lymphocytes to the site of injury (Hopkins and Rothwell 1995; Ridet *et al.*, 1997; Raivich *et al.*, 1999). Initially this production of pro-inflammatory cytokines can be beneficial in recruiting immune-responsive cells, such as microglia and lymphocytes to the site of injury and attenuation of CNS damage, however, prolonged release of these cytokines may induce chronic inflammation and neurodegeneration, as these pro-inflammatory cytokines are harmful to both neurons and oligodendrocytes (Oleszak *et al.*, 1998). Reactive astrocytes are also able to produce nitric oxide which causes damage to a number of cells, including neurons and oligodendrocytes (Estévez *et al.*, 1998). In contrast, reactive astrocytes also produce anti-inflammatory cytokines which are likely to contribute to limiting the neuroinflammation in the affected area and aid in the regeneration of neurons (Nair *et al.*, 2008). In addition, reactive astrocytes produce a number of growth factors which are able to promote oligodendrocytes to produce myelin (Moore *et al.*, 2011). Reactive gliosis is thought to be an attempt by the CNS to isolate the injured area (Fitch and Silver 1997) and therefore protect the unaffected area, however, astrogliosis also prevents axonal regeneration.

1.4.3.3 Oligodendrocytes (OLGs)

OLGs are the glial cells of the CNS that are able to wrap long segments of axons with a multilayered sheath of extended cell membrane. This ability of oligodendrocytes to form the myelin sheath, provides electrical insulation around nerve fibres, thereby making rapid transmission of electrical signals in the brain possible (Jessen 2004). Myelin was first understood to enable 'saltatory' impulse propagation in axons more than 60 years ago before it was recognised by electron microscopy as a specialised outgrowth of glia (Geren and Raskind 1953). OLGs are able to myelinate several axons simultaneously. Mature oligodendrocytes make myelin by wrapping axons with their own cell membrane in a spiral shape, which eventually becomes a multilayered sheath covering

a long segment of axon. These myelinated axons are flanked by nodes of Ranvier, the sites at which sodium channels are concentrated and the action potentials are generated (Nave 2010).

The proliferation and differentiation of OLG lineage cells is controlled by further growth factors and cytokines, including platelet-derived growth factor and brain-derived neurotrophic factor. This myelination of neurons prevents the consumption of large amounts of ATP, as in electrically active but unmyelinated fibers the restoration of ion gradients by sodium and potassium-ATPase consumes a large amount of available ATP. Myelination strongly reduces this energy consumption because action potentials and ion currents are restricted to less than 0.5% of the axon's surface. Furthermore, myelination of axons provides up to a 100-fold increase in conduction velocity (Nave 2010). Additional functions of OLGs are still not fully elucidated, but there is evidence that these cells communicate lifelong with axons, and that glia are required for the long-term integrity and survival of axons (Griffiths *et al.*, 1998; Lappe-Siefke *et al.*, 2003; Edgar *et al.*, 2004; Kassmann and Nave 2008). Subsequently, OLGs may also be neurotrophic.

1.4.4 Endothelial cells (ECs)

Brain ECs comprise a key component of the BBB (Figure 1.3) and contribute to the immune response of the CNS by responding to, transporting and secreting cytokines. A unique feature of brain ECs is their ability to change cell membrane composition depending in whether the membrane is facing the blood or the brain, with their lipid, receptor and transport compositions differing depending on this (Verma *et al.*, 2006). This polarisation is important in preventing harmful substances from entering the brain.

Brain ECs lack fenestrations, exhibit low pinocytotic but high efflux transporter activity and this limits transcellular diffusion (Fenstermacher *et al.*, 1988; Sedlakova *et al.*, 1999; Oldendorf *et al.*, 2004; Verma *et al.*, 2006). Brain ECs are exposed to an array of endogenous and exogenous neuromodulatory substances, immune cells, neurotransmitters and hormones, environmental stresses, and potentially toxic compounds at both the brain and blood side of the membranes. These brain ECs have the potential to receive signals from one compartment, e.g. the blood, and to secrete into the other, e.g. the brain (Verma *et al.*, 2006). Brain ECs secrete an array of cytokines, with IL-1 α , IL-10 and granulocyte-macrophage colony-stimulating factor preferentially secreted from brain ECs facing the blood. Exposure of brain ECs to IL-1 β , TNF- α , IFN- γ , or LPS decreases the transendothelial electrical resistance allowing leukocytes to enter the brain (Wong *et al.*, 2004).

1.4.5 The blood brain barrier (BBB)

Cells at three key interfaces form barriers between the blood and the CNS; BBB, blood-CSF barrier and the arachnoid barrier, in order to limit and regulate molecular exchange at the interfaces between the blood and the neural tissue or its fluid spaces (Ransohoff *et al.*, 2003; Abbott *et al.*, 2010). In the brain and spinal cord the BBB is created by ECs that form the walls of the capillaries. The combined surface area of these microvessels constitutes the largest interface for BBB exchanges and is the major site of blood-CNS exchange (Abbott *et al.*, 2010). A second interface is formed by the epithelial cells of the choroid plexus facing the CSF fluid, which forms the blood-CSF barrier (BCSFB). The CSF is secreted across the choroid plexus epithelial cells into the brain ventricular system (Brown *et al.*, 2004), whilst the remainder of the interstitial fluid (ISF), is secreted across the capillary endothelium of the BBB (Cserr *et al.*, 1981; Abbott 2004; Dolman *et al.*, 2005).

The third interface is provided by the avascular arachnoid epithelium, underlying the dura, and completely enclosing the CNS; this completes the seal between the extracellular fluids of the CNS and that of the rest of the body (Abbott *et al.*, 2006). Although the arachnoid also forms a barrier layer, it does not provide a significant surface for blood-CNS exchange due to its avasculature nature and relatively small surface area (Kandel *et al.*, 2000). At all three interfaces, the barrier function is not fixed, but can be modulated and regulated, both in physiology and pathology (Abbott *et al.*, 2006).

The BBB is composed of three cellular elements of the brain microvasculature: (1) ECs, (2) astrocyte end-feet and (3) pericytes (PCs) (Ballabh *et al.*, 2004) (Figure 1.3). The brain ECs differ from ECs in the rest of the body by the absence of fenestrations, more extensive tight junctions (TJ), and sparse pinocytotic vesicular transport. EC TJs limit the paracellular flux of hydrophilic molecules across the BBB. In contrast, small lipophilic substances, such as O₂ and CO₂ diffuse freely across plasma membranes along their concentration gradient (Grieb *et al.*, 1985). Nutrients including glucose and amino acids enter the brain via transporters, whereas receptor-mediated endocytosis mediates the uptake of larger molecules, including insulin, leptin and iron transferrin (Pardridge *et al.*, 1985; Zhang and Pardridge 2001).

TJ and adherens junction (AJ) proteins between adjacent ECs form a diffusion barrier which selectively prevents most blood-borne substances from entering the brain (Schulze and Firth 1993; Kniessel and Wolburg 2000; Mrass and Weninger 2006).

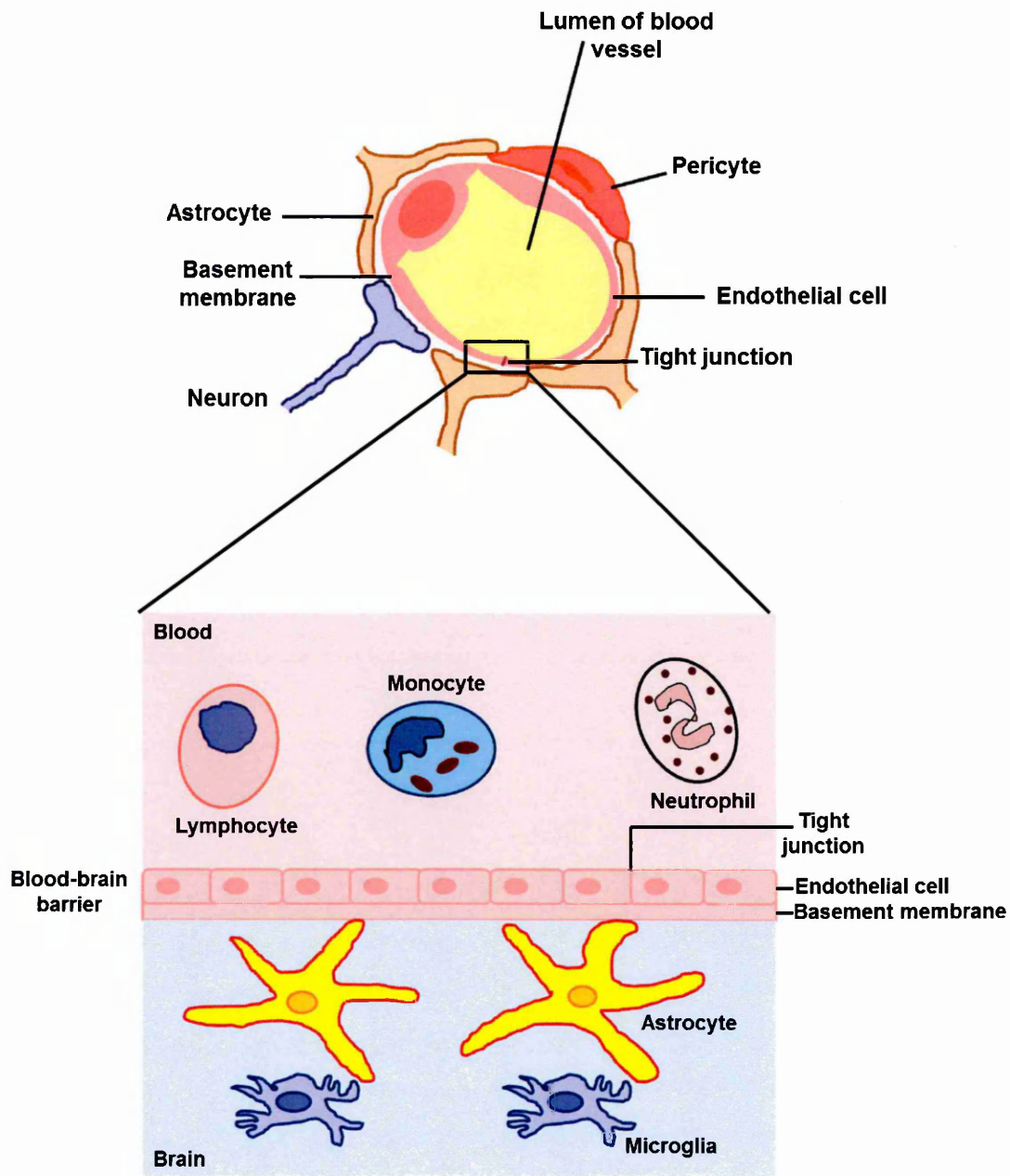


Figure 1.3: Schematic diagram of the blood-brain barrier (BBB). Endothelial cells line the BBB with associated tight junctions, forming a barrier between the circulation and the brain parenchyma. This prevents the entry of lymphocytes, monocytes and neutrophils. A thin basement membrane surrounds the endothelial cells and pericytes. This prevents the infiltration of pathogens and restricts antibody-mediated immune responses from entering into the central nervous system, and thus protects against a full-blown immune response (adapted from Francis *et al.*, 2003).

Extremely tight 'tight junctions' are a key feature of the BBB and significantly reduce permeation of polar solutes between the ECs from the blood plasma to the brain extracellular fluid (Begley and Brightman 2003; Wolburg *et al.*, 2009). AJs are essential for barrier formation of TJs and disruption of AJs results in barrier disruption (Wolburg and Lippoldt 2002). TJs are zipper-like structures that link two adjacent cells and are formed by the close interaction and the assembly into macromolecular complexes of at least three families of transmembrane proteins: claudins, occludin and junctional adhesion molecules (JAMs) (Wolburg and Lippoldt 2002; Wolburg *et al.*, 2009).

Astrocytic end-feet tightly ensheath the vessel wall and appear to be critical for the induction and maintenance of the TJ barrier. Induction and maintenance of many BBB properties, including formation of TJs and the polarised expression of transporters in the endothelial membranes, depends on close association with astrocytes (Rubin *et al.*, 1991; Wolburg *et al.*, 2009).

PCs are cells that wrap around ECs of microvessels including capillaries, venules, and arterioles. They are thought to provide structural support and vasodynamic capacity to the microvasculature (Ballabh *et al.*, 2004). PCs are the least studied cellular component of the BBB but appear to play a key role in angiogenesis, structural integrity and differentiation of the vessel, and formation of endothelial TJs (Balabanov and Dore-Duffy 1998; Allt and Lawrenson 2001). The BBB also consists of the capillary basement membrane (BM), in which PCs embed.

The BBB is present in all brain regions, except for the circumventricular organs, such as the pineal gland. Blood vessels in these areas of the the brain have fenestrations that permit diffusion of blood-borne molecules across the vessel wall (Ballabh *et al.*, 2004).

All components of the BBB are essential for the normal function and stability of the BBB. A number of CNS pathologies involve dysfunction of the BBB, including MS (Correale and Villa 2007), Parkinson's disease (PD) and Alzheimer's disease (AD) (Desai *et al.*, 2007; Zlokovic 2008), and hypoxia and ischaemia (Kaur and Ling 2008). The barrier dysfunction can range from mild and transient TJ opening to chronic barrier breakdown (Förster 2008).

1.4.5.1 BBB disruption and multiple sclerosis

Despite the presence of this highly regulated BBB, leukocyte entry into the CNS is an early event in MS. The entry of pro-inflammatory leukocytes into the CNS is thus considered an early phenomenon that can trigger early events leading to neuroinflammation, BBB disruption and MS plaque formation (Raine *et al.*, 1990;

Engelhardt 2006). Immune cells of MS subjects express inflammatory cytokines, ROS and enzymes that can facilitate their migration to the CNS by influencing barrier function, either directly or indirectly (Larochelle *et al.*, 2011). Acute MS lesions, featuring areas of demyelination, axonal loss and immune cell infiltrates, display BBB disruption as evidenced by *in vivo* gadolinium uptake on MRI and post-mortem evidence of focal micro-vascular leakage (Larochelle *et al.*, 2011).

Whether BBB dysfunction precedes immune cell infiltration or is the consequence of perivascular leukocyte accumulation remains to be established. While it has been suggested that BBB dysfunction can precede immune infiltration and demyelination in MS, leukocyte migration both directly and indirectly, modified BBB permeability (Larochelle *et al.*, 2011). An example of this is the clinical use of Natalizumab, an anti- $\alpha_4\beta_1$ integrin antibody known to restrict leukocyte migration to the CNS, which decreases lesion genesis and the number of lesions showing gadolinium enhancement (Polman *et al.*, 2006). A number of different BBB dysfunctions have been reported in MS, including breakdown of the BBB (Minagar and Alexander 2003), TJ abnormalities (McQuaid *et al.*, 2009), and down-regulation of laminin in the BM (Oki *et al.*, 2004).

1.5 Autoimmune mechanisms in MS

The immunopathogenesis of MS is complex and involves a number of different immune cells, most notably T cells, B cells and macrophages (Frohman *et al.*, 2006). Until recently, MS was considered to be a T cell mediated disease (Sospedra and Martin 2008). However, the role of B cells in MS pathogenesis is becoming increasingly apparent. In particular, deposition of antibody and complement is observed in the most common pathological pattern of MS lesions as well as the presence of oligoclonal IgG bands on IEF of CSF (Lucchinetti *et al.*, 2000).

1.5.1 T cells in MS

CD4+ T cells reactive with epitopes of several myelin proteins, including MBP and other myelin antigens are found in the blood and CSF as well as in MS lesions (Frohman *et al.*, 2006; Chitnis 2007; Sospedra and Martin 2008). This involvement of the CD4+ T cell-mediated process is consistent with the association of genetic risk with MHC class II molecules, with many studies confirming that HLA class II genes confer the largest genetic risk factor for MS (see section 1.3.3). CD4+ T cell reactivity is restricted by MS-associated MHC class II molecules (Sospedra and Martin 2005). However, the antigen specificity of T cells in patients with MS is very similar to that of T cells from healthy individuals (Sospedra and Martin 2005). It is possible that the HLA

molecules associated with MS might contribute to T cell population expansion and antigenic spread because of preferential binding of certain myelin epitopes (McFarland and Martin 2007). This is supported by the substantial increase in the frequency of high-avidity CD4+ T cells which recognise myelin epitopes in patients with MS (Bielekova *et al.*, 2000).

CD8+ T cells are easily demonstrated in inflammatory lesions (Traugott *et al.*, 1983; Babbe *et al.*, 2000). CD8+ T cells are present at the lesion edge as well as in perivascular regions, whereas CD4+ T cells are generally only present at the lesion edge (McFarland and Martin 2007). In addition, a higher frequency of CD8+ T cells recognising myelin proteins in patients with MS than in healthy controls, has been reported (Crawford *et al.*, 2004). It is hypothesised that CD4+ T cells initiate the MS lesion, followed by the clonal expansion of CD8+ T cells, which amplify and mediate the damage. This is supported by a study which showed that CD8+ T cells can directly attach to and damage axons (Medana *et al.*, 2001).

1.5.2 B cells in MS

B cells are important in the pathogenesis of MS, as they: (1) act as APCs for the activation of encephalitogenic T cells and therefore influence their differentiation; (2) are a precursor of plasma cells that secrete autoreactive antibodies and (3) are able to produce cytokines that activate macrophages and stimulate further proliferation of immune cells (Antel and Bar-Or 2006; Racke 2008).

Evidence of B cell activity associated with MS was first observed in 1950 when intrathecal Ig synthesis was reported in patients with MS (Kabat *et al.*, 1950). These Igs are observed on IEF of CSF, whereby clear OCBs can be seen, and are observed in up to 90% of patients with definite MS, although are not specific for the disease (Compston and Coles 2002). Increased Ig levels in CSF in patients with MS is one of the important findings used in the diagnosis of MS (Berger and Reindl 2007; Weber and Hemmer 2010). The presence of OCBs are associated with a worse prognosis in patients than those without (Zeman *et al.*, 1996; Villar *et al.*, 2002). Furthermore, clonally expanded populations of memory B cells and plasma cells are found in MS lesions and in the CSF of MS patients with Serafini and colleagues being the first to report the formation of B-cell follicle-like structures in the brains of patients with MS (Zeman *et al.*, 1996; Baranzini *et al.*, 1999; Villar *et al.*, 2002; Hauser *et al.*, 2008).

The target antigen of these OCB antibodies has not yet been fully characterised, despite many attempts. Of the candidate autoantigens, MBP is the most extensively studied. MBP is one of the principal components of the myelin sheath and is the

second most abundant protein in the CNS (Boggs 2006). MOG is present on the outer layer of the myelin sheath and is thus more accessible to antibody binding (Brunner *et al.*, 1989). Both MBP and MOG can act as autoantigens to trigger an animal model of MS in rodents, experimental autoimmune encephalomyelitis (EAE) (Gold *et al.*, 2006). Antibodies specific for MOG are present in active demyelinating lesions (Genain *et al.*, 1999). In terms of MS, changes in the structure of myelin through postranslational modification (PTM) of its component proteins including MBP and MOG may play an important role in disease pathogenesis, through the generation of novel epitopes to which the immune system is no longer tolerant. Citrullination is one possible PTM which may be responsible for these changes to the structure of proteins in MS.

1.5.3 Peptidylarginine deiminases (PADs) and citrullination

Citrulline is a non-standard amino acid and proteins containing citrulline can only be generated by PTM of arginine residues, in a process called citrullination or deimination, in which the guanidino group of arginine is hydrolysed to a ureido group and ammonia, yielding a deiminated amino acid (citrulline) (Anzilotti *et al.*, 2010). This PTM is carried out by a family of five citrullinating enzymes known as peptidylarginine deiminases 1, 2, 3, 4 and 6 (PADs), first described in 1977, the genes of which are located at a single locus on chromosome 1 at position 1p35-36 in the human genome, and are highly conserved showing 59-71% sequence homology at the protein level (Rogers *et al.*, 1977; Vossenaar *et al.*, 2003; Chavanas *et al.*, 2004). PAD1 and PAD3 are the most closely related isozymes, with 68% sequence homology (Vossenaar *et al.*, 2003; Chavanas *et al.*, 2004). These isoenzymes show a high level of tissue specific expression and require higher calcium levels than are normally physiologically present, to be active (Takahara *et al.*, 1986; Vossenaar *et al.*, 2003). The result of this citrullination is a reduction in the net positive charge of the protein, which can have dramatic effects on protein folding and protein-protein interactions due to interruption in electrostatic interactions (Tarcza *et al.*, 1996).

PAD1 is mainly expressed in the epidermis and uterus (Terakawa *et al.*, 1991; Rus'd *et al.*, 1999), and is thought to play an important role in terminal differentiation of keratinocytes, as during this process both keratins and the keratin-associated protein, filaggrin, are citrullinated (Senshu *et al.*, 1996; Senshu *et al.*, 1999). However, the exact role of citrullination in this process remains to be elucidated. PAD2 is the most widely expressed PAD, and is expressed in skeletal muscle, brain, spleen, secretory glands and macrophages (Watanabe *et al.*, 1988; Akiyama *et al.*, 1990; Urano *et al.*, 1990; Vossenaar *et al.*, 2004). PAD2 is known to citrullinate both MBP in the CNS and vimentin in skeletal muscle and macrophages (Vossenaar *et al.*, 2004). PAD3 is

believed to play an important role in hair follicle formation due to its ability to deiminate trichohyalin, an abundant arginine-rich structural protein present in the inner root and medulla of hair follicles (Mechin *et al.*, 2007).

PAD4 is the best characterised isoenzyme, and has been shown to be important in a number of processes, most importantly transcriptional regulation of genes. PAD4 is the only isoenzyme to carry a functional nuclear localization signal which enables it to translocate from the cytoplasm to the nucleus, and has been shown to regulate chromatin structure and function through its ability to deiminate histone proteins, and therefore plays an important role in transcriptional regulation (Hagiwara *et al.*, 2002; Nakashima *et al.*, 2002; Cuthbert *et al.*, 2004; Wang *et al.*, 2004)

1.5.3.1 PADs and citrullination in MS

In MS, PAD2 and PAD4 are of greatest interest due to their localisation in the brain and in macrophages. A number of PAD substrates that may be important in MS have been identified. These include MBP, GFAP, a number of nuclear proteins and, most recently, members of the CXC chemokine family. Several studies have documented that MBP in CNS tissue of MS patients is more highly citrullinated compared with MBP from control subjects (Moscarello *et al.*, 1994; Wood *et al.*, 1996). For example, MBP isolated from the CNS of MS patients was found to be more highly citrullinated than MBP isolated from CNS tissue of adults without neurological disease, and was similar in the extent of citrullination to that observed in children aged less than 4 years, indicating a role for citrullination in the development of mature myelin (Moscarello *et al.*, 1994; Wood *et al.*, 1996). By using MBP isolated from NAWM of patients with MS and controls, post mortem, and fractionation of the samples by column chromatography, Moscarello *et al.* found that 18% of MBP was citrullinated in control tissue compared with 45% of MBP in patients with MS (Moscarello *et al.*, 1994). Further studies by the same group found that in Marburg's disease as much as 90% of MBP is citrullinated, demonstrating that almost all the MBP is citrullinated (Wood *et al.*, 1996). This study found that citrullinated MBP in both controls and patients with chronic MS contained six citrulline residues and 13 arginine residues, whereas citrullinated MBP in patients with Marburg disease contained 18 citrulline residues and only one arginine residue.

Using immunoslot blots with antibodies specific to PAD2 and PAD4, Wood *et al.* (2008) found that levels of both PAD2 and PAD4 in myelin isolated from the NAWM of seven patients with MS was significantly higher than levels observed in six control subjects. The same method was also applied using an F95 antibody, specific for citrullinated proteins, which showed increased citrulline in the myelin isolated from NAWM of these patients compared with control tissue (Wood *et al.*, 2008). In addition to this, the

authors were able to demonstrate that MBP is citrullinated *in vitro* in the presence of recombinant PAD2 and PAD4 through measuring the specific activities of these enzymes following the addition of increasing amount of unmodified MBP (Wood *et al.*, 2008). By using mass spectrometric analysis of intact human MBP and its citrullinated forms, it was demonstrated that PAD2 can citrullinate 18 out of 19 arginine residues, whereas PAD4 can only citrullinate 15 out of the 19 arginine residues present in MBP (Wood *et al.*, 2008) .

By subjecting homogenates of NAWM from 12 MS patients and normal white matter from three controls to immunoslot blots, and measuring PAD2 levels using anti-PAD2 antibody in both MS and control white matter, PAD2 in MS NAWM was found to be three-fold higher than in control subjects, with a two-fold increase in citrullination compared with control subjects (Mastronardi *et al.*, 2007). To determine whether the increase in citrullination was due to citrullination of MBP, western blot analysis was carried out using whole MBP extracted from white matter and antibodies against MBP and citrulline, which confirmed the increase was consistent with increased citrullination of MBP (Mastronardi *et al.*, 2007).

GFAP has now been identified as a second substrate of PADs and has been found to be citrullinated in higher amounts in the NAWM of patients with SPMS compared with equivalent control brain tissue (Nicholas *et al.*, 2004). Using antibodies against citrullinated proteins and GFAP together, and with the aid of confocal microscopy, Nicholas *et al.* 2004 found that tissue taken from the NAWM of three patients with SPMS was highly citrullinated compared with NAWM taken from three patients with other neurological diseases (ONDs), and that this citrullination was demonstrated to co-localize with GFAP.

By fractionation of NAWM from MS patients and controls into a membrane-containing fraction, non-microsomal fraction and a nuclear fraction, followed by quantitation of the amount of PAD 1-4 antibody binding, PAD4 was found to be elevated in NAWM from 17 patients with MS compared with nine control subjects (Mastronardi *et al.*, 2006). The nuclear fraction contained a 3.5-fold increase in the level of PAD1–4 in patients with MS compared with controls. Through western blot analysis, using anti-PAD4 antibody, this was attributable to increased PAD4 in the MS NAWM. Using an antibody against citrullinated proteins, this increase in PAD4 was found to be accompanied by an increase in citrullinated proteins in tissue taken from patients with MS, whereby strong nuclear labeling in NAWM from MS patients was observed compared with the controls (Mastronardi *et al.*, 2006). This increase in PAD4 was also accompanied by an increase in nuclear histone H3 citrullination, as demonstrated by staining MS and control tissue with an antibody against citrullinated protein, which revealed increased

nuclear staining of cells in the MS white matter compared with the control white matter (Mastronardi *et al.*, 2006). These findings were confirmed by western blot analysis, which showed a great abundance of citrullinated H3 in MS NAWM, with only traces in white matter from controls (Mastronardi *et al.*, 2006). This citrullination of histones greatly affects the chromatin structure and function, as deimination of arginine residues of histones decreases their positive charge, which compromises their ability to interact with DNA and possibly result in apoptosis of affected cells (Wang *et al.*, 2004; Moscarello *et al.*, 2007)

Excess citrullination has been reported in the CNS in postmortem MS brain tissue (Nicholas and Whitaker 2002; Mastronardi *et al.*, 2006). Recently, using proton MR spectroscopy, Oguz *et al.* (2009) found that citrulline peaks occurred more frequently in 27 patients with early-onset MS compared with 23 control cases. This further suggests a role for increased citrullination of myelin proteins in MS and, possibly, other demyelinating diseases.

Chemokines are the most recently described substrates of PAD. Chemokines are a family of secreted proteins that activate and attract leukocytes to sites of inflammation and have been demonstrated to play a role in the recruitment of leukocytes across the BBB in MS (Rot and von Andrian 2004; Charo and Ransohoff 2006). Proost *et al.* were the first to identify citrullination of the chemokine CXC ligand 8 (CXCL8), expressed by human peripheral blood mononuclear cells (PBMCs) (Proost *et al.*, 2008). Further chemokines have since been reported to be citrullinated, including CXCL10, CXCL11, CXCL12 and, most recently, Mortier *et al.* identified a further chemokine that is also citrullinated, CXCL5 (Loos *et al.*, 2008; Struyf *et al.*, 2009; Mortier *et al.*, 2010). All these chemokines have been previously reported to play a role in the migration of T cells and monocytes into the CNS (Loos *et al.*, 2008; Struyf *et al.*, 2009; Mortier *et al.*, 2010), as well as CXCL12 having a proposed role in engraftment of neural stem cells (Carbajal *et al.*, 2010). Thus, studies on citrullination of chemokines are highly relevant to understanding the pathogenesis of MS and other inflammatory neurological diseases. In general, the effect of citrullination of these chemokines leads to a decrease in their proteolytic cleavage, resulting in a reduction in their binding affinity and intracellular signaling through the corresponding chemokine receptor. The heparin-binding capacity of both citrullinated CXCL10 and CXCL11 are significantly reduced compared with their native form, and since sequestration of chemokines and the formation of a chemokine gradient is essential for inflammatory cell recruitment, reduced binding of the citrullinated forms to the glycosaminoglycan (GAG) in the extracellular matrix would also contribute to decreased inflammatory cell recruitment (Loos *et al.*, 2008). In functional *in vivo* and *in vitro* assays, citrullination of chemokines

led to decreased inflammatory cell migration when compared to the noncitrullinated proteins, suggesting that PAD enzymes play an anti-inflammatory role through citrullination of chemokines (Loos *et al.*, 2008; Proost *et al.*, 2008; Struyf *et al.*, 2009; Mortier *et al.*, 2010). Using freshly isolated monocytes and activated lymphocytes, Struyf *et al.* found that CXCL12–1Cit was significantly less chemotactic for both monocytes and lymphocytes, and that CXCL12–5Cit was inactive *in vitro* (Struyf *et al.*, 2009). The authors concluded that citrullination appears to reduce the activity of chemokines leading to downregulation of inflammation. Therefore, citrullination of chemokines may be a mechanism for resolution of inflammation. IFN-g-induced CXCL10 is expressed in actively demyelinating MS lesions, predominantly by macrophages within the plaque and by reactive astrocytes in the surrounding parenchyma and this promotes the recruitment of activated CD4+ T cells expressing CXCR3 across the BBB (Simpson *et al.*, 2000a; Simpson *et al.*, 2000b). Citrullination of locally expressed chemokines may therefore be an important mechanism to reduce further T-cell and monocyte migration into the CNS. Based on current findings, it appears that there may be many more CNS proteins that undergo citrullination in MS that have yet to be identified.

1.5.3.2 Citrullination and experimental autoimmune encephalomyelitis (EAE)

EAE has been widely used as an animal model for MS for many years. There are several variations of EAE induction by immunisation of the animal with either myelin proteins or by adoptive transfer of myelin-specific CD8+ T cells (Mix *et al.*, 2010). MBP and MOG as well as smaller encephalitogenic peptides of MBP, MOG and PLP can act as autoantigens to trigger EAE (Gold *et al.*, 2006; Mix *et al.*, 2010). Transgenic animal models of spontaneous demyelination have also been developed in an attempt to imitate MS without the bias of a specific peptide for induction (Mastronardi *et al.*, 1993; Ellmerich *et al.*, 2005; Pöllinger *et al.*, 2009; Mix *et al.*, 2010). Although EAE models do not directly mimic the complex pathogenesis of MS, their similarities have allowed the investigation of CNS inflammation and tests for potential MS therapies. There is now an emerging understanding of the role of protein deimination in the CNS derived from studies on EAE models of MS.

Using antibodies against citrullinated proteins, MBP and GFAP, it has been demonstrated that citrullinated proteins are present in both the brain and spinal cord of mice with MOG-induced EAE, and that citrullination co-localises with both MBP and GFAP, indicating both oligodendrocytes and astrocytes as cell types with citrullinated proteins (Nicholas *et al.*, 2005). Raijmakers *et al.* 2005 were the first to report hypercitrullination of CNS proteins in PLP-induced EAE. This study found that during

development of EAE in mice, citrullination of proteins occurred in the spinal cord and correlated with areas of demyelination. The amount of citrullinated proteins was highest in the relapse phase of EAE, compared with acute-phase EAE, which was thought to be due to remyelination attempts, as increased citrullination is associated with myelination during development of the CNS (Cao *et al.*, 1999). By using specific antibodies, the citrullinated proteins were identified as MBP and GFAP. Using immunoblotting of spinal cord tissue, it was determined that this increase in citrullination was not due to an increase in the levels of PAD2 and PAD4. No citrullination was found in control mice (Rajmakers *et al.*, 2005). Based on this, the authors concluded that the hypercitrullination observed in EAE must be mediated by activating PAD2 and PAD4 already present in the CNS rather than *de novo* synthesis of the enzymes. In a study by Nicholas *et al.* 2005, GFAP was found to be citrullinated in higher amounts in the CNS of animals with EAE compared with equivalent control brain tissue (Nicholas *et al.*, 2005).

Musse *et al.* (2008) investigated the role of PAD2 in demyelinating disease, by developing transgenic mice overexpressing *PAD2*. These mice displayed a more severe clinical disease course than spontaneously demyelinating transgenic mice, with clinical symptoms presenting at 6 weeks compared with 3 months. Levels of PAD2 were compared with control mice, with PAD2 transgenic mice showing significantly increased PAD2 activity at 2 months of age, along with an approximately 2.5-fold increase in citrullinated MBP at 3 months of age. Histochemical staining with Luxol fast blue of the optic nerve of these mice showed areas of myelin breakdown, along with a reduction in myelin. All these changes were more pronounced in homozygous mice possessing 30 copies of the cDNA encoding the *PAD2* gene, compared with the heterozygotes possessing only 15 copies of this gene. *PAD2* mRNA levels showed similar changes with a four-fold increase in *PAD2* mRNA in transgenic compared with non-transgenic mice, which increased to 5.3-fold in homozygous *PAD2* transgenic mice. In addition, when assessing MBP isolated from PAD2 knockout mice, the authors demonstrated the ability of PAD4 to citrullinate MBP in the absence of PAD2 (Musse *et al.*, 2008).

1.5.3.3 Proteolytic enzyme action on citrullinated MBP

Since citrullination alters the charge of the protein, as for each arginine converted to citrulline there is a loss of one positive charge, MBP becomes partially unfolded and its interaction with phospholipids is weakened following citrullination, therefore the myelin sheaths formed are not as tightly packed as in normal myelin (Beniac *et al.*, 2000). Citrullination of MBP increases its susceptibility to degradation by proteinases, which

are reported to be elevated in the CNS in MS, in particular around active plaques and in the CSF (Einstein *et al.*, 1972; Cuzner and Davison 1973; Richards and Cuzner 1978). Macrophages and reactive astrocytes have been previously demonstrated to produce the proteinase cathepsin D (Prineas and Wright 1978; Allen and McKeown 1979). Studies carried out by Cao *et al.* (1999) showed that MBP-C6, the citrullinated isomer of MBP, which contains six citrulline residues, is digested four-times faster by cathepsin D than the unmodified form of MBP, and 35-times faster in MBP-C18, which contains 18 citrulline residues, releasing numerous peptides through cleavage at the Phe–Phe linkages in the MBP protein. The peptides generated by cathepsin D cleavage, which contain the immunodominant epitopes of MBP, have been detected in the CSF of patients with MS (Whitaker 1977; Whitaker and Granum 1980). By incubating various MBP species, containing different amounts of citrulline per mole of MBP, with cathepsin D, Pritzker and colleagues (2000) were able to demonstrate that the MBP species containing the greatest amount of citrulline per mole of MBP were digested at a much faster rate, as determined by mass spectrometric analysis of MBP peptides following digestion (Pritzker *et al.*, 2000).

In addition, using a 3D-atomic structure model of human MBP, the authors were also able to test the effects of deimination of specific arginine residues to citrulline residues and found that the molecule became significantly more extended and open in structure the more citrullinated it was (Pritzker *et al.*, 2000). Following this study, the authors concluded that this more open structure would allow cathepsin D better access to Phe–Phe linkages in MBP, which would account for the increased digestion of citrullinated MBP.

Using Cys scanning, spin labeling, electron paramagnetic resonance spectroscopy and site-specific proteolysis, Musse *et al.* (2006) were able to demonstrate that in the membrane-bound state the primary immunodominant epitope, V83-Y92, of recombinant murine MBP-C6 is more highly surface exposed than unmodified recombinant murine MBP. In addition, in the presence of cathepsin D, the recombinant murine MBP-C6 demonstrated enhanced proteolysis. These results suggest that citrullination of MBP not only impedes membrane adhesion and assembly activity of this protein into myelin, but also exposes an immunodominant epitope in the membrane-bound protein to proteases. From this study, the authors concluded that greater surface exposure and greater cleavage of the citrullinated protein by enzymes would lead to increased release of the immunodominant epitope, which could prime the innate immune-derived cells of the CNS and sensitize peripheral T cells (Musse *et al.*, 2006; Musse and Harauz 2007).

1.5.3.4 Regulation of PAD and citrullination

It is not yet known whether excess citrullination is a primary or secondary event to the inflammatory process in MS, or whether the regulation of PAD isoforms may be part of the genetic susceptibility to MS. Single nucleotide polymorphisms in the *PAD4* gene, associated with the autoimmune disease RA, increase mRNA stability, suggesting that this could result in more PAD4 protein expression and, therefore, increased citrullination of proteins (Suzuki *et al.*, 2003). Increased PAD2 protein expression in human astrocytes *in vitro* has also been reported in response to increased intracellular calcium levels when cells were subjected to elevated pressure and in response to hypoxia (Sambandam *et al.*, 2004; Bhattacharya *et al.*, 2006a; Bhattacharya *et al.*, 2006b). A number of pathological processes, including excitotoxicity, occur in the CNS in MS, which would lead to raised intracellular calcium ions in neurons and glia (Shideman 2006; Smith 2007). Large numbers of activated macrophages are present in inflammatory demyelinating sites within MS lesions as well as activated microglia. Since these cells contain PAD enzymes and there is increased cell death owing to raised intracellular calcium ions, this would lead to activation of PAD enzymes when released from dying cells (Bhattacharya *et al.*, 2006a). Thus, myelin proteins may be citrullinated both intracellularly, during myelin degradation following phagocytosis, as well as extracellularly, following release of PAD enzymes from dying cells. In addition, significant hypomethylation of the *PAD2* promoter has also been found to occur in MS NAWM compared with controls, which may lead to increased PAD2 expression and subsequent increase in citrullination, as hypomethylation leads to increased gene transcription (Mastronardi *et al.*, 2007).

PAD enzymes are dependent on the presence of calcium. X-ray crystallographic structural analysis of human PAD4 in calcium-free and calcium-bound forms, suggests that binding of calcium to the C-terminal domain is critical for both substrate specificity and binding (Arita *et al.*, 2003; Arita *et al.*, 2004). The binding of calcium to PAD4 leads to conformational changes around the substrate binding site, which then allows PAD4 to interact with arginine residues in other proteins (Arita *et al.*, 2004). Only the crystal structure of PAD4 has been elucidated as yet, however, due to human PAD4 and PAD2 showing more than 50% sequence homology, it is assumed that PAD2 will have a similar crystal structure and mechanism for activity (Vossenaar *et al.*, 2003). In the absence of high levels of intracellular calcium, PAD2 would not undergo these conformational changes which are essential for activation of the enzyme.

The cytosolic and nucleoplasmic calcium concentration is much too low (approximately 100-fold) for PAD activity under normal physiological conditions (Takahara *et al.*,

1986). However, there are numerous events which can lead to raised intracellular calcium. For example during cell death the integrity of the plasma membrane is lost (Schwab *et al.*, 2002; Tombal *et al.*, 2002), causing influx of calcium from the extracellular space and subsequent activation of intracellular PAD (Asaga *et al.*, 1998; Hagiwara *et al.*, 2002; Nakashima *et al.*, 2002; Vossenaar *et al.*, 2004). Artificially raising the cytosolic and nucleoplasmic calcium concentration by including calcium ionophores in the media of the cells should induce activation of PAD and subsequent citrullination of intracellular proteins (Vossenaar *et al.*, 2003).

1.5.3.5 Citrullination in rheumatoid arthritis (RA)

RA is a common autoimmune disease characterised by chronic inflammation of the synovial joints, which leads to destruction of the joints (van Venrooij *et al.*, 2011). Antibodies to citrullinated proteins have been reported in RA, since the 1960s (Nienhuis *et al.*, 1964). Since this discovery multiple citrullinated protein targets have been identified that are specific to RA-related autoimmunity, including vimentin, fibronectin and filaggrin amongst others (Klareskog *et al.*, 2008). Testing of ACPAs in individuals with RA is now one of the prime biomarkers used in the diagnosis of RA (Whiting *et al.*, 2010). Furthermore, the detection of ACPAs in the sera of a blood donor may indicate that this individual will develop RA in later life (Rantapää-Dahlqvist *et al.*, 2003; Jørgensen *et al.*, 2008). The detection of ACPA production also precedes the initial inflammatory cytokine response seen in pre-morbid RA patient sera by several years (Jørgensen *et al.*, 2008). It is also associated with a more destructive erosive form of the disease (van der Linden *et al.*, 2009).

The conversion of arginine to citrulline has been shown to enable a high-affinity peptide interaction with the RA-associated HLA-DRB1*0401 MHC class II molecule (Hill *et al.*, 2003). In this study Hill *et al.* (2003) demonstrated that converting arginine to citrulline significantly increases the vimentin-MHC affinity, leading to the activation of CD4⁺ T cells in HLA-DRB1*0401 transgenic mice. Unmodified vimentin did not induce T cell activation; however, citrullinated vimentin stimulated a strong proliferative response followed by the production of IFN- γ , showing that citrullination is required in order to elicit a CD4⁺ T cell response to vimentin in these transgenic mice. Furthermore, genetic susceptibility to RA is associated with MHC class II molecules that contain an amino acid motif known as the shared epitope (Gregersen *et al.*, 2005). Competition assays showed that the citrulline-containing vimentin bound with higher affinity to MHC class II molecules that contained this shared epitope compared to uncitrullinated vimentin. The authors concluded that this novel peptide-MHC interaction is dependent on both citrullination and a shared RA epitope (Hill *et al.*, 2003).

Following on from the above study, James *et al* (2010) were able to show that binding of arginine-substituted peptides to another RA-associated HLA-DRB1*1001 MHC class II molecule blocked peptide binding, suggesting that arginine is not accepted within the binding pockets of HLA-DRB1*1001. However, peptides with single citrulline substitutions bound to recombinant HLA-DRB1*1001 were accepted within the binding pocket, which was significantly enhanced by further citrulline substitutions (James *et al.*, 2010). Unmodified and citrullinated joint-associated peptide sequences were synthesised and used to stimulate CD4⁺ T cells from RA patients and controls. Three of these sequences elicited CD4⁺ T cell responses. T cell clones specific for these sequences only proliferated in response to citrullinated peptides and not unmodified peptides. The author concluded this generation of “altered-self” peptides suggests that citrullination must be an important factor in the initiation or progression of RA (James *et al.*, 2010).

1.5.3.6 Citrullination in other neurological diseases (ONDs)

Citrullination has also been shown to occur in ONDs including AD, PD and sporadic Creutzfeldt-Jakob disease (sCJD) (Ishigami and Maruyama 2010; Jang *et al.*, 2010; Nicholas 2011). AD is the most common neurodegenerative disease, leading to progressive dementia. Ishigami *et al.* (2005) showed, using western blot analysis with an anti-modified citrulline antibody, the presence of multiple citrullinated proteins in post-mortem hippocampal brain tissue from ten AD cases, whereas no citrullinated proteins were found in age-matched controls. Two-dimensional gel electrophoresis (2-DE) and subsequent MALDI-TOF mass spectrometry identified two of these proteins as vimentin and GFAP. Using immunohistochemistry citrullinated proteins were observed throughout the hippocampus in these AD cases with no citrullinated proteins detected in age-matched controls. PAD2 immunoreactivity was observed throughout both the AD and control hippocampal areas, although PAD2 enrichment did coincide with areas of positive citrullinated proteins. Dual immunofluorescence staining revealed that citrullinated proteins and PAD2 co-localised with GFAP-positive astrocytes. The authors of this study concluded that these results suggest a role for PAD and citrullination in AD (Ishigami *et al.*, 2005). Furthermore, Satoh *et al.* (2010) more recently showed the presence of serum ACPAs in eight out of forty-two patients with AD, using a commercially available enzyme-linked immunosorbent assay (ELISA) containing artificially engineered cyclic citrullinated peptides optimised for use in detecting RA-specific ACPAs, further implicating a role for citrullination in the pathogenesis of this disease (Satoh *et al.*, 2010).

PD is a neurodegenerative disease, characterised by a slow and progressive degeneration of dopaminergic neurons in the substantia nigra (SN) (Hirsch and Hunot 2009). Nicholas (2011) recently showed using dual immunofluorescence and an established monoclonal antibody against peptidyl-citrulline moieties, the presence of citrullinated proteins co-localised with GFAP-positive astrocytes in the SN of post-mortem brain tissue from five PD cases and five age-matched controls. Interestingly, this same study showed that citrullinated proteins co-localised to the cytoplasm of neurons in the SN of brain tissue from these PD cases, whereas none of the neurons from control SN brain tissue expressed citrullinated proteins (Nicholas 2011). The significance of these findings are not yet known, however the author of this study concluded that the results indicate that citrullination may be involved in the pathogenesis of PD.

Prion diseases are a group of progressive neurodegenerative diseases that affect the CNS in humans and animals, with sCJD accounting for approximately 85% of human prion cases (Jang *et al.*, 2010). Using western blot analysis Jang *et al.* (2010) showed that the expression of PAD2 was significantly increased in the frontal cortex of post-mortem tissue from four sCJD cases compared to four controls. Furthermore, immunohistochemistry revealed increased immunoreactivity of PAD2 in the brains of sCJD compared to controls, and was co-localised to reactive GFAP-positive astrocytes. PAD2 activity was also shown to be significantly elevated by 3.1-fold in sCJD brains compared to control brains. Western blot analysis also showed a significant increase in citrullinated proteins in sCJD compared to control brains, with immunohistochemistry showing the co-localisation of PAD2 and citrullinated proteins with GFAP-positive astrocytes. Lastly, a number of citrullinated proteins were identified using 2-DE and MALDI-TOF, including vimentin, GFAP and enolase (Jang *et al.*, 2010).

1.5.4 Hypothesis

An increase in intracellular calcium levels in the CNS during inflammation and/or polymorphisms in the PAD2 or 4 genes, leads to increased citrullination of MBP and other CNS proteins by PAD enzymes in MS. This could directly lead to demyelination through affecting the structural conformation of the myelin sheath. Secondary to this, citrullination of CNS proteins by PADs could also result in the generation of novel epitopes, to which the immune system is not tolerised. This could result in an autoantibody response against self proteins, leading to demyelination. The resultant antibody response to citrullinated proteins could be a useful diagnostic indicator of MS.

1.5.5 Aim of the thesis

To determine the role of PADs and citrullination in the pathogenesis of MS.

1.5.6 Objectives of the thesis

1. To compare PAD2 and PAD4 expression by cells of the CNS *in vitro* and determine factors involved in their modulation.
2. To determine cell types expressing PAD2 and PAD4 in the CNS *in vivo* in control white matter, MS NAWM and MS lesional brain tissue, and determine the distribution of citrullinated proteins.
3. To identify, using mass spectrometry, citrullinated proteins in MS lesional brain tissue.
4. To develop an ELISA method for the detection of ACPA in MS serum or CSF, specifically targeted to citrullinated MBP, and or other citrullinated proteins isolated above using mass spectrometry.
5. To examine ACPA antibodies in paired serum and CSF samples from MS, ONDs and controls, using the above ELISA techniques, and from this determine whether antibody levels correlate with the diagnosis of MS on clinical and CSF criteria.

Chapter 2

***In vitro* investigation of the effects of
pro-inflammatory cytokines on the
expression of PAD2 and PAD4**

2.1 Introduction

Although increases in PAD expression and the subsequent increase in citrullination are implicated in the pathogenesis of MS, little is known about the regulation of these enzymes during inflammation. It is well-reported that a number of pro-inflammatory cytokines are up-regulated in MS, particularly in and around lesions. Therefore, the effect of a number of pro-inflammatory cytokines implicated in MS pathogenesis on the modulation of PAD2 and PAD4 were investigated as these may be important regulators of PAD gene expression.

IL-1 β is predominantly produced by monocytes and macrophages but is also produced by brain endothelial cells, B cells and activated T cells (Corsini *et al.*, 1996), and has been found to be increased in the CSF of MS patients with active disease (Hauser *et al.*, 1990). In MS lesions there is increased expression of IL-1 β (Cannella and Raine 1995) and it is also up-regulated in the CNS during the induction of EAE (Kennedy *et al.*, 1992; Bauer *et al.*, 1993). TNF- α is produced by a number of cells including monocytes, macrophages, NK cells, astrocytes and microglia (Imitola *et al.*, 2005). Expression of TNF- α in the CNS is up-regulated in MS lesions (Cannella and Raine 1995; Algeciras *et al.*, 2008), and it is expressed by macrophages, microglia, and astrocytes within the MS plaque border in chronic active MS lesions (Hofman *et al.*, 1989; Selmaj *et al.*, 1991; Cannella and Raine 1995). TNF- α is also expressed by leukocytes within the perivascular cuff (Merrill 1992; Woodroffe and Cuzner 1993). An increased expression of TNF- α in the CSF of patients with active disease and in progressive forms of the disease compared to stable MS has been reported (Hauser *et al.*, 1990; Sharief and Hentges 1991).

IL-6 is synthesised by various cells including macrophages, T cells, astrocytes and microglia (Imitola *et al.*, 2005). In MS, the highest numbers of IL-6 expressing cells are found in inactive demyelinated lesions (Schönrock *et al.*, 2000), with IL-6 expression also reported in the cells of perivascular cuffs (Woodroffe and Cuzner 1993). IFN- γ , which is produced by activated T lymphocytes and NK cells (Ali Shokrgozar *et al.*, 2009), has been found to be increased in patient plasma preceding relapse (Beck *et al.*, 1988; Lu *et al.*, 1993) and has an activating role in sustaining inflammation in MS (Hofstetter *et al.*, 2006). It has also been found within the cells of the inflammatory cuffs in post-mortem MS CNS tissue (Woodroffe and Cuzner 1993; Simpson *et al.*, 2000b). IFN- γ levels are significantly higher in clinically isolated syndrome (CIS) patients in the acute phase and during relapses in RRMS (Frisullo *et al.*, 2008). IFN- γ is expressed in the CNS at the onset of EAE and increases during peak disease and decreases during remission (Issazadeh *et al.*, 1995; Begolka and Miller 1998).

Dysregulation of cytokine expression in MS is not restricted to pro-inflammatory mediators but is also observed in anti-inflammatory cytokines. IL-4 is produced by T cells and increased expression is found in both acute and chronic MS lesions (Cannella and Raine 1995). IL-10 is produced by monocytes, macrophages, B and T cells (Imitola *et al.*, 2005). Peripheral blood mononuclear cells (PBMCs) from patients with RRMS have decreased levels of IL-10 mRNA prior to the onset of an exacerbation (Rieckmann *et al.*, 1994). Levels of IL-10 mRNA are significantly lower in PBMCs from patients with SPMS compared to RRMS; however levels of IL-10 mRNA in RRMS decrease significantly six weeks prior to a clinical relapse (Van Boxel-Dezaire *et al.*, 1999).

TGF- β is produced by T cells, and has been shown to be significantly down-regulated in lymphocytes of MS patients with clinically active disease compared to stable MS (Mokhtarian *et al.*, 1994) and has been observed in microglia within the plaque edge of acute active lesions (Peress *et al.*, 1996) and surrounding the blood vessels within the extracellular matrix (ECM) of acute lesions (Cannella and Raine 1995). TGF- β mRNA in PBMCs of RRMS patients is significantly down-regulated compared to control PBMCs (Rieckmann *et al.*, 1994). Increased expression of TGF- β is also associated with the recovery phase in EAE (Iwahashi *et al.*, 1997).

This chapter describes the investigation of the *in vitro* effects of four pro-inflammatory cytokines (IL-1 β , TNF- α , IL-6 and IFN- γ) which, as outlined above, are up-regulated in MS, on the modulation of PAD2 and PAD4 gene expression in an astrocytoma cell line (U373-MG), three preparations of primary human astrocytes (MS16, EP14, EP15), a human foetal microglial cell line (CHME3), and a human brain endothelial cell line (hCMEC/D3). Initial experiments were undertaken to determine any effects of these cytokines on cell viability. In addition, the *in vitro* effects of three anti-inflammatory cytokines, IL-4, IL-10 and TGF- β , which have differential expression in MS, on the proliferative capacity of a human foetal microglial cell line (CHME3), and modulation of PAD2 gene expression was also investigated.

2.1.4 Aim of the study

To determine the gene expression of PAD2 and 4, their modulation and the subcellular localisations of PAD2 and PAD4 proteins.

2.1.5 Objectives of the study

1. Optimise the method of quantitative real-time polymerase chain reaction (qPCR) for the detection of PAD2 and PAD4 gene expression.
2. Determine the modulating effect of cytokine treatment on gene expression of PAD2 and PAD4 in all cell lines utilised in this study and assess the effect of single and co-treatment of cells with cytokines on proliferation or cell death.
3. Determine the subcellular localisation and distribution of PAD2 and PAD4.

2.2 Materials and methods

2.2.1 Suppliers used in this chapter

Abcam, 330 Cambridge Science Park, Cambridge, CB4 0FL, UK; **Bioline UK Ltd**, 16 The Edge Business Centre, Humber Rd., London, NW2 6EW; **Applied Biosystems**, Lingley House, 120 Birchwood Boulevard, Warrington, WA3 7QH, UK; **Fisher Scientific Inc**, Bishop Meadow Rd., Loughborough, Leicestershire, LE11 5RG, UK; **Invitrogen**, 3 Fountain Drive, Inchinnan Business Park, Paisley, PA4 9RF, UK; **Lonza**, Muenchensteinerstrasser 38, CH – 4002, Basel, Switzerland; Millipore, Suite 3 & 5, Building 6, Croxley Green Business Park, Watford, WD18 8YH, UK; **MWG-Biotech Ltd**, Mill Cart, Featherstone Rd., Wolverton Mill South, Milton Keynes, MK6 5RD; **NUNC**, supplied through Fisher Scientific Inc; **Peptotech EC Ltd**, Peptotech House, 29 Margravine Rd., London, W6 8LL, UK; **Sigma-Aldrich**, The Old Brickyard, New Rd., Gillingham, Dorset, SP8 4XT, UK; **Vector Laboratories Ltd.**, 3 Accent Park, Bakewell Road, Orton Southgate, Peterborough, PE2 6XS, U.K; **VWR International**, Hunter Boulevard, Magna Park, Lutterworth, Leicestershire, LE17 4XN, UK.

2.2.2 Cell culture

The culture of mammalian cells *in vitro* is a technique which enables the investigation of specific cell behavior under particular conditions. An example of this is the treatment of cells with cytokines or drugs, and the effect of this on specific gene or protein expression within the treated cells compared to untreated cells. Mammalian cells are broadly grouped into two categories: primary and secondary cultures.

Primary cultures are cells that are taken directly from living tissues, such as biopsy material, and established for growth *in vitro*. These cells are more heterogeneous and have undergone very few population doublings and are therefore more representative of the true *in vivo* state of the tissue of origin. However, these primary cells can only be used for a limited number of passages (sub-culture) before dying.

Secondary cultures or cell lines are cells that are immortalised. Although these cells are not as representative of normal tissue as primary cells they are useful in producing reproducible data due to the fact that these cultures contain a more homogenous population of cells.

CNS tumour cells such as glioma cell lines used here are transformed cells which grow and divide indefinitely in culture.

2.2.2.1 Collagen coating

For culture of hCMEC/D3 cell line, plasticware was coated with collagen type I from rat tail (3.41 mg/mL) (VWR, UK), which was diluted 1:30 in autoclaved distilled H₂O (dH₂O). Prior to use, the collagen solution was filtered through a 0.2 µm filter. Enough collagen solution was added to cover the bottom of a flask or a plate, and then incubated at 37°C for 1 hr. Following this, the excess collagen was removed and hCMEC/D3 cells were seeded.

2.2.2.2 Recovery of cryofrozen cells

Cells were stored long-term in 10% v/v dimethyl sulphoxide (DMSO) (Sigma, UK) in liquid nitrogen, until required for experimental work. Vials containing 1 mL of 1 x 10⁶ cells were removed from liquid nitrogen and placed in a 37°C incubator for 1-2 minutes to thaw. Following this, the contents of the vials were transferred into T25 flasks containing 9 mL of the appropriate, pre-warmed, complete cell culture medium and placed in a humidified incubator at 37°C containing 95% air and 5% CO₂. The following day, cells had adhered to the bottom of the flask and medium was replaced.

2.2.2.3 Cell harvesting and serial passage of cells

A number of different primary and secondary cell lines were used for this study with specific media requirements (see table 2.1). Primary adult human astrocytes were isolated from either CNS NAWM obtained at autopsy from UK MS Society Tissue Bank (donor labelled MS16) or from normal tissue taken during temporal lobectomy resections for treatment of epilepsy at King's College Hospital (KCH, London; donor labelled either EP14 or EP15) (MS16, EP14 and EP15 were a kind gift from Dr I. Romero, Open University UK). The human foetal microglia cell line, CHME3, was obtained following transfection of human foetal-brain derived macrophages with a plasmid encoding for the large T antigen of SV40 (Janabi *et al.*, 1995) (a kind gift from Prof. M. Tardieu, Faculté de Médecine Paris-Sud, France). The human brain endothelial cell line, hCMEC/D3, is a parent cell line obtained following lentiviral infection of pre-confluent human brain endothelial cells (Weksler *et al.*, 2005).

Briefly, cells were cultured as monolayers in either 25cm² or 75cm² filter-cap flasks (Falcon, UK) containing specified media and kept in a humidified incubator at 37°C containing 95% air and 5% CO₂. Cell media was changed twice weekly and cells were passaged when 80~90% confluent. Cells were passaged by aspirating medium from the flasks and washing twice with 5 mL or 10 mL (for T25 or T75, respectively) of Dulbecco's phosphate buffered saline (DPBS) without calcium and magnesium to

remove remaining media. This was then followed by the addition of 3-5 mL of 0.5% trypsin and 0.2% ethylenediaminetetraacetic acid (EDTA) solution (Sigma-Aldrich, UK) and incubation for 5 minutes in a humidified incubator at 37°C containing 95% air and 5% CO₂ to remove cells from the bottom of the flask. Trypsinisation was then stopped by neutralising trypsin/EDTA with 3-5 mL complete media, which was mixed with the cell suspension by gentle pipetting and then transferred to a sterile 15 mL centrifuge tube. Suspended cells were then centrifuged at 1000 rpm to pellet the cells, and the supernatant was aspirated to remove the trypsin/EDTA containing medium.

The cell pellet was then re-suspended in a known volume of fresh pre-warmed culture medium, and cells counted (see section 2.2.2.4) if required for experimental purposes, or suspended in the appropriate amount of complete media and seeded at a 1:6 split ratio to further propagate cells. Primary cells and cell lines were used between passages 5 and 8, except for U373-MG and hCMEC/D3 cell lines.

2.2.2.4 Cell counting

Cells were counted by removing 10 µL of cell suspension and adding to 10 µL of 0.4% Trypan blue, and mixed thoroughly. Trypan blue stain is based on the principle that live (viable) cells do not take up certain dyes, whereas dead (non-viable) cells do, as the dye can enter into cells with compromised membranes and is the method used with the Countess® automated cell counting platform (Invitrogen, UK). 10 µL of this mixture was then transferred onto a cell counting chamber slide and inserted into the Countess® Automated Cell Counter (<http://www.invitrogen.com/1/1/1306-trypan-blue-stain-0-4-use-the-countess-automated-cell-counter.html>). The automated cell counter then counts the number of cells in total, the number of live cells/mL and the number of dead cells/mL. The number of live cells/mL is then used to calculate the amount of media to add to the cells to make the appropriate cell concentration for each experiment.

2.2.2.5 Reconstitution of cytokines

Recombinant cytokines IL-1β (10 µg), TNF-α (50 µg), IL-6 (20 µg), IFN-γ (100 µg), IL-4 (20 µg), IL-10 (10 µg) and TGF-β (5 µg) (all from Peprotech, UK) were reconstituted from lyophilised powder in 100 µL, 500 µL, 200 µL, 1000 µL, 200 µL, 100 µL and 50 µL PBS, respectively, to give final stock concentrations of 100 µg/mL. These stock solutions of cytokines were stored in 20 µL aliquots at -20°C until required for further dilution on the day of experiments.

Table 2.1: Human primary and secondary cell lines used in this study and their culture medium composition.

Cell	Cell type	Origin	Source	Culture medium composition
U373-MG	Astrocytoma cell line	Human 61 year-old Caucasian male	European Collection of Cell Cultures (ECACC), UK	500 mL MEM 10% (v/v) HI FCS (Invitrogen, UK) 1% (v/v) Penicillin/streptomycin (100 U/mL/ 50 µg/mL) 1% (v/v) L-Glutamine (2 mM) 1% (v/v) Sodium pyruvate (1 mM) (Sigma- Aldrich, UK) 1% (v/v) Non-essential amino acids (Sigma-Aldrich, UK)
MS16 EP14 EP15	Primary human astrocytes	Human	Dr. I. A. Romero, Open University, Milton Keynes, UK	250 mL MEM- α , high glucose, Glutamax (Invitrogen, UK) 250 mL F-10 Hams (Invitrogen, UK) 10% (v/v) HI FCS (Invitrogen, UK) 1% (v/v) Human AB serum (Sigma Aldrich, UK) 1% (v/v) Penicillin/streptomycin (100 U/mL/ 50 µg/mL) (Invitrogen, UK) 1% (v/v) Fungizone (Invitrogen, UK)

Key: HI FCS; heat inactivated foetal calf serum, MEM; Minimal essential medium.

Table 2.1 (continued): Human primary and secondary cell lines used in this study and their complete culture medium composition.

Cell	Cell type	Origin	Obtained from	Culture medium composition
CHME3	Microglial cell line	Human foetal	Prof. M. Tardieu, Faculté de Médecine Paris-Sud, France	500 mL DMEM, high glucose, Glutamax (Invitrogen, UK) 10% (v/v) HI FCS (Invitrogen, UK) 1% (v/v) Penicillin/streptomycin (100 U/ML/100 µg/mL) (Invitrogen, UK) 1% (v/v) Fungizone (Invitrogen, UK)
hCMEC/D3	Brain endothelial cell line	Human	Dr. I. A. Romero, Open University, Milton Keynes, UK	500 mL EGM-2 supplemented with hydrocortisone, EGF vascular, gentamycin, ascorbic acid, human EGF, long R Insulin-GF, heparin, and human FGF-β (Lonza, UK) Penicillin/Streptomycin (Invitrogen, UK) 2% HI FCS (Invitrogen, UK)

Key: DMEM; Dulbecco's modified Eagle's medium, EGF; endothelial growth factor, EGM; endothelial growth media, FGF; fibroblast growth factor, GF; growth factor.

2.2.2.6 Cytokine treatment of cells

For qPCR analysis, cells were seeded into 24-well plates at a density of 1×10^5 cells per well, in 1 mL of complete media and left to adhere to the plate for 24 hours in a humidified incubator prior to treatment with cytokines. Following this, media was aspirated from the wells, and cells washed twice with DPBS to ensure no serum remained, as this could influence the results of the cytokine treatments. Subsequently, cells were treated in triplicate with serum free media (containing no FCS or human AB serum) containing 0, 1, 10 and 100 ng/mL of IL-1 β , TNF- α , IL-6 and IFN- γ , respectively, for 24 hours in a humidified incubator.

Following this, media was aspirated from the untreated and treated cells and plates washed twice with DPBS. 0.33 mL Tri Reagent (Sigma Aldrich, UK) was added to each well of the treated and untreated cells and the triplicate samples were pooled. Total RNA was extracted from each cell lysate sample according to the manufacturers' instructions (see section 2.2.3.1). Three independent experiments were performed and in each experiment, treatments were carried out in triplicate to allow statistical analysis to be performed.

2.2.2.7 Cell viability and proliferation assay

When examining the effects of specific conditions on the behavior of mammalian cells *in vitro*, it is vital to determine if these conditions are having an effect on cell viability and proliferation. This can be determined through the use of a colourimetric MTS ([3-(4,5-dimethylthiazol-2-yl)-5-(3-carboxymethoxyphenyl)-2-(4-sulfophenyl)-2H-tetrazolium) assay, whereby MTS is bio-reduced by viable cells into a formazan product which is soluble in culture medium. The absorbance of the formazan product can then be measured directly enabling fold-change in cell numbers to be determined.

Cellular proliferation was determined using the MTS based assay (Figure 2.1) according to the manufacturers' instructions (Promega, UK). MTS along with an electron coupling reagent, phenazine methosulphate (PMS), is bio-reduced by dehydrogenase enzymes found in metabolically active cells to a formazan product. The absorbance of the formazan product at 490 nm is directly proportional to the number of living cells in culture.

Using the Cell Titer 96® Aqueous Cell Viability kit (Promega, UK), which is an MTS-based assay, cells were assessed for viability following treatment with pro-inflammatory cytokines. Briefly, cells were seeded into 96-well plates at a density of 2.5×10^4 cells per well in 100 μ L complete media and left to adhere to the plate for 24 hours in a

humidified incubator. Medium was then aspirated from the well, and cells were washed twice with 100 μ L DPBS. Following this, cells were treated in triplicate with cytokines, 100 μ L per well, (see section 2.2.2.6) and left in a humidified incubator for 24 hours.

20 μ L of MTS/ phenazine methosulphate (PMS) solution (1 mL of PMS solution in 20 mL of MTS solution) was aseptically added to triplicate wells of the experimental samples. The plate was then incubated in a humidified incubator, and absorbance of the wells were measured at 490 nm using a Wallac Victor² plate reader spectrophotometer every hour between 1 and 4 hours. Following optimisation, readings were taken at 2 hours, as this was determined to be when maximal reaction had occurred. These absorbance readings were then used in order to calculate fold-change in cell number following treatment with varying concentrations (1, 10 and 100 ng/mL) of cytokines IL-1 β , TNF- α , IL-6 and IFN- γ , compared with untreated cells. Three independent experiments were performed.

2.2.3 The principles of standard polymerase chain reaction (PCR) and quantitative real-time PCR (qPCR)

Quantitative real-time polymerase chain reaction (qPCR) is widely used in gene expression studies in order to detect and quantify particular genes of interest, and is an improvement from traditional PCR. Prior to PCR, mRNA is converted to complementary DNA (cDNA) through the action of the enzyme reverse transcriptase, which elongates and copies the single-strand RNA using deoxynucleotide triphosphates (dNTPs) to make long single-stranded cDNA sequences of the entire length of RNA. This cDNA can then undergo traditional PCR or qPCR. In PCR primers are designed to bind to the 3' and 5' ends of a specific DNA sequence initiating the activity of DNA polymerase, which copies the target sequence into double-stranded DNA. This double-stranded DNA product or amplicon then undergoes many repeats or cycles of thermal cycling, which consist of heating to denature the hydrogen bonds of the alpha-DNA helix thus separating the strands, and cooling to anneal primers and encouraging polymerization, resulting in the synthesis of over a billion copies of target DNA exponentially (<http://gene-quantification.de/real-time-pcr-guide-bio-rad.pdf>). The amplified product of known length, denoted by the distance between the primers on the target sequence of the gene, is produced and can be measured and semi-quantified by agarose gel electrophoresis. This traditional method of PCR has poor precision, low sensitivity, relies on good band resolution, and the use of hazardous chemicals, e.g. ethidium bromide. In addition, because traditional PCR measures the end-point of the assay, the results between replicates can be highly variable (Figure 2.2).

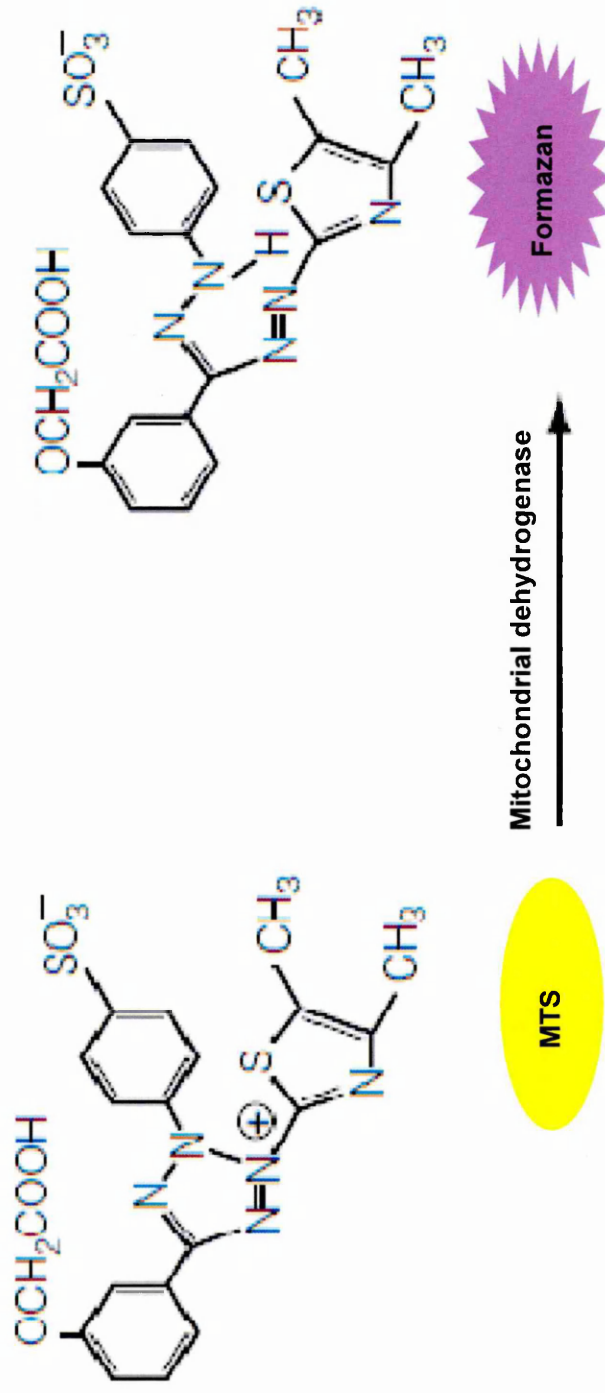


Figure 2.1: Chemical structures showing the conversion of MTS tetrazolium salt to formazan product. In the presence of mitochondrial dehydrogenase MTS (yellow) is reduced to formazan product (purple). The quantity of this formazan product is measured at 490nm and the absorbance readings obtained is directly proportional to the number of living cells in culture. Adapted from <http://www.promega.com/~media/Files/Resources/Protocols/Technical%20Bulletins/0/CellTiter%20Aqueous%20Non-Radioactive%20Cell%20Proliferation%20systems%20protocol.pdf>

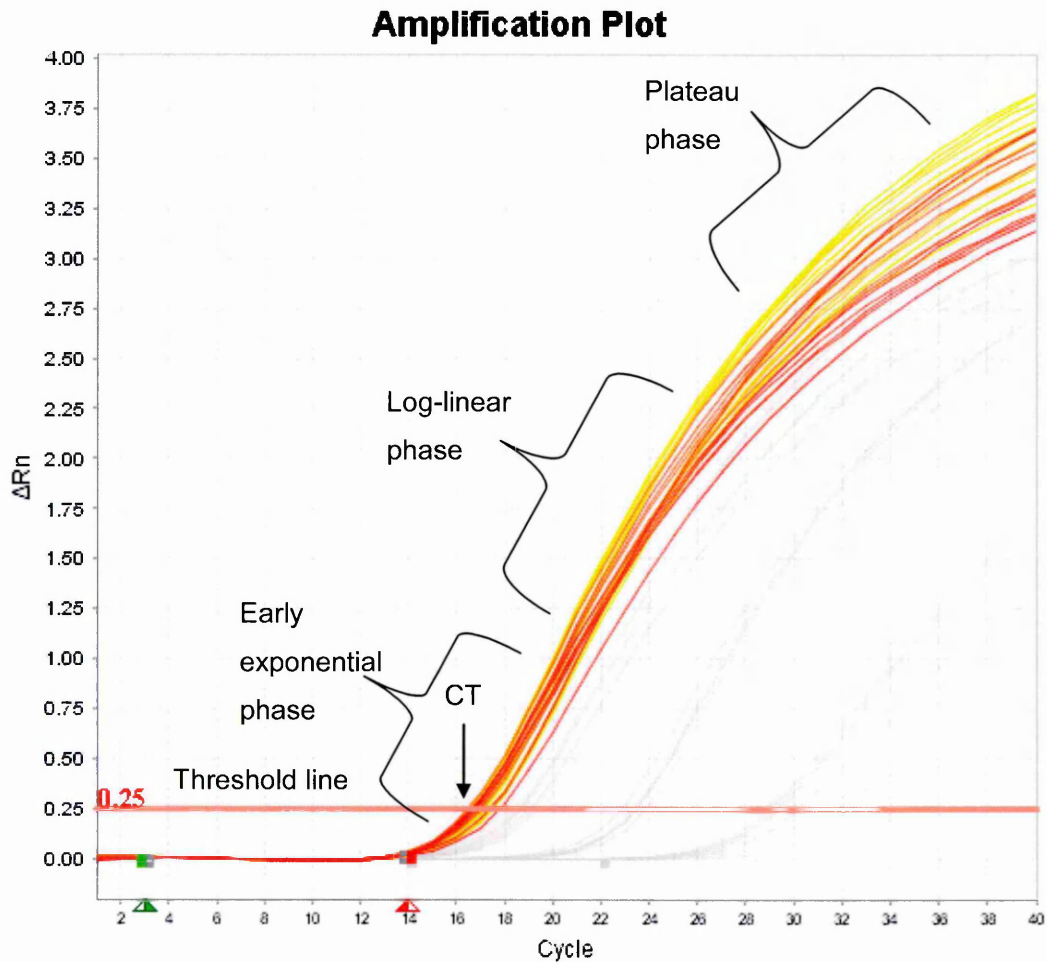


Figure 2.2: qPCR amplification plot. PCR consists of three amplification stages; exponential, linear and plateau. In the exponential phase, reagents are in abundance with PCR product doubling every cycle. During the linear phase these reagents begin to deplete and the PCR reaction begins to slow down. Finally in the plateau phase all reagents are depleted and the PCR reaction stops. qPCR measures PCR amplification during the exponential phase which generates more precise and accurate data, whereas traditional PCR measures the amount of accumulated PCR product at the end of the PCR cycles (the plateau phase) which shows much greater variability between triplicate samples.

Key: CT; Cycle Threshold.

qPCR measures amplification cycle by cycle in real-time, rather than at the end point of the assay, as occurs in traditional PCR, through the use of fluorescently labeled molecules which accumulate after each amplification cycle. In qPCR the PCR products are quantified in the exponential phase of the reaction where there is a doubling of the PCR product every cycle, which provides more precise and accurate data for quantification (Figure 2.2). Within this exponential phase two values are calculated: the threshold line and the cycle threshold (CT). The threshold line is the level where the reaction reaches a fluorescence intensity which is significantly higher than background levels, usually ten times the standard deviation of the baseline (Wong and Medrano 2005), and the CT is the PCR cycle at which the sample reaches this threshold (Figure 2.2).

There are two distinct detection chemistries employed in qPCR, namely probe- or non-probe based chemistries, also referred to as 'specific' and non-specific', respectively (Bustin and Mueller 2005). Probe-based detection methods use amplicon-specific fluorescent probes that only generate a fluorescent signal when bound to their complementary target sequence. This type of detection chemistry is very specific as a particular gene sequence must be present in order for the probe to bind. In comparison, non-probe-based methods rely on fluorescent dyes that intercalate to double-stranded DNA, when in free solution this dye exhibits little fluorescence but during DNA polymerisation increasing amounts of the dye binds to nascent DNA resulting in an increase in fluorescent signal. This method is much less specific because the dye binds to any double-stranded DNA, including any mispriming events or primer dimers as well as the target sequence and therefore requires verification of the PCR product through the generation of a melt curve of the amplicon where fluorescence is plotted as a function of temperature.

PCR products can either be quantified using absolute or relative quantification. Absolute quantification requires the use of standards of known target copy number to generate a standard curve from which the absolute quantity of the mRNA from a target gene of an unknown sample can be determined. This method of quantification is most commonly employed when determining viral load or tumour load in bodily fluids (Bustin and Mueller 2005). Relative quantification determines the changes in mRNA expression of a target gene across multiple samples and expresses it relative to an internal reference gene e.g. housekeeping gene. There are many mathematical algorithms that have been developed to produce the corrected relative expression ratio, the most common of which is the comparative delta CT method (Livak and Schmittgen 2001). However, in order for the comparative delta CT method to be valid, the primer amplification efficiencies of each target and reference gene must be approximately

equal, therefore it is important that primer efficiencies are determined prior to qPCR of unknown samples. Relative quantification is most commonly used when comparing expression levels of mRNA targets between different biological conditions and validating gene knockdown experiments.

qPCR using Taqman® probes

qPCR is used for the detection and quantification of gene expression. RNA is first reverse transcribed into complementary DNA (cDNA). The target DNA molecule is then amplified by PCR and quantified in real-time by the accumulation of fluorescence after each cycle of amplification (Figure 2.3). Taqman® probes have three levels of specificity to ensure that only the gene of interest is amplified. In addition to the forward and reverse primers of traditional PCR, an oligonucleotide probe designed to bind only to a portion of the target DNA sequence is also added to the reaction, which provides further specificity compared to standard PCR and non-probe dye intercalating chemistries, such as SYBR Green (Bustin *et al.*, 2005).

The Taqman® probe is an oligonucleotide that contains a fluorescent reporter dye bound to the 5' end and a quencher on the 3' end (Figure 2.3). The probe is designed to bind to a specific region of the target DNA sequence downstream from the primer binding site. While the probe is intact, the proximity of the quencher dye greatly reduces the fluorescence emitted by the reporter dye by fluorescence resonance energy transfer (FRET). If the target sequence is present, the probe anneals downstream from the primer site. During amplification the DNA polymerase elongates cleaving the probe due to its 5' nuclease activity, resulting in the separation of the reporter from the quencher, with a subsequent increase in the reporter dye fluorescence. As the primer extends, the probe is completely removed from the target strand enabling primer extension to the end of the template strand. This fluorescent signal is captured by the PCR instrument. With each cycle, additional reporter molecules are cleaved from their respective probes, resulting in an increase in fluorescence intensity. This increase in reporter fluorescence intensity is directly proportional to the number of amplicons generated.

2.2.3.1 Total RNA extraction

RNA was extracted from cells following cytokine treatment for 24 hours using Tri Reagent following the manufacturers' instructions (Sigma-Aldrich, UK). Briefly, cells were washed twice with DPBS followed by the addition of 0.33 mL of Tri Reagent to each well for 5 minutes at RT, in order to lyse the cells (total of 1 mL Tri Reagent per condition as 3 wells) and then transferred to sterile 1.5 mL microcentrifuge tubes.

Subsequently, 0.2 mL of chloroform was added to samples, mixed vigorously and left to stand for 15 minutes at RT followed by centrifugation at 12,000 g for 15 minutes at 4°C.

The colourless upper aqueous phase was then transferred into a RNA-free clean microcentrifuge tube and 0.5 mL of isopropanol was then added to precipitate the RNA, which was left to stand for 15 minutes at RT, followed by centrifugation at 12,000 g for 15 minutes. The supernatant was removed and the RNA pellet was washed in 1mL of 75% ethanol followed by vortexing and centrifugation at 12,000g for 15 minutes. Lastly, the 75% ethanol was removed and the RNA pellet was air-dried for 5-10 minutes and then resuspended in 10-30 µL of diethylpyrocarbonate (DEPC)-treated water for subsequent complementary DNA (cDNA) synthesis. DEPC inactivates any RNase enzymes which may be present in the water (Invitrogen, UK).

2.2.3.2 Agarose gel electrophoresis of total RNA

RNA samples were run on a 1% agarose gel to check the quality and purity of the total RNA extracted (e.g. no degradation or contamination of RNA). This separation is based on the principle that 28S rRNA will migrate at 5 kb and 18S rRNA will migrate at 2 kb, and are present in a 2:1 ratio (Sambrook and Russell 2001).

A 1% pre-stained agarose gel was prepared by the addition of 0.5 g agarose (Bioline, UK) in 50 mL Tris-acetate-EDTA (TAE) buffer (89 mM Tris-HCL pH 7.8, 89 mM borate, 2 mM EDTA), followed by heating in a microwave oven for 1 min to dissolve the agarose. The solution was then allowed to cool, followed by the addition of 3.5 µL ethidium bromide (from 10mg/mL stock concentration), and poured into a sealed gel tray. An 8-well gel comb was inserted into the agarose solution and the gel was left to set for ~30 minutes. Agarose gels were then submerged in an electrophoresis tank containing TAE buffer covering 2-3 mm above the gel. Experimental samples (2 µL RNA with 2 µL sample buffer) were then loaded into each well and run for 20 minutes at 100V. Gel images were captured using a UVP epi II dark room using Labworks software version 4.0.

2.2.3.3 cDNA synthesis

RNA extracted from both cytokine treated and untreated cells was converted to cDNA prior to carrying out qPCR. RNase-free filter tips and tubes were used throughout the cDNA synthesis procedure.

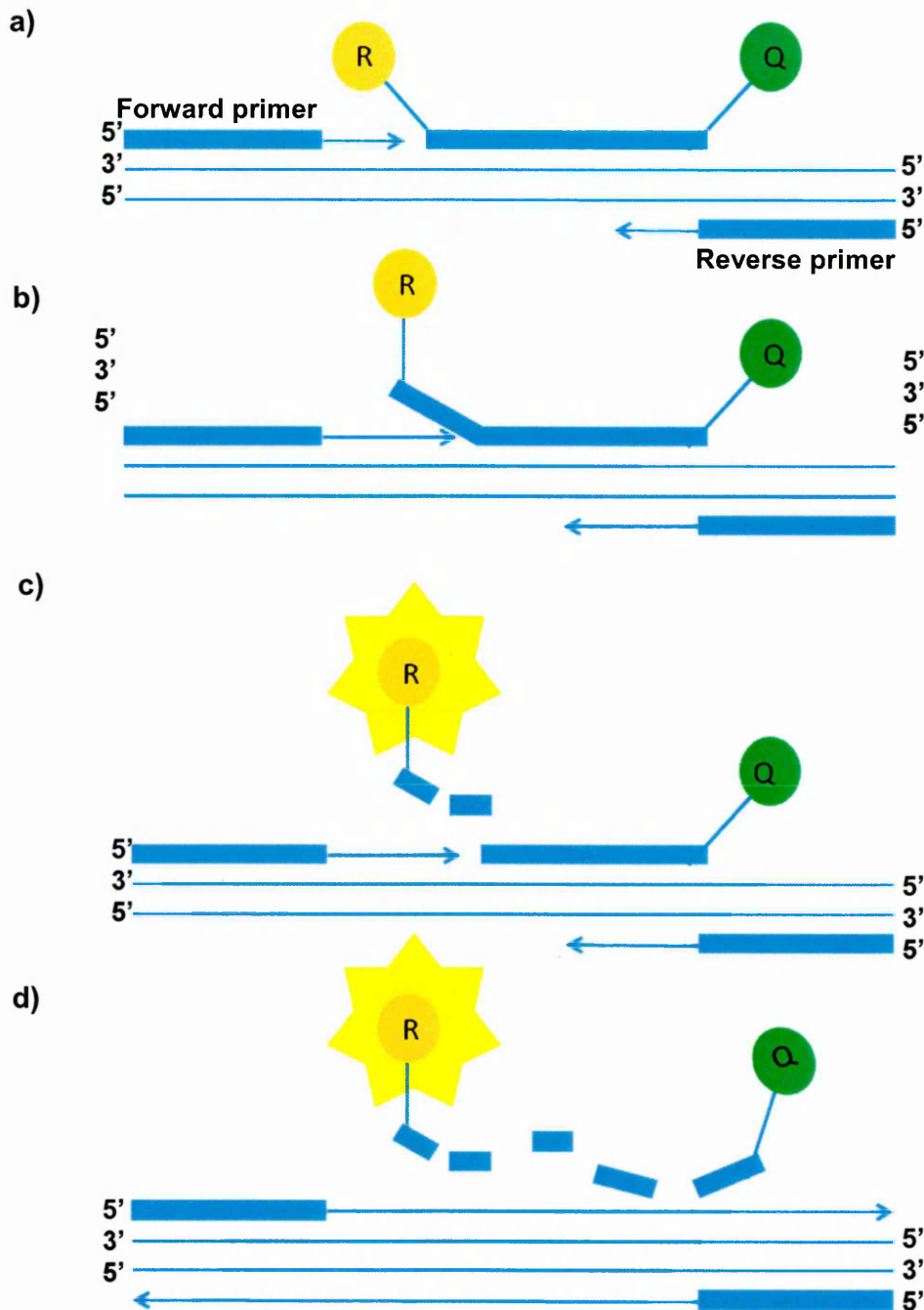


Figure 2.3: A schematic diagram showing the principles of qPCR using Taqman® probes. (a) Sequence-specific forward and reverse primers, along with a sequence-specific probe, hybridise to the DNA template. **(b-c)** During amplification, the 5' nuclease activity of the Taq DNA polymerase cleaves the probe as the primer is extended, separating the reporter (R) dye from the quencher (Q) leading to an increase in the reporter dye signal. **(d)** Lastly, the probe is fully removed from the target DNA sequence, allowing primer extension to continue and synthesis of the full amplicon sequence. Adapted from <http://www.clinchem.org/content/46/1/24/F1.small.gif>.

Briefly, 4 μL of 5x first strand buffer, 2 μL of 0.1 M dithiothreitol (DTT) (Invitrogen, UK), 1 μL of deoxynucleotide triphosphates (dNTPs) (Bioline, UK), 0.5 μL of RNase inhibitor (Invitrogen, UK), 0.5 μL of random hexamers (Invitrogen, UK), 9 μL of DEPC-treated water (Invitrogen, UK), 1 μL of reverse transcriptase (Invitrogen, UK) and 1 μL of RNA were mixed in RNase-free PCR tubes (Sigma, UK) on ice. Control samples were also prepared containing RNA without the addition of the RT enzyme and also a negative control containing no RNA sample. The samples were then placed on a heating block where they were heated for 2 hrs at 42°C, then 5 minutes at 95°C to inactivate the reverse transcriptase enzyme followed by 4°C and then stored at -20°C.

2.2.3.4 qPCR

Forward and reverse PCR primers along with probes for both housekeeping and target genes of interest were pre-designed and ordered from Applied Biosystems, UK (see Table 2.2 for full gene name, function and primer details).

PCR reactions were prepared on ice and performed in a volume of 10 μL , containing 0.5 μL FAM-labelled probe, 2.5 μL DEPC-treated water (Invitrogen, UK), 5 μL 2x Taqman® mastermix (ABI, UK) and 1 μL cDNA template. Reactions were performed in duplicate and three independent experiments were performed for each culture condition.

Amplification was carried out in an ABI 7900 sequence detector, using the following programme: 50°C for 2 minutes, 95°C for 2 minutes, followed by 40 cycles of denaturation at 95°C for 15 seconds and an annealing/elongation step at 60°C for 1 minute. At each step of the experiment, emitted fluorescence was measured in real-time resulting in an amplification plot on the ABI Prism 7900HT sequence detection system software 2.2.1. The relative mRNA level of each target gene was then calculated using the resulting cycle threshold (CT) values and the 2- delta delta cycle threshold ($2^{-\Delta\Delta\text{CT}}$) (see section 2.2.3.5).

2.2.3.5 Relative quantification using comparative CT method

The comparative CT method is a mathematical model that calculates changes in gene expression as a relative fold difference between an experimental and control (calibrator) sample normalised to an endogenous reference gene (Livak and Schmittgen 2001; Wong and Medrano 2005).

Table 2.2: qPCR housekeeping and target gene information.

Gene symbol	Gene name	mRNA accession number	Function	Assay ID	Exon boundary	Assay location	Amplicon length	Source
PADI2	Peptidylarginine deiminase, type II	NM_007365.2	Catalyzes the post-translational deimination of proteins by converting arginine residues into citrullines	Hs00247108_m1	1-2	176	79	ABI
PADI4	Peptidylarginine deiminase, type IV	NM-012387.2	Catalyzes the post-translational deimination of proteins by converting arginine residues into citrullines	Hs012387.2-m1 *Hs01057479_m1 *Hs01057476_m1	1-2 4-5 15-16	125 436 1785	71 73 73	ABI
GAPDH	Glyceraldehyde-3-phosphate dehydrogenase	NM_002046.4	Oxidoreductase in glycolysis and gluconeogenesis	Hs99999905_m1	3-3	229	122	ABI
PPIA	Peptidylprolyl isomerase A (Cyclophilin A)	NM_021130.3	Accelerates the folding of proteins.	Hs99999904_m1	4-4	433	98	ABI
HPRT1	Hypoxanthine phosphoribosyl-transferase 1	NM_000194.2	Generation of purine nucleotides in the purine salvage pathway	Hs99999909_m1	6-7	649	100	ABI

*Additional PAD4 primer and probes tested.

Prior to data analysis, the baseline and threshold was manually determined on each amplification plot for each target and reference gene. For data analysis, the means of each duplicate target and housekeeping C_T value for each sample were first averaged to account for any inter-assay variability. Following this the target mean C_T values for each sample were then normalised to the mean C_T values of two housekeeping genes to give the ΔC_T , as follows:

$$\Delta C_T = C_T \text{ target gene} - C_T \text{ reference gene}$$

For relative or semi-quantitative analysis of mRNA expression, the C_T values of the test samples in experimental conditions i.e. treated, were represented relative to their expression in control conditions i.e. untreated. An average ΔC_T of control samples for each repeat was then taken as the ΔC_T calibrator value from which the test sample ΔC_T values were normalised. Test samples were presented as relative fold-change from controls. The $\Delta\Delta C_T$ was then calculated as follows:

$$\Delta\Delta C_T = \Delta C_T \text{ calibrator} - \Delta C_T \text{ calibrator}$$

$$\Delta\Delta C_T = \Delta C_T \text{ sample} - \Delta C_T \text{ calibrator}$$

Following this, the untreated control sample or calibrator then has a $\Delta\Delta C_T$ value which equals 0. In order to account for the exponential nature of the PCR reaction, these values are then converted into linear form, as follows:

$$2^{-\Delta\Delta C_T}$$

By raising the $\Delta\Delta C_T$ to $2^{-\Delta\Delta C_T}$, this converts the $\Delta\Delta C_T$ value of the calibrator to 1, so that the fold-change in gene expression relative to the untreated control, equals 1. For the treated samples, the $2^{-\Delta\Delta C_T}$ indicates the fold-change in gene expression relative to the untreated control i.e. 1 (Livak and Schmittgen 2001).

2.2.3.6 Determination of primer efficiencies

In order for the comparative C_T method to be valid (see section 2.2.3.5), the primer efficiencies of the target genes and the reference or housekeeping genes must be approximately equal, therefore it is imperative to determine the primer efficiencies prior to data analysis (Livak and Schmittgen 2001). When primers are 100% efficient there should be a doubling of PCR product every cycle within the exponential phase of the reaction (Figure 2.1) (Livak and Schmittgen 2001). A sensitive method for determining primer efficiency is to carry out serial template dilutions of cDNA and examine the resultant ΔC_T . The data collected during this exponential phase can be log-transformed and plotted with slope of the regression line, which represents the samples amplification efficiency (Wong and Medrano 2005). Generally, a primer efficiency



between 90-110% is considered acceptable, although all target genes and housekeeping genes should be within 5% of one another in order to use the comparative C_T method (Livak and Schmittgen 2001).

In order to assess primer efficiencies a two-fold serial dilution of template cDNA ranging from 1:1 to 1:32 in DEPC-treated water was performed and subjected to qPCR. The resulting C_T values of all target and reference genes were plotted against log dilution factor. A linear trend line was then added to the graph, and from this, the slope of the line was determined and then calculated into percentage primer efficiency. The linear correlation was also determined, which indicates how good one value is at predicting another, with an R^2 value of >0.99 providing good confidence in correlating two values.

2.2.3.8 Selection of housekeeping genes

To achieve accurate, relative quantification of an mRNA target it is necessary to normalise to at least one reference gene, which is constitutively expressed and is not affected by the experimental treatment under study, and therefore can be used to correct for differences in the amount of total nucleic acid added to each reaction (Vandesompele *et al.*, 2002). There is not one specific gene that meets this criterion, therefore it is imperative to validate the expression stability of at least one control gene with experimental samples, prior to use for normalisation (Andersen *et al.*, 2004). Vandesompele *et al.* (2002) recommend the use of at least three internal control genes for normalisation. However, this is often impractical due to time and money constraints. Three commonly used reference genes; glyceraldehyde-3-phosphate dehydrogenase (GAPDH), cyclophilin A (PPIA), and hypoxanthine guanine phosphoribosyl transferase 1 (HPRT1), were assessed by qPCR to determine which of these reference genes were most stable, under the experimental conditions used in this chapter.

The geNorm programme was then used to select the two most stable reference genes (Vandesompele *et al.*, 2002). This programme determines the expression stability of reference genes on the basis of non-normalised expression levels. For each reference gene, the pair-wise variation with other reference genes is determined, resulting in a gene expression stability measure (M). Those with the lowest M values have the most stable expression, with increasing variation in ratio corresponding to decreasing expression stability. Prior to input into the geNorm programme, the C_T values were transformed using the ΔC_T method (see section 2.2.3.5). ΔC_T was calculated by subtracting the lowest C_T value from all other C_T values, followed by the equation $2^{-\Delta\Delta C_T}$ applied to each experimental sample. Following this, geNorm software then calculated the average M value for each reference gene in ranked order, followed by exclusion of

the gene with the highest M value (i.e. least stable) resulting in the display of the two most stable genes. An M value of <1.5 is considered a stable reference gene.

2.2.4 Traditional PCR

Untreated control cDNA from EP14 primary human astrocytes and U373-MG astrocytoma cell line were subjected to standard PCR (see section 2.2.3). All reagents were purchased from Bioline, UK, except for PCR primers which were designed and ordered from Applied Biosystems, UK. PCR reactions were prepared on ice and performed in a volume of 25 μ L, containing 2.5 μ L ImmunBuffer, 0.5 μ L 50 mM MgCl₂, 0.5 μ L dNTP mix, 1 μ L forward primer, 1 μ L reverse primer, 0.5 μ L Immolase DNA polymerase, 17 μ L DEPC-treated water (Invitrogen, UK) and 2 μ L cDNA template. Amplification was carried out in a Primus 96 Plus Thermal Cycler (MWG-Biotech, UK), using the following programme: 95°C for 10 minutes, followed by 35 cycles of: 95°C for 30 seconds, 55°C for 30 seconds and 72°C for 90 seconds. Samples were then stored at 4°C until the products were run on a gel.

2.4.4.1 Optimisation of traditional PCR for PAD4

Initially two forward and reverse primer sets (Table 2.3) were used to test for the presence of PAD4 product using cDNA from U373-MG and EP14 cells. Optimisation of forward and reverse primer sets predominantly involved testing different concentrations of MgCl₂ and different temperatures of the annealing and extension cycles, using cDNA from U373-MG astrocytoma cell line as a positive control for PAD4 as this cell line had been reported previously to express PAD4 mRNA (Chang and Han 2006).

2.4.4.2 Agarose gel of PCR products

PCR products were run on a 3% agarose gel to check that products were of the correct size specific to the primers. A 3% pre-stained agarose gel was prepared by the addition of 1.5 g of agarose to 50 mL of TAE buffer (see section 2.2.3.2). Samples (10 μ L with 3 μ L sample buffer) and ladder (Bioline, UK) were loaded into wells and run for ~90 minutes at 80V. The gel was then visualised using the UVP image analysis programme for the presence of a band at the expected size indicating no DNA contamination and the specificity of the primers.

Table 2.3: Details of PAD4 primers tested in traditional PCR, including details of the primer sequences for the forward and reverse primers used.

Gene symbol	Gene name	mRNA accession number	Primer set	Primer sequence (5'-3')	Position	Product size (bp)
PADI4	Peptidylarginine deiminase, type IV	NM-012387.2	1	ACCCCAGAGCAGCCCAC	56	600
				TGTCCATCTCAGACCTGGCC	656	
PADI4	Peptidylarginine deiminase, type IV	NM-012387.2	2	AAGTGCAGCGTAGTCTTGGGTC	698	600
				GGTATTCCCTTGCCCCCTGACTG	1298	

2.2.5 Immunocytochemistry

Antibodies are routinely used to detect the cellular localisation of proteins (or antigens) in cells, tissues or biological fluids. The detection of an antigen using antibodies in cultured cells is referred to as immunocytochemistry (ICC) whereas the detection of an antigen using antibodies in tissues is known as immunohistochemistry (IHC). In this chapter ICC was utilised.

Immunofluorescence is dependent on the coupling of fluorophores to antibodies, which when bound to the antigen of interest and excited by a light source, such as UV light, emits light, which can then be visualised using either a fluorescence or confocal microscope revealing the location of the antigen of interest. Prior to antibody application the cells and/or tissues are subjected to fixation, permeabilisation and if necessary blocking. Fixation preserves both the cellular and subcellular structure in addition to the antigenicity of the antigen(s) of interest. Fixatives either form cross-linkages to preserve the tissue structure e.g. aldehydes such as glutaraldehyde or formalin, or remove lipids and dehydrate cells whilst precipitating proteins and fixing them in their usual cellular localisation e.g. organic solvents such as acetone, ethanol, methanol (Delves *et al.*, 2006).

Both fixation methods can result in denaturation of the protein/antigen of interest. Fixatives which form cross-linkages may reduce the access of antibodies to some cell components, and therefore ICC may require a permeabilisation step to allow access of the antibody to the target protein/antigen. Detergents, such as Triton X-100 or Tween-20, are used for this permeabilisation step. A blocking step is often employed using bovine serum albumin (BSA) or serum from the species in which the secondary antibody is made. This prevents non-specific binding of the labelled secondary antibody and particularly binding to endogenous Fc receptors (FcRs) present on the surface of some cells (Buchwalow *et al.*, 2011).

Washing of the cells and/or tissues is performed following each of these steps to remove unbound reagents. There are two types of immunofluorescence: direct and indirect. In the direct method of immunofluorescence, the primary antibody directed against the antigen of interest is directly conjugated with a fluorochrome (Figure 2.4). Although this method involves fewer steps, the technique is limited as only a limited number of antibodies can access the antigen of interest leading to low sensitivity. Based on this, indirect immunofluorescence is often the preferred method utilised.

This method of immunofluorescence is most commonly employed and is called the double-layer technique because it uses two antibodies, the primary antibody, which

recognises the antigen of interest; the secondary antibody, which is directed against the species of Ig in which the primary antibody was raised (Figure 2.4). An example of this is the application of a monoclonal mouse anti-GFAP IgG antibody to cells or tissues, which can then be visualised by the addition of a fluorochrome-conjugated rabbit anti-mouse IgG. There are a number of advantages to this technique, in particular: several fluorescently labelled secondary antibodies can bind to the primary antibody, increasing the intensity of fluorescence and therefore the sensitivity of staining is greatly increased compared to the direct method; a single secondary antibody can be used to detect a range of primary antibodies, thereby reducing overall costs. Dual labelling of cells or tissues for two antigens can be performed providing the primary antibodies are raised in different species, otherwise the secondary antibody will be unable to discriminate between the two primary antibodies. In addition, the emission wavelengths of each of the fluorophore conjugated secondary antibodies must also be different otherwise discrimination between the two antigens of interest will not be possible. For example, GFAP and PAD2 can be detected in the same cell by using a monoclonal mouse and polyclonal rabbit primary antibody, respectively. In addition, the fluorescently labelled secondary antibodies must also be species specific, so directed against mouse and rabbit IgG, respectively each labelled with a different fluorophore.

2.2.5.1 Indirect immunofluorescence

In order to determine the cellular and subcellular localisation of PAD2 and PAD4, ICC was carried out on U373-MG, EP14 and EP15 cells. Cells were seeded into 8-well chamber slides (NUNC, Labtech International, UK) at a density of 1×10^4 cells/mL and 400 μ L per well and left to adhere to the chamber slide for 24 hours in an incubator at 37°C containing 95% air and 5% CO₂. Following this, media was aspirated from the chamber slides and cells washed three times in PBS for 5 minutes each. Cells were then fixed with acetone for 5 minutes and subsequently left to air dry for 10-15 minutes at RT. Prior to this a number of fixatives were tested in the initial optimisation procedure and acetone was found to provide substantially better staining than ethanol, methanol, or 4% paraformaldehyde (PFA). The chamber slide dividers were then removed and a wax pen was used to draw around each well of the chamber slide to ensure antibody solution remained within each well. The cells were stained for S100- β , GFAP, PAD2 and PAD4 using monoclonal mouse anti-human GFAP, polyclonal rabbit anti-human PAD2 and polyclonal rabbit anti-human PAD4, respectively (Table 2.4). Preliminary experiments were performed to determine the optimum concentration for ICC, with each antibody diluted within a range recommended by the supplier. Primary antibodies (20 μ L per well, diluted in DPBS with 0.5% Triton® X-100) were applied to

each well and incubated in a humidified chamber for 2 hrs at RT. The negative controls with the primary antibody omitted were incubated with 20 μ L PBS with 0.5% Triton® X-100. Cells were then washed three times in PBS, to remove any unbound antibody, for 5 minutes each. In order to detect any bound antigen, secondary antibodies FITC conjugated to rabbit anti-mouse IgG (for mouse monoclonal antibodies) or Alexa Fluor 568® conjugated to goat anti-rabbit IgG (for polyclonal antibodies) were then applied. Fluorochrome conjugated secondary antibodies (20 μ L per well, diluted in PBS) were applied to each well and incubated in the dark in a humidified chamber for 90 minutes at RT. Following this, cells were washed three times in DPBS, to remove any unbound secondary antibody, for 5 minutes each.

Subsequently, slides were mounted using Vectashield™ hard-set mounting medium with 4', 6-diamidino-2-phenylindole (DAPI) (Vector Laboratories, UK), which stains the cell nuclei blue. The edges of the coverslips were then sealed with nail varnish, and slides wrapped in foil and stored at 4°C until analysed. Images were captured using an upright Olympus BX60 fluorescent microscope, equipped with a cool-snap pro (Cybernetics) digital camera to acquire images into Labworks™ where they were saved without further manipulation.

2.2.6 Statistical analysis

MTS assay data was analysed using one-way ANOVA followed by a Dunnett's post-hoc test. Statistical significance was set at $p < 0.05$ and data are represented as mean \pm SEM. qPCR data was analysed using the non-parametric Kruskal-Wallis test followed by a Conover post-hoc test. In order to carry out statistical analysis, the $2^{-\Delta\text{CT}}$ was calculated to determine the relative gene expression. Each treated condition was then compared to the control. Statistical significance was set at $p < 0.05$ and data are represented as mean \pm SEM.

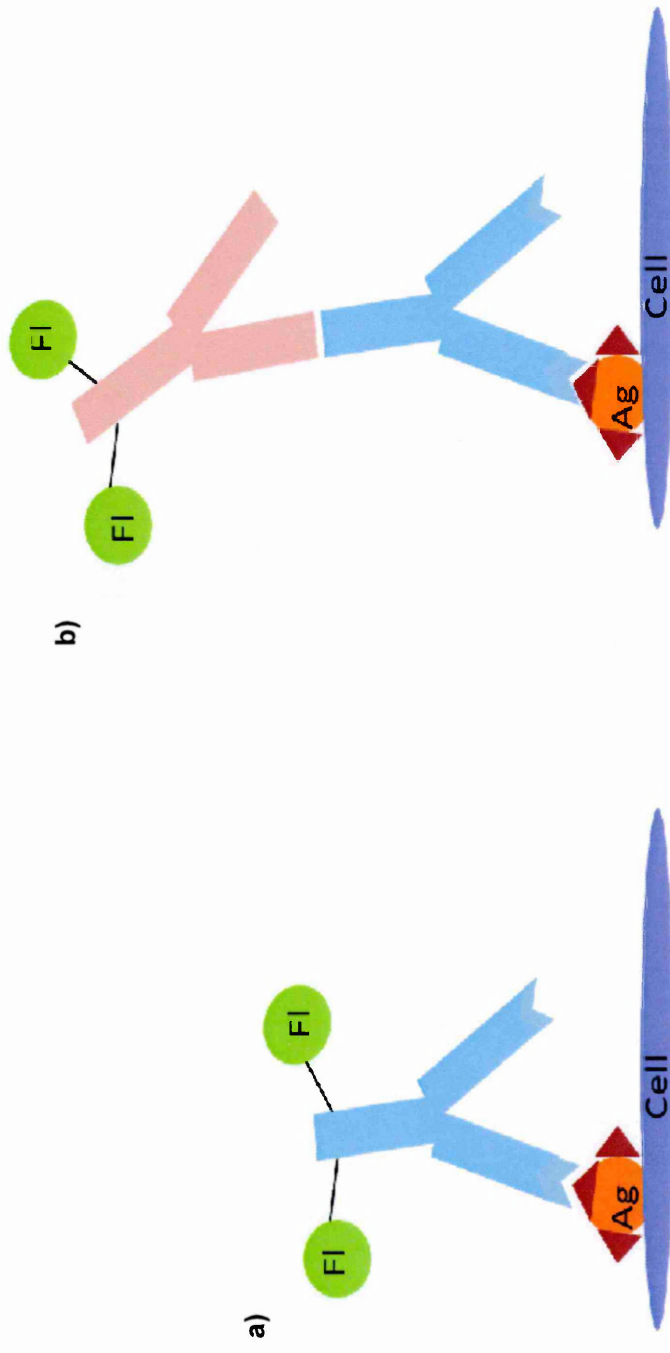


Figure 2.4: Direct and indirect immunofluorescence staining of a membrane antigen (Ag). (a) Cells are fixed to a microscope slide. In the direct method, cells are stained with an antibody directed against the antigen that is labelled with a fluorochrome (FI). (b) In the indirect method, cells are first incubated with an unlabelled primary antibody directed against the antigen of interest and then stained with a fluorochrome-labelled secondary antibody which is specific for the primary antibody. Fluorescence is then observed using a confocal or fluorescence microscope. Ag; antigen, FI; fluorophore.

Table 2.4: Details of primary and secondary antibodies used for immunocytochemical detection of GFAP, PAD2 and PAD4.

Primary antibodies					Secondary polyclonal antibodies				
Immunogen	Species	Clonality	Dilution	Source	Immunogen	Species	Conjugate	Dilution	Source
S100-β	Mouse	Monoclonal	1 in 500 1 in 1000	Sigma, UK	Mouse IgG	Rabbit	FITC	1:40	Dako, UK
GFAP	Mouse	Monoclonal	1:100 1:200 1:500	Millipore, UK	Mouse IgG	Rabbit	FITC	1:40	Dako, UK
GFAP	Rabbit	Polyclonal	1:500 1:1000	Abcam, UK	Rabbit IgG	Goat	Alexa fluor® 568	1:600	Molecular Probes, Invitrogen, UK
PAD2	Rabbit	Polyclonal	1:50 1:100 1:200	Abcam, UK	Rabbit IgG	Goat	Alexa fluor® 568	1:600	Molecular Probes, Invitrogen, UK
PAD4	Rabbit	Polyclonal	1:50 1:100 1:200	Abcam, UK	Rabbit IgG	Goat	Alexa fluor® 568	1:600	Molecular Probes, Invitrogen, UK

Key: GFAP; glial fibrillary acidic protein, PAD; peptidylarginine deiminase.

The optimal antibody titre was determined in preliminary experiments. The optimum concentration for each antibody used in this thesis is highlighted in bold.

2.3 Results

2.3.1 Effect of pro-inflammatory cytokines on the viability of CNS cells

Due to preliminary qPCR data (not shown) indicating a down-regulation in the expression of PAD2 and PAD4 in cells following cytokine treatment, the effect of pro-inflammatory cytokines on the viability of cells was examined to ensure down-regulation was not due to significant apoptosis of cells.

2.3.1.1 U373-MG astrocytoma cell line

Treatment of an astrocytoma cell line (U373-MG) with 100 ng/mL of TNF- α for 24 hours resulted in a small 7% decrease in number of viable cells compared to untreated control, whereas treatment with 100 ng/mL of IFN- γ resulted in a 16% decrease in number viable cells compared to control. Treatment with IL-1 β and IL-6 alone did not affect cell viability (Figure 2.5a). Treatment of U373-MG cells with 100 ng/mL of IL-1 β , TNF- α or IL-6 alone for 48 hours resulted in only small, 5 to 8% decreases in the number of viable cells, whereas 100ng/mL of IL-1 β caused a 20% reduction in the number of viable cells (Figure 2.5b).

2.3.1.2 EP14 primary human astrocyte cells

Treatment of primary human astrocytes (EP14) with IL-1 β , TNF- α , IL-6 or IFN- γ for 24 hours did not affect cell viability (Figure 2.6a). Co-treatment of EP14 cells with IL-1 β and TNF- α or IL-1 β and IFN- γ did not have an effect on cell viability, whereas dual treatment with 100 ng/mL of TNF- α and IFN γ resulted in a small 6% reduction in the number of viable cells compared to control cells (Figure 2.6b).

2.3.1.3 EP15 primary human astrocyte cells

Treatment of primary human astrocytes (EP15) with IL-1 β , TNF- α , IL-6 or IFN- γ did not alter the viability of the cells (Figure 2.7a). However, co-treatment of EP15 cells showed dramatic increases in cell proliferation (Figure 2.7b). Co-treatment of cells with IL-1 β and TNF- α resulted in a maximal 44% increase in cell number at 10 ng/mL (Figure 2.7b), similarly co-treatment with IL-1 β and IFN- γ resulted in a maximal 100% increase in cell number at 100 ng/mL. Furthermore, a maximal 61% increase in viable cells was observed following dual treatment with 100 ng/mL of TNF- α and IFN- γ .

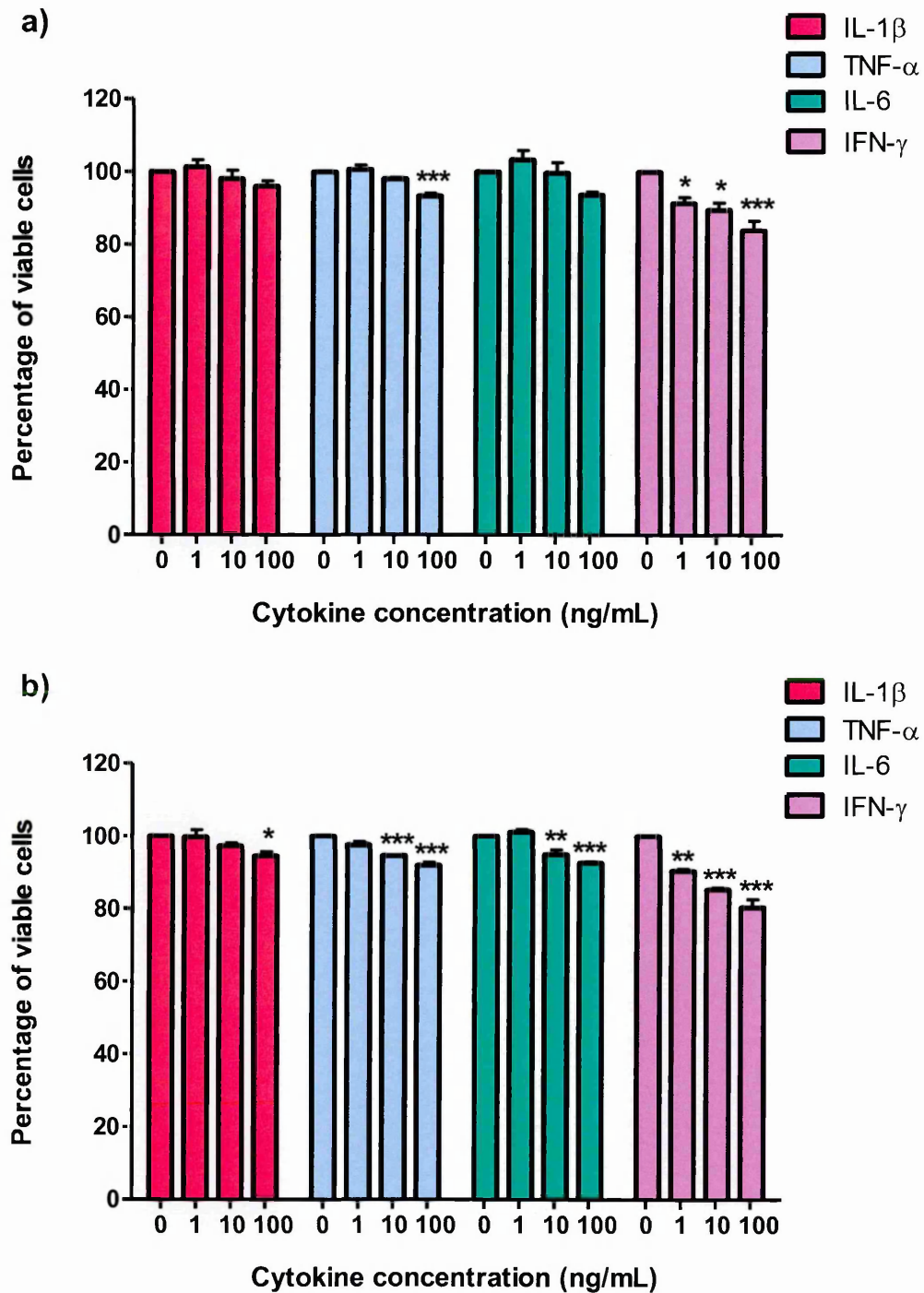


Figure 2.5: Effect of cytokine treatment on viability of an astrocytoma cell line (U373-MG). (a) 24 hour treatment with single cytokines IL-1 β , TNF- α , IL-6 and IFN- γ , and (b) 48 hour treatment with single cytokines IL-1 β , TNF- α , IL-6 and IFN- γ at 0-100 ng/mL. Data presented as the mean \pm SEM. Significant difference from control, * p <0.05, ** p <0.01, *** p <0.001 (ANOVA with Dunnett's test, n =3).

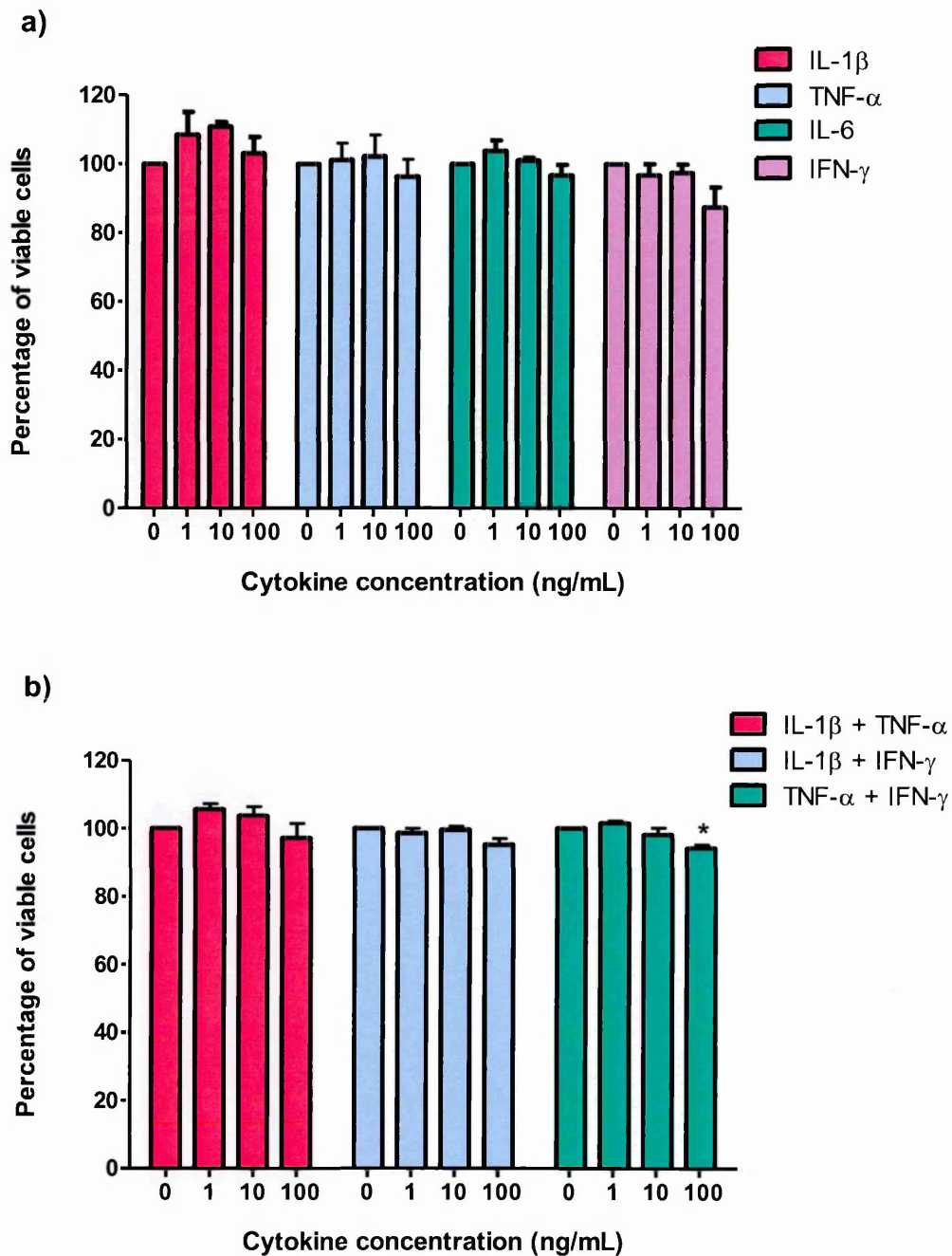


Figure 2.6: Effect of cytokines on the viability of primary adult human astrocytes (EP14). 24 hour treatment with (a) single cytokines IL-1 β , TNF- α , IL-6 and IFN- γ , and (b) dual cytokines IL-1 β + TNF- α , IL-1 β + IFN- γ and TNF- α + IFN- γ at 0-100 ng/mL. Data presented as the mean \pm SEM. Significant difference from control, * $p < 0.05$ (ANOVA with Dunnett's test, $n=3$).

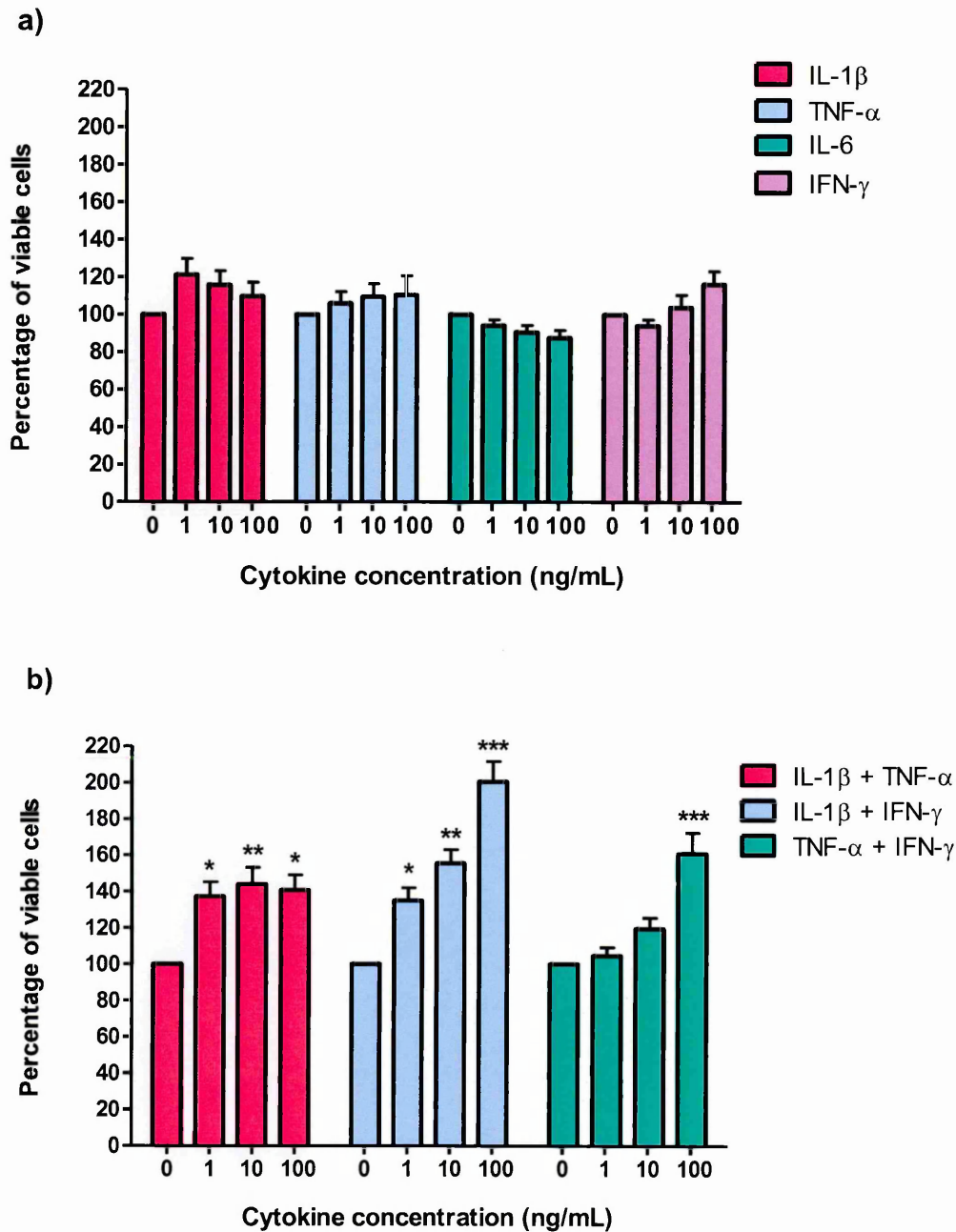


Figure 2.7: Effect of cytokines on the viability of primary adult human astrocytes (EP15). 24 hour treatment with (a) single cytokines IL-1 β , TNF- α , IL-6 and IFN- γ , and (b) dual cytokines IL-1 β + TNF- α , IL-1 β + IFN- γ and TNF- α + IFN- γ at 0-100 ng/mL. Data presented as the mean \pm SEM. Significant difference from control, * p <0.05, ** p <0.01, *** p <0.001 (ANOVA with Dunnett's test, n =3).

2.3.1.4 MS16 primary human astrocytes

IL-1 β treatment of primary human astrocytes (MS16) resulted in an increase in cell number, with a maximal 66% increase observed at 1 ng/mL, similarly TNF- α treatment resulted in an increase in viable cells, with a maximal 40% increase at 100 ng/mL (Figure 2.8a). IL-6 treatment resulted in an increase in viable cells, with a maximal 20% increase observed at 1 ng/mL. Treatment with IFN- γ did not alter the cell viability or proliferation. Co-treatment of MS16 cells with IL-1 β and TNF- α resulted in an increase in cell proliferation at all concentrations, with a maximal 187% increase observed at 10 ng/mL. Dual treatment with IL-1 β and IFN- γ resulted in an increase in cell proliferation at all concentrations tested, with a maximal 136% increase observed at 100 ng/mL (Figure 2.8b).

2.3.1.5 CHME3 human foetal microglial cell line

Treatment of human foetal microglial cell line (CHME3) with IL-1 β at 100 ng/mL resulted in a 16% decrease in viable cells compared to control, similarly treatment with TNF- α at 100 ng/mL resulted in a 19% decrease in viable cells compared to control (Figure 2.9a). Treatment with 100 ng/mL of IL-6 resulted in a 17% decrease in viable cells. IFN- γ treatment resulted in a decrease in the viability of cells at all concentrations tested, with a maximal 14% decrease observed at 100 ng/mL.

Co-treatment of CHME3 cells with IL-1 β and TNF- α or IL-1 β and IFN- γ did not have an effect on cell viability (Figure 2.9b). A decrease in the number of viable cells was observed following dual treatment with 10 and 100 ng/mL of TNF- α and IFN- γ , with a maximal 22% reduction observed at 100 ng/mL. Single treatment of CHME3 cells with IL-4, IL-10 and TGF- β did not alter cell viability.

2.3.1.6 hCMEC/D3 human brain endothelial cell line

Treatment of a brain endothelial cell line (hCMEC/D3) with IL-1 β , TNF- α , IL-6 or IFN- γ for 24 hours did not affect cell viability (Figure 2.10a). Following co-treatment of hCMEC/D3 cells with IL-1 β and TNF- α , a maximal 22% decrease in cell viability was observed at 100 ng/mL (Figure 2.10b). Co-treatment with IL-1 β and IFN- γ did not alter cell viability. A decrease in cell viability was observed following dual treatment with TNF- α and IFN- γ , with a maximal 20% decrease at 100 ng/mL.

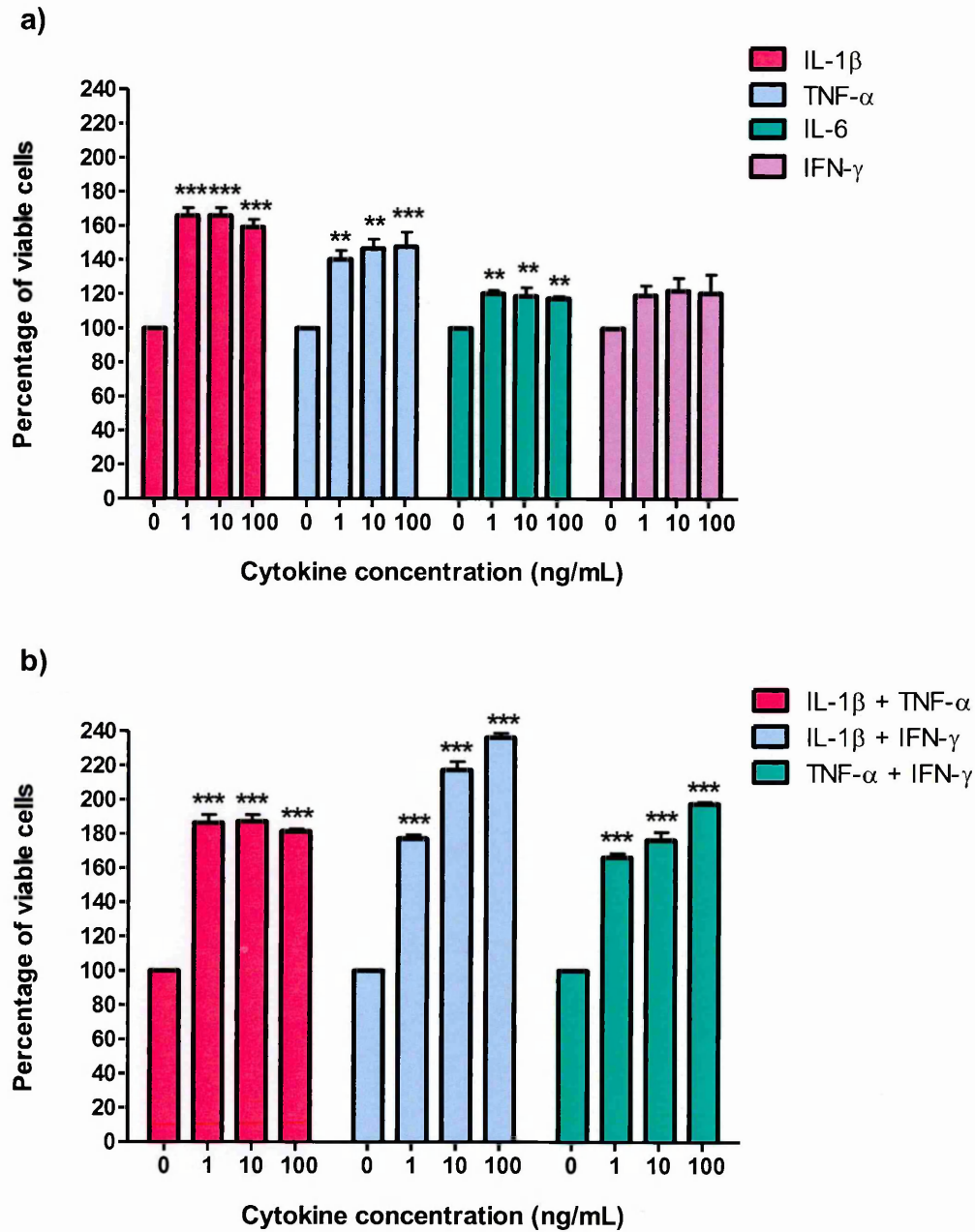


Figure 2.8: Effect of cytokines on the viability of primary adult human astrocytes (MS16). 24 hour treatment with (a) single cytokines IL-1 β , TNF- α , IL-6 and IFN- γ , and (b) dual cytokines IL-1 β + TNF- α , IL-1 β + IFN- γ and TNF- α + IFN- γ at 0-100 ng/mL. Data presented as the mean \pm SEM. Significant difference from control, * p <0.05, ** p <0.01, *** p <0.001 (ANOVA with Dunnett's test, n =3).

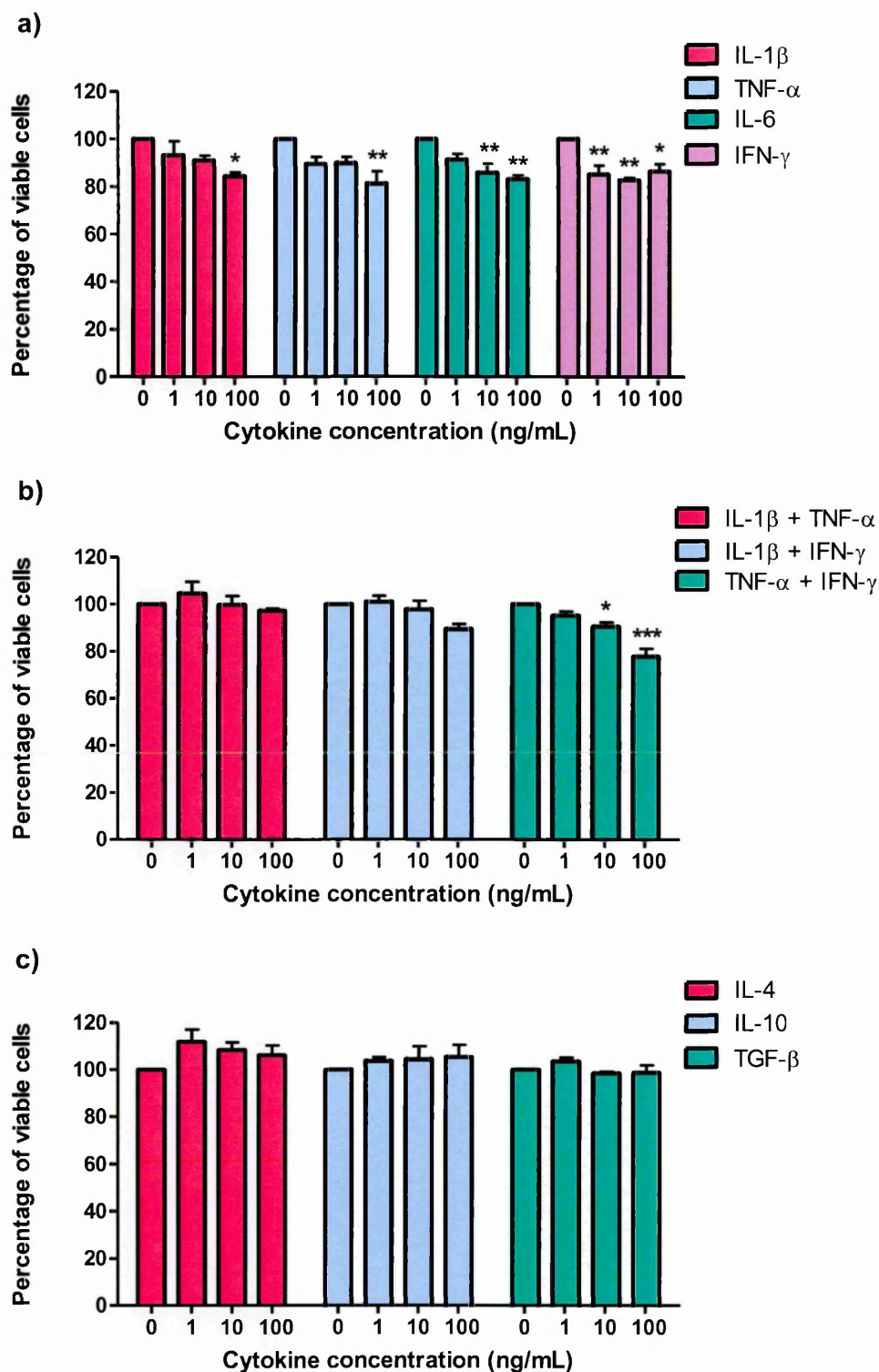


Figure 2.9: Effect of cytokines on the viability of CHME3. 24 hour treatment with (a) single cytokines IL-1 β , TNF- α , IL-6 and IFN- γ , and (b) dual cytokines IL-1 β + TNF- α , IL-1 β + IFN- γ and TNF- α + IFN- γ and (c) single cytokines IL-4, IL-10 and TGF- β at 0-100 ng/mL. Data presented as the mean \pm SEM. Significant difference from control, * p <0.05, ** p <0.01, *** p <0.001 (ANOVA with Dunnett's test, n =3).

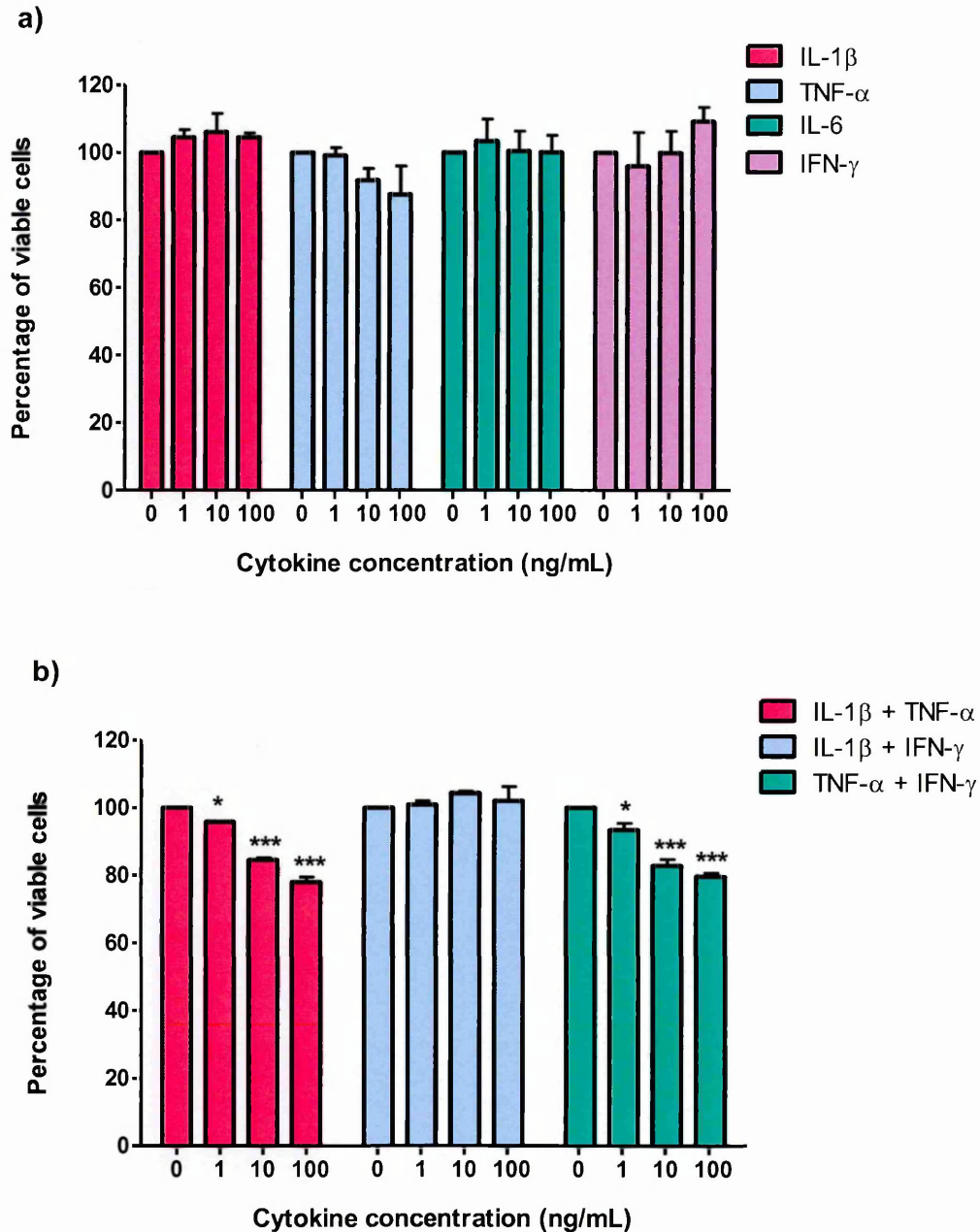


Figure 2.10: Effect of cytokines on the viability of hCMEC/D3 cells. 24 hour treatment with **(a)** single cytokines IL-1 β , TNF- α , IL-6 and IFN- γ , and **(b)** dual cytokines IL-1 β + TNF- α , IL-1 β + IFN- γ and TNF- α + IFN- γ at 0-100 ng/mL. Data presented as the mean \pm SEM. Significant difference from control, * p <0.05, *** p <0.001 (ANOVA with Dunnett's test, n =3).

2.3.2 RNA integrity

All RNA experimental samples showed clear bands at 5 kb and 2 kb indicating 28s and 18s ribosomal RNA in a ratio of 2:1 indicating no degradation or contamination, showing their suitability to be transcribed into cDNA and subjected to qPCR (Figure 2.11; Figure 2.12).

2.3.3 Selection of housekeeping genes

Three widely used housekeeping genes (GAPDH, PPIA, and HPRT1) were tested for their stability across the experimental conditions and hence suitability as reference genes for normalisation of target gene expression in qPCR experiments. Using geNorm (see section 2.2.3.8), the expression stability measure (M) of the two most stable genes were determined in each cell line following cytokine treatment. Ideally reference genes should have an M-value of less than 1.5, indicating that the expression is stable following cytokine treatment. Once determined these reference genes can then be used for normalisation (Vandesompele *et al.*, 2002).

In separate experiments, astrocyte preparations (EP14, EP15, MS16), CHME3, and hCMEC/D3 cells were treated with varying concentrations (1, 10 and 100 ng/mL) of single cytokines; IL-1 β , TNF- α , IL-6 and IFN- γ and dual cytokines; IL-1 β + TNF- α , IL-1 β + IFN- γ , and TNF- α + IFN- γ for 24 hours and then subjected to qPCR. The raw ΔC_T values from each experiment were then transformed using the relative quantification ΔC_T method (see section 2.2.3.5) and subjected to geNorm analysis (Table 2.5). Following this, it was determined that GAPDH was the least stably expressed gene in all cell lines tested. Following the elimination of GAPDH, the M-value of the two most stably expressed genes in the cells was calculated to be less than 1.5 (0.158, 0.425, 0.323, 0.246 and 0.405, respectively). This demonstrated the suitability of PPIA and HPRT1 to be used as reference genes, therefore both PPIA and HPRT1 were used in subsequent qPCR experiments.

2.3.4 Primer efficiencies

Once appropriate housekeeping genes had been selected, the amplification efficiency of four primer pairs was determined. cDNA from CHME3 was subjected to a two-fold serial dilution followed by qPCR using the standard curve method (see section 2.2.3.6). The resulting primer efficiencies ranged from 90 (PPIA) to 95% (HPRT1 and PAD4), with correlation coefficients between 0.957 (PPIA) and 0.999 (PAD4) (Table 2.6; Figure 2.13).

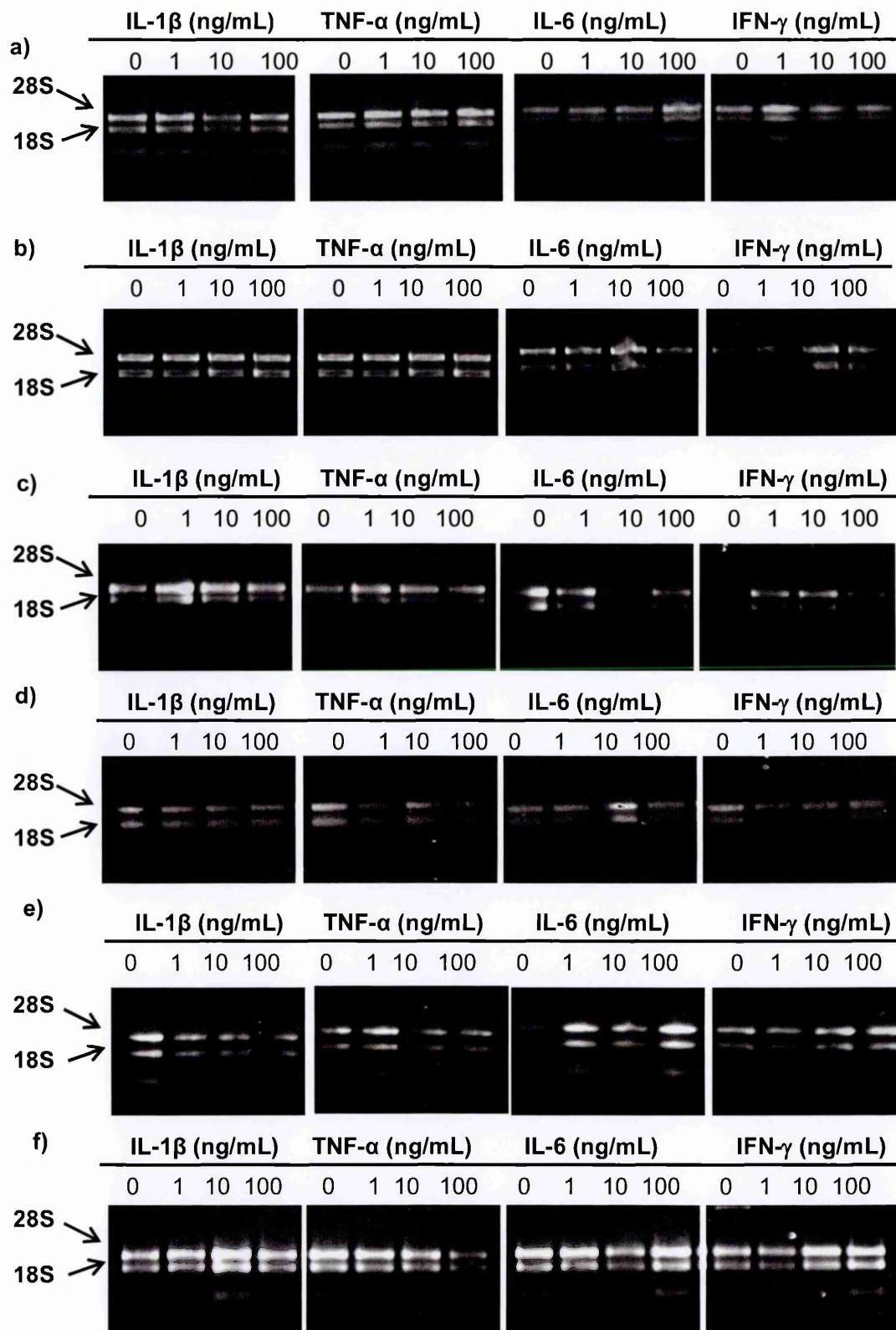


Figure 2.11: RNA extractions of CNS cells following treatment with varying concentrations (0, 1, 10 and 100 ng/mL) of single cytokines; IL-1 β , TNF- α , IL-6 and IFN- γ . (a) U373-MG, (b) EP14, (c) EP15, (d) MS16, (e) CHME3 and (f) hCMEC/D3.

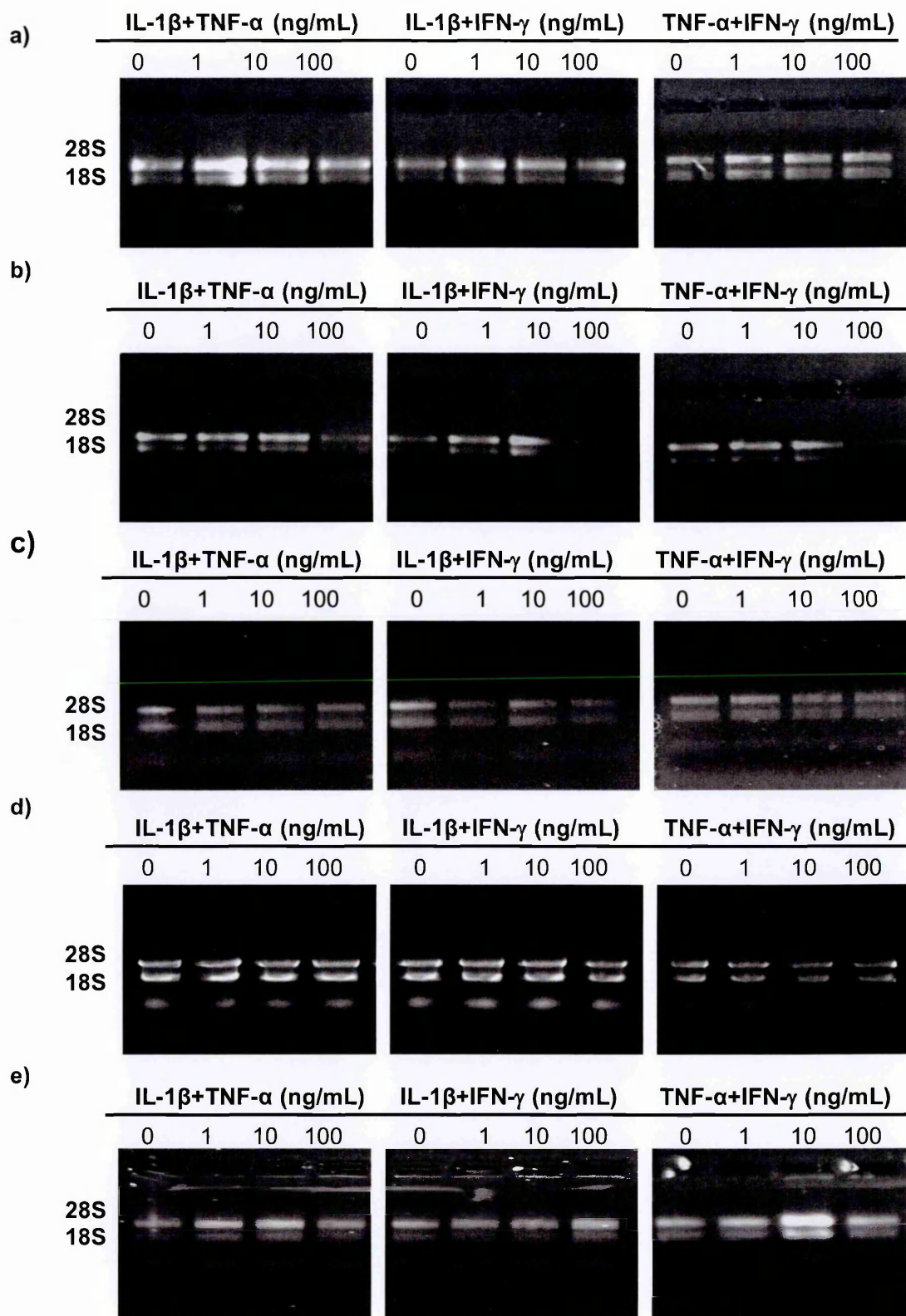


Figure 2.12: RNA extractions of CNS cells following treatment with varying concentrations (0, 1, 10 and 100 ng/mL) of dual cytokines; IL-1 β + TNF- α , IL-1 β + IFN, and TNF- α + IFN- γ . (a) EP14, (b) EP15, (c) MS16, (d) CHME3 and (e) hCMEC/D3.

Table 2.5: Validation of reference genes using the GeNorm analysis programme.

Cell line	Reference gene	Cytokine treatment	Mean independent experiment values	Overall mean M value
EP14	PPIA & HPRT1	IL-1 β	0.150	0.158
		TNF- α	0.194	
		IL-6	0.149	
		IFN- γ	0.136	
EP15	PPIA & HPRT1	IL-1 β	0.364	0.425
		TNF- α	0.399	
		IL-6	0.430	
		IFN- γ	0.507	
MS16	PPIA & HPRT1	IL-1 β	0.402	0.323
		TNF- α	0.188	
		IL-6	0.312	
		IFN- γ	0.392	
CHME3	PPIA & HPRT1	IL-1 β	0.266	0.246
		TNF- α	0.212	
		IL-6	0.289	
		IFN- γ	0.217	
hCMEC/D3	PPIA & HPRT1	IL-1 β	0.476	0.405
		TNF- α	0.303	
		IL-6	0.524	
		IFN- γ	0.316	

Table 2.6: Summary of the primer efficiencies of all housekeeping and target genes used in qPCR.

Gene name	Slope of curve	Correlation coefficient	Primer efficiency (%)
GAPDH	-1.0540	0.9815	95
PPIA	-0.9014	0.9572	90
HPRT1	-0.9487	0.9942	95
PAD2	-1.0926	0.9918	91
PAD4	-1.0518	0.9992	95

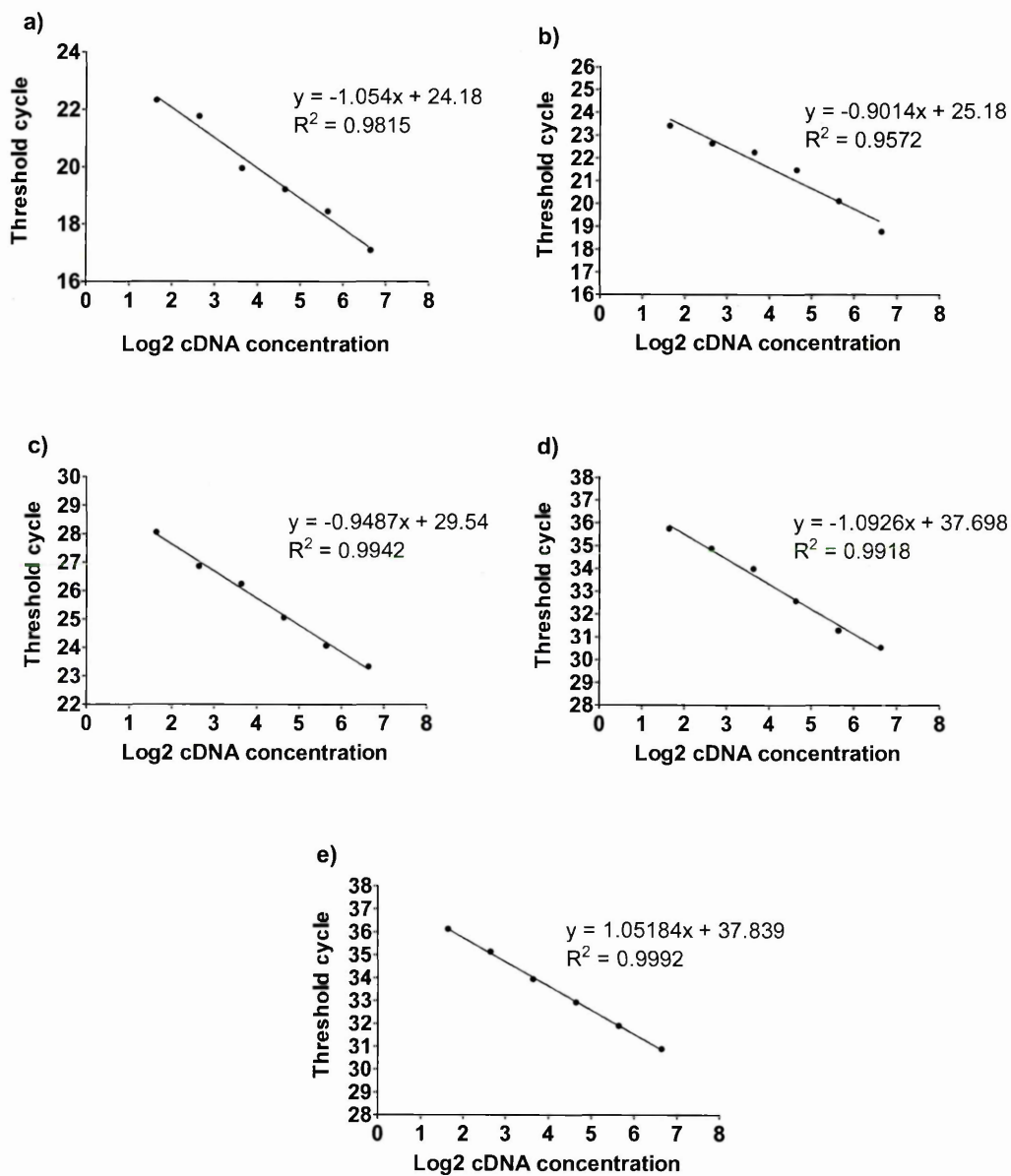


Figure 2.13: Standard curves showing the primer efficiencies following qPCR of serially diluted cDNA from CHME3. (a) GAPDH, (b) PPIA, (c) HPRT1, (d) PAD2 and (e) PAD4.

In order for the comparative CT method to be valid the primer efficiencies of the target genes and reference (housekeeping) genes must be approximately equal (see section 2.2.3.5) (Livak and Schmittgen 2001). It is generally recommended that to use the comparative CT method, primer efficiencies must be within 5% of one another. The primer efficiencies of the target genes and housekeeping genes in this case were within 5% of one another, therefore it was decided that the comparative CT method could be used for analysis of qPCR data. Once the primer efficiencies had been determined, the baseline and CT thresholds were set for each primer-probe pair (Figure 2.14).

2.3.5 Modulation of gene expression by pro-inflammatory cytokines

The effects of pro-inflammatory cytokines on the modulation of PAD2 and PAD4 were investigated in the cells of the CNS following treatment for 24 and 48 hours with both single (IL-1 β , TNF- α , IL-6 and IFN- γ) and dual cytokines (IL-1 β + TNF- α , IL-1 β + IFN- γ , and TNF- α + IFN- γ). Following this, qPCR was carried out to determine the influence of these cytokines on the expression of PAD2 and PAD4. The data obtained was then transformed and quantified through the comparative CT method (see section 2.2.3.5) using normalisation against two suitable housekeeping genes (see section 2.2.3.8). Treatments were applied to wells in triplicate and cells pooled together for qPCR, which was performed in duplicate. Three independent experiments were carried out for each cell type in order to perform statistical analyses to compare treated to untreated control samples.

2.3.5.1 Basal expression of PAD2 and PAD4 in cells of the CNS

The $2^{-\Delta CT}$ values obtained for untreated control cells of the CNS (Figure 2.15) show that PAD2 is most highly expressed in astrocytes from MS case (MS16) ($2^{-\Delta CT}=0.111$), followed by considerably lower expression in control astrocytes (EP14) ($2^{-\Delta CT}=0.006$) and EP15 cells ($2^{-\Delta CT}=0.002$). CHME3 cells ($2^{-\Delta CT}=0.003$), hCMEC/D3 cells ($2^{-\Delta CT}=0.001$) and U373-MG cells ($2^{-\Delta CT}=0.0001$) all showed low levels of PAD2 expression. The $2^{-\Delta CT}$ values obtained for untreated control astrocytoma cell line, U373-MG, shows that PAD4 is expressed at a considerably lower level than PAD2 ($2^{-\Delta CT}=0.000005$). PAD4 was undetectable in all the primary human astrocytes tested (EP14, EP15, and MS16), therefore modulation of PAD4 following treatment with pro-inflammatory cytokines was not investigated in these cells.

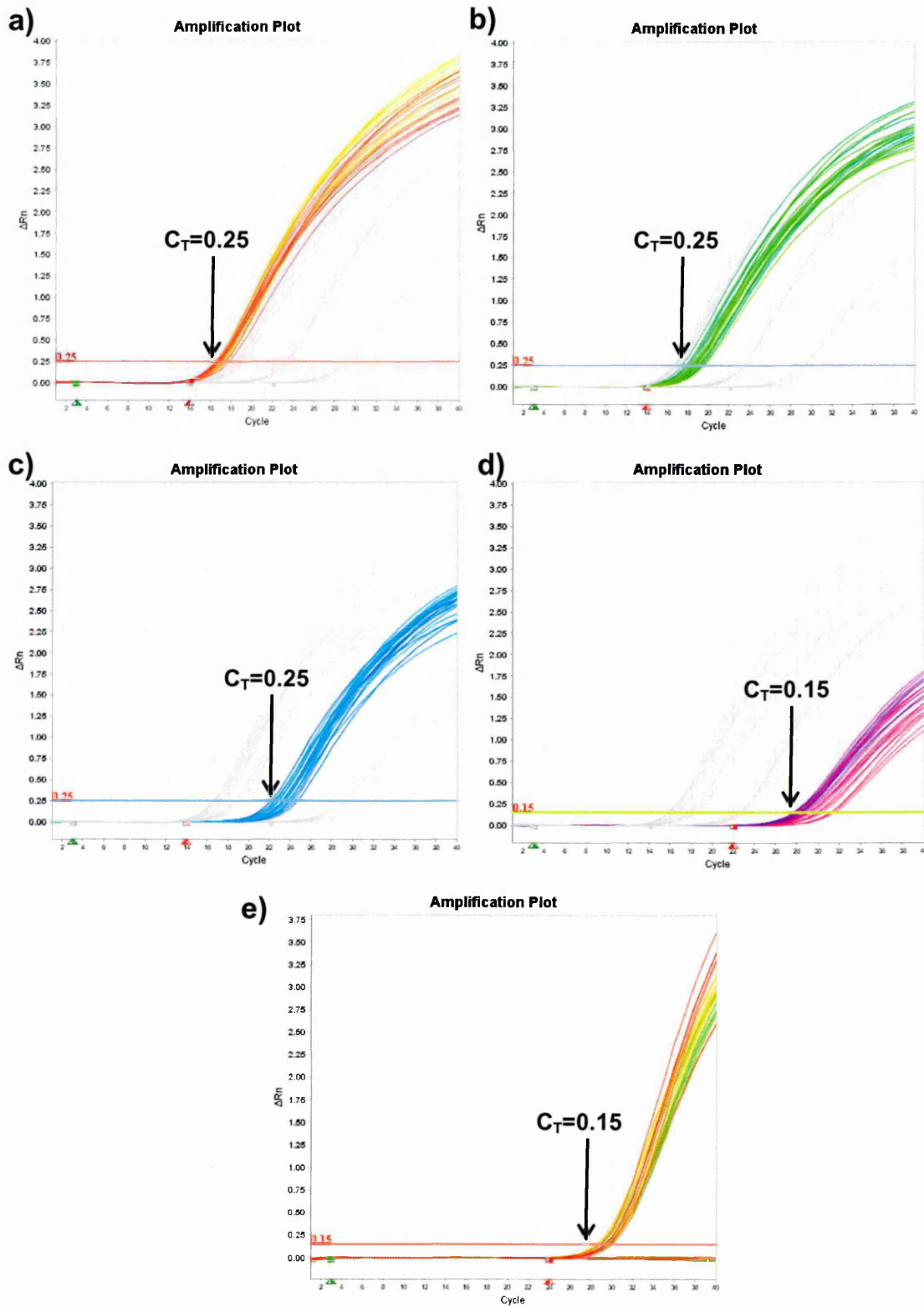


Figure 2.14: Amplification curves generated following qPCR of target and housekeeping genes. (a) GAPDH, (b) PPIA, (c) HPRT1, (d) PAD2 and (e) PAD4. C_T ; cycle threshold.

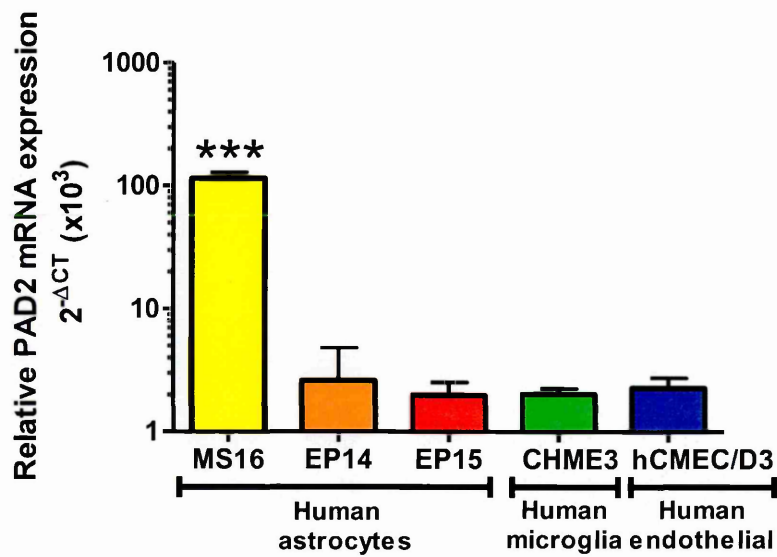


Figure 2.15: Basal expression of PAD2 mRNA in different preparations of primary human astrocytes, a human foetal microglial cell line (CHME3) and a human brain endothelial cell line (hCMEC/D3). Data presented as the mean ± SEM. Significant difference between MS16 and other cells tested is indicated, *** $p < 0.001$ (Kruskal-Wallis with Conover-Inman, $n = 21$).

2.3.5.2 U373-MG astrocytoma cell line

The expression of PAD2 in the astrocytoma cell line (U373-MG) was significantly down-regulated following treatment with IL-1 β , at 1, 10 and 100 ng/mL (4.7-fold ($P < 0.0001$), 3.2-fold ($p = 0.0002$) and 2.9-fold ($p = 0.0006$), respectively) (Figure 2.16a). Treatment with IL-1 β resulted in down-regulation of PAD4, but this only reached weak statistical significance at 1 ng/mL (1.8-fold ($p = 0.0468$)). A concentration-dependent decrease in PAD2 expression was observed following TNF- α treatment, with statistical significance reached at 10 and 100 ng/mL compared to control (2.3-fold and 3.6-fold ($p = 0.0052$ and $p = 0.0009$) respectively). Down-regulation of PAD4 was observed following treatment with 100 ng/mL TNF- α , however, statistical significance was not reached. Down-regulation of PAD2 and PAD4 was observed following treatment with 100 ng/mL IL-6, however, this was not significant. Treatment with IFN- γ resulted in a significant down-regulation at 1, 10 and 100 ng/mL (1.7-fold, 3.0-fold and 5.2-fold ($p = 0.0243$, $p = 0.002$ and $p = 0.0002$), respectively). Similarly, PAD4 was also down-regulated following treatment with IFN- γ , resulting in statistical significance at 1, 10 and 100 ng/mL (2.1-fold, 2.9-fold and 3.2-fold ($p = 0.0125$, $p = 0.0157$ and $p = 0.0125$), respectively).

Unlike at 24 hours, treatment with IL-1 β for 48 hours in the astrocytoma cell line (U373-MG) cells showed down-regulation at 1 and 100 ng/mL and statistical significance was reached (Figure 2.16b). Treatment with IL-1 β did not alter the expression of PAD4 at 48 hours, which was similar to the pattern observed at 24 hours. TNF- α treatment for 48 hours resulted in a concentration-dependent decrease in the expression of PAD2, with statistical significance obtained at 10 and 100 ng/mL (1.2-fold and 2.3-fold ($p = 0.0455$ and $p = 0.0033$), respectively).

Similar to 24 hours, treatment with TNF- α for 48 hours resulted in a decrease in PAD4 expression at 100 ng/mL (2.2-fold ($p = 0.0108$)). The expression of PAD2 did not alter following treatment with IL-6 for 48 hours, whereas PAD4 showed a concentration-dependent decrease with statistical significance reached at 100 ng/mL (2.0-fold ($p = 0.0157$)) which is similar to results from 24 hour treatment. Treatment with IFN- γ for 48 hours resulted in a concentration-dependent down-regulation in the expression of PAD2 similar to the pattern observed at 24 hours, with statistical significance at 10 and 100 ng/mL (4.2-fold and 8.4-fold ($p = 0.0017$ and $p = 0.0002$), respectively). PAD4 down-regulation was also observed following treatment with IFN- γ , with statistical significance reached at 10 and 100 ng/mL (2.9-fold and 2.7-fold ($p = 0.0053$ and $p = 0.0091$), respectively), which is similar to the pattern observed at 24 hours.

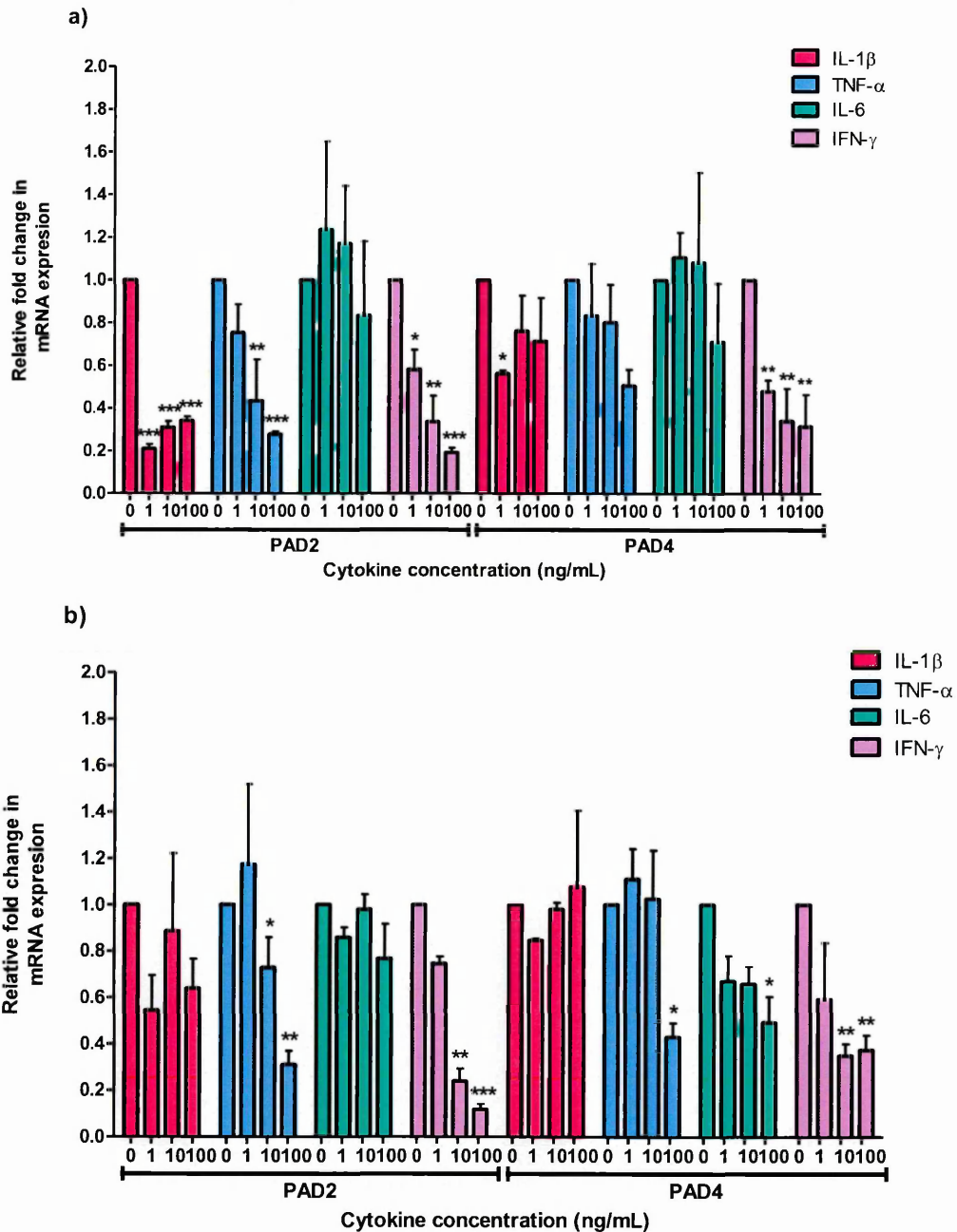


Figure 2. 16: Relative fold change in mRNA levels of PAD2 and PAD4 in U373-MG astrocytoma cells following cytokine treatment. Cells were treated with varying concentrations of IL-1 β , TNF- α , IL-6 and IFN- γ for **(a)** 24 hours and **(b)** 48 hours. Data presented as the mean \pm SEM. Significant difference from control, * p < 0.05, ** p < 0.01, *** p < 0.001 (Kruskal-Wallis with Conover-Inman, $n=3$).

2.3.5.3 Primary astrocytes derived from normal white matter (EP14 and EP15)

IL-1 β treatment resulted in down-regulation of PAD2 expression in primary human astrocytes (EP14 and EP15), with significance reached at 1 and 10 ng/mL compared to untreated control cells (5.60-fold ($p=0.0157$) and (4.36-fold ($p=0.0216$), respectively) (Figure 2.17a). Treatment with TNF- α resulted in down-regulation of PAD2 expression at all concentrations tested, however, statistical significance was only reached at 10 ng/mL where there was a 6.4-fold decrease in PAD2 ($p=0.0163$). Statistical significance was not reached at 1 and 100 ng/mL. Down-regulation of PAD2 expression was also observed following treatment with IL-6 at 1 and 10 ng/mL, although statistical significance was only reached at 10 ng/mL (3.8-fold ($p=0.0483$)). Treatment with IFN- γ resulted in an apparent down-regulation of PAD2 expression at 10 and 100 ng/mL, although statistical significance was not reached.

Treatment of primary human astrocytes (EP14 and EP15) with IL-1 β and TNF- α at 1ng/mL resulted in a 1.5-fold increase in PAD2 expression, however, a 1.6-fold and 2.7-fold decrease in PAD2 expression was observed at 10 and 100 ng/mL, respectively, although not statistically significant (Figure 2.17b). Down-regulation of PAD2 was observed following treatment with IL-1 β and IFN- γ with statistical significance reached at 10 and 100 ng/mL compared to control (1.6-fold ($P=0.0002$ and 2.7-fold ($p=0.0023$), respectively). A concentration-dependent decrease in PAD2 expression was observed following treatment with 1, 10 and 100 ng/mL TNF- α and IFN- γ , with statistical significance reached at 10 and 100 ng/mL (7.3-fold ($p=0.217$) and 34.7 ($p=0.009$), respectively).

2.3.5.4 Primary astrocytes derived from white matter from a case of MS (MS16)

Treatment of primary human astrocytes (MS16) with IL-1 β resulted in significant down-regulation of PAD2 expression at 1, 10 and 100 ng/mL compared to control (5.2-fold ($p=0.0046$), 3.2-fold ($p=0.0098$) and 3.6-fold ($p=0.0142$), respectively) (Figure 2.18a). A concentration-dependent decrease in PAD2 expression was observed following TNF- α treatment with statistical significance reached at 1, 10 and 100 ng/mL compared to control (4.5-fold ($p=0.004$), 5.4-fold ($p=0.0013$) and 7.5-fold ($p=0.0005$), respectively). IL-6 treatment did not affect the expression of PAD2 compared to control. Treatment with IFN- γ resulted in a concentration-dependent decrease in the expression of PAD2 resulting in significant down-regulation at 100 ng/mL (4.2-fold ($p=0.0242$)).

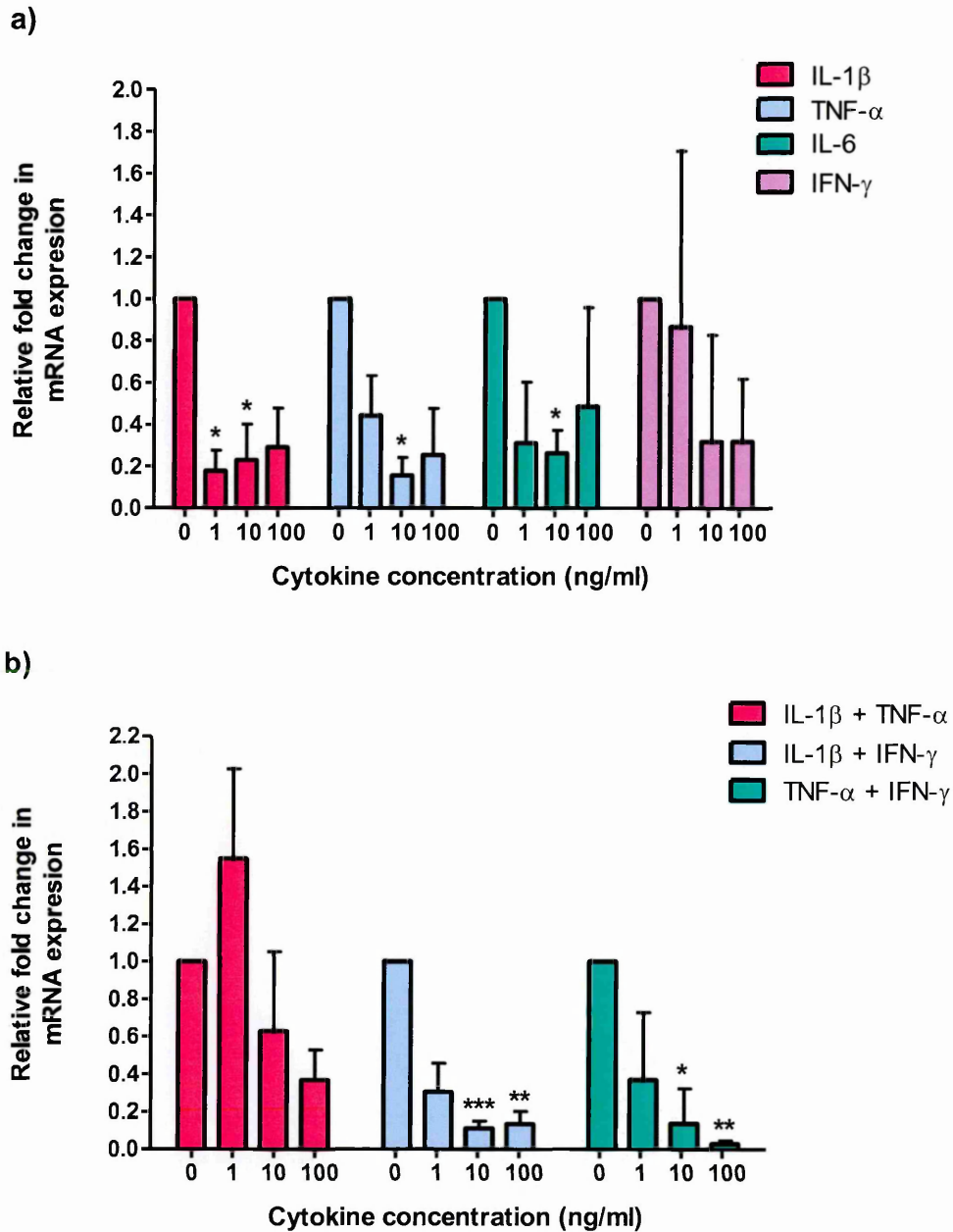
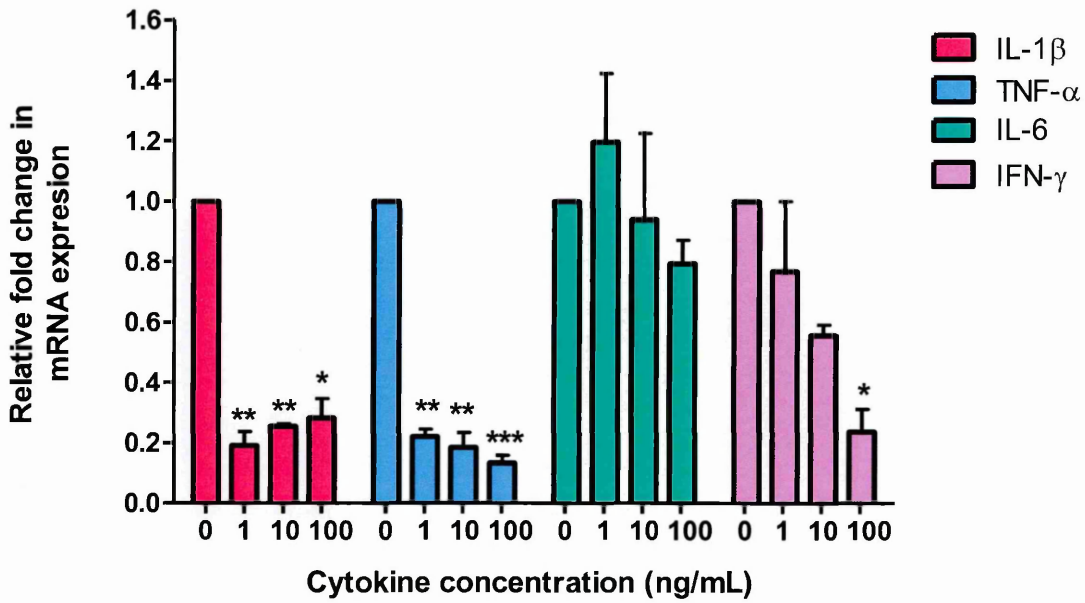


Figure 2.17: Relative fold change in mRNA levels of PAD2 in primary astrocytes from two control cases (EP14 and EP15) following cytokine treatment. Cells were treated for 24 hours with varying concentrations (0, 1, 10 and 100 ng/mL) of **(a)** single cytokines IL-1 β , TNF- α , IL-6 and IFN- γ , and **(b)** dual cytokines IL-1 β + TNF- α , IL- β + IFN- γ , and TNF- α + IFN- γ . Data presented as the mean \pm SEM. Significant difference from control, * p < 0.05, ** p < 0.01, *** p < 0.001 (Kruskal-Wallis with Conover-Inman, $n=3$).

a)



b)

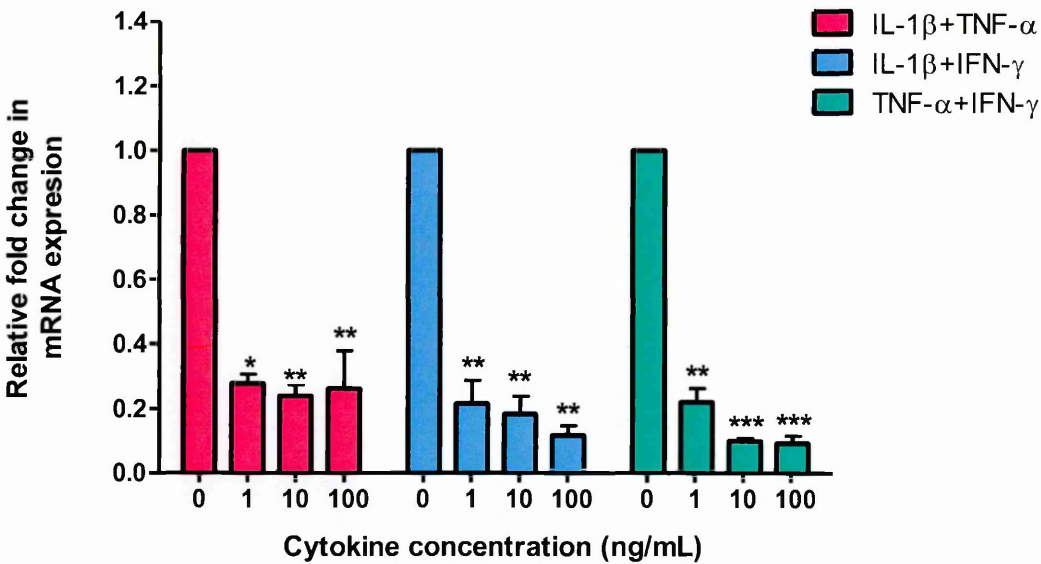


Figure 2.18: Relative fold change in mRNA levels of PAD2 in primary astrocytes from an MS case (MS16) following cytokine treatment. Cells were treated for 24 hours with varying concentrations (0, 1, 10 and 100 ng/mL) of (a) single cytokines IL-1 β , TNF- α , IL-6 and IFN- γ , and (b) dual cytokines IL-1 β + TNF- α , IL- β + IFN- γ , and TNF- α + IFN- γ . Data presented as the mean \pm SEM. Significant difference from control, * $p < 0.05$, ** $p < 0.01$, *** $p < 0.001$ (Kruskal-Wallis with Conover-Inman, $n=3$).

Co-treatment of primary human astrocytes (MS16) with IL-1 β and TNF- α resulted in significant down-regulation of PAD2 expression at 1, 10 and 100 ng/mL compared to control (3.6-fold ($p=0.0115$), 4.2-fold ($p=0.0024$) and 3.8-fold ($p=0.0079$), respectively) (Figure 2.18b). Significant concentration-dependent down-regulation of PAD2 expression was observed following co-treatment with IL-1 β and IFN- γ at 1, 10 and 100 ng/mL compared to control (4.7-fold ($p=0.0099$), 5.5-fold ($p=0.0036$) and 8.6-fold ($p=0.001$), respectively). Co-treatment with TNF- α and IFN- γ resulted in significant down-regulation in PAD2 expression at 1, 10 and 100 ng/mL (4.55-fold ($p=0.0036$), 10.1-fold ($p=0.0003$) and 10.8-fold ($p=0.0002$), respectively).

2.3.5.5 CHME3 human foetal microglial cell line

Down-regulation of PAD2 expression was observed following treatment of CHME3 cells with 1, 10 and 100 ng/mL IL-1 β , with statistical significance reached at 10 and 100 ng/mL (2.0-fold ($p=0.0014$) and 1.9-fold ($p=0.0029$), respectively) (Figure 2.19a). A significant concentration-dependent decrease in the expression of PAD2 was observed following treatment with TNF- α (1.6-fold ($p=0.0311$), 2.4-fold ($p=0.001$) and 3.2-fold ($p=0.0001$), respectively). Down-regulation of PAD2 expression was observed following treatment with IL-6 and IFN- γ alone, but the decreases were not significant.

A concentration-dependent decrease in PAD2 expression following co-treatment of CHME3 cells with IL-1 β and TNF- α was observed at all concentrations tested, with significance reached at 1, 10 and 100 ng/mL compared to control (1.9-fold ($p=0.0118$), 2.8-fold ($p=0.0009$) and 3.6-fold ($p=0.0005$), respectively) (Figure 2.19b). A significant down-regulation in PAD2 expression was observed following co-treatment with 1, 10 and 100 ng/mL IL-1 β and TNF- α compared to control (1.6-fold ($p=0.0133$), 2.5-fold ($p=0.0002$) and 2.2 ($p=0.0004$), respectively). Significant concentration-dependent down-regulation in the expression of PAD2 was observed following co-treatment with TNF- α and IFN- γ at 1, 10, and 100 ng/mL compared to control (2.6-fold ($p=0.0006$), 3.4-fold ($p=0.0003$) and 5.8-fold ($p<0.0001$), respectively).

Treatment of CHME3 with IL-4 induced a non-significant up-regulation of PAD2 expression at 1 and 10 ng/mL, with down-regulation observed at 100 ng/mL (Figure 2.19c). Treatment with IL-10 resulted in down-regulation of PAD2 at 10 and 100 ng/mL, but statistical significance was not reached. A concentration-dependent decrease in PAD2 expression was observed following treatment with TGF- β resulting in significant down-regulation at 1, 10 and 100 ng/mL compared to control (1.9-fold ($p=0.0289$), 2.2-fold ($p=0.0013$) and 4.0-fold ($p=0.0002$), respectively).

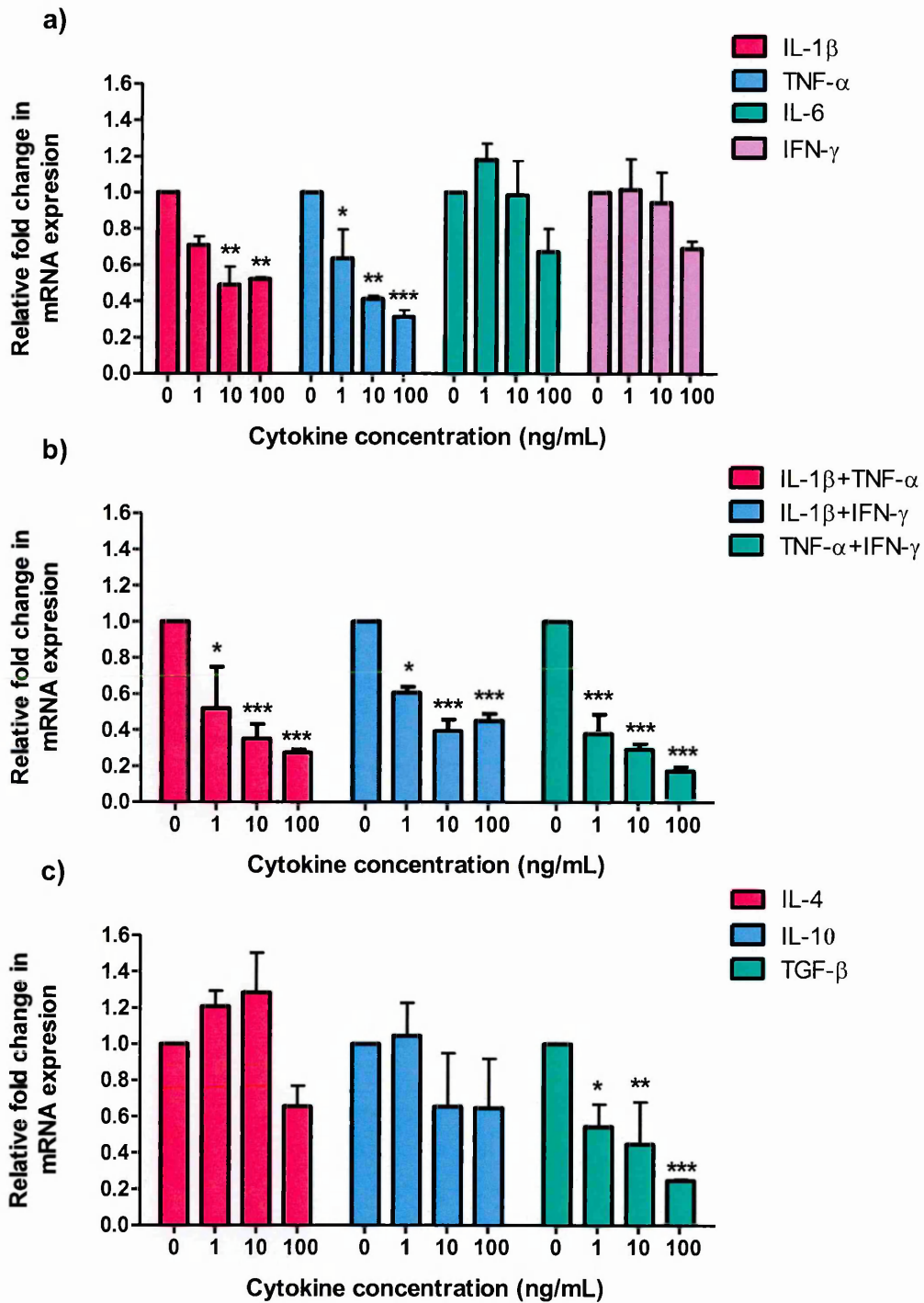


Figure 2.19: Relative fold change in mRNA levels of PAD2 in CHME3 following cytokine treatment. Cells were treated for 24 hours with varying concentrations (0, 1, 10 and 100 ng/mL) of **(a)** single cytokines IL-1 β , TNF- α , IL-6 and IFN- γ , **(b)** dual cytokines IL-1 β + TNF- α , IL- β + IFN- γ , and TNF- α + IFN- γ , and **(c)** single cytokines IL-4, IL-10 and TGF- β . Data presented as the mean \pm SEM. Significant difference from control, * p < 0.05, ** p < 0.01, *** p < 0.001 (Kruskal-Wallis with Conover-Inman, $n=3$).

2.3.5.6 hCMEC/D3 brain endothelial cell line

IL-1 β and IFN- γ treatment of the brain endothelial cell line (hCMEC/D3) did not alter the expression of PAD2 (Figure 2.20a). However, a concentration-dependent decrease in the expression of PAD2 was observed following treatment with TNF- α , although statistical significance was only reached at 100 ng/mL (6.6-fold ($p=0.036$)). Treatment with IL-6 resulted in a concentration-dependent non-significant decrease in the expression of PAD2.

A concentration-dependent decrease in the expression of PAD2 in hCMEC/D3 was observed following co-treatment with IL-1 β and TNF- α reaching statistical significance at 100 ng/mL (5.6-fold ($p=0.0424$)) (Figure 2.20b). Co-treatment with IL-1 β and IFN- γ resulted in a non-significant down-regulation of PAD2 at 10 and 100 ng/mL. A statistically significant decrease in the expression of PAD2 was observed following co-treatment with TNF- α and IFN- γ at 1, 10 and 100 ng/mL (4.3-fold ($p=0.0018$), 4.1-fold ($p=0.0274$) and 9.2-fold ($p=0.0052$), respectively).

2.3.6 Standard PCR of PAD4

Due to the inability to detect PAD4 mRNA in primary human astrocytes using qPCR, standard PCR was carried to confirm whether absence of PAD4 was due to a polymorphism preventing primers binding in qPCR or due to no PAD4 gene expression in these cells. Following optimisation of the standard PCR protocol, primer set 2 (Table 2.3) was used for the detection of PAD4. Standard PCR confirmed a product of 600 base pairs in the U373-MG astrocytoma cell line indicating presence of the PAD4 gene expression, whereas no product was found in the EP14 primary human astrocytes indicating the absence or undetectable levels of PAD4 gene expression (Figure 2.21).

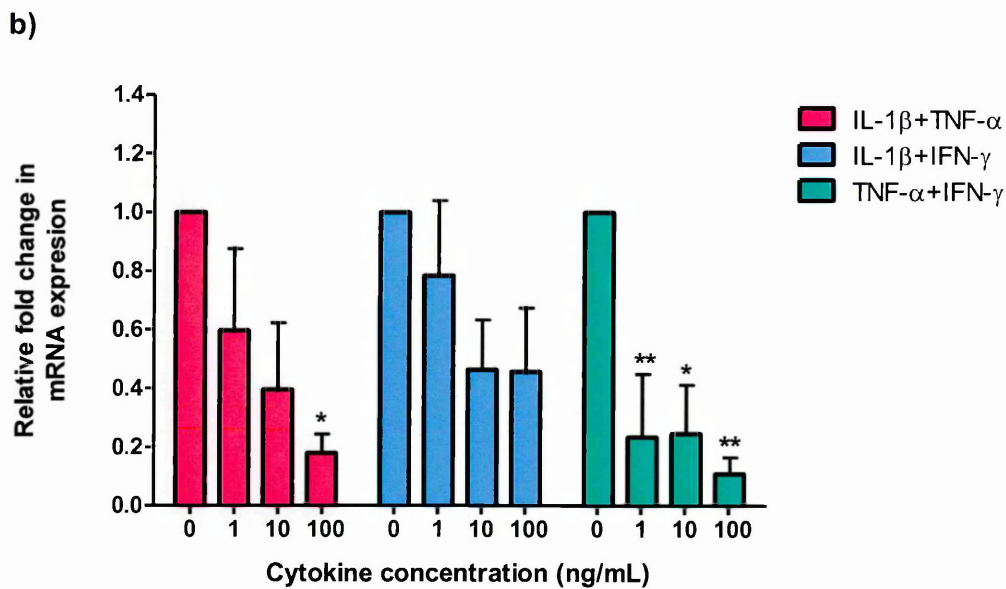
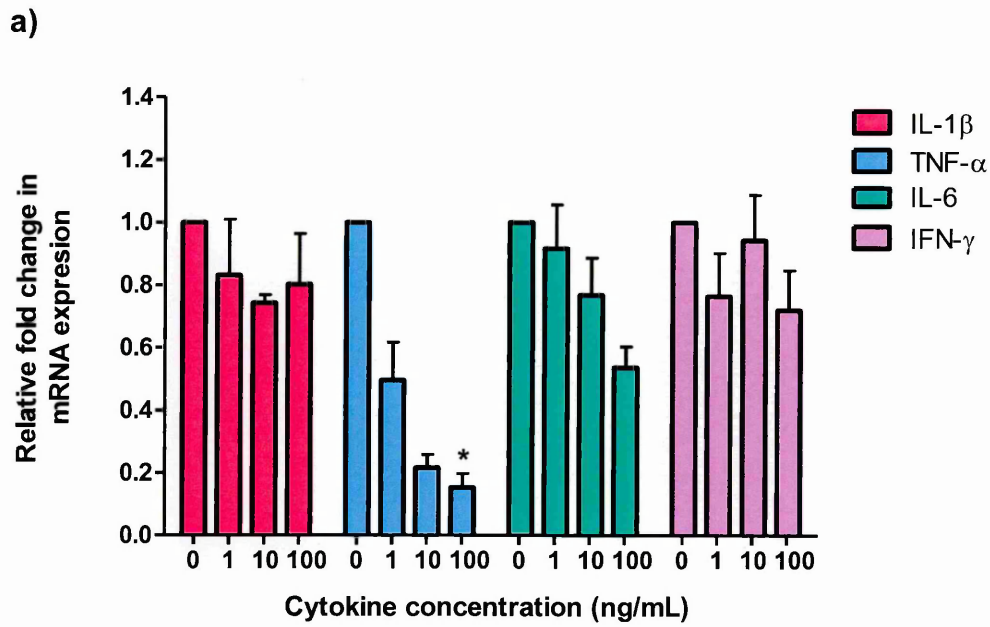


Figure 2.20: Relative fold change in mRNA levels of PAD2 in hCMEC/D3 endothelial cells following cytokine treatment. Cells were treated for 24 hours with varying concentrations (0, 1, 10 and 100 ng/mL) of (a) single cytokines IL-1 β , TNF- α , IL-6 and IFN- γ , and (b) dual cytokines IL-1 β and TNF- α , IL-1 β and IFN- γ , and TNF- α and IFN- γ . Data presented as the mean \pm SEM. Significant difference from control, * p < 0.05, ** p < 0.01, *** p < 0.001 (Kruskal-Wallis with Conover-Inman, $n=3$).

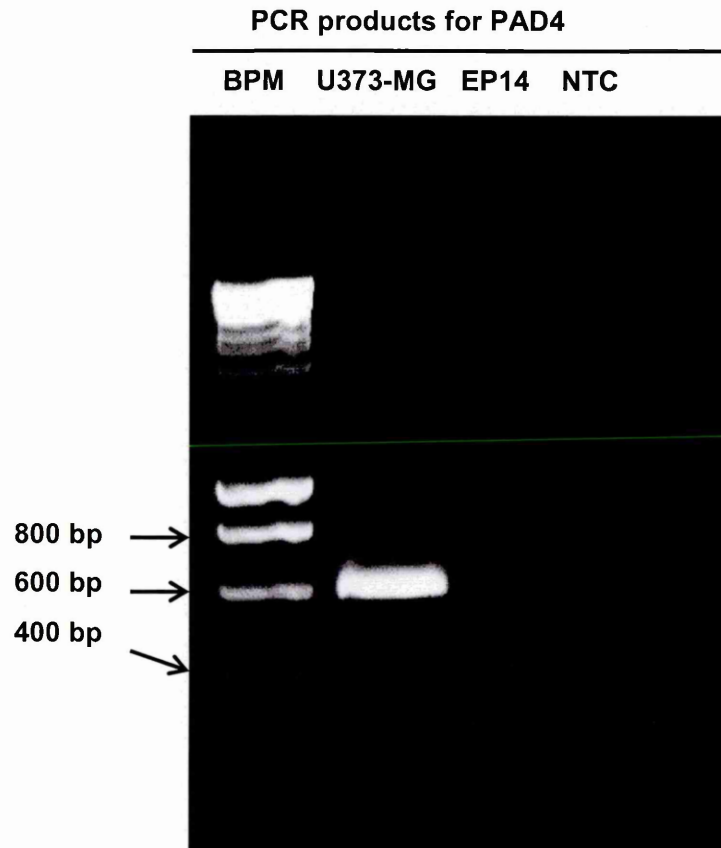


Figure 2.21: Agarose gel electrophoresis of standard PCR products. The presence of PAD4 in U373-MG cells (600 bp) and absence in EP14 cells is observed. BPM; base pair marker, NTC; no template control.

2.3.7 Immunocytochemical detection of PAD2 and PAD4

ICC was performed on astrocytes (EP14, EP15) and U373-MG cells in order to identify the cellular localisation of PAD2 and PAD4 following fixation in acetone to enable the intracellular localisation of astrocyte-specific markers (GFAP and S-100 β) and PAD2 and PAD4 (Figures 2.22 and 2.25).

Negative controls were also performed whereby the primary antibody was omitted. Fluorescence microscopy demonstrated characteristic staining of both the processes and cell bodies of astrocytes in EP14 cells with an anti-GFAP and anti-S100 β antibody (Figure 2.22 a, b).

PAD2 showed strong cytoplasmic staining in EP14, EP15 and U373-MG cells (Figure 2.23 a-c). PAD4 demonstrated weaker cytoplasmic staining and more intense nuclear staining in EP14, EP15 and U373-MG cells (Figure 2.24 a-c). A second PAD4 antibody was also tested using acetone and ethanol as fixatives, which showed weak cytoplasmic staining (Figure 2.25 a, b).

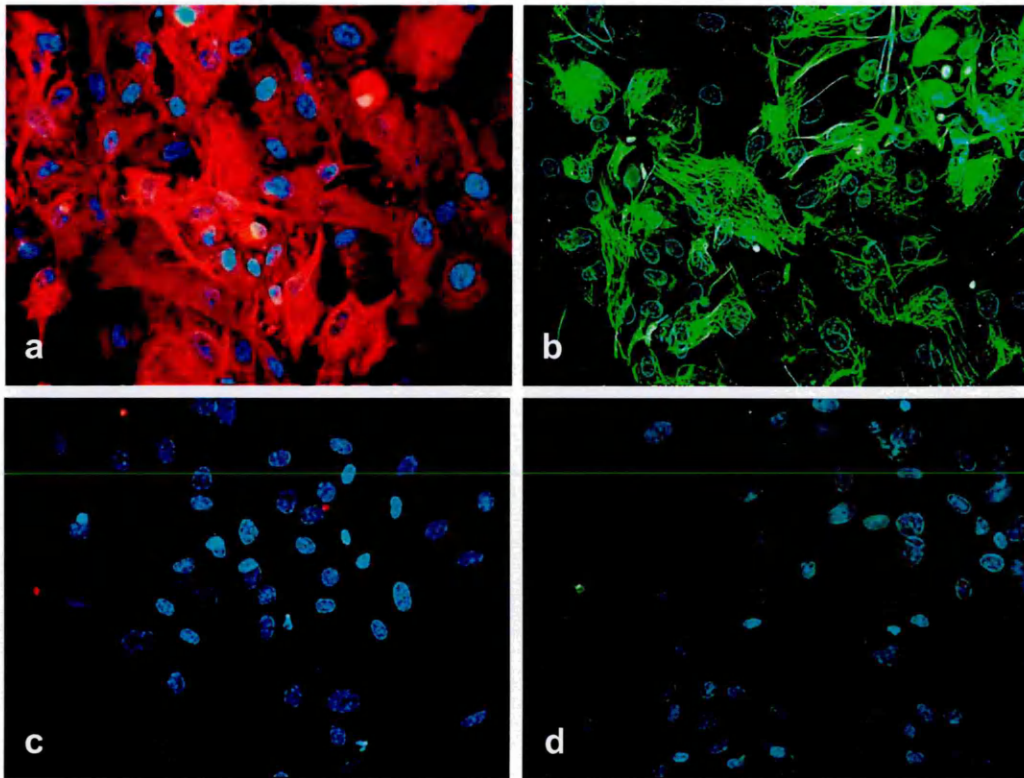


Figure 2.22: Single label immunofluorescence for GFAP and S-100 β in EP14 primary human astrocytes. Cells were fixed in acetone and labelled for **(a)** GFAP using primary polyclonal rabbit anti-human GFAP antibody and secondary antibody Alexa fluor 568 goat anti-rabbit IgG, **(b)** S-100 β using primary monoclonal mouse anti-human S-100 β antibody and secondary antibody FITC goat anti-mouse IgG, **(c)** negative control with secondary Alexa fluor 568 goat anti-rabbit IgG alone, and **(d)** negative control with secondary FITC goat anti-mouse antibody alone. Nuclei were counterstained with DAPI (x400 magnification).

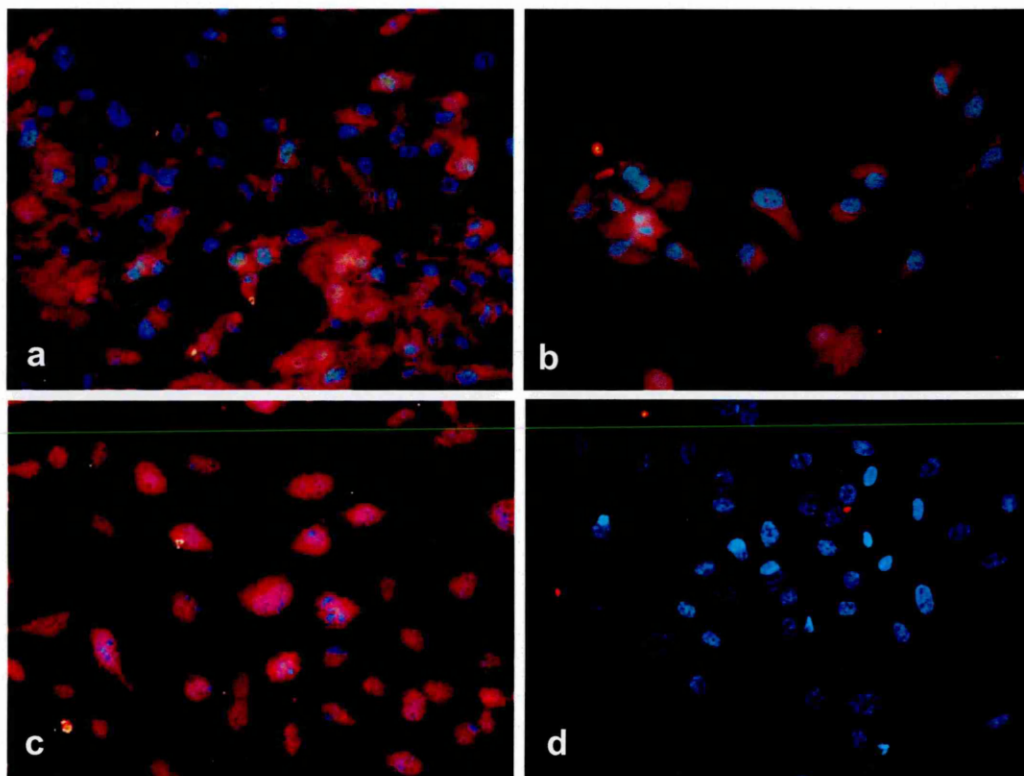


Figure 2.23: Single label immunofluorescence for PAD2 in different preparations of primary human astrocytes and an astrocytoma cell line. Cells were fixed in acetone and labelled for PAD2 using primary polyclonal rabbit anti-human PAD2 antibody and secondary Alexa fluor 568 goat anti-rabbit IgG in **(a)** EP14, **(b)** EP15, **(c)** U373-MG and **(d)** negative control with secondary antibody only. Nuclei were counterstained with DAPI (x400 magnification).

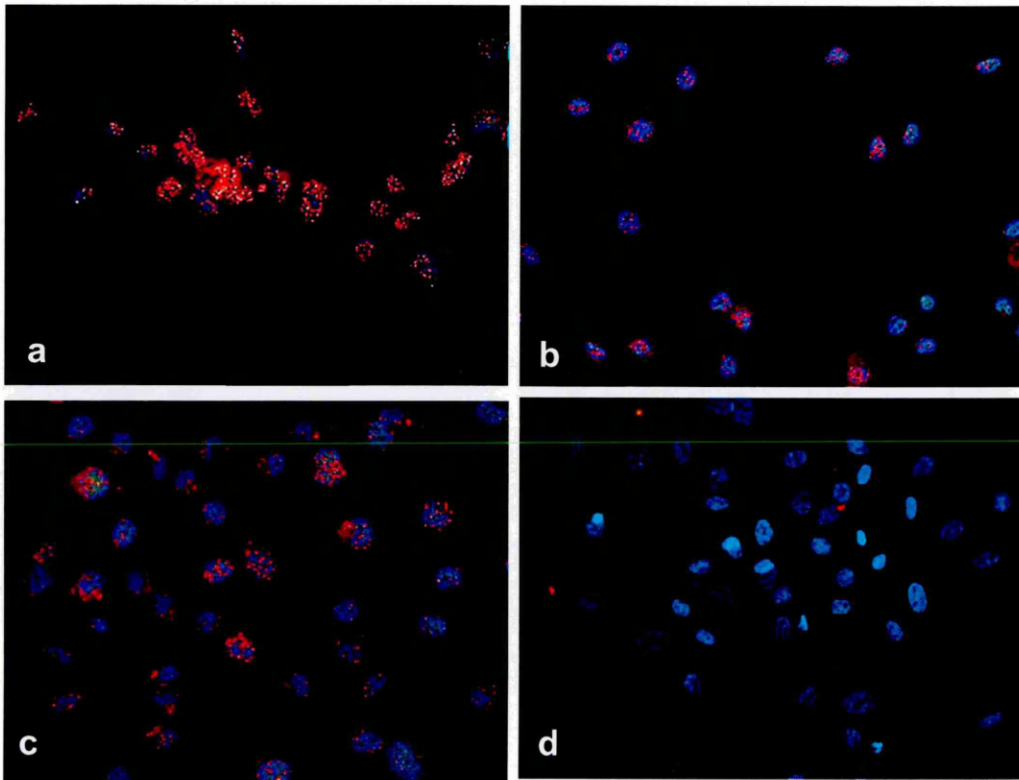


Figure 2.24: Single label immunofluorescence for PAD4 in different preparations of primary human astrocytes and an astrocytoma cell line. Cells were fixed in acetone and labelled for PAD4 using primary polyclonal rabbit anti-human PAD4 antibody and secondary Alexa fluor 568 goat anti-rabbit IgG in **(a)** EP14, **(b)** EP15, **(c)** U373-MG and **(d)** negative control with secondary antibody only. Nuclei were counterstained with DAPI (x400 magnification).

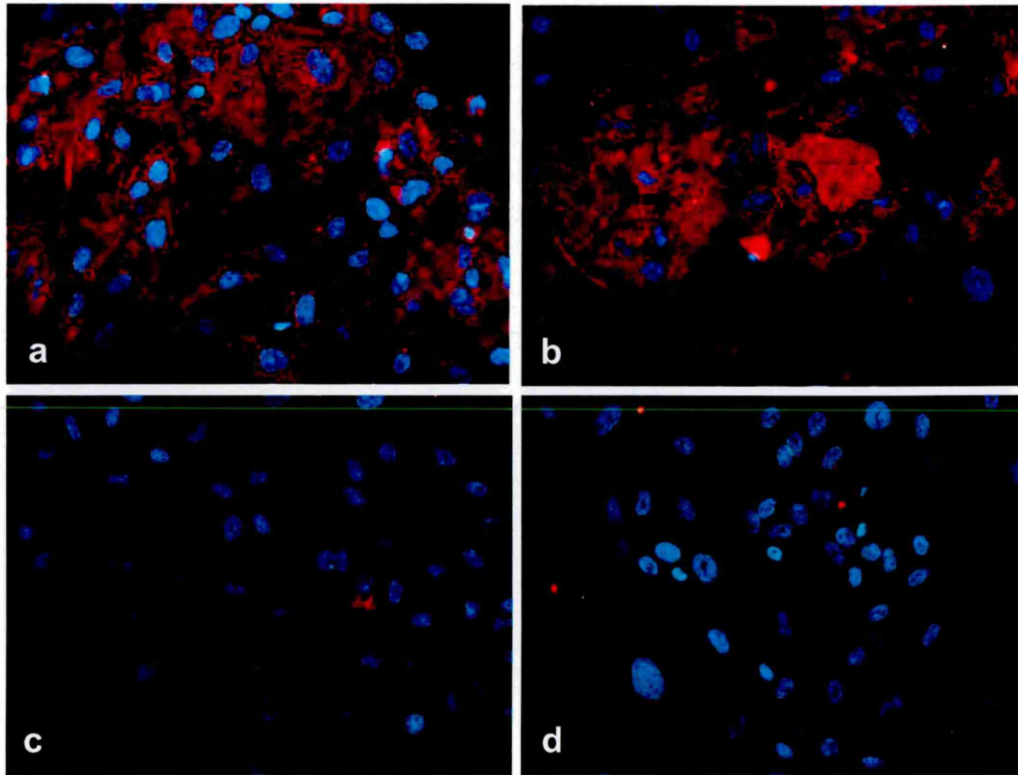


Figure 2.25: Single label immunofluorescence for PAD4 using a different primary antibody from Sigma, UK in EP14 primary human astrocytes. Cells were labelled for PAD4 using primary monoclonal mouse anti-human PAD4 antibody and secondary Alexa fluor 568 goat anti-mouse IgG following fixation with **(a)** ethanol, **(b)** acetone, and negative controls with secondary antibody only following fixation with **(c)** ethanol, and **(d)** acetone. Nuclei were counterstained with DAPI (x400 magnification).

2.4 Discussion

2.4.1 IL-1 β , TNF- α , IL-6 and IFN- γ differentially affect cellular proliferation in an astrocytoma cell line, primary human astrocytes, microglial cell line and brain endothelial cell line

Preliminary qPCR results showed down-regulation of PAD2 mRNA following cytokine treatment, therefore the effect of cytokines on the viability of cells was investigated to ensure this down-regulation was not due to significant cell death occurring in response to cytokine treatment. MS16 showed greater proliferation following treatment with single pro-inflammatory cytokines compared to normal astrocytes, EP14 and EP15 (Table 2.7). The astrocytoma cell line, U373-MG, showed a decrease in viable cells. A previous study, using qPCR, has shown that both U373-MG and primary human astrocytes prepared from patients with epilepsy constitutively express mRNA encoding the IFN- γ receptor (IFNGR). However, using post-mortem brain tissue from a patient with MS, strong up-regulation of IFNGR on activated astrocytes in affected areas in MS was seen compared to U373-MG and astrocytes extracted from patients with epilepsy (Hashioka *et al.*, 2009). Therefore, this increased proliferation in MS16 may be due greater sensitivity of these cells to IFN- γ as a result of up-regulated expression of cytokine receptors on astrocytes in MS tissue. Although there are no studies reporting differences in receptor expression for IL-1 β and TNF- α in astrocytes prepared from individuals with MS compared to controls, it could be hypothesised that these cytokine receptors may also be up-regulated in MS16. However, due to the astrocytes in this study being isolated from only one MS case and two control cases, it is difficult to make any firm conclusions, and more astrocyte preparations from a larger number of MS and control cases would have to be investigated. Furthermore, co-treatment with pro-inflammatory cytokines showed significant additive increases in proliferation of both MS16 and EP15 primary human astrocytes.

Single cytokine treatments caused some reduction in the percentage of viable cells in the human foetal microglia cell line, CHME3. Previous studies have shown microglia to express receptors for IL-1, IL-6 and TNF- α (Lee *et al.*, 2002). Co-treatment with TNF- α + IFN- γ resulted in a further additive reduction in the percentage of viable cells, whereas co-treatments with either IL-1 β + TNF- α or IL-1 β + IFN- γ did not affect the cell viability. Treatment with anti-inflammatory cytokines IL-4, IL-10 and TGF- β did not affect the proliferation or viability of CHME3 cells. Single-cytokine treatments did not affect the proliferation or viability of human brain endothelial cell line, hCMEC/D3, except following treatment with TNF- α which resulted in a small decrease in the

percentage of viable cells. Co-treatments with IL-1 β + TNF- α and TNF- α + IFN- γ resulted in a similar reduction in the percentage of viable cells. This reduction was no greater than TNF- α alone, indicating only TNF- α is exerting an effect on cell viability. This suggests that hCMEC/D3 cell lines are only sensitive to TNF- α .

The use of housekeeping genes in subsequent qPCR experimental results enables any differences in cell number to be accounted for when quantifying the mRNA levels of PAD2 and PAD4 genes, as data is expressed relative to HK gene level.

2.4.2 IL-1 β , TNF- α and IFN- γ differentially modulate the gene expression of PAD2 and PAD4 in an astrocytoma cell line, primary human astrocytes, microglial cell line and brain endothelial cell line

In this present study, following optimisation and validation of the qPCR method for detection of PAD2 and PAD4, it was found that PAD2 was constitutively expressed in an astrocytoma cell line, primary human astrocytes, a human foetal microglial cell line and a human adult brain endothelial cell line. This agreed with previous immunocytochemical studies which have shown expression of PAD2 in glial cells (Akiyama *et al.*, 1990), in particular microglia (Vincent *et al.*, 1992; Asaga *et al.*, 2002; Asaga and Ishigami 2007) and astrocytes (Vincent *et al.*, 1992; Asaga and Senshu 1993; Asaga and Ishigami 2000; Asaga *et al.*, 2001). This is the first study to report the expression of PAD2 mRNA in brain endothelial cells.

The most prominent initial finding was that the basal expression of PAD2 mRNA was significantly higher in primary human astrocytes isolated from the NAWM of an MS post-mortem case (MS16) than primary human astrocytes isolated from brains following a temporal lobectomy for the treatment of epilepsy (EP14 and EP15), and also compared to expression in the human foetal microglial and human brain endothelial cell lines. This higher level of PAD2 gene expression in astrocytes extracted from a patient with MS is not surprising, as previous studies have shown increased PAD2 activity in patients with MS compared to control individuals (Wood *et al.*, 2008), although this is the first study to show PAD2 mRNA expression is specifically increased in the astrocytes of an MS patient. However, this result should be considered with caution due to these cells being isolated from one MS case. For the result to be validated further studies would have to be carried to determine the basal expression of PAD2 mRNA in astrocytes extracted from the NAWM of a number of MS CNS cases, and other factors controlled for such as death to autopsy interval time, age and sex of the patient etc. This increase in basal PAD2 mRNA expression in MS16 may be due to hypoxia of the post-mortem brain tissue prior to extraction of the

astrocytes which has been shown to raise intracellular calcium levels resulting in increased expression of PAD2 mRNA (Sambandam *et al.*, 2004). In comparison, EP14 and EP15 primary human astrocyte preparations are extracted from living individuals undergoing surgery for treatment of epilepsy, and therefore would not be exposed to hypoxia to the same extent.

Initial experiments showed that PAD4 mRNA could only be detected in the astrocytoma cell line, U373-MG, and was undetectable in primary human astrocytes, EP14 and EP15. Due to the PAD4 gene being highly polymorphic, it was initially thought that the reason for this may be that the primary human astrocytes contained a polymorphism in the PAD4 gene which was preventing the original PAD4 primers from being able to bind and therefore amplify the PAD4 gene. Single nucleotide polymorphisms in the PAD4 gene are associated with the autoimmune disease RA (Suzuki *et al.*, 2003). Therefore a further two primer and probe sets were tested covering different exon boundaries to see if amplification of PAD4 occurred using different primer sets, targeting a different region of the PAD4 gene. However, the PAD4 gene was still undetectable in primary human astrocytes. Lastly, standard PCR was carried out to amplify a larger portion of the PAD4 mRNA to determine if PAD4 was present at the mRNA level. Using U373-MG as a positive control, results showed that U373-MG expressed the PAD4 gene which was indicated by a product at 600 base pairs whereas again, this PAD4 product was undetectable in primary human astrocytes (EP14). This confirmed that PAD4 was either absent or not expressed at a level detectable using qPCR or standard PCR in the primary human astrocytes. It was not surprising that PAD4 was expressed at a high enough level to be detected by qPCR in the astrocytoma cell line, as previous studies have shown PAD4 to be significantly expressed in various cancers but not in corresponding normal tissues (Chang and Han 2006; Wang *et al.*, 2010). Chang *et al.* (2006) were able to show moderate expression of PAD4 at the protein level in human brain astrocytoma cells compared to no expression in normal tissues. Previous studies have shown PAD4 to be predominantly expressed by white blood cells, in particular neutrophils (Asaga *et al.*, 2001), macrophages and monocytes (Vossenaar and van Venrooij 2004; Vossenaar *et al.*, 2004). Therefore, it was not surprising that PAD4 was not detected in primary human astrocytes.

Immunocytochemistry confirmed the expression of PAD2 protein in the astrocytoma cell line, U373-MG and the three different preparations of primary human astrocytes (EP14, EP15 and MS16). However, contrary to the qPCR findings in the present study, where no PAD4 mRNA was identified in the primary human astrocytes, the PAD4 protein was found to be expressed in all preparations of primary human astrocytes

(EP14, EP15 and MS16). PAD2 showed positive diffuse staining in the cytoplasm, whereas PAD4 showed strong punctate nuclear staining. This pattern of staining was expected as PAD4 is the only PAD to carry a nuclear localisation signal to translocate it to the nucleus of a cell (Nakashima *et al.*, 2002). However, a recent study has also shown PAD2 to be present in the nucleus (Jang *et al.*, 2011). In the present study, the conflicting data from qPCR and immunocytochemical studies does not allow for clear conclusions to be drawn. The staining was not caused by non-specific staining of the secondary antibody, as the negative control cells showed no positive staining. The staining pattern of PAD4 seemed specific to nuclear proteins, which was expected, as PAD4 is known to reside in the nucleus and is involved in the citrullination of histones (Hagiwara *et al.*, 2002; Nakashima *et al.*, 2002; Cuthbert *et al.*, 2004; Wang *et al.*, 2004).

In terms of reliability of the qPCR data the PAD4 primer-probes are validated by the supplier, ABI, however, in-house validation by target detection would have been useful to confirm the reliability of the procedure. However, the fact that the PAD4 gene was also not detected in the primary human astrocytes using standard PCR whereas the astrocytoma cell line as a positive control, where a band corresponding to PAD4 appeared at 600 base pairs, further confirms the absence of PAD4 mRNA in primary human astrocytes. The correlation between mRNA and protein expression is not always invariant, and Gygi *et al.*, (1999) described how mRNA is an insufficient predictor of protein expression. Post-transcriptional mechanisms controlling the translation rate of the proteins, the half-lives of specific mRNAs or proteins, and the intracellular location and molecular association of the protein products may all contribute to the disparity between mRNA and protein quantification (Gygi *et al.*, 1999). Through isolation of PBMCs from the peripheral blood of patients with RA and controls followed by differentiation of monocytes into macrophages, Vossenaar *et al.* (2004) has shown the presence of PAD4 protein in the absence of PAD4 mRNA in macrophages, whereas PAD2 was expressed at both the mRNA and protein level in monocytes.

Due to PAD4 mRNA only being detected in the astrocytoma cell line and undetectable in the primary human astrocytes, it was decided that further qPCR experiments in the primary human astrocytes, human foetal microglial and human adult brain endothelial cell lines would focus on PAD2 expression. Therefore, all subsequent qPCR was carried out using PAD2-specific primers only, except in the astrocytoma cell line.

Under inflammatory conditions, PAD2 and PAD4 genes showed differential expression patterns in the astrocytoma cell line, U373-MG (Table 2.8). Single treatment with IL-1 β , TNF- α and IFN- γ all resulted in the significant down-regulation of PAD2 mRNA

following treatment for 24 hours. Down-regulation of PAD4 mRNA was also observed following treatment with IFN- γ and to a lesser extent following treatment with IL-1 β for 24 hours. No significant differences were observed by incubating the cells with cytokines for 48 hours compared to 24 hours, therefore, all subsequent cytokine experiments were carried out for 24 hours.

All primary human astrocytes and the human foetal microglial cell line, CHME3, showed significant down-regulation of PAD2 mRNA following single cytokine treatment with either IL-1 β or TNF- α alone. Co-treatment with IL-1 β and TNF- α , IL-1 β and IFN- γ , or TNF- α and IFN- γ all resulted in significant down-regulation of PAD2 gene expression. Interestingly, co-treatment with TNF- α and IFN- γ resulted in a similar down-regulation of PAD2 gene expression as observed following single treatment with TNF- α , suggesting the down-regulation is exerted by TNF- α . This pre-dominance of TNF- α actions was also observed following co-treatment with IL-1 β and TNF- α . Single treatment with IFN- γ produced variable results with significant down-regulation of PAD2 mRNA only reached following 100 ng/mL of treatment in the primary human astrocytes, MS16, which as suggested earlier could be due to increased expression of the IFNGR in MS.

In the human brain endothelial cell line, hCMEC/D3, only single treatment with TNF- α elicited significant down-regulation of PAD2 gene expression. Co-treatment with IL-1 β + TNF- α or TNF- α + IFN- γ , showed significant down-regulation of PAD2 mRNA similar to the down-regulation observed following single treatment with TNF- α . Similar to the above observations, this implicates TNF- α as the single cytokine exerting effects on the expression of PAD2 mRNA.

This decrease in PAD2 and PAD4 mRNA expression following treatment with pro-inflammatory cytokines was unexpected, since previous studies have shown significant up-regulation of pro-inflammatory cytokines (for review see Imitola *et al.*, 2005) along with an increase in the expression of both PADs and citrullinated proteins in MS brains by IHC (for review see (Bradford *et al.*, 2009). It was anticipated that pro-inflammatory cytokines may initially up-regulate PAD mRNA expression resulting in increased PAD protein expression and activation followed by subsequent increase in citrullinated proteins. Therefore, it was expected that incubation of cells with pro-inflammatory cytokines *in vitro* to mimic the *in vivo* situation in MS would result in an up-regulation of PAD gene expression.

Due to this down-regulation of PAD2 in all primary cells and cell lines tested following treatment with pro-inflammatory cytokines, the effect of anti-inflammatory cytokines on the expression of PAD2 mRNA was briefly investigated as these anti-inflammatory

cytokines are thought to have an opposing effect on PAD2 gene expression. Microglia are a major cell type known to express PAD2 (Vincent *et al.*, 1992; Asaga *et al.*, 2002; Asaga and Ishigami 2007), therefore the human microglial cell line, CHME3, was selected for anti-inflammatory cytokine treatment with IL-4, IL-10 or TGF- β alone. Treatment with either IL-4 or IL-10 did not modulate the expression of PAD2, whereas treatment with TGF- β resulted in down-regulation of PAD2 mRNA, by CHME3 cells.

A previous study has shown citrullination to be rapidly induced in HL-60 neutrophils following exposure to various inflammatory signals, including TNF- α , LPS, lipoteichoic acid and hydrogen peroxide (Neeli *et al.*, 2008). However, there are very few studies that have investigated the effects of cytokines on the expression of PAD2 and PAD4 directly as opposed to the resultant citrullinated proteins. One study has showed that TNF- α is essential for translocation of PAD4 to the nucleus (Mastronardi *et al.*, 2006). This same study also showed that transgenic mice over-expressing TNF- α have increased levels of citrullinated histones and elevated nuclear PAD4 in the CNS prior to demyelination (Mastronardi *et al.*, 2006). There are other studies which indicate a number of different factors are involved in the regulation of PADs, and therefore it is tempting to speculate that in order for the expression of PAD2 to become significantly up-regulated a number of other mediators have to be present, of these calcium seems to be most important.

Not only is calcium the indispensable factor in the environment of the deimination reaction (see section 1.5.3.6), but it is also considered as a major regulator of PAD genes at the transcriptional level (Ying *et al.*, 2009). Using normal human keratinocytes (NHEK) Dong *et al.*, (2005) have shown that the expression of PAD2 mRNA is enhanced 2-fold when these cells are cultured in 1.2 mM calcium compared to cells grown in media containing only 0.15 mM of calcium. It is thought that calcium could control the binding of transcriptional factors to the promoters of the PAD2 gene. In particular, the level of Sp1 and/or Sp3 recruitment to the promoter and the Sp1/Sp3 ratio has been shown to change according to the calcium concentration in the culture medium (Dong *et al.*, 2005). Studies of PAD1 in NHEK cells have shown that mutations of the binding sites of MZF-1- or Sp-1 transcription factors markedly reduced PAD1 promoter activity (Dong *et al.*, 2007). Interestingly, MZF1-binding sites have not been identified in the promoter region of PAD2, which shows that PAD isoforms are differentially regulated at the transcription level (Dong *et al.*, 2005). In this study, the culture media contained approximately 1.8 mM of calcium, which according to the above studies should be sufficient to induce the binding of transcriptional factors to the promoters of the PAD2 gene, and explains why PAD2 mRNA expression was observed in untreated cells used in this study. However, the subsequent down-regulation of

PAD2 observed following cytokine treatment suggests that the balance between anti- and pro-inflammatory cytokines does not control PAD2 expression *in vitro* which indicates that additional mediators and mechanisms must be involved in the modulation of PADs *in vivo*.

Additional mechanisms have also been shown to be important to the transcriptional regulation of the PAD2 gene. Methylation of the PAD2 promoter results in silencing of the PAD2 gene (Cedar 1988; Yeivin and Razin 1993) whereas hypomethylation of the PAD2 promoter increases transcription. A study by Mastronardi *et al.* (2007) has shown significant hypomethylation of the PAD2 promoter in MS NAWM compared with controls, which would allow for increased transcription of PAD2, leading to increased expression and subsequent increase in citrullination (Mastronardi *et al.*, 2007). PAD2 protein was shown to be up-regulated in MS NAWM compared to control white matter (Mastronardi *et al.*, 2007). This hypomethylation of the PAD2 promoter has also been shown to occur in PBMCs from patients with MS along with an increase in PAD2 mRNA expression (Calabrese *et al.*, 2012).

In this study only expression of PAD2 at the mRNA level under the influence of pro-inflammatory cytokines was studied. It would have been useful to have carried out western blotting to determine the expression of PAD2 at the protein level, as mRNA levels do not always reflect protein levels (Bhattacharya *et al.*, 2006). Furthermore, although this study showed the presence of PAD2 enzymes in astrocytes, microglia and brain endothelial cells, it would have been useful to detect the presence of citrullinated proteins within these cells using immunocytochemistry and/or western blotting which would indicate whether PAD2 was active in these cells or to directly measure PAD2 activity in these cells.

In addition to the direct role of calcium in the transcription of PADs, activation of the PAD enzymes are dependent on the presence of calcium. X-ray crystallographic structural analysis of human PAD4 in calcium-free and calcium-bound forms, suggests that binding of calcium to the C-terminal domain is critical for both substrate specificity and binding (Arita *et al.*, 2003; Arita *et al.*, 2004). The binding of calcium to PAD4 leads to conformational changes around the substrate binding site, which then allows PAD4 to interact with arginine residues in other proteins (Arita *et al.*, 2004). Only the crystal structure of PAD4 has been elucidated as yet, however, due to human PAD4 and PAD2 showing more than 50% sequence homology, it is assumed that PAD2 will have a similar crystal structure and mechanism of activity (Arita *et al.*, 2004). In the absence of high levels of intracellular calcium, PAD2 would not undergo these conformational changes which are essential for activation of the enzyme.

The cytosolic and nucleoplasmic calcium concentration is much too low (approximately 100-fold) for PAD activity under normal physiological conditions (Takahara *et al.*, 1986). However, there are numerous events which can lead to raised intracellular calcium. For example during cell death the integrity of the plasma membrane is lost, causing influx of calcium from the extracellular space and subsequent activation of intracellular PAD. Artificially raising the cytosolic and nucleoplasmic calcium concentration by including calcium ionophores in the media of the cells should induce activation of PAD and subsequent citrullination of intracellular proteins (Vossenaar *et al.*, 2003). Calcium ionophores, such as ionomycin, facilitate a sustained calcium influx from the extracellular to the intracellular environment (Schwab *et al.*, 2002).

In addition to the presence of calcium, a number of other environmental or chemical factors have been shown to increase the expression of PAD2 mRNA and/or protein. Hypoxia has been previously shown to lead to an increase in PAD2 mRNA followed by an increase in PAD2 protein expression in primary human astrocytes (Sambandam *et al.*, 2004). Furthermore, this increase in PAD2 at both the mRNA and protein level correlated with an increase in the amount of citrullinated GFAP as a product of increased PAD2 enzymatic activity. Interestingly, kainic acid-evoked neurodegeneration in the rat brain has been shown to increase the expression of PAD2 protein in activated microglia but not in astrocytes (Asaga *et al.*, 2002). This shows differential activation of PADs depending on the cell type in which they are expressed.

Prostaglandin D₂ has been shown to induce PAD activity in a macrophage cell line (Lee *et al.*, 2006). Activation of the prostaglandin D₂ receptor also results in intracellular calcium influx (Boie *et al.*, 1995). Exposure of a human monocytic cell line, THP-1, to silica has been shown to lead to increased PAD activity and increased citrullination, with the addition of a PAD inhibitor shown to significantly reduce PAD activity and citrullination. A raised intracellular calcium concentration was shown to occur in cells exposed to silica, with the addition of a calcium blocker shown to inhibit protein citrullination (Mohamed *et al.*, 2012).

Pressure has been shown to increase the expression of PAD2 protein in human astrocytes compared to untreated cells and is associated with an increase in intracellular calcium. However, PAD2 mRNA levels were similar between pressure-treated and untreated astrocytes, suggesting posttranscriptional control of PAD2 expression (Bhattacharya *et al.*, 2006b). Furthermore, another study by the same group showed pressure-treated rat astrocytes exhibited elevated PAD2 protein and citrullination without an apparent change in PAD2 mRNA (Bhattacharya *et al.*, 2006a).

Interestingly, recent publications have also suggested an anti-inflammatory role for PADs and subsequent citrullination of proteins. Ji *et al.* (2011) have shown the up-regulation of microRNA, in particular miR-34a, in RA synovial monocytes, which targets the PAD4 gene, leading to decreased expression of PAD4 in RA synovial monocytes compared to normal PBMCs, which would lead to decreased PAD4 expression in RA. Therefore, microRNAs may be important regulators of PADs in RA and other autoimmune disease, such as MS (Ji *et al.*, 2011). The authors of this paper suggested that this decrease in PAD4 expression may be responsible for aggravating RA activity, implicating an anti-inflammatory role for PAD. Two reports have recently demonstrated that citrullination reduced the pro-inflammatory activity of several chemokines, including CXCL8, CXCL10 and CXCL11, thus suggesting an anti-inflammatory role for PAD (Loos *et al.*, 2008; Proost *et al.*, 2008; Loos *et al.*, 2009).

Furthermore, activated PAD2 has been shown to suppress NF- κ B kinase activity in LPS-stimulated macrophages, which would lead to the down-regulation of pro-inflammatory gene expression induced by LPS (Lee *et al.*, 2010). The authors of this study propose that activation of PAD2 in inflammation might serve to self-limit inflammatory responses. These studies suggest that PADs may play an anti-inflammatory role in autoimmune diseases.

In the *in vivo* situation, it is also important to consider reciprocal communication between different cells, such as neurones and astrocytes (Carmignoto 2000), which may also be responsible for the modulation of PADs. Furthermore, it has been shown *in vitro* that when human monocytes come into contact with stimulated T cells, both PAD2 and PAD4 are up-regulated at both the mRNA and protein level (Ferrari-Lacraz *et al.*, 2010).

2.4.3 Conclusion

PAD2 was shown to be down-regulated following incubation with pro-inflammatory cytokines in different preparations of primary human astrocytes (MS16, EP14, EP15), a human foetal microglial cell line (CHME3) and a brain endothelial cell line (hCMEC/D3) *in vitro*. This indicates that the balance between pro- and anti-inflammatory cytokines does not control PAD expression and additional mechanisms must be involved in the up-regulation of PADs reported by others in MS tissue. Furthermore, additional studies investigating the PADs at the protein level in addition to activity would provide further insight. Evidence provided here suggests that the transcription of PAD2 is regulated at multiple levels, and may involve a number of regulatory mechanisms which are difficult to mimic *in vitro*. Lastly, PAD2 protein expression and subsequent activation may be controlled at the translational level independent of transcriptional regulation.

Table 2.7: Summary of significant effects of cytokines, single and co-treatment on proliferation of CNS cells.

Cytokine treatment	U373-MG	EP14	EP15	MS16	CHME3	hCMEC/D3
IL-1 β	↓ 100 (48 h)	no effect	no effect	↑ 1, 10 & 100	↓ 100	no effect
TNF- α	↓ 100 (24 h) ↓ 10 & 100 (48 h)	no effect	no effect	↑ 1, 10 & 100	↓ 100	no effect
IL-6	↓ 10 & 100 (48 h)	no effect	no effect	↑ 1, 10 & 100	↓ 10, 100	no effect
IFN- γ	↓ 1, 10 & 100 (24 & 48 h)	no effect	no effect	no effect	↓ 1, 10 & 100	no effect
IL-1 β + TNF- α	Not tested	no effect	↑ 1, 10 & 100	↑ 1, 10 & 100	no effect	↓ 1, 10 & 100
IL-1 β + IFN- γ	Not tested	no effect	↑ 1, 10 & 100	↑ 1, 10 & 100	no effect	no effect
TNF- α + IFN- γ	Not tested	↓ 100	↑ 100	↑ 1, 10 & 100	↓ 100	↓ 1, 10 & 100
IL-4	Not tested	Not tested	Not tested	Not tested	no effect	Not tested
IL-10	Not tested	Not tested	Not tested	Not tested	no effect	Not tested
TGF- β	Not tested	Not tested	Not tested	Not tested	no effect	Not tested

Table 2.8: A summary of the significant data obtained by qPCR for PAD2 and PAD4 mRNA expression following cytokine treatment, single and co-treatment, on CNS cells used in this study. PAD4 expression was only assessed in U373-MG cell line.

Cytokine treatment	U373-MG	EP14/EP15	MS16	CHME3	hCMEC/D3
IL-1 β	↓ 1, 10, 100 PAD2 (24 h)	↓ 1 & 10 PAD2	↓ 1, 10 & 100 PAD2	↓ 10 & 100 PAD2	No effect
TNF- α	↓ 10 & 100 PAD2 (24 & 48 h) ↓ 100 PAD4 (48 h)	↓ 10 PAD2	↓ 1, 10 & 100 PAD2	↓ 1, 10 & 100 PAD2	↓ 100 PAD2
IL-6	No effect	↓ 10 PAD2	No effect	No effect	No effect
IFN- γ	↓ 1, 10 & 100 PAD2 & PAD4 (24) ↓ 10 & 100 PAD2 & PAD4 (48 h)	No effect	No effect	↓ 100 PAD2	No effect
IL-1 β + TNF- α	Not tested	No effect	↓ 1, 10 & 100 PAD2	↓ 1, 10 & 100 PAD2	↓ 100 PAD2
IL-1 β + IFN- γ	Not tested	↓ 10 & 100 PAD2	↓ 1, 10 & 100 PAD2	↓ 1, 10 & 100 PAD2	No effect
TNF- α + IFN- γ	Not tested	↓ 10 & 100 PAD2	↓ 1, 10 & 100 PAD2	↓ 1, 10 & 100 PAD2	↓ 1, 10 & 100 PAD2
IL-4	Not tested	Not tested	Not tested	No effect	Not tested
IL-10	Not tested	Not tested	Not tested	No effect	Not tested
TGF- β	Not tested	Not tested	Not tested	No effect	Not tested

Chapter 3

***In vivo* investigation of citrullinated
proteins and PAD expression in
post-mortem brain tissue**

3.1 Introduction

Citrullination has been shown to be increased in NAWM of patients with SPMS compared to patients with other neurological diseases in a small scale study using 3 MS and 3 control cases (Nicholas *et al.*, 2004). Citrullination co-localised with GFAP, indicating astrocyte proteins as targets for citrullination (Nicholas *et al.*, 2004). Earlier studies documented MBP in CNS tissue of MS patients as more highly citrullinated compared with MBP from control subjects, indicating oligodendrocytes as cell types which also have citrullinated proteins (Moscarello *et al.*, 1994; Wood *et al.*, 1996). Citrullinated proteins have been identified in the brain and spinal cord of mice with MOG-induced EAE, and co-localised with MBP and GFAP (Nicholas *et al.*, 2005). Hypercitrullination occurs in the CNS during induction of EAE (Raijmakers *et al.*, 2006).

The enzymes which perform this citrullination, PAD2 and PAD4, have also been reported to be increased in MS tissue compared to controls (Mastronardi *et al.*, 2007; Wood *et al.*, 2008). Both PAD2 and PAD4 isolated from myelin in NAWM of MS cases had significantly higher levels than observed in myelin from control subjects (Wood *et al.*, 2008). Transgenic mice overexpressing *PAD2* displayed a more severe clinical EAE disease course associated with increased citrullinated MBP and demyelination (Musse *et al.*, 2008). Based on these studies it is clear that citrullination is important in MS. Apart for the small-scale study by Nicholas and colleagues (2004) using three MS brains with chronic lesions, extensive immunohistochemical studies have not been carried out investigating the distribution of citrullinated proteins and PAD2/PAD4 in active and chronic-active lesions in MS. This study builds from the previous chapter where PAD2 was shown to be expressed in primary human astrocytes, human adult brain endothelial cells and a microglial cell line.

This chapter describes the detailed investigation of the expression of citrullinated proteins and PADs in active and chronic active lesions, to further elucidate the role of citrullination of CNS proteins in MS pathogenesis.

3.1.1. Aim of the study

To determine the expression and distribution of citrullinated proteins and PAD2 in different lesion types in MS tissue.

3.1.2 Objectives of the study

1. Investigate the expression of citrullinated proteins in MS tissue compared to control tissue.
2. Investigate the cellular distribution of citrullinated proteins in different lesion types in MS tissue compared to control tissue.
3. Confirm the identity of proteins that are citrullinated through SDS-PAGE and western blotting.

3.2 Materials and methods

3.2.1 Suppliers used in this chapter

Abcam, 330 Cambridge Science Park, Cambridge, CB4 0FL, UK; **Applied Biosystems**, Lingley House, 120 Birchwood Boulevard, Warrington, WA3 7QH, UK; **Invitrogen**, 3 Fountain Drive, Inchinnan Business Park, Paisley, PA4 9RF, UK; **Millipore**, Suite 3 & 5, Building 6, Croxley Green Business Park, Watford, WD18 8YH, UK; **Sigma-Aldrich**, The Old Brickyard, New Road, Gillingham, Dorset, SP8 4XT, UK; **LI-COR Biosciences Ltd**, St. John's Innovation Centre, Cowley Road, Cambridge, CB4 0WS, UK; **Vector Laboratories Ltd.**, 3 Accent Park, Bakewell Road, Orton Southgate, Peterborough, PE2 6XS, U.K; **VWR International**, Hunter Boulevard, Magna Park, Lutterworth, Leicestershire, LE17 4XN, UK.

3.2.2 Source of MS and control tissue and ethical approval

Eighteen blocks of snap-frozen autopsy CNS tissue from 12 clinically and neuropathologically confirmed MS cases, together with 9 blocks from six normal control cases, obtained from the UK Multiple Sclerosis Society Tissue Bank, Imperial College, London, were investigated for the presence of citrullinated proteins. Informed consent and ethical approval for this study was obtained from the Multi-Centre Research Ethics Committee (MREC) (See Appendix I). The MS cases included 10 females, mean age 67.7 years (range 37-86) and 2 males, mean age 58.5 years (range 55-62) (Table 3.1). The control cases included 3 females, mean age 69 years (range 60-78) and 3 males, mean age 58 years (range 35-75) (Table 3.2). Tissue was received fresh from autopsy ≤ 24 h death-autopsy interval for 11 out of 12 MS cases. All of the MS cases had a confirmed diagnosis of SPMS. Control and MS blocks were matched for CNS location as far as possible.

The UK Multiple Sclerosis Society Tissue Bank initially prepared the tissue used in this study. Tissue blocks were prepared by cutting the whole brain into anterior and posterior halves by a single cut through the mamillary bodies. One centimetre thick coronal slices were then cut through the entire brain. The slices were then numbered based on whether they were taken anteriorly to the mamillary bodies and therefore from the frontal pole or posteriorly to the mammillary bodies and therefore from the occipital pole. The former were numbered A1, A2 etc and the latter were numbered P1, P2 etc. The coronal slices were then laid on a grid and divided into 2cm² blocks, frozen by immersion in isopentane, pre-cooled on dry ice and then stored in air-tight containers at -85°C (Dr. Abhi Vora, The UK Multiple Sclerosis Tissue Bank).

Table 3.1: Clinical data of patients with multiple sclerosis included in this study.

Case number	Region	Age	Gender	Diagnosis	Total disease duration (years)	Cause of death	Death to tissue preservation interval (hours)
MS050	P1E4 P5D7	72	Female	SPMS	41	Bronchopneumonia, multiple sclerosis	8
MS051	A1B6	73	Female	SPMS	43	Bronchopneumonia	19
MS057	A2D5 P1C4	77	Female	SPMS	Unknown	General deterioration, lung infection, treatment withheld	9
MS058	P1C3 P1D3	51	Female	SPMS	21	Multiple sclerosis	15
MS060	P1C2 P1C7	55	Male	SPMS	43	Aspiration of gastric contents, multiple sclerosis	16
MS067	P2C7	86	Female	SPMS	36	Bronchopneumonia	11
MS071	P2C3	78	Female	SPMS	42	Metastatic carcinoma of the bronchus	5

Key: MS; multiple sclerosis, SPMS; secondary progressive multiple sclerosis

Table 3.1 (continued): Clinical data of patients with multiple sclerosis included in this study.

Case number	Region	Age	Gender	Diagnosis	Total disease duration (years)	Cause of death	Death to tissue preservation interval (hours)
MS080	P2D4	71	Female	SPMS	35	Bowel blockage, post-operative complication, heart failure	24
MS090	A1E6	62	Male	SPMS	39	Multiple sclerosis	17
MS092	A2E3 P1B1 P1D1	37	Female	SPMS	17	Multiple sclerosis	26
MS103	P1B3 P1D3	77	Female	SPMS	21	Pneumonia	7
MS159	P1B2	55	Female	SPMS	25	Amitriptyline overdose	24

Key: MS; multiple sclerosis, SPMS; secondary progressive multiple sclerosis

Table 3.2: Clinical data of control cases included in this study.

Case number	Region	Age	Gender	Diagnosis	Total disease duration (years)	Cause of death	Death to tissue preservation interval (hours)
CO14	P2A2	64	Male	Normal	N/A	Cardiac failure	18
CO22	A1A3 P1C2 P1C3	69	Female	Normal	N/A	Lung cancer	33
CO25	P1C2	35	Male	Normal	N/A	Carcinoma of the tongue	22
CO26	P1B1	78	Female	Normal	N/A	Myeloid leukaemia	33
CO28	A1E1 P1C3	60	Female	Normal	N/A	Ovarian cancer	13
CO30	A1C3	75	Male	Normal	N/A	Cerebrovascular accident, aspiration, pneumonia	17

Key: CO; control, SPMS; secondary progressive multiple sclerosis

Each patient is given an ID code and the four digits following that relate to the coronal section and the grid reference where the tissue block was taken from, e.g. MS058 P1C3, is patient ID: MS058, and the coronal section is P1 and therefore derived from the first section posterior to the mamillary bodies, and the block was taken from grid coordinates C3 (Figure 3.1).

These brain blocks were then mounted using Cryo-M-bed mounting media and cut into 10 μ M sections using a cryostat and transferred onto polysine coated glass slides (VWR, UK) where they were left to dry for approximately 30 minutes. Slides were then stored at -80°C until required.

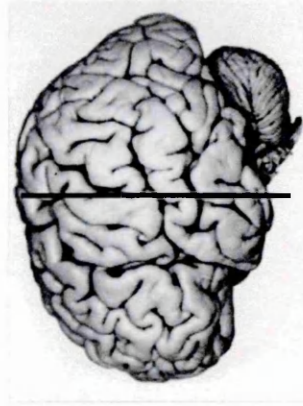
3.2.3 Characterisation of tissue blocks

In order to characterise each tissue block, cryostat sections (10 μ m) were processed for haematoxylin and eosin (H&E), oil red-O (ORO), myelin oligodendrocyte glycoprotein (MOG), MHC class II (HLA-DR), CD3 (T cell) and CD20 (B cell) to evaluate general histology and extent of cellular activation within each block. H&E stain was utilised to determine the extent of inflammation. Both ORO and MOG were used in order to assess the extent of demyelination. An antibody directed against HLA-DR was employed to determine the state of activation of microglia and macrophages, in addition to B and T cells (anti-CD3 and CD20).

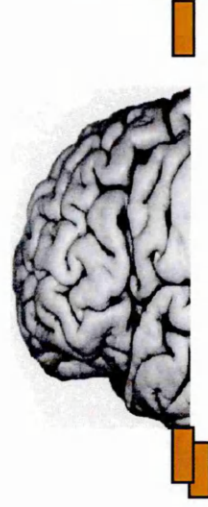
3.2.3.1 Haematoxylin and eosin (H&E)

H&E is the most common stain used in histology and exploits the different acidic and basic properties of the cell's nucleus and cytoplasm (Ross and Pawlina 2006). Haematoxylin stains the nucleus whereas eosin stains the cytoplasm and the connective tissue, therefore allowing excellent insight into the overall tissue architecture as well as demonstrating any inflammatory processes which may be taking place (Bancroft and Gamble 2008). Dyes used in histology are broadly classified into two groups; acidic or basic. An acidic dye carries a net negative charge on its coloured portion whereas a basic dye carries a net positive charge on its coloured portion. Haematoxylin is used to stain the nuclei of cells, but first requires oxidation either naturally or through chemical oxidising agents, followed by combining with a mordant which gives the dye-mordant complex a positive charge, as haematoxylin stains poorly itself (Bancroft and Gamble 2008). This then enables the dye-mordant complex to bind to anionic sites within the tissue, in particular nuclear chromatin, which results in a deep blue to a black colour of nuclei within tissue sections.

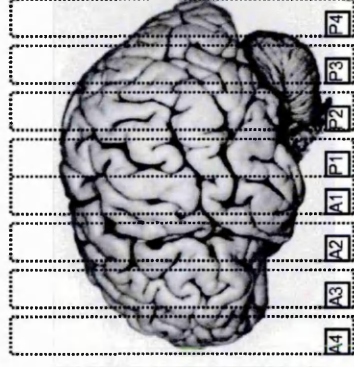
The brain is divided into anterior and posterior regions



Each region is coronally sliced into 1 cm sections



Slices within the frontal or occipital poles are numbered



Slices are further divided into 2cm² blocks and given a grid reference number

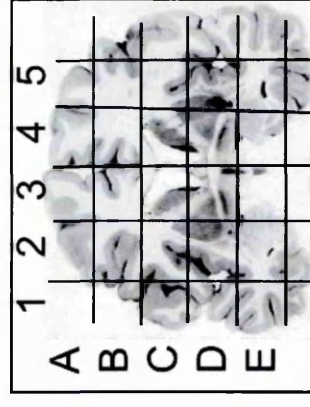


Figure 3.1: Schematic diagram illustrating the coronal slicing of brains and preparation of tissue blocks by the UK MS Society Tissue Bank. The whole brain is first divided into the anterior and posterior segments. Following this each segment is then coronally sliced into 1cm thick slices. Slices are then numbered based on whether they were cut anterior or posterior to the mammillary bodies. The first slice anterior to the mammillary bodies is labelled A1, the next A2, etc, and the first slice posterior is labelled P1, the next P2, etc. Lastly, the slices are then placed onto a grid where they are further cut into 2cm² blocks and given a further number based on the co-ordinates on the grid from which the block is cut. Images courtesy of the UK MS Society Tissue Bank.

Harris's haematoxylin is the most commonly used haematoxylin that has undergone oxidation through the use of mercuric oxide. Following nuclear staining, the cytoplasm and connective tissue is counterstained with eosin, which is an acidic dye, which gives varying shades and intensities of pink, orange and red (Ross and Pawlina 2006). Eosin Y is the most widely used eosin (Bancroft and Gamble 2008).

Prior to staining, frozen sections were fixed in 4% paraformaldehyde (PFA) for 1 hr at 4°C. Following fixation, slides were immersed in Harris's haematoxylin for 1 min and then rinsed in tap water until the water ran clear. Slides were then immersed in eosin Y for 40 secs and then rinsed in tap water until the water ran clear. Following this, slides were subjected to dehydration in increasing concentrations of ethanol (50, 70, 80, 95 and 100%) for 2 minutes in each concentration, followed by xylene for 5 minutes. This last step was then repeated a further time. Lastly, slides were then mounted using DPX mounting medium. Slides were then left to harden in the fume hood for at least 30 minutes and then examined using light microscopy with an Olympus BX60 microscope with a CoolSNAP-Pro (Media Cybernetics) imaging system.

3.2.3.2 Oil Red O (ORO)

In demyelination there is release of proteins and lipids, which undergo enzymatic degradation, mainly within macrophages but also in some astrocytes (Li *et al.*, 2008). Active MS lesions are characterised by the presence of lipid-laden foamy macrophages, which acquire their distinctive morphology by ingestion and accumulation of vast amounts of myelin-derived lipids (Li *et al.*, 1996; Boven *et al.*, 2006). In order to visualise these breakdown products within macrophages, ORO is used. ORO is a fat-soluble dye used to stain neutral triglycerides and lipids on frozen sections (Ross and Pawlina 2006). This technique relies on the fact that the dye is soluble in the lipid in the tissue (Bancroft and Gamble 2008).

Prior to staining, an ORO solution was prepared by adding 1 g of powder (Sigma Aldrich, UK) to 60 mL of triethyl phosphate (TEP) and 40 mL of dH₂O, placed on a stirrer and heated to 100°C for 5 minutes. Following this, the ORO solution was then filtered through filter paper (Whatman, UK) whilst still hot and a second time when cold.

Prior to staining, frozen sections were fixed in 4% PFA at 4°C for 1 hr. Following fixation, slides were washed in tap water, rinsed in 60% TEP, and stained in the filtered ORO solution for 10-15 minutes at RT. Once stained, the slides were briefly rinsed in 60% TEP, and then in tap water. Nuclei were then counterstained with Harris's haematoxylin (diluted with dH₂O to 20% v/v) and then briefly washed in dH₂O. Lastly,

slides were mounted using aqueous mountant glycerol gelatin, as any alcoholic or organic mountant will dissolve the lipids from the tissue.

3.2.3.3 Sudan black B staining

Sudan black B (SBB) is a fat-soluble dye used for staining of neutral triglycerides and lipids on frozen tissue sections, and is most commonly used to reduce autofluorescence of tissue due to the presence of lipofuscin (Schnell *et al.*, 1999). Lipofuscin is a fluorescent pigment which accumulates with age in the cytoplasm of cells, and because of its broad excitation and emission spectra often overlaps with those of all commonly used fluorophores, which is detrimental when using fluorescence microscopy (Viegas *et al.*, 2009). Using a concentration of 1% SBB has previously been shown to be sufficient to quench this lipofuscin autofluorescence (Schnell *et al.*, 1999).

Prior to staining, a 1% SBB solution was freshly prepared by adding 1 g of powder (Sigma Aldrich, UK) to 100 mL of 70% ethanol, placed on a stirrer in the dark for 2 hours at RT. Following this, the SBB solution was filtered through filter paper (Whatman, UK), wrapped in foil and kept at 4°C until it was used in immunohistochemistry (see section 3.2.5).

3.2.4 Tissue grading

3.2.4.1 H&E and ORO stains

In order to examine levels of inflammation, H&E stained slides were graded according to the extent of perivascular cuffing observed, using a five-point scale (negative, +, ++, +++, +++) with + indicating a few immune cell infiltrates around the blood vessel through to a ++++ indicating a large collection of immune cell infiltrates several layers deep around the blood vessel (Figures 3.2 and 3.3).

ORO was used in order to assess the extent of myelin loss and sections were graded using a four-point scale, with negative indicating complete absence of ORO-positive cells through to 3+ where ORO-positive cells were present throughout the lesion area (Figure 3.4). Blocks displaying ORO-positive cells throughout the lesion were classified as active, whereas blocks displaying ORO-positive cells around the lesion edge were classified as chronic-active (Lucchinetti *et al.*, 2005).

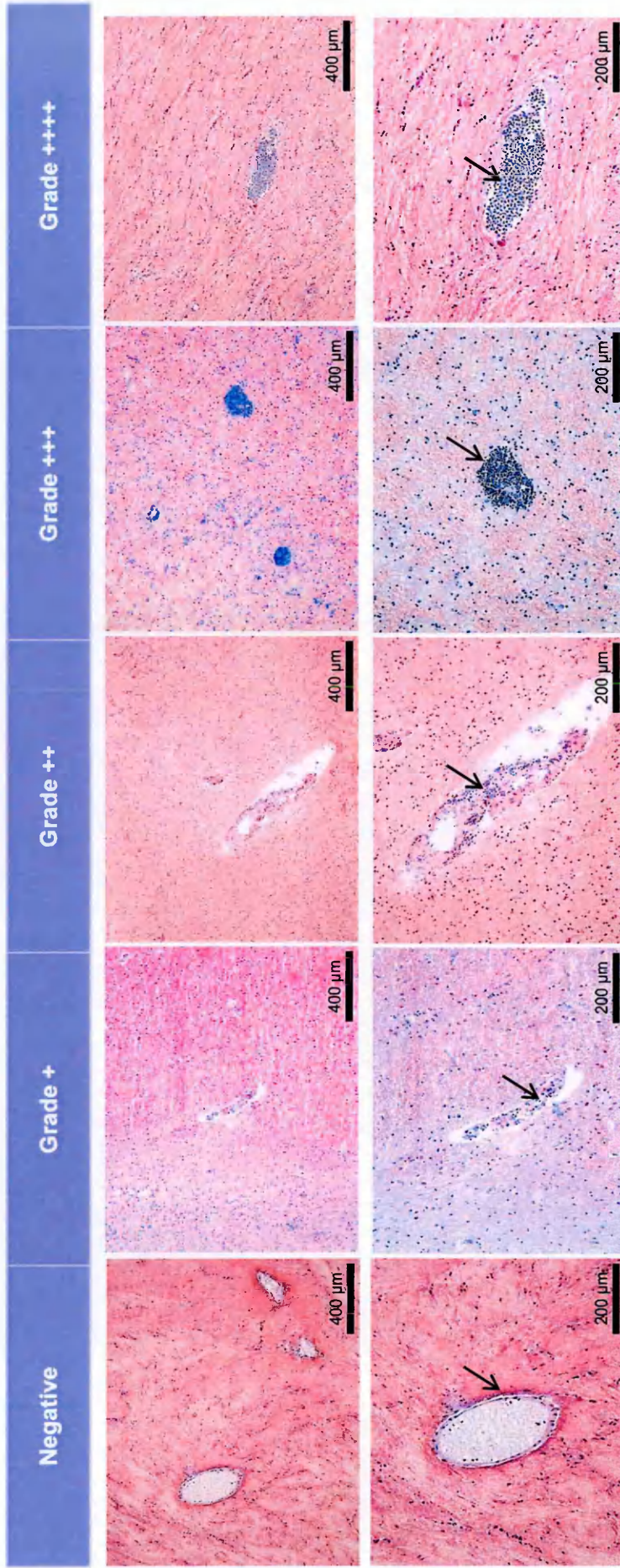


Figure 3.2: Haematoxylin and eosin staining showing the different grades of inflammation observed in CNS white matter. Control tissue (CO22 P1C3) showed no inflammation whereas the majority of MS tissue showed an inflammatory burden of + (MS058 P1C3), ++ (MS090 A1E6), +++ (MS092 P1B1) and ++++ (MS058 P1D3). The black arrows indicate leukocytes that have breached the blood-brain barrier. The upper panel shows a lower magnification and the lower panel shows a higher magnification of the same region.

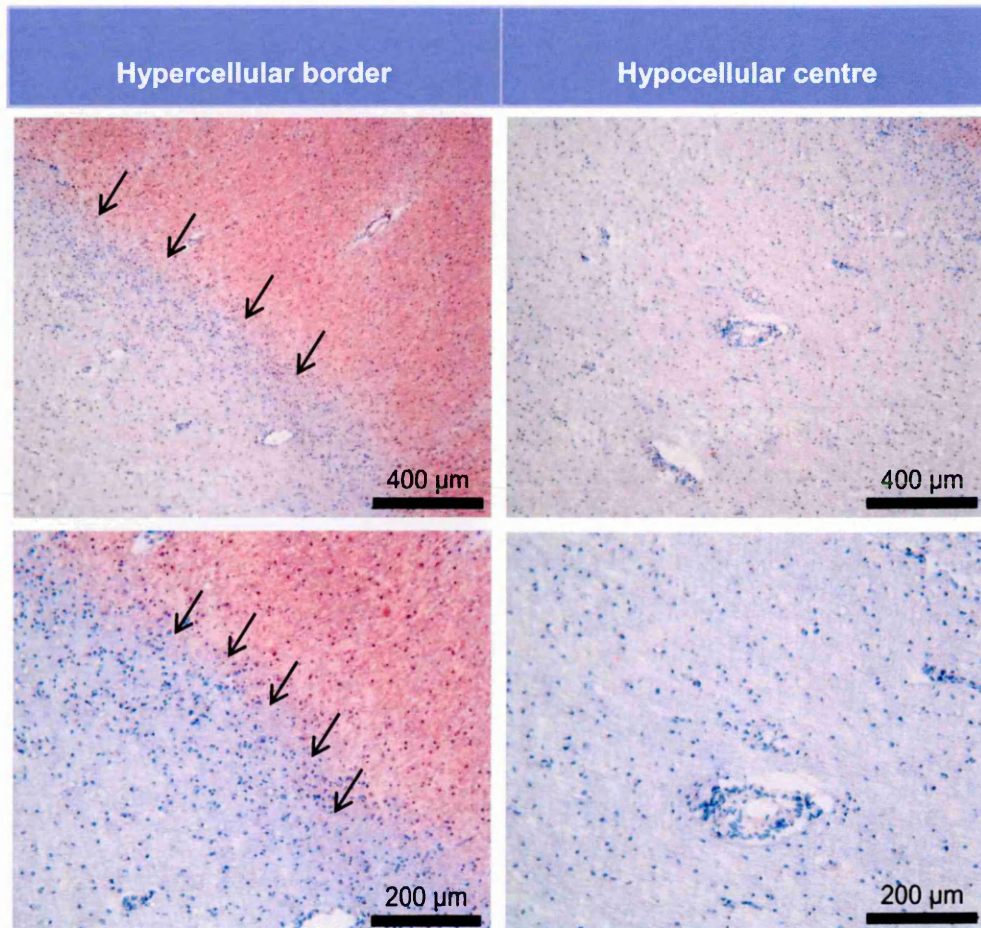


Figure 3.3: Haematoxylin and eosin staining showing the hypercellular border surrounding a lesion and the hypocellular centre of the same lesion (MS058 P1C3). The black arrows indicate the hypercellular lesion edge where there is a gathering of leukocytes. The upper panel shows a lower magnification and the lower panel show a higher magnification of the same region.

3.2.4.2 HLA-DR expression

In order to determine the extent of cellular activation, an antibody against HLA-DR was utilised. HLA-DR is a cell surface receptor encoded by the MHC II complex on chromosome 6 region 6p21.31. There are usually very low levels of MHC class II expression in healthy control tissues, whereas in autoimmune diseases the expression of MHC class II can greatly increase (Power *et al.*, 1993). An example of this is in active lesions in MS where there is an abundance of MHC class II positive cells in and around the lesion (Woodroffe *et al.*, 1986; Boyle and McGeer 1990).

Lesions were classified based on a study by Bö and colleagues (1994), in actively demyelinating lesions HLA-DR positive cells are evenly distributed within the lesion, whereas in chronic active lesions HLA-DR positive cells are located at lesion edges rather than centrally (Bo *et al.*, 1994). Lastly, in chronic inactive lesions there is little or no HLA-DR positive cells either inside the lesion, at the edges of, or outside the demyelinated lesions.

3.2.4.3 MOG expression

In order to assess the extent of myelin loss an antibody against MOG was used. MOG is a type I membrane glycoprotein preferentially localised at the outermost surface of the myelin sheath and oligodendrocytes (Brunner *et al.*, 1989). MOG is a useful marker for classifying the type of lesion in MS based on the extent of demyelination and also remyelination. In a chronic inactive plaque there is no evidence of active myelin breakdown, whereas in an active lesion there is substantial pallor of myelin staining (Lucchinetti *et al.*, 2005). Therefore MOG can be extremely useful in determining whether the plaque is chronic inactive or active.

3.2.4.4 Classification of lesion type

H&E, ORO, HLA-DR and MOG staining were all used in order to classify the MS lesions as active, chronic active or chronic inactive. In this study no blocks were found to contain chronic inactive lesions. MOG was used in order to assess the extent of demyelination. If there was complete MOG loss the lesion was classified as chronic whereas if MOG was disrupted along with inflammation as shown through H&E staining the lesion was classified as active. HLA-DR was used to assess cellular reactivity. In the case of positive HLA-DR staining at the lesion edge in the chronic lesion the lesion was classified as chronic-active whereas if positive HLA-DR staining was observed throughout the tissue the lesion was classified as active.

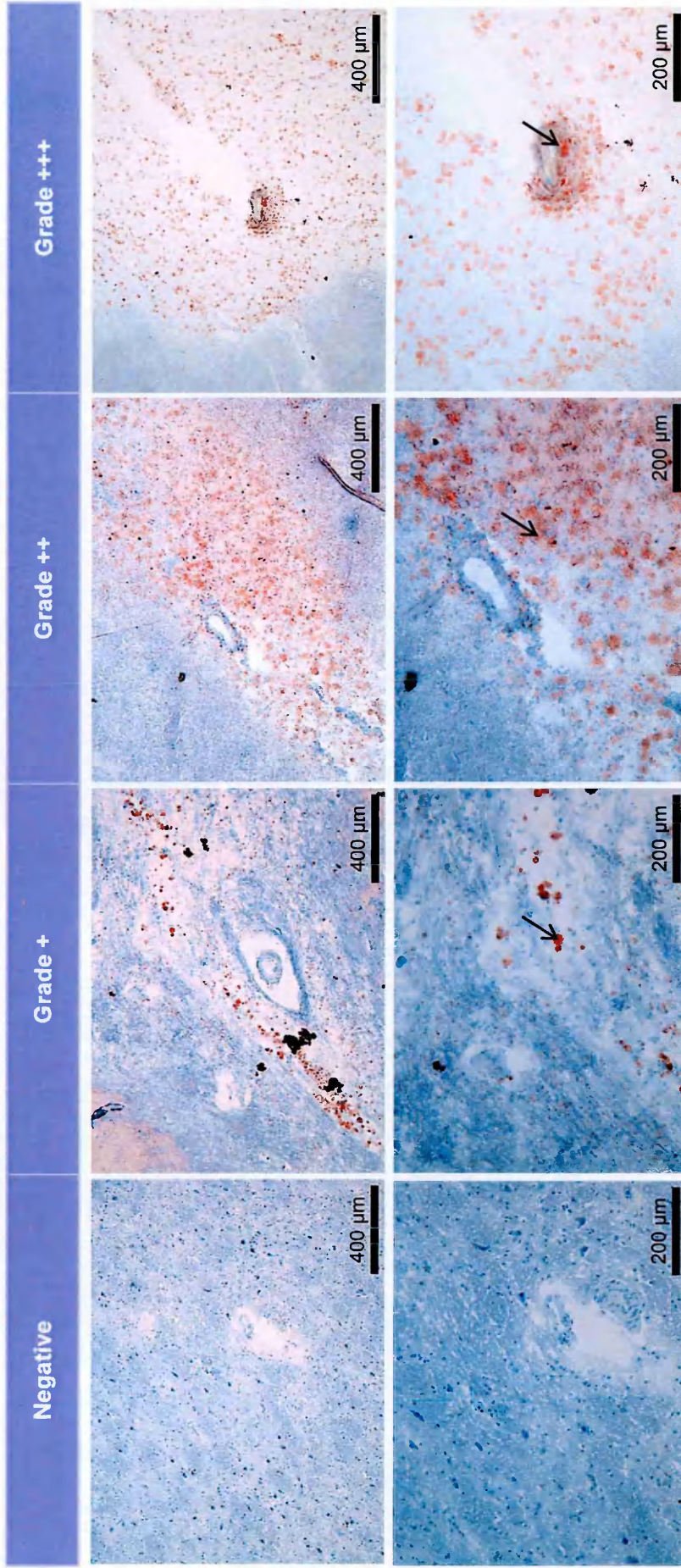


Figure 3.4: Oil red O (ORO) showing the different grades of lipid-laden macrophages in the white matter tissue. Control tissue (CO22 P1C3) and some MS tissue showed no ORO positive cells whereas some MS tissue showed a few ORO positive cells graded as + (MS058 P1C3), ++ (MS051 A1B6) and +++ (MS058 P1D3). The black arrows indicate lipid-laden macrophages engulfing myelin. The upper panel shows a lower magnification and the lower panel show a higher magnification of the same region.

In some instances ORO staining of lipid-laden macrophages was also used in the classification of lesions. In the chronic-active lesion, lipid-laden macrophages are sometimes observed around the edge of the lesion whereas in active lesions there are lipid-laden macrophages throughout the lesion.

3.2.5 Immunohistochemistry

This procedure was similar to ICC performed on cells *in vitro*. For full details refer to chapter 2 (see section 2.2.5).

3.2.5.1 Single label immunofluorescence

Prior to staining, sections were fixed in ice-cold acetone in Coplin jars for 10 minutes at RT, and then air-dried for 20 minutes. Sections were then treated with 5% goat serum/1% BSA in phosphate buffered saline (PBS) for 30 min at room temperature (RT) to prevent non-specific binding of the primary and secondary antibodies. Table 3.2 provides a summary of the primary and secondary antibodies used in the study. Primary antibodies were initially optimised by selecting a range of dilutions based on an initial recommendation by the manufacturer, except anti-HLA-DR and vWF which was previously optimised by Dr. H. Denney and anti-MOG which was given as a gift from Dr. Stephen McQuaid and used at his recommended dilution. Following this, sections were then incubated with the primary antibody diluted in 0.3% goat serum in PBS overnight at 4°C, washed in PBS and incubated in the appropriate secondary antibody diluted in 1% BSA in PBS for 1 h at RT. Cell nuclei were counterstained with diamidino-2-phenylindole (DAPI), included in the mountant (Vector Laboratories, UK). For controls, the primary antibody was replaced with either an isotype control (IC) or omission of the primary antibody to ensure the absence of non-specific binding from the secondary antibody (Table 3.3). Where there was more than one primary antibody with the same isotype, the IC was used at the most concentrated primary antibody dilution

Following this, sections were blocked with 3% BSA plus 0.3% Triton X-100 in PBS (pH 7.4) (180 µL per section) for 30 minutes at RT. Sections were then washed in PBS three times, 10 minutes per wash. Primary antibodies (180 µL per tissue section, diluted in PBS in 0.3% Triton® X-100) were applied to each section and incubated in a humidified slide tray for 2 hrs or overnight (O/N). The negative controls with the primary antibody omitted were incubated with 180 µL PBS with 0.3% Triton® X-100. Following this, slides were then washed three times in PBS, to remove any unbound antibody, for 10 minutes per wash. Secondary antibodies (180 µL per tissue section, diluted in PBS with 0.3% Triton® X-100) were applied to each tissue section and incubated as before

for 1 hr at RT. Slides were then washed three times in PBS, to remove any unbound antibody, for 10 minutes per wash. Lastly, slides were immersed in 1% Sudan Black B (SBB) for 5 minutes in the dark at RT, and then rinsed briefly in PBS, 8-10 times. Slides were mounted using Vectashield™ hard-set mounting medium with 4', 6-diamidino-2-phenylindole (DAPI). The edges of the coverslips were sealed with nail varnish, slides were wrapped in foil and stored at 4°C until analysed.

3.2.5.2 Dual labeling immunofluorescence

Prior to carrying out dual immunostaining, serial sections were single-labeled with each mouse or rabbit primary antibody followed by secondary antibodies to anti-rabbit Ig and anti-mouse Ig respectively to ensure that no cross-reactivity was observed between the primary antibody and the inappropriate secondary antibody. To determine the cellular localisation of citrullination, the following sequential dual-label immunofluorescence protocol was carried out.

Sections were co-incubated with both a monoclonal and polyclonal antibody overnight at 4°C and then detected by co-incubating the appropriate secondary antibodies against mouse and rabbit immunoglobulins for 1 h at RT. Following three 5 min washes in PBS, sections were placed in 1% SBB for 5 minutes, followed by 8-10 washes in PBS and then mounted in Vectorshield mountant with DAPI (Vector Laboratories, Peterborough, UK).

Dual staining was performed with polyclonal antibodies to the astrocytic marker, glial fibrillary acidic protein (GFAP), endothelial marker von Willebrand Factor (vWF), PAD2 and PAD4 with mouse IgM anti-human citrullinated proteins (F95). Rabbit polyclonal anti-PAD2 and anti-PAD4 were used in dual staining with the marker for activated macrophage/microglial cells with mouse monoclonal anti-HLA-DR, T cells with mouse monoclonal anti-CD3, endothelial cells with mouse monoclonal anti-vWF and astrocytes with mouse monoclonal anti-GFAP, respectively. Prior to carrying out dual staining, serial sections were single-label immunostained with each mouse or rabbit primary antibody with secondary antibodies to anti-rabbit Ig and anti-mouse Ig respectively to ensure that no cross-reactivity was observed between the primary antibody and the inappropriate secondary antibody. Omission of either primary antibody from the protocol but with the secondary antibody resulted in no signal detection in the channel used to detect that antigen, indicating no non-specific binding of the secondary antibody. Due to cross-reactivity when carrying out dual staining with mouse IgM anti-human citrullinated proteins and mouse anti-human HLA-DR, CD3 and MOG these markers were stained using single label immunofluorescence of serial sections.

Table 3.3: Details of the primary and secondary antibodies used in immunohistochemistry.

Primary antibodies						Secondary antibodies				
Immunogen	Species	Clonality	Dilution	Source		Immunogen	Species	Conjugate	Dilution	Source
Citrullinated protein (F95)	Mouse	Monoclonal (IgM)	1 in 250 (unknown) 1 in 500 (unknown) 1 in 1000 (unknown)	Dr. A. Nicholas		Mouse IgM	Goat	FITC	1 in 250	Invitrogen
						Mouse IgM	Goat	Alexa 568	1 in 500	Invitrogen
CD3	Mouse	Monoclonal (IgG1 kappa)	1 in 50 (0.625µg/mL)	BD Biosciences		Mouse IgG	Goat	Alexa 568	1 in 500 1 in 1000	Invitrogen
HLA-DR	Mouse	Monoclonal (IgG2b)	1 in 50 (500 ng/mL)	Novocastra		Mouse IgG	Goat	Alexa 568	1 in 500 1 in 1000	Invitrogen
CD20	Mouse	Monoclonal (IgG2a kappa)	1 in 200 1 in 400 1 in 600	Dako		Mouse IgG	Goat	Alexa 568	1 in 500 1 in 1000	Invitrogen
vWF	Mouse	Monoclonal (IgG1 kappa)	1:100 (2.4 µg/mL)	Dako		Mouse IgG	Goat	Alexa 568	1 in 500 1 in 1000	Invitrogen
vWF	Rabbit	Polyclonal (IgG)	1:250 1:500 1:1000	Dako		Rabbit IgG	Goat	Alexa 568	1 in 500 1 in 1000	Invitrogen

Key: HLA; human leukocyte antigen, vWF; von Willebrand Factor.

Table 3.3 (continued): Details of the primary and secondary antibodies used in immunohistochemistry.

Primary antibodies						Secondary antibodies					
Immunogen	Species	Clonality	Dilution	Source		Immunogen	Species	Conjugate	Dilution	Source	
GFAP	Mouse	Monoclonal (IgG1 kappa)	1:500 (2 µg/mL)	Millipore		Mouse IgG	Goat	Alexa 568	1 in 500 1 in 1000	Invitrogen	
GFAP	Rabbit	Polyclonal (IgG)	1 in 100 1 in 500 1:1000	Abcam		Rabbit IgG	Goat	Alexa 568	1 in 500 1 in 1000	Invitrogen	
MOG	Mouse	Monoclonal	1 in 100	Dr. Stephen McQuaid		Mouse IgG	Goat	Alexa 568	1 in 500 1 in 1000	Invitrogen	
Neurofilament	Mouse	Monoclonal (IgG1 kappa)	1 in 200 (25 µg/mL)	Abcam		Mouse IgG	Goat	Alexa 568	1 in 500 1 in 1000	Invitrogen	
PAD2	Rabbit	Polyclonal (IgG)	1 in 50 (10 µg/mL) 1 in 100 (5 µg/mL) 1 in 200 (2.5 µg/mL)	Abcam		Rabbit IgG	Goat	Alexa 488	1 in 500 1 in 1000	Invitrogen	
PAD4	Rabbit	Polyclonal (IgG)	1 in 50 (2 µg/mL) 1 in 100 (1 µg/mL) 1 in 200 (0.5 µg/mL)	Abcam		Rabbit IgG	Goat	Alexa 488	1 in 500 1 in 1000	Invitrogen	

Key: GFAP; glial fibrillary acidic protein, PAD; peptidylarginine deiminase.

Table 3.3 (continued): Details of the primary and secondary antibodies used in immunohistochemistry.

Primary antibodies				Secondary antibodies					
Immunogen	Species	Clonality	Dilution	Source	Immunogen	Species	Conjugate	Dilution	Source
Mouse IgG1 kappa	Mouse	Monoclonal	1 in 20 (25 µg/mL)	Abcam	Mouse IgG	Goat	Alexa 568	1 in 500	Invitrogen
Mouse IgG2b kappa	Mouse	Monoclonal	1 in 2000 (500 ng/mL)	Abcam	Mouse IgG	Goat	Alexa 568	1 in 500	Invitrogen
Mouse IgM	Mouse	Monoclonal	1 in 500 (unknown) 1 in 1000	Abcam	Mouse IgG	Goat	FITC	1 in 250	Invitrogen
Rabbit IgG	Rabbit	Polyclonal	1 in 40 (5 µg/mL)	Abcam	Rabbit IgG	Goat	Rabbit 488	1 in 500	Invitrogen

Key: Ig; immunoglobulin.

3.2.5.3 Semi-quantification of citrullination immunoreactivity

Sections of MS and control white matter were anonymised by coding by a third party and then scored by two independent blinded observers. Single-labelled immunostaining for F95 on these sections was graded on a five-point scale: sections devoid of F95-immunoreactivity were graded 0, sections displaying low level punctate F95 staining were graded +, sections showing slightly more elongated fibre staining were ++, with more intensive staining were given +++ and sections with extensive staining were graded ++++ (Figure 3.5).

3.2.6.1 Image analysis and capture

Confocal laser scanning microscopy (CLSM) is a powerful tool in the biological field, mainly in the imaging of single optical sections from fixed and immunofluorescently labelled specimens, in particular cells and tissues (Paddock 1999b). Furthermore, CSLM can also be used for time-lapse imaging of living cells (Paddock 2000). These cells or tissues can be labelled with up to three fluorescent probes, which can then be excited or illuminated by either a multi-wavelength laser or multiple lasers capable of excitation at several wavelengths. The use of more than one fluorescent probe in a single specimen is often utilised for mapping the relative distribution of three proteins within cells and tissue (Paddock 1999a). Only light emitted from a particular focal plane reaches the detector due to the presence of mirrors and filters which only direct specific light to the detector (Figure 3.6). In fluorescence microscopy approximately 90% of the fluorescence signal elicited by illuminating a spot in the plane of focus comes from out-of-focus light along with scattered light, which can interfere with the in-focus detail, greatly reducing the contrast and creating a high background level (Conchello and Lichtman 2005).

However, this is overcome in confocal microscopy through the use of a pinhole in front of the detector which rejects both out-of-focus light collected by the objective and scattered light around the illuminated spot (Conchello and Lichtman 2005). This removal of out-of-focus and scattered light in each image plane enables the acquisition of images of thin sections of a thick specimen, providing greater contrast and resolution. Through computationally combining data from a series of images of these thin sections a three-dimensional high resolution image can be constructed (Conchello and Lichtman 2005).

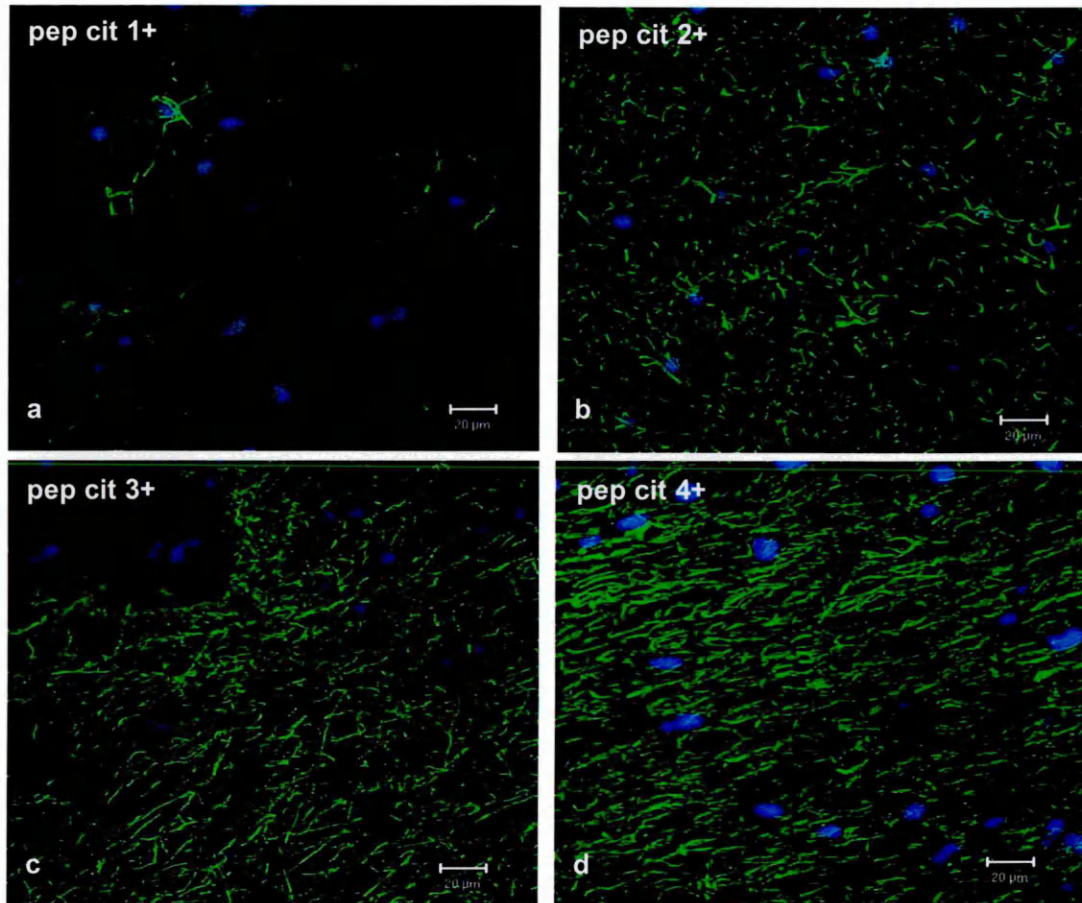


Figure 3.5: Levels of citrullinated protein (pep cit) in control, NAWM and multiple sclerosis lesions by single staining immunofluorescence and confocal microscopy. DAPI counterstaining (blue) shows the location of cell nuclei. Levels of peptidyl-citrulline staining were graded (a) 1+ single astrocytes were observed (CO22 P1C2), (b) 2+ levels of staining became more diffuse (CO22 P1C3), (c) 3+ pattern is more dense and filamentous (MS90 A1E6) and (d) 4+ widespread filamentous staining was observed together with an increase in intensity of staining (MS58 P1C3). Scale bar is 20 µm.

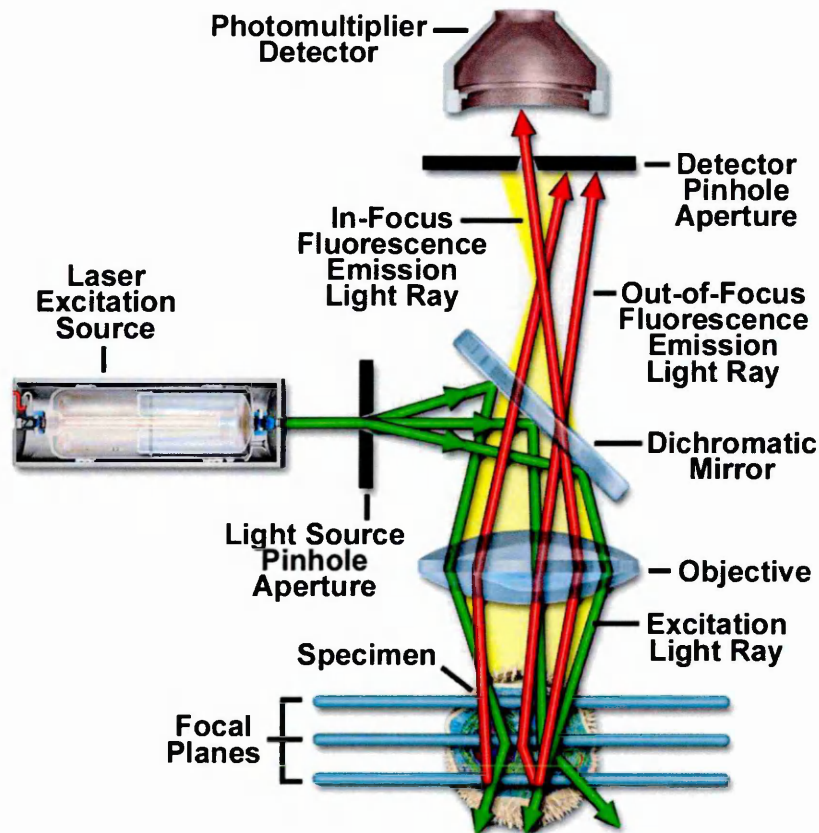


Figure 3.6: Schematic diagram showing the optical pathway and principal components in a laser scanning confocal microscope. Light emitted by the laser passes through a light source pinhole aperture and is reflected by a dichromatic mirror towards the microscope objective and into the sample. The microscope objective focuses the laser to a particular focal plane in the specimen that becomes confocal with the pinhole apertures of the light source and detector (Claxton *et al.*, 2006). On excitation at the correct wavelength the sample fluoresces and the emitted light passes through the dichromatic mirror and is focused into the detector pinhole aperture (Claxton *et al.*, 2006). Refocusing the objective moves the excitation and emission points in a specimen to a new plane. Emitted fluorescence that occurs at points above and below the objective focal plane is obstructed from detection as it is unable to pass through the detector pinhole aperture. Therefore, only information from the focal region of interest reaches the detector (Paddock 1999a). Focused light that passes through the detector pinhole aperture is detected by a photomultiplier detector, which produces a signal directly proportional to the brightness of the light. This signal is then converted to an image directly processed by the adjoining computer, which builds up the image a pixel at a time resulting in a high-resolution image representative of the objective focal slice. From <http://www.olympusconfocal.com/theory/LSCMIntro.pdf>

3.2.6.2 Light and fluorescence microscopy

For grading of sections an upright Olympus BX60 microscope was used. Images of ORO and H&E on sections were also taken using an upright Olympus BX60 microscope, equipped with a cool-snap pro (Cybernetics) digital camera to acquire images into labworks™ where they were saved without further manipulation.

3.2.6.3 Confocal scanning laser microscopy

All immunofluorescent images were captured using a Zeiss 510 CSLM equipped with a krypton/argon laser. Fluorophores were excited at wavelengths of 488 or 568 nm. Colocalisation studies of the dual-labelled samples utilised the colocalisation software available with the Zeiss 510 CSLM. Individual pixels were scanned for each channel within set intensity thresholds. Colocalised pixels were represented as yellow in the composite image.

3.2.3 qPCR using Taqman® probes

RNA was isolated from homogenised CNS tissue (2 x 30 µm sections) collected from 12 MS and 6 control blocks using TRI-reagent, followed by cDNA synthesis and subjected to qPCR. For full details refer to chapter 2 (section 2.2.3).

3.2.3.1 Statistical analysis for qPCR data

qPCR data was analysed using a non-parametric Kruskal-Wallis test followed by Conover-Inman multiple comparisons test. To carry out this test, $2^{-\Delta CT}$ for each sample was calculated to determine the relative gene expression. Comparisons were then made between control, NAWM and MS lesional tissue. Significance was set at $p < 0.05$.

3.2.4 Western blotting

Western blotting, also called immunoblotting, is a widely used analytical technique in the detection of specific proteins in a given sample of tissue homogenate or cell extract (Kurien and Scofield 2006). It uses gel electrophoresis to separate native proteins by three-dimensional structures or denatured proteins by the length of the polypeptide chain (Figure 3.7). These separated proteins are then transferred onto a membrane where they are probed with antibodies specific to the target protein. Specific antibody binding is then detected using a range of methods, most commonly chemiluminescence with an enzyme-labelled secondary antibody, or a fluorescently labelled secondary antibody.

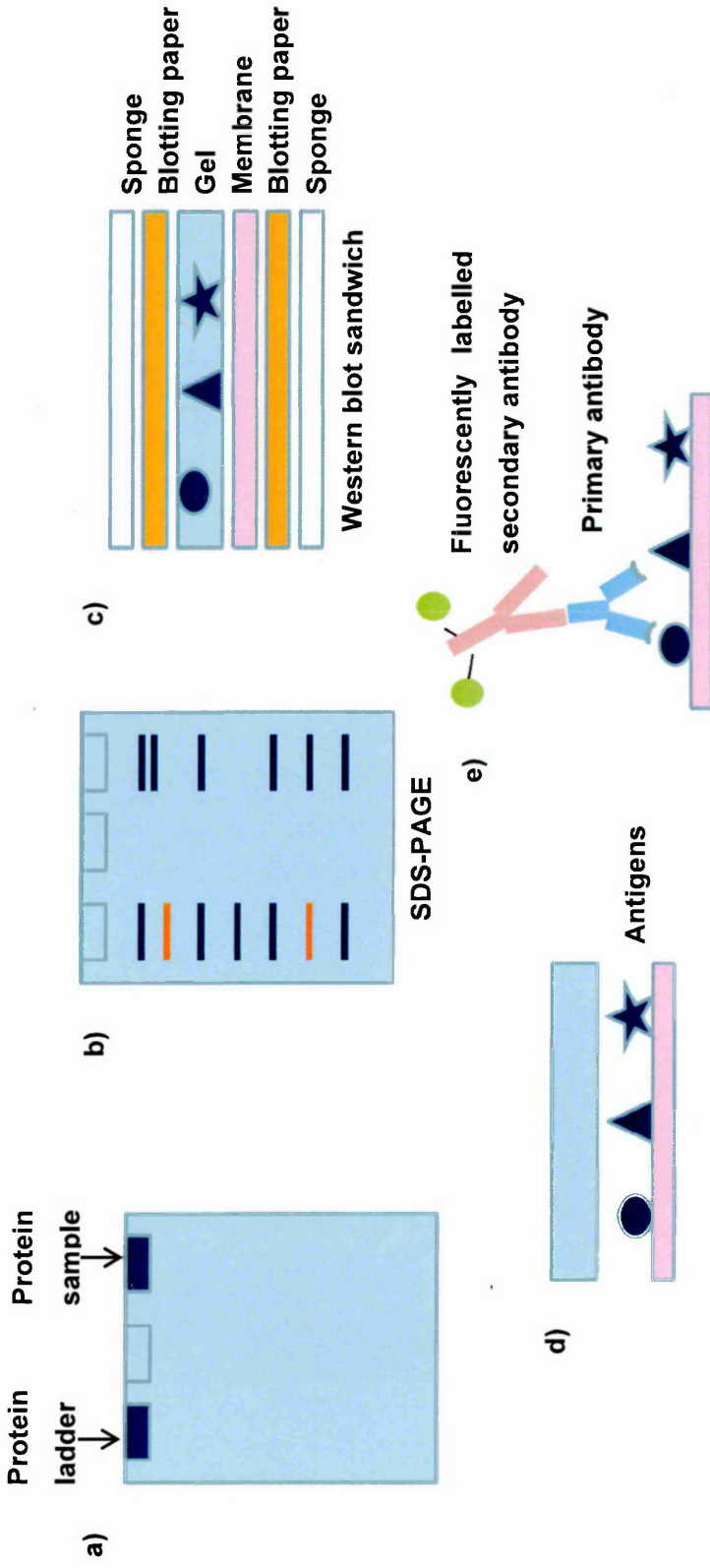


Figure 3.7: Schematic representation of western blotting and detection procedure. (a) Proteins denatured by SDS are loaded into the wells of an SDS-PAGE gel along with a protein ladder containing standards of known molecular weights. (b) These proteins are then fractionated by gel electrophoresis on the basis of size with lower molecular weight proteins migrating faster through the gel matrix than higher molecular weight proteins. (c) Following this, the gel is then electroblotted onto a membrane, (d) resulting in the transfer of all proteins onto the membrane. (e) The resulting blot is then immunoprobed with a primary antibody specific to the target protein, followed by incubation with a fluorescently labelled secondary antibody. The target protein is then visualised using the LI-COR Odyssey® Imaging System.

The most commonly employed type of gel electrophoresis is sodium dodecyl sulphate-polyacrylamide gel electrophoresis (SDS-PAGE) (Laemmli 1970). In SDS-PAGE proteins are first denatured by the addition of SDS and reduced through the use of reducing agents to remove the secondary and tertiary structure of the protein, enabling the proteins to be separated based on their molecular weight. These proteins then become negatively charged by SDS binding and move towards the positively charged electrode through the acrylamide of the gel. Smaller proteins migrate faster whereas larger proteins migrate slower, thus separating the proteins based on their size.

In order to make these proteins accessible to antibodies for detection, they are electroblotted using an electric current to pull the proteins from the gel onto a nitrocellulose or polyvinylidene difluoride (PVDF) membrane. Although there are a number of membranes available, including nitrocellulose and PVDF, nitrocellulose is the most commonly used. PVDF membranes have high protein binding capacity and are strong; however they are expensive and have a short shelf-life. Nitrocellulose membranes have a lower binding capacity and are often brittle when dry, but are relatively inexpensive and have the longest shelf-life. Supported nitrocellulose membranes, such as Hybond-C extra, have improved mechanical strength thereby making them less brittle.

Once electroblotting is complete, it is often useful to check the effectiveness of the protein transfer through staining the membrane with Ponceau S, which enables visualisation of the protein bands (Salinovich and Montelaro 1986). Ponceau S is highly sensitive, detecting as little as 250 ng protein, and is water-soluble therefore can be easily removed through washing with tap water without affecting with probing of the membrane (Salinovich and Montelaro 1986).

Following electroblotting, the membrane is blocked in order to prevent non-specific binding of the primary antibody with either bovine serum albumin (BSA) or non-fat milk powder dissolved in Tris-buffered saline (TBS) with a detergent such as Tween 20 or Triton X-100. These proteins then bind to membrane in areas where the transferred proteins have not attached. This prevents non-specific binding of the primary antibody. The membrane is then probed with a primary antibody against the target protein of interest, such as a mouse anti-human GFAP, followed by the addition of a secondary antibody, such as a goat anti-mouse IgG, which is either tagged with an enzyme e.g. horseradish peroxidase (HRP) or a fluorescent molecule. With the addition of a substrate, HRP catalyses the oxidation of luminal to 3-aminophthalate, which results in the emission of luminescence measured through X-ray film exposure, the intensity produced is directly correlated with the amount of protein on the membrane. A second method of detection involves the use of secondary antibodies directly conjugated with

near infrared (IR) fluorophores. These antibodies are available with an excitation at 679nm and emission at 700, and an excitation at 778 nm and an emission at 800 nm, therefore, allowing simultaneous detection of two targets on the same blot (Schutz-Geschwender *et al.*, 2004). The Odyssey Infrared Imaging System (LI-COR Biosciences, UK) instrument is equipped with two separate lasers and detectors, which allows simultaneous detection of both fluorescent signals at the same time (Figure 3.8).

3.2.4.1 Protein extraction

Protein was extracted, using Tri Reagent, according to the manufacturers' instructions. Briefly, 2x30 μ m tissue sections from each block were placed in 1 mL of Tri Reagent in an Eppendorf tube and then vortexed for approximately 5 minutes in order to lyse cells. Subsequently, this cell lysate was transferred into clean 1.5 mL microcentrifuge tubes where 0.2 ml of chloroform was added per ml of Tri Reagent, mixed vigorously and left to stand for 15 minutes at RT followed by centrifugation at 12,000 g for 15 minutes at 4°C. The colourless aqueous phase containing RNA was then transferred into new Eppendorf tubes.

The remaining white cloudy phase containing DNA was then precipitated by adding 0.3 mL of 100% ethanol per ml of Tri Reagent used in the original sample preparation, followed by gentle inversion and leaving at RT for 2-3 minutes. Samples were then centrifuged at 2,000 g for 5 minutes at 4°C, leaving a pellet containing DNA and supernatant containing protein. The DNA pellet was then removed and protein was precipitated by the addition of 1.5 ml of 2-isopropanol per ml of Tri Reagent. Samples were then left at RT for 10 minutes, followed by centrifugation at 12,000 g for 10 minutes at 4°C. The supernatant was removed and the pellet containing protein was washed three times in 2 ml of 0.3 M guanidine hydrochloride/95% ethanol per ml of Tri Reagent. During each wash, samples were left for 20 minutes at RT followed by centrifugation at 7,500 g for 5 minutes at 4°C. Following this, 2 ml of 100% ethanol was added per ml of Tri Reagent and the protein pellet was vortexed and left to stand at RT for 20 minutes. Samples were then centrifuged at 7,500 g for 5 minutes at 4°C, followed by removal of the ethanol. Protein pellets were air-dried in a fume hood for 5-10 minutes and then dissolved in 70 μ L 1% sodium lauryl sulphate (SDS) through gently pipetting up and down. Samples were then stored at -20°C overnight. The following day samples were placed on a 60°C heatblock for 10 minutes and dissolved further. Protein samples were then stored at -80°C until required.

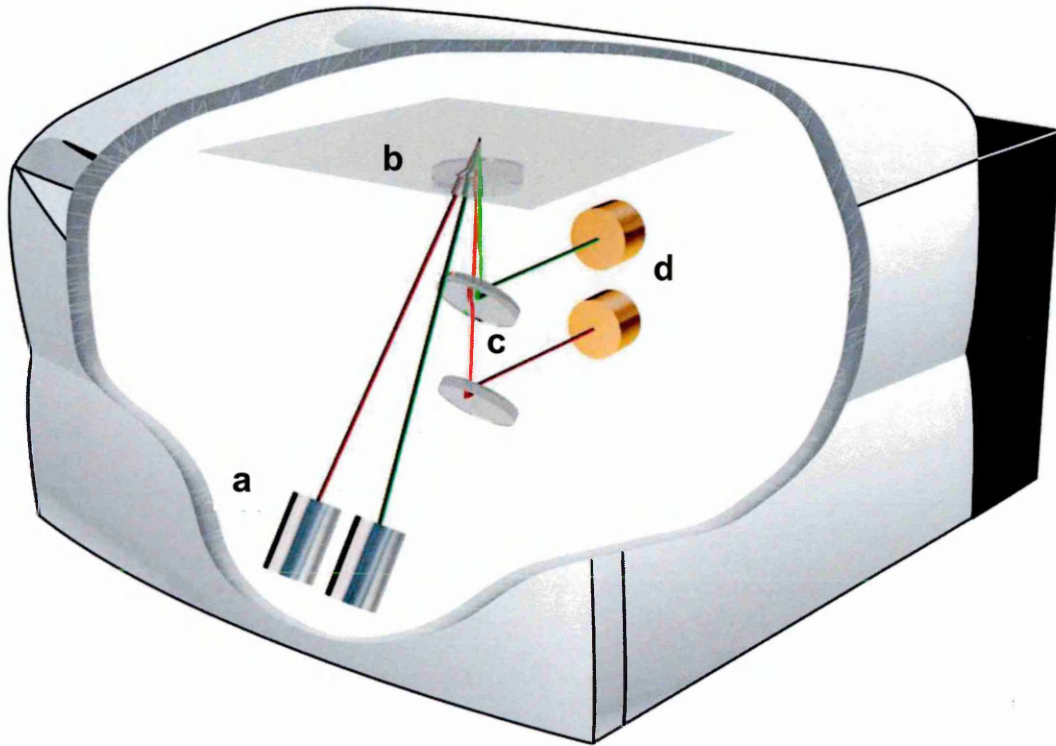


Figure 3.8: Schematic diagram showing the principal components of the Odyssey Infrared Imaging System (LI-COR Biosciences, UK). (a) Beams from the 685 nm and 785 nm lasers are focused to form an excitation spot simultaneously on the scanning surface where the blot is placed. (b) A microscope objective focusses the excitation spot and collects light from the fluorescent infrared dyes at the same time. (c) This light then passes through a dichroic mirror where it is split into two separate fluorescent signals. (d) Each fluorescent signal then passes through two independent light paths, where it is focused on separate avalanche photodiodes and detected. This information is processed in real-time by the adjoining computer, resulting in two 16-bit red and green images depicting fluorescent bands of proteins of interest. These images can be viewed one channel at a time or together overlaid, with signal bands in the same position given a yellow colour.

Adapted from <http://psf.cobre.ku.edu/Odyssey.pdf>

3.2.4.2 Bicinchoninic Acid (BCA) assay for measurement of protein concentration

Prior to western blotting, protein samples underwent protein concentration determination using the BCA protein assay kit according to the manufacturers' instructions. This method relies on the formation of a Cu^{2+} -protein complex under alkaline conditions, followed by the reduction of Cu^{2+} to Cu^{1+} . The amino acids cysteine, cystine, tryptophan, and tyrosine, along with the peptide bonds are responsible for this reduction from Cu^{2+} to Cu^{1+} . The amount reduced is proportional to the amount of protein present. BCA forms a purple-blue complex with the reduced Cu^{1+} , which exhibits a strong linear absorbance at 570 nm with increasing protein concentrations. A standard curve can be constructed using known concentrations of protein, such as BSA, the readings of which can be used to construct a graph. The concentration of unknown samples can then be determined directly from the graph using the slope of the line. The BCA assay is a highly advantageous method for protein determination based on its ability to form a stable colour complex and ability to be used in determining a broad range of protein concentrations (<http://www.sigmaaldrich.com/life-science/proteomics/protein-quantitation/bicinchoninic-acid-kit.html>).

Briefly, BSA protein standards of concentrations ranging from 0.1 to 200 mg/mL were prepared, with dilutions made in 1% SDS. BCA reagent (10 mL BCA solution + 200 μL copper (II) sulphate pentahydrate solution (4% w/v)) was then prepared and stored in the dark until use. 200 μL of the BCA working reagent was added to 20 μL of each protein standard and blank in triplicate and the unknown protein samples in duplicate in a 96-well plate, mixed and left to incubate in the dark for 30 minutes at RT.

Following this the absorbance of each well was measured at 570nm using a Wallac Victor plate reading spectrophotometer. These readings were then used to plot a standard curve (Figure 3.9) and unknown protein concentrations were determined using linear regression analysis, as follows:

$$y = mx + c$$

y = absorbance; **m** = gradient; **x** = protein concentration; **c** = y intercept.

3.2.4.3 Optimisation of western blotting

Prior to carrying out western blotting of all the MS, NAWM and control block extracted protein samples various parameters were optimised (Table 3.4).

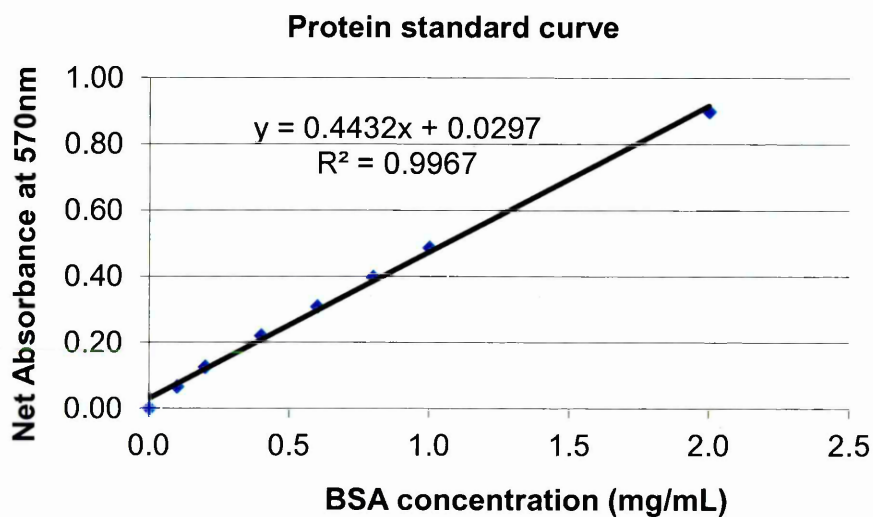


Figure 3.9: An example of a standard curve used in the determination of the protein concentration of unknown samples using BSA as a standard. The concentration (x value) of protein in an unknown sample can be determined through using the absorbance value at 570 nm (y value) and rearranging the equation to $x = (y - 0.0297) / 0.4432$.

3.2.4.4 Sodium Dodecyl Sulphate Polyacrylamide Gel Electrophoresis (SDS-PAGE)

Protein samples (30 µg) were fractionated on a pre-cast 10% Bis-Tris gel using Sodium Dodecyl Sulphate Polyacrylamide Gel Electrophoresis (SDS-PAGE) first developed by Laemmli (Laemmli 1970). All reagents for SDS-PAGE were purchased from Invitrogen, UK, unless stated otherwise. Protein samples were prepared by adding 50 µL protein sample to 25 µL LDS sample buffer, 10 µL sample reducing agent, and 15 µL dH₂O. Samples were then reduced by placing on a heat block at 100°C for 5 minutes. Pre-cast mini gels were placed into a Novex electrophoresis tank containing NuPage MOPS SDS running buffer (25 mL 20X NuPage MOPS SDS running buffer, 475 mL dH₂O, 250 µL NuPage anti-oxidant). 30 µg of each protein sample was loaded per well along with 10 µL of 2-colour protein marker standard (LI-COR, UK), and electrophoresis carried out at 150V and 300 mA for approximately 90 minutes, until the dye front reached the bottom of the gel.

3.2.4.5 Protein electroblotting

Fractionated proteins were transferred onto Hybond-C Extra nitrocellulose membrane (NCM). A piece of NCM was soaked for 10 minutes in cold transfer buffer (150 mL methanol, 1275 mL H₂O and 1500 µL anti-oxidant), along with two pieces of blotting paper and two pieces of sponge per mini-gel. The transfer cassette was then assembled whilst submerged in the transfer buffer to ensure no air bubbles were allowed to form in any of the layers. One sponge was placed on the open transfer cassette, followed by a piece of blotting paper and the NCM, the gel, a second piece of blotting paper and another sponge. The cassette was then closed and placed into the tank containing the transfer buffer, ensuring the NCM was positioned closest to the anode. Protein was transferred from the SDS-PAGE gel to NCM at 100 V for 60 minutes on ice.

To verify the proteins had transferred successfully onto the NCM, blots were briefly immersed in Ponceau S red in order to visualise the proteins, following by rinsing under running tap water to remove the stain.

3.2.4.6 Immunoprobng

Prior to probing with antibodies, blots were blocked for 90 minutes with gentle agitation, in 5% BSA in Tris-buffered saline (TBS) and 0.05% polyoxyethylene sorbitan monolaurate (Tween-20). Following this, the membrane was washed three times for 10 minutes each in TBS with 0.05% Tween-20 (TBS-T), with gentle agitation. The primary

antibody was then diluted to an appropriate concentration in TBS-T with or without non-fat milk powder (Table 3.3) and incubated overnight at 4°C. For negative controls, primary antibody was omitted, and the membrane was incubated with TBS-T alone. The next day, the membrane was washed three times for 10 minutes each in TBS-T, with gentle agitation, to remove any unbound antibody. Labelled secondary antibodies were then diluted to an appropriate concentration in TBS-T (Table 3.3) and placed onto the blots and incubated for 2 hours with gentle agitation. The membrane was then washed twice for 5 minutes each in TBS-T on the shaker followed by one final wash for 5 minutes in TBS only with gentle agitation. The blot was then visualised using the LICOR Odyssey® Imaging System (see section 3.2.4) whereby the optimum exposure time for each laser was determined and then set for all subsequent western blots.

3.2.4.7 Statistical analysis of western blot data

Densitometric data was analysed using a non-parametric Kruskal-Wallis test followed by Conover-Inman test. Comparisons were then made between control, NAWM and MS lesional tissue. Significance was set at $p < 0.05$.

Table 3.4: Details of the primary and secondary antibodies used in western blotting for analysis of protein expression in MS and control tissue.

Primary antibodies					Secondary antibodies					
Immunogen	Species	Clonality	Dilution	Source	Immunogen	Species	Clonality	Conjugate	Dilution	Source
Citrullinated protein (F95)	Mouse	Monoclonal	1 in 100 1 in 500 1:1000	Dr. A. Nicholas	Mouse IgM	Goat	Polyclonal	Alexa 680	1 in 3,000 1 in 10,000 1 in 20,000 1 in 30,000 1 in 50,000	Invitrogen
PAD2	Rabbit	Polyclonal	1 in 500	Abcam	Rabbit IgG	Goat	Polyclonal	Alexa 680	1 in 3,000 1 in 10,000 1 in 30,000	Invitrogen
GFAP	Mouse	Monoclonal	1:1000	Abcam	Mouse IgG	Goat	Monoclonal	IR 800CW	1:10,000	Invitrogen
GFAP	Rabbit	Polyclonal	1:1000	Abcam	Rabbit IgG	Goat	Polyclonal	IR 800CW	1 in 3,000 1 in 10,000 1 in 30,000	Invitrogen
β -actin	Mouse	Monoclonal	1:1000	Abcam	Mouse IgG	Goat	Polyclonal	IR 800CW	1 in 10,000	Invitrogen
β -actin	Rabbit	Polyclonal	1:1000	Abcam	Rabbit IgG	Goat	Polyclonal	IR 800 CW	1 in 10,000	Invitrogen

Key: GFAP; glial fibrillary acidic protein, PAD; peptidylarginine deiminase.

The optimal antibody titre was determined in preliminary experiments. The optimum concentration for each antibody used in this thesis is highlighted in bold.

3.3 Results

3.3.1 Tissue classification

Initially 40 MS and control blocks were assessed for level of inflammation and those displaying the greatest inflammation were chosen for the study. The majority of MS patient tissue blocks displayed varying degrees of perivascular cuffs except for two blocks which displayed no inflammation (MS051 A1B6 and MS057 A2D5) (Table 3.4). Most blocks displayed cuffs graded at +/++, except for four blocks which displayed cuffs graded ++/+++ (MS058 P1C3; MS092 P1B1; MS092 P1D1 and MS159 P1B) and two blocks which displayed cuffs at +++/++++ (MS058 P1D3 and MS159 P1B2). The majority of tissue blocks were negative for ORO lipid-laden macrophages. However, five blocks displayed weak ORO positive staining which was very sparse and were graded as +. Only one block displayed more extensive ORO positive staining and was graded at ++ (MS051 A1B6) and a further patient block showed widespread ORO positive staining and was graded at +++ (Table 3.4). Five blocks were classified as containing active lesions, i.e. ongoing demyelination with or without ORO positive macrophages and increased HLA-DR staining in the absence of a hypocellular region. 13 blocks were classified as containing chronic-active lesions, i.e. MOG loss with or without ORO positive macrophages and a rim of HLA-DR positive cells bordering the lesion with hypercellularity. 5 blocks were classified as NAWM, i.e. displayed minimal inflammation, no ORO positive macrophages, normal MOG and resting microglia (as shown by HLA-DR staining). Control blocks were negative for both perivascular cuffs and ORO positive macrophages and displayed resting microglia with low levels of HLA-DR staining along with normal MOG staining.

3.3.2 Isotype and negative controls

In order to determine the level of background staining isotype controls (IC) were tested on the NAWM of an MS tissue block. The IgM IC corresponding to the F95 monoclonal antibody showed a non-specific homogenous green hue (Figure 3.10a). The IgG_{1κ} IC corresponding to GFAP, CD3, VWF and NF monoclonal antibodies produced a very faint red hue (Figure 3.10b). The HLA-DR IC, IgG_{2b}, showed a general widespread red hue which was not specific (Figure 3.10c). No specific staining was observed in tissues incubated with the CD20 IC, IgG_{2a} (Figure 3.10d). No isotype control was available for the monoclonal antibody for MOG, therefore omission of the antibody served as a negative control. Omission of the primary antibody for MOG did not show any background staining from the secondary antibody (Figure 3.10e).

Table 3.5: Tissue classification of MS and control blocks based upon H&E, ORO, HLA-DR and MOG staining. For each block the classification given by the MS Society Tissue Bank is documented and then the score for each of the staining criteria with re-classification of lesion type. H&E was graded for perivascular cuffing indicating extent of inflammation using a five-point scale (-, +, ++, +++, +++++) and ORO was graded using a four-point scale indicating extent of ORO positive cells (negative, +, ++, +++). MOG staining was assessed based upon whether it was normal, disrupted or negative. Lesions were classified as active, chronic active or chronic inactive. MS tissue with normal myelin and minimal inflammation was classified as NAWM.

Case number	Region	Brain bank classification	H&E	ORO	HLA-DR	MOG	Re-classification of lesion
MS050	P1E4	NAWM	+	-	Mostly resting, some rounded up microglia	Disrupted in lesion	Active
	P5D7	Lesion	+	+	Activated rounded up microglia at border	Negative in lesion	Chronic active
MS051	A1B6	Lesion	-	++	Activated rounded microglia and flattened in lesion	Disrupted in lesion	Active
MS057	A2D5	NAWM	-	-	Mostly resting microglia, with small area of activated microglia at border	Negative in lesion	Chronic active
	P1C4	NAWM	+	-	Activated rounded up microglia at border	Negative in lesion	Chronic active
			+	-	Activated rounded up microglia at border	Negative in lesion	Chronic active
			+	+	Flattened microglia in lesion	Disrupted in lesion	Active

Table 3.5 (continued): Tissue classification of MS and control blocks based upon H&E, ORO, HLA-DR and MOG staining. For each block the classification given by the MS Society Tissue Bank is documented and then the score for each of the staining criteria with re-classification of lesion type. H&E was graded for perivascular cuffing indicating extent of inflammation using a five-point scale (-, +, ++, +++) and ORO was graded using a four-point scale indicating extent of ORO positive cells (negative, +, ++, +++). MOG staining was assessed based upon whether it was normal, disrupted or negative. Lesions were classified as active, chronic active or chronic inactive. MS tissue with normal myelin and minimal inflammation was classified as NAWM.

Case number	Region	Brain bank classification	H&E	ORO	HLA-DR	MOG	Re-classification of lesion
MS058	P1C3	Lesion	++/+++	-	Activated rounded up microglia at border	Negative in lesion	Chronic active
		Lesion	++/+++ +++/>++++	+ +++	Activated rounded up microglia Activated rounded up microglia	Disrupted in lesion Disrupted in lesion	Active Active
	P1D3	Lesion	+ +	+ +	Activated rounded up microglia	Negative in lesion	Chronic active
		Lesion	+ +	- -	Activated rounded up microglia Resting microglia	Negative in lesion Normal	Chronic active NAWM
MS060	P1C2	Lesion	+	-	Activated rounded up microglia	Negative in lesion	Chronic active
	P2C7	Lesion	+	-	Resting microglia	Normal	NAWM
MS067	P2C7	NAWM	+	-	Resting microglia	Normal	NAWM
MS071	P2C3	NAWM	-	-	Resting microglia	Normal	NAWM
MS080	P2D4	Lesion	+	-	Activated rounded up microglia	Negative in lesion	Chronic active
MS090	A1E6	Lesion	++	+	Activated rounded up microglia, flattened within lesion centre	Negative in lesion	Chronic active

Table 3.5 (continued): Tissue classification of MS and control blocks based upon H&E, ORO, HLA-DR and MOG staining. For each block the classification given by the MS Society Tissue Bank is documented and then the score for each of the staining criteria with re-classification of lesion type. H&E was graded for perivascular cuffing indicating extent of inflammation using a five-point scale (-, +, ++, +++, +++++) and ORO was graded using a four-point scale indicating extent of ORO positive cells (negative, +, ++, +++). MOG staining was assessed based upon whether it was normal, disrupted or negative. Lesions were classified as active, chronic active or chronic inactive. MS tissue with normal myelin and minimal inflammation was classified as NAWM.

Case number	Region	Brain bank classification	H&E	ORO	HLA-DR	MOG	Re-classification of lesion
MS092	A2E3	Lesion	++	-	Activated rounded up microglia	Negative in lesion	Chronic active
	P1B1	Lesion	+++	-	Activated rounded up microglia, flattened within lesion centre	Negative in lesion	Chronic active
	P1D1	Lesion	++/+++	+	Activated rounded up microglia, flattened within lesion centre	Negative in lesion	Chronic active
MS103	P1B3	NAWM	-	-	Resting microglia	Normal	NAWM
	P1D3	NAWM	-	-	Resting microglia	Normal	NAWM
MS159	P1B2	NAWM	++/+++	-	Resting microglia, activated rounded up microglia in centre of lesion	Negative in lesion	Chronic active
CO14	P2A2	Control	-	-	Low numbers of resting microglia	Normal	N/A
CO22	A1A3	Control	-	-	Low numbers of resting microglia around blood vessels	Normal	N/A

Table 3.5 (continued): Tissue classification of MS and control blocks based upon H&E, ORO, HLA-DR and MOG staining. For each block the classification given by the MS Society Tissue Bank is documented and then the score for each of the staining criteria with re-classification of lesion type. H&E was graded for perivascular cuffing indicating extent of inflammation using a five-point scale (-, +, ++, +++) and ORO was graded using a four-point scale indicating extent of ORO positive cells (negative, +, ++, +++). MOG staining was assessed based upon whether it was normal, disrupted or negative. Lesions were classified as active, chronic active or chronic inactive. MS tissue with normal myelin and minimal inflammation was classified as NAWM.

Case number	Region	Brain bank classification	H&E	ORO	HLA-DR	MOG	Re-classification of lesion
CO22	P1C2	Control	-	-	Low numbers of resting microglia	Normal	N/A
	P1C3	Control	-	-	Resting microglia evenly distributed	Normal	N/A
CO25	P1C2	Control	-	-	Resting microglia evenly distributed	Normal	N/A
CO26	P1B1	Control	-	-	Low numbers of resting microglia	Normal	N/A
CO28	A1E1	Control	-	-	Small areas of resting microglia	Normal	N/A
	P1C3	Control	-	-	Low numbers of resting microglia	Normal	N/A
CO30	A1C3	Control	-	-	Low numbers of resting microglia	Normal	N/A

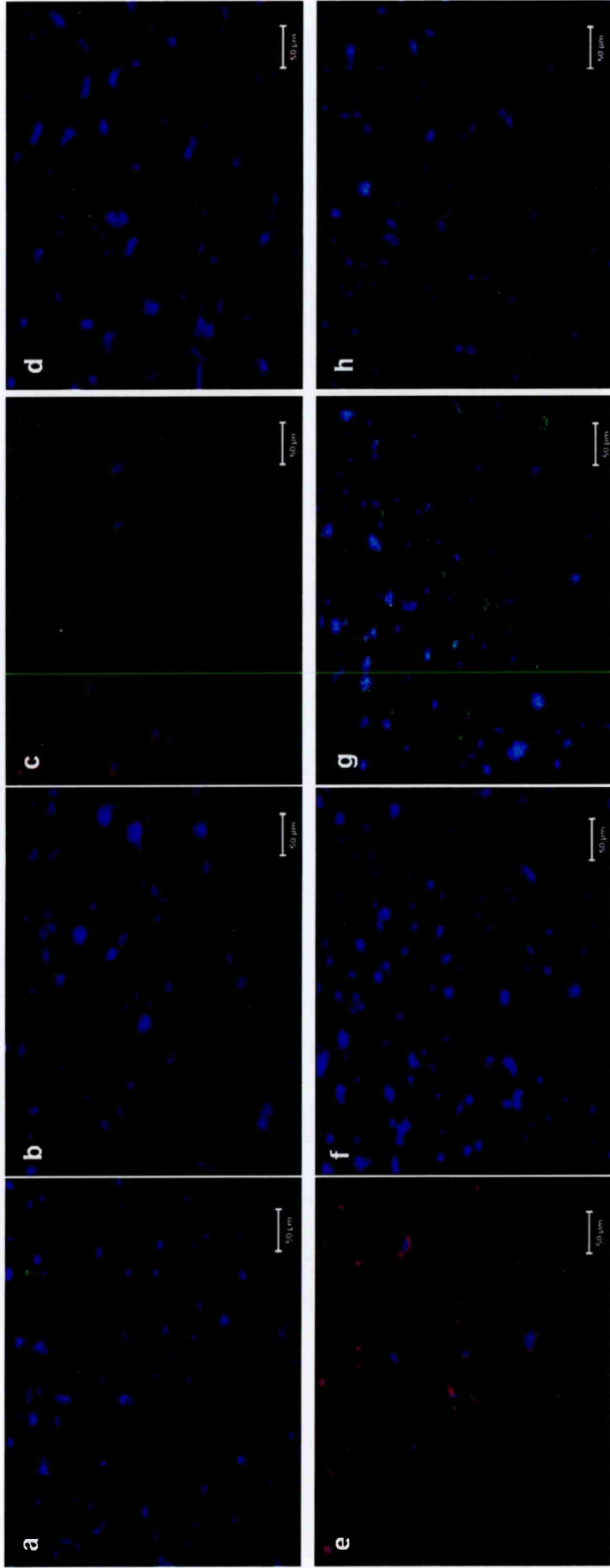


Figure 3.10: The levels of non-specific staining using isotype controls: (a) IgM, (b) IgG1 κ , (c) IgG2 κ , (d) IgG2a, (e) no primary, (f) IgG, (g) IgG and (h) IgG. Nuclei were counterstained with DAPI (blue). Scale bar is 50 μ m.

The rabbit polyclonal antibodies for GFAP, PAD2 and PAD4 were all the same class, however, were tested individually at their specific concentrations due to the use of different secondary antibodies. The rabbit IgG IC concentration corresponding to the anti-GFAP antibody showed some non-specific staining (Figure 3.10f). The IgG IC concentration corresponding to PAD2 antibody showed significant cell-specific staining, which was also seen to a lesser extent in the lower concentration IgG IC corresponding to PAD4 antibody (Figure 3.10f; Figure 3.10g).

3.3.3 Expression of citrullinated proteins in MS, NAWM and control tissue

Levels of citrullinated proteins were graded from 1+ to 4+ (Figure 3.15 a-d). Intense immunoreactivity for citrullinated proteins was seen in both active and chronic active lesions of MS tissue blocks, as compared to NAWM and control white matter tissue. The highest levels of citrullination (3+ and 4+) were observed in lesions, whereas both control and NAWM were rated predominantly 2+ except for one control case which was graded 1+ (Figure 3.11). Strong peptidyl-citrulline immunoreactivity was observed in active lesions with ongoing demyelination, and was associated with areas of activated microglia (Figure 3.12 a-c). Using dual label immunofluorescence for peptidyl-citrulline and GFAP, the intensity of GFAP staining was markedly upregulated in MS specimens, and was colocalised with F95 immunoreactivity (Figure 3.12 d). Strong peptidyl-citrulline immunoreactivity was also observed in active lesions with thinning of the myelin sheath, as assessed by disrupted MOG staining, and was associated with areas of activated microglia HLA-DR, with GFAP colocalised with F95 immunoreactivity (Figure 3.13 4a-d). Citrullination was absent in lesions with complete myelin loss (Figure 3.13 a, c; Figure 3.14 a, c). In chronic active lesions, peptidyl-citrulline immunoreactivity was either weak or absent in areas of complete myelin loss and no microglia, with strongest peptidyl-citrulline immunoreactivity observed in areas with intact or thinning myelin and activated microglia at the lesion edge (Figure 3.15 a-d). NAWM showed weak peptidyl-citrulline immunoreactivity, with strongest immunoreactivity observed at the abluminal region of blood vessels (Figure 3.16 a-d). Control white matter showed areas with peptidyl-citrulline immunoreactivity, with colocalisation with GFAP positive astrocyte cell bodies (Figure 3.17 a-d). Myelin was intact and normal in these cases, with microglia associated with these areas of peptidyl-citrulline immunoreactivity being resting with fine processes (Figure 3.17 a-c).

3.3.4 Expression of PAD2 in MS, NAWM and control tissue

PAD2 consistently showed high immunoreactivity within the lumen of blood vessels, but was not colocalised with endothelial cells (Figure 3.18 a,b). PAD2 did colocalise

with activated microglia (Figure 3.18 c,d). However, PAD2 was shown not to be associated with either GFAP or with citrullinated proteins in astrocytes (Figure 3.18 e-h). In addition to this, PAD2 was not expressed by CD3+ T cells or in myelin (Figure 3.18 i-l). There were no obvious differences in intensity or distribution of PAD2 immunoreactivity between control, NAWM and lesions except within lesions where the green background hue was stronger. The IC for PAD2 antibody showed a high level of staining within the tissue, but was weaker than staining with the PAD2 antibody (Figure 3.19 a-b). PAD4 staining was difficult to detect and was similar to the staining pattern observed when using the corresponding IC (Figure 3.19 c-d).

3.3.5 qPCR analysis of mRNA expression of PAD2 and PAD4 in MS, NAWM and control tissue

PAD2 was shown to be expressed at the mRNA level in control white matter, MS NAWM and MS lesion brain tissue (Figure 3.20). There was significantly less PAD2 mRNA in the MS NAWM compared to both control white matter and MS lesional brain tissue ($p=0.0093$ and $p=0.0369$, respectively).

3.3.6 Western blot analysis of expression of citrullinated proteins in MS, NAWM and control tissue

Following initial optimisation, western blot analysis of proteins from control white matter, MS NAWM and MS lesions all showed multiple bands for citrullinated proteins using the F95 antibody to detect peptidyl citrulline moieties (Nicholas and Whitaker 2002) (Figure 3.21b). In control white matter, MS NAWM and MS lesions, seven major bands were detected, including one at the expected 50 kDa molecular weight for GFAP and one at 18.5 kDa molecular weight suggestive of citrullinated MBP (Figure 3.21b) (Harauz *et al.*, 2004; Boggs 2006). The remaining unidentified bands were seen at 250, 75, 15 and 10 kDa. Among these bands from brain tissue, two bands at ~48 and ~50 kDa were most prominent, which were positively identified as citrullinated GFAP isoforms by overlay of the two antibodies (F95 and anti GFAP) (Figure 3.22a) (Ferguson *et al.*, 2009). Densitometric analysis of these bands showed no significant differences in the proportion of these citrullinated proteins between control white matter and MS NAWM, or control white matter and MS lesion (Figure 3.23 a, b). A strong single band at 75 kDa (Ishigami *et al.*, 2002) was observed when proteins extracted from MS lesional and control tissue were immunoprobed with the PAD2 antibody, confirming the specificity of the antibody (Figure 3.22b).

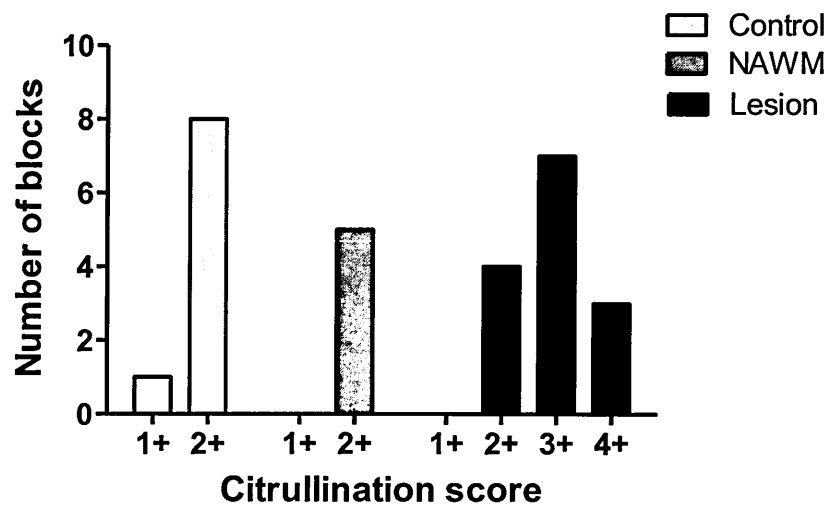


Figure 3.11: Level of citrullinated proteins scored from each block of control white matter, NAWM and lesions from MS cases. Anonymised blocks were blindly graded by two independent researchers (control white matter, $n=9$; MS NAWM, $n=5$; MS lesion, $n=14$). Any discrepancies between blocks were reviewed again and a consensus agreement reached between the two raters. Levels of citrullinated proteins were highest in MS lesions compared to control white matter and MS NAWM.

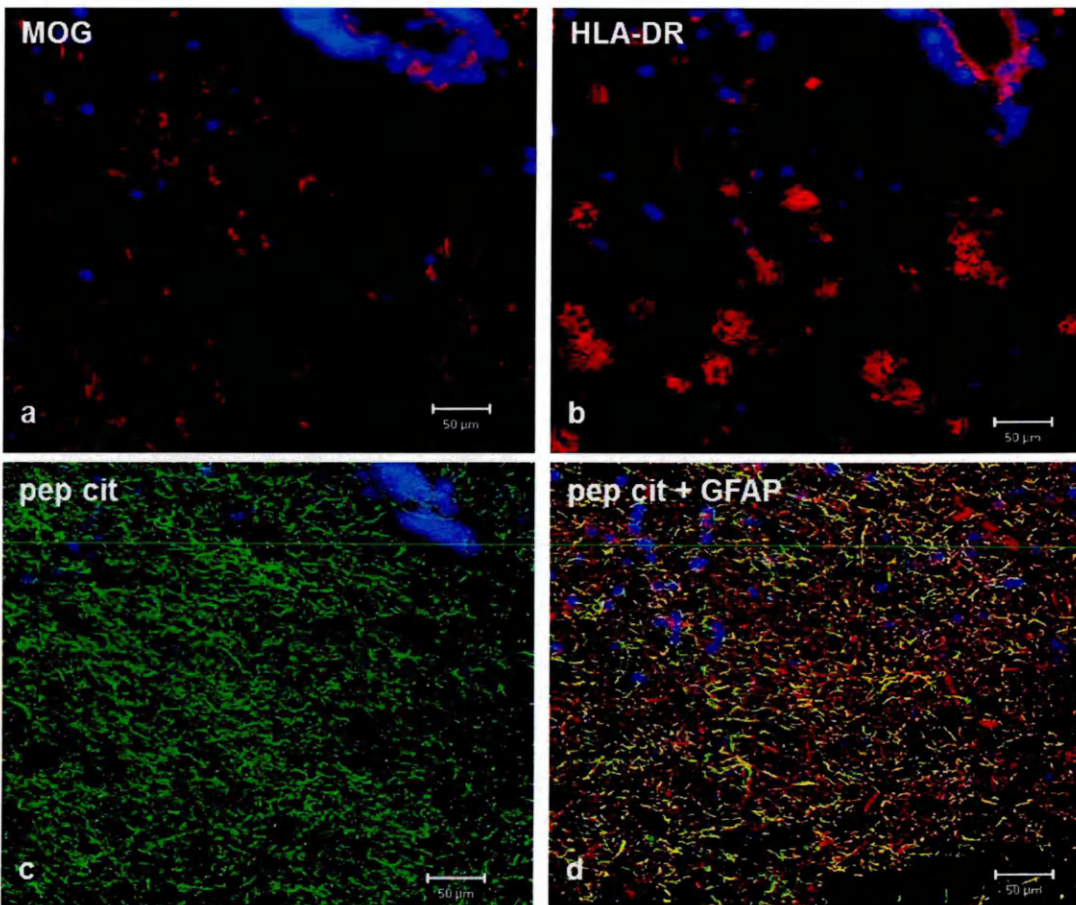


Figure 3.12: Citrullinated protein expression in areas of demyelination in an active MS lesion. Citrullination (pep cit; green), myelin (MOG; red), microglia (HLA-DR; red) and GFAP (red) in an active MS lesion (MS51 A1B6), visualised using single and dual staining immunofluorescence microscopy of serial tissue sections combined with DAPI (blue) demonstrating cell nuclei. **(a)** Ongoing demyelination was observed along with **(b)** activated microglia and **(c)** associated with strong immunoreactive staining for citrullination. **(d)** Citrullination (green) was predominantly co-localised (yellow) to within astrocytes (GFAP; red) at the centre of the lesion. *Scale bar is 50 μm.*

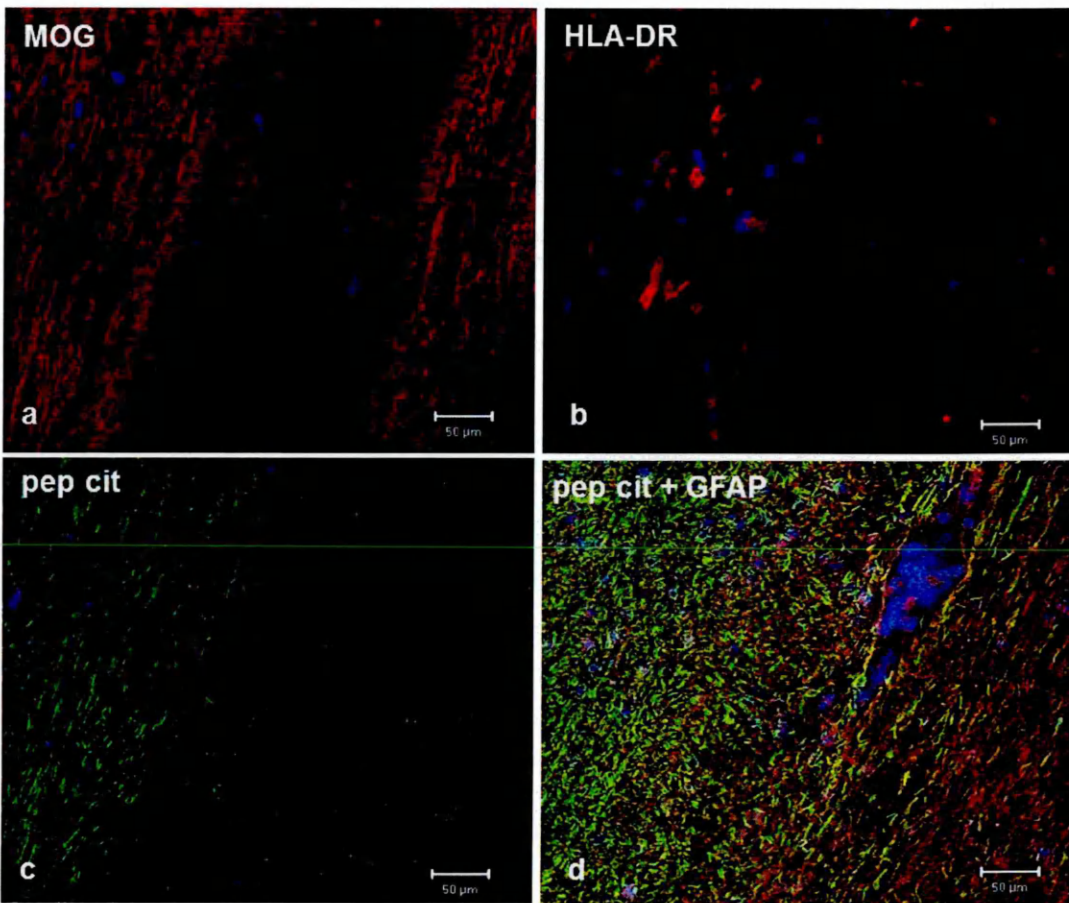


Figure 3.13: Differential citrullinated protein expression in an active MS lesion.

Citrullination (pep cit; green), myelin (MOG; red), microglia (HLA-DR; red) and GFAP (red) in an active MS lesion (MS58 P1D3), visualised using single and dual staining immunofluorescence microscopy of serial tissue sections combined with DAPI (blue) demonstrating cell nuclei. **(a)** Ongoing demyelination was observed along with **(b)** activated microglia and **(c)** strong immunoreactive staining for citrullination. Areas with complete myelin loss were associated with absence of citrullinated proteins. **(d)** Citrullination (green) was predominantly co-localised (yellow) to within astrocytes (GFAP; red). *Scale bar is 50 µm.*

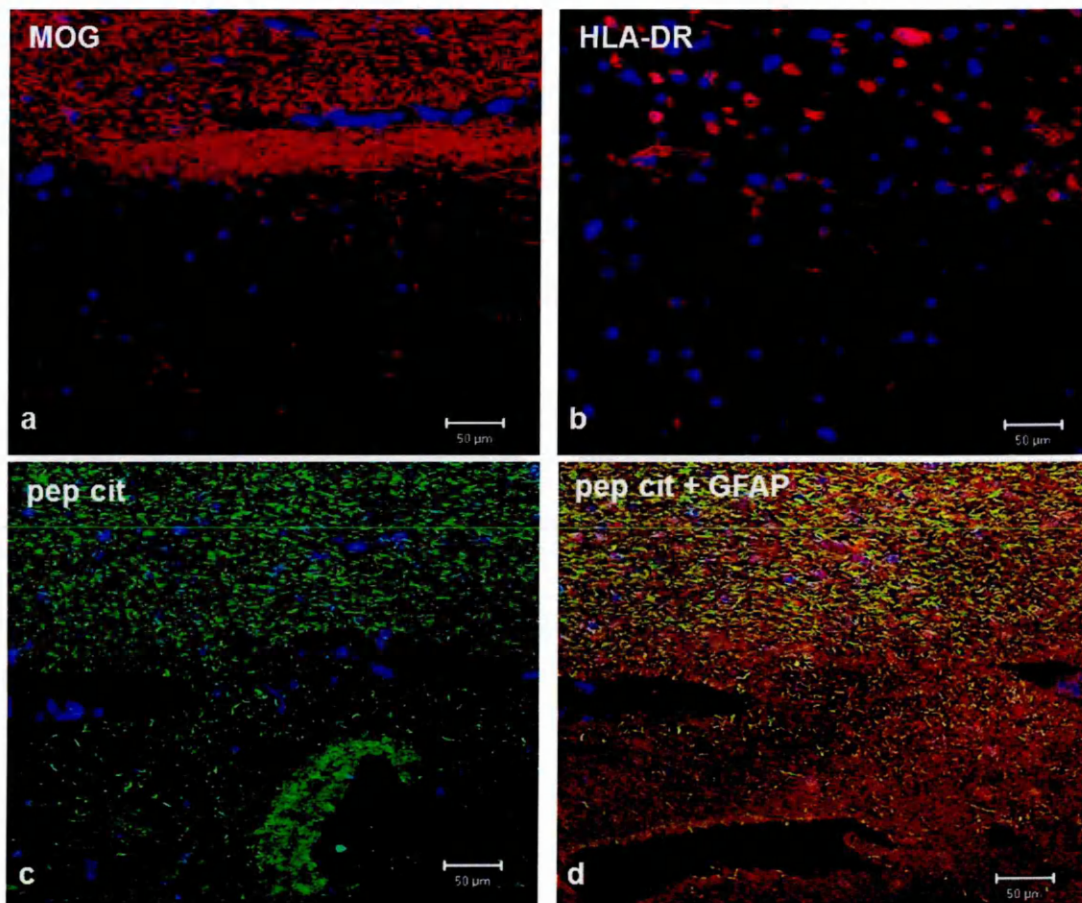


Figure 3.14: Citrullinated protein expression in areas of demyelination in an active MS lesion. Citrullination (pep cit; green), myelin (MOG; red), microglia (HLA-DR; red) and GFAP (red) in a chronic active MS lesion (MS58 P1D3), visualised using single and dual staining immunofluorescence microscopy of serial tissue sections combined with DAPI (blue) demonstrating cell nuclei. **(a)** Complete myelin loss was observed along with **(b)** activated microglia and **(c)** absence of immunoreactive staining for citrullination. **(d)** Low levels of citrullination (green) was observed in absence of extensive astrocyte processes (GFAP; red). Scale bar is 50 µm.

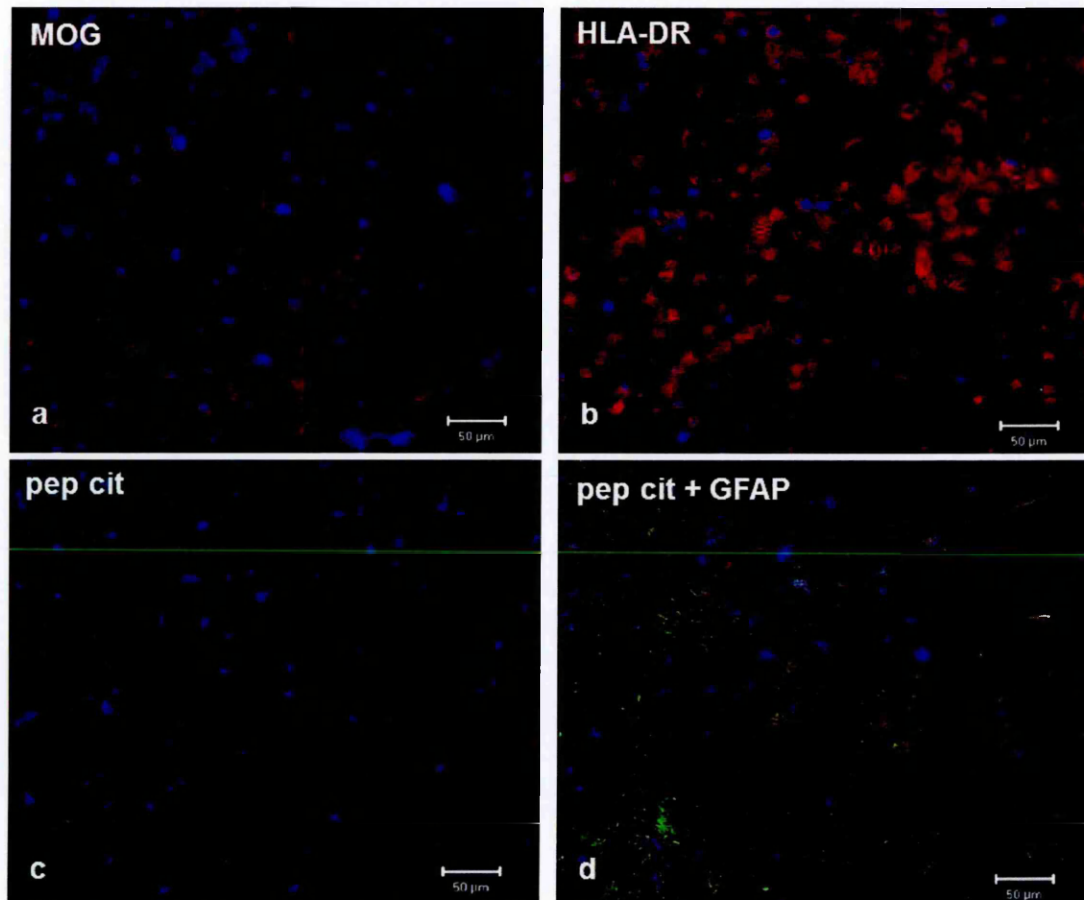


Figure 3.15: Citrullinated protein expression in a chronic active MS lesion. Citrullination (pep cit; green), myelin (MOG; red), microglia (HLA-DR; red) and GFAP (red) in a chronic active MS lesion (MS58 P1D3), visualised using single and dual staining immunofluorescence microscopy of serial tissue sections combined with DAPI (blue) demonstrating cell nuclei. **(a)** In areas of intact myelin **(b)** activated microglia were observed along with **(c)** strong immunoreactive staining for citrullination which was predominantly **(d)** co-localised (yellow) to within astrocytes (GFAP; red). Areas of complete myelin loss were associated with absence of both microglia and citrullination. Scale bar is 50 µm.

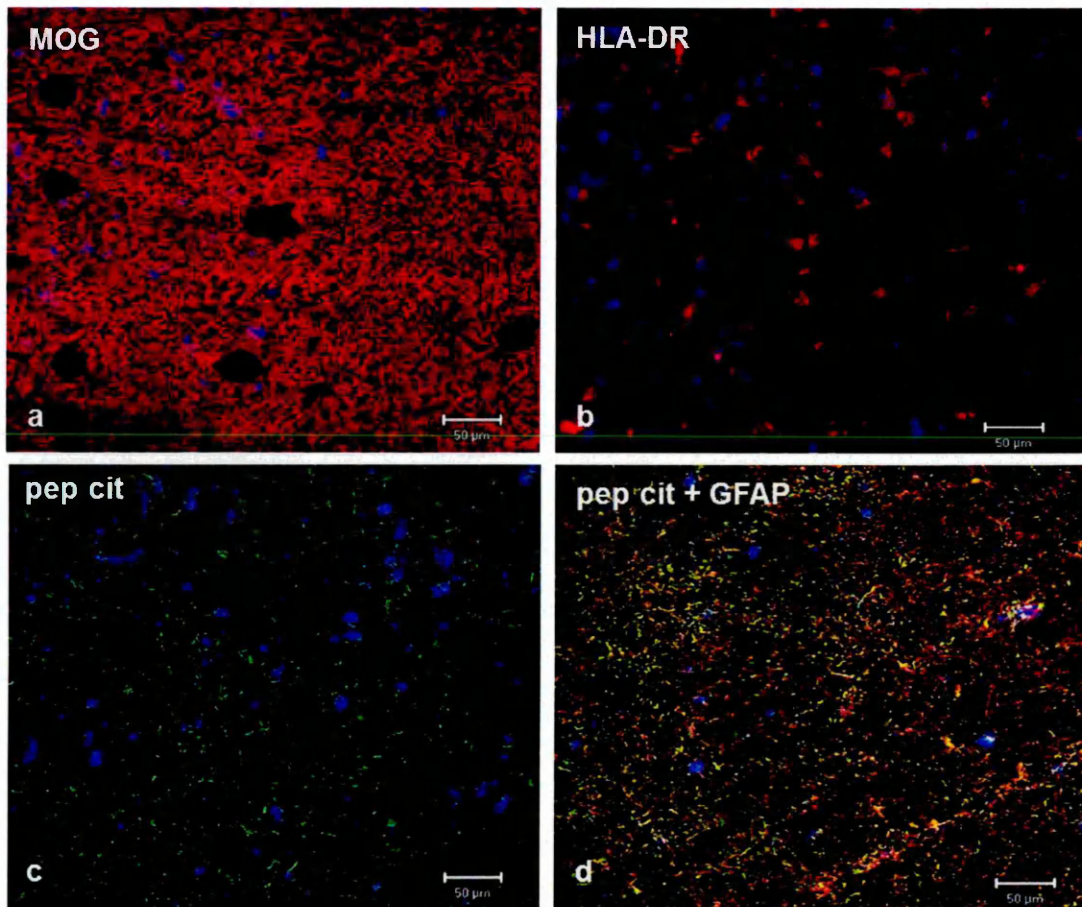


Figure 3.16: Citrullinated protein expression in MS NAWM. Citrullination (pep cit; green), myelin (MOG; red), microglia (HLA-DR; red) and GFAP (red) in MS NAWM (MS71 P2C3), visualised using single and dual staining immunofluorescence microscopy of serial tissue sections combined with DAPI (blue) demonstrating cell nuclei. (a) Intact myelin (b) with resting microglia were observed along with (c) weak immunoreactive staining for citrullination (2+) which was predominantly (d) co-localised (yellow) to within astrocytes (GFAP; red). Scale bar is 50 μm.

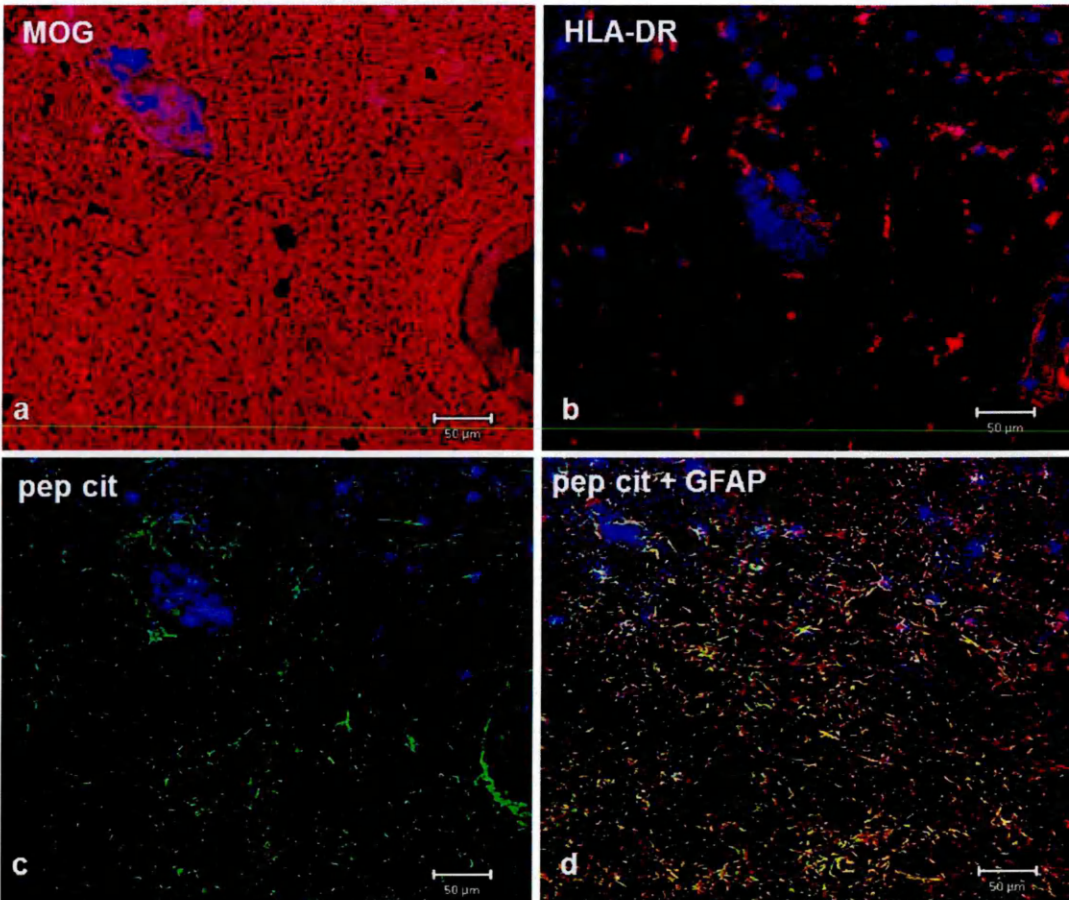


Figure 3.17: Citrullinated protein expression in control white matter. Citrullination (pep cit; green) in control white matter (CO22 P1C3; visualised using single and dual staining immunofluorescence microscopy of serial tissue sections combined with DAPI (blue) demonstrating cell nuclei. **(a)** Intact myelin was observed throughout with **(b)** low level of resting microglia along with **(c)** weaker immunoreactive staining for citrullination which was predominantly (2+) **(d)** co-localised (yellow) to within astrocytes (GFAP; red). *Scale bar is 50 µm.*

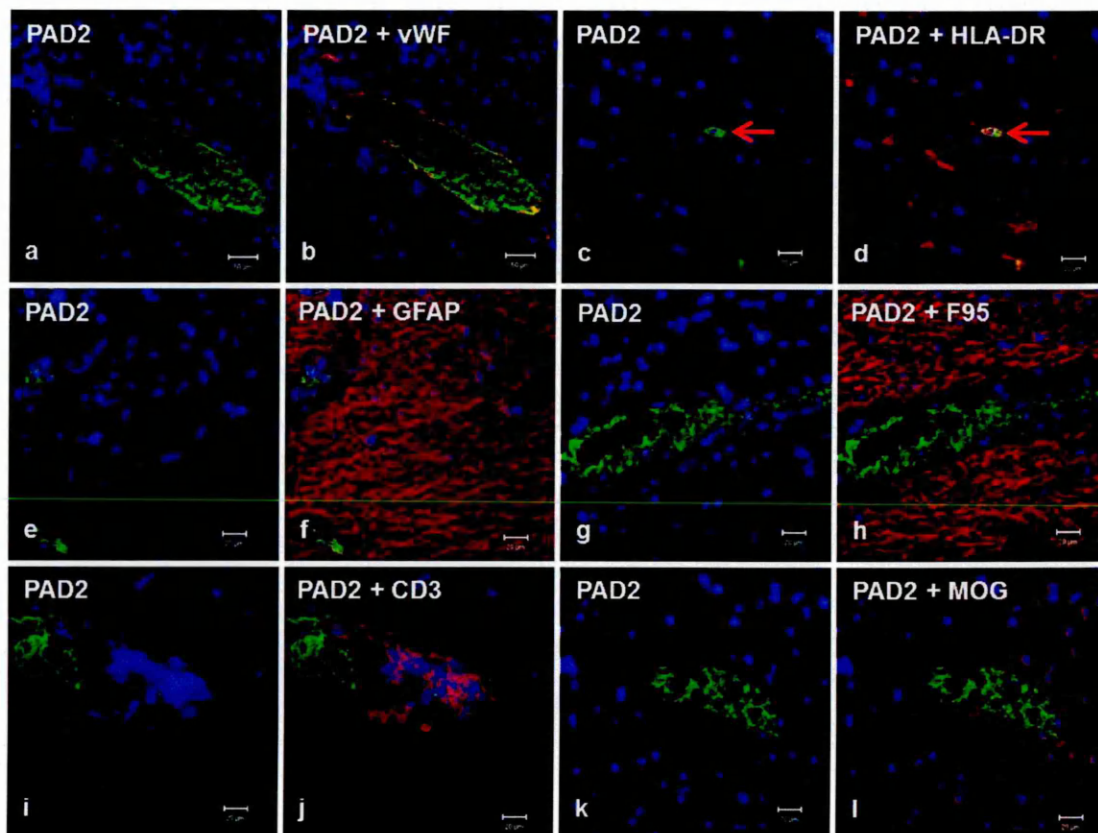


Figure 3.18: Localisation of peptidylarginine deiminase 2 (PAD2) in MS lesions, visualised using double staining immunohistochemistry and confocal microscopy. (a, b) Strong immunoreactivity for PAD2 within the lumen of a blood vessel. (c, d) PAD2 co-localised with HLA-DR positive cells within a white matter lesion, as indicated by red arrow. (e, f) No immunoreactivity for PAD2 within astrocytes in a white matter lesion. (g, h) No co-localisation of PAD2 with citrullinated proteins in a white matter lesion. (i-j) Strong PAD2 immunoreactivity within the lumen of a blood vessel not associated with CD3+ T cells. (k, l) Strong PAD2 immunoreactivity within the lumen of a blood vessel not associated with areas of MOG staining. Scale bar is 20 μ m.

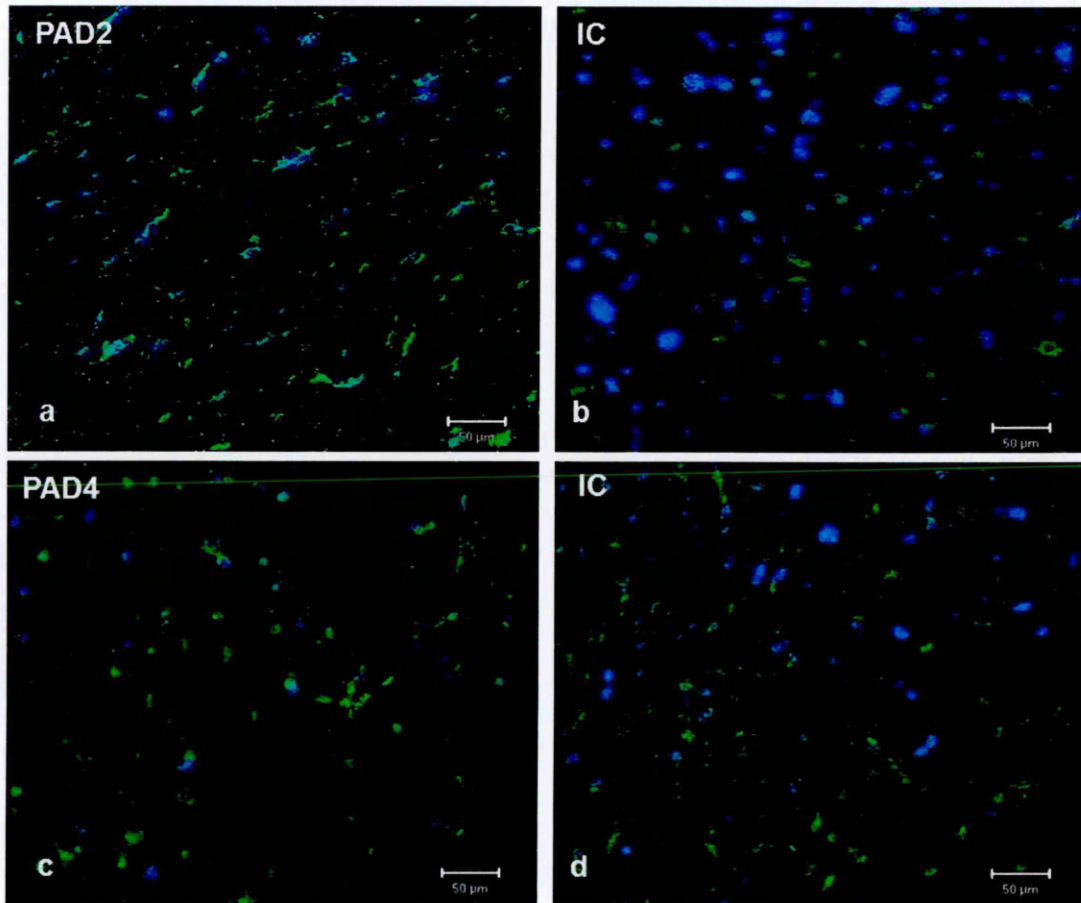


Figure 3.19: Expression of PAD2 and PAD4 in MS NAWM (MS103 P1D3). (a) Low level PAD2 expression was observed throughout the tissue but the expression pattern was similar to (b) the corresponding isotype control (IC). (c) Specific PAD4 staining was difficult to detect and was similar to (d) the corresponding IC. *Scale bar is 50 µm.*

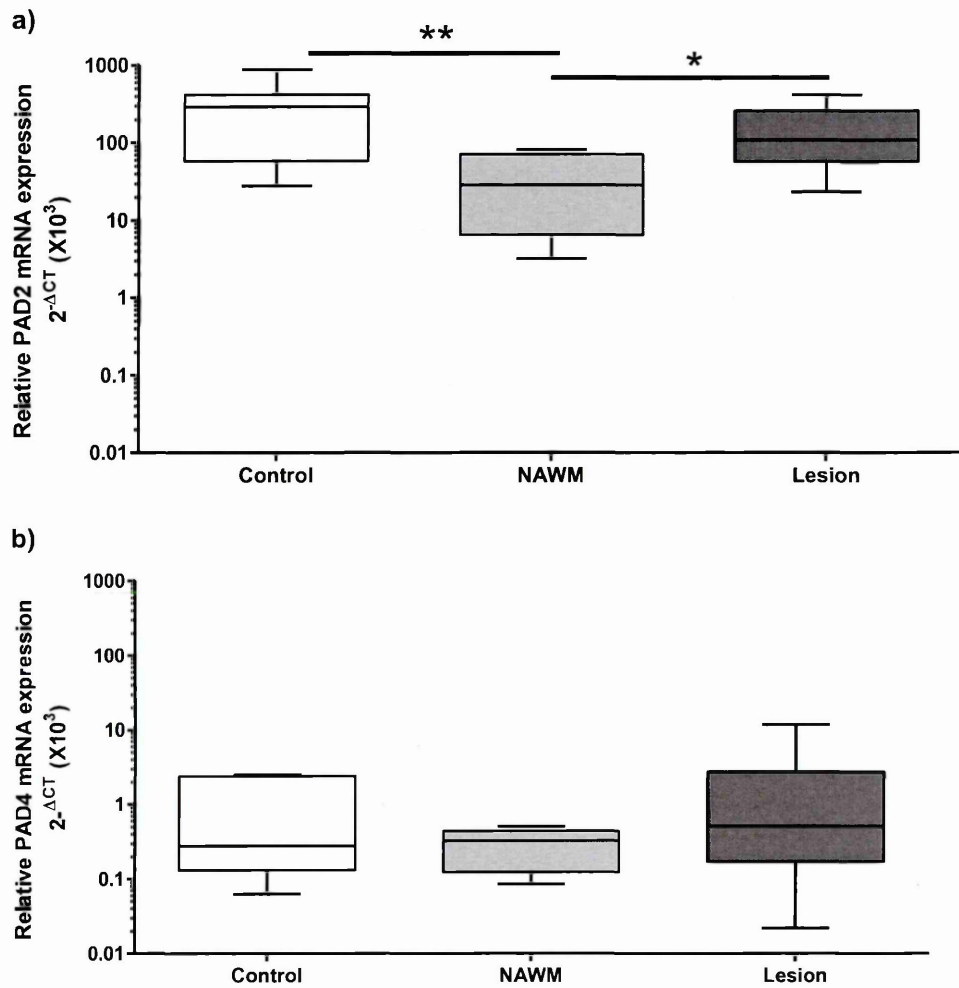


Figure 3.20: qPCR analyses showing PAD2 and PAD4 mRNA expression in control, NAWM and lesion brain tissue (Log scale). mRNA expression of **(a)** PAD2 and **(b)** PAD4. Note the difference in scale bars, showing much greater expression of PAD2 compared to PAD4. Data are represented as the mean (control white matter, $n=9$; MS NAWM, $n=5$; MS lesion, $n=14$) \pm SEM. Statistically significant differences between control white matter, MS NAWM and MS lesional tissue are marked by asterisks ($*p < 0.05$, $**p < 0.01$).

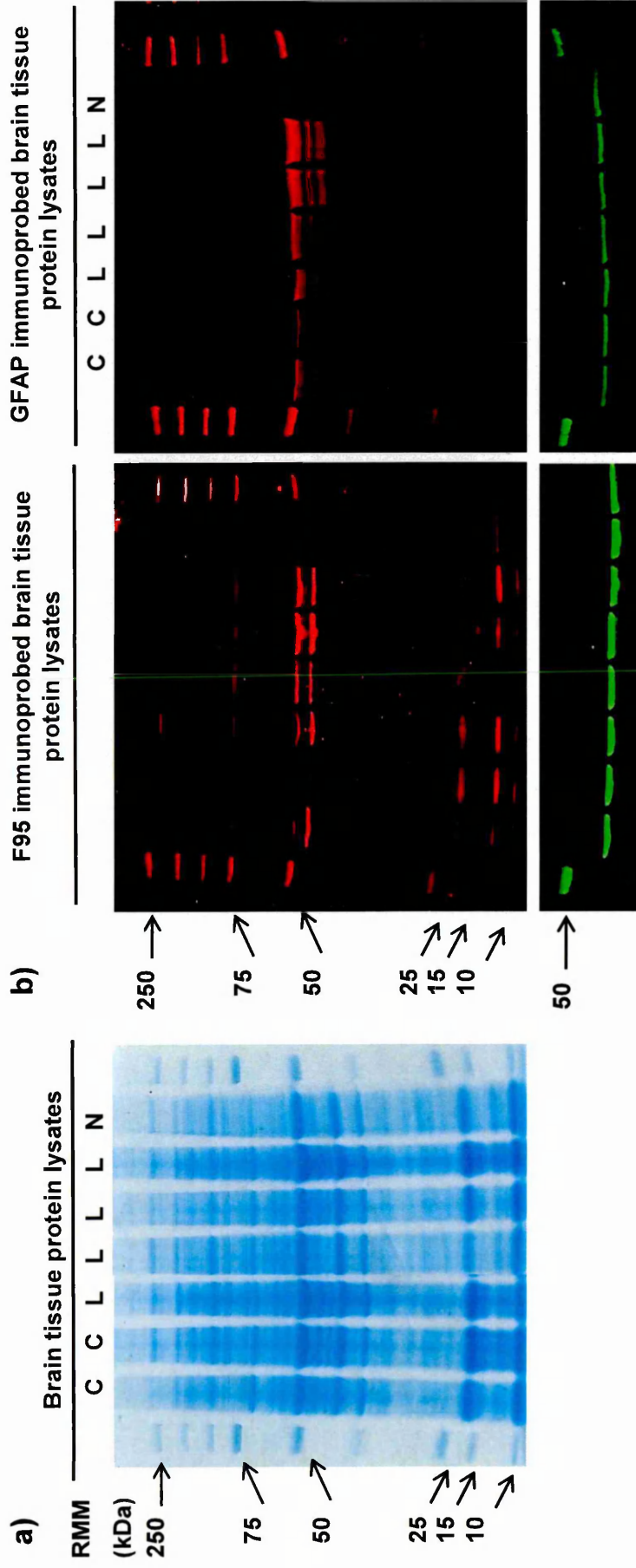


Figure 3.21: Coomassie blue stain of SDS-PAGE and subsequent western blotting of proteins extracted from control white matter, MS NAWM and MS lesional brain tissue. (a) Coomassie stain of SDS-PAGE of control (C), NAWM (N) and lesion (L) brain tissue showing equal loading of protein samples (30 µg/lane). (b) F95 and GFAP immunoprobed western blot of SDS-PAGE separated brain proteins (red). Equal loading was verified by β-actin immunoprobing (green).

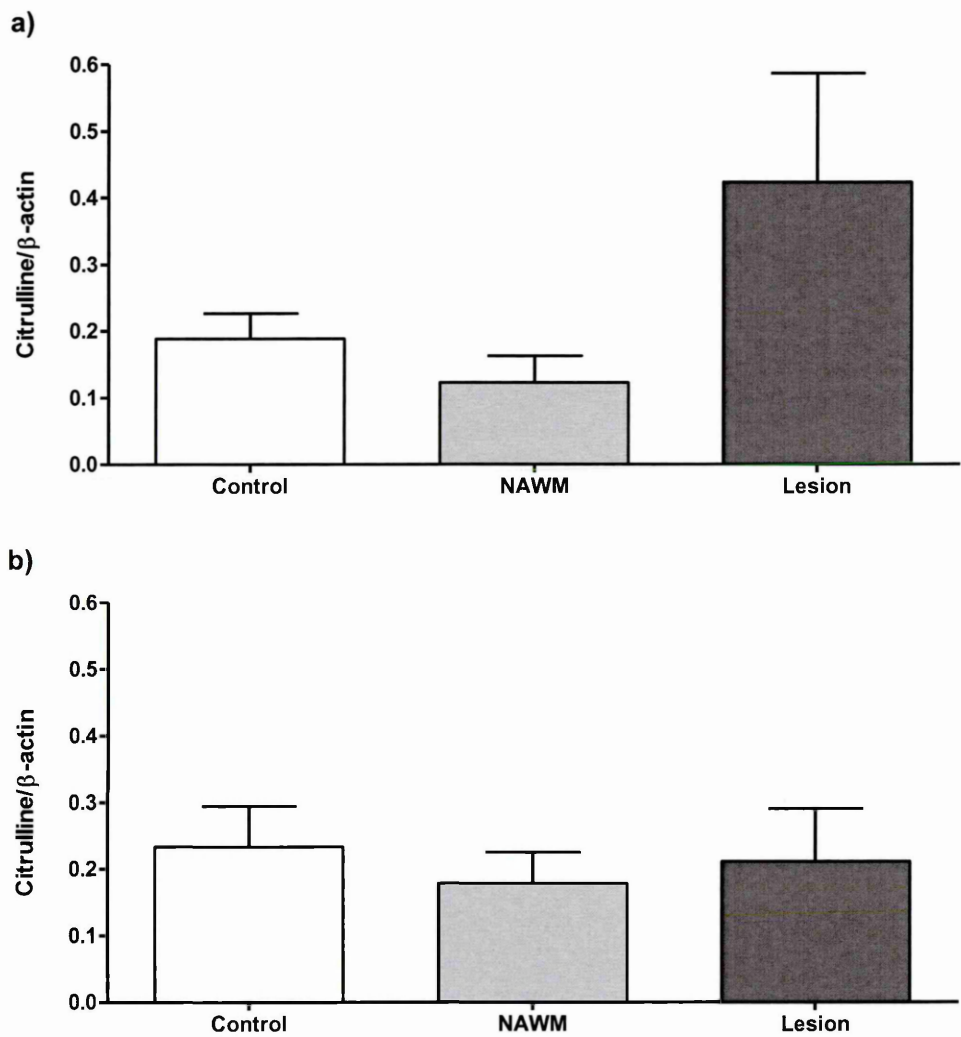


Figure 3.23: Levels of citrullinated GFAP and MBP in control white matter, MS NAWM and MS lesional brain tissue. Densitometric analysis values expressed as the density ratio of target (citrulline) to loading control (β -actin) in arbitrary units in (a) GFAP and (b) MBP of control white matter, MS NAWM and MS lesional brain tissue. Data are presented as the mean (n = control 9 blocks; NAWM 5 blocks; lesion 14 blocks) \pm SEM. No significant differences in levels of citrullinated GFAP and MBP were observed between control, MS NAWM and MS lesional tissue.

3.4 Discussion

3.4.1 The expression of citrullinated proteins is increased in MS

In this study, high levels of citrullinated proteins were found in areas of ongoing demyelination and myelin thinning. In comparison, much lower levels of citrullination were consistently found in the NAWM of MS and control white matter tissue where there is no demyelination. This suggests that the process of citrullination is intimately linked with that of demyelination, which is the hallmark of MS. A striking finding from this study is the increased expression of citrullinated GFAP in both active and chronic active lesions in brain tissue taken from patients with MS. It is not known whether these findings represent an increase in the amount of naturally occurring citrullinated GFAP overall, or if more arginine residues in these GFAP proteins are citrullinated in the disease state.

Citrullination was not shown to be associated with MOG, which was unexpected as MOG is a predicted target of citrullinated proteins. However, this inability to detect citrullinated MOG may be due to under exposure during image capture, as low exposure times were used to capture images of citrullinated GFAP due to the brightness of citrullinated GFAP. By over-exposing the images citrullinated MOG may have been detectable. Unfortunately, interpretation of results regarding citrulline and MOG co-localisation was difficult due to the inability to carry out dual-staining as a result of cross-reactivity of secondary antibodies when carrying out staining on the same section. Furthermore, the majority of previous studies have identified MBP as citrullinated in MS (Wood and Moscarello 1989; Moscarello *et al.*, 1994; Wood *et al.*, 1996). Therefore, it may also have been useful to have carried out dual-staining with anti-human MBP and anti-human peptidyl-citrulline, although interpretation may have also been difficult due to these two antibodies only being available as monoclonal antibodies.

Due to increasing histological evidence indicating that non-lesional NAWM in MS patients has underlying pathology (Nicholas *et al.*, 2004; Kutzelnigg *et al.*, 2005; Frischer *et al.*, 2009; van der Valk and Amor 2009), the NAWM was also examined for the presence of citrullinated proteins. However, in this study we were unable to identify a difference in levels of citrullination between control white matter and MS NAWM compared to MS lesional brain tissue. This finding was unexpected as previously Nicholas and colleagues (2004), using three control and three MS blocks, were able to show increased expression of citrullinated GFAP in the NAWM of brain tissue taken from patients with SPMS. However, our study examined both active and chronic active

plaques as opposed to old chronic active plaques, which may account for this difference. In addition, in this study additional markers were used to assess the underlying pathology of the lesion and surrounding NAWM, most importantly cellular activation of microglia, myelin thinning and demyelination.

Western blotting showed the presence of multiple citrullinated proteins, with bands at ~48 and ~50 kDa, identified as GFAP isoforms and a band at ~18.5 kDa identified as MBP (see chapter 4) (Harauz *et al.*, 2004; Boggs 2006; Ferguson *et al.*, 2009). Additional bands of unidentified citrullinated proteins were observed at 250, 75, 15 and 10 kDa. Western blot analysis and subsequent densitometry of bands corresponding to citrullinated GFAP and citrullinated MBP did not show a difference between levels of citrullination in the three tissue groups. However, this is most likely due to carrying out western blotting using brain extracts of the whole tissue section, as only a small area of the section demonstrated high levels of citrullination microscopically. Using immunoprecipitation with F95 antibody to isolate the citrullinated proteins, as has been used in previous studies (Nicholas *et al.*, 2004; Nicholas *et al.*, 2005) would address this issue. In addition, in immunostaining only a few citrullinated proteins are needed to provide a positive signal, whereas in western blotting a much greater amount of the protein of interest is needed (Keilhoff *et al.*, 2008).

Although previous studies have identified citrullination of MBP in MS, this is the first study that has shown directly that high levels of citrullination are associated with areas of ongoing demyelination and not in areas of complete myelin loss. These findings provide evidence to suggest that citrullination of MBP precedes the actual loss of myelin. Previously, using MBP isolated from NAWM of MS cases and controls, and fractionation of the samples by column chromatography, Moscarello *et al.* (1994) found that 18% of MBP was citrullinated in control tissue compared to 45% of MBP in patients with MS. Further studies by the same group found that in Marburg's disease, as much as 90% of MBP is citrullinated (Wood *et al.*, 1996). This study found that citrullinated MBP in both control and patients with chronic MS contained 6 citrulline residues and 13 arginine residues, whereas citrullinated MBP in patients with Marburg disease contained 18 citrulline residues and only 1 arginine residue (Wood *et al.*, 1996). A number of studies have shown that deiminated MBP is unable to compact lipid bilayers, causing membrane destabilisation, thereby, possibly promoting demyelination (Brady *et al.*, 1981; Wood and Moscarello 1989; Boggs *et al.*, 1999; Beniac *et al.*, 2000). In addition, deiminated MBP is more susceptible to proteolytic digestion by myelin-associated proteases (Cao *et al.*, 1999; Pritzker *et al.*, 2000; D'Souza and Moscarello 2006; Musse *et al.*, 2006). This greater surface exposure and greater enzymatic cleavage of the citrullinated protein would lead to increased release of the

immunodominant epitope, which could prime the innate immune cells of the CNS and sensitize peripheral blood T cells (Musse *et al.*, 2006; Musse and Harauz 2007). Furthermore, proteolytic breakdown of MBP would allow access of PAD2 to the MBP protein, enabling citrullination to take place more readily than when myelin is intact. During demyelination there may be an increase in extracellular calcium, as a result of cell death, leading to activation of PAD2. These results reported in this thesis support previous studies as at sites of ongoing demyelination there is an increase in citrullinated proteins.

GFAP is the main intermediate filament protein in mature astrocytes and is involved in a number of structural and functional processes, including motility, proliferation, vesicle trafficking, autophagy and synaptic interactions with neurons (Middeldorp and Hol 2011). GFAP is also thought to play an important role in astrocyte motility, with motility of GFAP^{-/-} astrocytes shown to be greatly reduced compared to GFAP-expressing astrocytes (Lepekhin *et al.*, 2001). Vesicle trafficking has also been shown to be reduced in astrocytes from mice with double knock-out of GFAP and vimentin (Potokar *et al.*, 2007; Potokar *et al.*, 2008). Neuronal activity is closely linked to the release and uptake of the neurotransmitter glutamate, which requires the interaction between astrocytes and neurons. Glutamate transporters have been identified on neuronal and astrocytic membranes and are important for removal of extracellular glutamate (Pines *et al.*, 1992; Storck *et al.*, 1992; Rothstein *et al.*, 1994). GFAP plays a key role in modulating astrocytic and neuronal glutamate transporter trafficking and function and in the control of glutamine production. In cortical and hippocampal synaptosomal preparations from adult GFAP^{-/-} mice a reduced glutamate uptake was found together with decreased glutamate transport activity (Hughes *et al.*, 2004). GFAP is subjected to multiple post-translational modifications that have important consequences for its structure and functions. Although the exact effect of citrullination of GFAP in astrocytes is currently unknown, it may have detrimental effects on a number of these physiological processes described above, such as reducing astrocyte motility and vesicle trafficking, preventing the phosphorylation of GFAP during cell proliferation (Inagaki *et al.*, 1994), or affect the ability of astrocytes to effectively remove glutamate from the extracellular environment leading to neuronal glutamate excitotoxicity, contributing to pathological processes in MS (Bak *et al.*, 2006).

Traditionally MS is believed to be induced by primarily targeting myelin sheaths and/or oligodendrocytes (Noseworthy *et al.*, 2000). However, recent studies into other demyelinating diseases, such as neuromyelitis optica (NMO), have shown that direct targeting of myelin or oligodendrocytes is not essential and that initial antibodies targeting the astrocytic antigen aquaporin-4 (AQP-4) result in destruction of astrocytes

which is then followed by degeneration and primary demyelination (Lennon *et al.*, 2004; Lennon *et al.*, 2005; Roemer *et al.*, 2007). Astrocyte injury has also been suggested as an important early step in the cascade of lesion formation in brain inflammation, and that this may also be the case in the development of lesions in MS (Sharma *et al.*, 2010). At present potential pathological alterations of astrocytes in MS lesions have not received major attention; however, the high levels of citrullinated GFAP in MS lesions requires further investigation of how this might affect astrocyte function in the pathogenesis of MS.

3.4.2 PAD2 protein expression is associated with microglia and the lumen of blood vessels

PAD2 mRNA was shown to be expressed in control white matter, MS NAWM and in MS lesions. Interestingly, there was significantly less PAD2 mRNA in the MS NAWM compared to both control white matter and MS lesional brain tissue. These results are not unexpected as the expression of mRNA is an insufficient predictor of protein expression (see chapter 2) (Gygi *et al.*, 1999). However, PAD2 protein expression within control white matter, MS NAWM and lesional tissue showed the strongest immunoreactivity within the lumen of the blood vessels and in microglia. No staining for PAD2 was observed in GFAP-positive astrocytes. Previous studies have shown PAD2 to be present in both GFAP-positive astrocytes (Inagaki *et al.*, 1994; Ishigami *et al.*, 2005; Jang *et al.*, 2008; Jang *et al.*, 2011) and microglia (Asaga *et al.*, 2002). Ishigami *et al.* (2005) were able to demonstrate co-localisation of PAD2 with GFAP-positive astrocytes in brain tissue from patients with Alzheimer's Disease (AD). Another group have shown PAD2 to be widely distributed in both astrocytes and neurons in brain tissue from scrapie-infected mice (Jang *et al.*, 2008; Jang *et al.*, 2011). These studies also showed PAD2 to co-localise with citrullinated GFAP-positive astrocytes (Ishigami *et al.*, 2005; Jang *et al.*, 2008; Jang *et al.*, 2011). However, despite testing of several concentrations of anti-PAD2 antibody, blocking steps and fixatives, specific staining of astrocytes was not obtained. Western blotting of control and MS lesional brain tissue produced a single band at ~75 kDa which confirmed the antibody did recognise PAD2 as previous studies have shown PAD2 to be 665 amino acids in length with a predicted molecular mass of 75 kDa (Ishigami *et al.*, 2002; Ishigami *et al.*, 2005). The inability to detect PAD2 in frozen sections, as used in this study, may be due to the fact that in previous successful studies paraffin embedded tissue was used. Unlike previous studies which have shown increased expression of PAD2 in MS brain tissue compared to control brain tissue (Mastronardi *et al.*, 2006; Wood *et al.*, 2008), in this study there were no obvious differences in expression levels between control, MS NAWM and MS

lesional tissue, except for a higher background staining level in lesions, which may indicate PAD2 localisation to myelin. However, this requires further investigation.

In order for PAD2 to become active, raised intracellular calcium ions must be present. There are many physiological and pathological conditions that could lead to raised intracellular calcium and subsequent activation of PAD2 in both neurons and glia, including hypoxia and excitotoxicity (see chapter 2) (Sambandam *et al.*, 2004; Shideman *et al.*, 2006; Smith 2007). If large numbers of activated macrophages containing PAD enzymes are present at inflammatory demyelinating sites in MS white matter, this could result in increased cell death in these areas, due to raised intracellular calcium ions, which would activate PAD enzymes, present both intracellularly and extracellularly, when released from dying cells (Bhattacharya *et al.*, 2006a; Bhattacharya *et al.*, 2006b). In addition, the *PAD2* promoter has been found to be hypomethylated in the white matter of subjects with MS compared to control subjects. Recently this hypomethylation of the *PAD2* promoter has also been found to occur in peripheral blood mononuclear cells taken from patients with MS and is associated with significantly increased peripheral *PAD2* expression in these individuals as compared to controls (Mastronardi *et al.*, 2007; Calabrese *et al.*, 2012). Taken together it seems that hypomethylation of the *PAD2* promoter could be a principal event in inducing the transcription of *PAD2* and subsequent increased activity of the enzyme through increases in intracellular calcium ions leading to citrullination of CNS proteins in MS. A recent study has also shown that upon contact with stimulated T cells, expression of *PAD2* is upregulated in human monocytes (Ferrari-Lacraz *et al.*, 2010), which may also be the case in lesions when macrophages and microglia come into contact with activated T cells. Therefore, there are many factors within the MS tissue, particularly the lesion, which could lead to activation of *PAD2* and subsequent citrullination of CNS proteins.

3.4.3 Conclusion

In conclusion, the increase in citrullinated proteins in areas of myelin thinning and loss within and surrounding MS lesions, along with co-localisation of citrullinated proteins with GFAP-positive astrocytes, supports the hypothesis that citrullination of proteins is important in the pathogenesis of MS, both in terms of citrullination of MBP preceding demyelination and citrullination of GFAP and its possible effect(s) on astrocyte function(s). It is difficult to draw any firm conclusions regarding the expression of *PAD2* in MS brain tissue compared to control tissue due to the inability to detect expression in GFAP-positive astrocytes, although this has been reported by others previously.

Chapter 4

Investigation of the presence of anti-citrullinated protein antibodies in MS and other neurological conditions

4.1 Introduction

Self-reactive antibodies have been implicated in the pathogenesis of MS for many years, since intrathecal Ig synthesis was reported in patients with MS (Kabat *et al.*, 1950) and has remained a hallmark finding in the diagnosis of the disease (Berger and Reindl 2007). Since this discovery, many studies have been carried out to identify the target antigens, with limited success. Whilst the presence of antibodies in the CSF is associated with the diagnosis of MS, it is still unclear whether these Igs actively contribute to the pathogenesis or progression of the disease (Weber *et al.*, 2011). Antibodies are also frequently observed in acute lesions of MS patients (Weber *et al.*, 2011). Furthermore, in newly diagnosed patients, histopathological biopsy studies demonstrate heterogeneity of acute lesions between individual patients suggesting at least four distinct patterns of acute demyelinating lesions exist (Lucchinetti *et al.*, 2000; Lassmann *et al.*, 2001). The most frequent pattern is characterized by significant antibody deposits and complement activation (pattern II) (Lucchinetti *et al.*, 2000). In contrast, in acute lesions of patients with established MS, a more homogenous pattern was observed (Breij *et al.*, 2008). Complement activation supports the role of pathogenic antibodies and antibody-mediated effector functions and is found in areas of demyelination (Storch *et al.*, 1998; Lucchinetti *et al.*, 2000). Furthermore, patients with pattern II histopathologic lesions respond well to plasma exchange therapy, further implicating the role of antibodies in MS (Keegan *et al.*, 2005). In further support of this, clonally expanded populations of memory B cells and plasma cells are found in MS lesions and in the CSF of MS patients with Serafini and colleagues being the first to report the formation of B-cell follicle-like structures in the brains of patients with MS (Baranzini *et al.*, 1999; Villar *et al.*, 2002; Serafini *et al.*, 2004).

It has proven challenging to definitively identify the target antigen to which these autoantibodies bind. There is evidence that autoantibodies derived from patients with MS bind lipids (Brennan *et al.*, 2011), carbohydrates (Lolli *et al.*, 2005; Schwarz *et al.*, 2006) and DNA (Williamson *et al.*, 2001), however, the majority of research has focused on components of the myelin sheath, in particular MBP, MOG, and PLP as possible targets of these autoantibodies, with MBP being the most extensively studied. MBP is one of the principal components of the myelin sheath and is the second most abundant protein in the CNS (Boggs 2006). MOG is present on the outer layer of the myelin sheath and is thus more accessible to antibody binding (Brunner *et al.*, 1989). Both MBP and MOG can act as autoantigens to trigger EAE (Gold *et al.*, 2006), yet no unequivocal evidence of this CNS reactivity has been established to date in MS. In active demyelinating MS lesions, antibodies to myelin, especially to MOG, were found by immunohistochemical analysis (Genain *et al.*, 1999) and IgGs extracted from

inflamed CNS also recognised MOG (O'Connor *et al.*, 2005). Elevated antibody titres against MBP and/or MOG were also reported in the serum and CSF of MS patients (Reindl *et al.*, 1999; Schmidt *et al.*, 2001) and in serum of children with the first episode of CNS demyelination (Brilot *et al.*, 2009; Selter *et al.*, 2010). Furthermore, serum antibodies to MBP and MOG were observed in sub-groups of patients with MS (Lalive *et al.*, 2006; Zhou *et al.*, 2006). Intrathecal IgG from MS patients demonstrate reactivity to several myelin epitopes including: MBP, MOG, MAG and PLP (Archelos *et al.*, 2000; Cross *et al.*, 2001) suggesting that these may contribute to MS pathogenesis. However, myelin-specific antibodies can also be detected in other neurological diseases and healthy controls (Karni *et al.*, 1999; Lampasona *et al.*, 2004), suggesting that these targets are not specifically predictive of disease.

Breakdown in immunological self-tolerance, leading to the production of autoantibodies in MS, might arise from immune recognition of self-proteins that have undergone post-translational modification under pathophysiological conditions (Carillo-Vico *et al.*, 2009). Such modifications might change the structure of the component proteins of myelin, such as MBP and MOG, through the generation of novel epitopes to which the immune system is no longer tolerant resulting in the production of autoantibodies against these modified epitopes. Citrullination is one possible PTM which may be responsible for these changes in MS (Moscarello *et al.*, 2007; Musse and Harauz 2007). Interest in citrullination in MS first developed from studies showing increased citrullination of MBP in patients, particularly those with hyperacute Marburg's syndrome (Wood and Moscarello 1989; Moscarello *et al.*, 1994; Wood *et al.*, 1996). Since these earlier findings, a number of studies have shown increased citrullination to occur in MS brain post-mortem tissue compared to control brain tissue (Nicholas *et al.*, 2004; Mastronardi *et al.*, 2006; Mastronardi *et al.*, 2007; Wood *et al.*, 2008; Oguz *et al.*, 2009). A study by Musse *et al.* (2006) showed that citrullination of membrane bound MBP in MS exposes an immunodominant epitope, which is highly susceptible to cleavage by myelin-associated proteases, which may result in its release and priming of the immune system (Cao *et al.*, 1999; Musse *et al.*, 2006). Furthermore, peripheral T cells from patients with MS have shown enhanced reactivity to citrullinated MBP compared to non-citrullinated MBP and control individuals (Tranquill *et al.*, 2000).

Antibodies to citrullinated proteins have been reported in another autoimmune disease, RA, targeting multiple RA-specific proteins, including vimentin, fibronectin and filaggrin amongst others (Klareskog *et al.*, 2008). Testing of ACPAs in individuals with RA is now one of the prime biomarkers used in the diagnosis of RA, with the ability to predict disease onset and is associated with a more severe disease course (Whiting *et al.*, 2010).

Previous studies investigating the presence of autoantibodies to citrullinated peptides in MS patients are limited. A study by De Seze *et al.* (2001) using paired CSF and serum samples from 60 patients with MS and 30 other neurological disease (OND) controls, followed by incubation with both citrullinated and non-citrullinated MBP peptides in an enzyme-linked immunosorbent assay (ELISA), did not demonstrate any difference in antibody responses to citrullinated MBP peptides between individuals with MS and OND controls (De Seze *et al.*, 2001). A more recent study using serum from 85 patients with MS and a commercially available RA specific ELISA kit coated with cyclic-citrulline containing peptides, showed only 3 patients demonstrated serum reactivity to these citrulline containing peptides (Bodil Roth *et al.*, 2008). However this low positivity amongst patients with MS is most likely attributed to the fact that the antigen used in this assay was developed to diagnose RA.

Based on these previous studies and studies in chapter 3 of this thesis showing extensive citrullination within the CNS associated with demyelination in MS, a study was carried out to further identify proteins that are specifically citrullinated in MS. This predominantly involved the use of mass spectrometry for peptide identification, with the aim of being able to use these newly identified citrullinated peptides to coat the wells of an ELISA plate to develop an assay more specific for ACPA in MS patients.

The conversion of an arginine to citrulline results in a 0.984 Da mass increase and loss of one positive charge per modified citrulline (György *et al.*, 2006). This latter change has a substantial effect on the acidity of the amino acid side chain, changing the isoelectric point (*pI*) from 11.41 for arginine to 5.91 for citrulline (Orgován and Noszál 2011). Both the mass difference and the shift from a basic to a neutral pH will have consequences on the detection of citrullinated proteins and peptides, by mass spectrometry (De Ceuleneer *et al.*, 2012).

The most common detection method for citrullinated proteins is western blotting, whereby a tissue extract containing citrullinated proteins is separated by SDS-PAGE, followed by electrophoretic transfer to a membrane which is then incubated with a primary antibody against citrullinated proteins followed by a labelled secondary antibody for immunodetection. Although very specific, this method only gives an indication of citrullination state, but not of the identity of the citrullinated protein, nor of the location of the citrullinated residues within this protein. Two SDS-PAGE analyses of the same sample are often executed concurrently. One gel being used for the determination of the citrullination status by blotting followed by immunodetection with an antibody specific for citrullinated proteins and the other stained and matched with the blot, after which proteins of interest are excised and identified using mass spectrometry.

This chapter describes the investigation of novel citrullinated proteins in post-mortem MS brain tissue utilising SDS-PAGE and mass spectrometry to follow on from the previous chapter (chapter 3) whereby multiple citrullinated protein bands were observed following western blotting of proteins extracted from control, MS NAWM and MS lesional brain tissue. Mass spectrometry was employed to ascertain the identities of these citrullinated proteins, with the aim of being able to use these newly identified citrullinated peptides to develop an assay to measure ACPAs in individuals with MS.

4.1.1 Aim of the study

To identify novel citrullinated proteins in MS brain tissue and determine if antibodies against these citrullinated proteins are present in MS patient serum and CSF.

4.1.2 Objectives of the study

1. Identify novel citrullinated proteins in MS brain tissue using MALDI-MS.
2. Develop an ELISA method for the detection of ACPAs in MS serum and CSF, specifically targeted to citrullinated MBP and/or other CNS proteins.
3. Detect the presence of ACPAs in paired patient serum and CSF samples from MS patients, ONDs and non-neurological patient controls using this developed ELISA technique and determine whether antibody levels can be used to identify patients with MS.

4.2 Materials and methods

4.2.1 Suppliers used in this chapter

Axis-Shield Plc, Luna Place, The Technology Park, Dundee, DD2 1XA, Scotland; **eBioscience Ltd**, 2nd floor, Titan Court, 3 Bishop Square, Hatfield, AL10 9NA, UK; **Millipore Ltd**, Suite 3 & 5, Building 6, Croxley Green Business Park, Watford, WD18 8YH, UK; **Pepceuticals Ltd**, 4 Feldspar Close, Warrens Park, Enderby, Leicestershire, LE19 4JS, UK; **Peprotech EC Ltd**, Peprotech House, 29 Margravine Road, London, W6 8LL, UK; **Sigma-Aldrich**, The Old Brickyard, New Road, Gillingham, Dorset, SP8 4XT, UK; **Waters Corporation**, Floats Road, Manchester, M23 9LZ, UK.

4.2.2 Reconstitution of human MBP

Recombinant human MBP (Sigma, UK) (1 mg) was reconstituted in 1000 μ L sterile H₂O to give a final concentration of 1mg/mL. This stock solution of MBP was stored in 20 μ L aliquots at -20°C until required.

4.2.3 Sodium Dodecyl Sulphate Polyacrylamide Gel Electrophoresis (SDS-PAGE)

MS tissue protein extract (MS058 P1C3) which had showed the most extensive citrullination by immunohistochemical and western blot analysis (Chapter 3) (30 μ g) (see sections 3.2.4.1 and 3.2.4.2) and pure MBP (10 μ g) (Sigma, UK) as a positive control were fractionated on pre-cast 10% Bis-Tris gels using SDS-PAGE (see section 3.2.4.4). Following SDS-PAGE, the gel was stained using Instant Blue (Expedion, UK) for 1 hr at RT in order to visualise the protein bands. Protein bands of interest were then excised from the gel using a sterile blade and placed into Eppendorf tubes and stored at -80°C.

4.2.4 In-gel digest and extraction of peptides

Prior to carrying out an in-gel tryptic digest 10 mM dithiothreitol (DTT) solution in 25 mM NH₂CO₃ (1.5 mg DTT in 1 mL 25 mM (NH₄)₂CO₃) and 55 mM idoacetamide solution was made in 25 mM (NH₄)₂CO₃ (10 mg idoacetamide in 1 mL 25 mM (NH₄)₂CO₃) were prepared. The first step involves the reduction and alkylation of gel pieces. Briefly, each gel piece was rehydrated in 40 μ L 10 mM DTT, vortexed followed by pulse-centrifugation. The sample was then incubated on a heat block at 56°C for 45 minutes. Following this, the supernatant was then removed and 40 μ L 55 mM

idoacetamide was added to each gel piece, vortexed followed by pulse-centrifugation. The sample was then placed in the dark and left to incubate for 30 minutes to allow the reaction to proceed. Following this, the supernatant was discarded and the gel piece was washed by the addition of 100 μL 25 mM $(\text{NH}_4)_2\text{CO}_3$, vortexed for 10 minutes followed by pulse-centrifugation. The supernatant was then removed and 200 μL 100% acetonitrile (ACN) was added to the gel piece, vortexed briefly and then left to stand for approximately 10 minutes until the gel pieces started to shrink and turn white. Lastly, the supernatant was removed and samples were subjected to Speed Vac for approximately 10 minutes until the gel pieces were dry.

Once the gel pieces had been successfully reduced and alkylated the tryptic digest was performed. Briefly, 25 μL (10 $\mu\text{g}/\text{mL}$) trypsin solution (Promega trypsin made up in 25 mM $(\text{NH}_4)_2\text{CO}_3$; pH 8.1) was added to each gel piece and samples were allowed to rehydrate for 1 hour on ice. Following this the excess trypsin solution was removed and the gel piece was covered with ~ 40 μL 25 mM $(\text{NH}_4)_2\text{CO}_3$. The gel pieces were then incubated on a shaker overnight at 37°C.

The next day, peptides were extracted from the gel pieces. Briefly, gel pieces were subjected to pulse-centrifugation, and following this the supernatant was removed and transferred to a clean Eppendorf tube. 30 μL 50% ACN 0.1% TFA was added to each gel piece, vortexed for 15 minutes and then subjected to pulse-centrifugation. The supernatant was then removed and added to the supernatant from the previous step. The step with the addition of 50% ACN 0.1% TFA was then repeated. The resulting extract was then subjected to Speed Vac centrifuge to reduce the sample to approximately 10 μL .

In-gel digests were also performed with Lysine C (Lys C) (Promega, UK), which digests proteins at the carboxyl side of lysine residues allowing for the detection of peptides with probable arginine modifications. In this instance the same procedure as above was followed except the $(\text{NH}_4)_2\text{CO}_3$ buffer was replaced with 25 mM Tris-HCl (pH 9.3) and the Lys C was incubated with the gel piece for 18 hours at 37°C.

4.2.5 Mass spectrometry

Mass spectrometry is used to measure the molecular mass of a sample within approximately 0.01-0.2% of the total mass, which enables detection of minor mass changes such as post-translational modifications or amino acid substitutions (Karas *et al.*, 1990).

4.2.5.1 Principles of MALDI mass spectrometry

Matrix assisted laser desorption ionisation (MALDI) is a useful tool for the analysis of non-volatile organic compounds of high M_r . This ionisation technique is used for the analysis of proteins, peptides, glycoproteins, oligosaccharides and oligonucleotides (Yan *et al.*, 2000). A basic mass spectrometer consists of three main components: the ionisation source, a mass analyser that measures the mass-to-charge ratio (m/z) of the ionised analytes, and a detector that registers the numbers of ions at each m/z value (Aebersold and Mann 2003). Experimental samples are mixed with an organic compound with a strong absorption at the appropriate laser wavelength and then spotted onto a stainless steel target plate and left to air-dry. The matrix and sample are mixed with approximately 100-1000-fold molar excess of the matrix. The required amount of the sample is low, between 0.5 and 2.0 μL of the analyte/matrix mixture is usually sufficient (Schiller *et al.*, 2004). Once the solvent has evaporated and the matrix has crystallised, the plate is placed into the mass spectrometer, where ionisation begins. The laser beam hits the sample-matrix crystal in pulses, leading to absorption of the laser energy by the matrix. UV lasers are most commonly used in MALDI and emit light at a fixed wavelength, usually a nitrogen laser at a wavelength of 337 nm is used (El-Aneed *et al.*, 2009) (Figure 4.1a). Energy is then transferred from the matrix molecules to the sample within the matrix, and both sample and matrix desorb from the condensed state and enter the vapour phase. During this process ion formation occurs whereby protons transfer from the matrix to the sample. Following this, under a high potential, the ions accelerate down a vacuumed drift scope tube. The ions are then passed through a series of extraction and focusing electrodes and lenses in the analyser region, where separation according to mass (m) –to-charge (z) ratio (m/z) occurs, before the ions are detected.

MALDI is a soft ionisation method that enables the analysis of biomolecules of higher molecular weights without major degradation, reducing the risk of fragmentation and produces singly-charged ions (Schiller *et al.*, 2004). Mass analysers with high m/z capabilities are therefore used in addition to MALDI, such as the time-of-flight (TOF) analyser or quadrupoles, which all separate ions based on their m/z ratio, however, they differ in their m/z range coverage, accuracy or resolution. The TOF mass analyser measures the time for ions to travel between the accelerator electrode and the detector, i.e. along the drift tube, and from this determines the m/z value (Figure 4.1b). Equally charged low mass ions arrive at the detector in a shorter time than high mass ions.

The laser pulses produce discrete groups of ions intermittently, which facilitates measurement of the flight time. The resolution of the TOF is improved by the addition

of a reflectron, which focuses the energy spread of the ions (El-Aneed *et al.*, 2009). These reflectrons are repelling devices that cause the ion to change direction and accelerate back towards the detector. Ions with higher kinetic energy will penetrate deeper into the ion mirror and therefore travel further into the reflectron and have a longer flight path. This leads to all ions of a specific m/z ratio arriving at the detector in a narrower time span, which improves the TOF spectrum.

These analysers can be used alone or joined together to take advantage of the strengths of each to form a hybrid. Tandem (MS-MS) mass spectrometers have more than one analyser and are useful in acquiring structural and sequence data, for example the quadrupole-time-of-flight version. Ion mobility separation (IMS) is used extensively to assess the structure and identity of a large number of molecular analytes and can also be incorporated into modern mass spectrometers. Hybrid IMS-MS instruments that have taken multiple forms, and recent advances have seen improvements in both the IMS and MS stages in modern instrumentation. Among these hybrid instruments, the quadrupole (Q)-IM-TOF MS instrument, known as the Synapt 2 HDMS system, has been recently developed (Waters Corporation, UK). This instrument consists of four components: ionisation source for ion generation, a modified quadrupole mass analyser for ion selection, tri-wave IMS which uses time-varying potential 'waves' to drive ions through the drift tube, and a high-performance TOF mass analyser for high-resolution mass analysis (Zhong *et al.*, 2011).

MALDI can be used in either positive or negative ion mode, depending on whether the sample either gains or loses a proton respectively, i.e. $(M+H)^+$ or $(M-H)^-$, where M represents the molecular ion. Positive mode is generally used for protein and peptide analysis. In positive mode, other species commonly identified are $(M+NH_4)^+$ salt adducts, such as $(M+Na)^+$. Traces of doubly charged molecular ions at half the m/z value, or dimers at twice the m/z value, can sometimes be identified. Since spectra are primarily recorded in the positive ion detection mode cationising agents are often added to the matrix to increase the ion yield, such as TFA in a concentration of 0.1% (Schiller *et al.*, 2004).

There are numerous detectors available to suit the type of analyser used, but detection of ions is always based on their charge, their mass or their velocity. The ion current is monitored by the detector, which also amplifies it and transmit signals to the data system, which records it as a mass spectra.

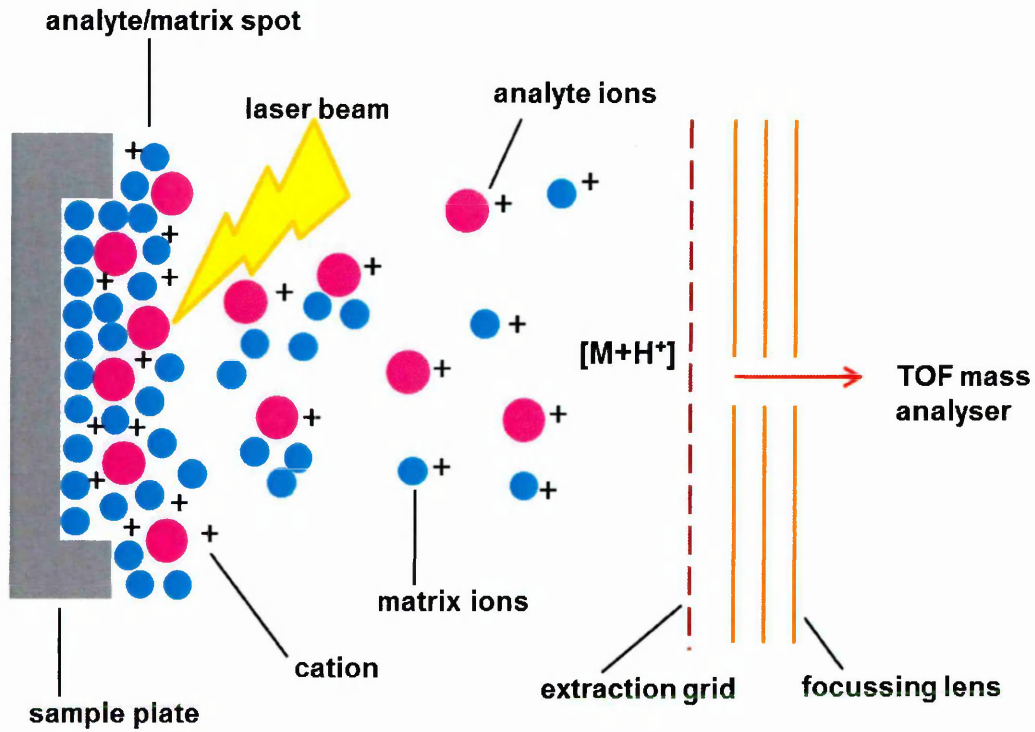
Figure 4.1: Schematic diagram demonstrating MALDI-TOF mass spectrometer and a TOF mass spectrometer.

a) Prior to MALDI mass spectrometry analysis the sample is mixed with a matrix and spotted onto a target plate and left to air dry. Once dry the matrix crystallises and forms co-crystals with the sample. The target plate is then inserted into the mass spectrometer, where a laser is fired onto the sample. Desorption occurs as the matrix absorbs the laser energy, causing rapid heating and subsequent sublimation of matrix molecules. Matrix and analyte clusters expand into the vapour phase, and are ejected from the target surface. Excited matrix molecules are stabilised by proton transfer to the analyte, and cation attachment to the analyte occurs. The matrix evaporates away to leave free analyte ions.

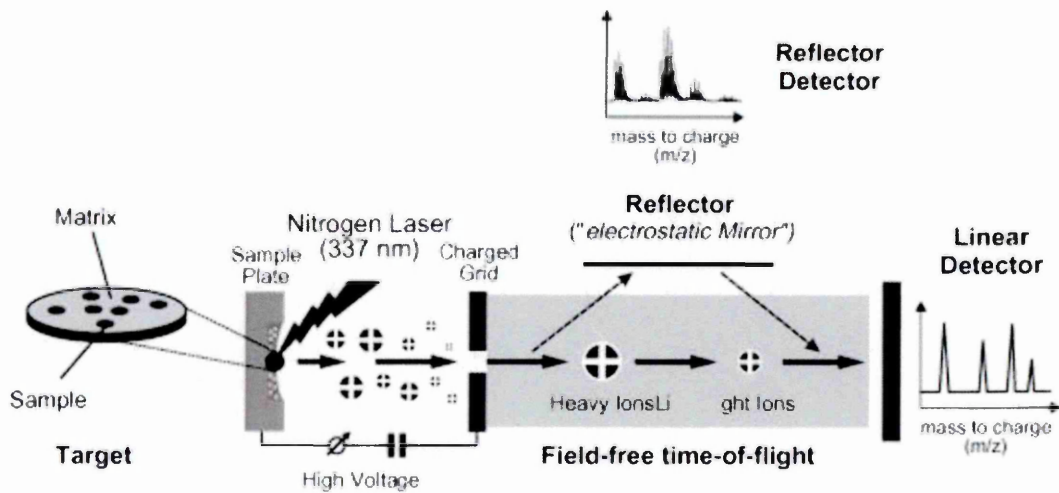
b) Singly charged ions generated from the desorption-ionisation process pass through a charged grid, and are accelerated into the TOF drift tube, which is under a high vacuum. The length of this tube is typically 0.5-3 m long, and since the separation of ions is achieved over this distance, determines the possible mass resolution achieved. In order to improve resolution, longer flight tubes can be used or an “electrostatic mirror” can be incorporated to reflect ions at the end of the flight tube to reach a “reflector-detector”, thereby lengthening the field-free path travelled. Equally charged low mass ions reach the end of the flight tube in a shorter time than high mass ions, and as they are equally charged, separation based on mass is achieved. A detector at the end of the tube produces a signal upon impact of each ion, and m/z spectra are produced from this signal as a function of time.

$[M+H^+]$ = ion formed by interaction of a molecule with a proton; TOF = time-of-flight

a)



b)



(Adapted from Schiller *et al.*, 2004)

The m/z values are plotted against their intensities, and the resulting spectra show the molecular mass of the sample components and their relative abundance. From this spectra, peptide mass fingerprinting can be carried out to identify the protein. This set of masses, typically obtained by MALDI-TOF, is then compared to the theoretically expected tryptic peptide masses for each entry in the database (Cottrell 2011). The proteins can be ranked according to the number of peptide matches. When high mass accuracy is achieved, at least 5 peptide masses need to be matched to the protein (Cottrell 2011).

In MALDI, resulting spectra usually only contain the ionised molecule with very little fragmentation data and therefore MS spectra are of little use for structural characterisation. In these cases, induced fragmentation is required using collision-induced dissociation (CID) and tandem mass spectrometry (Mann *et al.*, 2001). This is carried out by first selecting and focussing the precursor ion in the first mass spectrometer analyser (e.g. quadrupole) followed by transfer of the precursor ion to the CID collision cells where it interacts with a collision gas and fragments. The resulting fragments are then separated in the second mass analyser (e.g. TOF) producing the typical MS/MS spectrum which can be used for sequencing, structural elucidation and analyte identification through fragment fingerprinting (Zhong *et al.*, 2011). Tandem mass spectra data contains structural information related to the sequence of the peptide, rather than only the mass, therefore databases can also be searched to identify peptide sequences which match known sequences (Cottrell 2011).

Multiple collisions impart energy onto the molecule until it fragments, where several bonds along the backbone can be broken by these collisions (Figure 4.2). CID fragments peptide ions by cleaving at the N-C bonds. The most common ion types are the b and y ions, which denote fragmentation at the amide bond with charge retention on the N or C terminus, respectively (Mann *et al.*, 2001). These b and y fragment ions provide sequence information which can then be searched against a protein database (Creese *et al.*, 2011).

Protein identification using peptide CID spectra are more clear-cut than those achieved by mass mapping because, in addition to the peptide mass, the peak pattern in the CID spectrum also provides information about the peptide sequence (Aebersold and Mann 2003). The CID spectra are scanned against comprehensive protein sequence databases, such as Mascot, using one of a number of different algorithms to find a positive identification with a known peptide.

4.2.5.2 Matrix requirements for MALDI mass spectrometry

The type of matrix selected for use in MALDI mass spectrometry (MALDI-MS) is very important and greatly affects the results obtained. Different matrices are selected dependent on the sample being analysed. For peptides and protein samples, α -cyano-4-hydroxycinnamic acid (α -CHCA) is most commonly used. The matrices consist of small organic compounds which absorb the laser energy at the selected wavelength and should mix well with the analyte resulting in homogenous co-crystallisation (Schiller *et al.*, 2004). In addition, the matrix should also separate the analyte molecules from each other to prevent cluster formation and avoiding direct laser hits on the analyte that would lead to intense fragmentation (Pan *et al.*, 2007).

MALDI preparations should ideally have a low concentration of analyte molecules and an excess of matrix on the target plate, usually matrix and sample are mixed with ~100-1000-fold excess of the matrix, which helps to prevent fragmentation of the analyte (Schiller *et al.*, 2004). Most importantly, a matrix should be selected that has good absorption properties with the laser used, and that mixes well with the analyte to give homogenous co-crystallisation.

4.2.5.3 Use of Zip Tips® in sample preparation for analysis by mass spectrometry

Mass spectrometry is often complicated by the presence of salts and contaminants in the sample, which can obscure the protein of interest, particularly when it is present at low concentrations. To concentrate and purify samples for optimal results with MALDI-quadrupole/TOF (MALDI-QTOF) analysis, Zip Tips® (Millipore, UK) were used prior to spotting samples onto the target plate. Zip Tips® are 10 μ L pipette tips that contain chromatography resin.

Various resins are available for different applications, and for concentrating small proteins, Zip Tips® with 0.6 μ L of a C18 resin were used, composed of 15 μ m silica with 20 nm pores.

Citrullinated protein digested samples were analysed by MALDI-MS both with, and without, the use of Zip Tips® in the sample preparation stage. Preliminary experiments were thus performed where samples were compared after being mixed with matrix and spotted onto the target plate, or first passed through a Zip Tip® according to the following protocol.

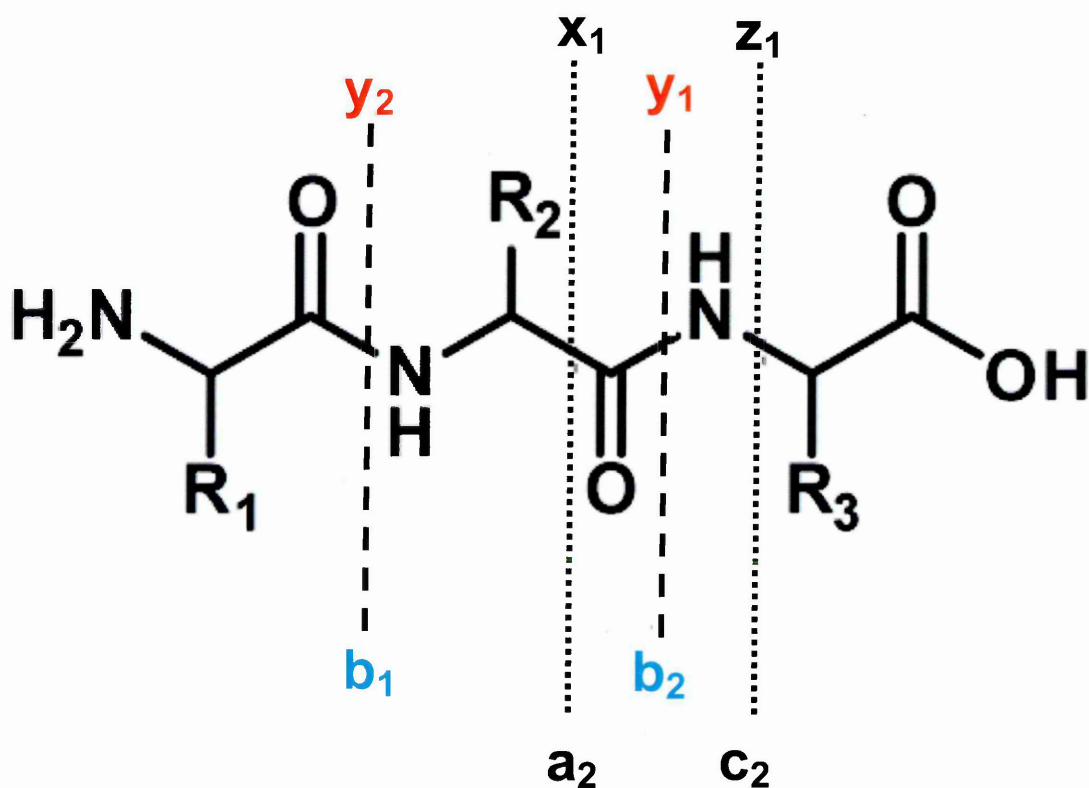


Figure 4.2: Nomenclature for the product ions generated in the fragmentation of peptide molecules. Collision-induced dissociation (CID) causes a single cleavage to occur randomly at the various amide bonds in the peptide molecules. This process generates a series of fragments that differ by a single amino acid residue. Peptide fragments are named according to whether the fragments contains the N- or C-terminus, the peptide bond that is cleaved, and the position along the peptide chain. The b-ion type contains the N-terminus whereas the y-ion type contains the C-terminus. The subscript number is the residue number relative to the terminus that the fragment contains. Additional ion types correspond to cleavage at different positions in the backbone (dotted lines).

(adapted from <http://www.lamondlab.com/MSResource/LCMS/MassSpectrometry/peptideFragmentation.php>).

The Zip Tip® was wetted twice with 10 µL ACN, which was then expelled before two equilibrium steps involving slow uptake and expulsion of 10 µL equilibration/wash solution (0.1% TFA in dH₂O). The digest sample was then cycled slowly through the Zip Tip® between 8 and 10 times in an Eppendorf tube and then expelled. Three x 10 µL of wash solution (0.1% TFA in dH₂O) were then drawn up and ejected, followed by 2 µL of elution solution (0.1% v/v TFA, 50% v/v ACN, 50% v/v methanol, 12.5 mg/mL α-CHCA) which was aspirated and cycled 3 to 4 times into a clean Eppendorf tube before being spotted directly onto a target plate.

4.2.2.4 MALDI-MS/MS of peptides

Preliminary data supported the use of Zip Tips® in the preparation of samples prior to mass spectrometry; therefore all subsequent experiments were performed following sample preparation with Zip Tips® (see section 4.2.2.3).

Peptide mass fingerprints of pure MBP samples were initially acquired by MALDI-MS using a Q-Star Pulsar *i* Quadrupole time-of-flight mass spectrometer (Applied Biosystems, UK). Initially peptide mass fingerprints of unknown samples were also acquired using the above instrument, however, due to the higher resolution achieved and ability to perform IMS-MS/MS subsequent experimental samples were analysed using HDMS SYNAPT™ G2 system (Waters Corporation, UK).

MALDI IMS/MS and MALDI IMS-MS/MS were performed using a HDMS SYNAPT™ G2 system (Waters Corporation, UK). Laura Cole (Sheffield Hallam University) provided support for acquisition of mass spectra and data interpretation. The instrument was used in positive ionisation mode. In order to achieve good quality MS/MS spectra, spectra were acquired by manually moving the laser position and adjusting the collision energy to achieve good signal to noise for product ions across the full *m/z* range of the spectrum. Collision energies were adjusted from 70 to 100 eV during acquisition and acquisition times were generally 5-10 seconds per spectrum. The resulting peaks obtained from the MS/MS spectra were uploaded in a text file format to perform a Mascot (Matrix Science, UK) search which used the UniProt database in order to generate a sequence match. Searches were performed with either Trypsin or Lys C specificity and two missed cleavages were allowed. Mass deviations for precursor ions and for fragment ions were set at 10 ppm and 0.75 Da, respectively.

4.2.6 Enzyme-linked immunosorbant assay (ELISA)

ELISA is used for both the detection and quantification of a specific antigen or antibody in a range of biological samples. In this method, an enzyme, which reacts with a

colourless substrate to produce a coloured product, is covalently linked to a specific antibody that recognises a target antigen or antibody (Berg *et al.*, 2002). If the antigen or antibody is present, the antibody-enzyme complex will bind to it, and the enzyme component of the antibody-enzyme complex will catalyse the reaction generating the coloured product. The presence of the coloured product indicates the presence of the antigen or antibody. There are several types of ELISAs, but an indirect ELISA and a sandwich ELISA are most commonly used. An indirect ELISA is used to detect the presence of an antibody whereas a sandwich ELISA is generally used for the detection of an antigen. This chapter uses an indirect ELISA (Figure 4.3). In the indirect ELISA specific proteins (antigens) are absorbed to the bottom of a well of a 96-well plate, serum or CSF containing antibodies of interest are then added to the coated well and allowed to bind to the antigen. Enzyme-linked antibodies that recognise human immunoglobulins are then added and bind to the target antibody. At each stage of the assay washes are performed to remove unbound antigen and antibodies. Lastly, a substrate is applied, resulting in a colour change which can be measured and is directly proportional to the amount of antibody present (Berg *et al.*, 2002).

4.2.6.1 CSF and serum samples and ethical approval

In total paired CSF and serum samples were collected from 197 patients attending the Neurology Department at the Royal Hallamshire Hospital (RHH), Sheffield (Table 4.1). Ethical approval for this study was obtained from the Leeds West Research Ethics Committee (See Appendix 2). Informed consent was obtained from each patient participant by Consultant Neurologist, Dr Basil Sharrack. There were 36 patients with definite MS, 23 patients with inflammatory CNS, 69 patients with CNS disorders, 14 patients with idiopathic intracranial hypertension (IIH), 33 patients with headache/migraine, and 20 control individuals.

4.2.6.2 Preparation and storage of CSF and serum samples

Following collection of paired CSF and serum samples from the RHH, CSF and blood samples were centrifuged for ten minutes at 3000 rpm (Sorvall RT 6000D) at 4°C. CSF was then aliquoted into 1 mL Eppendorf tubes and stored at -80°C. Serum was removed from the top layer of the serum separator tube (SST) gold-topped tube and aliquoted into 500 µL Eppendorf tube for storage at -80°C.

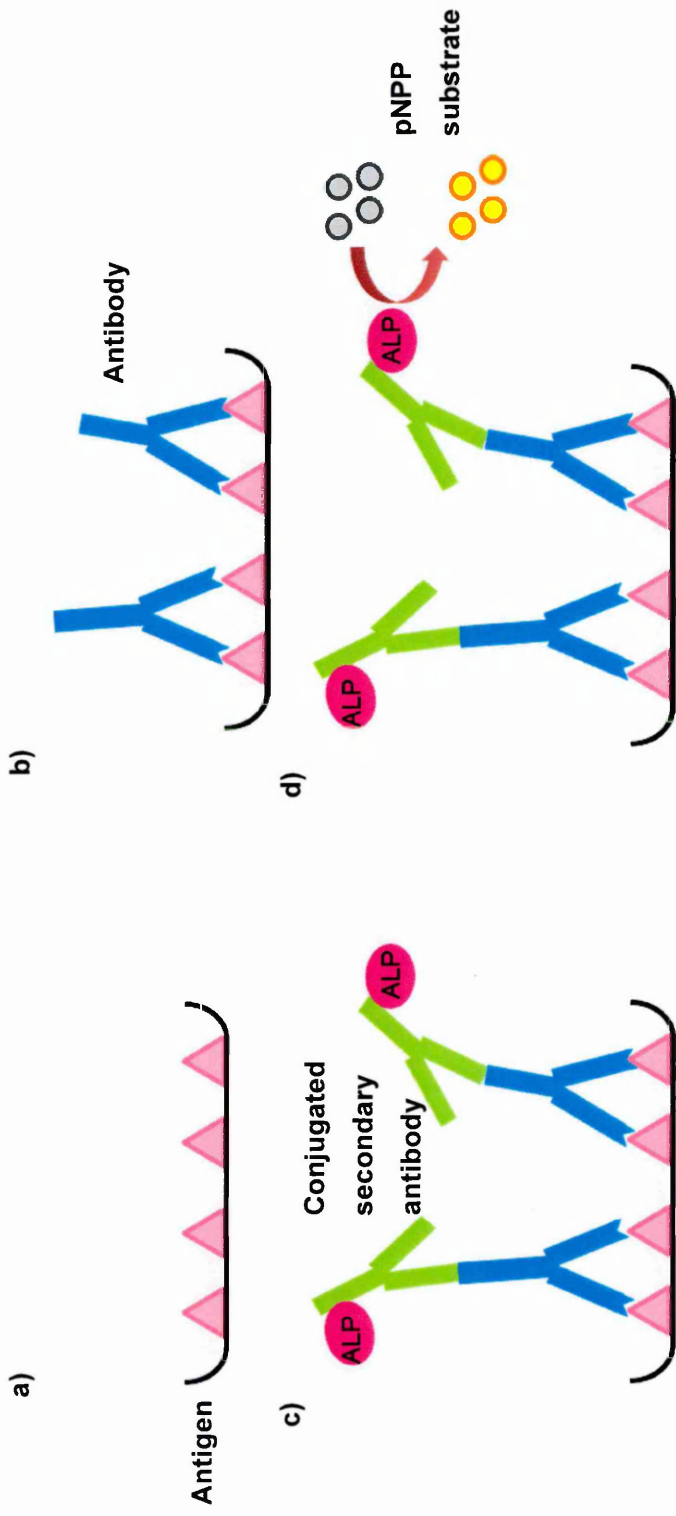


Figure 4.3: Indirect ELISA. (a) Antigens are coated on the surface of a well, (b) followed by the addition of serum or CSF containing specific antibodies which bind directly to the antigens (c) An enzyme-linked antibody (e.g. ALP; alkaline phosphatase) is then added which binds specifically to the patient antibody and (d) upon the application of a substrate solution (p-nitrophenyl phosphate (pNPP)) a colorimetric product is created. The colour formation is proportional to the amount of specific patient antibody present.

(adapted from <http://www.ncbi.nlm.nih.gov/books/NBK22420/figure/A515/?report=objectonly>).

Table 4.1: Summary of clinical details of patients participating in this study.

Group	Mean age (range) years	Sex		Ratio female to male	Mean serum IgG (g/L)	Mean CSF IgG (mg/L)	Albumin/IgG ratio	Oligoclonal bands		Total number in group
		Female	Male					+	-	
MS	46 (30-70)	24	12	2:1	9.6 (6.3-14.6)	53.7 (10-288)	1.1 (0.5-3.1)	23	11	36
Inflammatory CNS	45 (21-63)	15	8	1.9:1	10.1 (3.1-30.4)	41.3 (13-115)	0.8 (0.4-2.4)	6	15	23
Non-inflammatory CNS disorders	55 (22-86)	38	31	1:0.8	10.9 (6.4-19.9)	27.3 (9-59)	0.5 (0.4-1.1)	0	39	69
IIH	33 (23-57)	14	0	1:0	9.7 (7.1-12.4)	15.4 (4-27)	0.4 (4-27)	4	10	14
Headache or migraine	43 (19-77)	24	9	2.7:1	9.6 (6.4-12.3)	30.3 (7-182)	0.7 (0.4-4.2)	1	26	33
Control	40 (19-80)	12	8	1.5:1	9.9 (6.4-13.3)	23.9 (9-55)	0.5 (0.4-0.7)	0	17	20

Key: CNS; central nervous system, MS; multiple sclerosis, IIH; idiopathic intracranial hypertension, Ig; immunoglobulin.

4.2.6.3 Detection of ACPAs using a commercial ACPA ELISA used for detection of these antibodies in RA

Patient CSF and serum samples were tested for the presence of RA-specific anti-cyclic citrullinated peptide (CCP) antibodies using a commercially available ELISA kit according to the manufacturers' instructions (Axis-Shield, UK). Briefly, 100 μ L serum samples and controls (diluted 1:100 in sample diluent), along with calibrators, were loaded in duplicate into a 96-well ELISA plate and left to incubate for 1 hour at RT. Subsequently, the contents were aspirated and wells washed four times with wash buffer, through quick inversion and blotting on a paper towel. 100 μ L of conjugated secondary antibody was then added to each well and left to incubate for 30 minutes at RT, this was then aspirated and the plate washed four times, as described above. Following this, 100 μ L of substrate was added to each well, and left to incubate for 30 minutes avoiding direct sunlight. 100 μ L stop solution was added to each well and left for 10 minutes at RT, and then the absorbance of wells was measured at 450 nm using a Wallac® plate reader. The OD reading of each patient sample was then plotted on a graph, grouped into disease type.

4.2.6.4 Antigens

As novel citrullinated peptides were not identified through mass spectrometry, three MBP peptide sequences containing citrulline residues were designed based on previous publications (Tranquill *et al.*, 2000; De Seze *et al.*, 2001) and the resulting peptides synthesised (Pepceuticals, UK) (Table 4.2).

4.2.6.5 Optimisation of ELISA

Initially eight known MS patient sera and CSF were used for optimisation, as this disease group was most likely to have the highest level of ACPAs. 1, 5 and 10 μ g/well of peptides 1 and 2 were used to coat the 96-well plates. CSF samples were used both neat and diluted 1:5, whereas serum was diluted 1:50 and 1:200 before analysis by ELISA.

4.2.6.6 ELISA

ELISA was performed using 96-well microtitre plates (eBioscience, UK) coated with 500 μ g/mL MBP-peptide solution in PBS overnight at 4°C (5 μ g/well). Following this plates were washed five times with 0.1% PBS-Tween (PBS-T) and blocked with 5% BSA (Sigma, UK) in PBS for 2 hours at RT. Following this, plates were washed five times with 0.1% PBS-T, followed by incubation with 100 μ L of CSF (diluted 1:5) or

seum (diluted 1 in 50) in 0.5% BSA in 0.1% PBS-T per well for 1 hour at RT. Plates were then washed five times with PBS-T, and incubated for a further one hour at RT with alkaline phosphatase-conjugated goat anti-human IgG (Fc specific) secondary antibody (Sigma, UK). Reaction products were then visualised with p-nitrophenylphosphate substrate (Sigma, UK) and the optical density was determined at 405 nm after 90 minutes. All data were corrected by subtraction of the mean background values i.e. absorbance of wells coated with citrullinated MBP peptides and no serum/CSF. All samples were run in duplicate and an average OD value taken to allow for intra-assay variability.

4.2.6.7 Statistical analysis

Data obtained from the ELISA was analysed for any statistical significance between absorbance of the three peptides and between disease groups using a General Linear Model (GLM) followed by univariate analysis. To determine any correlation between absorbance of wells linear regression analysis was carried out. Statistical significance was set at $p < 0.05$.

Table 4.2: Citrullinated MBP peptides used as the antigenic substrate in ELISA assays.

Peptides	Amino-acid sequence
Peptide 1 (MBP ₁₈₋₃₈)	ASTMDHACitHGFLPRHRDTGIL
Peptide 2 (MBP ₁₁₅₋₁₃₁)	SWGAEQGQCitPGFGYGGCitA
Peptide 3 (MBP ₁₅₁₋₁₇₀)	SKIFKLGGCitDSRSGSPMARCit

Key: MBP; myelin basic protein

4.3 Results

4.3.1 Identification of citrullinated peptides

Initially an in-gel tryptic digest was performed using pure MBP followed by analysis on the QStar *i* Pulsar MALDI-TOF-MS as a positive control to ensure the technique was performed correctly. MS spectra obtained showed multiple peptide peaks which correctly corresponded to a number of theoretical digest peaks for MBP (Figure 4.4). Subsequently, in-gel tryptic digest was performed using SDS-PAGE bands excised at ~18.5 and ~50 kDa from MS058 P1D3 (Figure 4.5a-b) followed by analysis on the QStar *i* Pulsar MALDI-TOF-MS. MS spectra obtained showed a number of peptide peaks which corresponded to a number of theoretical digest peaks for human GFAP (Figure 4.6a). However, MS spectra from an in-gel tryptic digest of a ~ 18.5 kDa band did not produce any peptide peaks which corresponded to theoretical digest peaks for MBP (Figure 4.6b). Trypsin cleaves polypeptides at both the lysine and arginine residues, and is therefore unable to cleave arginine residues that have been post-translationally modified to citrulline; therefore subsequent in-gel digests were performed using the endoproteinase Lys C which cleaves the carboxylic bond of lysine residues in proteins (Wada and Kadoya 2003) and analysis was performed using the Synapt G2 MALDI-IMS-MS. Initially an $(\text{NH}_4)_2\text{CO}_3$ buffer was used during the in-gel digest and subsequent extraction of peptides; however, this produced very poor MS spectra (Figure 4.7a). Subsequently, changing the buffer to Tris-HCl produced high quality MS spectra with a number of peaks (Figure 4.7b). MALDI-MS without prior sample preparation using a Zip-Tip® resulted in a high background noise with dominant MALDI matrix adduct signals and smaller peptide signals observed at m/z 1491 and 1897 (Figure 4.8a). Sample preparation with a Zip-Tip® prior to sample spotting resulted in a low background noise with a significant reduction in the MALDI matrix adduct signals and a significant increase in peptide intensity at m/z 1491 and 1897 (Figure 4.8b).

A number of MBP and GFAP peptides were positively identified from in-gel digests of bands corresponding to ~18.5 and ~15 kDa and ~48 and ~50 kDa, respectively (Table 4.3). An example of MS spectra showing a peak corresponding to GFAP is shown in Figure 4.9a with subsequent MS/MS spectra showing positive identification of GFAP (Figure 4.9b). An example of MS spectra showing a peak corresponding to MBP is shown in Figure 4.10a with subsequent MS/MS spectra showing positive identification of MBP (Figure 4.10b). Citrullinated peptides were not identified.

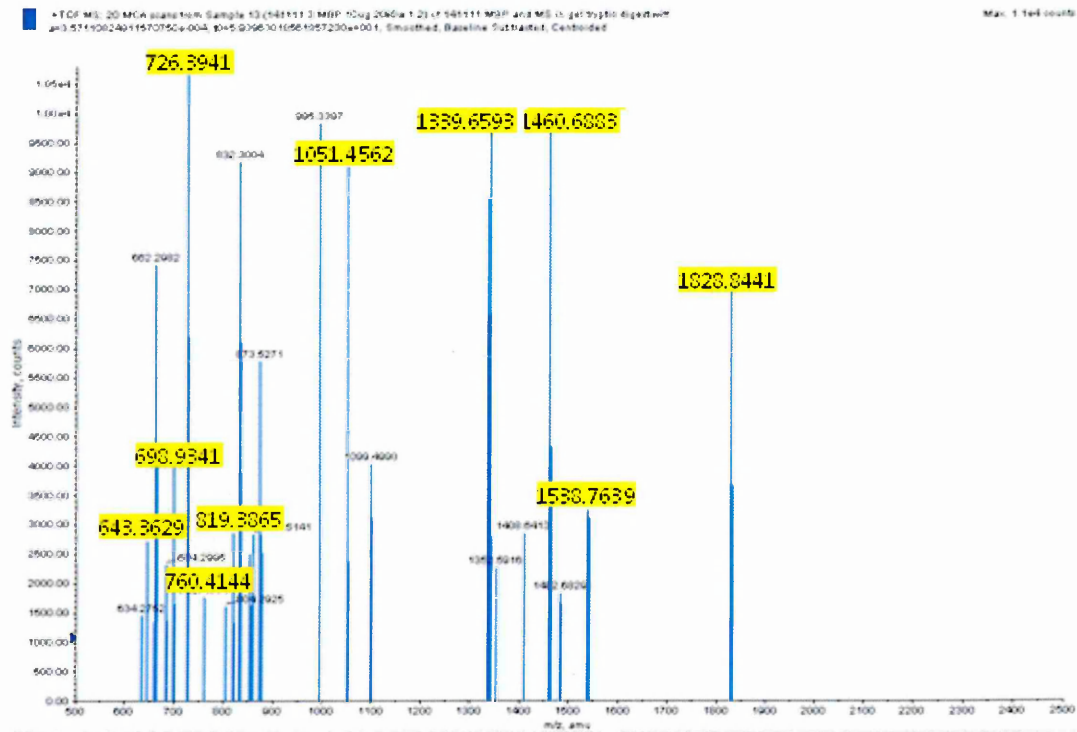


Figure 4.4: MALDI mass spectrum obtained following in-gel digestion of recombinant human MBP. MBP tryptic peptides at m/z 643, 698, 726, 760, 819, 1051, 1339, 1460, 1538 and 1828 are highlighted based on theoretical human MBP tryptic digest peaks from Mascot.

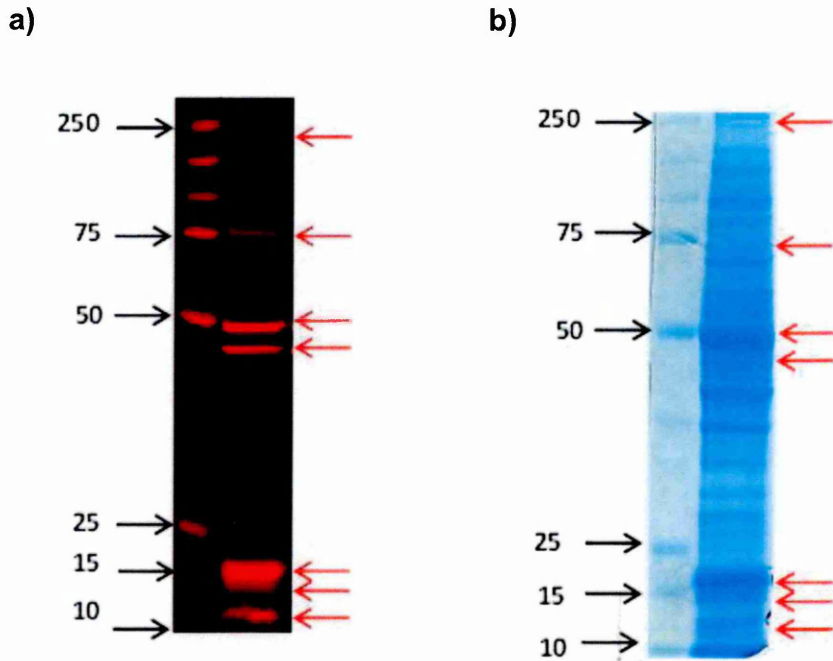
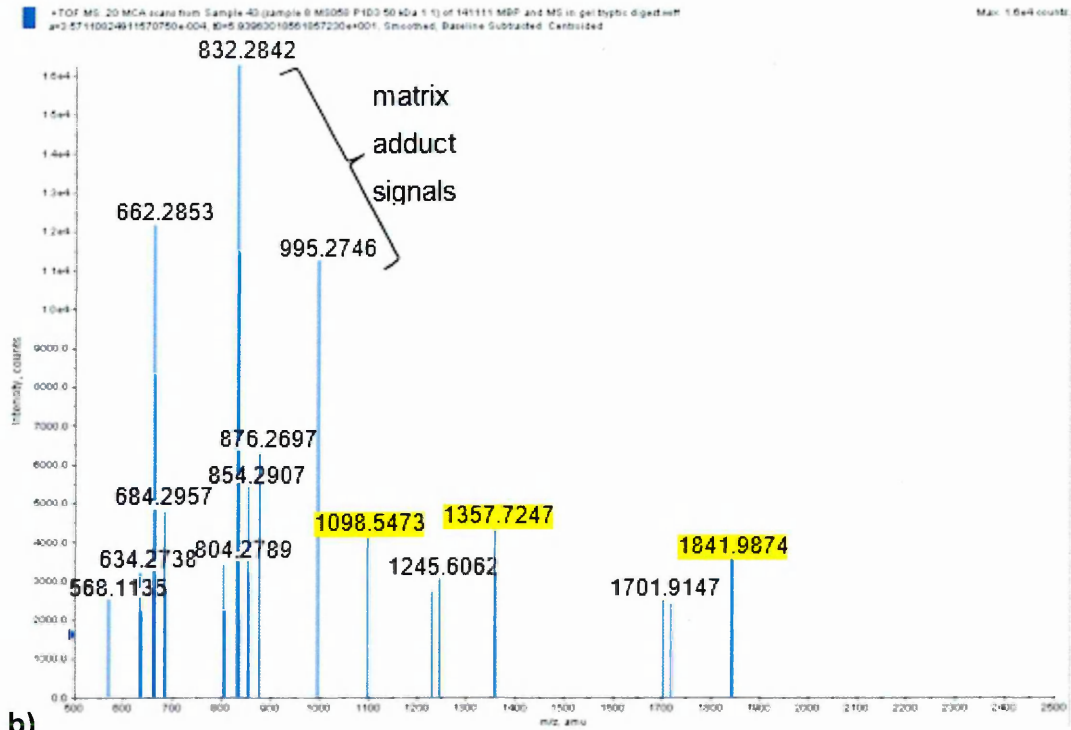


Figure 4.5: Western blotting of MS brain tissue showing citrullinated proteins identified with F95 mAb and corresponding Instant Blue® SDS-PAGE gel. (a) western blot showing the presence of citrullinated protein bands using protein extracted from MS058 P1D3 and **(b)** corresponding Instant Blue® SDS-PAGE gel. Red arrows indicate bands of interest that were excised for in-gel digestion and subsequent mass spectrometry for protein identification.

a)



b)

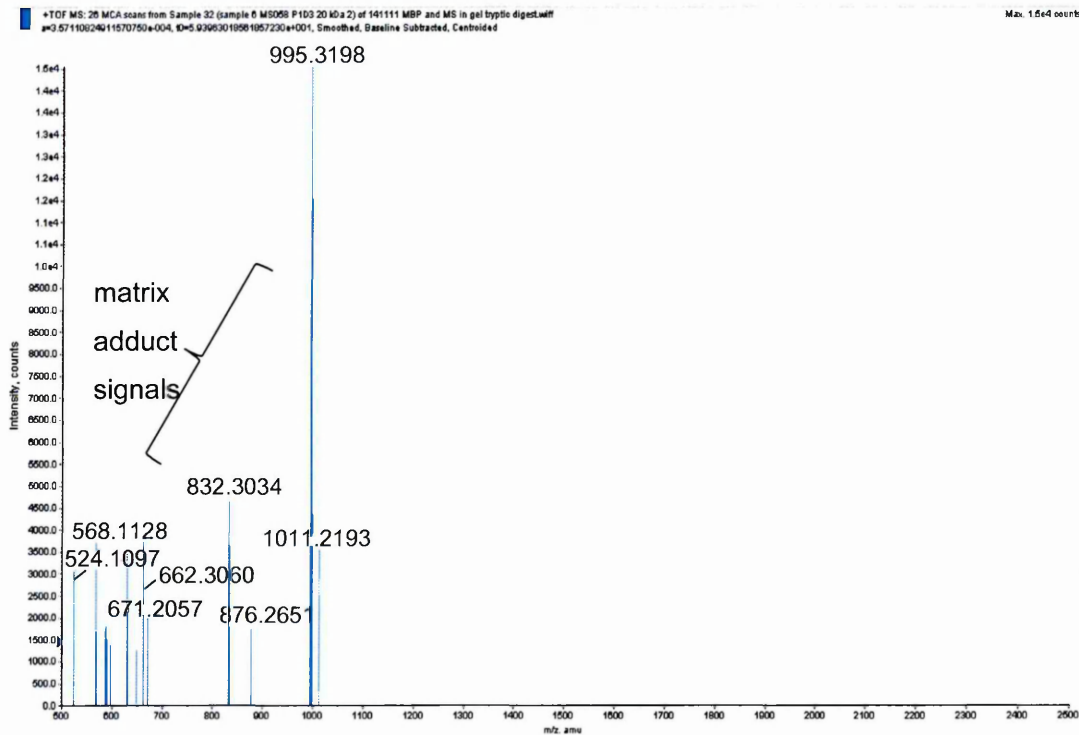
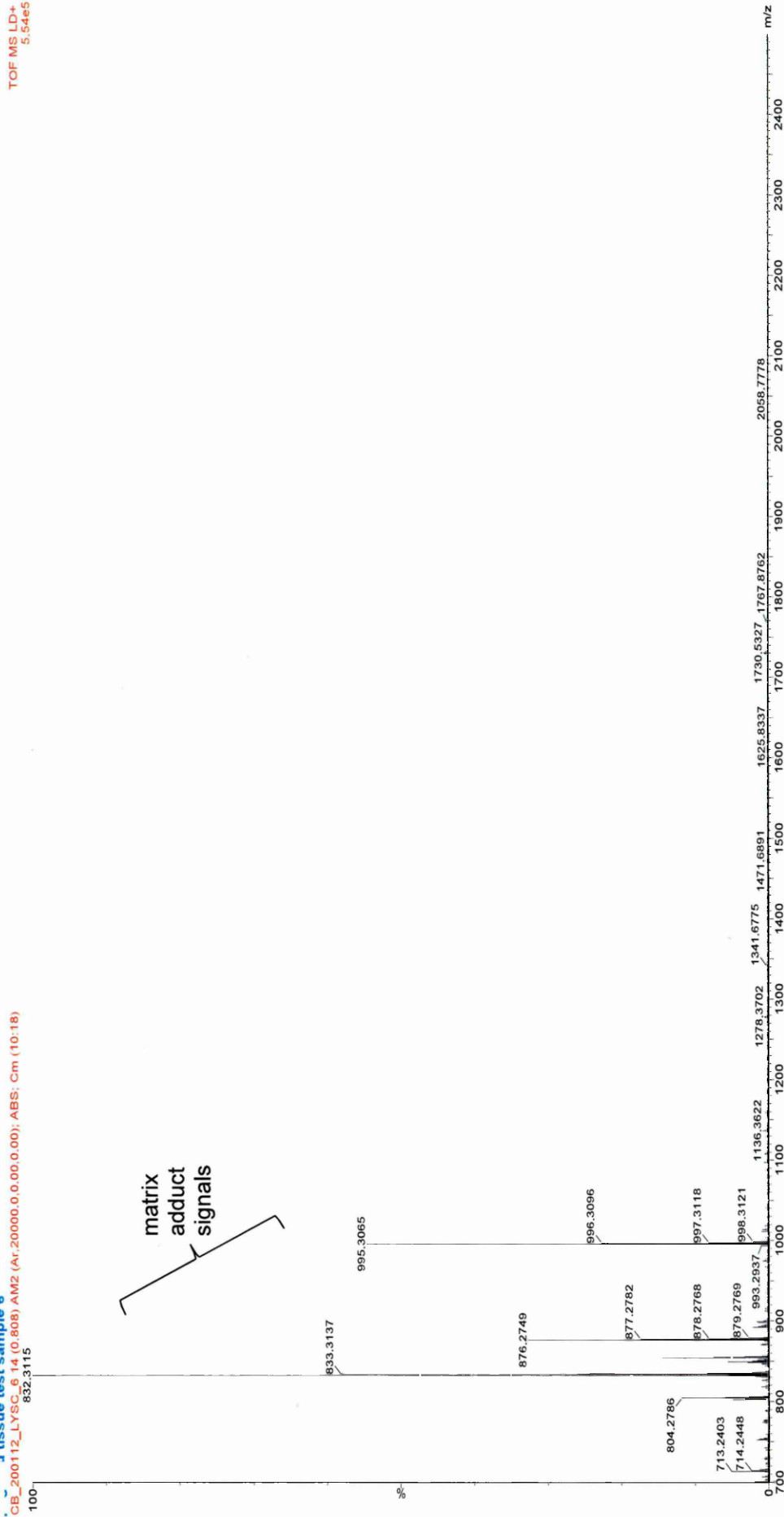


Figure 4.6: MALDI mass spectrum obtained following in-gel digest of MS brain tissue. (a) MALDI-MS peptide profile obtained from in-gel digestion of a 50 kDa band showing GFAP tryptic peptides at m/z 1098, 1357 and 1841 highlighted. **(b)** MALDI-MS peptide profile obtained from in-gel digestion of a 20 kDa band showing no MBP tryptic peptides.

a) **d** tissue test sample 6
CB_200112_LYSC_6_14 (0.806) AM2 (Ar:200000.0.0.0.0.0.0); ABS; Cm (10:18)
832.3115



b) ma Peg cal and sample 6
70312_ZIPTIP_MB_P1D3_11 (0.544) AM2 (Ar:20000.0,0.00,0.00); ABS; Cm (8:12)

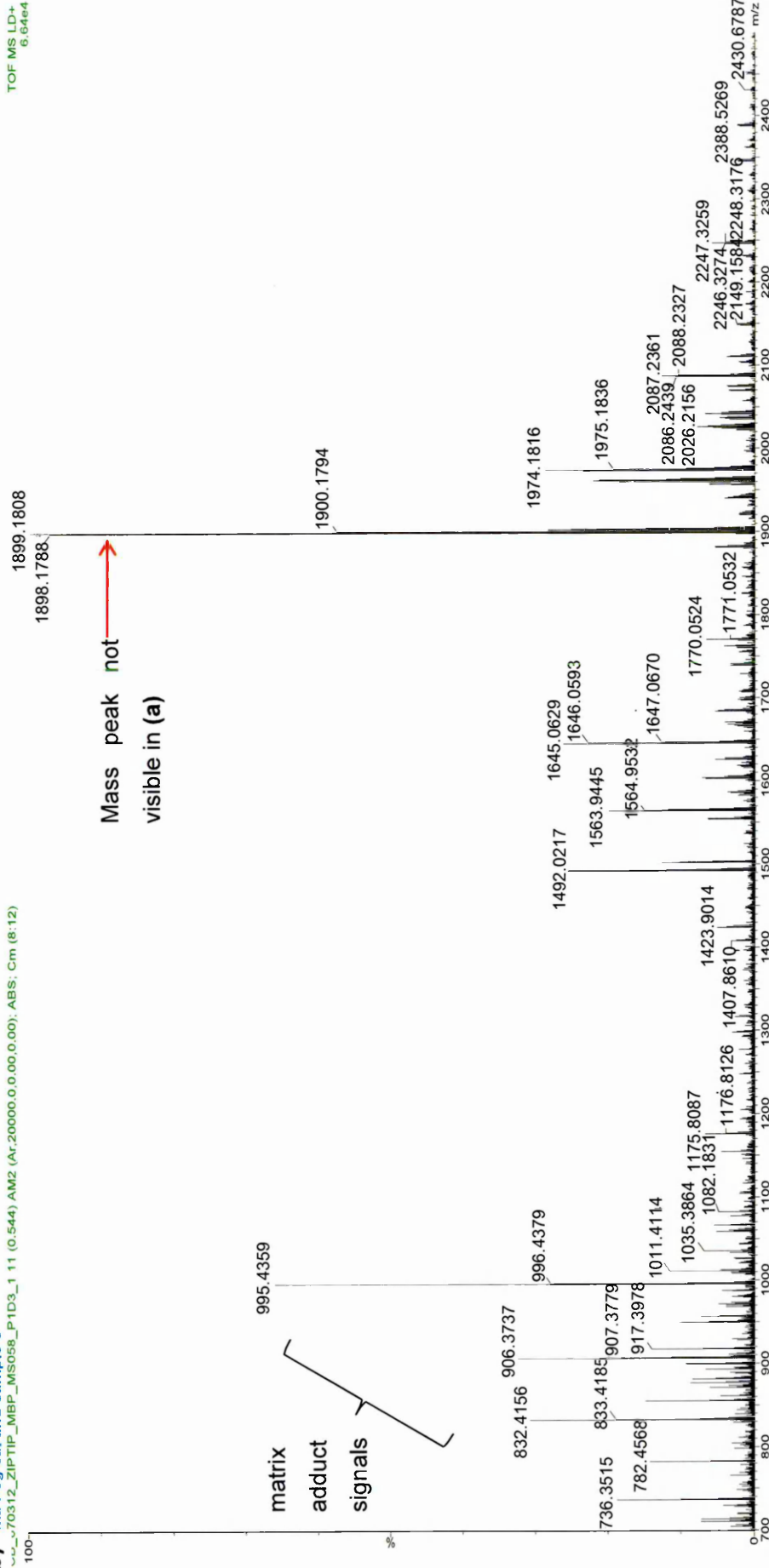
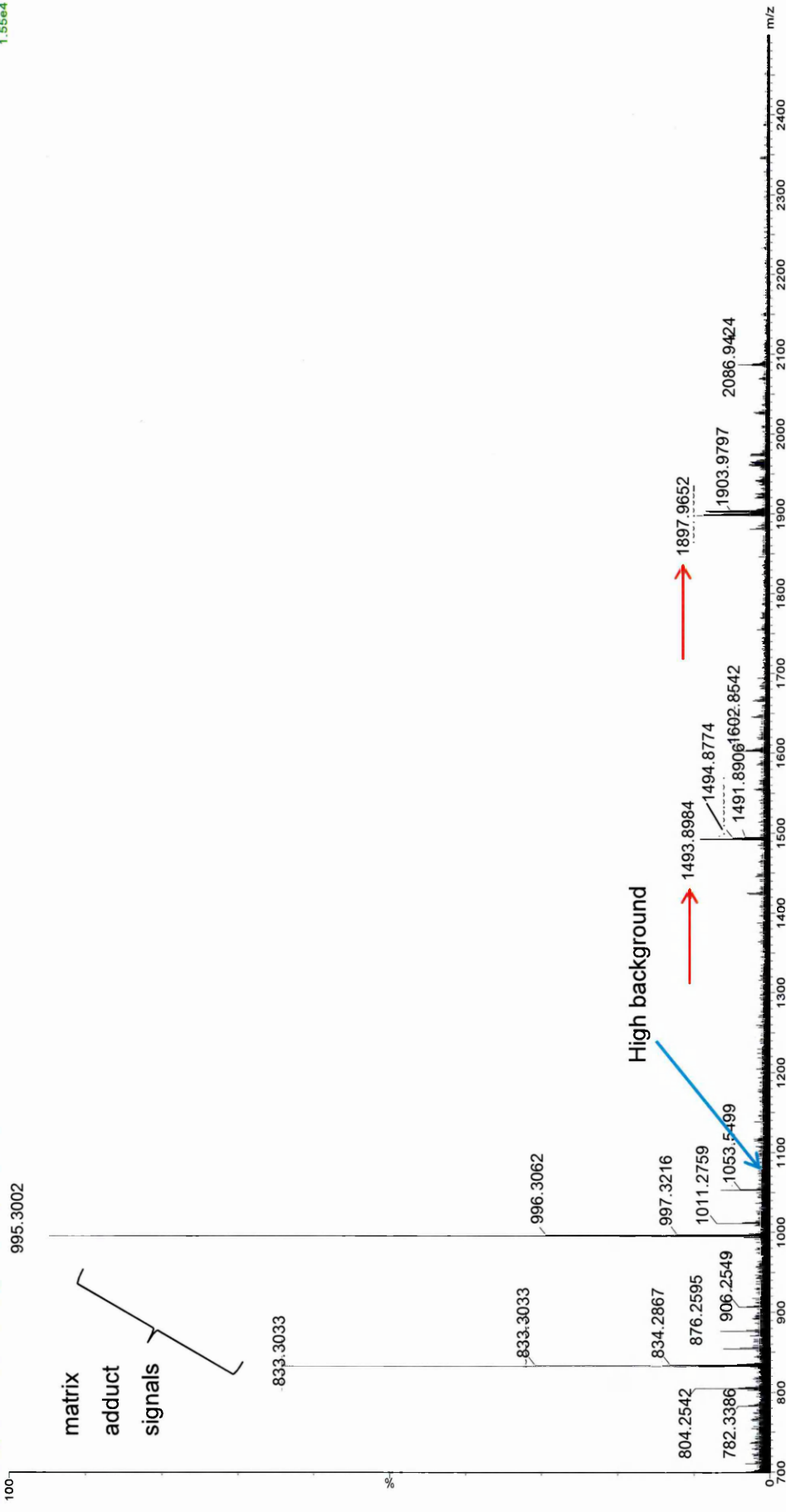


Figure 4.7: MALDI MS spectrum produced when using different buffers during in-gel digestion and subsequent peptide extraction. (a) 25 mM $(\text{NH}_4)_2\text{CO}_3$ buffer compared to (b) 25 mM Tris buffer during in-gel digestion with Lys C and subsequent peptide extraction.

a)

0503012_MS058 P1D3 AND MBP_8 13 (0.665) Cm (12:16)

TOF MS LD+
1.56e4



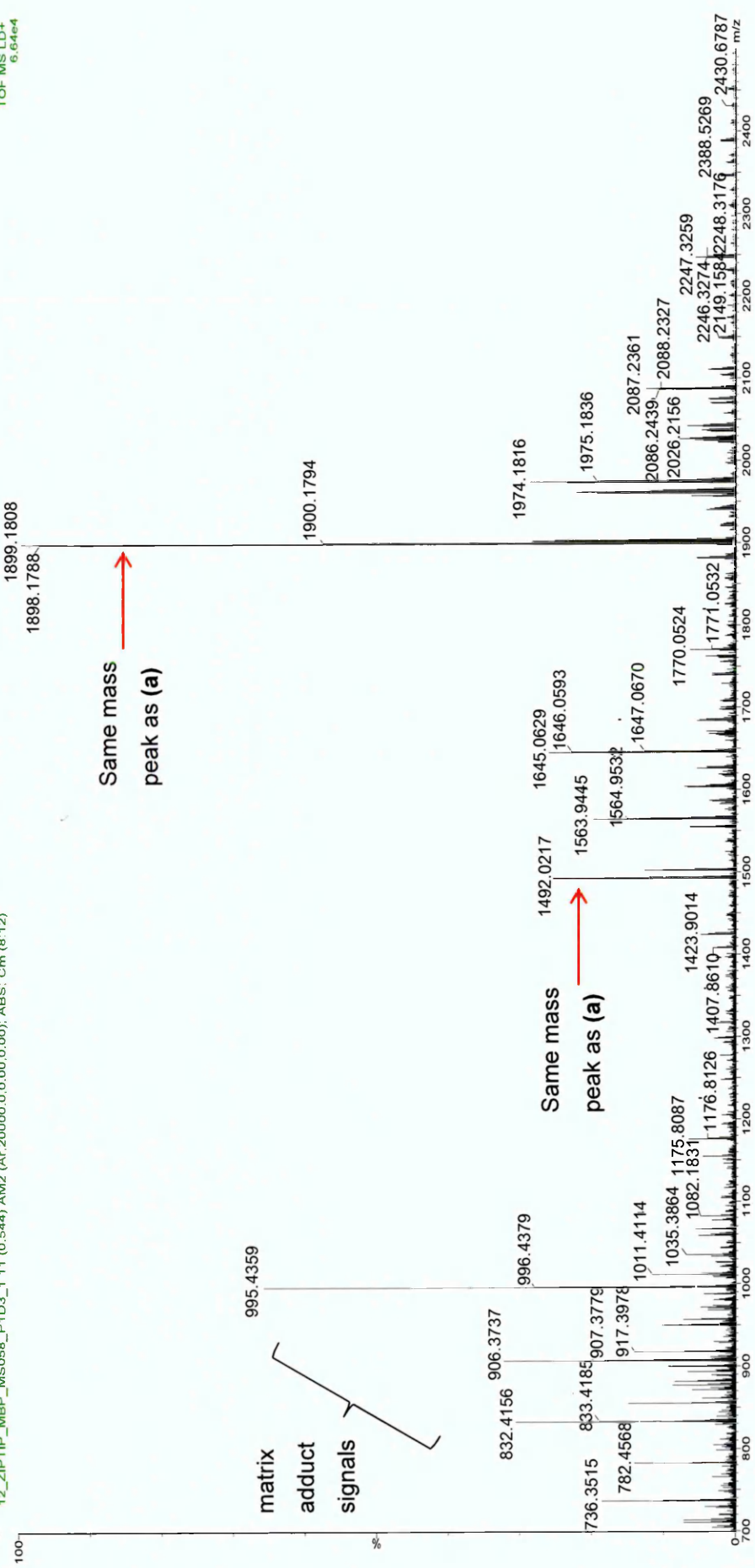


Figure 4.8: Comparison between MS spectra produced with and without sample clean-up using Zip Tips®. MALDI-MS spectra produced when (a) spotting sample directly onto target plate and (b) following post-sample clean-up using Zip Tips®.

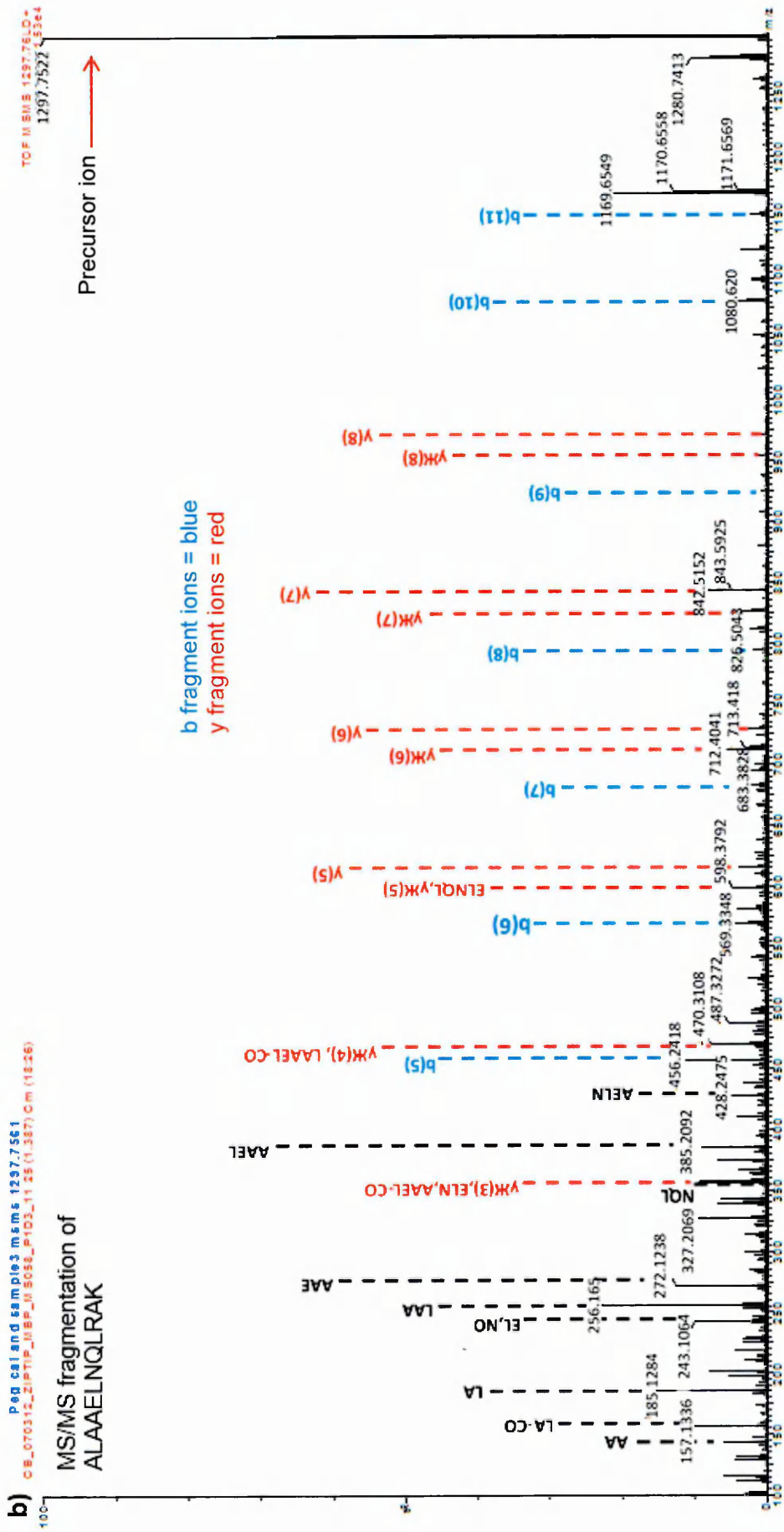


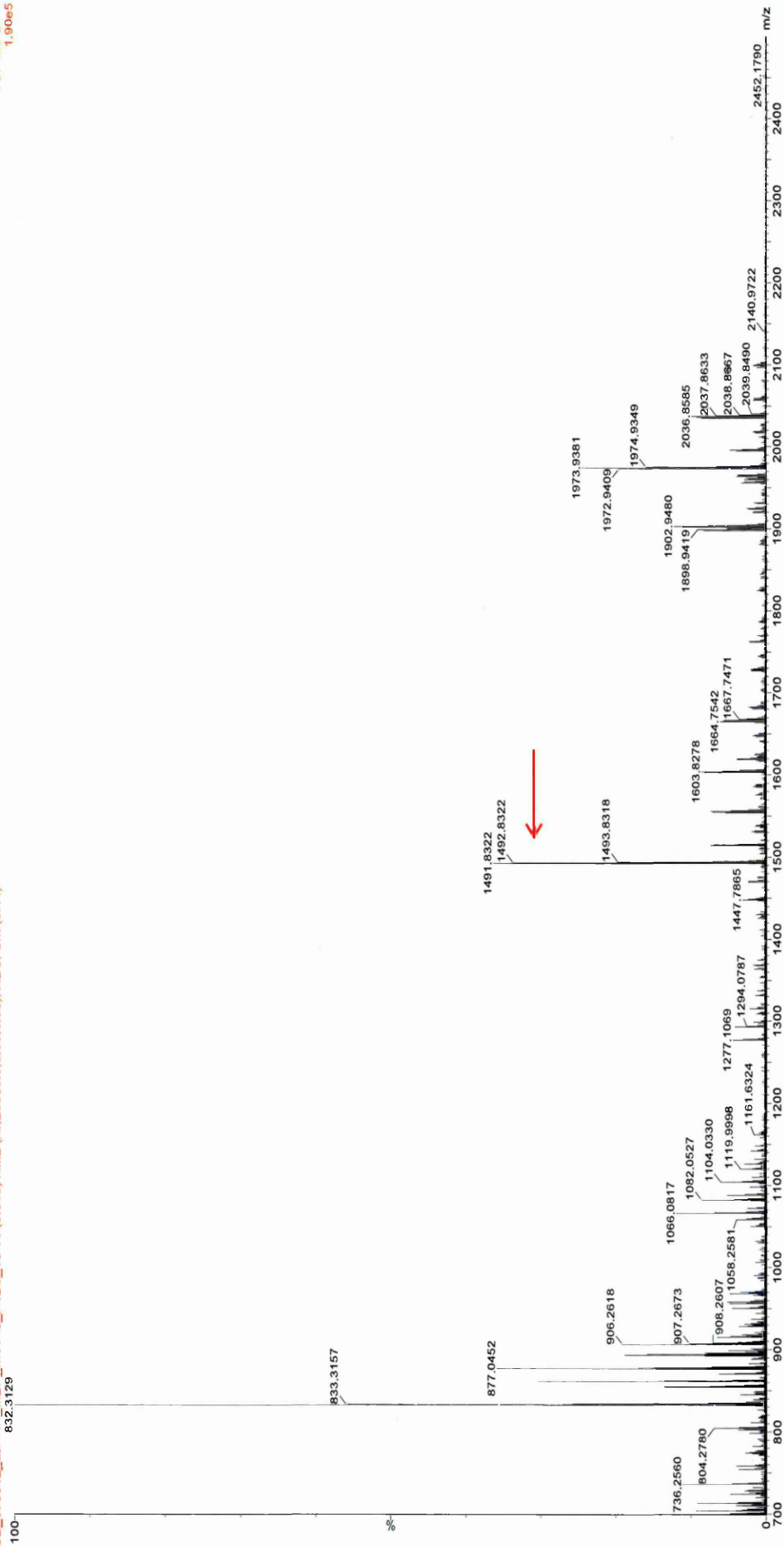
Figure 4.9: An example of peptide identification. (a) MS spectrum of the peak observed at m/z 1297.76 (red arrow) and subsequent (b) MS/MS spectra. This peptide was identified by Mascot search as arising from human GFAP (ALAAELNQLRAK).

a)

eg cal and samples

CB_070312_ZIP115_MBP_MS056_P1D3_16 11 (0.515), AM2 (Ar.200000.0.0.00.0.00); ABS; Cm (8.14)
832.3129

TOF MS LD+
1.90e5



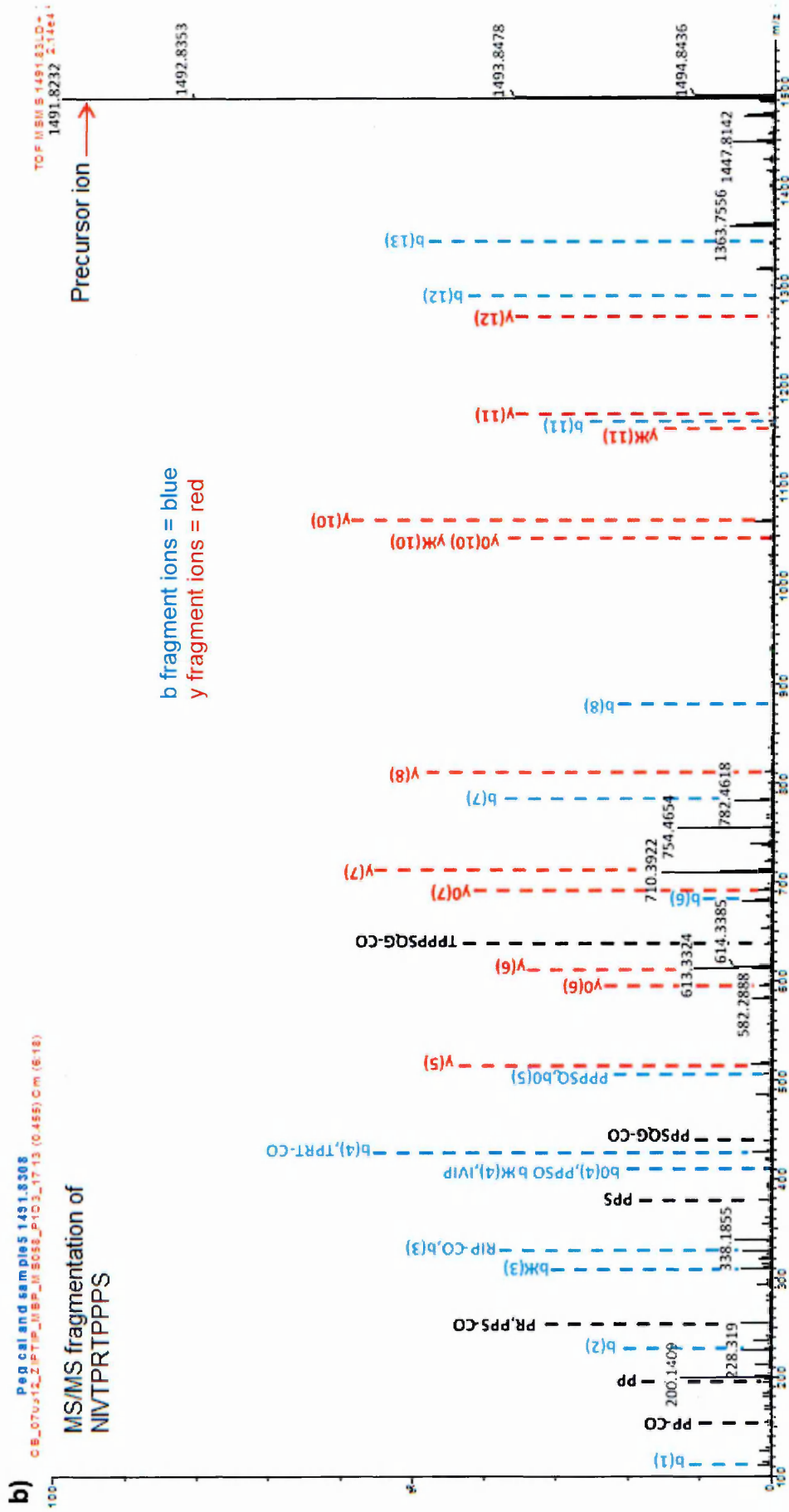


Figure 4.10: An example of peptide identification. (a) MS spectrum of the peak observed at m/z 1491.83 (red arrow) and subsequent (b) MS/MS spectra. This peptide was identified by Mascot search as arising from human MBP (NIVTPRTPPSQGK).

Table 4.3: List of peptides identified using MALDI-IMS-MS/MS and Mascot. Following MS/MS a peptide peak list consisting of peptide mass values was exported into Mascot where peptide identification was performed, resulting in protein identification including the peptide amino acid sequence, score and Mascot threshold score. A protein score of ≥ 30 is considered a good score if two or more peptides are identified within the same sample. Individual ions scores of >16 indicate identity or extensive homology ($p < 0.05$) (Mascot threshold score at 95% significance).

Protein	Accession number	Mass (Da)	Observed m/z with MALDI/MS	Expected m/z with MALDI/MS	Mass error (ppm)	Amino acid sequence	Protein score	Mascot threshold score at 95% significance
GFAP	P1436	49.880	1161.6376	1160.6303	0.12	VRFLEQQNK	32	>19
			1161.6392	1160.6319	1.5	VRFLEQQNK	31	>18
			1297.7561	1296.7488	-1.93	ALAAELNQLRAK	76	>13
			1297.7612	1296.7513	2.0	ALAAELNQLRAK	72	>13
			1297.7612	1296.7539	2.0	ALAAELNQLRAK	72	>13
			1405.8020	1404.7947	-2.06	LALDIEIATYRK	44	>12
			2074.1060	2073.0987	1.0	FADLTDAARAELLRQAK	65	>16
			2102.0259	2101.0186	-3.61	DEMARHLQEYQDLLNVK	62	>13
			MBP	P02686	33.117	1491.8308	1490.8235	2.0
1491.8317	1490.8244	2.6				NIVTPRTPPPSQGK	38	>16
1897.9371	18.96.9298	3.5				SHGRTQDENPVVHFFK	76	>15

Key: GFAP; glial fibrillary acidic protein, MALDI/MS; Matrix-Assisted Laser Desorption/Ionisation-Mass Spectrometry, MBP; myelin basic protein.

4.3.2 Detection of RA-specific ACPAs

No significant differences in patient sera immunoreactivity were observed between the disease groups, with the mean absorbance readings of ~0.10 for all groups (Figure 4.11a). The inflammatory CNS disease group and the MS group showed slightly higher CSF immunoreactivity to citrullinated proteins compared to the other disease groups; however there was no statistical significance (Figure 4.11b).

4.3.3 Optimisation of MBP ELISA

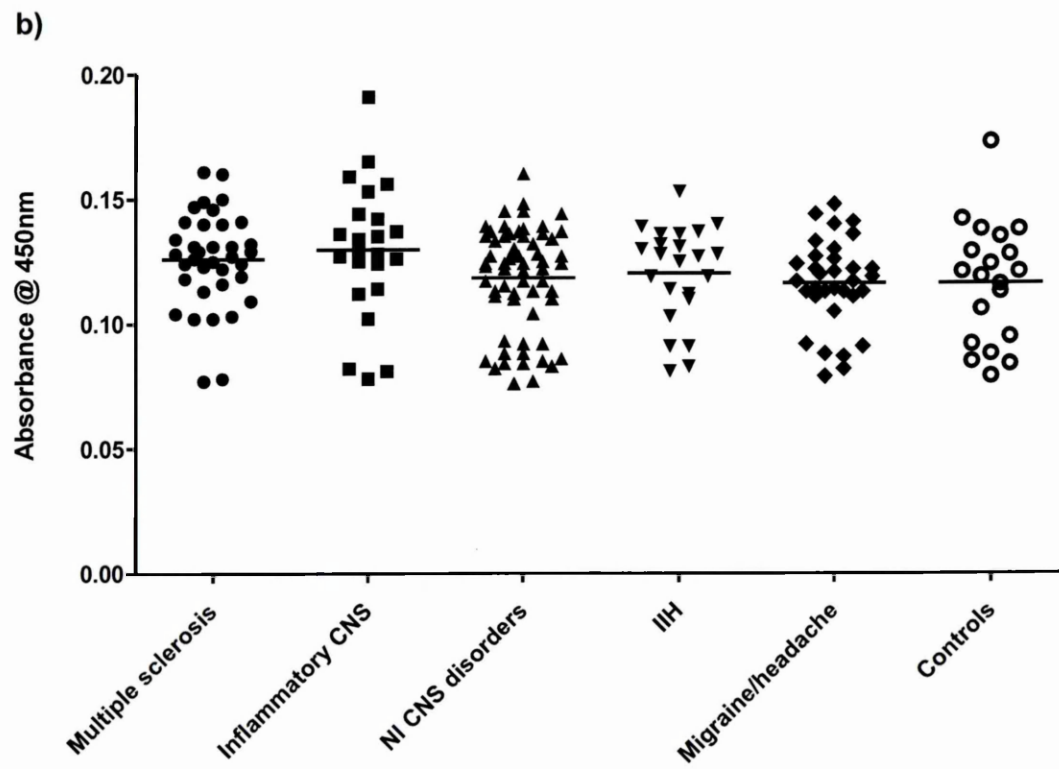
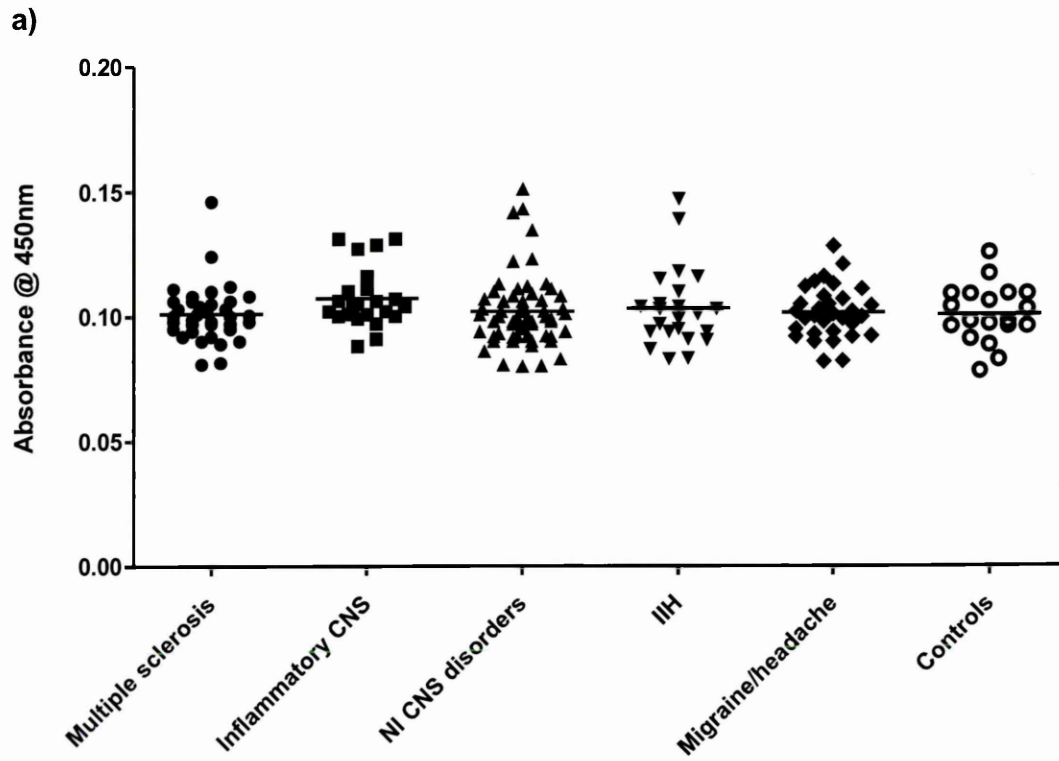
Initial optimisation using eight known MS patient serum samples and citrullinated MBP (cit-MBP) peptide 1 showed that diluting the serum 1 in 50 produced higher absorbance readings than a 1 in 200 dilution, with a greater spread of data points (Figure 4.12a-b). There was very little difference in the absorbance values obtained when coating the ELISA plate with 1, 5 or 10 µg peptide 1 (Figure 4.12a). Much higher absorbance values were obtained when using the secondary antibody diluted 1 in 1000 compared to 1 in 5000 (Figure 4.11a). Similar results for these variables were obtained when using peptide 2 to coat the ELISA plates (Figure 4.13a-b).

The corresponding CSF samples from the 8 MS patients were also used for optimisation and cit-MBP peptide 1. Using neat CSF produced higher absorbance values than using CSF diluted 1 in 5 (Figure 4.12c-d). Lower absorbance values were obtained when coating the ELISA plate with 1 µg of peptide 1, whereas similar absorbance readings were observed when using either 5 or 10 µg peptide 1 (Figure 4.12c-d). Higher absorbance values were obtained when using the secondary antibody at a 1 in 1,000 dilution compared to 1 in 5,000 (Figure 4.12c-d) as expected. Identical results were obtained when using cit-MBP peptide 2 to coat the ELISA plates (Figure 4.13c-d).

Based on these results it was decided that serum would be diluted 1 in 50 and CSF would be diluted 1 in 5 for all subsequent analyses by ELISA. It was decided that 5 µg of peptide would be used to coat the ELISA plates and the secondary antibody would be used at a dilution of 1 in 1000.

Figure 4.11: Analysis of immune response by ELISA to RA-specific citrullinated peptides in patients with MS, other neurological disorders and controls. (a) sera and (b) CSF. Data is presented as a scatter plot with each symbol representing an individual patient ($n=197$). The solid line indicates the mean absorbance value. Data was analysed for any statistical significance between absorbance values for each peptide and between disease groups using a General Linear Model followed by univariate analysis using SPSS. Statistical significance was set at $p<0.05$.

Key: CNS; central nervous system, IIH; idiopathic intracranial hypertension, NI; non-inflammatory.



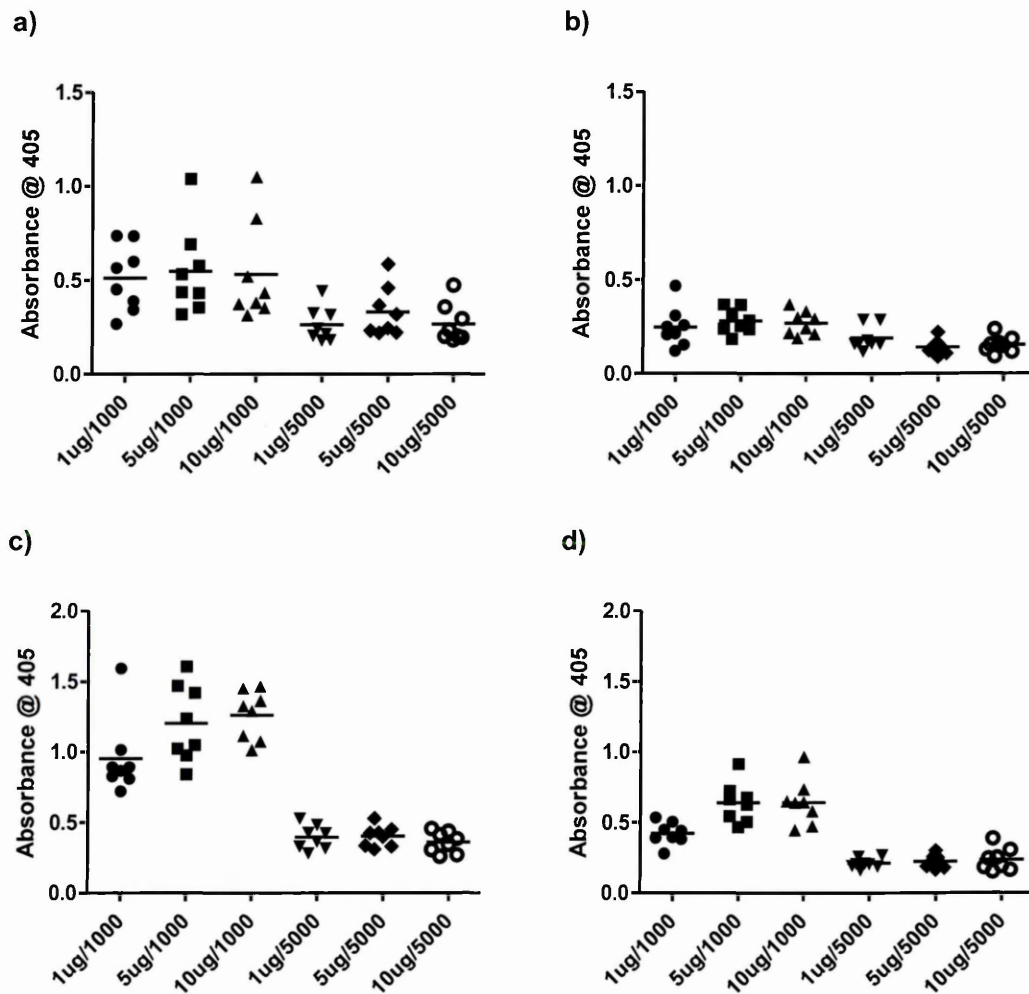


Figure 4.12: Optimisation of citrullinated MBP peptide ELISA. (a) serum 1 in 50 (b) serum 1 in 200 (c) CSF neat and (d) CSF 1 in 5. Wells were coated with 1, 5 or 10 μ g peptide 1 and following incubation with either sera or CSF antibodies were detected using a secondary antibody at a concentration of 1 in 1,000 or 1 in 5,000. Data is presented as a scatter plot with each symbol representing an individual patient ($n=8$). The solid line indicates the mean absorbance value.

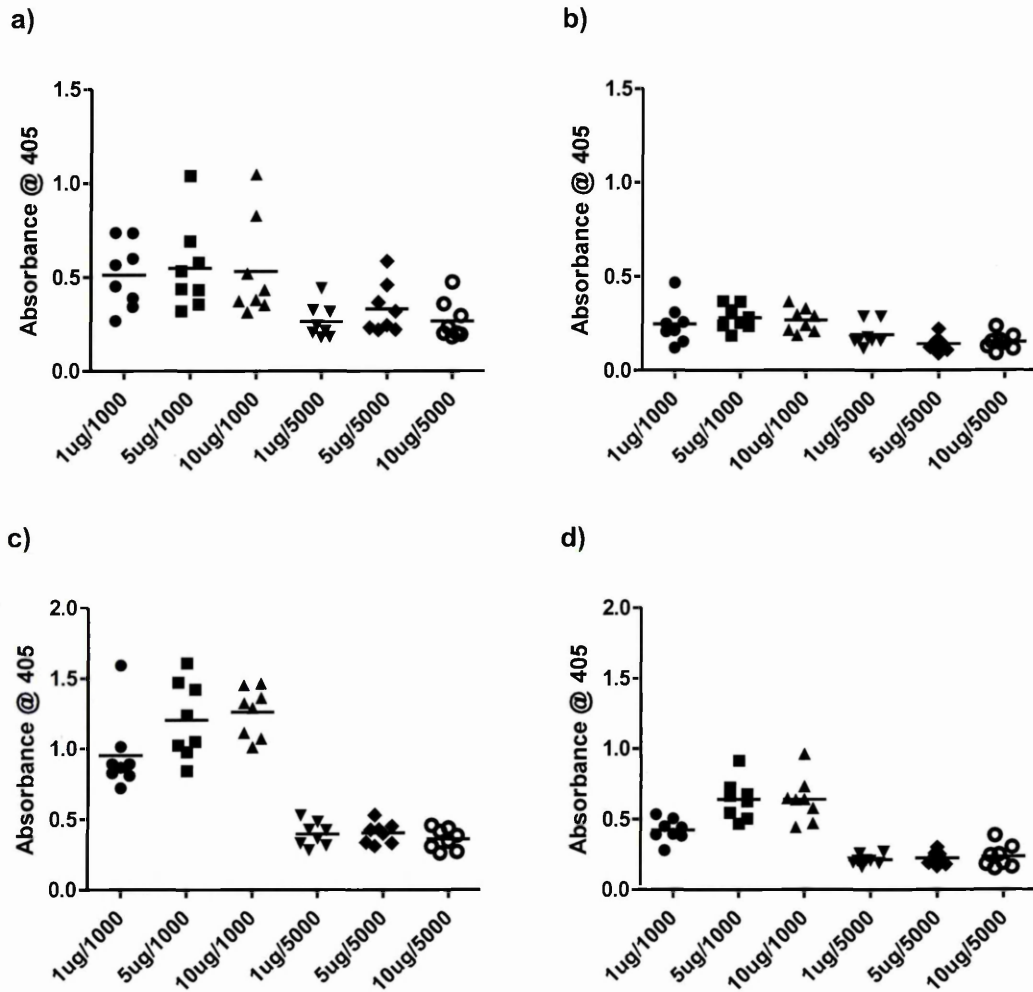


Figure 4.13: Optimisation of citrullinated MBP peptide ELISA. (a) serum 1 in 50 (b) serum 1 in 200 (c) CSF neat and (d) CSF 1 in 5. Wells were coated with 1, 5 or 10 μ g peptide 2 and following incubation with either sera or CSF antibodies were detected using a secondary antibody at a concentration of 1 in 1,000 or 1 in 5,000. Data is presented as a scatter plot with each symbol representing an individual patient ($n=8$). The solid line indicates the mean absorbance value.

4.3.4 Detection of MS-specific ACPAs

Serum immunoreactivity towards cit-MBP peptide 1 was slightly higher in patients with CNS disorders and controls compared to other disease groups, however these results were not statistically significant (Figure 4.14a). This higher serum immunoreactivity in CNS disorders and controls was also observed against peptide 2 and 3, however statistical significance was not reached (Figure 4.14b-c).

CSF immunoreactivity towards cit-MBP peptide 1 was slightly higher in patients with IHH compared to other disease groups and controls, however, this difference was not statistically significant (Figure 4.15a). Interestingly, CSF immunoreactivity towards both cit-MBP peptide 2 and 3 was higher in patients with MS compared to other disease groups and controls, however this difference was not statistically significant (Figure 4.15b-c).

Using linear regression analysis, a strong relationship was shown to exist between serum immunoreactivity for peptide 1 and 2 ($R^2 = 0.9120$) (Figure 4.16a). This strong relationship was also observed between serum immunoreactivity for peptide 1 and 3 ($R^2 = 0.8268$) (Figure 4.16b). Lastly, a strong relationship between serum immunoreactivity of peptide 2 and 3 was also observed ($R^2 = 0.8453$) (Figure 4.16c). This showed that where high absorbance readings were observed against one peptide it was highly likely that a high absorbance reading would also be observed against a different peptide.

A weak relationship was observed in CSF absorbance values between peptide 1 and 2 ($R^2=0.1415$) (Figure 4.17a). A weak relationship was also observed in CSF absorbance values between peptide 1 and 3 ($R^2 = 0.2721$) (Figure 4.17b). Lastly, a weak relationship was also shown to exist between CSF absorbance values between peptide 2 and 3 ($R^2=0.3139$) (Figure 4.17c).

No statistically significant relationship was observed between high immunoreactivity to peptide 1 and the presence or absence of OCBs (Figure 4.18a). A statistically significant relationship was shown to exist between high immunoreactivity to peptide 2 and the presence of OCBs ($p=0.002$) compared to readings obtained from individuals who tested negative for OCBs (Figure 4.18b). This relationship was also shown to exist between high immunoreactivity to peptide 3 and the presence of OCBs ($p=0.004$) compared to readings obtained from individuals who tested negative for OCBs (Figure 4.18c).

No relationship was observed between the albumin/IgG ratio and serum immunoreactivity towards peptides 1, 2 and 3 ($R^2 = 0.01518, 0.01682$ and 0.008834 ,

respectively) (Figure 4.19a-c). A weak correlation was found between the albumin/IgG ratio and CSF reactivity to peptide 1, 2 and 3 ($R^2 = 0.08996$, $R^2 = 0.1698$ and $R^2 = 0.3004$, respectively) (Figure 4.20a-c). This showed that the albumin/IgG ratio did not affect the level of ACPAs detected.

A weak relationship was shown to exist between the serum IgG concentration and serum immunoreactivity to peptides 1, 2 and 3 ($R^2 = 0.1190$, $R^2 = 0.1279$ and $R^2 = 0.1475$, respectively) (Figure 4.21a-c). Similarly, a weak relationship was also exhibited between the CSF IgG concentration and corresponding CSF immunoreactivity to peptides 1, 2 and 3 ($R^2 = 0.1631$, $R^2 = 0.1722$ and $R^2 = 0.4959$, respectively) (Figure 4.22a-c), but was strongest for peptide 3.

Figure 4.14: Analysis of immune response by ELISA to different citrullinated MBP peptides in the sera of patients with MS, other neurological disorders and controls. (a) peptide 1 (b) peptide 2 and (c) peptide 3. Data is presented as a scatter plot with each symbol representing an individual patient ($n=197$). The solid line indicates the mean absorbance value. Data was analysed for any statistical significance between absorbance of peptides and between disease groups using a General Linear Model followed by univariate analysis. Statistical significance was set at $p<0.05$.

Key: CNS; central nervous system, IHH; idiopathic intracranial hypertension, NI; non-inflammatory.

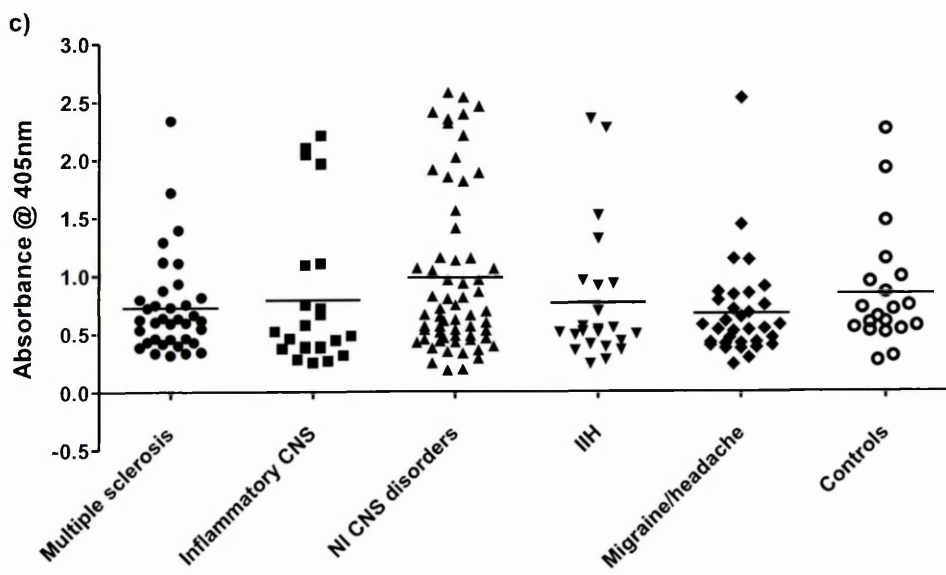
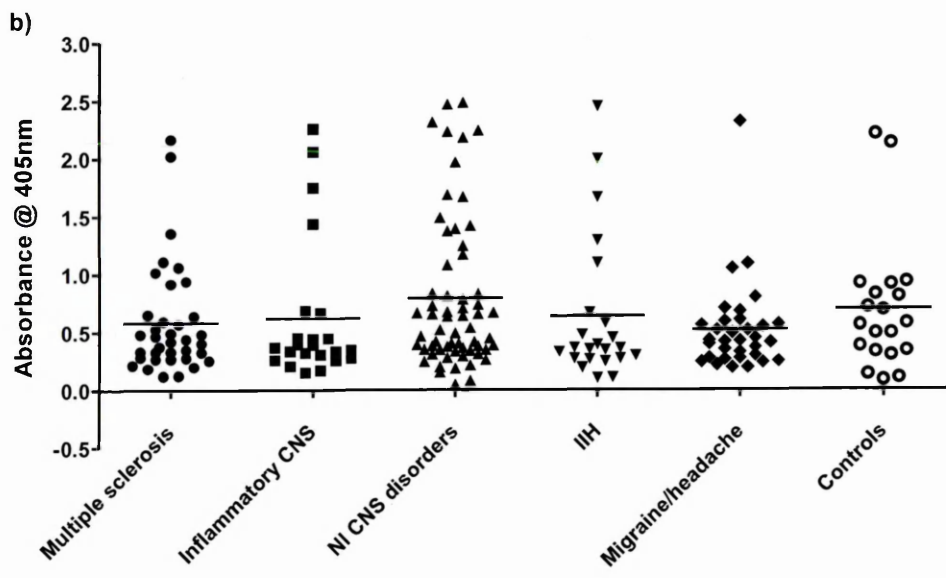
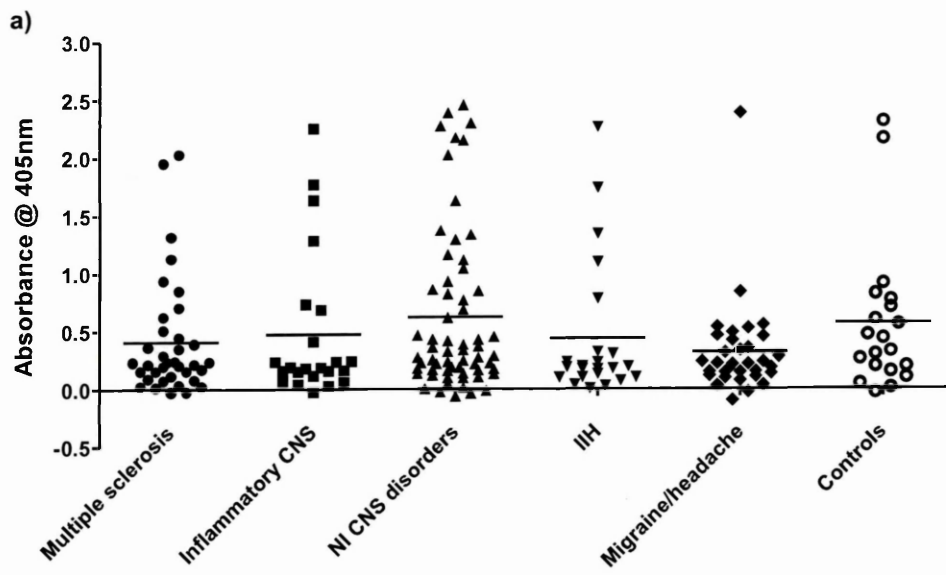
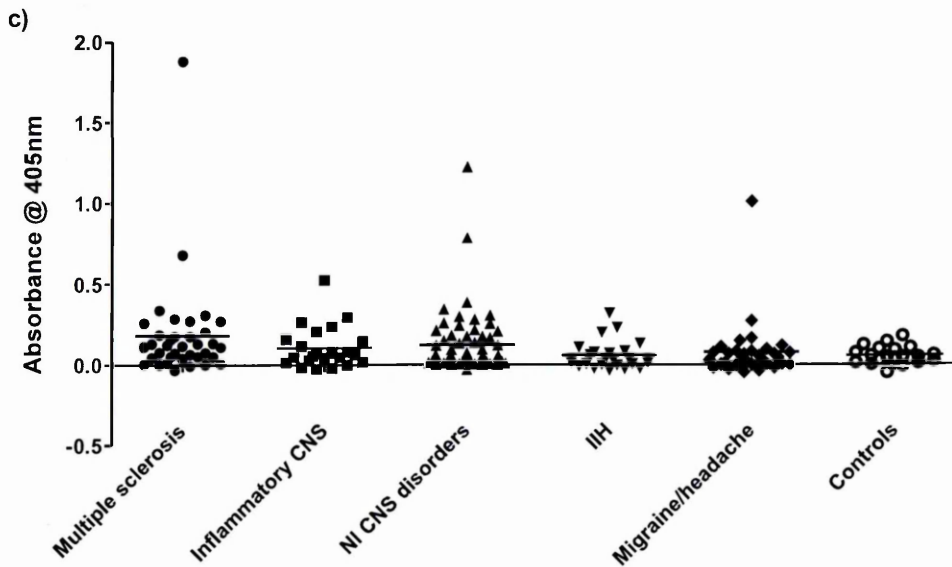
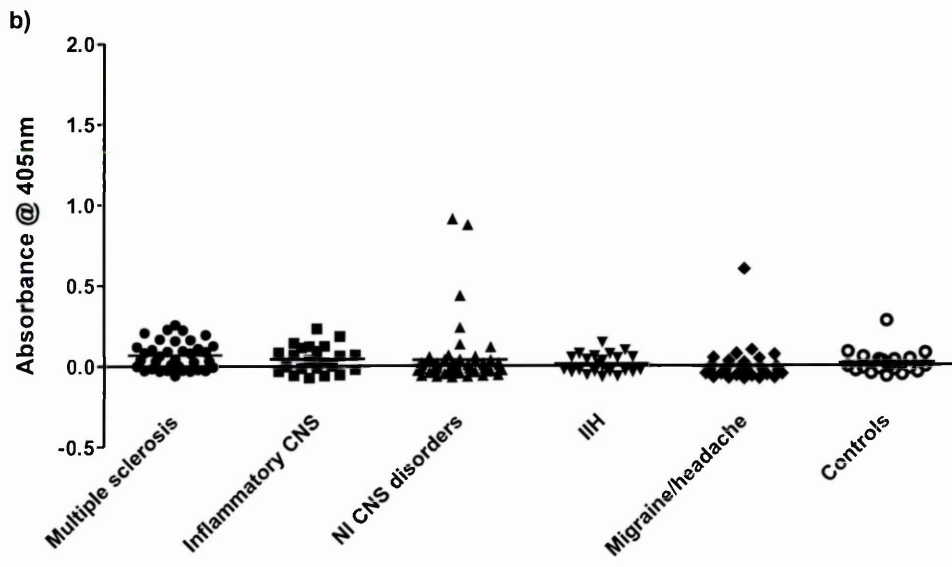
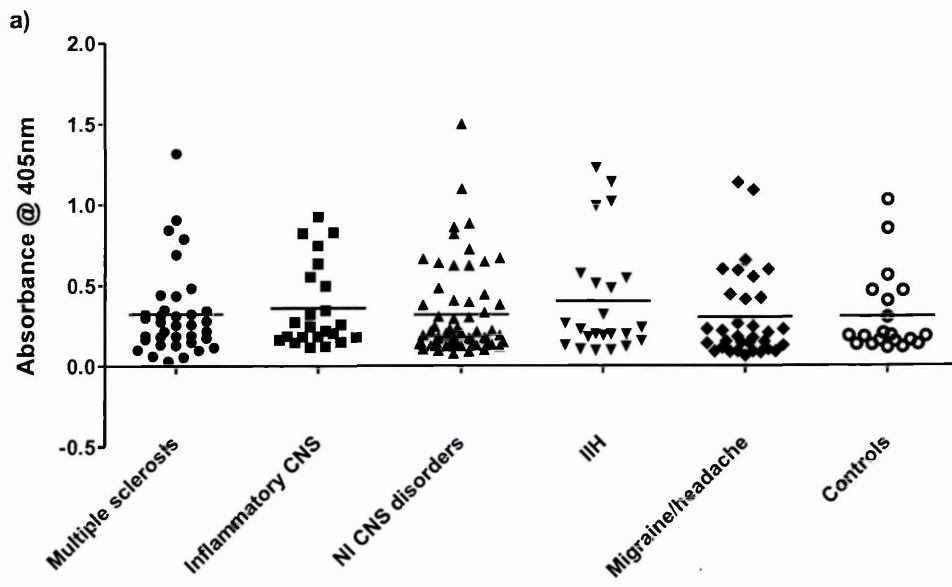


Figure 4.15: Analysis of immune response by ELISA to different citrullinated MBP peptides in the CSF of patients with MS, other neurological disorders and controls. (a) peptide 1 (b) peptide 2 and (c) peptide 3. Data is presented as a scatter plot with each symbol representing an individual patient ($n=197$). The solid line indicates the mean absorbance value. Data was analysed for any statistical significance between absorbance of peptides and between disease groups using a General Linear Model followed by univariate analysis. Statistical significance was set at $p<0.05$.

Key: CNS; central nervous system, IIH; idiopathic intracranial hypertension, NI; non-inflammatory.



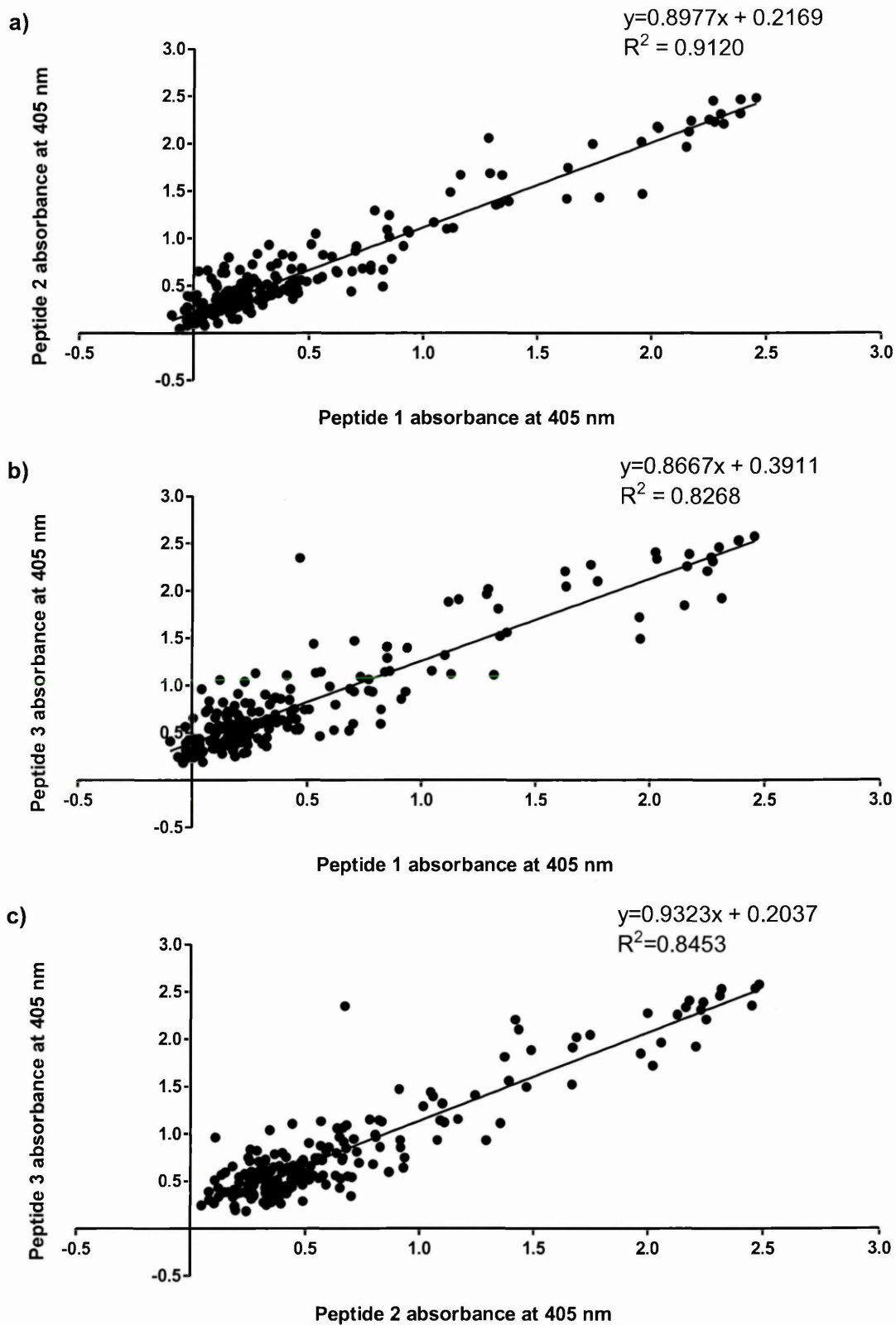


Figure 4.16: Correlation between patient sera antibodies against different cit-MBP peptides by ELISA. (a) peptide 1 versus peptide 2, (b) peptide 3 versus peptide 1 and (c) peptide 3 versus peptide 2 ($n=197$). Correlation coefficients (R^2) were determined using linear regression analysis.

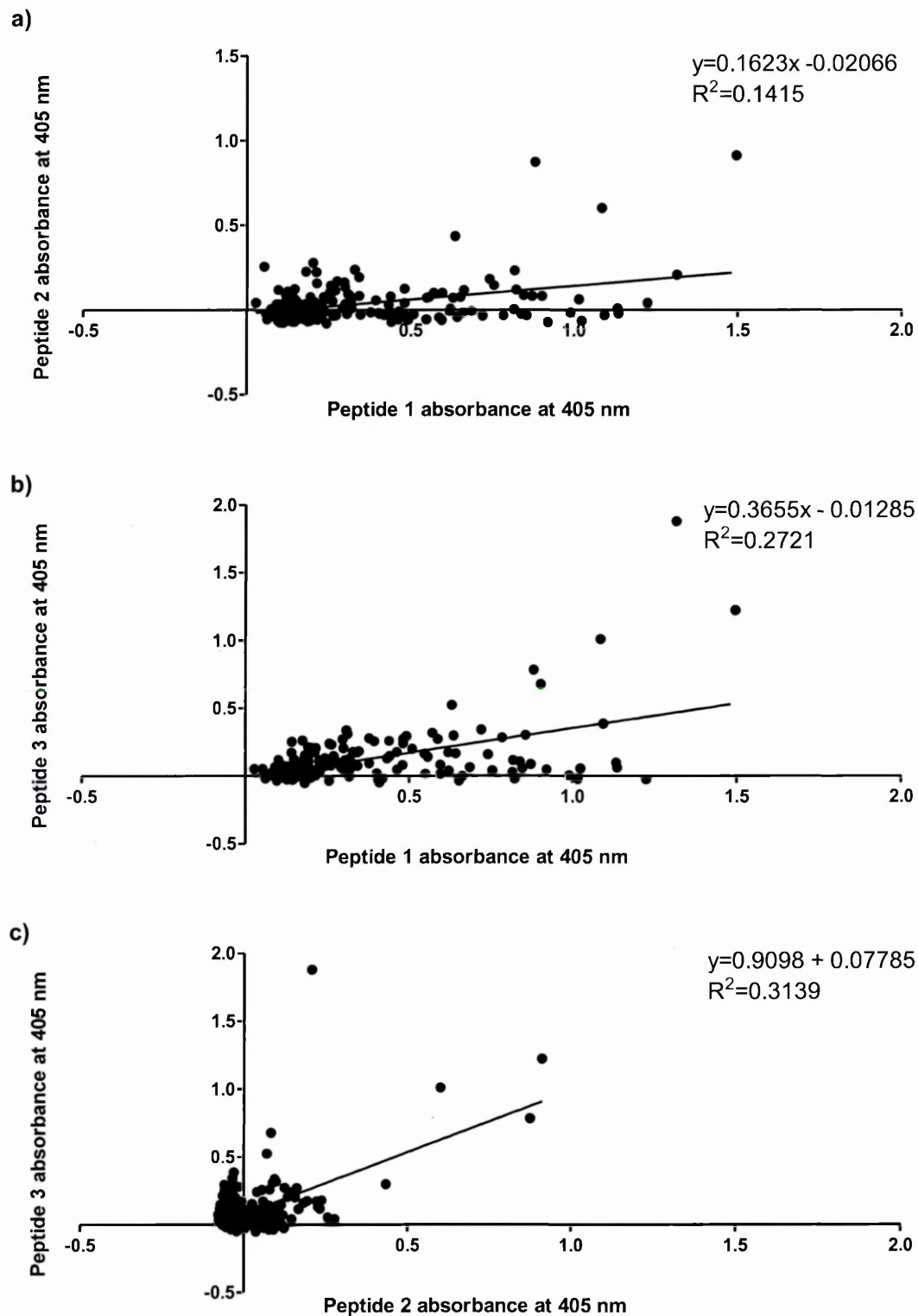
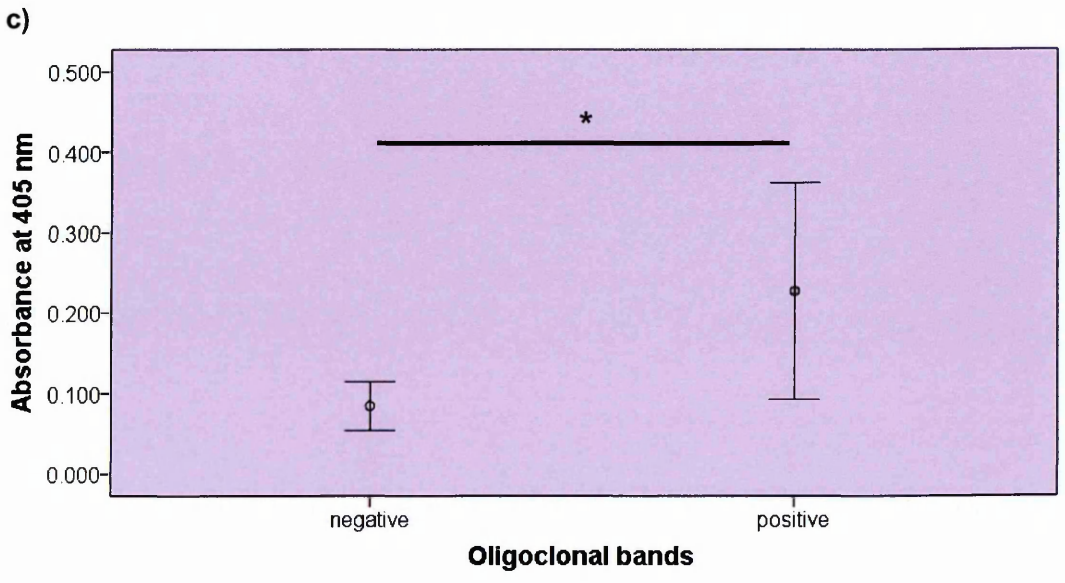
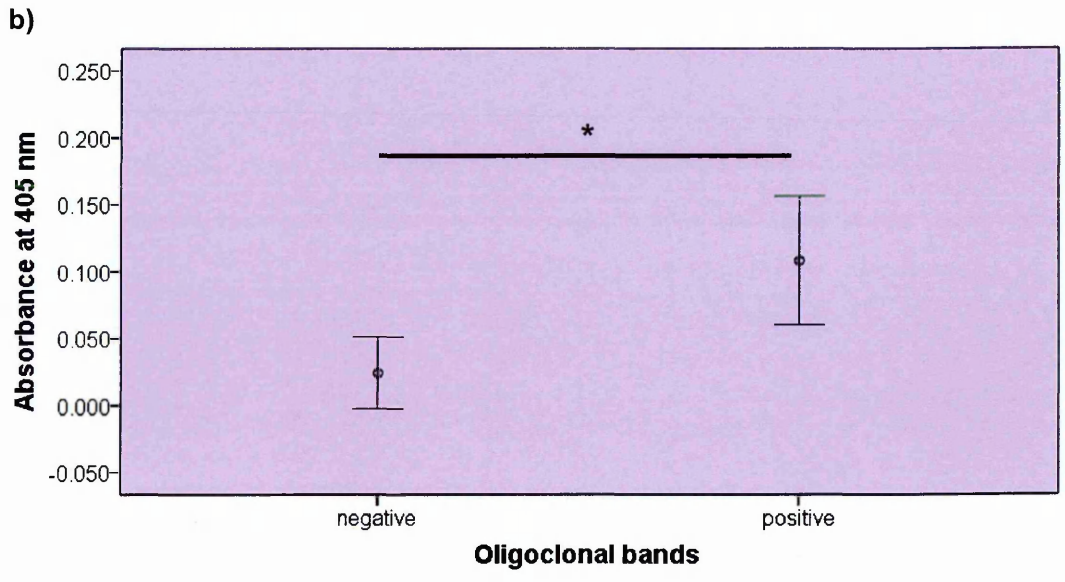
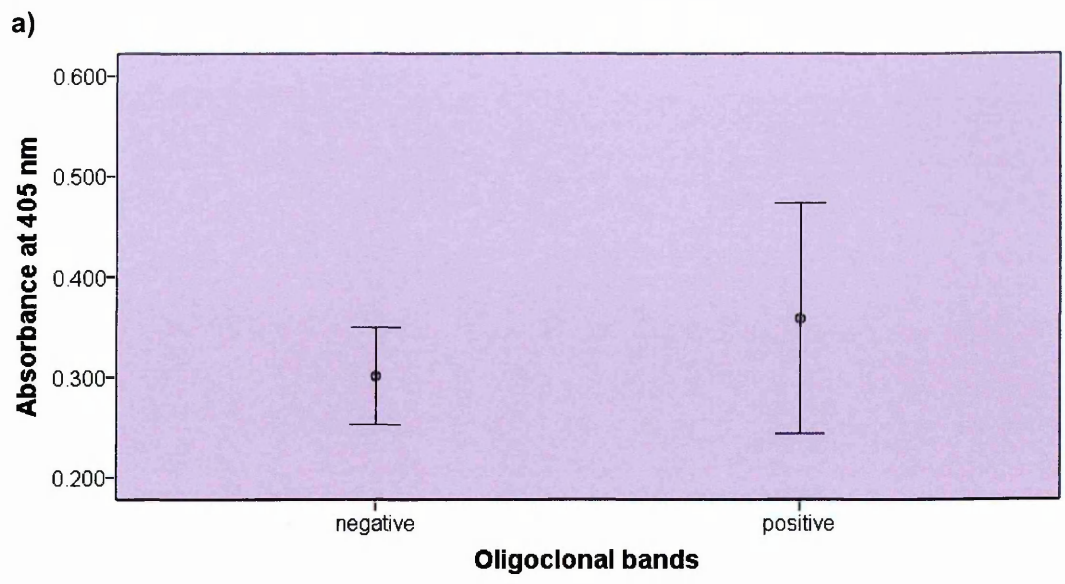


Figure 4.17: Correlation between patient CSF antibodies against different cit-MBP peptides by ELISA. (a) peptide 1 versus peptide 2, (b) peptide 3 versus peptide 1 and (c) peptide 3 versus peptide 2 ($n=197$). Correlation coefficients (R^2) were determined using linear regression analysis.

Figure 4.18: CSF Absorbance values by ELISA from patients with and without oligoclonal bands (OCBs). (a) peptide 1, (b) peptide 2, (c) peptide 3. Data is presented as the spread of absorbance values with each bar representing 95% confidence interval for the mean of each group ($n=138$; 34 positive for OCBs and 118 negative for OCBs). The central circle represents the mean. Data was analysed for any statistical significance between absorbance of peptides and between disease groups using a General Linear Model followed by univariate analysis. Statistical significance was set at $*p<0.05$.



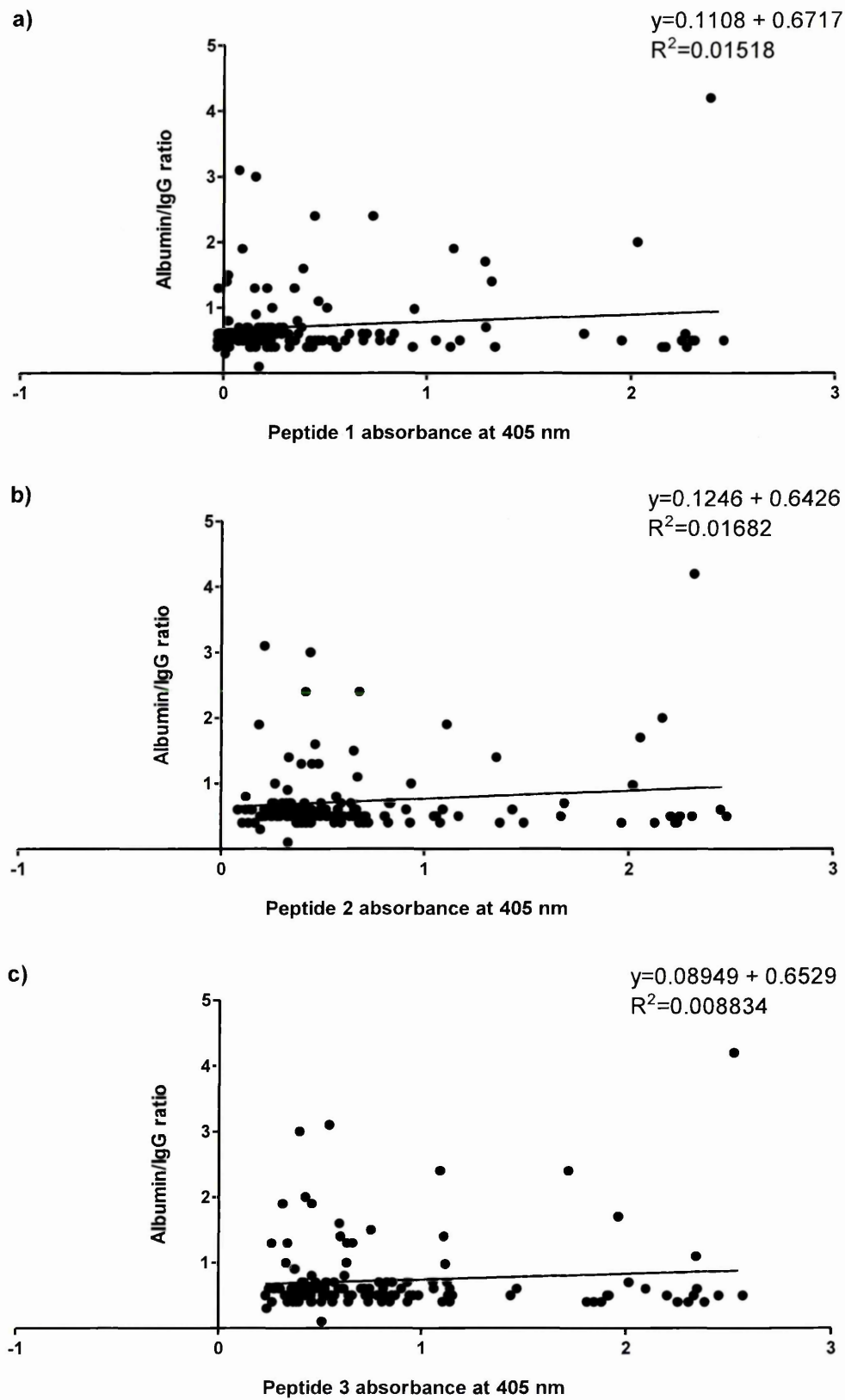


Figure 4.19: Correlation between patient albumin/IgG ratio and patient serum antibodies to cit-MBP peptides. (a) peptide 1, (b) peptide 2 and (c) peptide 3 ($n=137$). Correlation coefficients (R^2) were determined using linear regression analysis.

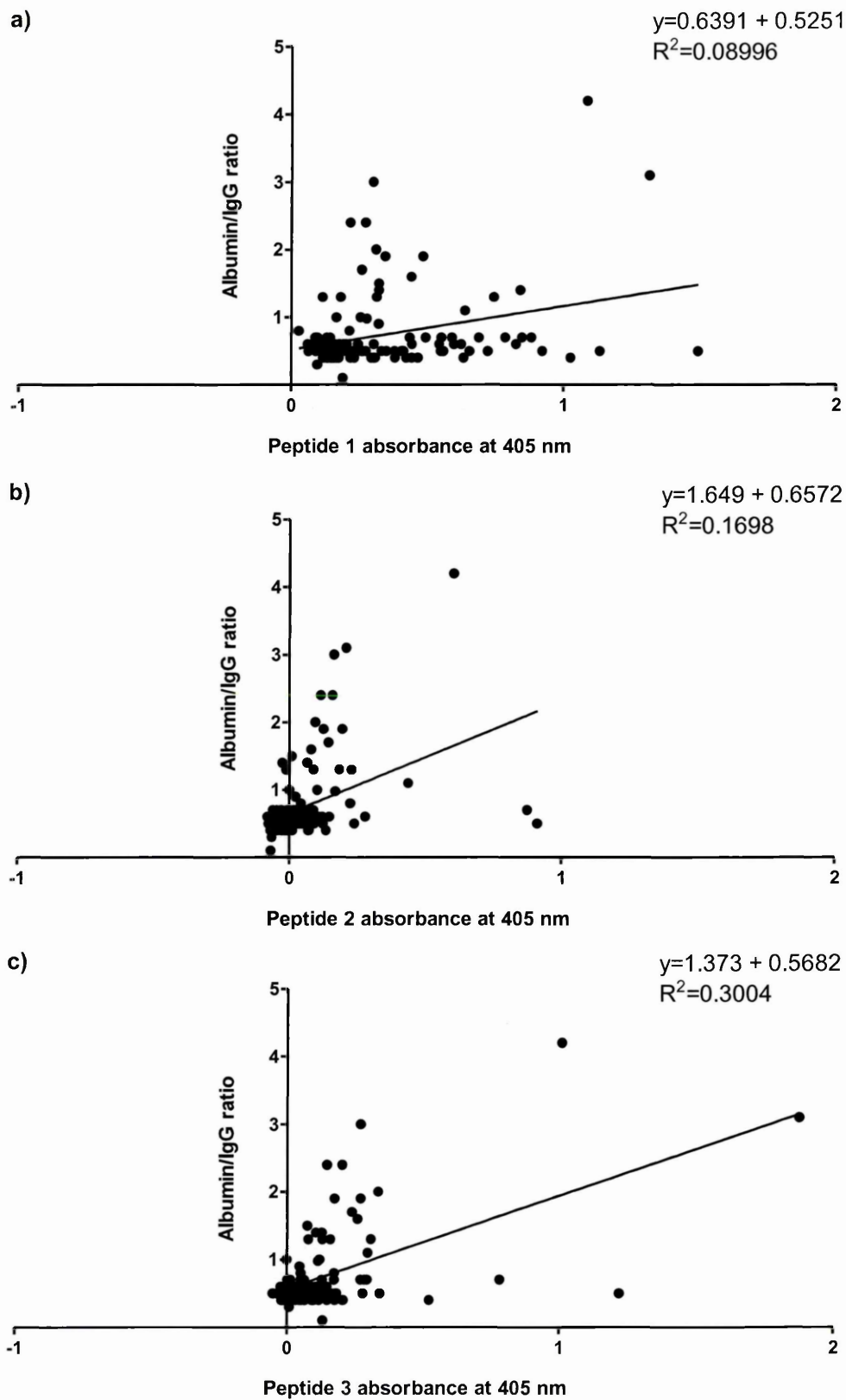


Figure 4.20: Correlation between patient albumin/IgG ratio and patient CSF antibodies to cit-MBP peptides. (a) peptide 1, (b) peptide 2 and (c) peptide 3 ($n=137$). Correlation coefficients (R^2) were determined using linear regression analysis.

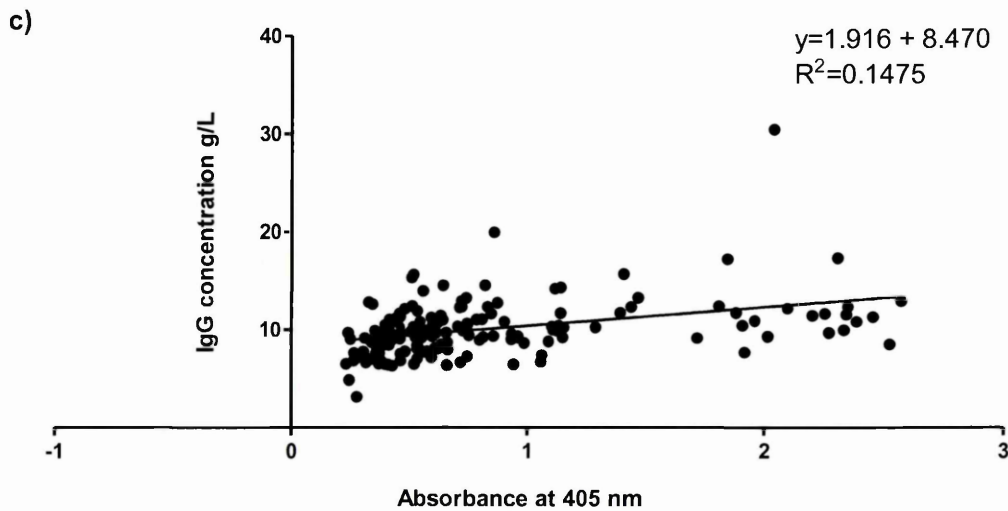
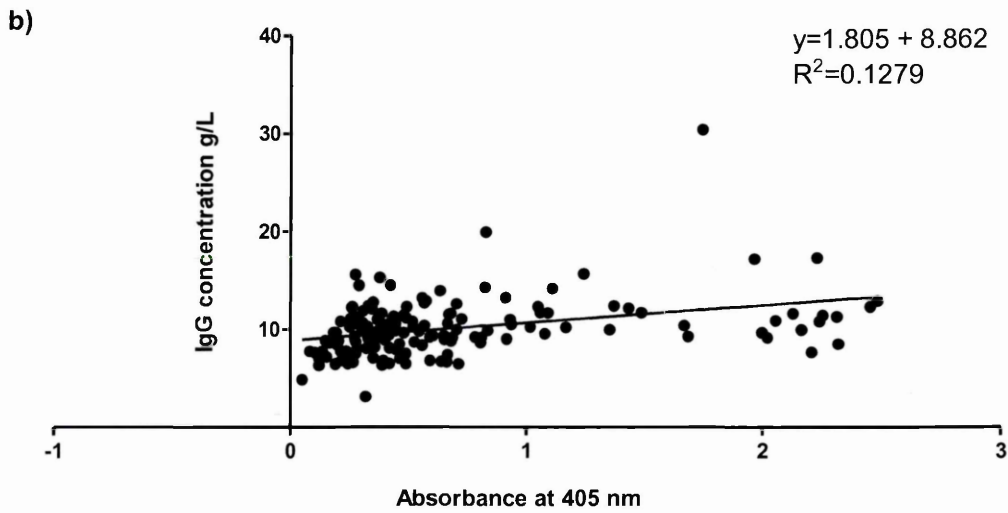
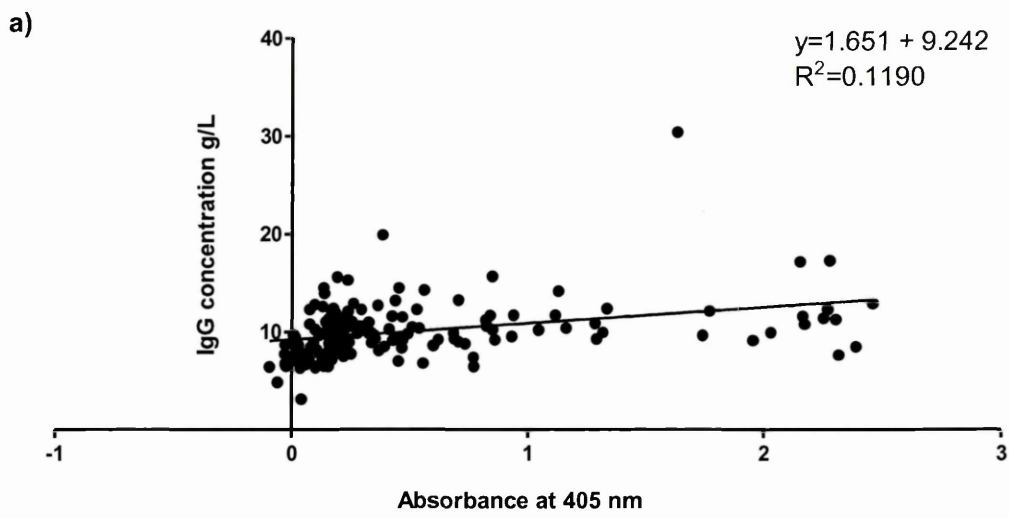


Figure 4.21: Correlation between patient serum IgG concentration and patient serum antibodies to cit-MBP peptides. (a) peptide 1, (b) peptide 2 and (c) peptide 3 ($n=158$). Correlation coefficients (R^2) were determined using linear regression analysis.

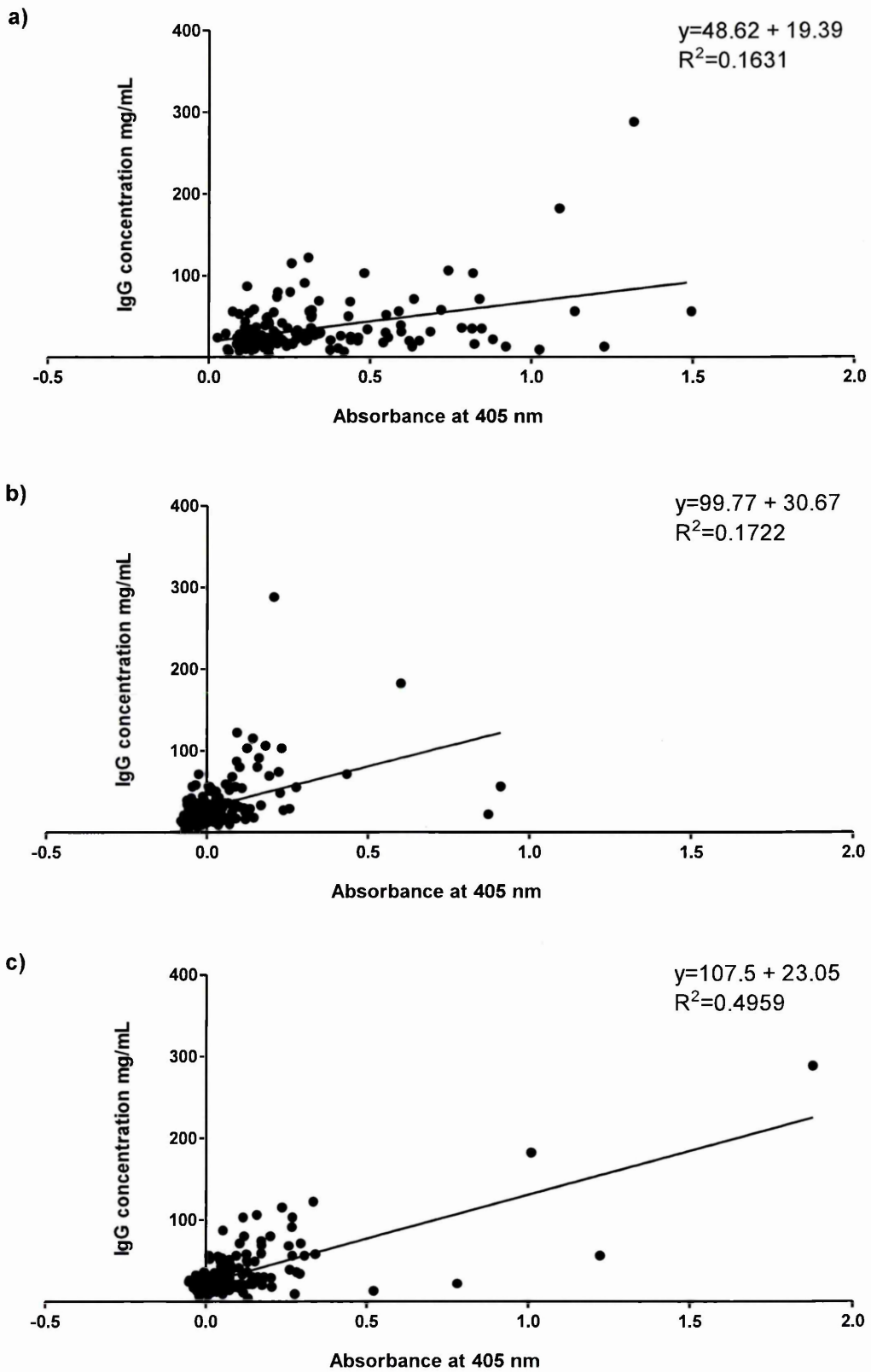


Figure 4.22: Correlation between patient CSF IgG concentration and patient CSF antibodies to cit-MBP peptides. (a) peptide 1, (b) peptide 2 and (c) peptide 3 ($n=152$). Correlation coefficients (R^2) were determined using linear regression analysis.

4.4 Discussion

4.4.1 Citrullinated peptide detection by mass spectrometry

Mass spectrometry was able to confirm the presence of GFAP and MBP from excised bands; however, no citrullinated peptides were identified. The positive identification of GFAP from bands excised at both ~48 and ~50 kDa confirmed previous results of the immunohistochemistry and western blotting where citrullinated GFAP was readily detectable in MS tissue (Chapter 3). The positive identification of MBP from bands excised at both ~15 and ~18.5 kDa confirmed that MBP is also citrullinated.

The detection of citrullinated peptides through MS/MS is difficult due to the 1 Da shift following citrullination, which often falls within the isotope peak range of the uncitrullinated peptide, if both are present in the same sample, which is a problem most likely to occur in *in vivo* tissue samples (De Ceuleneer *et al.*, 2012). In this case, both versions of the peptides will therefore be selected for MS/MS, since the *m/z* window used for data-dependent analysis is usually wide enough to encompass isotope peaks to enhance sensitivity. Fragment peaks from both peptides will consequently be present in the MS/MS spectrum and may hamper correct interpretation (De Ceuleneer *et al.*, 2012). Furthermore, citrullination is a PTM known to be of low abundance and difficult to detect (Hermansson *et al.*, 2010), therefore when in a mixed sample containing unmodified proteins, the peptide peaks containing citrulline may be much smaller and become masked by the large unmodified peptide peaks, again making detection of citrullinated peptides difficult.

A further difficulty in relying upon this 1 Da mass shift to detect citrullinated peptides is that some peptides may contain asparagine or glutamine, which upon deamidation yield the same mass shift as citrullination, and also have a similar retention time shift compared to the unmodified peptide (Hermansson *et al.*, 2010). Although MS/MS can distinguish between deamidation and deimination (citrullination), MS/MS data on citrullinated peptides from *in vivo* samples is frequently missing or of poor quality therefore resulting in the incorrect selection of deamidated peptides for subsequent peptide identification (Hermansson *et al.*, 2010).

Mass spectrometry has become the method of choice for the analysis of post-translationally modified proteins and peptides. Peptides carrying a given PTM are, however, usually present in small amounts and in heterogenous mixtures, making their characterisation challenging. Therefore, methods which allow a more targeted analysis of PTM polypeptides have been developed (Stensland *et al.*, 2009). A specific

modification can pinpoint the presence of citrullinated peptides much more clearly than the method relying on the 1 Da mass shift (De Ceuleneer *et al.*, 2011).

Methods are now available which can specifically modify citrulline residues to enable their detection. An example of this is the modification of the ureido group of a citrulline residue by 2,3-butanedione and antipyrine, which results in a specific +238 Da mass shift that is easily detected by a mass spectrometer. In a recent study a synthetic peptide sequence (human vimentin 65-77) containing a citrulline residue was modified in this manner and analysed by QTOF instrumentation. Fragmentation of a doubly charged peptide observed at 790.918 produced a modification-derived fragment ion at m/z 201.104 as the dominant signal. However, sequence-specific fragments containing modified citrulline were of very low intensity. As the fragment at m/z 201.1 is derived from chemically modified citrulline residues, it may be used as a particular signature ion for the detection of peptides carrying derivatised citrulline residues. However, the favoured generation of this fragment resulted in a lack of b- and y-ions and therefore compromises peptide identification, as there was not sufficient information to identify the sequence of the selected precursor ion and citrullination site (Stensland *et al.*, 2009). In addition, this modification requires large amounts of peptides, where the amount of citrullinated peptides will only be a fraction of the total protein content of the sample (De Ceuleneer *et al.*, 2012). Thus future work could apply to the use of 2,3-butanedione with CNS cell extracts to increase the sensitivity of the mass spectrometry detection of citrullinated CNS proteins.

An alternative approach would be to select only citrullinated proteins prior to mass spectrometry analysis, through the selective immobilisation of specifically modified citrullinated peptides with 4-hydroxyphenylglyoxal immobilised on beads (Tutturen *et al.*, 2010). With this technique, citrullinated peptides could selectively be enriched from protein digests by cross-linking them to beads with guanidine and afterwards cleaving the modified peptide. This results in a less complex mixture of citrullinated peptides that can then be spotted onto a MALDI plate.

A previous study has shown that with very low peptide concentration samples, reducing the matrix concentration further improves peptide ionisation and peptide fragmentation (Zhu and Papayannopoulos 2003). In this study, three additional peptides from a BSA trypsin digest were observed with 2 mg/mL α -CHCA compared with 5 mg/mL α -CHCA, with the presence of more abundant and numerous MS/MS fragment ions from these peptides, resulting in more complete peptide sequences allowing for higher protein scores to be obtained (Zhu and Papayannopoulos 2003). In this study 5 mg/mL α -CHCA was used, reducing the matrix concentration to 2 mg/mL may have improved the mass spectra obtained and subsequent protein identifications.

It may have also been useful to remove abundant proteins from the MS tissue extract prior to SDS-PAGE and in-gel digestion using a multiple affinity removal spin cartridge for the depletion of high-abundant proteins (Hermansson *et al.*, 2010). This would have left an enriched pool of low-abundant proteins, which would have prevented abundant proteins from interfering with identifications of less abundant proteins in the sample.

Hermansson and colleagues (2010), using synovial tissue extracts and subsequent in-gel digestion of bands which matched the *in vitro* citrullinated fibrinogen α - and β -chains in size, were excised and in-gel digested with endoproteinase Lys C. The resulting peptide mixtures were subjected to HPLC-MS/MS and analysed for presence of citrullinated peptides. This approach identified the α - and β -chains of fibrinogen in the sample but no citrullinated peptides were detected by global MS/MS analysis, which indicated low levels of citrullination and the necessity to apply a targeted approach.

The method of peptide fragmentation is also important in the identification of citrullinated peptides, as many PTMs are not stable. A recent study showed that citrullinated BSA peptides were unstable following CID, with only two small signals assigned to fragments which had maintained the citrulline modification (Stensland *et al.*, 2009). In the same study electron-transfer dissociation (ETD)-based fragmentation maintained the modification and resulted in spectra with nearly complete sequence coverage compared to CID-based fragmentation and the identification of three additional citrullination sites (Stensland *et al.*, 2009). Therefore, it may have been useful to compare different fragmentation techniques.

Analysis of citrulline-containing peptides is also possible without chemical derivatisation. With modern LC/MS/MS instrumentation citrullinated peptides can be separated from their non-deiminated counterparts and the high resolution and mass accuracy allow their identification by CID (Stensland *et al.*, 2009). The slight change in hydrophobicity caused by the loss of a protonated arginine side chain will cause a higher retention on reverse phase-LC (RP-LC) columns for citrullinated peptides. However, this approach requires extensive optimisation for every peptide of interest and is therefore less practical for use in a shotgun proteome analysis (Hermansson *et al.*, 2010). It may have been useful to have carried out RP-LC prior to mass spectrometry to separate the non-citrullinated and citrullinated peptides. However, this equipment was not available.

4.4.2 ACPAs were not significantly different in MS

In this study there were no significant differences in the level of ACPAs in patients with MS compared to those with other ONDs and non-neurological controls using a commercial ELISA designed for RA. On the basis of ACPA in RA it was anticipated that antibodies towards citrullinated MBP may be raised at disease onset, as immunohistochemistry results on MS CNS tissue suggests citrullination (see chapter 3) precedes demyelination, it was predicted that antibodies towards citrulline would occur early in the disease course and contribute to the demyelination which is a classical hallmark of MS. ACPAs were slightly higher against citrullinated MBP peptides 2 and 3 in CSF from patients with MS compared to other neurological disease and non-neurological controls, but this was not significant. Interestingly, higher CSF ACPA levels towards both citrullinated MBP peptides 2 and 3 were significantly associated with patients that tested positive for OCBs, whereas those with lower ACPA levels were significantly associated with patients that tested negative for OCBs. This provided a good indication that absorbance values were not due to non-specific binding of IgG in the CSF. Furthermore, these results suggest that the antibody response towards citrullinated proteins is restricted to the CSF, i.e. intrathecal antibody production, and is not a peripheral immune response and indicates that patients with these OCBs contain antibodies against citrulline residues. In addition, these findings also support the B cell follicle hypothesis (Serafini *et al.*, 2004).

MBP has been described as a potential target for autoimmune reactivity in MS (Reindl *et al.*, 1999). However, previous studies have also failed to detect significantly high levels of ACPAs towards MBP in serum and CSF of MS patients compared to ONDs and controls (De Seze *et al.*, 2001). In fact De Seze and colleagues (2001) showed that the physiological substitution of only one arginine residue with citrulline at the MBP₁₂₂ position of this peptide dramatically reduced the immune response in MS patients, whereas this response did not alter the immune recognition in sera and CSF of patients with ONDs (De Seze *et al.*, 2001). In comparison, this group did not detect any significant modification of immune reactivity to the citrullinated MBP₁₅₁₋₁₇₀ epitope in either CSF or sera of MS patients. Whereas, a previous study showed a higher peripheral T-cell response to the citrullinated MBP₁₅₁₋₁₇₀ epitope in MS compared to control subjects (Tranquill *et al.*, 2000). However, in this latter study, comparative evaluation between unmodified and citrullinated MBP epitopes was not performed. The current study and previous studies have only focussed on physiologically citrullinated MBP peptides, and not on the entire human MBP-C8.

In addition, immunohistochemical and western blot studies using an antibody specific to all deca-citrullinated peptides have shown the predominance of citrullinated GFAP

as opposed to MBP in MS brain tissue, therefore the predominant immune response to citrullinated proteins may be directed towards GFAP positive astrocytes rather than MBP. However, due to being unable to identify citrullinated GFAP peptides through mass spectrometry in this study, and therefore determine which specific arginine amino acids are citrullinated in GFAP, specific citrullinated GFAP peptides could not be used to coat the wells of an ELISA plate for this study and no other studies have reported this information to date.

Previous ELISA studies have included controls and compared binding to BSA and the specific peptide to check for non-specific binding of patient antibodies by coating wells with BSA (De Seze *et al.*, 2001). This control procedure was not carried out in this study, but a blocking step was employed prior to incubation with patient serum and CSF which should have prevented any non-specific binding of antibodies. In addition, there were weak correlations observed between ACPA levels in CSF and all three citrullinated MBP peptides, i.e. a high ACPA response of a patient to peptide 1 did not predict a high ACPA response to peptides 2 and 3, suggesting that the antibody binding within the wells was not due to non-specific binding. However, there were strong correlations between ACPA levels in serum for all three citrullinated MBP peptides, i.e. where there was a high ACPA response to peptide 1 this was also observed towards peptides 2 and 3. This could indicate non-specific binding of patient serum antibodies to the citrullinated peptides, but could also indicate a genuine antibody response to all citrullinated peptides.

Although antibody reactivities would be attractive for use as biomarkers to predict relapses or progression in MS, no antibody that is specific to MS has yet been identified. This may be in part due to shortcomings in the assays used to determine antibody responses to CNS proteins. Especially to membrane proteins which are highly folded, and are the conformational epitope targets of autoantibodies, which are not preserved in conventional assays such as ELISA or western blot. This problem has been recently overcome by cell-based assays, in which MOG is expressed by a transfected cell line. Serum antibodies to native MOG were observed in a subgroup of patients using this assay (Lalivie *et al.*, 2006; Zhou *et al.*, 2006). Interestingly, high antibody titres to native MOG were recently reported in two independent studies in paediatric CIS, ADEM, and MS (O'Connor *et al.*, 2007; McLaughlin *et al.*, 2009). The use of whole myelin particles also revealed a more frequent positive reactivity in MS and CIS patients (Vogt *et al.*, 2009).

Previous studies have shown sample antigenicity is affected by changes in the composition of the buffers used to immobilise proteins to the ELISA plate wells (Miura *et al.*, 2012). Furthermore, to develop a more sensitive and reliable ELISA-based

diagnostic tests for RA, synthetic cyclic citrullinated filaggrin peptides were used in the anti-CCP assay (Schellekens *et al.*, 2001). This cyclisation forces the peptide to adopt a β -hairpin conformation, as cysteine-bridged cyclic peptides have been shown to mimic the β -turn structure of the antigenic epitope, and therefore antibodies bind these with enhanced affinity (Dorow *et al.*, 1985). Furthermore, in these cyclic peptides, the citrulline moiety is optimally exposed for antibody binding (Vossenaar and van Venrooij 2004). In this current study only linear citrullinated peptides were used to coat the ELISA wells, therefore, the use of CCPs may be necessary in order for sufficient binding of antibodies to occur. Another possible reason for the low level reactivity to citrullinated peptides in the CSF of patients with MS may be that these autoantibodies are largely bound to their tissue targets, rather than freely soluble within the CSF (Cross and Waubant 2011).

Furthermore, MS is very heterogenous with respect to histopathological changes (Lucchinetti *et al.*, 2000), CSF phenotype (Cepok *et al.*, 2001), disease course (Noseworthy *et al.*, 2000), and response to therapy. Accordingly, different mechanisms may play a role in demyelination. Not all patients might have a prominent antibody response, or specific autoantibodies may characterise distinct clinical entities (Weber *et al.*, 2011).

4.4.3 Conclusion

The identification of citrullinated proteins by mass spectrometry is inherently difficult, as shown by this study and previous studies, due to low levels of citrullinated peptides in tissue extracts and the small mass shift caused by the conversion of arginine to citrulline within the protein. The results of the ELISA assay employing citrullinated MBP peptides showed increased reactivity of MS patient CSF Igs towards certain citrullinated MBP peptides which has provided promising preliminary results. However, further controls and optimisation of the assay is needed to further define these antibody specificities, and possibly the recruitment of larger patient groups. Future research to investigate specific arginine residues that are citrullinated in GFAP may provide a better target to which antibodies towards citrulline residues may bind, as results of western blotting and immunohistochemistry on MS post-mortem brain tissue have indicated that citrullination occurs to a much greater extent in GFAP as opposed to MBP, as described in chapter 3.

Chapter 5

General Discussion

5.1 General Discussion

The main overall aim of this thesis was to investigate the role of PADs and citrullination in the pathogenesis of MS. This involved a four-pronged approach. The first part of this study involved an *in vitro* investigation into the expression of PADs in cells of the CNS and treatment of these cells with pro-inflammatory cytokines to determine if cytokines are involved in the modulation of PADs. The second part of the study involved a detailed investigation into the expression of PADs and citrullinated protein in post-mortem MS and control brain tissue in order to determine the cell types which have citrullinated proteins and determine any differences in the levels of citrullination between MS and control individuals. The third part involved using mass spectrometry to identify any novel citrullinated proteins from MS brain tissue extracts, which could be used to develop an in-house ELISA assay for the detection of ACPAs in individuals with MS. The final part involved the determination of ACPAs in the serum and CSF of individuals with MS, other neurological diseases and controls, using ELISA, in order to determine if higher levels are associated with MS.

Previous studies have shown an increase in PAD2 and PAD4 expression along with an increase in citrullination in MS brain tissue compared to control brain tissue (Moscarello *et al.*, 1994; Wood *et al.*, 1996; Wood *et al.*, 2008). Due to this direct association between the expression of PADs and the increase in citrullination, a number of studies have attempted to understand what factors lead to this increase in the PAD enzymes. Studies have identified that PADs are calcium-dependent enzymes and therefore high levels of PAD are required for their subsequent activation (Vossenaar *et al.*, 2004). Other studies have identified additional environmental conditions which can lead to PAD activation, including hypoxia, kainic acid and pressure (Asaga *et al.*, 2002; Sambandam *et al.*, 2004; Bhattacharya *et al.*, 2006a; Bhattacharya *et al.*, 2006b). However, studies investigating the involvement of pro-inflammatory cytokines, which are significantly increased in MS brains (for review see (Imitola *et al.*, 2005), in the modulation of PADs are limited. A previous study has shown citrullination to be rapidly induced in neutrophils following exposure to the pro-inflammatory cytokine TNF- α (Neeli *et al.*, 2008). Furthermore, TNF- α has been shown to be necessary for translocation of PAD4 to the nucleus (Mastronardi *et al.*, 2006).

The findings reported in this thesis suggest that pro-inflammatory cytokines are either not involved in the modulation of PAD2 or implicate an anti-inflammatory role for PAD2, as significant down-regulation in PAD2 mRNA expression was observed following cytokine treatment with IL-1 β , TNF- α and IFN- γ in astrocytes and microglia. Down-regulation of PAD2 mRNA in brain endothelial cells was only observed following

treatment with TNF- α . Overall, dual treatment of these cytokines also resulted in significant down-regulation in PAD2 mRNA in astrocytes, microglia and brain endothelial cells. This indicates that pro-inflammatory cytokines are not involved in the up-regulation of PAD2 and that additional mechanisms may be involved in the modulation of PAD2. Additional mechanisms have been identified which are important in this transcriptional regulation of PAD2 at the mRNA level. Previously, the PAD2 promoter in MS brains has been shown to be hypomethylated compared to control brains, leading to increased transcription of PAD2 (Mastronardi *et al.*, 2007). Furthermore, PAD2 protein was also shown to be upregulated in MS NAWM compared to control white matter (Mastronardi *et al.*, 2007). Calcium has also been shown to be involved in the recruitment of transcription factors to the PAD2 gene, resulting in the transcription of PAD2 (Dong *et al.*, 2005). It is difficult to reproduce *in vitro* the complex inflammatory milieu within the CNS during inflammation and demyelination, however, based on the data obtained in this thesis pro-inflammatory cytokines downregulate PAD2 mRNA expression.

A limitation of this current study is that only PAD2 mRNA expression was investigated. mRNA levels do not always reflect protein levels (Bhattacharya *et al.*, 2006). Previous studies investigating PAD2 expression have shown that the enzyme can be present at the protein level and absent at the mRNA level (Vossenaar *et al.*, 2004). mRNA is much less stable than protein, therefore, protein expression may have given a better indication of whether cytokines are involved in the modulation of PAD2, as proteins have a much longer half-life than mRNA (Gygi *et al.*, 1999). Furthermore, PAD2 activity was not investigated, which would have provided information on the actual activity of the enzymes, and hence ability to citrullinate CNS proteins.

This study investigated single cell types grown in media, and did not determine the effects of co-cultures on the expression of PAD2 mRNA. It is important to consider the reciprocal communication between different cell types, such as astrocytes and neurons, in the *in vivo* situation (Carmignoto 2000). Expression of PADs may require communication between these different cell types in order for modulation of PAD2 to occur. In normal physiology, astrocytes have been shown to play a decisive role as the linker between neurons and blood vessels (Zonta *et al.*, 2003; Fellin and Carmignoto 2004; Fellin 2009) and to act to supply oxygen and energy via internal stores and vasodilation to support neuronal activity (Zonta *et al.*, 2003; Brown and Ransom 2007). These mechanisms are involved in increases in intracellular Ca²⁺ in astrocytes, and these events trigger Ca²⁺ waves to neighbouring astrocytes (Cornell-Bell *et al.*, 1990; Zonta *et al.*, 2003; Fiacco and McCarthy 2006). Therefore Ca²⁺ signalling as a result of

interactions of astrocytes with neurons may be necessary in order for PAD2 to become activated *in vitro*.

Previous studies have shown the expression of citrullinated proteins to be increased in MS brain tissue compared to control brains, and that this is associated with increased expression of PAD2 and PAD4 enzymes in the brains of these individuals (Mastronardi *et al.*, 2006; Wood *et al.*, 2008). The results from this thesis confirmed previous findings, that citrullination is increased in MS brain tissue compared to control brain tissue. However, this study also identified that citrullination is highest in the lesion edges where myelin is either thinning or where active demyelination is occurring rather than associated with areas of complete myelin loss. The findings of this study indicate that citrullination of MBP precedes demyelination in MS, which agrees with the proposed hypothesis that citrullination of MBP precedes myelin loss leading to a conformational change in the structure of myelin resulting in direct demyelination and also exposure of new epitopes not recognized by the immune system as self. This contributes to earlier studies which have shown that up to 45-90% of MBP in patients with MS is citrullinated compared to only 18% in control individuals (Moscarello *et al.*, 1994; Wood *et al.*, 1996). A number of studies have shown that deiminated MBP is unable to compact lipid bilayers, causing membrane destabilisation, thereby, possibly promoting demyelination (Brady *et al.*, 1981; Wood and Moscarello 1989; Boggs *et al.*, 1999; Beniac *et al.*, 2000). In addition, deiminated MBP is more susceptible to proteolytic digestion by myelin-associated proteases (Cao *et al.*, 1999; Pritzker *et al.*, 2000; D'Souza and Moscarello 2006; Musse *et al.*, 2006). This greater surface exposure and greater enzymatic cleavage of the citrullinated protein would lead to increased release of the immunodominant epitope, which could prime the innate immune cells of the CNS and sensitize peripheral blood T cells (Musse *et al.*, 2006; Musse and Harauz 2007). These results reported in this thesis support previous studies as at sites of ongoing demyelination there is an increase in citrullinated proteins.

Previous studies have focused on citrullination and its association with MBP (Moscarello *et al.*, 1994; Wood *et al.*, 1996; Mastronardi and Moscarello 2005; Wood *et al.*, 2008); however, in this study citrullination was shown to be predominantly associated with GFAP, the structural component of astrocytes. This agrees with a previous study carried out by Nicholas *et al.* (2004) which also showed the co-localisation of citrulline with GFAP in the NAWM of MS brain tissue. However, Nicholas *et al.* (2004) showed increased citrullination in the NAWM, whereas in this study the highest levels of citrullination were observed in areas of myelin thinning and ongoing demyelination. The reasons for this difference between this latter study and this study

are unclear, except that in the study by Nicholas *et al.* (2004) only three MS blocks were used as opposed to this study where 12 blocks were used. In addition, Nicholas *et al.* did not characterise the tissue sections using H&E, ORO, HLA-DR and MOG or any other markers prior to staining for citrullinated proteins. Due to the tissue sections in this latter study not undergoing classification, it seems possible that the NAWM may have actually contained lesions.

Similarly, post-mortem immunohistochemical studies investigating citrullination in sCJD have also shown increased citrullinated proteins in sCJD infected brains compared to control brains, with these citrullinated proteins mostly co-localised with GFAP-positive astrocytes (Jang *et al.*, 2010). Reactive gliosis is accompanied by activation and upregulation of various proteins with potent biological effects, including L-type Ca^{2+} channels, various receptors, PAD2 and its well known substrates including GFAP (Aronica *et al.*, 2001; Jang *et al.*, 2008). Although citrullinated forms of astrocyte-specific GFAP have been reported in various neurodegenerative conditions, a functional role for citrullinated GFAP in the CNS has not been elucidated (Nicholas *et al.*, 2004; Ishigami *et al.*, 2005; Jang *et al.*, 2008). It remains unknown whether the accumulation level of citrullination is different amongst different neurodegenerative conditions and whether specific citrullinated proteins are present in these neurodegenerative conditions.

GFAP is the main intermediate filament protein in mature astrocytes and is involved in a number of structural and functional processes, including motility, proliferation, vesicle trafficking, autophagy and synaptic interactions with neurons (Middeldorp and Hol 2011). GFAP is also thought to play an important role in astrocyte motility, with motility of GFAP^{-/-} astrocytes shown to be greatly reduced compared to GFAP-expressing astrocytes (Lepekhn *et al.*, 2001). Vesicle trafficking has also been shown to be reduced in astrocytes from mice with double knock-out of GFAP and vimentin (Potokar *et al.*, 2007; Potokar *et al.*, 2008). Neuronal activity is closely linked to the release and uptake of the neurotransmitter glutamate, which requires the interaction between astrocytes and neurons. Glutamate transporters have been identified on neuronal and astrocytic membranes and are important for removal of extracellular glutamate (Pines *et al.*, 1992; Storck *et al.*, 1992; Rothstein *et al.*, 1994). GFAP plays a key role in modulating astrocytic and neuronal glutamate transporter trafficking and function and in the control of glutamine production. In cortical and hippocampal synaptosomal preparations from adult GFAP^{-/-} mice a reduced glutamate uptake was found together with decreased glutamate transport activity (Hughes *et al.*, 2004). GFAP is subjected to multiple post-translational modifications that have important consequences for its structure and functions. Although the exact effect of citrullination of GFAP in astrocytes

is currently unknown, it may have detrimental effects on a number of these physiological processes described above, such as reducing astrocyte motility and vesicle trafficking, preventing the phosphorylation of GFAP during cell proliferation (Inagaki *et al.*, 1994), or affect the ability of astrocytes to effectively remove glutamate from the extracellular environment leading to neuronal glutamate excitotoxicity, contributing to pathological processes in MS (Bak *et al.*, 2006).

Previous studies have shown the increased expression of PAD2 and PAD4 at both the mRNA and protein level in MS lesions compared to controls; with studies showing its co-localisation with astrocytes and microglia (Vincent *et al.*, 1992; Asaga *et al.*, 2001; Ishigami *et al.*, 2002). In this study no difference in the expression of PAD2 at the protein level was observed between MS lesional tissue, MS NAWM and control brain tissue. Furthermore, PAD2 expression was shown to co-localise with some but not all microglia and was not co-localised with astrocytes. PAD4 staining was very difficult to identify above background level. These findings were unexpected as based on previous studies it was anticipated that PAD2 would be upregulated in MS lesions and would be associated with microglia and astrocytes. However, there were difficulties with the anti-human PAD2 antibody used even following stringent optimisation, as staining was generally weak even when the highest concentration of antibody was applied to the tissue section. A second primary antibody against PAD2 was also tested with similar results. Furthermore, the isotype control also showed very high levels of staining. Although the staining was less intense than for the PAD2 antibody, the results of the PAD2 staining should still be treated with caution. Similarly, a second antibody against human PAD4 was also tested, but specific staining above background levels was not observed, and corresponding isotype control showed similar non-specific staining. Obtaining anti-human PAD2 and PAD4 primary antibodies was problematic as the majority of previously published work showing high immunostaining for these enzymes used antibodies that had been produced in-house by the research groups themselves and were not available commercially. Furthermore, both PAD2 and PAD4 mRNA was shown to be present in control, MS NAWM and MS lesional brain tissue; although the expression of PAD2 was relatively low and PAD4 was 100-fold lower than the expression of PAD2 mRNA.

Through the use of western blotting of brain homogenates from an MS brain block known to contain high levels of citrullinated proteins, multiple proteins in the brain were shown to be citrullinated. Mass spectrometry identified four of the proteins as GFAP and MBP isoforms, however, the remaining three proteins were not identified. Furthermore, specific citrullinated residues were not identified by mass spectrometry. Previous studies have been able to identify citrullinated proteins through the use of

mass spectrometry. However these studies have applied different approaches in order to identify these citrullinated proteins.

Based on previous studies showing the effects of citrullination on the structure of MBP (Pritzker *et al.*, 2000), along with the high levels of citrullination observed in this study, and the possibility of citrullination introducing new epitopes that are not recognised as being self by the immune system, it was anticipated that antibodies may be produced directed specifically against citrullinated proteins. In addition, citrullinated peptides have been shown to have increased binding to HLA-DR (Hill *et al.*, 2003; James *et al.*, 2010). Furthermore, in RA, ACPAs have been shown to present specifically in RA and are now routinely used in the diagnosis of this disease. Testing for the presence of antibodies towards citrullinated MBP peptides in paired CSF and serum from individuals with MS, ONDs and controls, did not show any significant differences in serum or CSF reactivity between these groups. Previous studies have also failed to identify any significant reactivity towards citrullinated proteins in the serum and CSF of individuals with MS (De Seze *et al.*, 2001). A previous study by Tranquill *et al.* (2000) showed a higher peripheral T-cell response to citrullinated MBP in patients with MS compared to control, although a comparison in reactivity towards unmodified MBP was not carried out in this study (Tranquill *et al.*, 2000). This lack of association of the presence of ACPAs and diagnosis of MS may be due to a number of factors. In this thesis citrullinated proteins were shown to be predominantly associated with GFAP, rather than MBP, however due to the inability to identify which amino acids are citrullinated in GFAP peptides could not be synthesised containing citrulline residues for coating the ELISA plates. Therefore, a greater reactivity of MS patient CSF and serum towards citrullinated proteins may have been observed if citrullinated GFAP peptides were used. In addition, the RA-specific ACPA test utilises CCPs to coat the ELISA plates, as this has been shown to optimally expose the peptide for antibody binding (Dorow *et al.*, 1985; Vossenaar *et al.*, 2004). It is also possible that any autoantibodies present in patient CSF and serum may be bound to their tissue targets, rather than freely soluble, which would account for the low reactivity observed (Cross and Waubant 2011).

5.1.1 Future work

Although conflicting results exist, accumulating evidence strongly supports a role for PADs and subsequent citrullination of CNS proteins in the pathogenesis of MS, and certainly warrants further investigation. It is important that future research focusses on determining the mechanisms that trigger the activation of PADs and subsequent citrullination.

Since the addition of pro-inflammatory cytokines to CNS cells used in this thesis did not result in upregulation of PADs, it is worth investigating additional factors which may be involved in the regulation of these enzymes. However, due to the known differential expression of mRNA and protein, it may be worth assessing the expression of PAD2 and PAD4 protein following cytokine treatment rather than just mRNA as measured in this study. It would also be useful to determine PAD2 and PAD4 activity as the mRNA levels do not necessarily reflect the activity of the enzymes. Although the calcium concentration of the cell culture media was the concentration known to activate PADs, incubation with calcium ionophores may also be necessary to modulate the mRNA and subsequent activation of PADs. Due to the close relationship of astrocytes with neurons co-culture of these cells may provide more information on the modulation of PADs (Zonta *et al.*, 2003; Fellin and Carmignoto 2004; Fellin 2009).

There are no publications investigating the effects of citrullination on the structure and function of GFAP, therefore it would be useful to investigate these effects.

In terms of the variable results obtained with western blotting of citrullinated proteins from MS, NAWM and control brain tissues, immunoprecipitation using the F95 antibody to specifically obtain citrullinated proteins would provide better quantitative data. It may also be useful to assess PAD2 and PAD4 enzyme activity in these tissue sections. Testing of further PAD2 primary antibodies is needed in order to make concrete conclusions.

Immunoprecipitation of citrullinated proteins from MS brain tissue using an F95 primary antibody to capture citrullinated proteins may also be useful prior to mass spectrometry and make identification of citrullinated proteins easier. Performing in-gel digestion using both LysC and Trypsin may assist in identifying citrullinated proteins from the unmodified proteins as different cleavage products will be generated. Performing liquid chromatography prior to mass spectrometry may further enhance separation of citrullinated peptides from non-citrullinated peptides before performing MS/MS.

In terms of the patient study, greater serum and CSF antibody reactivities may be observed if the ELISA plates are coated with cyclic citrullinated MBP and GFAP, as this has been shown to enhance antibody binding in RA-patients, therefore this is also worth investigating in MS patients.

5.1.2 Conclusions

This thesis has investigated in detail the expression of PADs and citrullination in MS. Evidence presented here has shown that citrullination is increased in MS lesions compared to control and NAWM, and is associated with GFAP-positive astrocytes and

myelin breakdown. *In vitro* studies have shown this increase in citrullination is not due to the modulation of PADs by pro-inflammatory cytokines. Lastly, although there is serum and CSF reactivity observed towards citrullinated MBP peptides in patients with MS, this reactivity is not significantly different from serum and CSF from ONDs and controls. Due to the inability to detect significant serum and CSF reactivity towards citrullinated MBP in patients with MS, definitive conclusions cannot be made regarding the role of citrullination of proteins in MS. However, the evidence based on immunohistochemistry and western blotting indicates citrullination is involved in MS pathogenesis (Figure 5.1). The most interesting finding in this thesis is the dominant colocalisation of citrullinated proteins within astrocytes in MS lesions, which may result in significant changes in both the astrocyte structure and function, which could have important implications in MS (Figure 5.1). The results of this thesis indicate that further investigations into the role of citrullination in MS are required.

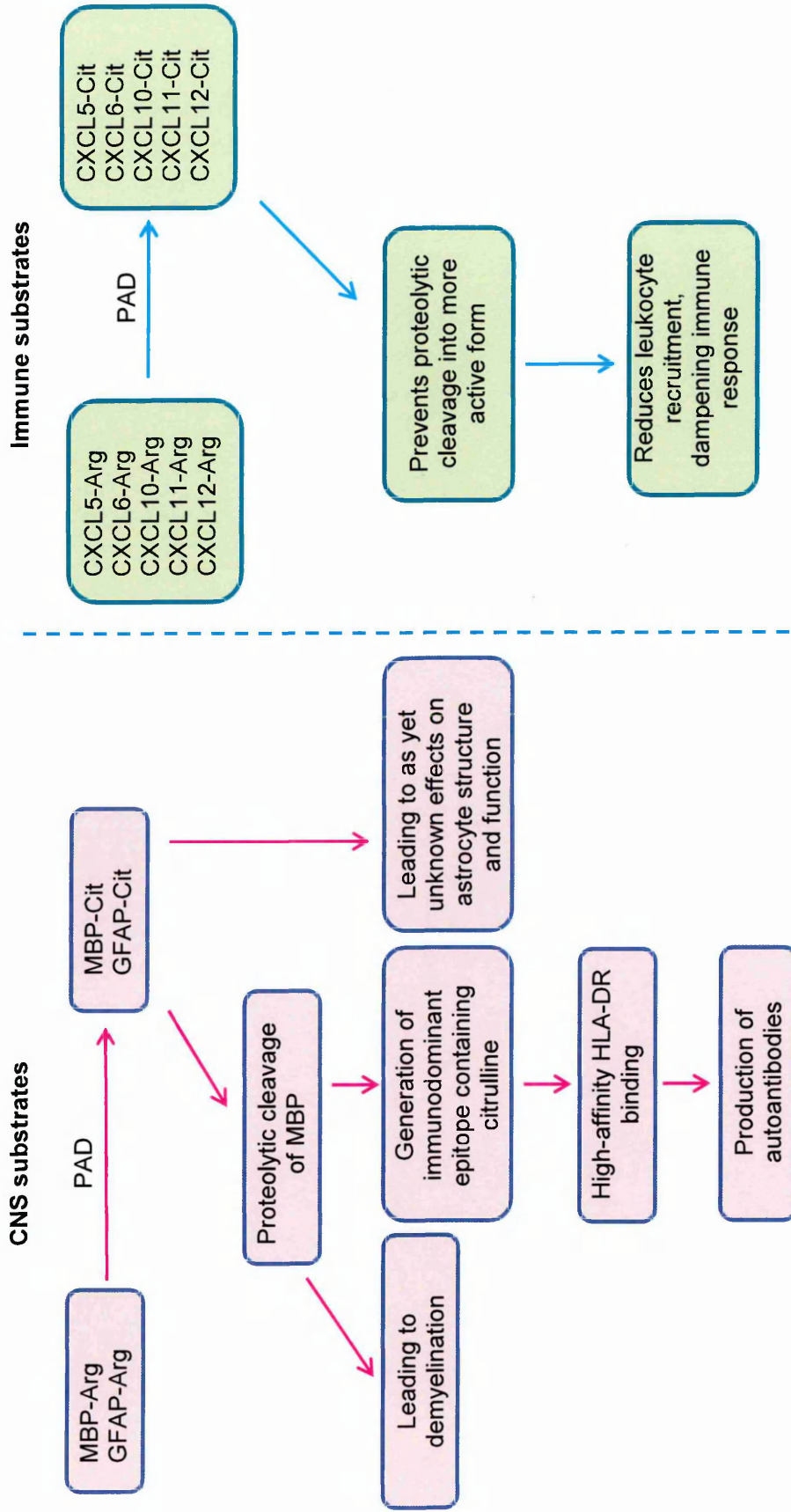


Figure 5.1: Overview of the effects of citrullination on the immune response in MS. This study has identified two major citrullinated proteins in MS, MBP and GFAP, which have the potential to influence the disease process. The conversion of arginine to citrulline in MBP alters the charge of the protein, as for each arginine converted to citrulline there is a loss of one positive charge, leading to partial unfolding of the protein and weakening interaction with phospholipids, therefore myelin sheaths are not as tightly packed as in normal myelin (Beniac *et al.*, 2000). Citrullination of MBP increases its susceptibility to degradation by proteinases, such as cathepsin D which has been shown to release numerous peptides at the Phe-Phe linkages in the MBP protein, in particular generating immunodominant epitopes containing citrulline (Cao *et al.*, 1999). Conversion of arginine to citrulline has been shown to enable a high-affinity peptide interaction with the rheumatoid arthritis-associated HLA-DRB1*401 MHC class II molecule and subsequent activation of CD4+ T cells (Hill *et al.*, 2003). Overall, this could lead to the production of autoantibodies targeting the myelin sheath. Although less is known regarding the conversion of arginine to citrulline in GFAP it is expected to have implications on the structure and function of GFAP positive astrocytes. Secondary to this, recent evidence has identified the CXC chemokines as targets for citrullination, which has been shown to prevent proteolytic cleavage of chemokines into their more active form resulting in reduced leukocyte recruitment and therefore may also play a role in disease pathogenesis (Loos *et al.*, 2008; Proost *et al.*, 2009; Loos *et al.*, 2008; Struyf *et al.*, 2009; Mortier *et al.*, 2010).

Key: Arg; arginine, Cit; citrulline, HLA; human leukocyte antigen, GFAP; glial fibrillary acidic protein; MBP, myelin basic protein.

Chapter 6

References

Abbott, N. J. (2004). Evidence for bulk flow of brain interstitial fluid: Significance for physiology and pathology. *Neurochemistry International*, **45** (4), 545-552.

Abbott, N. J., Patabendige, A. A. K., Dolman, D. E. M., Yusof, S. R. and Begley, D. J. (2010). Structure and function of the blood–brain barrier. *Neurobiology of Disease*, **37** (1), 13-25.

Abbott, N. J., Rönnbäck, L. and Hansson, E. (2006). Astrocyte–endothelial interactions at the blood–brain barrier. *Nature Reviews Neuroscience*, **7** (1), 41-53.

Abraham, C. and Cho, J. M. (2009). Inflammatory bowel disease. *New England Journal of Medicine*, **361**, 2066-2078.

Acheson, E. D., Bachrach, C. A. and Wright, F. M. (1960). Some comments on the relationship of the distribution of multiple sclerosis to latitude, solar radiation, and other variables. *Acta Psychiatrica Scandinavica Supplement*, **35** (147), 132-147.

Aebersold, R. and Mann, M. (2003). Mass spectrometry-based proteomics. *Nature*, **422** (6928), 198-207.

Akiyama, K., Inoue, K. and Senshu, T. (1990). Immunocytochemical demonstration of skeletal muscle type peptidylarginine deiminase in various rat tissues. *Cell Biology International Reports*, **14** (3), 267-273.

Alaedini, A. and Green, P. H. R. (2005). Narrative review: Celiac disease: Understanding a complex autoimmune disorder. *Annals of Internal Medicine*, **142** (4), 289-298.

Algeciras, M. E., Takahara, H. and Bhattacharya, S. K. (2008). Mechanical stretching elevates peptidyl arginine deiminase 2 expression in astrocytes. *Current Eye Research*, **33** (11), 994-1001.

Ali Shokrgozar, M., Sarial, S., Amirzargar, A., Shokri, F., Rezaei, N., Arjang, Z., Radfar, J., Yousefi-behzadi, M., Ali Sahraian, M. and Lotfi, J. (2009). IL-2, IFN- γ , and IL-12 gene polymorphisms and susceptibility to multiple sclerosis. *Journal of Clinical Immunology*, **29** (6), 747-751.

Allen, I. V. and McKeown, S. R. (1979). A histological, histochemical and biochemical study of the macroscopically normal white matter in multiple sclerosis. *Journal of the Neurological Sciences*, **41** (1), 81-91.

Allt, G. and Lawrenson, J. (2001). Pericytes: Cell biology and pathology. *Cells Tissues Organs*, **169** (1), 1-11.

Alonso, A. and Hernan, M. A. (2008). Temporal trends in the incidence of multiple sclerosis: A systematic review. *Neurology*, **71** (2), 129-135.

Amadori, A., Zamarchi, R., De Silvestro, G., Forza, G., Cavatton, G., Danieli, G. A., Clementi, M. and Chieco-Bianchi, L. (1995). Genetic control of the CD4/CD8 T-cell ratio in humans. *Nature Medicine*, **1** (12), 1279-1283.

Andersen, C. L., Jensen, J. L. and Ørntoft, T. F. (2004). Normalization of real-time quantitative reverse transcription-PCR data: A model-based variance estimation approach to identify genes suited for normalization, applied to bladder and colon cancer data sets. *Cancer Research*, **64** (15), 5245-5250.

- Anderson, M. S., Venanzi, E. S., Klein, L., Chen, Z., Berzins, S. P., Turley, S. J., von Boehmer, H., Bronson, R., Dierich, A. and Benoist, C. (2002). Projection of an immunological self shadow within the thymus by the aire protein. *Science*, **298** (5597), 1395-1401.
- Antel, J. and Bar-Or, A. (2006). Roles of immunoglobulins and B cells in multiple sclerosis: From pathogenesis to treatment. *Journal of Neuroimmunology*, **180** (1-2), 3-8.
- Anzilotti, C., Pratesi, F., Tommasi, C. and Migliorini, P. (2010). Peptidylarginine deiminase 4 and citrullination in health and disease. *Autoimmunity Reviews*, **9** (3), 158-160.
- Aravalli, R. N., Peterson, P. K. and Lokensgard, J. R. (2007). Toll-like receptors in defense and damage of the central nervous system. *Journal of Neuroimmune Pharmacology*, **2** (4), 297-312.
- Arita, K., Hashimoto, H., Shimizu, T., Nakashima, K., Yamada, M. and Sato, M. (2004). Structural basis for Ca²⁺-induced activation of human PAD4. *Nature Structural & Molecular Biology*, **11** (8), 777-783.
- Arita, K., Hashimoto, H., Shimizu, T., Yamada, M. and Sato, M. (2003). Crystallization and preliminary X-ray crystallographic analysis of human peptidylarginine deiminase V. *Acta Crystallographica Section D: Biological Crystallography*, **59** (12), 2332-2333.
- Arnold, B., Schönrich, G. and Hämmerling, G. J. (1993). Multiple levels of peripheral tolerance. *Immunology Today*, **14** (1), 12-14.
- Aronica, E., Yankaya, B., Jansen, G. H., Leenstra, S., Van Veelen, C. W. M., Gorter, J. A. and Troost, D. (2001). Ionotropic and metabotropic glutamate receptor protein expression in glioneuronal tumours from patients with intractable epilepsy. *Neuropathology and Applied Neurobiology*, **27** (3), 223-237.
- Asaga, H., Akiyama, K., Ohsawa, T. and Ishigami, A. (2002). Increased and type II-specific expression of peptidylarginine deiminase in activated microglia but not hyperplastic astrocytes following kainic acid-evoked neurodegeneration in the rat brain. *Neuroscience Letters*, **326** (2), 129-132.
- Asaga, H. and Ishigami, A. (2000). Protein deimination in the rat brain: Generation of citrulline-containing proteins in cerebrum perfused with oxygen-deprived media. *Biomedical Research-Tokyo*, **21** (4), 197-206.
- Asaga, H. and Ishigami, A. (2007). Microglial expression of peptidylarginine deiminase 2 in the prenatal rat brain. *Cellular & Molecular Biology Letters*, **12** (4), 536-544.
- Asaga, H., Nakashima, K., Senshu, T., Ishigami, A. and Yamada, M. (2001). Immunocytochemical localization of peptidylarginine deiminase in human eosinophils and neutrophils. *Journal of Leukocyte Biology*, **70** (1), 46-51.
- Asaga, H. and Senshu, T. (1993). Combined biochemical and immunocytochemical analyses of postmortem protein deimination in the rat spinal cord. *Cell Biology International*, **17** (5), 525-532.

Asaga, H., Yamada, M. and Senshu, T. (1998). Selective deimination of vimentin in calcium ionophore-induced apoptosis of mouse peritoneal macrophages. *Biochemical and Biophysical Research Communications*, **243** (3), 641-646.

Aschner, M. (2000). Neuron-astrocyte interactions: Implications for cellular energetics and antioxidant levels. *Neurotoxicology*, **21** (6), 1101.

Aschner, M., Allen, J., Kimelberg, H., LoPachin, R. and Streit, W. (1999). Glial cells in neurotoxicity development. *Annual Review of Pharmacology and Toxicology*, **39** (1), 151-173.

Asseman, C., Mauze, S., Leach, M. W., Coffman, R. L. and Powrie, F. (1999). An essential role for interleukin 10 in the function of regulatory T cells that inhibit intestinal inflammation. *The Journal of Experimental Medicine*, **190** (7), 995-1004.

Aulchenko, Y. S., Hoppenbrouwers, I. A., Ramagopalan, S. V., Broer, L., Jafari, N., Hillert, J., Link, J., Lundström, W., Greiner, E. and Sadovnick, A. D. (2008). Genetic variation in the KIF1B locus influences susceptibility to multiple sclerosis. *Nature Genetics*, **40** (12), 1402-1403.

Avery, D. T., Ellyard, J. I., Mackay, F., Corcoran, L. M., Hodgkin, P. D. and Tangye, S. G. (2005). Increased expression of CD27 on activated human memory B cells correlates with their commitment to the plasma cell lineage. *The Journal of Immunology*, **174** (7), 4034-4042.

Babbe, H., Roers, A., Waisman, A., Lassmann, H., Goebels, N., Hohlfeld, R., Friese, M., Schröder, R., Deckert, M. and Schmidt, S. (2000). Clonal expansions of CD8 T cells dominate the T cell infiltrate in active multiple sclerosis lesions as shown by micromanipulation and single cell polymerase chain reaction. *The Journal of Experimental Medicine*, **192** (3), 393-404.

Baccarelli, A., Wright, R. O., Bollati, V., Tarantini, L., Litonjua, A. A., Suh, H. H., Zanobetti, A., Sparrow, D., Vokonas, P. S. and Schwartz, J. (2009). Rapid DNA methylation changes after exposure to traffic particles. *American Journal of Respiratory and Critical Care Medicine*, **179** (7), 572-578.

Bach, J. F. (2002). The effect of infections on susceptibility to autoimmune and allergic diseases. *New England Journal of Medicine*, **347** (12), 911-920.

Bak, L. K., Schousboe, A. and Waagepetersen, H. S. (2006). The glutamate/GABA-glutamine cycle: Aspects of transport, neurotransmitter homeostasis and ammonia transfer. *Journal of Neurochemistry*, **98** (3), 641-653.

Balabanov, R. and Dore-Duffy, P. (1998). Role of the CNS microvascular pericyte in the blood-brain barrier. *Journal of Neuroscience Research*, **53** (6), 637-644.

Balato, A., Unutmaz, D. and Gaspari, A. A. (2009). Natural killer T cells: An unconventional T-cell subset with diverse effector and regulatory functions. *Journal of Investigative Dermatology*, **129** (7), 1628-1642.

Ballabh, P., Braun, A. and Nedergaard, M. (2004). The blood-brain barrier: An overview: Structure, regulation, and clinical implications. *Neurobiology of Disease*, **16** (1), 1-13.

Ballestar, E. (2010). Epigenetics lessons from twins: Prospects for autoimmune disease. *Clinical Reviews in Allergy and Immunology*, **39** (1), 30-41.

Banchereau, J. and Steinman, R. M. (1998). Dendritic cells and the control of immunity. *Nature*, **392** (6673), 245-252.

Bancroft, J. D. and Gamble, M. (2008). *Theory and practice of histological techniques*. 6th ed., China, Churchill Livingstone.

Banwell, B., Ghezzi, A., Bar-Or, A., Mikaeloff, Y. and Tardieu, M. (2007). Multiple sclerosis in children: Clinical diagnosis, therapeutic strategies, and future directions. *Lancet Neurology*, **6** (10), 887-902.

Baranzini, S. E., Jeong, M. C., Butunoi, C., Murray, R. S., Bernard, C. C. A. and Oksenberg, J. R. (1999). B cell repertoire diversity and clonal expansion in multiple sclerosis brain lesions. *The Journal of Immunology*, **163** (9), 5133-5144.

Barcellos, L. F., Sawcer, S., Ramsay, P. P., Baranzini, S. E., Thomson, G., Briggs, F., Cree, B. C. A., Begovich, A. B., Villoslada, P. and Montalban, X. (2006). Heterogeneity at the HLA-DRB1 locus and risk for multiple sclerosis. *Human Molecular Genetics*, **15** (18), 2813-2824.

Barnett, M., Williams, D., Day, S., Macaskill, P. and McLeod, J. (2003). Progressive increase in incidence and prevalence of multiple sclerosis in newcastle, australia: A 35-year study. *Journal of the Neurological Sciences*, **213** (1-2), 1-6.

Barrett, J. C., Clayton, D. G., Concannon, P., Akolkar, B., Cooper, J. D., Erlich, H. A., Julier, C., Morahan, G., Nerup, J. and Nierras, C. (2009). Genome-wide association study and meta-analysis find that over 40 loci affect risk of type 1 diabetes. *Nature Genetics*, **41** (6), 703-707.

Batista, F. D. and Harwood, N. E. (2009). The who, how and where of antigen presentation to B cells. *Nature Reviews Immunology*, **9** (1), 15-27.

Bauer, J., Berkenbosch, F., Van Dam, A. M. and Dijkstra, C. D. (1993). Demonstration of interleukin-1 [beta] in lewis rat brain during experimental allergic encephalomyelitis by immunocytochemistry at the light and ultrastructural level. *Journal of Neuroimmunology*, **48** (1), 13-21.

Bauer, U. M., Daujat, S., Nielsen, S. J., Nightingale, K. and Kouzarides, T. (2002). Methylation at arginine 17 of histone H3 is linked to gene activation. *EMBO reports*, **3** (1), 39-44.

Beck, J., Rondot, P., Catinot, L., Falcoff, E., Kirchner, H. and Wietzerbin, J. (1988). Increased production of interferon gamma and tumor necrosis factor precedes clinical manifestation in multiple sclerosis: Do cytokines trigger off exacerbations? *Acta Neurologica Scandinavica*, **78** (4), 318-323.

Begley, D. J. and Brightman, M. W. (2003). Structural and functional aspects of the blood-brain barrier. *Progress in Drug Research*, **61** , 39-78.

Begolka, W. S. and Miller, S. (1998). Cytokines as intrinsic and exogenous regulators of pathogenesis in experimental autoimmune encephalomyelitis: Immunoregulation of experimental autoimmune encephalomyelitis. *Research in Immunology*, **149** (9), 771-781.

Belz, G. T., Heath, W. R. and Carbone, F. R. (2002). The role of dendritic cell subsets in selection between tolerance and immunity. *Immunology and Cell Biology*, **80** (5), 463-468.

Bengtsson, A., Rylander, L., Hagmar, L., Nived, O. and Sturfelt, G. (2002). Risk factors for developing systemic lupus erythematosus: A case-control study in southern Sweden. *Rheumatology*, **41** (5), 563-571.

Beniac, D. R., Wood, D. D., Palaniyar, N., Ottensmeyer, F. P., Moscarello, M. A. and Harauz, G. (2000). Cryoelectron microscopy of protein-lipid complexes of human myelin basic protein charge isomers differing in degree of citrullination. *Journal of Structural Biology*, **129** (1), 80-95.

Bennett, C. L., Christie, J., Ramsdell, F., Brunkow, M. E., Ferguson, P. J., Whitesell, L., Kelly, T. E., Saulsbury, F. T., Chance, P. F. and Ochs, H. D. (2001). The immune dysregulation, polyendocrinopathy, enteropathy, X-linked syndrome (IPEX) is caused by mutations of FOXP3. *Nature Genetics*, **27** (1), 20-21.

Benveniste, E. N. (1997). Cytokines: Influence on glial cell gene expression and function. *Chemical Immunology*, **69**, 31-75.

Berg, J. M., Tymoczko, J. L. and Stryer, L. (2002). *Biochemistry*. 5th ed., New York, W. H. Freeman.

Berger, A. (2000). Science commentary: Th1 and Th2 responses: What are they? *BMJ: British Medical Journal*, **321** (7258), 424.

Berger, T. and Reindl, M. (2007). Multiple sclerosis: Disease biomarkers as indicated by pathophysiology. *Journal of the Neurological Sciences*, **259** (1-2), 21-26.

Bertrams, J., Kuwert, E. and Liedtke, U. (1972). HL-A antigens and multiple sclerosis. *Tissue Antigens*, **2** (5), 405-408.

Bessis, A., Béchade, C., Bernard, D. and Roumier, A. (2006). Microglial control of neuronal death and synaptic properties. *Glia*, **55** (3), 233-238.

Bettelli, E., Korn, T. and Kuchroo, V. K. (2007). Th17: The third member of the effector T cell trilogy. *Current Opinion in Immunology*, **19** (6), 652-657.

Bhattacharya, S. K., Bhat, M. B. and Takahara, H. (2006a). Modulation of peptidyl arginine deiminase 2 and implication for neurodegeneration. *Current Eye Research*, **31** (12), 1063-1071.

Bhattacharya, S. K., Crabb, J. S., Bonilha, V. L., Gu, X., Takahara, H. and Crabb, J. W. (2006b). Proteomics implicates peptidyl arginine deiminase 2 and optic nerve citrullination in glaucoma pathogenesis. *Investigative Ophthalmology & Visual Science*, **47** (6), 2508-2514.

Bianchi, M. E. (2007). DAMPs, PAMPs and alarmins: All we need to know about danger. *Journal of Leukocyte Biology*, **81** (1), 1-5.

Bielekova, B., Goodwin, B., Richert, N., Cortese, I., Kondo, T., Afshar, G., Gran, B., Eaton, J., Antel, J. and Frank, J. A. (2000). Encephalitogenic potential of the myelin basic protein peptide (amino acids 83-99) in multiple sclerosis: Results of a phase II clinical trial with an altered peptide ligand. *Nature Medicine*, **6** (10), 1167-1175.

- Bielig, H., Rompikuntal, P., Dongre, M., Zurek, B., Lindmark, B., Ramstedt, M., Wai, S. and Kufer, T. (2011). NOD-like receptor activation by outer membrane vesicles from vibrio cholerae non-O1 non-O139 strains is modulated by the quorum-sensing regulator HapR. *Infection and Immunity*, **79** (4), 1418-1427.
- Bignami, A., Eng, L. F., Dahl, D. and Uyeda, C. T. (1972). Localization of the glial fibrillary acidic protein in astrocytes by immunofluorescence. *Brain Research*, **43** (2), 429-435.
- Bird, A. (2002). DNA methylation patterns and epigenetic memory. *Genes & Development*, **16** (1), 6-21.
- Bjorkman, P. J. (1997). MHC restriction in three dimensions: A view of T cell receptor/ligand interactions. *Cell*, **89** (2), 167-170.
- Blank, M., Barzilai, O. and Shoenfeld, Y. (2007). Molecular mimicry and auto-immunity. *Clinical Reviews in Allergy and Immunology*, **32** (1), 111-118.
- Bö, L., Dawson, T. M., Wesselingh, S., Möurk, S., Choi, S., Kong, P. A., Hanley, D. and Trapp, B. D. (1994). Induction of nitric oxide synthase in demyelinating regions of multiple sclerosis brains. *Annals of Neurology*, **36** (5), 778-786.
- Bö, L., Geurts, J., Mörk, S. and Valk, P. (2006). Grey matter pathology in multiple sclerosis. *Acta Neurologica Scandinavica*, **113**, 48-50.
- Bo, L., Mork, S., Kong, P. A., Nyland, H., Pardo, C. A. and Trapp, B. D. (1994). Detection of MHC class II-antigens on macrophages and microglia, but not on astrocytes and endothelia in active multiple sclerosis lesions. *Journal of Neuroimmunology*, **51** (2), 135-146.
- Bodansky, H., Staines, A., Stephenson, C., Haigh, D. and Cartwright, R. (1992). Evidence for an environmental effect in the aetiology of insulin dependent diabetes in a transmigratory population. *British Medical Journal*, **304** (6833), 1020-1022.
- Bodil Roth, E., Theander, E., Londos, E., Sandberg-Wollheim, M., Larsson, A., Sjöberg, K. and Stenberg, P. (2008). Pathogenesis of autoimmune diseases: Antibodies against transglutaminase, peptidylarginine deiminase and protein-bound citrulline in primary sjögren's syndrome, multiple sclerosis and alzheimer's disease. *Scandinavian Journal of Immunology*, **67** (6), 626-631.
- Boehmer, H., Kisielow, P., Kishi, H., Scott, B., Borgulya, P. and Teh, H. S. (1989). The expression of CD4 and CD8 accessory molecules on mature T cells is not random but correlates with the specificity of the $\alpha\beta$ receptor for antigen. *Immunological Reviews*, **109** (1), 143-152.
- Boggs, J. (2006). Myelin basic protein: A multifunctional protein. *Cellular and Molecular Life Sciences*, **63** (17), 1945-1961.
- Boggs, J. M., Rangaraj, G., Koshy, K. M., Ackerley, C., Wood, D. D. and Moscarello, M. A. (1999). Highly deiminated isoform of myelin basic protein from multiple sclerosis brain causes fragmentation of lipid vesicles. *Journal of Neuroscience Research*, **57** (4), 529-535.

Borchers, A. T., Naguwa, S. M., Shoenfeld, Y. and Gershwin, M. E. (2010). The geoepidemiology of systemic lupus erythematosus. *Autoimmunity Reviews*, **9** (5), A277-A287.

Bottini, N., Vang, T., Cucca, F. and Mustelin, T. (2006). Role of PTPN22 in type 1 diabetes and other autoimmune diseases. In: *Seminars in Immunology*, Elsevier, 207-213.

Boven, L. A., Van Meurs, M., Van Zwam, M., Wierenga-Wolf, A., Hintzen, R. Q., Boot, R. G., Aerts, J. M., Amor, S., Nieuwenhuis, E. E. and Laman, J. D. (2006). Myelin-laden macrophages are anti-inflammatory, consistent with foam cells in multiple sclerosis. *Brain*, **129** (2), 517-526.

Boyle, E. and McGeer, P. (1990). Cellular immune response in multiple sclerosis plaques. *The American Journal of Pathology*, **137** (3), 575-584.

Bradford, C., Cross, A., Haddock, G. and Woodroffe, M. (2009). Citrullination in MS: Potential for a new diagnostic test. *British Journal of Neuroscience Nursing*, **5** (1), 1-13.

Brady, G. W., Murthy, N. S., Fein, D. B., Wood, D. and Moscarello, M. (1981). The effect of basic myelin protein on multilayer membrane formation. *Biophysical Journal*, **34** (2), 345-350.

Breij, E. C. W., Brink, B. P., Veerhuis, R., Van Den Berg, C., Vloet, R., Yan, R., Dijkstra, C. D., Van Der Valk, P. and Bö, L. (2008). Homogeneity of active demyelinating lesions in established multiple sclerosis. *Annals of Neurology*, **63** (1), 16-25.

Brennan, K. M., Galban-Horcajo, F., Rinaldi, S., O'Leary, C. P., Goodyear, C. S., Kalna, G., Arthur, A., Elliot, C., Barnett, S. and Linington, C. (2011). Lipid arrays identify myelin-derived lipids and lipid complexes as prominent targets for oligoclonal band antibodies in multiple sclerosis. *Journal of Neuroimmunology*, **238** (1-2), 87-95.

Breton, C. V., Salam, M. T., Vora, H., Gauderman, W. J. and Gilliland, F. D. (2011). Genetic variation in the glutathione synthesis pathway, air pollution, and children's lung function growth. *American Journal of Respiratory and Critical Care Medicine*, **183** (2), 243-248.

Brilot, F., Dale, R. C., Selter, R. C., Grummel, V., Reddy Kalluri, S., Aslam, M., Busch, V., Zhou, D., Cepok, S. and Hemmer, B. (2009). Antibodies to native myelin oligodendrocyte glycoprotein in children with inflammatory demyelinating central nervous system disease. *Annals of Neurology*, **66** (6), 833-842.

Broadley, S., Deans, J., Sawcer, S., Clayton, D. and Compston, D. (2000). Autoimmune disease in first-degree relatives of patients with multiple sclerosis. *Brain*, **123** (6), 1102-1111.

Brown, A. M. and Ransom, B. R. (2007). Astrocyte glycogen and brain energy metabolism. *Glia*, **55** (12), 1263-1271.

Brown, P., Davies, S., Speake, T. and Millar, I. (2004). Molecular mechanisms of cerebrospinal fluid production. *Neuroscience*, **129** (4), 955-968.

Brownell, B. and Hughes, J. T. (1962). The distribution of plaques in the cerebrum in multiple sclerosis. *Journal of Neurology, Neurosurgery & Psychiatry*, **25** (4), 315-320.

Brück, W., Porada, P., Poser, S., Rieckmann, P., Hanefeld, F., Kretzschmarch, H. A. and Lassmann, H. (1995). Monocyte/macrophage differentiation in early multiple sclerosis lesions. *Annals of Neurology*, **38** (5), 788-796.

Brück, W., Schmied, M., Suchanek, G., Brück, Y., Breitschopf, H., Poser, S., Piddlesden, S. and Lassmann, H. (1994). Oligodendrocytes in the early course of multiple sclerosis. *Annals of Neurology*, **35** (1), 65-73.

Brunner, C., Lassmann, H., Waehneltd, T. V., Matthieu, J. M. and Lington, C. (1989). Differential ultrastructural localization of myelin basic protein, myelin/oligodendroglial glycoprotein, and 2',3'-cyclic nucleotide 3'-phosphodiesterase in the CNS of adult rats. *Journal of Neurochemistry*, **52** (1), 296-304.

Burnet, F. M. (1976). A modification of jerne's theory of antibody production using the concept of clonal selection. *CA: A Cancer Journal for Clinicians*, **26** (2), 119-121.

Bustin, S. and Mueller, R. (2005). Real-time reverse transcription PCR (qRT-PCR) and its potential use in clinical diagnosis. *Clinical Science*, **109** , 365-379.

Bustin, S., Benes, V., Nolan, T. and Pfaffl, M. (2005). Quantitative real-time RT-PCR—a perspective. *Journal of Molecular Endocrinology*, **34** (3), 597-601.

Cafferty, W. B. J., Yang, S. H., Duffy, P. J., Li, S. and Strittmatter, S. M. (2007). Functional axonal regeneration through astrocytic scar genetically modified to digest chondroitin sulfate proteoglycans. *The Journal of Neuroscience*, **27** (9), 2176-2185.

Calabrese, R., Zampieri, M., Mechelli, R., Annibaldi, V., Guastafierro, T., Ciccarone, F., Coarelli, G., Umeton, R., Salvetti, M. and Caiafa, P. (2012). Methylation-dependent PAD2 upregulation in multiple sclerosis peripheral blood. *Multiple Sclerosis Journal*, **18** (3), 299-304.

Cammer, W. and Tansey, F. A. (1988). Carbonic anhydrase immunostaining in astrocytes in the rat cerebral cortex. *Journal of Neurochemistry*, **50** (1), 319-322.

Cannella, B. and Raine, C. S. (1995). The adhesion molecule and cytokine profile of multiple sclerosis lesions. *Annals of Neurology*, **37** (4), 424-435.

Cao, L., Goodin, R., Wood, D., Moscarello, M. A. and Whitaker, J. N. (1999). Rapid release and unusual stability of immunodominant peptide 45-89 from citrullinated myelin basic protein. *Biochemistry*, **38** (19), 6157-6163.

Carbajal, K. S., Schaumburg, C., Strieter, R., Kane, J. and Lane, T. E. (2010). Migration of engrafted neural stem cells is mediated by CXCL12 signaling through CXCR4 in a viral model of multiple sclerosis. *Proceedings of the National Academy of Sciences*, **107** (24), 11068.

Carmignoto, G. (2000). Reciprocal communication systems between astrocytes and neurones. *Progress in Neurobiology*, **62** (6), 561-581.

Castagnetta, L. A., Carruba, G., Granata, O. M., Stefano, R., Miele, M., Schmidt, M., Cutolo, M. and Straub, R. H. (2003). Increased estrogen formation and estrogen to androgen ratio in the synovial fluid of patients with rheumatoid arthritis. *The Journal of Rheumatology*, **30** (12), 2597-2605.

Cedar, H. (1988). DNA methylation and gene activity. *Cell*, **53** (1), 3-4.

Cederbom, L., Hall, H. and Ivars, F. (2000). CD4 CD25 regulatory T cells down-regulate co-stimulatory molecules on antigen-presenting cells. *European journal of immunology*, **30** (6), 1538-1543.

Cepok, S., Jacobsen, M., Schock, S., Omer, B., Jaekel, S., Bøddeker, I., Oertel, W. H., Sommer, N. and Hemmer, B. (2001). Patterns of cerebrospinal fluid pathology correlate with disease progression in multiple sclerosis. *Brain*, **124** (11), 2169-2176.

Cepok, S., Rosche, B., Grummel, V., Vogel, F., Zhou, D., Sayn, J., Sommer, N., Hartung, H. P. and Hemmer, B. (2005). Short-lived plasma blasts are the main B cell effector subset during the course of multiple sclerosis. *Brain*, **128** (7), 1667-1676.

Cepok, S., von Geldern, G., Grummel, V., Hochgesand, S., Celik, H., Hartung, H. P. and Hemmer, B. (2006). Accumulation of class switched IgD-IgM-memory B cells in the cerebrospinal fluid during neuroinflammation. *Journal of Neuroimmunology*, **180** (1-2), 33-39.

Cepok, S., Zhou, D., Vogel, F., Rosche, B., Grummel, V., Sommer, N. and Hemmer, B. (2003). The immune response at onset and during recovery from borrelia burgdorferi meningoradiculitis. *Archives of Neurology*, **60** (6), 849-855.

Chang, A., Tourtellotte, W. W., Rudick, R. and Trapp, B. D. (2002). Premyelinating oligodendrocytes in chronic lesions of multiple sclerosis. *New England Journal of Medicine*, **346** (3), 165-173.

Chang, X. and Han, J. (2006). Expression of peptidylarginine deiminase type 4 (PAD4) in various tumors. *Molecular Carcinogenesis*, **45** (3), 183-196.

Chaplin, D. D. (2010). Overview of the immune response. *Journal of Allergy and Clinical Immunology*, **125** (2), S3-S23.

Charo, I. F. and Ransohoff, R. M. (2006). The many roles of chemokines and chemokine receptors in inflammation. *New England Journal of Medicine*, **354** (6), 610-621.

Chavanas, S., Méchin, M. C., Takahara, H., Kawada, A., Nachat, R., Serre, G. and Simon, M. (2004). Comparative analysis of the mouse and human peptidylarginine deiminase gene clusters reveals highly conserved non-coding segments and a new human gene, PADI6. *Gene*, **330**, 19-27.

Chitnis, T. (2007). The role of CD4 T cells in the pathogenesis of multiple sclerosis. *International Review of Neurobiology*, **79**, 43-72.

Claxton, N. S., Fellers, T. J. and Davidson, M. W. (2006). Laser scanning confocal microscopy. *Olympus.Available online at <http://www.olympusconfocal.com/theory/LSCMIntro.pdf>*, .

Compston, A. and Coles, A. (2002). Multiple sclerosis. *Lancet*, **359** (9313), 1221-1231.

Compston, A. and Coles, A. (2008). Multiple sclerosis. *Lancet*, **372**, 1502-1517.

Compston, A. and Confavreux, C. (1998). Distribution of multiple sclerosis. *McAlpine's multiple sclerosis*, 63-100.

- Conchello, J. A. and Lichtman, J. W. (2005). Optical sectioning microscopy. *Nature Methods*, **2** (12), 920-931.
- Cooper, G. S., Wither, J., Bernatsky, S., Claudio, J. O., Clarke, A., Rioux, J. D. and Fortin, P. R. (2010). Occupational and environmental exposures and risk of systemic lupus erythematosus: Silica, sunlight, solvents. *Rheumatology*, **49** (11), 2172-2180.
- Cornell-Bell, A. H., Finkbeiner, S. M., Cooper, M. S. and Smith, S. J. (1990). Glutamate induces calcium waves in cultured astrocytes: Long-range glial signaling. *Science*, **247** (4941), 470-473.
- Correale, J. and Villa, A. (2007). The blood-brain-barrier in multiple sclerosis: Functional roles and therapeutic targeting. *Autoimmunity*, **40** (2), 148-160.
- Corsini, E., Dufour, A., Ciusani, E., Gelati, M., Frigerio, S., Gritti, A., Cajola, L., Mancardi, G., Massa, G. and Salmaggi, A. (1996). Human brain endothelial cells and astrocytes produce IL-1 β but not IL-10. *Scandinavian Journal of Immunology*, **44** (5), 506-511.
- Costenbader, K. H., Chang, S. C., Vivo, I. D., Plenge, R. and Karlson, E. W. (2010). Genetic polymorphisms in PTPN22, PADI-4, and CTLA-4 and risk for rheumatoid arthritis in two longitudinal cohort studies: Evidence of gene-environment interactions with heavy cigarette smoking. *Arthritis Research and Therapy*, **10** (3), 52-63.
- Costenbader, K. H., Gay, S., Riquelme, M. E. A., Iaccarino, L. and Doria, A. (2012). Genes, epigenetic regulation and environmental factors: Which is the most relevant in developing autoimmune diseases? *Autoimmunity Reviews*, **11** (8), 604-609.
- Cottrell, J. S. (2011). Protein identification using MS/MS data. *Journal of Proteomics*, **74** (10), 1842-1851.
- Crawford, M. P., Yan, S. X., Ortega, S. B., Mehta, R. S., Hewitt, R. E., Price, D. A., Stastny, P., Douek, D. C., Koup, R. A. and Racke, M. K. (2004). High prevalence of autoreactive, neuroantigen-specific CD8 T cells in multiple sclerosis revealed by novel flow cytometric assay. *Blood*, **103** (11), 4222-4231.
- Creese, A. J., Grant, M. M., Chapple, I. L. C. and Cooper, H. J. (2011). On-line liquid chromatography neutral loss-triggered electron transfer dissociation mass spectrometry for the targeted analysis of citrullinated peptides. *Analytical Methods*, **3** (2), 259-266.
- Criswell, L. A., Pfeiffer, K. A., Lum, R. F., Gonzales, B., Novitzke, J., Kern, M., Moser, K. L., Begovich, A. B., Carlton, V. E. H. and Li, W. (2005). Analysis of families in the multiple autoimmune disease genetics consortium (MADGC) collection: The PTPN22 620W allele associates with multiple autoimmune phenotypes. *The American Journal of Human Genetics*, **76** (4), 561-571.
- Cross, A. H. and Waubant, E. (2011). MS and the B cell controversy. *Biochimica et Biophysica Acta*, **1812** (2), 231-238.
- Cserr, H., Cooper, D., Suri, P. and Patlak, C. (1981). Efflux of radiolabeled polyethylene glycols and albumin from rat brain. *American Journal of Physiology-Renal Physiology*, **240** (4), F319-F328.

Cuthbert, G. L., Daujat, S., Snowden, A. W., Erdjument-Bromage, H., Hagiwara, T., Yamada, M., Schneider, R., Gregory, P. D., Tempst, P. and Bannister, A. J. (2004). Histone deimination antagonizes arginine methylation. *Cell*, **118** (5), 545-553.

Cutolo, M., Sulli, A., Capellino, S., Villaggio, B., Montagna, P., Seriolo, B. and Straub, R. (2004). Sex hormones influence on the immune system: Basic and clinical aspects in autoimmunity. *Lupus*, **13** (9), 635-638.

Cuzner, M. L. and Davison, A. N. (1973). Changes in cerebral lysosomal enzyme activity and lipids in multiple sclerosis. *Journal of the Neurological Sciences*, **19** (1), 29-36.

D'Souza, C. A. and Moscarello, M. A. (2006). Differences in susceptibility of MBP charge isomers to digestion by stromelysin-1 (MMP-3) and release of an immunodominant epitope. *Neurochemical Research*, **31** (8), 1045-1054.

Davalos, D., Grutzendler, J., Yang, G., Kim, J. V., Zuo, Y., Jung, S., Littman, D. R., Dustin, M. L. and Gan, W. B. (2005). ATP mediates rapid microglial response to local brain injury in vivo. *Nature Neuroscience*, **8** (6), 752-758.

De Ceuleneer, M., De Wit, V., Van Steendam, K., Van Nieuwerburgh, F., Tilleman, K. and Deforce, D. (2011). Modification of citrulline residues with 2, 3-butanedione facilitates their detection by liquid chromatography/mass spectrometry. *Rapid Communications in Mass Spectrometry*, **25** (11), 1536-1542.

De Ceuleneer, M., Van Steendam, K., Dhaenens, M. and Deforce, D. (2012). In vivo relevance of citrullinated proteins and the challenges in their detection. *Proteomics*, **12** (6), 752-760.

De Seze, J., Dubucquoi, S., Lefranc, D., Virecoulon, F., Nuez, I., Dutoit, V., Vermersch, P. and Prin, L. (2001). IgG reactivity against citrullinated myelin basic protein in multiple sclerosis. *Journal of Neuroimmunology*, **117** (1-2), 149-155.

Dean, G., Yeo, T., Goris, A., Taylor, C., Goodman, R., Elian, M., Galea-Debono, A., Aquilina, A., Felice, A. and Vella, M. (2008). HLA-DRB1 and multiple sclerosis in Malta. *Neurology*, **70** (2), 101-105.

Delves, P., Martin, S., Burton, D. and Roitt, I. (2006). *Roitt's essential immunology*. 11th ed., Oxford, Blackwell Publishing Ltd.

Desai, B. S., Monahan, A. J., Carvey, P. M. and Hendey, B. (2007). Bloodbrain barrier pathology in alzheimer's and parkinson's disease: Implications for drug therapy. *Cell Transplantation*, **16** (3), 285-299.

Detels, R., Brody, J. A. and Edgar, A. H. (1972). Multiple sclerosis among american, japanese and chinese migrants to california and washington. *Journal of Chronic Diseases*, **25** (1), 3-10.

Didier, M., Harandi, M., Aguera, M., Bancel, B., Tardy, M., Fages, C., Calas, A., Stagaard, M., Møllgård, K. and Belin, M. (1986). Differential immunocytochemical staining for glial fibrillary acidic (GFA) protein, S-100 protein and glutamine synthetase in the rat subcommissural organ, nonspecialized ventricular ependyma and adjacent neuropil. *Cell and Tissue Research*, **245** (2), 343-351.

Dolman, D., Drndarski, S., Abbott, N. J. and Rattray, M. (2005). Induction of aquaporin 1 but not aquaporin 4 messenger RNA in rat primary brain microvessel endothelial cells in culture. *Journal of Neurochemistry*, **93** (4), 825-833.

Dong, S., Kojima, T., Shiraiwa, M., Méchin, M. C., Chavanas, S., Serre, G., Simon, M., Kawada, A. and Takahara, H. (2005). Regulation of the expression of peptidylarginine deiminase type II gene (PADI2) in human keratinocytes involves Sp1 and Sp3 transcription factors. *Journal of Investigative Dermatology*, **124** (5), 1026-1033.

Dong, S., Ying, S., Kojima, T., Shiraiwa, M., Kawada, A., Méchin, M. C., Adoue, V., Chavanas, S., Serre, G. and Simon, M. (2007). Crucial roles of MZF1 and Sp1 in the transcriptional regulation of the peptidylarginine deiminase type I gene (PADI1) in human keratinocytes. *Journal of Investigative Dermatology*, **128** (3), 549-557.

Dorow, D., Shi, P., Carbone, F., Minasian, E., Todd, P. and Leach, S. (1985). Two large immunogenic and antigenic myoglobin peptides and the effects of cyclisation. *Molecular Immunology*, **22** (11), 1255-1264.

Dunkelberger, J. R. and Song, W. C. (2009). Complement and its role in innate and adaptive immune responses. *Cell Research*, **20** (1), 34-50.

Ebers, G. C., Koopman, W. J., Hader, W., Sadovnick, A. D., Kremenchutzky, M., Mandalfino, P., Wingerchuk, D. M., Baskerville, J. and Rice, G. P. A. (2000). The natural history of multiple sclerosis: A geographically based study. *Brain*, **123** (3), 641-649.

Ebers, G. C., Sadovnick, A. D. and Risch, N. J. (1995). A genetic basis for familial aggregation in multiple sclerosis. *Nature*, **377** , 150-151.

Eddleston, M. and Mucke, L. (1993). Molecular profile of reactive astrocytes—implications for their role in neurologic disease. *Neuroscience*, **54** (1), 15-36.

Edgar, J. M., McLaughlin, M., Yool, D., Zhang, S. C., Fowler, J. H., Montague, P., Barrie, J. A., McCulloch, M. C., Duncan, I. D. and Garbern, J. (2004). Oligodendroglial modulation of fast axonal transport in a mouse model of hereditary spastic paraplegia. *The Journal of Cell Biology*, **166** (1), 121-131.

Egerton, M., Scollay, R. and Shortman, K. (1990). Kinetics of mature T-cell development in the thymus. *Proceedings of the National Academy of Sciences*, **87** (7), 2579-2582.

Einstein, E. R., Csejtey, J., Dalal, K. B., Adams, C. W. M., Bayliss, O. B. and Hallpike, J. F. (1972). Proteolytic activity and basic protein loss in and around multiple sclerosis plaques: Combined biochemical and histochemical observations. *Journal of Neurochemistry*, **19** (3), 653-662.

El-Aneed, A., Cohen, A. and Banoub, J. (2009). Mass spectrometry, review of the basics: Electrospray, MALDI, and commonly used mass analyzers. *Applied Spectroscopy Reviews*, **44** (3), 210-230.

Ellmerich, S., Mycko, M., Takacs, K., Waldner, H., Wahid, F. N., Boyton, R. J., King, R. H. M., Smith, P. A., Amor, S. and Herlihy, A. H. (2005). High incidence of spontaneous disease in an HLA-DR15 and TCR transgenic multiple sclerosis model. *The Journal of Immunology*, **174** (4), 1938-1946.

Eng, L. F. (1985). Glial fibrillary acidic protein (GFAP): The major protein of glial intermediate filaments in differentiated astrocytes. *Journal of Neuroimmunology*, **8**, 203-214.

Engelhardt, B. (2006). Molecular mechanisms involved in T cell migration across the blood–brain barrier. *Journal of Neural Transmission*, **113** (4), 477-485.

Estévez, A. G., Spear, N., Manuel, S. M., Radi, R., Henderson, C. E., Barbeito, L. and Beckman, J. S. (1998). Nitric oxide and superoxide contribute to motor neuron apoptosis induced by trophic factor deprivation. *The Journal of Neuroscience*, **18** (3), 923-931.

Fairweather, D. L., Frisancho-Kiss, S. and Rose, N. R. (2008). Sex differences in autoimmune disease from a pathological perspective. *The American Journal of Pathology*, **173** (3), 600-609.

Fehling, H. J., Krotkova, A., Saint-Ruf, C. and von Boehmer, H. (1995). Crucial role of the pre-T-cell receptor α gene in development of $\alpha\beta$ but not $\gamma\delta$ T cells. *Nature*, **375**, 795-798.

Fellin, T. (2009). Communication between neurons and astrocytes: Relevance to the modulation of synaptic and network activity. *Journal of Neurochemistry*, **108** (3), 533-544.

Fellin, T. and Carmignoto, G. (2004). Neurone-to-astrocyte signalling in the brain represents a distinct multifunctional unit. *The Journal of Physiology*, **559** (1), 3-15.

Fenstermacher, J., Gross, P., Sposito, N., Acuff, V., Pettersen, S. and Gruber, K. (1988). Structural and functional variations in capillary systems within the brain. *Annals of the New York Academy of Sciences*, **529** (1), 21-30.

Ferguson, B., Matyszak, M. K., Esiri, M. M. and Perry, V. H. (1997). Axonal damage in acute multiple sclerosis lesions. *Brain*, **120** (3), 393-399.

Ferguson, C. J., Lenk, G. M. and Meisler, M. H. (2009). Defective autophagy in neurons and astrocytes from mice deficient in PI (3, 5) P2. *Human Molecular Genetics*, **18** (24), 4868-4878.

Ferrari-Lacraz, S., Sebbag, M., Chicheportiche, R., Foulquier, C., Serre, G. and Dayer, J. M. (2010). Upon contact with stimulated T cells, expression of peptidylarginine deiminase 2 and 4 is upregulated in human monocytes. *Annals of the Rheumatic Diseases*, **69** (Suppl 2), A2.

Fiacco, T. A. and McCarthy, K. D. (2006). Astrocyte calcium elevations: Properties, propagation, and effects on brain signaling. *Glia*, **54** (7), 676-690.

Finckh, A., Cooper, G. S., Chibnik, L. B., Costenbader, K. H., Watts, J., Pankey, H., Fraser, P. A. and Karlson, E. W. (2006). Occupational silica and solvent exposures and risk of systemic lupus erythematosus in urban women. *Arthritis & Rheumatism*, **54** (11), 3648-3654.

Fitch, M. T. and Silver, J. (1997). Glial cell extracellular matrix: Boundaries for axon growth in development and regeneration. *Cell and Tissue Research*, **290** (2), 379-384.

Fogdell, A., Hillert, J., Sachs, C. and Olerup, O. (1995). The multiple sclerosis-and narcolepsy-associated HLA class II haplotype includes the DRB5^{A*} 0101 allele. *Tissue Antigens*, **46** (4), 333-336.

Förster, C. (2008). Tight junctions and the modulation of barrier function in disease. *Histochemistry and Cell Biology*, **130** (1), 55-70.

Fraga, M. F., Ballestar, E., Paz, M. F., Ropero, S., Setien, F., Ballestar, M. L., Heine-Suñer, D., Cigudosa, J. C., Urioste, M. and Benitez, J. (2005). Epigenetic differences arise during the lifetime of monozygotic twins. *Proceedings of the National Academy of Sciences of the United States of America*, **102** (30), 10604-10609.

Francis, K., van Beek, J., Canova, C., Neal, J. W. and Gasque, P. (2003). Innate immunity and brain inflammation: The key role of complement. *Expert Reviews in Molecular Medicine*, **2** (1), 1-19.

Franke, A., McGovern, D. P. B., Barrett, J. C., Wang, K., Radford-Smith, G. L., Ahmad, T., Lees, C. W., Balschun, T., Lee, J. and Roberts, R. (2010). Genome-wide meta-analysis increases to 71 the number of confirmed crohn's disease susceptibility loci. *Nature Genetics*, **42** (12), 1118-1125.

Freedman, D. M., Dosemeci, M. and Alavanja, M. C. R. (2000). Mortality from multiple sclerosis and exposure to residential and occupational solar radiation: A case-control study based on death certificates. *Occupational and Environmental Medicine*, **57** (6), 418-421.

Friese, M. A. and Fugger, L. (2009). Pathogenic CD8 T cells in multiple sclerosis. *Annals of Neurology*, **66** (2), 132-141.

Frischer, J. M., Bramow, S., Dal-Bianco, A., Lucchinetti, C. F., Rauschka, H., Schmidbauer, M., Laursen, H., Sorensen, P. S. and Lassmann, H. (2009). The relation between inflammation and neurodegeneration in multiple sclerosis brains. *Brain*, **132** (5), 1175-1189.

Frisullo, G., Nociti, V., Iorio, R., Patanella, A. K., Marti, A., Caggiula, M., Mirabella, M., Tonali, P. A. and Batocchi, A. P. (2008). IL17 and IFN [gamma] production by peripheral blood mononuclear cells from clinically isolated syndrome to secondary progressive multiple sclerosis. *Cytokine*, **44** (1), 22-25.

Frohman, E. M., Racke, M. K. and Raine, C. S. (2006). Multiple sclerosis--the plaque and its pathogenesis. *New England Journal of Medicine*, **354** (9), 942-955.

Gallucci, S., Lolkema, M. and Matzinger, P. (1999). Natural adjuvants: Endogenous activators of dendritic cells. *Nature Medicine*, **5** (11), 1249-1255.

Gandhi, R., Laroni, A. and Weiner, H. L. (2010). Role of the innate immune system in the pathogenesis of multiple sclerosis. *Journal of Neuroimmunology*, **221** (1), 7-14.

Gardiner-Garden, M. and Frommer, M. (1987). CpG islands in vertebrate genomes. *Journal of Molecular Biology*, **196** (2), 261-282.

Genain, C. P., Cannella, B., Hauser, S. L. and Raine, C. S. (1999). Identification of autoantibodies associated with myelin damage in multiple sclerosis. *Nature Medicine*, **5** (2), 170-175.

Gerem, B. B. and Raskind, J. (1953). Development of the fine structure of the myelin sheath in sciatic nerves of chick embryos. *Proceedings of the National Academy of Sciences of the United States of America*, **39** (8), 880-884.

Geurts, J. J. G., Bö, L., Pouwels, P. J. W., Castelijns, J. A., Polman, C. H. and Barkhof, F. (2005). Cortical lesions in multiple sclerosis: Combined postmortem MR imaging and histopathology. *American Journal of Neuroradiology*, **26** (3), 572-577.

Ghodke, Y., Joshi, K., Chopra, A. and Patwardhan, B. (2005). HLA and disease. *European Journal of Epidemiology*, **20** (6), 475-488.

Gilmore, C. P. (2008). *Spinal cord grey matter pathology in multiple sclerosis*, .

Glezer, I., Simard, A. and Rivest, S. (2007). Neuroprotective role of the innate immune system by microglia. *Neuroscience*, **147** (4), 867-883.

Godfrey, D. I., MacDonald, H. R., Kronenberg, M., Smyth, M. J. and Van Kaer, L. (2004). NKT cells: What's in a name? *Nature Reviews Immunology*, **4** (3), 231-237.

Gold, R., Linington, C. and Lassmann, H. (2006). Understanding pathogenesis and therapy of multiple sclerosis via animal models: 70 years of merits and culprits in experimental autoimmune encephalomyelitis research. *Brain*, **129** (8), 1953-1971.

Goldacre, M. J., Seagroatt, V., Yeates, D. and Acheson, E. D. (2004). Skin cancer in people with multiple sclerosis: A record linkage study. *British Medical Journal*, **58** (2), 142-144.

Goldsby, R., Kindt, T., Osborne, B. and Kuby, J. (2003). *Immunology*. 5th ed., New York, W. H. Freeman.

Gourley, M. and Miller, F. W. (2007). Mechanisms of disease: Environmental factors in the pathogenesis of rheumatic disease. *Nature Clinical Practice Rheumatology*, **3** (3), 172-180.

Graeber, M. B. and Kreutzberg, G. W. (1988). Delayed astrocyte reaction following facial nerve axotomy. *Journal of Neurocytology*, **17** (2), 209-220.

Gray, D., Siepmann, K. and Wohlleben, G. (1994). CD40 ligation in B cell activation, isotype switching and memory development. In: *Seminars in Immunology*, Elsevier, 303-310.

Green, A. and Patterson, C. C. (2001). Trends in the incidence of childhood-onset diabetes in Europe 1989–1998. *Diabetologia*, **44** , 3-8.

Gregersen, P. K. and Olsson, L. M. (2009). Recent advances in the genetics of autoimmune disease. *Annual Review of Immunology*, **27** , 363-391.

Gregersen, P. K., Silver, J. and Winchester, R. J. (2005). The shared epitope hypothesis. An approach to understanding the molecular genetics of susceptibility to rheumatoid arthritis. *Arthritis & Rheumatism*, **30** (11), 1205-1213.

Gregory, P. D., Wagner, K. and Hörz, W. (2001). Histone acetylation and chromatin remodeling. *Experimental Cell Research*, **265** (2), 195-202.

- Grieb, P., Forster, R., Strome, D., Goodwin, C. and Pape, P. (1985). O₂ exchange between blood and brain tissues studied with ¹⁸O₂ indicator-dilution technique. *Journal of Applied Physiology*, **58** (6), 1929-1941.
- Griffiths, I., Klugmann, M., Anderson, T., Yool, D., Thomson, C., Schwab, M. H., Schneider, A., Zimmermann, F., McCulloch, M. and Nadon, N. (1998). Axonal swellings and degeneration in mice lacking the major proteolipid of myelin. *Science*, **280** (5369), 1610-1613.
- Gygi, S. P., Rochon, Y., Franza, B. R. and Aebersold, R. (1999). Correlation between protein and mRNA abundance in yeast. *Molecular and Cellular Biology*, **19** (3), 1720-1730.
- György, B., Tóth, E., Tarcsa, E., Falus, A. and Buzás, E. I. (2006). Citrullination: A posttranslational modification in health and disease. *The International Journal of Biochemistry & Cell Biology*, **38** (10), 1662-1677.
- Hafler, D. A., Compston, A., Sawcer, S., Lander, E. S., Daly, M. J., De Jager, P. L., De Bakker, P., Gabriel, S. B., Mirel, D. B. and Ivinson, A. J. (2007). Risk alleles for multiple sclerosis identified by a genomewide study. *The New England Journal of Medicine*, **357** (9), 851-862.
- Hagiwara, T., Nakashima, K., Hirano, H., Senshu, T. and Yamada, M. (2002). Deimination of arginine residues in nucleophosmin/B23 and histones in HL-60 granulocytes. *Biochemical and Biophysical Research Communications*, **290** (3), 979-983.
- Hammond, S., English, D. and McLeod, J. (2000). The age-range of risk of developing multiple sclerosis evidence from a migrant population in australia. *Brain*, **123** (5), 968-974.
- Harauz, G., Ishiyama, N., Hill, C., Bates, I. R. and Libich, D. S. (2004). Myelin basic protein--diverse conformational states of an intrinsically unstructured protein and its roles in myelin assembly and multiple sclerosis. *Micron*, **35** (7), 503-542.
- Harris, D. P., Haynes, L., Sayles, P. C., Duso, D. K., Eaton, S. M., Lepak, N. M., Johnson, L. L., Swain, S. L. and Lund, F. E. (2000). Reciprocal regulation of polarized cytokine production by effector B and T cells. *Nature Immunology*, **1** (6), 475-482.
- Hashioka, S., Klegeris, A., Schwab, C. and McGeer, P. L. (2009). Interferon- γ -dependent cytotoxic activation of human astrocytes and astrocytoma cells. *Neurobiology of Aging*, **30** (12), 1924-1935.
- Hauser, S. L., Waubant, E., Arnold, D. L., Vollmer, T., Antel, J., Fox, R. J., Bar-Or, A., Panzara, M., Sarkar, N. and Agarwal, S. (2008). B-cell depletion with rituximab in relapsing-remitting multiple sclerosis. *The New England Journal of Medicine*, **358** (7), 676-688.
- Hauser, S., Doolittle, T., Lincoln, R., Brown, R. and Dinarello, C. (1990). Cytokine accumulations in CSF of multiple sclerosis patients. *Neurology*, **40** (11), 1735-1735.
- Haynes, S. E., Hollopeter, G., Yang, G., Kurpius, D., Dailey, M. E., Gan, W. B. and Julius, D. (2006). The P2Y₁₂ receptor regulates microglial activation by extracellular nucleotides. *Nature Neuroscience*, **9** (12), 1512-1519.

Hermansson, M., Artemenko, K., Ossipova, E., Eriksson, H., Lengqvist, J., Makrygiannakis, D., Catrina, A. I., Nicholas, A. P., Klareskog, L. and Savitski, M. (2010). MS analysis of rheumatoid arthritic synovial tissue identifies specific citrullination sites on fibrinogen. *Proteomics-Clinical Applications*, **4** (5), 511-518.

Hickey, W. F. (1999). The pathology of multiple sclerosis: A historical perspective1. *Journal of Neuroimmunology*, **98** (1), 37-44.

Hill, J. A., Southwood, S., Sette, A., Jevnikar, A. M., Bell, D. A. and Cairns, E. (2003). Cutting edge: The conversion of arginine to citrulline allows for a high-affinity peptide interaction with the rheumatoid arthritis-associated HLA-DRB1* 0401 MHC class II molecule. *The Journal of Immunology*, **171** (2), 538-541.

Hirsch, E. C. and Hunot, S. (2009). Neuroinflammation in parkinson's disease: A target for neuroprotection? *Lancet Neurology*, **8** (4), 382-397.

Hofman, F. M., Hinton, D. R., Johnson, K. and Merrill, J. E. (1989). Tumor necrosis factor identified in multiple sclerosis brain. *The Journal of Experimental Medicine*, **170** (2), 607-612.

Hofstetter, H. H., Toyka, K. V. and Gold, R. (2006). Permanent effector phenotype of neuroantigen-specific T cells acquired in the central nervous system during experimental allergic encephalomyelitis. *Neuroscience Letters*, **391** (3), 127-130.

Holmes, J., Madgwick, T. and Bates, D. (1995). The cost of multiple sclerosis. *British Journal of Medical Economics*, **8**, 181-193.

Hopkins, S. J. and Rothwell, N. J. (1995). Cytokines and the nervous system I: Expression and recognition. *Trends in Neurosciences*, **18** (2), 83-88.

Hoppenbrouwers, I. A., Aulchenko, Y. S., Ebers, G. C., Ramagopalan, S. V., Oostra, B. A., van Duijn, C. M. and Hintzen, R. Q. (2008). EVI5 is a risk gene for multiple sclerosis. *Genes and Immunity*, **9** (4), 334-337.

Huang, C. Y., Sleckman, B. P. and Kanagawa, O. (2005). Revision of T cell receptor α chain genes is required for normal T lymphocyte development. *Proceedings of the National Academy of Sciences of the United States of America*, **102** (40), 14356-14361.

Huang, Q. Q. and Pope, R. M. (2010). Toll-like receptor signaling: A potential link among rheumatoid arthritis, systemic lupus, and atherosclerosis. *Journal of Leukocyte Biology*, **88** (2), 253-262.

Hughes, E. G., Maguire, J. L., McMinn, M. T., Scholz, R. E. and Sutherland, M. L. (2004). Loss of glial fibrillary acidic protein results in decreased glutamate transport and inhibition of PKA-induced EAAT2 cell surface trafficking. *Molecular Brain Research*, **124** (2), 114-123.

Illingworth, R. S. and Bird, A. P. (2009). CpG islands—'a rough guide'. *FEBS Letters*, **583** (11), 1713-1720.

Imitola, J., Chitnis, T. and Khoury, S. J. (2005). Cytokines in multiple sclerosis: From bench to bedside. *Pharmacology & Therapeutics*, **106** (2), 163-177.

Inagaki, M., Imakamura, Y., Takeda, M., Nishimura, T. and Inagaki, N. (1994). Glial fibrillary acidic protein: Dynamic property and regulation by phosphorylation. *Brain Pathology*, **4** (3), 239-243.

Irving, B. A., Alt, F. W. and Killeen, N. (1998). Thymocyte development in the absence of pre-T cell receptor extracellular immunoglobulin domains. *Science*, **280** (5365), 905-908.

Ishigami, A. and Maruyama, N. (2010). Importance of research on peptidylarginine deiminase and citrullinated proteins in age-related disease. *Geriatrics & Gerontology International*, **10** (s1), S53-S58.

Ishigami, A., Ohsawa, T., Asaga, H., Akiyama, K., Kuramoto, M. and Maruyama, N. (2002). Human peptidylarginine deiminase type II: Molecular cloning, gene organization, and expression in human skin. *Archives of Biochemistry and Biophysics*, **407** (1), 25-31.

Ishigami, A., Ohsawa, T., Hiratsuka, M., Taguchi, H., Kobayashi, S., Saito, Y., Murayama, S., Asaga, H., Toda, T., Kimura, N. and Maruyama, N. (2005). Abnormal accumulation of citrullinated proteins catalyzed by peptidylarginine deiminase in hippocampal extracts from patients with alzheimer's disease. *Journal of Neuroscience Research*, **80** (1), 120-128.

Israeli, E., Agmon-Levin, N., Blank, M. and Shoenfeld, Y. (2009). Adjuvants and autoimmunity. *Lupus*, **18** (13), 1217-1225.

Issazadeh, S., Mustafa, M., Ljungdahl, Å., Höjeberg, B., Dagerlind, Å., Elde, R. and Olsson, T. (1995). Interferon γ , interleukin 4 and transforming growth factor β in experimental autoimmune encephalomyelitis in lewis rats: Dynamics of cellular mRNA expression in the central nervous system and lymphoid cells. *Journal of Neuroscience Research*, **40** (5), 579-590.

Iwahashi, T., Koh, C. S., Inoue, A. and Yanagisawa, N. (1997). Tumor necrosis factor- α and transforming growth factor- β production by isolated mononuclear cells from the spinal cords of lewis rats with experimental autoimmune encephalomyelitis. *The Tohoku Journal of Experimental Medicine*, **183** (2), 123-133.

Jack, C. S., Arbour, N., Blain, M., Meier, U. C., Prat, A. and Antel, J. P. (2007). Th1 polarization of CD4 T cells by toll-like receptor 3-activated human microglia. *Journal of Neuropathology & Experimental Neurology*, **66** (9), 848-859.

James, E. A., Moustakas, A. K., Bui, J., Papadopoulos, G. K., Bondinas, G., Buckner, J. H. and Kwok, W. W. (2010). HLA-DR1001 presents "altered-self" peptides derived from joint-associated proteins by accepting citrulline in three of its binding pockets. *Arthritis & Rheumatism*, **62** (10), 2909-2918.

Janabi, N., Peudenier, S., Héron, B., Ng, K. H. and Tardieu, M. (1995). Establishment of human microglial cell lines after transfection of primary cultures of embryonic microglial cells with the SV40 large T antigen. *Neuroscience Letters*, **195** (2), 105-108.

Jang, B., Jin, J. K., Jeon, Y. C., Cho, H. J., Ishigami, A., Choi, K. C., Carp, R. I., Maruyama, N., Kim, Y. S. and Choi, E. K. (2010). Involvement of peptidylarginine deiminase-mediated post-translational citrullination in pathogenesis of sporadic creutzfeldt-jakob disease. *Acta Neuropathologica*, **119** (2), 199-210.

- Jang, B., Kim, E., Choi, J. K., Jin, J. K., Kim, J. I., Ishigami, A., Maruyama, N., Carp, R. I., Kim, Y. S. and Choi, E. K. (2008). Accumulation of citrullinated proteins by up-regulated peptidylarginine deiminase 2 in brains of scrapie-infected mice: A possible role in pathogenesis. *The American Journal of Pathology*, **173** (4), 1129-1142.
- Jang, B., Shin, H., Choi, J., Du Phuong, T. N., Jeong, B., Ishigami, A., Maruyama, N., Carp, R., Kim, Y. and Choi, E. (2011). Subcellular localization of peptidylarginine deiminase 2 and citrullinated proteins in brains of scrapie-infected mice: Nuclear localization of PAD2 and membrane fraction-enriched citrullinated proteins. *Journal of Neuropathology and Experimental Neurology*, **70** (2), 116-124.
- Jessen, K. R. (2004). Glial cells. *The international journal of biochemistry & cell biology*, **36** (10), 1861-1867.
- Ji, J. D., Kim, T. H., Lee, B., Na, K. S., Choi, S. J., Lee, Y. H. and Song, G. G. (2011). Integrated analysis of MicroRNA and mRNA expression profiles in rheumatoid arthritis synovial monocytes. *Journal of Rheumatic Diseases*, **18** (4), 253-263.
- Joncker, N. T. and Raulet, D. H. (2008). Regulation of NK cell responsiveness to achieve self-tolerance and maximal responses to diseased target cells. *Immunological Reviews*, **224** (1), 85-97.
- Jørgensen, K. T., Wiik, A., Pedersen, M., Hedegaard, C. J., Vestergaard, B. F., Gislefoss, R. E., Kvien, T. K., Wohlfahrt, J., Bendtzen, K. and Frisch, M. (2008). Cytokines, autoantibodies and viral antibodies in premonitory and postdiagnostic sera from patients with rheumatoid arthritis: Case-control study nested in a cohort of norwegian blood donors. *Annals of the Rheumatic Diseases*, **67** (6), 860-866.
- Joshi, N. S. and Kaech, S. M. (2008). Effector CD8 T cell development: A balancing act between memory cell potential and terminal differentiation. *The Journal of Immunology*, **180** (3), 1309-1315.
- Kabat, E. A., Freedman, D. A., Murray, J. P. and Knaub, V. (1950). A study of the crystalline albumin, gamma globulin and total protein in the cerebrospinal fluid of one hundred cases of multiple sclerosis and in other diseases. *The American Journal of the Medical Sciences*, **219** (1), 55-64.
- Kandel, E. R., Schwartz, J. H. and Jessell, T. M. (2000). *Principles of neural science*. 4th ed., New York, McGraw-Hill Companies.
- Karlson, E. W., Chang, S. C., Cui, J., Chibnik, L. B., Fraser, P. A., De Vivo, I. and Costenbader, K. H. (2010). Gene-environment interaction between HLA-DRB1 shared epitope and heavy cigarette smoking in predicting incident rheumatoid arthritis. *Annals of the Rheumatic Diseases*, **69** (01), 54-60.
- Karni, A., Bakimer-Kleiner, R., Abramsky, O. and Ben-Nun, A. (1999). Elevated levels of antibody to myelin oligodendrocyte glycoprotein is not specific for patients with multiple sclerosis. *Archives of Neurology*, **56** (3), 311-315.
- Karouzakis, E., Gay, R. E., Michel, B. A., Gay, S. and Neidhart, M. (2009). DNA hypomethylation in rheumatoid arthritis synovial fibroblasts. *Arthritis & Rheumatism*, **60** (12), 3613-3622.
- Kassmann, C. M. and Nave, K. A. (2008). Oligodendroglial impact on axonal function and survival-a hypothesis. *Current Opinion in Neurology*, **21** (3), 235-241.

- Kaur, C. and Ling, E. (2008). Blood brain barrier in hypoxic-ischemic conditions. *Current Neurovascular Research*, **5** (1), 71-81.
- Keegan, M., König, F., McClelland, R., Brück, W., Morales, Y., Bitsch, A., Panitch, H., Lassmann, H., Weinshenker, B. and Rodriguez, M. (2005). Relation between humoral pathological changes in multiple sclerosis and response to therapeutic plasma exchange. *The Lancet*, **366** (9485), 579-582.
- Keilhoff, G., Prell, T., Langnaese, K., Mawrin, C., Simon, M., Fansa, H. and Nicholas, A. P. (2008). Expression pattern of peptidylarginine deiminase in rat and human schwann cells. *Developmental Neurobiology*, **68** (1), 101-114.
- Kennedy, A. D. and DeLeo, F. R. (2009). Neutrophil apoptosis and the resolution of infection. *Immunologic Research*, **43** (1), 25-61.
- Kennedy, M. K., Torrance, D. S., Picha, K. S. and Mohler, K. M. (1992). Analysis of cytokine mRNA expression in the central nervous system of mice with experimental autoimmune encephalomyelitis reveals that IL-10 mRNA expression correlates with recovery. *The Journal of Immunology*, **149** (7), 2496-2505.
- Kepp, O., Galluzzi, L. and Kroemer, G. (2011). Mitochondrial control of the NLRP3 inflammasome. *Nature Immunology*, **12** (3), 199-200.
- Kettenmann, H. and Verkhratsky, A. (2008). Neuroglia: The 150 years after. *Trends in Neurosciences*, **31** (12), 653-659.
- Khuder, S. A., Peshimam, A. Z. and Agraharam, S. (2002). Environmental risk factors for rheumatoid arthritis. *Reviews on Environmental Health*, **17** (4), 307-315.
- Kidd, D., Barkhof, F., McConnell, R., Algra, P., Allen, I. and Revesz, T. (1999). Cortical lesions in multiple sclerosis. *Brain*, **122** (1), 17-26.
- Kivity, S. and Ehrenfeld, M. (2010). Can we explain the higher prevalence of autoimmune disease in women? *Expert Review of Clinical Immunology*, **6** (5), 691-694.
- Klareskog, L., Rönnelid, J., Lundberg, K., Padyukov, L. and Alfredsson, L. (2008). Immunity to citrullinated proteins in rheumatoid arthritis. *Annual Review of Immunology*, **26**, 651-675.
- Klein, U. and Dalla-Favera, R. (2008). Germinal centres: Role in B-cell physiology and malignancy. *Nature Reviews Immunology*, **8** (1), 22-33.
- Kniesel, U. and Wolburg, H. (2000). Tight junctions of the blood–brain barrier. *Cellular and Molecular Neurobiology*, **20** (1), 57-76.
- Kondrashova, A., Reunanen, A., Romanov, A., Karvonen, A., Viskari, H., Vesikari, T., Ilonen, J., Knip, M. and Hyöty, H. (2005). A six-fold gradient in the incidence of type 1 diabetes at the eastern border of finland. *Annals of Medicine*, **37** (1), 67-72.
- König, R., Fleury, S. and Germain, R. (1996). The structural basis of CD4-MHC class II interactions: Coreceptor contributions to T cell receptor antigen recognition and oligomerization-dependent signal transduction. *Current Topics in Microbiology and Immunology*, **205**, 19-46.

Korthäuer, U., Graf, D., Mages, H. W., Brière, F., Padayachee, M., Malcolm, S., Ugazio, A. G., Notarangelo, L. D., Levinsky, R. J. and Kroccek, R. A. (1993). Defective expression of T-cell CD40 ligand causes X-linked immunodeficiency with hyper-IgM. *Nature*, **361**, 539-541.

Kurien, B. T. and Scofield, R. H. (2006). Western blotting. *Methods*, **38** (4), 283-293.

Kurtzke, J. F., Beebe, G. W. and Norman Jr, J. E. (1979). Epidemiology of multiple sclerosis in US veterans: 1. race, sex, and geographic distribution. *Neurology*, **29** (9, Part 1), 1228.

Kutzelnigg, A., Faber-Rod, J. C., Bauer, J., Lucchinetti, C. F., Sorensen, P. S., Laursen, H., Stadelmann, C., Brück, W., Rauschka, H. and Schmidbauer, M. (2007). Widespread demyelination in the cerebellar cortex in multiple sclerosis. *Brain Pathology*, **17** (1), 38-44.

Kutzelnigg, A., Lucchinetti, C. F., Stadelmann, C., Brück, W., Rauschka, H., Bergmann, M., Schmidbauer, M., Parisi, J. E. and Lassmann, H. (2005). Cortical demyelination and diffuse white matter injury in multiple sclerosis. *Brain*, **128** (11), 2705-2712.

Kwan, J. and Killeen, N. (2004). CCR7 directs the migration of thymocytes into the thymic medulla. *The Journal of Immunology*, **172** (7), 3999-4007.

Ladeby, R., Wirenfeldt, M., Dalmau, I., Gregersen, R., García-Ovejero, D., Babcock, A., Owens, T. and Finsen, B. (2005). Proliferating resident microglia express the stem cell antigen CD34 in response to acute neural injury. *Glia*, **50** (2), 121-131.

Laemmli, U. K. (1970). Cleavage of structural proteins during the assembly of the head of bacteriophage T4. *Nature*, **227** (5259), 680-685.

Lalive, P. H., Menge, T., Delarasse, C., Della Gaspera, B., Pham-Dinh, D., Villoslada, P., von Büdingen, H. C. and Genain, C. P. (2006). Antibodies to native myelin oligodendrocyte glycoprotein are serologic markers of early inflammation in multiple sclerosis. *Proceedings of the National Academy of Sciences of the United States of America*, **103** (7), 2280-2285.

Lambrecht, B. N. and Hammad, H. (2009). Biology of lung dendritic cells at the origin of asthma. *Immunity*, **31** (3), 412-424.

Lamkanfi, M. (2011). Emerging inflammasome effector mechanisms. *Nature Reviews Immunology*, **11** (3), 213-220.

Lampasona, V., Franciotta, D., Furlan, R., Zanaboni, S., Fazio, R., Bonifacio, E., Comi, G. and Martino, G. (2004). Similar low frequency of anti-MOG IgG and IgM in MS patients and healthy subjects. *Neurology*, **62** (11), 2092-2094.

Lappe-Siefke, C., Goebbels, S., Gravel, M., Nicksch, E., Lee, J., Braun, P. E., Griffiths, I. R. and Nave, K. A. (2003). Disruption of Cnp1 uncouples oligodendroglial functions in axonal support and myelination. *Nature Genetics*, **33** (3), 366-374.

Larochelle, C., Alvarez, J. I. and Prat, A. (2011). How do immune cells overcome the blood-brain barrier in multiple sclerosis? *FEBS Letters*, **585** (23), 3770-3780.

LaRosa, D. F. and Orange, J. S. (2008). 1. lymphocytes. *Journal of Allergy and Clinical Immunology*, **121** (2), S364-S369.

- Lassmann, H. (2004). Cellular damage and repair in multiple sclerosis. *Myelin biology and disorders*, **2**, 733-762.
- Lassmann, H., Brück, W. and Lucchinetti, C. (2001). Heterogeneity of multiple sclerosis pathogenesis: Implications for diagnosis and therapy. *Trends in molecular medicine*, **7** (3), 115-121.
- Lawson, L., Perry, V., Dri, P. and Gordon, S. (1990). Heterogeneity in the distribution and morphology of microglia in the normal adult mouse brain. *Neuroscience*, **39** (1), 151-170.
- Lee, H. J., Joo, M., Abdolrasulnia, R., Young, D. G., Choi, I., Ware, L. B., Blackwell, T. S. and Christman, B. W. (2010). Peptidylarginine deiminase 2 suppresses inhibitory κ B kinase activity in lipopolysaccharide-stimulated RAW 264.7 macrophages. *Journal of Biological Chemistry*, **285** (51), 39655-39662.
- Lehnardt, S. (2010). Innate immunity and neuroinflammation in the CNS: The role of microglia in Toll-like receptor-mediated neuronal injury. *Glia*, **58** (3), 253-263.
- Leibowitz, U., Kahana, E. and Alter, M. (1973). The changing frequency of multiple sclerosis in Israel. *Archives of Neurology*, **29** (2), 107-110.
- Lennon, V. A., Kryzer, T. J., Pittock, S. J., Verkman, A. and Hinson, S. R. (2005). IgG marker of optic-spinal multiple sclerosis binds to the aquaporin-4 water channel. *The Journal of Experimental Medicine*, **202** (4), 473-477.
- Lennon, V. A., Wingerchuk, D. M., Kryzer, T. J., Pittock, S. J., Lucchinetti, C. F., Fujihara, K., Nakashima, I. and Weinshenker, B. G. (2004). A serum autoantibody marker of neuromyelitis optica: Distinction from multiple sclerosis. *The Lancet*, **364** (9451), 2106-2112.
- Lepikhin, E. A., Eliasson, C., Berthold, C. H., Berezin, V., Bock, E. and Pekny, M. (2001). Intermediate filaments regulate astrocyte motility. *Journal of Neurochemistry*, **79** (3), 617-625.
- Levings, M. K., Sangregorio, R., Sartirana, C., Moschin, A. L., Battaglia, M., Orban, P. C. and Roncarolo, M. G. (2002). Human CD25 CD4 T suppressor cell clones produce transforming growth factor β , but not interleukin 10, and are distinct from type 1 T regulatory cells. *The Journal of Experimental Medicine*, **196** (10), 1335-1346.
- Li, H., Cuzner, M. and Newcombe, J. (1996). Microglia-derived macrophages in early multiple sclerosis plaques. *Neuropathology and Applied Neurobiology*, **22** (3), 207-215.
- Li, H., Newcombe, J., Groome, N. and Cuzner, M. (2008). Characterization and distribution of phagocytic macrophages in multiple sclerosis plaques. *Neuropathology and Applied Neurobiology*, **19** (3), 214-223.
- Lin, J. P., Cash, J. M., Doyle, S. Z., Peden, S., Kanik, K., Amos, C. I., Bale, S. J. and Wilder, R. L. (1998). Familial clustering of rheumatoid arthritis with other autoimmune diseases. *Human Genetics*, **103** (4), 475-482.
- Liu, Y. J., Johnson, G. D., Gordon, J. and MacLennan, I. (1992). Germinal centres in T-cell-dependent antibody responses. *Immunology Today*, **13** (1), 17-21.

- Livak, K. J. and Schmittgen, T. D. (2001). Analysis of relative gene expression data using real-time quantitative PCR and the 2- $^{-\Delta\Delta CT}$ method. *Methods*, **25** (4), 402-408.
- Lolli, F., Mulinacci, B., Carotenuto, A., Bonetti, B., Sabatino, G., Mazzanti, B., D'Ursi, A. M., Novellino, E., Pazzagli, M. and Lovato, L. (2005). An N-glycosylated peptide detecting disease-specific autoantibodies, biomarkers of multiple sclerosis. *Proceedings of the National Academy of Sciences of the United States of America*, **102** (29), 10273.
- Loos, T., Mortier, A., Gouwy, M., Ronsse, I., Put, W., Lenaerts, J. P., Van Damme, J. and Proost, P. (2008). Citrullination of CXCL10 and CXCL11 by peptidylarginine deiminase: A naturally occurring posttranslational modification of chemokines and new dimension of immunoregulation. *Blood*, **112** (7), 2648-2656.
- Loos, T., Opdenakker, G., Van Damme, J. and Proost, P. (2009). Citrullination of CXCL8 increases this chemokine's ability to mobilize neutrophils into the blood circulation. *Haematologica*, **94** (10), 1346-1353.
- Lowe, C. E., Cooper, J. D., Brusko, T., Walker, N. M., Smyth, D. J., Bailey, R., Bourget, K., Plagnol, V., Field, S. and Atkinson, M. (2007). Large-scale genetic fine mapping and genotype-phenotype associations implicate polymorphism in the IL2RA region in type 1 diabetes. *Nature Genetics*, **39** (9), 1074-1082.
- Lu, C. Z., Jensen, M. A. and Arnason, B. G. W. (1993). Interferon γ -and interleukin-4-secreting cells in multiple sclerosis. *Journal of Neuroimmunology*, **46** (1-2), 123-128.
- Lu, Q., Renaudineau, Y., Cha, S., Ilei, G., Brooks, W. H., Selmi, C., Tzioufas, A., Pers, J. O., Bombardieri, S. and Gershwin, M. E. (2010). Epigenetics in autoimmune disorders: Highlights of the 10th sjögren's syndrome symposium. *Autoimmunity Reviews*, **9** (9), 627-630.
- Lublin, F. D. and Reingold, S. C. (1996). Defining the clinical course of multiple sclerosis: Results of an international survey. *Neurology*, **46** (4), 907-911.
- Lucchinetti, C., Bruck, W., Parisi, J., Scheithauer, B., Rodriguez, M. and Lassman, H. (2000). Heterogeneity of multiple sclerosis lesions: Implications for the pathogenesis of demyelination. *Annals of Neurology*, **47** (6), 707-717.
- Lucchinetti, C. F., Parisi, J. and Bruck, W. (2005). The pathology of multiple sclerosis. *Neurologic Clinics*, **23** (1), 77-105.
- Lumsden, C. E. (1970). The neuropathology of multiple sclerosis. *Handbook of Clinical Neurology*, **9**, 217-309.
- Lundmark, F., Duvefelt, K., Jacobaeus, E., Kockum, I., Wallström, E., Khademi, M., Oturai, A., Ryder, L. P., Saarela, J. and Harbo, H. F. (2007). Variation in interleukin 7 receptor α chain (IL7R) influences risk of multiple sclerosis. *Nature Genetics*, **200** (39), 1108-1113.
- MacLennan, I. C. M. (1994). Germinal centers. *Annual Review of Immunology*, **12** (1), 117-139.

Mahnke, K., Bedke, T. and Enk, A. H. (2007). Regulatory conversation between antigen presenting cells and regulatory T cells enhance immune suppression. *Cellular Immunology*, **250** (1), 1-13.

Mahnke, K., Schmitt, E., Bonifaz, L., Enk, A. H. and Jonuleit, H. (2002). Immature, but not inactive: The tolerogenic function of immature dendritic cells. *Immunology and Cell Biology*, **80** (5), 477-483.

Malhotra, S., Luong, L., Bhatnagar, R. and Shnitka, T. (1997). Up-regulation of reactive astrogliosis in the rat glioma 9L cell line by combined mechanical and chemical injuries. *Cytobios*, **89** (357), 115-134.

Maloy, K. J. and Powrie, F. (2001). Regulatory T cells in the control of immune pathology. *Nature immunology*, **2** (9), 816-822.

Mann, M., Hendrickson, R. C. and Pandey, A. (2001). Analysis of proteins and proteomes by mass spectrometry. *Annual Review of Biochemistry*, **70** (1), 437-473.

Marín-Teva, J. L., Dusart, I., Colin, C., Gervais, A., van Rooijen, N. and Mallat, M. (2004). Microglia promote the death of developing purkinje cells. *Neuron*, **41** (4), 535-547.

Marzi, M., Vigano, A., Trabattoni, D., Villa, M., Salvaggio, A., Clerici, E. and Clerici, M. (1996). Characterization of type 1 and type 2 cytokine production profile in physiologic and pathologic human pregnancy. *Clinical & Experimental Immunology*, **106** (1), 127-133.

Mastronardi, F. G., Wood, D. D., Mei, J., Raijmakers, R., Tseveleki, V., Dosch, H., Probert, L., Casaccia-Bonnel, P. and Moscarello, M. A. (2006). Increased citrullination of histone H3 in multiple sclerosis brain and animal models of demyelination: A role for tumor necrosis factor-induced peptidylarginine deiminase 4 translocation. *The Journal of Neuroscience*, **26** (44), 11387-11396.

Mastronardi, F. G. and Moscarello, M. A. (2005). Molecules affecting myelin stability: A novel hypothesis regarding the pathogenesis of multiple sclerosis. *Journal of Neuroscience Research*, **80** (3), 301-308.

Mastronardi, F. G., Noor, A., Wood, D. D., Paton, T. and Moscarello, M. A. (2007). Peptidyl argininedeiminase 2 CpG island in multiple sclerosis white matter is hypomethylated. *Journal of Neuroscience Research*, **85** (9), 2006-2016.

Mastronardi, F., Ackerley, C., Arsenault, L., Roots, B. and Moscarello, M. (1993). Demyelination in a transgenic mouse: A model for multiple sclerosis. *Journal of Neuroscience Research*, **36** (3), 315-324.

McCarthy, M. (2000). The "gender gap" in autoimmune disease. *The Lancet*, **356** (9235), 1088.

McCormic, Z. D., Khuder, S. S., Aryal, B. K., Ames, A. L. and Khuder, S. A. (2010). Occupational silica exposure as a risk factor for scleroderma: A meta-analysis. *International Archives of Occupational and Environmental Health*, **83** (7), 763-769.

McDonald, W. I., Compston, A., Edan, G., Goodkin, D., Hartung, H. P., Lublin, F. D., McFarland, H. F., Paty, D. W., Polman, C. H. and Reingold, S. C. (2001). Recommended diagnostic criteria for multiple sclerosis: Guidelines from the

international panel on the diagnosis of multiple sclerosis. *Annals of Neurology*, **50** (1), 121-127.

McFarland, H. F. and Martin, R. (2007). Multiple sclerosis: A complicated picture of autoimmunity. *Nature Immunology*, **8** (9), 913-919.

McGargill, M. A., Derbinski, J. M. and Hogquist, K. A. (2000). Receptor editing in developing T cells. *Nature Immunology*, **1** (4), 336-341.

McLaughlin, K. A., Chitnis, T., Newcombe, J., Franz, B., Kennedy, J., McArdel, S., Kuhle, J., Kappos, L., Rostasy, K. and Pohl, D. (2009). Age-dependent B cell autoimmunity to a myelin surface antigen in pediatric multiple sclerosis. *The Journal of Immunology*, **183** (6), 4067-4076.

McMurray, R. W. (2001). Estrogen, prolactin, and autoimmunity: Actions and interactions. *International Immunopharmacology*, **1** (6), 995-1008.

McQuaid, S., Cunnea, P., McMahan, J. and Fitzgerald, U. (2009). The effects of blood-brain barrier disruption on glial cell function in multiple sclerosis. *Biochemical Society Transactions*, **37** (1), 331-331.

Mechin, M. C., Sebbag, M., Arnaud, J., Nachat, R., Foulquier, C., Adoue, V., Coudane, F., Duplan, H., Schmitt, A. M. and Chavanas, S. (2007). Update on peptidylarginine deiminases and deimination in skin physiology and severe human diseases. *International Journal of Cosmetic Science*, **29** (3), 147.

Meda, F., Folci, M., Baccarelli, A. and Selmi, C. (2011). The epigenetics of autoimmunity. *Cellular & Molecular Immunology*, **8** (3), 226-236.

Medana, I., Martinic, M. A., Wekerle, H. and Neumann, H. (2001). Transection of major histocompatibility complex class I-induced neurites by cytotoxic T lymphocytes. *The American Journal of Pathology*, **159** (3), 809-815.

Meinecke, I., Rutkauskaite, E., Gay, S. and Pap, T. (2005). The role of synovial fibroblasts in mediating joint destruction in rheumatoid arthritis. *Current Pharmaceutical Design*, **11** (5), 563-568.

Melief, C. J. M. (2003). Mini-review: Regulation of cytotoxic T lymphocyte responses by dendritic cells: Peaceful coexistence of cross-priming and direct priming? *European Journal of Immunology*, **33** (10), 2645-2654.

Menard, L., Saadoun, D., Isnardi, I., Ng, Y. S., Meyers, G., Massad, C., Price, C., Abraham, C., Motaghedi, R. and Buckner, J. H. (2011). The PTPN22 allele encoding an R620W variant interferes with the removal of developing autoreactive B cells in humans. *The Journal of Clinical Investigation*, **121** (9), 3635-3644.

Menard, L. C., Minns, L. A., Darche, S., Mielcarz, D. W., Foureau, D. M., Roos, D., Dzierszynski, F., Kasper, L. H. and Buzoni-Gatel, D. (2007). B cells amplify IFN- γ production by T cells via a TNF- α -mediated mechanism. *The Journal of Immunology*, **179** (7), 4857-4866.

Merrill, J. E. (1992). Proinflammatory and antiinflammatory cytokines in multiple sclerosis and central nervous system acquired immunodeficiency syndrome. *Journal of Immunotherapy*, **12** (3), 167-170.

- Metzger, T. C. and Anderson, M. S. (2011). Control of central and peripheral tolerance by aire. *Immunological Reviews*, **241** (1), 89-103.
- Middeldorp, J. and Hol, E. (2011). GFAP in health and disease. *Progress in Neurobiology*, **93** (3), 421-443.
- Miller, D. H. and Leary, S. M. (2007). Primary-progressive multiple sclerosis. *Lancet Neurology*, **6** (10), 903-912.
- Miller, J. F. A. P. (2002). The discovery of thymus function and of thymus-derived lymphocytes. *Immunological Reviews*, **185** (1), 7-14.
- Minagar, A. and Alexander, J. S. (2003). Blood-brain barrier disruption in multiple sclerosis. *Multiple Sclerosis*, **9** (6), 540-549.
- Misslitz, A., Pabst, O., Hintzen, G., Ohl, L., Kremmer, E., Petrie, H. T. and Förster, R. (2004). Thymic T cell development and progenitor localization depend on CCR7. *The Journal of Experimental Medicine*, **200** (4), 481-491.
- Mittelbronn, M., Dietz, K., Schluesener, H. and Meyermann, R. (2001). Local distribution of microglia in the normal adult human central nervous system differs by up to one order of magnitude. *Acta Neuropathologica*, **101** (3), 249-255.
- Miura, K., Aoun, K., Yoshida, S. and Kurosawa, Y. (2012). Autoantibodies directed against labile epitopes on cell surface proteins in autoimmune disease patients: Proposal of a novel ELISA for the detection of anti-endothelial cell antibodies. *Journal of Immunological Methods*, **382** (1-2), 32-39.
- Mix, E., Meyer-Rienecker, H., Hartung, H. P. and Zettl, U. K. (2010). Animal models of multiple sclerosis—Potentials and limitations. *Progress in Neurobiology*, **92** (3), 386-404.
- Mohamed, B. M., Verma, N. K., Davies, A. M., McGowan, A., Crosbie-Staunton, K., Prina-Mello, A., Kelleher, D., Botting, C. H., Causey, C. P. and Thompson, P. R. (2012). Citrullination of proteins: A common post-translational modification pathway induced by different nanoparticles in vitro and in vivo. *Nanomedicine*, **7** (8), 1181-1195.
- Mokhtarian, F., Shi, Y., Shirazian, D., Morgante, L., Miller, A. and Grob, D. (1994). Defective production of anti-inflammatory cytokine, TGF-beta by T cell lines of patients with active multiple sclerosis. *The Journal of Immunology*, **152** (12), 6003-6010.
- Moore, C. S., Abdullah, S. L., Brown, A., Arulpragasam, A. and Crocker, S. J. (2011). How factors secreted from astrocytes impact myelin repair. *Journal of Neuroscience Research*, **89** (1), 13-21.
- Mortier, A., Loos, T., Gouwy, M., Ronsse, I., Van Damme, J. and Proost, P. (2010). Posttranslational modification of the NH2-terminal region of CXCL5 by proteases or peptidylarginine deiminases (PAD) differently affects its biological activity. *Journal of Biological Chemistry*, **285** (39), 29750.
- Moscarello, M. A., Mastronardi, F. G. and Wood, D. D. (2007). The role of citrullinated proteins suggests a novel mechanism in the pathogenesis of multiple sclerosis. *Neurochemical Research*, **32** (2), 251-256.

- Moscarello, M. A., Wood, D. D., Ackerley, C. and Boulias, C. (1994). Myelin in multiple sclerosis is developmentally immature. *Journal of Clinical Investigation*, **94** (1), 146-154.
- Mrass, P. and Weninger, W. (2006). Immune cell migration as a means to control immune privilege: Lessons from the CNS and tumors. *Immunological Reviews*, **213** (1), 195-212.
- Munn, D. H., Sharma, M. D., Lee, J. R., Jhaver, K. G., Johnson, T. S., Keskin, D. B., Marshall, B., Chandler, P., Antonia, S. J. and Burgess, R. (2002). Potential regulatory function of human dendritic cells expressing indoleamine 2, 3-dioxygenase. *Science's STKE*, **297** (5588), 1867-1870.
- Musse, A. A., Boggs, J. M. and Harauz, G. (2006). Deimination of membrane-bound myelin basic protein in multiple sclerosis exposes an immunodominant epitope. *Proceedings of the National Academy of Sciences of the United States of America*, **103** (12), 4422-4427.
- Musse, A. A. and Harauz, G. (2007). Molecular "negativity" may underlie multiple sclerosis: Role of the myelin basic protein family in the pathogenesis of MS. *International Review of Neurobiology*, **79**, 149-172.
- Musse, A. A., Li, Z., Ackerley, C. A., Bienzle, D., Lei, H., Poma, R., Harauz, G., Moscarello, M. A. and Mastronardi, F. G. (2008). Peptidylarginine deiminase 2 (PAD2) overexpression in transgenic mice leads to myelin loss in the central nervous system. *Disease Models & Mechanisms*, **1** (4-5), 229-240.
- Nagasawa, T. (2006). Microenvironmental niches in the bone marrow required for B-cell development. *Nature Reviews Immunology*, **6** (2), 107-116.
- Nair, A., Frederick, T. J. and Miller, S. D. (2008). Astrocytes in multiple sclerosis: A product of their environment. *Cellular and Molecular Life Sciences*, **65** (17), 2702-2720.
- Naito, S., Namerow, N., Mickey, M. and Terasaki, P. (1972). Multiple sclerosis: Association with HL-A3. *Tissue Antigens*, **2** (1), 1-4.
- Nakashima, K., Hagiwara, T. and Yamada, M. (2002). Nuclear localization of peptidylarginine deiminase V and histone deimination in granulocytes. *Journal of Biological Chemistry*, **277** (51), 49562-49568.
- Napoli, I. and Neumann, H. (2009). Microglial clearance function in health and disease. *Neuroscience*, **158** (3), 1030-1038.
- Napoli, I. and Neumann, H. (2010). Protective effects of microglia in multiple sclerosis. *Experimental Neurology*, **225** (1), 24-28.
- Nave, K. A. (2010). Myelination and support of axonal integrity by glia. *Nature*, **468** (7321), 244-252.
- Neeli, I., Khan, S. N. and Radic, M. (2008). Histone deimination as a response to inflammatory stimuli in neutrophils. *The Journal of Immunology*, **180** (3), 1895-1902.
- Neidhart, M., Rethage, J., Kuchen, S., Künzler, P., Crowl, R. M., Billingham, M. E., Gay, R. E. and Gay, S. (2000). Retrotransposable L1 elements expressed in

rheumatoid arthritis synovial tissue: Association with genomic DNA hypomethylation and influence on gene expression. *Arthritis & Rheumatism*, **43** (12), 2634-2647.

Neumann, H., Kotter, M. and Franklin, R. (2009). Debris clearance by microglia: An essential link between degeneration and regeneration. *Brain*, **132** (2), 288-295.

Nicholas, A. P. (2011). Dual immunofluorescence study of citrullinated proteins in parkinson diseased substantia nigra. *Neuroscience Letters*, **495** (1), 26-29.

Nicholas, A. P., Sambandam, T., Echols, J. D. and Barnum, S. R. (2005). Expression of citrullinated proteins in murine experimental autoimmune encephalomyelitis. *The Journal of Comparative Neurology*, **486** (3), 254-266.

Nicholas, A. P., Sambandam, T., Echols, J. D. and Tourtellotte, W. W. (2004). Increased citrullinated glial fibrillary acidic protein in secondary progressive multiple sclerosis. *The Journal of Comparative Neurology*, **473** (1), 128-136.

Nicholas, A. P. and Whitaker, J. N. (2002). Preparation of a monoclonal antibody to citrullinated epitopes: Its characterization and some applications to immunohistochemistry in human brain. *Glia*, **37** (4), 328-336.

Nienhuis, R., Mandema, E. and Smids, C. (1964). New serum factor in patients with rheumatoid arthritis: The antiperinuclear factor. *Annals of the Rheumatic Diseases*, **23** (4), 302-305.

Nikbin, B., Bonab, M. M., Khosravi, F. and Talebian, F. (2007). Role of B cells in pathogenesis of multiple sclerosis. *International Review of Neurobiology*, **79** , 13-42.

Nile, C. J., Read, R. C., Akil, M., Duff, G. W. and Wilson, A. G. (2008). Methylation status of a single CpG site in the IL6 promoter is related to IL6 messenger RNA levels and rheumatoid arthritis. *Arthritis & Rheumatism*, **58** (9), 2686-2693.

Nimmerjahn, A., Kirchhoff, F. and Helmchen, F. (2005). Resting microglial cells are highly dynamic surveillants of brain parenchyma in vivo. *Science*, **308** (5726), 1314-1318.

Noonan, C. W., Kathman, S. J. and White, M. C. (2002). Prevalence estimates for MS in the united states and evidence of an increasing trend for women. *Neurology*, **58** (1), 136-138.

Noseworthy, J. H., Lucchinetti, C., Rodriguez, M. and Weinshenker, B. G. (2000). Multiple sclerosis. *New England Journal of Medicine*, **343** (13), 938-952.

Nurieva, R. I., Liu, X. and Dong, C. (2009). Yin–Yang of costimulation: Crucial controls of immune tolerance and function. *Immunological Reviews*, **229** (1), 88-100.

O'Connor, K. C., Appel, H., Bregoli, L., Call, M. E., Catz, I., Chan, J. A., Moore, N. H., Warren, K. G., Wong, S. J. and Hafler, D. A. (2005). Antibodies from inflamed central nervous system tissue recognize myelin oligodendrocyte glycoprotein. *The Journal of Immunology*, **175** (3), 1974-1982.

O'Callaghan, J. P. and Sriram, K. (2005). Glial fibrillary acidic protein and related glial proteins as biomarkers of neurotoxicity. *Expert Opinion on Drug Safety*, **4** (3), 433-442.

O'Connor, K. C., McLaughlin, K. A., De Jager, P. L., Chitnis, T., Bettelli, E., Xu, C., Robinson, W. H., Cherry, S. V., Bar-Or, A. and Banwell, B. (2007). Self-antigen tetramers discriminate between myelin autoantibodies to native or denatured protein. *Nature Medicine*, **13** (2), 211-217.

Oguz, K. K., Kurne, A., Aksu, A. O., Karabulut, E., Serdaroglu, A., Teber, S., Haspolat, S., Senbil, N., Kurul, S. and Anlar, B. (2009). Assessment of citrullinated myelin by 1H-MR spectroscopy in early-onset multiple sclerosis. *American Journal of Neuroradiology*, **30** (4), 716-721.

Okamoto, M., Wang, X. and Baba, M. (2005). HIV-1-infected macrophages induce astrogliosis by SDF-1 α and matrix metalloproteinases. *Biochemical and Biophysical Research Communications*, **336** (4), 1214-1220.

Oki, T., Takahashi, S., Kuwabara, S., Yoshiyama, Y., Mori, M., Hattori, T. and Suzuki, N. (2004). Increased ability of peripheral blood lymphocytes to degrade laminin in multiple sclerosis. *Journal of the Neurological Sciences*, **222** (1), 7-11.

Oksenberg, J. R. and Barcellos, L. F. (2005). Multiple sclerosis genetics: Leaving no stone unturned. *Genes and Immunity*, **6** (5), 375-387.

Oldendorf, W. H., Cornford, M. E. and Brown, W. J. (2004). The large apparent work capability of the blood-brain barrier: A study of the mitochondrial content of capillary endothelial cells in brain and other tissues of the rat. *Annals of Neurology*, **1** (5), 409-417.

Oleszak, E. L., Zaczynska, E., Bhattacharjee, M., Butunoi, C., Legido, A. and Katsetos, C. D. (1998). Inducible nitric oxide synthase and nitrotyrosine are found in monocytes/macrophages and/or astrocytes in acute, but not in chronic, multiple sclerosis. *Clinical and Diagnostic Laboratory Immunology*, **5** (4), 438-445.

Oliver, J. E. and Silman, A. J. (2009). Why are women predisposed to autoimmune rheumatic diseases. *Arthritis Research & Therapy*, **11** (5), 252-260.

O'Neill, L. A. (2008). The interleukin-1 receptor/Toll-like receptor superfamily: 10 years of progress. *Immunological Reviews*, **226** (1), 10-18.

O'Neill, L. A., Bryant, C. E. and Doyle, S. L. (2009). Therapeutic targeting of toll-like receptors for infectious and inflammatory diseases and cancer. *Pharmacological Reviews*, **61** (2), 177-197.

Orgován, G. and Noszál, B. (2011). The complete microspeciation of arginine and citrulline. *Journal of Pharmaceutical and Biomedical Analysis*, **54** (5), 965-971.

Orton, S. M., Herrera, B. M., Yee, I. M., Valdar, W., Ramagopalan, S. V., Sadovnick, A. D. and Ebers, G. C. (2006). Sex ratio of multiple sclerosis in Canada: A longitudinal study. *Lancet Neurology*, **5** (11), 932-936.

Paddock, S. W. (1999a). Confocal laser scanning microscopy. *BioTechniques*, **27**, 992-1007.

Paddock, S. W. (1999b). *Confocal microscopy methods and protocols*. New Jersey, Humana Press Inc.

- Paddock, S. W. (2000). Principles and practices of laser scanning confocal microscopy. *Molecular Biotechnology*, **16** (2), 127-149.
- Pan, C., Xu, S., Zhou, H., Fu, Y., Ye, M. and Zou, H. (2007). Recent developments in methods and technology for analysis of biological samples by MALDI-TOF-MS. *Analytical and Bioanalytical Chemistry*, **387** (1), 193-204.
- Pardridge, W. M., Eisenberg, J. and Yang, J. (1985). Human Blood—Brain barrier insulin receptor. *Journal of Neurochemistry*, **44** (6), 1771-1778.
- Parijs, L. V. and Abbas, A. K. (1998). Homeostasis and self-tolerance in the immune system: Turning lymphocytes off. *Science*, **280** (5361), 243-248.
- Pattison, D. J., Symmons, D. P. M., Lunt, M., Welch, A., Luben, R., Bingham, S. A., Khaw, K. T., Day, N. E. and Silman, A. J. (2004). Dietary risk factors for the development of inflammatory polyarthritis: Evidence for a role of high level of red meat consumption. *Arthritis & Rheumatism*, **50** (12), 3804-3812.
- Penkowa, M., Hidalgo, J. and Aschner, M. (2008). Immune and inflammatory responses in the central nervous system: Modulation by astrocytes. *NeuroImmune Biology*, **6**, 275-288.
- Peress, N. S., Perillo, E. and Seidman, R. J. (1996). Glial transforming growth factor (TGF)- β isotypes in multiple sclerosis: Differential glial expression of TGF- β 1, 2 and 3 isotypes in multiple sclerosis. *Journal of Neuroimmunology*, **71** (1), 115-123.
- Peterson, J. W., Bö, L., Mörk, S., Chang, A. and Trapp, B. D. (2001). Transected neurites, apoptotic neurons, and reduced inflammation in cortical multiple sclerosis lesions. *Annals of Neurology*, **50** (3), 389-400.
- Petrie, H., Livak, F., Schatz, D., Strasser, A., Crispe, I. and Shortman, K. (1993). Multiple rearrangements in T cell receptor alpha chain genes maximize the production of useful thymocytes. *The Journal of Experimental Medicine*, **178** (2), 615-622.
- Phillips, L. M. and Lampson, L. A. (1999). Site-specific control of T cell traffic in the brain: T cell entry to brainstem vs. hippocampus after local injection of IFN- γ . *Journal of Neuroimmunology*, **96** (2), 218-227.
- Piccio, L., Buonsanti, C., Mariani, M., Cella, M., Gilfillan, S., Cross, A. H., Colonna, M. and Panina-Bordignon, P. (2007). Blockade of TREM-2 exacerbates experimental autoimmune encephalomyelitis. *European Journal of Immunology*, **37** (5), 1290-1301.
- Pines, G., Danbolt, N. C., Bjørås, M., Zhang, Y., Bendahan, A., Eide, L., Koepsell, H., Storm-Mathisen, J., Seeberg, E. and Kanner, B. I. (1992). Cloning and expression of a rat brain L-glutamate transporter. *Nature*, **360**, 464-467.
- Podojil, J. R. and Miller, S. D. (2006). Immunopathological mechanisms in multiple sclerosis. *Drug Discovery Today: Disease Mechanisms*, **3** (2), 177-184.
- Pöllinger, B., Krishnamoorthy, G., Berer, K., Lassmann, H., Bösl, M. R., Dunn, R., Domingues, H. S., Holz, A., Kurschus, F. C. and Wekerle, H. (2009). Spontaneous relapsing-remitting EAE in the SJL/J mouse: MOG-reactive transgenic T cells recruit endogenous MOG-specific B cells. *The Journal of Experimental Medicine*, **206** (6), 1303-1316.

Polman, C. H., O'Connor, P. W., Havrdova, E., Hutchinson, M., Kappos, L., Miller, D. H., Phillips, J. T., Lublin, F. D., Giovannoni, G. and Wajgt, A. (2006). A randomized, placebo-controlled trial of natalizumab for relapsing multiple sclerosis. *New England Journal of Medicine*, **354** (9), 899-910.

Polman, C. H., Reingold, S. C., Edan, G., Filippi, M., Hartung, H. P., Kappos, L., Lublin, F. D., Metz, L. M., McFarland, H. F. and O'Connor, P. W. (2005). Diagnostic criteria for multiple sclerosis: 2005 revisions to the "McDonald criteria". *Annals of Neurology*, **58** (6), 840-846.

Potokar, M., Kreft, M., Li, L., Daniel Andersson, J., Pangršič, T., Chowdhury, H. H., Pekny, M. and Zorec, R. (2007). Cytoskeleton and vesicle mobility in astrocytes. *Traffic*, **8** (1), 12-20.

Potokar, M., Stenovec, M., Kreft, M., Kreft, M. E. and Zorec, R. (2008). Stimulation inhibits the mobility of recycling peptidergic vesicles in astrocytes. *Glia*, **56** (2), 135-144.

Power, C., Kong, P. A., Crawford, T. O., Wesselingh, S., Glass, J. D., McArthur, J. C. and Trapp, B. D. (1993). Cerebral white matter changes in acquired immunodeficiency syndrome dementia: Alterations of the blood-brain barrier. *Annals of Neurology*, **34** (3), 339-350.

Prineas, J. W. (1985). The neuropathology of multiple sclerosis. *Handbook of Clinical Neurology*, **3** (47), 213-257.

Prineas, J. W., Barnard, R. O., Revesz, T., Kwon, E. E., Sharer, L. and Cho, E. S. (1993). Multiple sclerosis. pathology of recurrent lesions. *Brain*, **116** , 681-693.

Prineas, J. W. and Wright, R. G. (1978). Macrophages, lymphocytes, and plasma cells in the perivascular compartment in chronic multiple sclerosis. *Laboratory Investigation*, **38** (4), 409-421.

Pritzker, L. B., Joshi, S., Gowan, J. J., Harauz, G. and Moscarello, M. A. (2000). Deimination of myelin basic protein. 1. effect of deimination of arginyl residues of myelin basic protein on its structure and susceptibility to digestion by cathepsin D. *Biochemistry*, **39** (18), 5374-5381.

Privat, A. (2003). Astrocytes as support for axonal regeneration in the central nervous system of mammals. *Glia*, **43** (1), 91-93.

Proost, P., Loos, T., Mortier, A., Schutyser, E., Gouwy, M., Noppen, S., Dillen, C., Ronsse, I., Conings, R. and Struyf, S. (2008). Citrullination of CXCL8 by peptidylarginine deiminase alters receptor usage, prevents proteolysis, and dampens tissue inflammation. *The Journal of Experimental Medicine*, **205** (9), 2085-2097.

Quintero, O. L., Amador-Patarroyo, M. J., Montoya-Ortiz, G., Rojas-Villarraga, A. and Anaya, J. M. (2011). Autoimmune disease and gender: Plausible mechanisms for the female predominance of autoimmunity. *Journal of Autoimmunity*, **38** (2-3), 109-119.

Racke, M. K. (2008). The role of B cells in multiple sclerosis: Rationale for B-cell-targeted therapies. *Current Opinion in Neurology*, **21** , S9-S18.

Raijmakers, R., Vogelzangs, , Raats, J., Panzenbeck, M., Corby, M., Jiang, H., Thibodeau, M., Haynes, N., van Venrooij, W. J., Pruijn, G. J. M. and Werneburg, B.

(2006). Experimental autoimmune encephalomyelitis induction in peptidylarginine deiminase 2 knockout mice. *The Journal of Comparative Neurology*, **498** (2), 217-226.

Raijmakers, R., Vogelzangs, J., Croxford, J. L., Wesseling, P., van Venrooij, W. J. and Pruijn, G. J. M. (2005). Citrullination of central nervous system proteins during the development of experimental autoimmune encephalomyelitis. *Journal of Comparative Neurology*, **486** (3), 243-253.

Raine, C., Cannella, B., Duijvestijn, A. and Cross, A. (1990). Homing to central nervous system vasculature by antigen-specific lymphocytes. II. Lymphocyte/endothelial cell adhesion during the initial stages of autoimmune demyelination. *Laboratory Investigation*, **63** (4), 476-489.

Raivich, G. and Banati, R. (2004). Brain microglia and blood-derived macrophages: Molecular profiles and functional roles in multiple sclerosis and animal models of autoimmune demyelinating disease. *Brain Research Reviews*, **46** (3), 261-281.

Raivich, G., Jones, L., Werner, A., Blüthmann, H., Doetschmann, T. and Kreutzberg, G. (1999). Molecular signals for glial activation: Pro- and anti-inflammatory cytokines in the injured brain. *Acta Neurochirurgica Supplement*, **73**, 21-30.

Rajewsky, K. (1996). Clonal selection and learning in the antibody system. *Nature*, **381**, 751-758.

Ramagopalan, S. V., Morris, A. P., Dymont, D. A., Herrera, B. M., DeLuca, G. C., Lincoln, M. R., Orton, S. M., Chao, M. J., Sadovnick, A. D. and Ebers, G. C. (2007). The inheritance of resistance alleles in multiple sclerosis. *PLoS genetics*, **3** (9), 1607-1613.

Randolph, G. J., Ochando, J. and Partida-Sánchez, S. (2008). Migration of dendritic cell subsets and their precursors. *Annual Review of Immunology*, **26**, 293-316.

Ranque, B. and Mouthon, L. (2010). Geoepidemiology of systemic sclerosis. *Autoimmunity Reviews*, **9** (5), A311.

Ransohoff, R. M., Kivisäkk, P. and Kidd, G. (2003). Three or more routes for leukocyte migration into the central nervous system. *Nature Reviews Immunology*, **3** (7), 569-581.

Ransohoff, R. M. and Perry, V. H. (2009). Microglial physiology: Unique stimuli, specialized responses. *Annual Review of Immunology*, **27**, 119-145.

Rantapää-Dahlqvist, S., de Jong, B. A. W., Berglin, E., Hallmans, G., Wadell, G., Stenlund, H., Sundin, U. and van Venrooij, W. J. (2003). Antibodies against cyclic citrullinated peptide and IgA rheumatoid factor predict the development of rheumatoid arthritis. *Arthritis & Rheumatism*, **48** (10), 2741-2749.

Ravichandran, K. S. (2003). "Recruitment signals" from apoptotic cells: Invitation to a quiet meal. *Cell*, **113** (7), 817-820.

Ravichandran, K. S. and Lorenz, U. (2007). Engulfment of apoptotic cells: Signals for a good meal. *Nature Reviews Immunology*, **7** (12), 964-974.

Reindl, M., Linington, C., Brehm, U., Egg, R., Dilitz, E., Deisenhammer, F., Poewe, W. and Berger, T. (1999). Antibodies against the myelin oligodendrocyte glycoprotein and

the myelin basic protein in multiple sclerosis and other neurological diseases: A comparative study. *Brain*, **122** (11), 2047-2056.

Richards, P. T. and Cuzner, M. L. (1978). Proteolytic activity in CSF. *Advances in Experimental Medicine and Biology*, **100**, 521-527.

Ridet, J., Privat, A., Malhotra, S. and Gage, F. (1997). Reactive astrocytes: Cellular and molecular cues to biological function. *Trends in Neurosciences*, **20** (12), 570-577.

Rieckmann, P., Albrecht, M., Kitze, B., Weber, T., Tumani, H., Broocks, A., Lüer, W. and Poser, S. (1994). Cytokine mRNA levels in mononuclear blood cells from patients with multiple sclerosis. *Neurology*, **44** (8), 1523-1523.

Robertson, N. P., O'riordan, J. I., Chataway, J., Kingsley, D. P. E., Miller, D. H., Clayton, D. and Compston, D. A. S. (1997). Offspring recurrence rates and clinical characteristics of conjugal multiple sclerosis. *The Lancet*, **349** (9065), 1587-1590.

Rock, R. B., Gekker, G., Hu, S., Sheng, W. S., Cheeran, M., Lokensgard, J. R. and Peterson, P. K. (2004). Role of microglia in central nervous system infections. *Clinical Microbiology Reviews*, **17** (4), 942-964.

Roemer, S. F., Parisi, J. E., Lennon, V. A., Benarroch, E. E., Lassmann, H., Bruck, W., Mandler, R. N., Weinshenker, B. G., Pittock, S. J. and Wingerchuk, D. M. (2007). Pattern-specific loss of aquaporin-4 immunoreactivity distinguishes neuromyelitis optica from multiple sclerosis. *Brain*, **130** (5), 1194-1205.

Rogers, G. E., Harding, H. W. J. and Llewellyn-Smith, I. J. (1977). The origin of citrulline-containing proteins in the hair follicle and the chemical nature of trichohyalin, an intracellular precursor. *Biochimica et Biophysica Acta (BBA)-Protein Structure*, **495** (1), 159-175.

Rojas-Villarraga, A., Toro, C. E., Espinosa, G., Rodríguez-Velosa, Y., Duarte-Rey, C., Mantilla, R. D., Iglesias-Gamarra, A., Cervera, R. and Anaya, J. M. (2010). Factors influencing polyautoimmunity in systemic lupus erythematosus. *Autoimmunity Reviews*, **9** (4), 229-232.

Rolls, A., Shechter, R. and Schwartz, M. (2009). The bright side of the glial scar in CNS repair. *Nature Reviews Neuroscience*, **10** (3), 235-241.

Ross, I. (2010). *A bird's-eye view of macrophage biology*. 1st Edition ed., Norfolk, UK, Caister Academic Press.

Ross, M. H. and Pawlina, W. (2006). *Histology: A text and atlas: With correlated cell and molecular biology*. 5th ed., London, Lippincott Williams & Wilkins.

Rot, A. and von Andrian, U. H. (2004). Chemokines in innate and adaptive host defense: Basic chemokines grammar for immune cells. *Annu.Rev.Immunol.*, **22**, 891-928.

Roth, S. Y., Denu, J. M. and Allis, C. D. (2001). Histone acetyltransferases. *Annual Review of Biochemistry*, **70** (1), 81-120.

Rothenberg, E. V. and Dionne, C. J. (2002). Lineage plasticity and commitment in T-cell development. *Immunological Reviews*, **187** (1), 96-115.

Rothstein, J. D., Martin, L., Levey, A. I., Dykes-Hoberg, M., Jin, L., Wu, D., Nash, N. and Kuncel, R. W. (1994). Localization of neuronal and glial glutamate transporters. *Neuron*, **13** (3), 713-725.

Rovaris, M., Confavreux, C., Furlan, R., Kappos, L., Comi, G. and Filippi, M. (2006). Secondary progressive multiple sclerosis: Current knowledge and future challenges. *Lancet Neurology*, **5** (4), 343-354.

Ruan, K., Fang, X. and Ouyang, G. (2009). MicroRNAs: Novel regulators in the hallmarks of human cancer. *Cancer Letters*, **285** (2), 116-126.

Rubin, L., Hall, D., Porter, S., Barbu, K., Cannon, C., Horner, H., Janatpour, M., Liaw, C., Manning, K. and Morales, J. (1991). A cell culture model of the blood-brain barrier. *The Journal of Cell Biology*, **115** (6), 1725-1735.

Rus'd, A. A., Ikejiri, Y., Ono, H., Yonekawa, T., Shiraiwa, M., Kawada, A. and Takahara, H. (1999). Molecular cloning of cDNAs of mouse peptidylarginine deiminase type I, type III and type IV, and the expression pattern of type I in mouse. *European Journal of Biochemistry*, **259** (3), 660-669.

Sadovnick, A. D., Armstrong, H., Rice, G. P. A., Bulman, D., Hashimoto, L., Party, D. W., Hashimoto, S. A., Warren, S., Hader, W. and Murrar, T. J. (1993). A population-based study of multiple sclerosis in twins: Update. *Annals of Neurology*, **33** (3), 281-285.

Sadovnick, A. D., Ebers, G. C., Dyment, D. A. and Risch, N. J. (1996). Evidence for genetic basis of multiple sclerosis. the canadian collaborative study group. *Lancet*, **347** (9017), 1728-1730.

Sakaguchi, S. (2004). Naturally arising CD4 regulatory T cells for immunologic self-tolerance and negative control of immune responses. *Annual Review of Immunology*, **22**, 531-562.

Sakaguchi, S., Yamaguchi, T., Nomura, T. and Ono, M. (2008). Regulatory T cells and immune tolerance. *Cell*, **133** (5), 775-787.

Salinovich, O. and Montelaro, R. C. (1986). Reversible staining and peptide mapping of proteins transferred to nitrocellulose after separation by sodium dodecylsulfate-polyacrylamide gel electrophoresis. *Analytical Biochemistry*, **156** (2), 341-347.

Sallusto, F. and Lanzavecchia, A. (2009). Heterogeneity of CD4 memory T cells: Functional modules for tailored immunity. *European Journal of Immunology*, **39** (8), 2076-2082.

Sambandam, T., Belousova, M., Accaviti-Loper, M. A., Blanquicett, C., Guercello, V., Raijmakers, R. and Nicholas, A. P. (2004). Increased peptidylarginine deiminase type II in hypoxic astrocytes. *Biochemical and Biophysical Research Communications*, **325** (4), 1324-1329.

Sambrook, J. and Russell, D. W. (2001). *Molecular cloning: A laboratory manual*. 3rd ed., New York, Cold Spring Harbour Laboratory Press. 1.

Satoh, K., Kawakami, A., Shirabe, S., Tamai, M., Sato, A., Tsujihata, M., Nagasato, K. and Eguchi, K. (2010). Anti-cyclic citrullinated peptide antibody (anti-CCP antibody) is

present in the sera of patients with dementia of Alzheimer's type in asian. *Acta Neurologica Scandinavica*, **121** (5), 338-341.

Schellekens, G. A., Visser, H., De Jong, B. A. W., Van Den Hoogen, F. H. J., Hazes, J. M. W., Breedveld, F. C. and Van Venrooij, W. J. (2001). The diagnostic properties of rheumatoid arthritis antibodies recognizing a cyclic citrullinated peptide. *Arthritis & Rheumatism*, **43** (1), 155-163.

Schiller, J., Süß, R., Arnhold, J., Fuchs, B., Lessig, J., Müller, M., Petkovic, M., Spalteholz, H., Zschörnig, O. and Arnold, K. (2004). Matrix-assisted laser desorption and ionization time-of-flight (MALDI-TOF) mass spectrometry in lipid and phospholipid research. *Progress in Lipid Research*, **43** (5), 449-488.

Schmidlin, H., Diehl, S. A. and Blom, B. (2009). New insights into the regulation of human B-cell differentiation. *Trends in Immunology*, **30** (6), 277-285.

Schmidt, S., Haase, C. G., Bezman, L., Moser, H., Schmidt, M., Köhler, W., Linington, C. and Klockgether, T. (2001). Serum autoantibody responses to myelin oligodendrocyte glycoprotein and myelin basic protein in X-linked adrenoleukodystrophy and multiple sclerosis. *Journal of Neuroimmunology*, **119** (1), 88-94.

Schmierer, K., Parkes, H. G., So, P. W., An, S. F., Brandner, S., Ordidge, R. J., Yousry, T. A. and Miller, D. H. (2010). High field (9.4 tesla) magnetic resonance imaging of cortical grey matter lesions in multiple sclerosis. *Brain*, **133** (3), 858-867.

Schnell, S. A., Staines, W. A. and Wessendorf, M. W. (1999). Reduction of lipofuscin-like autofluorescence in fluorescently labeled tissue. *Journal of Histochemistry & Cytochemistry*, **47** (6), 719-730.

Schönrock, L. M., Gawlowski, G. and Brück, W. (2000). Interleukin-6 expression in human multiple sclerosis lesions. *Neuroscience Letters*, **294** (1), 45-48.

Schotta, G., Lachner, M., Sarma, K., Ebert, A., Sengupta, R., Reuter, G., Reinberg, D. and Jenuwein, T. (2004). A silencing pathway to induce H3-K9 and H4-K20 trimethylation at constitutive heterochromatin. *Genes & Development*, **18** (11), 1251-1262.

Schulze, C. and Firth, J. A. (1993). Immunohistochemical localization of adherens junction components in blood-brain barrier microvessels of the rat. *Journal of Cell Science*, **104** (3), 773-782.

Schutz-Geschwender, A., Zhang, Y., Holt, T., McDermitt, D. and Olive, D. M. (2004). Quantitative, two-color western blot detection with infrared fluorescence. *LI-COR Biosciences*, .

Schwab, B. L., Guerini, D., Didszun, C., Bano, D., Ferrando-May, E., Fava, E., Tam, J., Xu, D., Xanthoudakis, S. and Nicholson, D. W. (2002). Cleavage of plasma membrane calcium pumps by caspases: A link between apoptosis and necrosis. *Cell Death and Differentiation*, **9** (8), 818-831.

Schwarz, M., Spector, L., Gortler, M., Weissshaus, O., Glass-Marmor, L., Karni, A., Dotan, N. and Miller, A. (2006). Serum anti-glc (α 1, 4) glc (α) antibodies as a biomarker for relapsing–remitting multiple sclerosis. *Journal of the Neurological Sciences*, **244** (1), 59-68.

- Sedlakova, R., Shivers, R. and Del Maestro, R. (1999). Ultrastructure of the blood-brain barrier in the rabbit. *Journal of Submicroscopic Cytology and Pathology*, **31** (1), 149-161.
- Sellner, J., Awad, A., Milo, R. and Hemmer, B. (2011). The increasing incidence and prevalence of female multiple sclerosis-A critical analysis of potential environmental factors. *Autoimmunity Reviews*, **10** (8), 495-502.
- Selmaj, K., Raine, C. S., Cannella, B. and Brosnan, C. F. (1991). Identification of lymphotoxin and tumor necrosis factor in multiple sclerosis lesions. *Journal of Clinical Investigation*, **87** (3), 949-954.
- Selmi, C., De Santis, M., Cavaciocchi, F. and Gershwin, M. E. (2010). Infectious agents and xenobiotics in the etiology of primary biliary cirrhosis. *Disease Markers*, **29** (6), 287-299.
- Selmi, C., Papini, A. M., Pugliese, P., Alcaro, M. C. and Gershwin, M. E. (2011). Environmental pathways to autoimmune diseases: The cases of primary biliary cirrhosis and multiple sclerosis. *Archives of Medical Science*, **7** (3), 368-380.
- Selter, R. C., Brilot, F., Grummel, V., Kraus, V., Cepok, S., Dale, R. C. and Hemmer, B. (2010). Antibody responses to EBV and native MOG in pediatric inflammatory demyelinating CNS diseases. *Neurology*, **74** (21), 1711-1715.
- Senshu, T., Akiyama, K. and Nomura, K. (1999). Identification of citrulline residues in the V subdomains of keratin K1 derived from the cornified layer of newborn mouse epidermis. *Experimental Dermatology*, **8** (5), 392-401.
- Senshu, T., Kan, S., Ogawa, H., Manabe, M. and Asaga, H. (1996). Preferential deimination of keratin K1 and filaggrin during the terminal differentiation of human epidermis. *Biochemical and Biophysical Research Communications*, **225** (3), 712-719.
- Serafini, B., Rosicarelli, B., Magliozzi, R., Stigliano, E. and Aloisi, F. (2004). Detection of ectopic B-cell follicles with germinal centers in the meninges of patients with secondary progressive multiple sclerosis. *Brain Pathology*, **14** (2), 164-174.
- Sharief, M. K. and Hentges, R. (1991). Association between tumor necrosis factor- α and disease progression in patients with multiple sclerosis. *New England Journal of Medicine*, **325** (7), 467-472.
- Sharma, R., Fischer, M. T., Bauer, J., Felts, P. A., Smith, K. J., Misu, T., Fujihara, K., Bradl, M. and Lassmann, H. (2010). Inflammation induced by innate immunity in the central nervous system leads to primary astrocyte dysfunction followed by demyelination. *Acta Neuropathologica*, **120** (2), 223-236.
- Shaw, P. J., Lamkanfi, M. and Kanneganti, T. (2010). NOD-like receptor (NLR) signaling beyond the inflammasome. *European Journal of Immunology*, **40** (3), 624-627.
- Shevach, E. M., Thornton, A. and Suri-Payer, E. (1998). T Lymphocyte-Mediated control of autoimmunity. In: *Novartis Foundation Symposium 215-Immunological Tolerance*, Wiley Online Library, 200-230.

- Shideman, C., Hu, S., Peterson, P. and Thayer, S. (2006). CCL5 evokes calcium signals in microglia through a kinase-, phosphoinositide-, and nucleotide-dependent mechanism. *Journal of Neuroscience Research*, **83** (8), 1471-1484.
- Shikama, N., Nusspaumer, G. and Holländer, G. A. (2009). Clearing the AIRE: On the pathophysiological basis of the autoimmune polyendocrinopathy syndrome type-1. *Endocrinology & Metabolism Clinics of North America*, **38** (2), 273-288.
- Shresta, S., Pham, C. T. N., Thomas, D. A., Graubert, T. A. and Ley, T. J. (1998). How do cytotoxic lymphocytes kill their targets? *Current Opinion in Immunology*, **10** (5), 581-587.
- Sigal, L. J., Crotty, S., Andino, R. and Rock, K. L. (1999). Cytotoxic T-cell immunity to virus-infected non-haematopoietic cells requires presentation of exogenous antigen. *Nature*, **402**, 25-29.
- Simpson, J., Rezaie, P., Newcombe, J., Cuzner, M. L., Male, D. and Woodroffe, M. N. (2000a). Expression of the [beta]-chemokine receptors CCR2, CCR3 and CCR5 in multiple sclerosis central nervous system tissue* 1. *Journal of neuroimmunology*, **108** (1-2), 192-200.
- Simpson, J., Newcombe, J., Cuzner, M. and Woodroffe, M. (2000b). Expression of the interferon- γ -inducible chemokines IP-10 and mig and their receptor, CXCR3, in multiple sclerosis lesions. *Neuropathology and Applied Neurobiology*, **26** (2), 133-142.
- Smith, K. J. (2007). Sodium channels and multiple sclerosis: Roles in symptom production, damage and therapy. *Brain Pathology*, **17** (2), 230-242.
- Sofroniew, M. V. (2009). Molecular dissection of reactive astrogliosis and glial scar formation. *Trends in Neurosciences*, **32** (12), 638-647.
- Sospedra, M. and Martin, R. (2005). Immunology of multiple sclerosis*. *Annual Review of Immunology*, **23**, 683-747.
- Sospedra, M. and Martin, R. (2008). Immunology of Multiple Sclerosis, in Raine, C.S., McFarland, H. and Hohlfeld, R. (eds), *Multiple Sclerosis: A Comprehensive Text*. 1st ed., London, Elsevier Limited, 192-213.
- Stahl, E. A., Raychaudhuri, S., Remmers, E. F., Xie, G., Eyre, S., Thomson, B. P., Li, Y., Kurreeman, F. A. S., Zhernakova, A. and Hinks, A. (2010). Genome-wide association study meta-analysis identifies seven new rheumatoid arthritis risk loci. *Nature Genetics*, **42** (6), 508-514.
- Staines, A., Hanif, S., Ahmed, S., McKinney, P., Shera, S. and Bodansky, H. (1997). Incidence of insulin dependent diabetes mellitus in karachi, pakistan. *Archives of Disease in Childhood*, **76** (2), 121-123.
- Starr, T. K., Jameson, S. C. and Hogquist, K. A. (2003). Positive and negative selection of T cells. *Annual Review of Immunology*, **21** (1), 139-176.
- Stensland, M., Holm, A., Kiehne, A. and Fleckenstein, B. (2009). Targeted analysis of protein citrullination using chemical modification and tandem mass spectrometry. *Rapid Communications in Mass Spectrometry*, **23** (17), 2754-2762.

- Stichel, C. and Müller, H. W. (1998). The CNS lesion scar: New vistas on an old regeneration barrier. *Cell and Tissue Research*, **294** (1), 1-9.
- Storch, M. K., Piddlesden, S., Haltia, M., Iivanainen, M., Morgan, P. and Lassmann, H. (1998). Multiple sclerosis: In situ evidence for antibody- and complement-mediated demyelination. *Annals of Neurology*, **43** (4), 465-471.
- Storck, T., Schulte, S., Hofmann, K. and Stoffel, W. (1992). Structure, expression, and functional analysis of a Na-dependent glutamate/aspartate transporter from rat brain. *Proceedings of the National Academy of Sciences*, **89** (22), 10955-10959.
- Struyf, S., Noppen, S., Loos, T., Mortier, A., Gouwy, M., Verbeke, H., Huskens, D., Luangsay, S., Parmentier, M. and Geboes, K. (2009). Citrullination of CXCL12 differentially reduces CXCR4 and CXCR7 binding with loss of inflammatory and anti-HIV-1 activity via CXCR4. *The Journal of Immunology*, **182** (1), 666.
- Surh, C. D. and Sprent, J. (1994). T-cell apoptosis detected in situ during positive and negative selection in the thymus. *Nature*, **372** (6501), 100-103.
- Süss, G. and Shortman, K. (1996). A subclass of dendritic cells kills CD4 T cells via Fas/Fas-ligand-induced apoptosis. *The Journal of Experimental Medicine*, **183** (4), 1789-1796.
- Suzuki, A., Yamada, R., Chang, X., Tokunishi, S., Sawada, T., Suzuki, M., Nagasaki, M., Nakayama-Hamada, M., Kawaida, R. and Ono, M. (2003). Functional haplotypes of PADI4, encoding citrullinating enzyme peptidylarginine deiminase 4, are associated with rheumatoid arthritis. *Nature Genetics*, **34** (4), 395-402.
- Swanson, K. A., Zheng, Y., Heidler, K. M., Mizobuchi, T. and Wilkes, D. S. (2004). CD11c cells modulate pulmonary immune responses by production of indoleamine 2, 3-dioxygenase. *American Journal of Respiratory Cell and Molecular Biology*, **30** (3), 311-318.
- Symons, D. (1995). Frequency of lupus in people of african origin. *Lupus*, **4** (3), 176-178.
- Takahara, H., Okamoto, H. and Sugawara, K. (1986). Affinity chromatography of peptidylarginine deiminase from rabbit skeletal muscle on a column of soybean trypsin inhibitor (kunitz)-sepharose. *Journal of Biochemistry*, **99** (5), 1417-1424.
- Takahashi, K., Rochford, C. D. P. and Neumann, H. (2005). Clearance of apoptotic neurons without inflammation by microglial triggering receptor expressed on myeloid cells-2. *The Journal of Experimental Medicine*, **201** (4), 647-657.
- Takahashi, T., Kuniyasu, Y., Toda, M., Sakaguchi, N., Itoh, M., Iwata, M., Shimizu, J. and Sakaguchi, S. (1998). Immunologic self-tolerance maintained by CD25⁺ CD4⁺ naturally anergic and suppressive T cells: Induction of autoimmune disease by breaking their anergic/suppressive state. *International Immunology*, **10** (12), 1969-1980.
- Takahashi, T., Tagami, T., Yamazaki, S., Uede, T., Shimizu, J., Sakaguchi, N., Mak, T. W. and Sakaguchi, S. (2000). Immunologic self-tolerance maintained by CD25⁺ CD4⁺ regulatory T cells constitutively expressing cytotoxic T lymphocyte-associated antigen 4. *The Journal of Experimental Medicine*, **192** (2), 303-310.

- Takami, N., Osawa, K., Miura, Y., Komai, K., Taniguchi, M., Shiraishi, M., Sato, K., Iguchi, T., Shiozawa, K. and Hashiramoto, A. (2006). Hypermethylated promoter region of DR3, the death receptor 3 gene, in rheumatoid arthritis synovial cells. *Arthritis & Rheumatism*, **54** (3), 779-787.
- Takeda, K. and Akira, S. (2005). Toll-like receptors in innate immunity. *International Immunology*, **17** (1), 1-14.
- Tarantini, L., Bonzini, M., Apostoli, P., Pegoraro, V., Bollati, V., Marinelli, B., Cantone, L., Rizzo, G., Hou, L. and Schwartz, J. (2009). Effects of particulate matter on genomic DNA methylation content and iNOS promoter methylation. *Environmental Health Perspectives*, **117** (2), 217-222.
- Tarcsa, E., Marekov, L. N., Mei, G., Melino, G., Lee, S. C. and Steinert, P. M. (1996). Protein unfolding by peptidylarginine deiminase. *Journal of Biological Chemistry*, **271** (48), 30709-30716.
- Terakawa, H., Takahara, H. and Sugawara, K. (1991). Three types of mouse peptidylarginine deiminase: Characterization and tissue distribution. *Journal of Biochemistry*, **110** (4), 661-666.
- Terness, P., Bauer, T. M., Röse, L., Dufter, C., Watzlik, A., Simon, H. and Opelz, G. (2002). Inhibition of allogeneic T cell proliferation by indoleamine 2, 3-Dioxygenase-expressing dendritic cells. *The Journal of Experimental Medicine*, **196** (4), 447-457.
- Thiagalingam, S. A. M., Cheng, K. H., Lee, H. J., Mineva, N., Thiagalingam, A. and Ponte, J. F. (2003). Histone deacetylases: Unique players in shaping the epigenetic histone code. *Annals of the New York Academy of Sciences*, **983** (1), 84-100.
- Thorsby, E. and Lie, B. A. (2005). HLA associated genetic predisposition to autoimmune diseases: Genes involved and possible mechanisms. *Transplant Immunology*, **14** (3-4), 175-182.
- Tobón, G. J., Youinou, P. and Saraux, A. (2010). The environment, geo-epidemiology, and autoimmune disease: Rheumatoid arthritis. *Journal of Autoimmunity*, **35** (1), 10-14.
- Tombal, B., Denmeade, S., Gillis, J. and Isaacs, J. (2002). A supramicromolar elevation of intracellular free calcium ($[Ca^{2+}]_i$) is consistently required to induce the execution phase of apoptosis. *Cell Death and Differentiation*, **9**, 561-573.
- Torgerson, T. R. and Ochs, H. D. (2007). Immune dysregulation, polyendocrinopathy, enteropathy, X-linked: Forkhead box protein 3 mutations and lack of regulatory T cells. *Journal of Allergy and Clinical Immunology*, **120** (4), 744-750.
- Tranquill, L. R., Cao, L., Ling, N. C., Kalbacher, H., Martin, R. M. and Whitaker, J. N. (2000). Enhanced T cell responsiveness to citrulline-containing myelin basic protein in multiple sclerosis patients. *Multiple Sclerosis*, **6** (4), 220-225.
- Trapani, J. A., Davis, J., Sutton, V. R. and Smyth, M. J. (2000). Proapoptotic functions of cytotoxic lymphocyte granule constituents in vitro and in vivo. *Current Opinion in Immunology*, **12** (3), 323-329.
- Trapp, B. D., Peterson, J., Ransohoff, R. M., Rudick, R., Mork, S. and Bo, L. (1998). Axonal transection in the lesions of multiple sclerosis. *The New England Journal of Medicine*, **338** (5), 278-285.

- Trapp, B. D., Wujek, J. R., Criste, G. A., Jalabi, W., Yin, X., Kidd, G. J., Stohlman, S. and Ransohoff, R. (2006). Evidence for synaptic stripping by cortical microglia. *Glia*, **55** (4), 360-368.
- Traugott, U., Reinherz, E. and Raine, C. (1983). Multiple sclerosis: Distribution of T cells, T cell subsets and Ia-positive macrophages in lesions of different ages. *Journal of Neuroimmunology*, **4** (3), 201-221.
- Tsacopoulos, M. and Magistretti, P. J. (1996). Metabolic coupling between glia and neurons. *The Journal of Neuroscience*, **16** (3), 877-885.
- Turvey, S. E. and Broide, D. H. (2010). Innate immunity. *Journal of Allergy and Clinical Immunology*, **125** (2), S24-S32.
- Tutturen, A. E. V., Holm, A., Jørgensen, M., Stadtmüller, P., Rise, F. and Fleckenstein, B. (2010). A technique for the specific enrichment of citrulline containing peptides. *Analytical Biochemistry*, **403** (1-2), 43-51.
- Ueno, T., Saito, F., Gray, D. H. D., Kuse, S., Hieshima, K., Nakano, H., Kakiuchi, T., Lipp, M., Boyd, R. L. and Takahama, Y. (2004). CCR7 signals are essential for cortex-medulla migration of developing thymocytes. *The Journal of Experimental Medicine*, **200** (4), 493-505.
- Urano, Y., Watanabe, K., Sakaki, A., Arase, S., Watanabe, Y., Shigemi, F., Takeda, K., Akiyama, K. and Senshu, T. (1990). Immunohistochemical demonstration of peptidylarginine deiminase in human sweat glands. *The American Journal of Dermatopathology*, **12** (3), 249-255.
- Van Boxel-Dezaire, A. H. H., Hoff, S. C. J., Van Oosten, B. W., Verweij, C. L., Dräger, A. M., Ader, H. J., Van Houwelingen, J. C., Barkhof, F., Polman, C. H. and Nagelkerken, L. (1999). Decreased interleukin-10 and increased interleukin-12p40 mRNA are associated with disease activity and characterize different disease stages in multiple sclerosis. *Annals of Neurology*, **45** (6), 695-703.
- van der Linden, M. P. M., van der Woude, D., Ioan-Facsinay, A., Levarht, E., Stoeken-Rijsbergen, G., Huizinga, T. W. J., Toes, R. E. M. and van der Helm-van Mil, A. (2009). Value of anti-modified citrullinated vimentin and third-generation anti-cyclic citrullinated peptide compared with second-generation anti-cyclic citrullinated peptide and rheumatoid factor in predicting disease outcome in undifferentiated arthritis and rheumatoid arthritis. *Arthritis & Rheumatism*, **60** (8), 2232-2241.
- van der Valk, P. and Amor, S. (2009). Preactive lesions in multiple sclerosis. *Current Opinion in Neurology*, **22** (3), 207-213.
- Van der Valk, P. and De Groot, C. (2000). Staging of multiple sclerosis (MS) lesions: Pathology of the time frame of MS. *Neuropathology and Applied Neurobiology*, **26** (1), 2-10.
- van Venrooij, W. J., van Beers, J. J. B. C. and Pruijn, G. J. M. (2011). Anti-CCP antibodies: The past, the present and the future. *Nature Reviews Rheumatology*, **7** (7), 391-398.
- Van Waesberghe, J., Kamphorst, W., De Groot, C., Van Walderveen, M., Castelijns, J., Ravid, R., Lycklama a Nijeholt, G., Van der Valk, P., Polman, C. and Thompson, A.

(1999). Axonal loss in multiple sclerosis lesions: Magnetic resonance imaging insights into substrates of disability. *Annals of Neurology*, **46** (5), 747-754.

Vandesompele, J., De Preter, K., Pattyn, F., Poppe, B., Van Roy, N., De Paepe, A. and Speleman, F. (2002). Accurate normalization of real-time quantitative RT-PCR data by geometric averaging of multiple internal control genes. *Genome Biology*, **3** (7), 1-11.

Vang, T., Congia, M., Macis, M. D., Musumeci, L., Orrú, V., Zavattari, P., Nika, K., Tautz, L., Taskén, K. and Cucca, F. (2005). Autoimmune-associated lymphoid tyrosine phosphatase is a gain-of-function variant. *Nature Genetics*, **37** (12), 1317-1319.

Verma, S., Nakaoke, R., Dohgu, S. and Banks, W. A. (2006). Release of cytokines by brain endothelial cells: A polarized response to lipopolysaccharide. *Brain, Behavior, and Immunity*, **20** (5), 449-455.

Viegas, M. S., Martins, T. C., Seco, F. and Do Carmo, A. (2009). An improved and cost-effective methodology for the reduction of autofluorescence in direct immunofluorescence studies on formalin-fixed paraffin-embedded tissues. *European Journal of Histochemistry*, **51** (1), 59-66.

Villar, L. M., Masjuan, J., González-Porqué, P., Plaza, J., Sádaba, M. C., Roldán, E., Bootello, A. and Alvarez-Cermeno, J. C. (2002). Intrathecal IgM synthesis predicts the onset of new relapses and a worse disease course in MS. *Neurology*, **59** (4), 555-559.

Vincent, S. R., Leung, E. and Watanabe, K. (1992). Immunohistochemical localization of peptidylarginine deiminase in the rat brain. *Journal of Chemical Neuroanatomy*, **5** (2), 159-168.

Vogt, M. H. J., Teunissen, C. E., Iacobaeus, E., Heijnen, D. A. M., Breij, E. C. W., Olsson, T., Brundin, L., Killestein, J. and Dijkstra, C. D. (2009). Cerebrospinal fluid anti-myelin antibodies are related to magnetic resonance measures of disease activity in multiple sclerosis. *Journal of Neurology, Neurosurgery & Psychiatry*, **80** (10), 1110-1115.

Völzke, H., Werner, A., Wallaschofski, H., Friedrich, N., Robinson, D. M., Kindler, S., Kraft, M., John, U. and Hoffmann, W. (2005). Occupational exposure to ionizing radiation is associated with autoimmune thyroid disease. *Journal of Clinical Endocrinology & Metabolism*, **90** (8), 4587-4592.

Vossenaar, E. R., Radstake, T. R. D., van der Heijden, A., van Mansum, M. A. M., Dieteren, C., de Rooij, D. J., Barrera, P., Zendman, A. J. W. and van Venrooij, W. J. (2004). Expression and activity of citrullinating peptidylarginine deiminase enzymes in monocytes and macrophages. *Annals of the Rheumatic Diseases*, **63** (4), 373-381.

Vossenaar, E. R. and van Venrooij, W. J. (2004). Citrullinated proteins: Sparks that may ignite the fire in rheumatoid arthritis. *Arthritis Research & Therapy*, **6** (3), 107-111.

Vossenaar, E. R., Zendman, A. J. W., van Venrooij, W. J. and Pruijn, G. J. M. (2003). PAD, a growing family of citrullinating enzymes: Genes, features and involvement in disease. *BioEssays*, **25** (11), 1106-1118.

Wada, Y. and Kadoya, M. (2003). In-gel digestion with endoproteinase LysC. *Journal of Mass Spectrometry*, **38** (1), 117-118.

- Wakasa, S., Shiiya, N., Tachibana, T., Ooka, T. and Matsui, Y. (2009). A semiquantitative analysis of reactive astrogliosis demonstrates its correlation with the number of intact motor neurons after transient spinal cord ischemia. *The Journal of Thoracic and Cardiovascular Surgery*, **137** (4), 983-990.
- Walker, L. S. K. and Abbas, A. K. (2002). The enemy within: Keeping self-reactive T cells at bay in the periphery. *Nature Reviews Immunology*, **2** (1), 11-19.
- Wallin, M. T., Page, W. F. and Kurtzke, J. F. (2003). Multiple sclerosis in US veterans of the vietnam era and later military service: Race, sex, and geography. *Annals of Neurology*, **55** (1), 65-71.
- Wang, L., Chang, X., Yuan, G., Zhao, Y. and Wang, P. (2010). Expression of peptidylarginine deiminase type 4 in ovarian tumors. *International Journal of Biological Sciences*, **6** (5), 454-464.
- Wang, Y., Wysocka, J., Sayegh, J., Lee, Y. H., Perlin, J. R., Leonelli, L., Sonbuchner, L. S., McDonald, C. H., Cook, R. G. and Dou, Y. (2004). Human PAD4 regulates histone arginine methylation levels via demethyliminination. *Science*, **306** (5694), 279-283.
- Washburn, T., Schweighoffer, E., Gridley, T., Chang, D., Fowlkes, B., Cado, D. and Robey, E. (1997). Notch activity influences the $\alpha\beta$ versus $\gamma\delta$ T cell lineage decision. *Cell*, **88** (6), 833-843.
- Watanabe, K., Akiyama, K., Hikichi, K., Ohtsuka, R., Okuyama, A. and Senshu, T. (1988). Combined biochemical and immunochemical comparison of peptidylarginine deiminases present in various tissues. *Biochimica et Biophysica Acta (BBA)-General Subjects*, **966** (3), 375-383.
- Weber, M. S. and Hemmer, B. (2010). Cooperation of B cells and T cells in the pathogenesis of multiple sclerosis. *Results and Problems in Cell Differentiation*, **51** , 115-126.
- Weber, M. S., Hemmer, B. and Cepok, S. (2011). The role of antibodies in multiple sclerosis. *Biochimica et Biophysica Acta (BBA)-Molecular Basis of Disease*, **1812** (2), 239-245.
- Wegmann, T. G., Lin, H., Guilbert, L. and Mosmann, T. R. (1993). Bidirectional cytokine interactions in the maternal-fetal relationship: Is successful pregnancy a TH2 phenomenon? *Immunology Today*, **14** (7), 353-356.
- Weksler, B. B., Subileau, E. A., Perriere, N., Charneau, P., Holloway, K., Leveque, M., Tricoire-Leignel, H., Nicotra, A., Bourdoulous, S. and Turowski, P. (2005). Blood-brain barrier-specific properties of a human adult brain endothelial cell line. *The FASEB Journal*, **19** , 1872-1874.
- Whitacre, C. C. (2001). Sex differences in autoimmune disease. *Nature Immunology*, **2** (9), 777-780.
- Whitaker, J. N. (1977). Myelin encephalitogenic protein fragments in cerebrospinal fluid of persons with multiple sclerosis. *Neurology*, **27** (10), 911.

- Whitaker, J. R. and Granum, P. E. (1980). An absolute method for protein determination based on difference in absorbance at 235 and 280 nm. *Analytical Biochemistry*, **109** (1), 156-159.
- Whiting, P. F., Smidt, N., Sterne, J., Harbord, R., Burton, A., Burke, M., Beynon, R., Ben-Shlomo, Y., Axford, J. and Dieppe, P. (2010). Systematic review: Accuracy of anti-citrullinated peptide antibodies for diagnosing rheumatoid arthritis. *Annals of Internal Medicine*, **152** (7), 456.
- Willer, C. J., Dyment, D. A., Risch, N. J., Sadovnick, A. D. and Ebers, G. C. (2003). Twin concordance and sibling recurrence rates in multiple sclerosis. *Proceedings of the National Academy of Sciences*, **100** (22), 12877-12882.
- Williamson, R. A., Burgoon, M. P., Owens, G. P., Ghausi, O., Leclerc, E., Firme, L., Carlson, S., Corboy, J., Parren, P. W. H. I. and Sanna, P. P. (2001). Anti-DNA antibodies are a major component of the intrathecal B cell response in multiple sclerosis. *Proceedings of the National Academy of Sciences*, **98** (4), 1793-1798.
- Wing, K. and Sakaguchi, S. (2009). Regulatory T cells exert checks and balances on self tolerance and autoimmunity. *Nature Immunology*, **11** (1), 7-13.
- Wolburg, H. and Lippoldt, A. (2002). Tight junctions of the blood–brain barrier: Development, composition and regulation. *Vascular Pharmacology*, **38** (6), 323-337.
- Wolburg, H., Noell, S., Mack, A., Wolburg-Buchholz, K. and Fallier-Becker, P. (2009). Brain endothelial cells and the glio-vascular complex. *Cell and Tissue Research*, **335** (1), 75-96.
- Wolfer, A., Wilson, A., Nemir, M., MacDonald, H. R. and Radtke, F. (2002). Inactivation of Notch1 impairs VDJ [beta] rearrangement and allows pre-TCR-independent survival of early [alpha][beta] lineage thymocytes. *Immunity*, **16** (6), 869-879.
- Wolswijk, G. (1998). Chronic stage multiple sclerosis lesions contain a relatively quiescent population of oligodendrocyte precursor cells. *The Journal of Neuroscience*, **18** (2), 601-609.
- Wong, D., Dorovini-Zis, K. and Vincent, S. R. (2004). Cytokines, nitric oxide, and cGMP modulate the permeability of an in vitro model of the human blood–brain barrier. *Experimental Neurology*, **190** (2), 446-455.
- Wong, M. L. and Medrano, J. F. (2005). Real-time PCR for mRNA quantitation. *BioTechniques*, **39** (1), 75-85.
- Wood, D. D., Ackerley, C. A., Brand, B., Zhang, L., Raijmakers, R., Mastronardi, F. G. and Moscarello, M. A. (2008). Myelin localization of peptidylarginine deiminases 2 and 4: Comparison of PAD2 and PAD4 activities. *Laboratory Investigation*, **88** (4), 354-364.
- Wood, D. D., Bilbao, J. M., O'Connors, P. and Moscarello, M. A. (1996). Acute multiple sclerosis (marburg type) is associated with developmentally immature myelin basic protein. *Annals of Neurology*, **40** (1), 18-24.
- Wood, D. D. and Moscarello, M. A. (1989). The isolation, characterization, and lipid-aggregating properties of a citrulline containing myelin basic protein. *Journal of Biological Chemistry*, **264** (9), 5121-5127.

- Woodrooffe, M. N., Bellamy, A. S., Feldmann, M., Davison, A. N. and Cuzner, M. L. (1986). Immunocytochemical characterisation of the immune reaction in the central nervous system in multiple sclerosis: Possible role for microglia in lesion growth. *Journal of the Neurological Sciences*, **74** (2), 135-152.
- Woodrooffe, M. N. and Cuzner, M. L. (1993). Cytokine mRNA expression in inflammatory multiple sclerosis lesions: Detection by non-radioactive in situ hybridization. *Cytokine*, **5** (6), 583-588.
- Yamaguchi, T., Hirota, K., Nagahama, K., Ohkawa, K., Takahashi, T., Nomura, T. and Sakaguchi, S. (2007). Control of immune responses by antigen-specific regulatory T cells expressing the folate receptor. *Immunity*, **27** (1), 145-159.
- Yang, Z., Wang, K., Li, T., Sun, W., Li, Y., Chang, Y. F., Dorman, J. S. and LaPorte, R. E. (1998). Childhood diabetes in china: Enormous variation by place and ethnic group. *Diabetes Care*, **21** (4), 525-529.
- Yeager, M. P., DeLeo, J. A., Hoopes, P. J., Hartov, A., Hildebrandt, L. and Hickey, W. F. (2000). Trauma and inflammation modulate lymphocyte localization in vivo: Quantitation of tissue entry and retention using indium-111-labeled lymphocytes. *Critical Care Medicine*, **28** (5), 1477.
- Yeivin, A. and Razin, A. (1993). Gene methylation patterns and expression. *Experientia. Supplementum*, (64), 523-568.
- Yeo, T. W., De Jager, P. L., Gregory, S. G., Barcellos, L. F., Walton, A., Goris, A., Fenoglio, C., Ban, M., Taylor, C. J. and Goodman, R. S. (2007). A second major histocompatibility complex susceptibility locus for multiple sclerosis. *Annals of Neurology*, **61** (3), 228-236.
- Ying, S., Dong, S., Kawada, A., Kojima, T., Chavanas, S., Méchin, M. C., Adoue, V., Serre, G., Simon, M. and Takahara, H. (2009). Transcriptional regulation of peptidylarginine deiminase expression in human keratinocytes. *Journal of Dermatological Science*, **53** (1), 2-9.
- Zeman, A. Z., Kidd, D., McLean, B. N., Kelly, M. A., Francis, D. A., Miller, D. H., Kendall, B. E., Rudge, P., Thompson, E. J. and McDonald, W. I. (1996). A study of oligoclonal band negative multiple sclerosis. *Journal of Neurology, Neurosurgery & Psychiatry*, **60** (1), 27-30.
- Zenewicz, L. A., Abraham, C., Flavell, R. A. and Cho, J. H. (2010). Unraveling the genetics of autoimmunity. *Cell*, **140** (6), 791-797.
- Zhang, D., Hu, X., Qian, L., O'Callaghan, J. P. and Hong, J. S. (2010). Astrogliosis in CNS pathologies: Is there a role for microglia? *Molecular Neurobiology*, **41** (2), 232-241.
- Zhang, H., Zhu, Z. and Meadows, G. G. (2011). Chronic alcohol consumption decreases the percentage and number of NK cells in the peripheral lymph nodes and exacerbates B16BL6 melanoma metastasis into the draining lymph nodes. *Cellular Immunology*, **266** (2), 172-179.
- Zhang, Y. and Pardridge, W. M. (2001). Rapid transferrin efflux from brain to blood across the blood-brain barrier. *Journal of Neurochemistry*, **76** (5), 1597-1600.

Zhong, Y., Hyung, S. J. and Ruotolo, B. T. (2011). Characterizing the resolution and accuracy of a second-generation traveling-wave ion mobility separator for biomolecular ions. *Analyst*, **136** (17), 3534-3541.

Zhou, D., Srivastava, R., Nessler, S., Grummel, V., Sommer, N., Brück, W., Hartung, H. P., Stadelmann, C. and Hemmer, B. (2006). Identification of a pathogenic antibody response to native myelin oligodendrocyte glycoprotein in multiple sclerosis. *Proceedings of the National Academy of Sciences*, **103** (50), 19057-19062.

Zhu, X. and Papayannopoulos, I. A. (2003). Improvement in the detection of low concentration protein digests on a MALDI TOF/TOF workstation by reducing α -cyano-4-hydroxycinnamic acid adduct ions. *Journal of Biomolecular Techniques*, **14** (4), 298-307.

Zinkernagel, R. M. and Doherty, P. C. (1997). The discovery of MHC restriction. *Immunology Today*, **18** (1), 14-17.

Zlokovic, B. V. (2008). The blood-brain barrier in health and chronic neurodegenerative disorders. *Neuron*, **57** (2), 178-201.

Zonta, M., Angulo, M. C., Gobbo, S., Rosengarten, B., Hossmann, K. A., Pozzan, T. and Carmignoto, G. (2003). Neuron-to-astrocyte signaling is central to the dynamic control of brain microcirculation. *Nature Neuroscience*, **6** (1), 43-50.

Zuvich, R. L., McCauley, J. L., Pericak-Vance, M. A. and Haines, J. L. (2009). Genetics and pathogenesis of multiple sclerosis. In: *Seminars in Immunology*, Elsevier, 328-333.



**Central Office for Research Ethics Committees
(COREC)**

CONDITIONS OF ETHICAL APPROVAL

Research Ethics Committee:	MREC FOR WALES
Research Tissue Bank:	THE UK MULTIPLE SCLEROSIS TISSUE BANK
REC reference number:	08/MRE09/31
Name of applicant:	PROFESSOR RICHARD REYNOLDS (DESIGNATED INDIVIDUAL : MR G. ROPER)
Date of approval:	08 MAY 2008

Ethical approval is given to the Research Tissue Bank ("the Bank") by the Research Ethics Committee ("the Committee") subject to the following conditions.

1. Further communications with the Committee

- 1.1 Further communications with the Committee are the personal responsibility of the applicant.

2. Duration of approval

- 2.1 Approval is given for a period of 5 years, which may be renewed on consideration of a new application by the Committee, taking account of developments in legislation, policy and guidance in the interim. New applications should include relevant changes of policy or practice made by the Bank since the original approval together with any proposed new developments.

3. Licensing

- 3.1 A copy of the Licence from the Human Tissue Authority (HTA) should be provided when available (if not already submitted).
- 3.2 The Committee should be notified if the Authority renews the licence, varies the licensing conditions or revokes the Licence, or of any change of Designated Individual. If the Licence is revoked, ethical approval would be terminated.

4. Generic ethical approval for projects receiving tissue

- 4.1 Samples of human tissue or other biological material may be supplied and used in research projects to be conducted within the establishment responsible for the Bank and/or by researchers and research institutions external to the Bank within the UK and in other countries in accordance with the following conditions
- 4.1.1 The research project should be within the fields of medical or biomedical research described in the approved application form.
 - 4.1.2 The Bank should be satisfied that the research has been subject to scientific critique, is appropriately designed in relation to its objectives and (with the exception of student research below doctoral level) is likely to add something useful to existing knowledge
 - 4.1.3 Where tissue samples have been donated with informed consent for use in future research ("broad consent"), the Bank should be satisfied that the use of the samples complies with the terms of the donor consent.
 - 4.1.4 All samples and any associated clinical information must be non-identifiable to the researcher at the point of release (i.e. anonymised or linked anonymised).
 - 4.1.5 Samples will not be released to any project requiring further data or tissue from donors or involving any other research procedures. Any contact with donors must be confined to ethically approved arrangements for the feedback of clinically significant information.
 - 4.1.6 A supply agreement must be in place with the researcher to ensure storage, use and disposal of the samples in accordance with the HTA Codes of Practice, the terms of the ethical approval and any other conditions required by the Bank.
- 4.2 A research project in the UK using tissue provided by a Bank in accordance with these conditions will be considered to have ethical approval from the Committee under the terms of this approval. In England, Wales and Northern Ireland this means that the researcher will not require a licence from the Human Tissue Authority for storage of the tissue for use in relation to this project.
- 4.3 The Bank may require any researcher to seek specific ethical approval for their project. Such applications should normally be made to the Committee and booked via the COREC Central Allocation System.
- 4.4 A Notice of Amendment form should be submitted to seek the Committee's agreement to change the conditions of generic approval.

5. Records

- 5.1 The Bank should maintain a record of all research projects to which tissue has been supplied. The record should contain at least the full title of the project, a summary of its purpose, the name of the Chief Investigator, the sponsor, the location of the research, the date on which the project was approved by the Bank, details of the tissue released and any relevant reference numbers.
- 5.2 The Committee may request access to these records at any time.

6. Annual reports

- 6.1 An annual report should be provided to the Committee listing all projects for which tissue has been released in the previous year. The list should give the full title of each project, the name of the Chief Investigator, the sponsor, the location of the research and the date of approval by the Bank. The report is due on the anniversary of the date on which ethical approval for the Bank was given.

6.2 The Committee may request additional reports on the management of the Bank at any time.

7. Substantial amendments

- 7.1 Substantial amendments should be notified to the Committee and ethical approval sought before implementing the amendment. A substantial amendment generally means any significant change to the arrangements for the management of the Bank as described in the application to the Committee and supporting documentation.
- 7.2 The COREC Notice of Amendment form should be used to seek approval. The form is available at <http://www.corec.org.uk/applicants/apply/amendments.htm#other>.
- 7.3 The following changes should always be notified as substantial amendments:
 - 7.3.1 Any significant change to the policy for use of the tissue in research, including changes to the types of research to be undertaken or supported by the Bank.
 - 7.3.2 Any significant change to the types of biological material to be collected and stored, or the circumstances of collection.
 - 7.3.3 Any significant change to informed consent arrangements, including new/modified information sheets and consent forms.
 - 7.3.4 A change to the conditions of generic approval.
 - 7.3.5 Any other significant change to the governance of the RTB.

8. Serious adverse events

- 8.1 The Committee should be notified as soon as possible of any serious adverse event or reaction, any serious breach of security or confidentiality, or any other incident that could undermine public confidence in the ethical management of the tissue. The criteria for notifying the Committee will be the same as those for notifying the Human Tissue Authority in the case of research tissue banks in England, Wales and Northern Ireland.

9. Other information to be notified

- 9.1 The Committee should be notified of any change in the contact details for the applicant or where the applicant hands over responsibility for communication with the Committee to another person at the establishment.

10. Closure of the Bank

- 10.1 Any plans to close the Bank should be notified to the Committee as early as possible and at least two months before closure. The Committee should be informed what arrangements are to be made for disposal of the tissue or transfer to another research tissue bank.
- 10.2 Where tissue is transferred to another research tissue bank, the ethical approval for the Bank is not transferable. Where the second bank is ethically approved, it should notify the responsible Research Ethics Committee. The terms of its own ethical approval would apply to any tissue it receives.

11. Breaches of approval conditions

- 11.1 The Committee should be notified as soon as possible of any breach of these approval conditions.
- 11.2 Where serious breaches occur, the Committee may review its ethical approval and may, exceptionally, suspend or terminate the approval.

Leeds (West) Research Ethics Committee

Room 22
Floor CD, Block 40
King Edward Home
Leeds General Infirmary
Leeds
LS1 3EX

Telephone: 0113 3923181

Facsimile: 0113 3926799

14 January 2010

Dr. Basil Sharrack
Consultant Neurologist
Department of Neurology
Royal Hallamshire Hospital
Glossop Road, Sheffield
S10 2JF

Dear Dr. Sharrack

Study Title: **Antibodies as indicators of specific neurological conditions.**

REC reference number: **10/H1307/1**

Protocol number: **1**

The Research Ethics Committee reviewed the above application at the meeting held on 08 January 2010. The Committee would like to thank Ms Bradford and Professor Woodroffe for attending to discuss the study. The recruitment procedure was

discussed; Ms Bradford confirmed that the clinicians would approach the potential participants and take consent.

Ms Bradford explained that the clinicians would decide whether a lumbar puncture is required and would be in a position within 3 months to know if a positive multiple sclerosis diagnosis is made. Ms Bradford confirmed that severity of symptoms would be assessed by EDSS; members commented that no mention is made in the application to routine clinical data being collected.

The Committee were concerned that the application indicated that 30 mls of CSF would be taken; Professor Woodroffe confirmed that only a 5mls sample would be required and a larger amount of blood.

Discussion took place on the storage of the samples at the end of the study; Professor Woodroffe confirmed that collection will be during Ms Bradford's second year of study, the samples would be analysed during her third year and the samples would be stored for a further year after which a decision would be made on whether to conduct a further ethics project.

Documents reviewed

The documents reviewed at the meeting were:

<i>Document</i>	<i>Version</i>	<i>Date</i>
Covering Letter		
1	23 November 2009	
REC application		
2.5	27 July 2009	
Protocol		

1	20 October 2009	
Investigator CV		
1	23 November 2009	
Participant Information Sheet: Information Sheet for Patients		
1	07 August 2009	
Participant Consent Form: Patient Consent Form		
1	01 October 2009	
Letter from Statistician		
1	19 November 2009	
Award Letter		
1	11 August 2008	
CV - Claire Bradford		
1	23 November 2009	
CV - Nicola Woodroffe		
1	23 November 2009	

Provisional opinion

The Committee would be content to give a favourable ethical opinion of the research, subject to receiving a complete response to the request for further information set out below.

The Committee delegated authority to confirm its final opinion on the application to a meeting of the sub-committee of the REC.

Further information or clarification required

- 1 The Committee considers that potential participants should not be excluded if they do not speak English, and that the translators who have been employed for clinical reasons could assist.
- 2 The participant information sheet should be simplified and should state that the study is for an educational qualification.
- 3 The consent form should follow NRES guidelines and should have the mandatory section on regulatory authorities.
- 4 Information should be provided on the routine clinical data to be recorded.
- 5 Please confirm that data transferred electronically will be encrypted.

When submitting your response to the Committee, please send revised documentation where appropriate underlining or otherwise highlighting the changes you have made and giving revised version numbers and dates.

If the committee has asked for clarification or changes to any answers given in the application form, please do not submit a revised copy of the application form; these can be addressed in a covering letter to the REC.

The Committee will confirm the final ethical opinion within a maximum of 60 days from the date of initial receipt of the application, excluding the time taken by you to respond

fully to the above points. A response should be submitted by no later than 14 May 2010.

Membership of the Committee

The members of the Committee who were present at the meeting are listed on the attached sheet.

Statement of compliance

The Committee is constituted in accordance with the Governance Arrangements for Research Ethics Committees (July 2001) and complies fully with the Standard Operating Procedures for Research Ethics Committees in the UK.

10/H1307/1

Please quote this number on all correspondence

Yours sincerely

Dr Rhona Bratt

Chair

Email: Elaine.hazell@leedsth.nhs.uk

Enclosures: List of names and professions of members who were present at the meeting and those who submitted written comments.

Copy to: Dr Ramila Patel

Leeds (West) Research Ethics Committee

Attendance at Committee meeting on 08 January 2010

Committee Members:

<i>Name</i>	<i>Profession</i>	<i>Present</i>	<i>Notes</i>
Miss Brygitta Atraszkiewicz			
Information Analyst	Yes		
Professor Howard Bird			
Consultant Rheumatologist	Yes		
Dr Rhona Bratt			
Retired Multimedia Project Manager	Yes		
Mr Stephen Bush			
Consultant in Emergency Medicine	Yes		
Dr Sheila E. Fisher			
NCRI Associate Director for PPI	Yes		
Dr Stella Kwan			
Senior Lecturer in Dental Public Health	No		
Mr Peter Margerison			
Retired Solicitor	No		
Miss Eve Miles			
Medical student	Yes		

Dr Wendy Neil			
Consultant Psychiatrist	No		
Dr Vera Neumann			
Consultant in Rehabilitation Medicine	Yes		
Dr Jane Orton			
Consultant Oncologist	Yes		
Dr Michael Rivlin			
Medical Ethics Lecturer Lay Member,	No		
Dr Ken Shenderey			
General Practitioner	No		
Revd. Chris Swift			
Hospital Chaplain	Yes		

Also in attendance:

<i>Name</i>	<i>Position (or reason for attending)</i>
Mrs Elaine Hazell	
REC Co-ordinator	
Ms Claire Kelly	
Assistant Co-ordinator	

Written comments received from:

<i>Name</i>	<i>Position</i>

Mr Peter Margerison	
Retired Solicitor	